23rd INTERNATIONAL MULTIDISCIPLINARY SCIENTIFIC GEOCONFERENCE - SGEM 2023

28 – 30 November 2023 – Vienna, Austria

CONFERENCE PROCEEDINGS OF SELECTED PAPERS in WATER RESOURCES. FOREST, MARINE AND OCEAN ECOSYSTEMS ISSUE 3.2

Editors-in-Chief:

- **Prof. DSc. Oleksandr Trofymchuk, National Academy of Sciences of Ukraine, UKRAINE**
- **Prof. Dr. hab. oec. Baiba Rivza, Latvian Academy of Sciences, LATVIA**

DISCLAIMER

The International Multidisciplinary Scientific GeoConference SGEM (Survey, Geology, Ecology and Management) are focused on GLOBAL WARMING, CLIMATE CHANGE, CO_2 REDUCTION, BIODIVERSITY, AND GREEN TECHNOLOGIES FOR A SUSTAINABLE FUTURE.

Authors are responsible for the content and accuracy of the written papers. Opinions expressed are not meant to represent or reflect the position of the SGEM International Scientific Committee members.

10/11 Gerlgasse, Vienna 1030, Austria
Published by STEF92 Technology
Total print: 5000

E-mail: **science@sgemviennagreen.org** | URL: **www.sgemviennagreen.org**

ISBN 978-619-7603-64-4
ISSN 1314-2704
DOI: 10.5593/sgem2023v/3.2

FOREWORD

The International Multidisciplinary Scientific GeoConference SGEM is focused on AGENDA 2030 Goals - GLOBAL WARMING, CLIMATE CHANGE, CO_2 REDUCTION, BIODIVERSITY, AND GREEN TECHNOLOGIES FOR A SUSTAINABLE FUTURE.

In an ever-evolving world, amidst the vast expanse of the universe, Earth remains our singular home — a beacon of life, mystery, and endless curiosity. It is with immense pride and anticipation that we present the **2023 Conference Proceedings in Earth and Planetary Science, a collective endeavor of minds passionate about our world and the celestial wonders beyond.**

The beauty of science, particularly in the realm of geosciences, lies in its ability to unite us. It transcends borders, politics, and cultural divides, binding us together in pursuit of knowledge, understanding, and enlightenment. This year, our focus aligns with the noble aspirations of Agenda 2030, reminding us that our planet's health and sustainability are integral to our shared future. Every paper within these pages stands as a testament to our collective commitment to that goal.

Moreover, this conference encapsulates the harmonious dance between the Earth as a place we live in and to care for, and the Planet, with its place in the Universe - different but intertwined, sharing the primary goal of interpreting, understanding and celebrating the Universe and our place in it. Like an artist who captures the majesty of a mountain range or the vastness of space, our researchers, too, paint with data, hypotheses, and discoveries, sketching a future where knowledge drives progress.

In a world where discord often grabs headlines, this gathering underscores that there exist realms untouched by strife, where camaraderie and cooperation reign supreme. This is the world of geosciences: a haven for curious minds, a frontier for explorers, a canvas for dreamers.

As you delve into these meticulously peer-reviewed articles, let them not only inform you but inspire you. Let them remind you of the magic that happens when diverse minds converge for a singular purpose. **And let them serve as a beacon of hope, signaling a future where science, with its inherent artistry, continues to light our way.**

In anticipation of the better future and optimism,
Sincerely yours,

Prof. DSc. Oleksandr Trofymchuk
Editor-in-Chief of XXIII SGEM GeoConference Proceedings
National Academy of Sciences of Ukraine, UKRAINE

Prof. Dr. hab. oec. Baiba Rivza
Editor-in-Chief of XXIII SGEM GeoConference Proceedings
Member of the Presidium of the Latvian Academy of Sciences, LATVIA
President of the Latvian Academy of Agricultural and Forestry Sciences
Vice-chair of the Latvian Council of Higher education
President of Latvian universities professors' association
Expert from the European Academy of Sciences Academic Advisory Board (EASAC)

CONFERENCE PROCEEDINGS CONTENTS

SECTION HYDROLOGY AND WATER RESOURCES

SECTION FOREST ECOSYSTEMS

SECTION

HYDROLOGY AND WATER RESOURCES

ACID AND HEAT TREATMENT OF GEORGIAN NATURAL HEULANDITE

Prof. Dr. Vladimer Tsitsishvili[1]

Dr. Bela Khutsishvili[2]

Prof. Dr. Marinela Panayotova[3]

Prof. Dr. Manabu Miyamoto[4]

Dr. Nato Mirdzveli[2]

[1] Georgian National Academy of Sciences, **Georgia**
[2] Petre Melikishvili Institute of Physical and Organic Chemistry, I. Javakhishvili Tbilisi State University, **Georgia**
[3] Department of Chemistry, University of Mining and Geology, St. Ivan Rilski, **Bulgaria**
[4] Department of Chemistry & Biomolecular Science, Faculty of Engineering, Gifu University, **Japan**

ABSTRACT

Natural zeolites, a family of hydrated aluminosilicates, are important raw materials for micro and nano technologies due to their molecular-sieve, ion-exchange and catalytic properties. Their porous crystalline framework is built from alternating SiO_4 and AlO_4^- tetrahedra forming cages and channels, and improvement of zeolite performance is possible by thermal and chemical treatment. The influence of hydrochloric acid and calcination on heulandite-containing tuff from the Georgian Dzegvi-Tedzami deposit was studied by the X-ray energy dispersion spectra and diffraction patterns, thermal analysis, adsorption of water, benzene and nitrogen. It was found that an acidic environment leads to significant dealumination and decationization without amorphization, but with gradual dissolution of the sample; there is also a sharp increase in the surface area and volume of micropores available for large molecules, and in the mesoporous system, pores with a diameter of 4 nm become predominant. Heat treatment leads to dehydration proceeding up to ≈800 ºC, amorphization starting at ≈250 ºC; the transition to the heulandite B at ≈340 ºC is not fixed, at ≈500 ºC wairakite is formed; at temperatures above ≈1000 ºC, amorphous aluminosilicate contains crystalline inclusions of cristobalite, α-quartz, albite, hematite and magnetite. It is also shown that heat treatment increases the acid resistance of heulandite by reducing the degree of dealumination of acid-treated samples.

Keywords: heulandite, dealumination, decationization, dehydration, amorphization

INTRODUCTION

Natural and synthetic zeolites, hydrated porous aluminosilicates of the general formula $M_x[Al_xSi_yO_{2(x+y)}]\cdot mH_2O$ ($M^+ = Na^+, K^+, \ldots ½Ca^{2+}, ½Mg^{2+}, ...$), have a wide application due to unique set of molecular-sieve, sorption, ion exchange and catalytic properties [1]. In general, synthetic zeolites are more suitable for use as adsorbents (in particular, for the sequestration of heavy metals in wastewater treatment) due to the high uniformity of pore size distribution and the presence of a single compensation cation, while natural varieties, although very attractive from an economic and environmental points of view,

demonstrate a lower sorption capacity (including with respect to most heavy metals [2]). The problem is related to the porous crystalline structure of zeolites, built from alternating SiO_4 and AlO_4^- tetrahedra, forming open framework uniform structures with cages and channels, and to improve the performance of the zeolite, its structure can be changed by thermal or chemical treatment. For example, acid treatment makes it possible to increase the surface area of the adsorbent and the effective porosity of the original natural zeolites [2-4], since exchangeable cations M^+ located in channels and cavities throughout the zeolite structure sometimes block the channel system [5]. However, concentrated acid solutions at high processing temperatures can cause significant aluminum leaching (dealumination) and even destruction of the zeolite crystal structure. As has been shown [6], hydrochloric and nitric acids are more efficient dealuminating agents than sulfuric and phosphoric acids, not to mention weak organic acids. The most widely used is hydrochloric acid, its effect on the structure and properties of zeolites is well known [7, 8]. On the other hand, heat treatment is also used to improve the properties of natural zeolites [4], while the stability of the zeolite framework plays an important role, and it can be assumed that preliminary heat treatment can affect the acid resistance of the sample.
The purpose of our work was to study changes in structure and properties of heulandite-containing tuff from the Tedzami-Dzegvi deposit (Eastern Georgia) caused by acid and heat treatment; this zeolite was selected to create new bactericidal zeolite filter materials for purification and desinfection of water from various sources.

MATERIALS AND METHODS

Samples of heulandite-containing tuff were collected in the southern section of the Tedzami-Dzegvi deposit, Eastern Georgia. According to the results of recent study [9], the sample contains up to ≈90% of zeolite phase consisting of high-silica heulandite mixed with chabazite in a ratio of 8:1. Zeolitic tuff was crushed on a standard crusher, fractionated to a particle size of 1-1.4 mm (14-16 mesh), washed with distilled water to remove clay impurities, and dried at a temperature of 95-100 °C.

Acid treatment of samples was carried out by mixing 10 g of original zeolitic tuff with 100 ml of 0.5, 1.0, and 2.0 N HCl solutions in a shaking water bath (OLS26 Aqua Pro, Grant Instruments, US) operating in linear mode at 75 ºC. To achieve maximum effect, acid treatment was carried out in three steps: the first lasted 1 hour, the second – 2 hours, and the third – 3 hours, each step was followed by washing with distilled water until no Cl^- ions were detected in the washing water by using $AgNO_3$ solution.

Calcination of prepared samples in the temperature range of 200-1100°C was carried out in muffle furnace B400/410 (Naberthem, Carl Stuart Group). Zeolite samples were placed in a muffle furnace in heat-resistant round-bottom cups, subjected to heat treatment under static conditions for 1 hour, and then, after a while, these cups was placed in desiccators with calcined $CaCl_2$ until complete cooling.

Chemical composition of samples was calculated from the X-ray energy dispersive (XR-ED) spectra obtained from scanning electron microscope JSM-6490LV (Jeol, Japan) equipped with INCA Energy 350 XRED analyzer (Oxford, UK). Powder X-ray diffraction (XRD) patterns were obtained from D8 Endeavor diffractometer (Bruker, Germany). Thermogravimetric analysis was based on weight loss (TG), difference thermal analysis (DTA) and difference thermogravimetric (DTG) curves recorded on an

STA 2500 Regulus thermal analyzer (NETZSCH group) at a heating rate of 10 ºC/min. The adsorption capacity for water and benzene vapors was measured under static conditions at room temperature; the samples weighed on an electronic analytical balance (FA 2204N, JOAN LAB, China) were placed in a desiccator and kept for 96 hours at a constant pressure of water vapor (relative pressure p/p_o=0.4 and saturated vapor pressure p/p_o=1.0) and benzene (p/p_o=1.0) and then the samples that absorbed the vapors were weighed again. Nitrogen adsorption/desorption isotherms were measured at 77 K using ASAP 2020 Plus analyzer (Micromeritics, USA) using Brunauer–Emmett–Teller (BET) and Barrett-Joyner-Halenda (BJH) models for data analysis.

RESULTS AND DISCUSSION

The results for chemical composition of the acid-treated samples calculated for 72 oxygen atoms in the unit cell are given in Table 1 in terms of averaged empirical formulas of dehydrated zeolites; the Si/Al molar ratio shows the degree of dealumination.

Table 1. Chemical composition of original and acid-treated samples.

Concentration of HCl solution	Empirical formula	Si/Al
0	$(Na_{1.96}K_{0.47}Ca_{1.49}Mg_{1.17})[Al_{7.8}Si_{28.2}O_{72}]$	3.6
0.5 N	$(Na_{0.62}K_{0.67}Ca_{0.71}Mg_{0.47})[Al_{4.59}Si_{31.4}O_{72}]$	6.85
1.0 N	$(Na_{0.47}K_{0.40}Ca_{0.65}Mg_{0.46})[Al_{4.26}Si_{31.7}O_{72}]$	7.45
2.0 N	$(Na_{0.096}K_{0.50}Ca_{0.61}Mg_{0.26})[Al_{3.43}Si_{32.6}O_{72}]$	9.5

The degree of decationization is shown in Figure 1 by a decrease in the total charge of the compensating ions Na^+, K+, Ca^{2+} and Mg^{2+}, as well as the share of each of these cations in compensating the negative charge of the zeolite framework as they are leached and replaced in the framework by H^+.

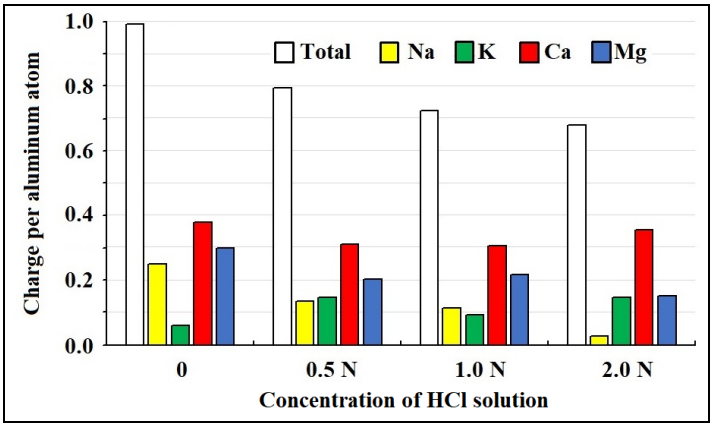

Figure 1. Cationic charge per Al atom of native (0) and acid-treated samples.

An increase in the Si/Al molar ratio by more than two and a half times indicates a rather high degree of acid-mediated dealumination; the total charge of metal cations per one aluminum atom monotonically decreases from ≈1 to ≈0.68 with increasing acid concentration. The contribution of Na^+ ions to compensate for the negative charge on aluminum atoms decreases, so that sodium is leached to the greatest extent (its content

decreased ≈9 times after treatment with 2.0 N solution); Mg^{2+} ions are washed out to a lesser extent, the content of Ca^{2+} ions decreased slightly (–7%), and K^{+} ions do not take part in the decationization process. This conclusion is consistent with the results of the study of decationization and dealumination of clinoptilolite tuff [7], but do not correspond to the data of work [8] that the removal of monovalent cations, such as Na^{+} and K^{+} ions, is insignificant for the temperatures of 25 – 100 ºC and changed little with acid concentration.

Powder XRD patterns show no changes after treatment with a dilute HCl solution (0.5 N), but treatment with concentrated solutions leads to a change in the intensity of some peaks (see Figure 2, left), and these changes are described in detail in our paper [9].

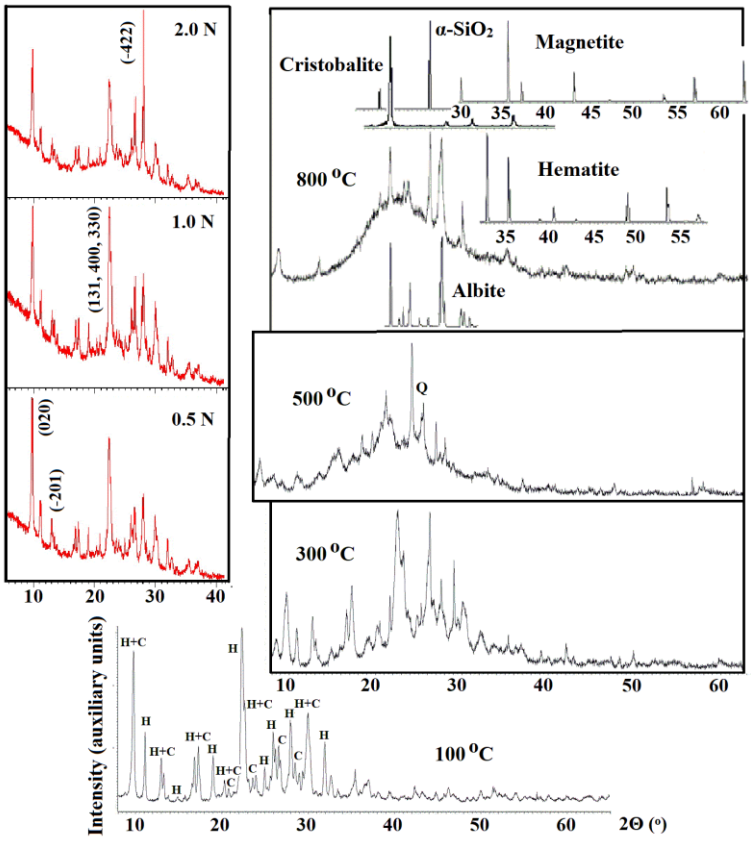

Figure 2. Powder XRD patterns of dried at 100 ºC sample (bottom, H – peaks of main heulandite phase, C – peaks of impurity chabazite phase), acid treated samples (left, numbers in parenthesis are Miller indices *hkl* of peaks changing intensity) and samples calcined at 300, 500 and 800 ºC (right).

No peak broadening is observed in XRD patterns of acid treated samples, so that the acidic environment does not cause amorphization of the crystal framework; the overall intensity of patterns decreases slightly with increasing acid concentration. The result obtained does not contradict the known ones, since in a recent work [6], the amorphization of clinoptilolite recorded using XRD patterns was noted only after treatment of the zeolite with solutions with a high concentration of hydrochloric acid (5 and 10 N).

XRD patterns do not change in the temperature range up to 200 ºC, at higher temperatures the peaks begin to broaden, than the intensity of the heulandite peaks decreases, and at ≈500 ºC a broad band and a sharp peak of quartz (2Θ = 26.6º) appear (Figure 2, right). Thermogravimetric curves show slow endothermic peaks at relatively low temperatures (DTA at 101.5 and 198.5 °C, DTG at 92.0 and 163.7 °C), but no sharp endothermic peak at ≈340 °C, which is associated with the transition to the structure of "sluggish" [10] heulandite B, first described by Koizumi [11]. Probably, the absence of a transition to heulandite B is explained by the lower aluminum content in Georgian heulandite (Si/Al=3.6) than in the low-silica samples studied in works [10-12].

It is believed that when heulandite is heated, the metastable phase of heulandite B exists in the temperature range of 340–470 °C, and at temperatures exceeding 500 °C a mixture of quartz (SiO_2) and minerals of the 9.GB.05 group such as wairakite ($Ca(Al_2Si_4O_{12})\cdot 2H_2O$) and/or anorthite ($Ca(Al_2Si_2O_8)$) starts to appear. The XRD patterns cannot unequivocally confirm the formation of these minerals, since the most intense peaks for wairakite and anorthite (2Θ ≈ 16 and 28º, respectively) overlap with the peaks of chabazite (reflection with *hkl*=113 giving an intense peak at 2Θ=16º [13]) and heulandite ((*hkl*=-422 at 2Θ=28.1º, and *hkl*=-441 at 2Θ=28.5º). However, the formation of wairakite containing "zeolite water" is confirmed by thermal analysis data: the measured total weight loss (15.09%) is in good agreement with the calculated one (15.5%) for 3 water molecules per aluminum atom, most of the water (≈60% of the total water content) is continuously lost at temperatures below ≈250 °C, and then part of the remainder (≈24%) is slowly dehydrated up to 650 °C, complete dehydration of the sample is achieved at ≈800 ºC; high-temperature endothermic peaks are registered (on the DTA curve at 730.5 °C, on the DTG curve at 717.7 and 778.8 °C). Complete amorphization of all zeolite phases (heulandite, wairakite, and chabazite) is completed at 1000°C; at higher temperatures, the amorphous aluminosilicate contains crystalline inclusions of cristobalite, α-quartz, albite, hematite and magnetite.

Water molecules have a small kinetic diameter of 0.266 nm and can freely pass through entrance windows into heulandite channels, and the adsorption of water vapor at a relative pressure p/p_o=0.4, corresponding to almost complete filling of micropores, is a measure of their volume available for small polar molecules [14], while adsorption at saturated water vapor pressure (p/p_o≈1) is a measure of the total pore volume. The kinetic diameter of the benzene molecule (0.585 nm) significantly exceeds the sizes of micropores and channels of heulandite, so that this non-polar molecule can be adsorbed only on the zeolite surface developed due to the presence of meso- and macropores; benzene adsorption capacity is a relative measure of surface area and its hydrophobicity. Results of measurements are shown in Figure 3.

The volume of micropores accessible for water molecules in native heulandite is about 60% of the total pore volume. Adsorption in micropores practically does not change as a result of acid treatment and decreases with an increase in the calcination temperature, reaching very low values (<0.3 mmol/g) at temperatures above 500 °C; it is in no way related to the aluminum content, as was noted in studies of water vapor adsorption on high-silica synthetic zeolites reviewed in [14].

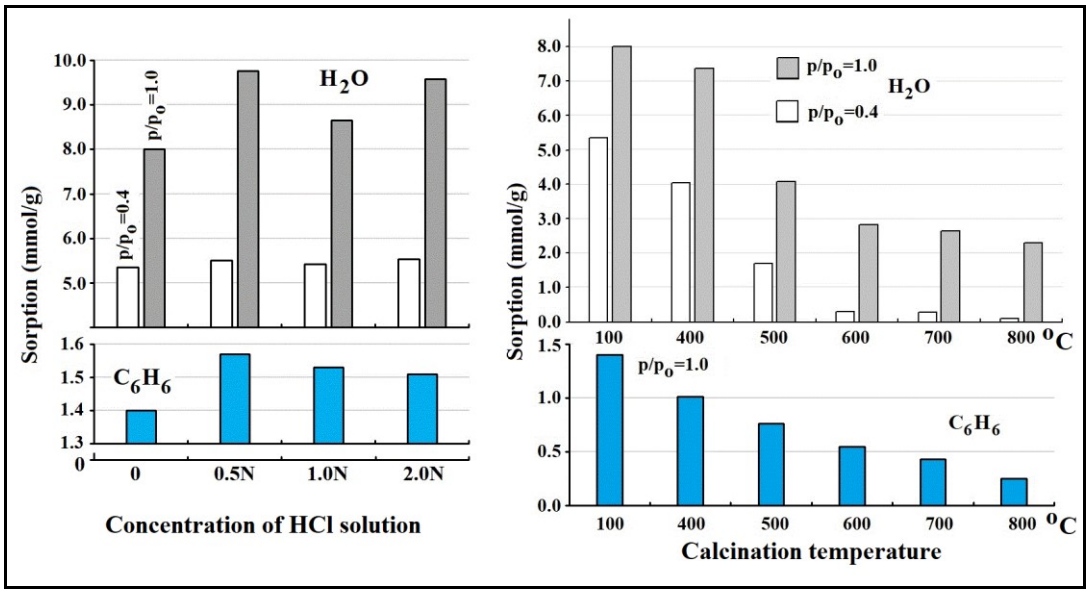

Figure 3. Water vapor (H_2O) and benzene (C_6H_6) adsorption capacity of acid-treated (left) and calcined (right) samples.

The adsorption capacity of all pores in acid treated samples changes nonmonotonically and decreases with an increase in the calcination temperature. Benzene adsorption changes insignificantly, but the results obtained indicate an increase in the hydrophobicity of the surface after acid treatment, while heat treatment leads to decrease of hydrophobicity.

In heulandite crystal structure, a 10-membered ring (0.75 x 0.31 nm) and one of the 8-membered rings (0.47 x 0.28 nm) cannot accommodate a nitrogen molecule (kinetic diameter 0.364 nm), which can pass only into one 8-membered ring (0.46 x 0.36 nm). The low-temperature adsorption-desorption isotherms of nitrogen on studied calcined samples correspond to the filling of micropores at low relative pressures ($p/p_o<0.3$) and demonstrate a hysteresis loop with a jump at p/p_0= 0.4-0.5 indicating the presence of developed system of mesopores; porosity parameters are given in Table 2, where S_{BET} is the BET surface area, V_p – total volume of pores, V_m – volume of micropores, D_{BJH} – the BJH desorption average pore diameter.

Table 2. Porosity parameters of initial, acid treated and calcined samples.

Parameter	Initial	Concentration of HCl (N)			Calcination temperature (°C)				
		0.5	1.0	2.0	400	500	600	700	800
S_{BET} (m^2/g)	12.8	127	155	175	11.4	10.5	9.45	9.16	6.52
V_p (mm^3/g)	89.5	109	113	126	89.2	92.8	82.2	78.0	83.8
V_m (mm^3/g)	6.47	78.2	85.6	88.9	6.0	5.7	5.1	5.0	3.5
D_{BJH} (nm)	17.2	13.1	11.6	11.1	17.6	17.6	17.2	16.1	20.1

The initial sample has a low surface area (12.8 m^2/g), and the fraction of micropores accessible to nitrogen molecules is only 7% of the total porosity. Under the influence of acid, the surface area and the volume of micropores accessible to nitrogen molecules increase sharply and continue to increase with increasing acid concentration in the treatment solution. A similar effect was noted in [6] for acid-treated clinoptilolite. The total pore volume increases monotonically with increasing acid concentration, while the

diameter of nanosized pores calculated using the BJH model sharply decreases. The pore size distribution has a maximum at ≈12 nm, after acid treatment, it disappears, but a sharp maximum appears at ≈4 nm (details are given in our work [9]). Heat treatment reduces the surface area and volume of micropores, while the volume, diameter and distribution of mesopores change only slightly.

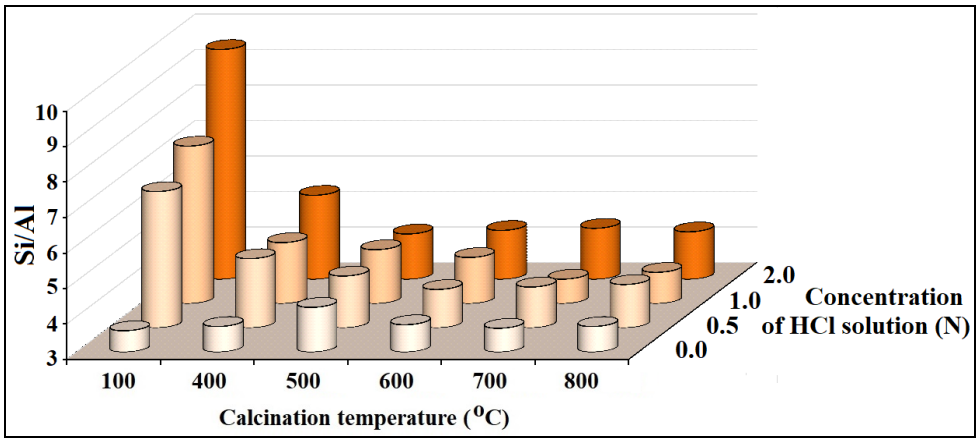

Figure 4. The Si/Al molar ratio calculated from XR-ED spectra in samples calcined at different temperatures and treated with HCl solutions of various concentrations.

According to measured changes in the Si/Al molar ratio in samples subjected to calcination and then treated with hydrochloric acid solutions, such pre-heat treatment significantly reduces the degree of dealumination, especially for samples amorphized by high-temperature calcination. Perhaps these results are not of practical importance, since at an annealing temperature of 600 °C and above, the corresponding samples lose their adsorption properties, but the structure and properties of the calcined and acid-treated samples require further study.

CONCLUSION

Acid treatment leads to significant dealumination and decationization of heulandite without amorphization, sharply increases the surface area and volume of micropores available for large molecules, and causes changes in the mesoporous system, leading to the prevalence of pores with a diameter up to 4 nm. Heat treatment causes dehydration continuing up to 800 °C, amorphization starting at 200 °C, formation of wairakite at 500°C, and does not lead to significant changes in pore systems. Heat treatment increases the acid resistance of heulandite by reducing the degree of dealumination after the sample is treated with hydrochloric acid solution The results obtained show the possibilities of obtaining effective molecular sieves, adsorbents and ion exchangers by modifying natural heulandite.

ACKNOWLEDGEMENTS

This work was supported by the International Science and Technology Center (ISTC) under the project GE-2506 “Scientific substantiation of the possibility of creating new bactericidal zeolite filter materials for purification-decontamination of water from various sources”.

REFERENCES

[1] Vasconcelos A.A., Len T., de Oliveira A.dN., da Costa A.A.F., da Silva Souza A.R., da Costa C.E.F., Luque R., da Rocha Filho G.N., Noronha R.C.R., do Nascimento L.A.S. Zeolites: A Theoretical and Practical Approach with Uses in (Bio)Chemical Processes. App. Sci., vol. 13/issue 3, #1897, 2023.

[2] de Magalhães L.F., da Silva G.R., Peres A.E.C. Zeolite Application in Wastewater Treatment. Adsorpt. Sci. Technol., vol. 2022, #4544104, pp. 1-34, 2022.

[3] Andrunik M., Bajda T. Removal of Pesticides From Waters by Adsorption: Comparison Between Synthetic Zeolites and Mesoporous Silica Materials. A Review. Materials (Basel), vol. 14/issue 13, #3532, pp. 1-38, 2021.

[4] Grela A., Kuc J., Bajda T. A Review of the Application of Zeolites and Mesoporous Silica Materials in the Removal of Non-Steroidal Anti-Flammatory Drugs and Antibiotics from Water. Materials, vol. 14/issue 17, # 4994, pp. 1-24, 2021.

[5] Wang S., Peng Y. Natural Zeolites as Effective Adsorbents in Water and Wastewater Treatment/ Chem. Eng. J.. vol. 156, pp. 1-24, 2010.

[6] Çakicioğlu-Özkan F., Becer M. Effect of the Acid Type on the Natural Zeolite Structure. J. Turk. Chem. Soc. B, vol. 2/issue 2, pp 69-74, 2019.

[7] Rozić M., Cerjan-Stefanović S., Kurajica S., Maeefat M.R., Margeta K., Farkas A. Decationization and Dealumination of Clinoptilolite Tuff and Ammonium Exchange on Acid-Modified Tuff. J. Colloid Interface Sci., vol. 284, pp 48-56, 2005.

[8] Cakicioglu-Ozkan F., Ulku S. The Effect of HCl Treatment on Water Vapor Adsorption Characteristics of Clinoptilolite Rich Natural Zeolite. Micropor. Mesopor. Mat., vol. 77, pp 47-53, 2005.

[9] Tsitsishvili V., Panayotova M., Mirdzveli N., Dzhakipbekova N., Panayotov V., Dolaberidze N., Nijaradze M. Acid Resistance and Ion-Exchange Capacity of Natural Mixtures of Heulandite and Chabazite. Minerals, vol. 13/issue 3, #364, pp 1-16, 2023.

[10] Mumpton F.A. Clinoptilolite Redefined. Amer. Mineral., vol. 45, pp 351-369, 1960.

[11] Koizumi M. The Differential Thermal Analysis Curves and the Dehydration Curves of Zeolites. Mineralogical J., vol. 1/issue 1, pp 36-47, 1953.

[12] Pechar F., Rykl D. Study of the Thermal Stability of the Natural Zeolite Heulandite. Chem. Pap., vol. 39/issue 3, pp 369-377, 1985.

[13] Dang L., Le S., Lobo R., Pham T. Hydrothermal Synthesis of Alkali-Free Chabazite Zeolites. J. Porous Mat., vol. 27, pp 1481-1489, 2020.

[14] Olson D.H., Haag W.O., Borghard W.S. Use of Water as a Probe of Zeolitic Properties: Interaction of Water with HZSM-5. Micropor. Mesopor. Mater., vol. 35/36, pp 435-446, 2000.

ADVANCED REMOVAL OF GAMMA HCH FROM WATER BY ULTRASONICATION, FENTON AND PHOTO FENTON ULTRASONICATION

Dr. Mihai Stefanescu[1]

Dr. Costel Bumbac[1]

Dr. Ionut Cristea[1]

[1] National Research and Development Institute for Industrial Ecology - ECOIND, **Romania**

ABSTRACT

Historical pollution with hexachlorocyclohexane (HCH) isomers of soil and groundwater unfortunately is an unsolved problem, especially in some countries where Lindane is still produced, as also in Europe in the surrounding areas of former production sites or landfilling sites usually due to inadequate long-term storage, treatment or recovery of these wastes. HCH removal technologies are usually dedicated to soil remediation, leachate treatment, water and wastewater treatment. This paper presents the research efforts to develop a treatment technology for gamma HCH removal from water matrices by advanced oxidation processes (AOPs) based on ultrasonication, Fenton and photo Fenton oxidation. Five treatment systems were assessed comparatively: direct ultrasonication, oxidation with hydrogen peroxide, ultrasonication with hydrogen peroxide, Fenton ultrasonication and Fenton ultrasonication followed by photo Fenton oxidation.

The energy (25-800 kJ) and amplitude of ultrasonic field, initial concentration of HCH (10 - 89 μg/L), hydrogen peroxide (1 - 4000 x stoichiometric dose), iron (Fe II) doses (1-15 mg/L) and UV irradiation time (30-60 min.) were the main experimental parameters evaluated. The ultrasonic frequency was constant - 20 kHz in all experiments. Best treatment performance of 99.9% HCH removal efficiency was achieved after application of a treatment train combining Fenton ultrasonication followed by Fenton UV photolysis at the main experimental parameters of: 200 kJ ultrasonic energy, 1000 x s peroxide dose, 5 mg Fe(II)/L and 30 minutes of UV irradiation.

Keywords: hexachlorocyclohexane, ultrasonication, AOPs, Fenton oxidation

INTRODUCTION

Hexachlorocyclohexane (HCH) was a very widespread insecticide in 20th century but nowadays its fabrication is stopped in Europe (all uses were banned since 2008). In Romania it was produce until 2006 and is still produced in some countries abroad. γHCH isomer (Lindane) is the one with application in agriculture. HCH isomers are a continuous pollution source for atmosphere, soil and underground water in case of inadequate storage of industrial waste and no interest of the landfill owner for capitalization (usually as trichlorobenzenes and derivates) [1]. In the year 2019 the HCH isomers waste around the world were as following: Türkiye 23500 t, Romania

310000 t, Slovakya 26000 t, Poland 35000 t, Germany 373000 t, France 330000 t, Spain 200000 t, USA 65000 t, India 56000 t, China 91200 t, Brasil 50000 t, South Africa 70000 t, Japan 76000 t [2].

HCH isomers have been included on persistent organic pollutants (POPs) list (Stockholm Convention), gamma HCH being the only one with pesticidal properties (approx. 10-12% of eight HCH isomers mixture) [3].

There are many chemical removal methods of POPs, including HCH, as advanced oxidation processes (AOPs) like ozonation, Fenton oxidation, UV and photocatalytic oxidation, ultrasonication, wet air oxidation, electrochemical oxidation or reductive methods like zerovalent iron technology (ZVI) [4]. For this paper work, ultrasonication is the main subject.

Ultrasonication has many applications (compound synthesis, cleaning, purification etc) including water treatment and soil remediation. *Ultrasonic cavitation* is the base of water and wastewater treatment.

Acoustic cavitation was the most studied because its applications in chemistry and environmental chemistry and the beginning of researchers was in 1880 with the discovery of piezoelectric effect by Curie brothers [5].

In the seventies were studied the effects of ultrasonication to the cellular degradation and in the nineties, it started the experiments of advanced removal of xenobiotics from water with high degree of mineralization.

The ultrasonic field has many industrial applications. The mechanical effect of acoustic cavitation leads to cellular membrane rupture having application in microbiology (proteins and enzymes formation, genetic enginering) or in wastewater treatment (increases biodegradability and the efficiency of secondary treatment stage in wastewater treatment plants) or in disinfection, both of wastewater and drinking water [6].

Four theories of ultrasonic cavitation effect in water are knows these days: theory of hot points; electric theory; theory of plasma discharges; supercritical theory.

The hot spots theory is generally accepted to explain the mechanism of sonochemical reactions. According to this theory, the ultrasonic field (16 kHz-100 MHz) generates inside the water volume rapid compressions and decompressions. These creates small bubbles which collapse and generate high pressures (>1000 at) and temperatures (>4700 ^{0}C) [7].

The organic pollutants bear these effects/actions being degraded because of physical and chemical interactions.

The main free reactive radicals in aqueous liquid after ultrasonication are HO• (hydroxyl radical is a very strong reactive reagent having the potential $\varepsilon_0 = 2.79$ V), H•, HOO• and O•.

The ultrasonication acts on water pollutants in three different ways [8]:

- mechanical effect (diminishing of particle size followed by solubilization increasing);

- chemical oxidation du to the free radical's action, OH• the most important having the oxidation potential higher than O_3, H_2O_2, NaOCl, Cl_2;
- thermal/pyrolytic effect (thermal degradation).

Hybrid technologies based on ultrasonication were studied for organic pollutants (pharmaceuticals, oils, dyeing, benzene, toluene, pesticides etc) removal from water (US + UV photolysis, US + Fenton oxidation, US + membrane processes, US + biological processes) [9].

Hydroxyl radical has non-selective attack which is extremely useful for an oxidant to be used on water treatment.

Degradation of HCH can be done by oxidative and reductive methods. In case of oxidative methods, they can be radical (dominant to HCH degradation) and non-radical. Hydroxyl (OH•) and sulphate ($SO_4^{\bullet-}$) radicals are the most representative for HCH oxidation.

Generally, most of proposed oxidative degradation mechanisms by hydroxyl radicals (from H_2O_2) lead to more stable trichlorobenzenes while the oxidation with sulphate radical (from peroxydisulphate) by dedydrochlorination leads to pentachlorocyclohexane and tetrachlorocyclohexadiene, before trichlorobenzene generation [10].

This paper is about advanced degradation of γHCH from synthetic aqueous solutions.

MATERIALS AND METHODS

The experiments were performed using an ultrasonic generator SONICS Vibracell 500 with 20 kHz stable frequency and 35 μm maximum amplitude. GC-MS analyse was used for samples γHCH determination.

Five experiments were performed in order to establish the main operating parameter of advanced lindane degradation in aqueous solutions:

- **Test 1**: direct ultrasonication (simple US) - it was studied the influence of ultrasonic energy (25÷800 kJ), amplitude (20-100%) and initial γHCH isomer concentration (9.77 – 88.89 μg/L);
- **Test 2**: oxidation with hydrogen peroxide (without ultrasonication) - the influence of active oxygen (O*) was studied (1÷4000 x *s* mg O*/L, *s* = stoichiometric dose for completely mineralization of HCH);
- **Test 3**: ultrasonication with hydrogen peroxide - the influence of H_2O_2 dose was studied (similar doses with previously test 2);
- **Test 4**: Fenton ultrasonication - the dose of Fe^{2+} (1 ÷ 15 mg Fe^{2+}/L) was studied keeping constantly the the ultrasonic energy level (200 kJ) and the dose of hydrogen peroxide (1000 x *s*);
- **Test 5**: ultrasonication + Fenton UV photolysis - the influence of catalyst and irradiation time (15 ÷ 60 min.) were studied.

The experimental results were centralized in tables.

RESULTS

- **Test 1 – Direct ultrasonication**

The influence of three main operational parameters (ultrasonic energy, ultrasonic amplitude and initial HCH concentration) was studied.

Tabel 1 emphasized the evolution of γHCH depending on **ultrasonic energy**.

Table 1 The influence of ultrasonic energy to γHCH degradation

Sample	E, kJ	Temperature, ^{0}C	pH, final	[γHCH] residual, μg/L	γHCH efficiency, %
E1	25	28.1	6.58	62.45	26.5
E2	50	30.5	6.14	70.50	17.0
E3	100	33.5	5.80	61.13	28.0
E4	150	34.3	5.62	15.22	82.0
E5	200	35.6	5.47	4.98	94.1
E6	400	35.5	5.12	5.84	93.1
E7	800	37.6	5.00	9.34	89.0

These tests were performed at the same initial γHCH concentration (85 μg/L) and amplitude (100%). The main experimental observations were as following:

- along the growth of ultrasonic energy from 25 kJ to 800 kJ the residual concentrations of γHCH decrease to minimum 4.98 μg/L (sample E5); the efficiency of degradation was maximum 94.1% for 200 kJ ultrasonic energy;
- the increase of energy led to pH decreasing (generation of acid species).

Table 2 shows **the influence of ultrasonic amplitude** on γHCH degradation.

Table 2 The influence of ultrasonic amplitude to γHCH degradation

Sample	A, %	[γHCH] residual, μg/L	γHCH efficiency, %
A1	100	62.45	26.5
A2	80	81.20	4.5
A3	40	83.44	1.8
A4	20	83.00	1.8

These tests were performed at the same initial γHCH concentration (85 μg/L) and 25 kJ energy.

The maximum amplitude was the best option from the point of view of HCH degradation efficiency and reaction time (lower amplitude means longer reaction time in order to have the final energy of 25 kJ).

Tabel 3 shows the efficiency of direct ultrasonication for **six initials γHCH concentration** in the same reaction conditions.

Table 3 The influence of initial γHCH concentration

Sample	[γHCH] initial, µg/L	[γHCH] residual, µg/L	γHCH efficiency, %
C1	88.89	66.77	24.9
C2	69.26	48.71	29.6
C3	49.44	37.77	23.5
C4	39.63	24.25	38.8
C5	14.72	8.22	44.1
C6	9.77	6.69	31.5

These tests were performed at the same initial ultrasonic energy (25 kJ) and 100% amplitude in order to find the treatment efficiency in the domain of low ultrasonic energy. 200 kJ energy was selected for the next experimental tests.

- **Test 2 – oxidation with hydrogen peroxide (without ultrasonication)**

All the experiments of Test 2 ÷ Test 4 were performed with the same initial stock solution of γHCH having 54.7 µg γHCH/L, 25 kJ energy and 100% amplitude.

Table 4 emphasized the influence of hydrogen peroxide dose on γHCH degradation efficiency.

Table 4 The influence of oxidant dose (H_2O_2)

Sample	O^* dose, mg/L	[γHCH] residual, µg/L	γHCH efficiency, %
H1	stoechiometric (s)	45.33	17.1
H2	100s	47.90	12.4
H3	1000s	42.98	21.4
H4	4000s	45.55	16.7

The maximum degradation of HCH was in case of sample H3 - η γHCH = 21.4% for 1000 x stoichiometric dose of O*. The application of high excess of oxidant is usual in case of some refractory pollutants like HCH isomers.

- **Test 3 – ultrasonication with hydrogen peroxide**

Ultrasonication (US) efficiency could be improve by adding oxidant, hydrogen peroxide in this case. Our experimental results are presented in table 5 in case of 25 kJ ultrasonic energy.

Table 5 Advanced oxidation system – US/H_2O_2

Sample	O^* dose, mg/L	[γHCH] residual, µg/L	γHCH efficiency, %
U1	stoechiometric (s)	43.10	21.2
U2	100s	43.20	21.2
U3	1000s	42.30	22.6
U4	4000s	41.49	24.1

The oxidant adds had a small influence on γHCH degradation, maximal value being 24.1% in case of sample U4.

- **Test 4 – Fenton ultrasonication results**

Fenton ultrasonication is a hybrid AOPs based on ultrasound and classic Fenton oxidation with hydrogen peroxide and iron (II). The influence of five iron doses was studied. The stock fresh solution of 1 g Fe^{2+}/L as $FeSO_4$ was used. Table 6 shows the degradation yields of γHCH with iron doses for a constant amount of hydrogen peroxide.

Table 6 Advanced oxidation system – US/H_2O_2

Sample	O^* dose, mg/L	Fe^{2+} dose, mg/l	[γHCH], µg/l	γHCH efficiency, %
F1	1000s	1	36.84	32.6
F2		5	30.16	44.8
F3		7.5	31.31	42.8
F4		15	31.80	41.9

The removal efficiencies of γHCH are double comparing with ordinary oxidation with hydrogen peroxide being 44.8% in case of sample F2 (5 mg Fe^{2+}/L).

- **Test 5 – Hybrid oxidation system Ultrasonication + Photo-Fenton oxidation**

The experiments were performed in two steps:

First step: Direct/simple ultrasonication;

Second step: Photo-Fenton oxidation

Three main tests were made taking into consideration the previous results in order to emphasized the influence of iron (II) dose and UV irradiation time. The ultrasonic energy was 200 kJ with 100% amplitude and peroxide dose 1000s, constant for all three tests. The results are shown in table 7.

Table 7 The influence of iron dose and UV irradiation time to γHCH degradation

Sample	O^* dose, mg/L	Fe^{2+} dose, mg/L	UV irradiation time, min.	[γHCH] residual, µg/L	γHCH efficiency, %
UV1	1000s	15	30	22.88	58.2
UV2		5	60	<0.1	99.9
UV3		5	90	<0.1	99.9

These results show that a triple dose of iron does not rise the efficiency of γHCH degradation (only 58.2%) but the increase of irradiation time did it (η γHCH > 99%).

DISCUSSION

HCH isomers are not easy to be degraded to harmless compounds by conventional water and wastewater treatment which led to new advanced degradation methods like AOPs. This paper is in the tendence of AOPs application in the field of refractory micropollutants (including POPs) degradation from aqueous matrix. There is preoccupation of scientists to combine modern water treatment technologies among themselves or with classic methods.

The final result of this paper work represents an argument in this sense: a combination between ultrasonication, Fenton oxidation and UV photolysis.

CONCLUSION

Gamma HCH is the only HCH isomer with application in agriculture. It is still used in some countries from Asia but can be detected in Europe in the proximities of old Lindane factories, in soil and underground water. Romania is one of European countries with historical pollution with HCH isomers.

In this context this paper shows the experimental results of γHCH degradation by advanced oxidation processes (AOPs) based on: ultrasonication, hydrogen peroxide, ultrasonication and hydrogen peroxide, Fenton ultrasonication and ultrasonication + UV Fenton photolysis. Five experimental tests were performed: direct ultrasonication (simple US), oxidation with hydrogen peroxide (without ultrasonication), ultrasonication with hydrogen peroxide, Fenton ultrasonication, ultrasonication + Fenton UV photolysis.

The ultrasonic energy, hydrogen peroxide dose and UV irradiation turned out to be the main influencing factors of γHCH removal. The aim of these preliminary tests was to obtain the best degradation efficiency of γHCH with minimal consumption of energy and reagents. The results had shown that the ultrasonic energy should be ≥200 kJ in order to have removal yield over 90%.

The most efficient oxidation system was ULTRASONICATION + UV Photo Fenton oxidation with 99.9% γHCH removal for 200 kJ ultrasonic energy, 6.76 mg O*/L oxidant dose, 5 mg Fe^{2+}/L catalyst and minimum 30 minutes of UV reaction time.

ACKNOWLEDGEMENTS

The work has been conducted with the support of Romanian Ministry of Research, Innovation and Digitalization, UEFISCDI, under the research project PN IV 584 PED/2022.

REFERENCES

[1] Waclawek S., Silvestri D., Hrabak P., Padil V.T., Torres-Mendieta R., Waclawek M., Cernik M., Chemical oxidation and reduction of hexachlorocyclohexane: A review, Water Research, vol. 162, pp 302-319, 2019;

[2] Berger M., Loffler D., Ternes T., Heininger P., Ricking M., Schwarzbauer J., Hexachlorocyclohexane derivatives in industrial waste and samples from a contaminated riverine system, Chemosphere, vol. 150, pp 219-226, 2016;

[3] Rostam A.B., Taghizadeh M., Advanced oxidation processes integrated by membrane reactors and bioreactors for various wastewater treatments: A critical review, Journal of Environmental Chemical Engineering, vol.8/issue104566, pp 1-15, 2020;

[4] Oliveira A.S., Saggioro E.M., Pavesi T., Moreira J.C., Ferreira L.F.V., Solar photochemistry for environmental remediation – Advanced oxidation Processes for industrial wastewater treatment/Molecular Photochemistry – Various aspects, pp 195-222, 2012;

[5] Parag R.G., Abhijeet M.K., A review of aplications of cavitation in biochemical engineering/biotechnology, Biochemical Engineering Journal, vol. 44, pp 60-72, 2009;

[6] Collin G.J., Gianluca L.P., Awang B., Duduku K., Sonophotocatalysis in advanced oxidation process: A shor review, Ultrasonics Sonochemistry, vol. 16, pp 583-589, 2009;

[7] Suslick K.S., McNamara W.B., Didenko Y., Hot spot conditions during multi-bubble cavitations, Sonochemistry and Sonoluminescence, pp 191-204, 1999;

[8] Madhavan J., Theerthagiri J., Balaji D., Sunitha S., Choi M.Y., Ashokkumar M., Hybrid advanced oxidation processes involving ultrasound: An overview, Molecules, vol. 24/issue 3341, pp 1-18, 2019;

[9] Kida M., Ziembowiez S., Koszelnik P., Application of an ultrasonic field for the removal of selected pesticides, E3S Web Conf., vol. 49, 2018;

[10] Ribeiro A.R., Nunes O.C., Pereira M.F.R., Silva A.M.T., An overview on the advanced oxidation processes applied for the treatment of water pollutants defined in the recently launched Directive 2013/39/EU, Environment International, vol. 75, pp 33-51, 2015.

ANALYSIS OF CHOSEN LOCALITY IN THE SOUTH MORAVIAN REGION IN TERMS OF RUNOFF AND EROSION CONDITIONS AND IN TERMS OF POLLUTION OF SURFACE WATER

Lukáš Buršík[1]

Prof. Dr. Miroslav Dumbrovský[1]

Dr. Veronika Sobotková[1]

Dr. Marcela Pavlíková[1]

[1] Brno University of Technology, **Czech Republic**

ABSTRACT

Firstly, this paper is focused on the analysis of runoff and erosion conditions in the chosen locality, which is in the South Moravian Region of the Czech Republic. The analysis was made using geographic information systems, mainly the ArcGIS Pro software program. Water erosion endangers more than fifty percent of arable land in the Czech Republic. Unfortunately, there is no systematic protection of the majority of soil erosion-threatened areas that would prevent further losses. One of the main causes of this is the fact that the Czech Republic has the largest blocks of arable land in Europe due to agricultural intensification production, which began with collectivization and subsequent consolidation of small fields into large ones. Instead of a colourful landscape mosaic, it is now made up of uniform fields. The consequence is a reduction in the natural resistance of the Czech landscape to water erosion, drought, and floods. Another problem facing agricultural areas is that pollutants are often introduced into the recipient via surface runoff or drainage water. Thus, secondly, this paper deals with the evaluation of water samples taken in the locality from a main drainage facility and a stream with the aim of investigating how agriculture affects water quality. Chemical parameters determining water pollution were selected, such as nitrogen or phosphorus content.

Keywords: water erosion, runoff, drainage water, water pollution, ArcGIS Pro

INTRODUCTION

The paper primarily deals with the analysis of runoff and erosion conditions in the chosen locality which is mostly done using the geographic information system ArcGIS Pro. This paper is also aimed at contamination of surface water by pollutants which are produced by an agricultural company that uses a part of the locality as a sod farm. For this reason, ten water samples were taken from a drain from which water flows into a watercourse that is used as a main drainage facility. The samples were subsequently analyzed in a chemical laboratory. These analyses were focused, among other parameters, on the nitrogen or phosphorus content.

Soil erosion by rainfall and runoff is one of the most threatening environmental problems in the world [1]. It is a significant global soil degradation threat to land, freshwater, and oceans, while wind and water are the major drivers [2]. Soil erosion is a threat to food security, especially in regions where the area of arable land is shrinking dramatically due to soil degradation [3]. Changes in future soil erosion rates are driven by climatic conditions, land use patterns, farmers' choices, socio-economic development, and importantly modified by agro-environmental policies [4]. The world is experiencing serious soil losses. Soil erosion has become an important environmental problem in certain regions, and it is strongly affected by climate and land-use changes [5]. Conservation management practices – including agroforestry, cover cropping, no-till, reduced tillage, and residue return – have been applied for decades to control surface runoff and soil erosion [6].

Water contamination, caused by natural and anthropogenic activities, possess a significant threat to public health globally [7]. The emission of nutrients and pesticides from agricultural soils endangers natural habitats [8].

MATERIALS AND METHODS

Description of Chosen Locality

The chosen locality can be found in the South Moravian Region (NUTS 3) of the Czech Republic, in the Brno-County District (NUTS 4). It is situated in proximity of the south-eastern border of the city of Brno (see Fig. 1), near a Brno Airport. The territory is a part of a fourth-order watershed that falls into the Morava River Basin. It extends into cadastral territories of three municipalities: Kobylnice (cadastral territory Kobylnice u Brna), Sokolnice (cadastral territory Sokolnice), and Šlapanice (cadastral territory Šlapanice u Brna). The area of the chosen locality covers approximately 215 hectares. Majority of the area (almost 66%) falls into cadastral territory Kobylnice u Brna. Roughly 22% falls into cadastral territory Šlapanice u Brna and about 12% falls into cadastral territory Sokolnice.

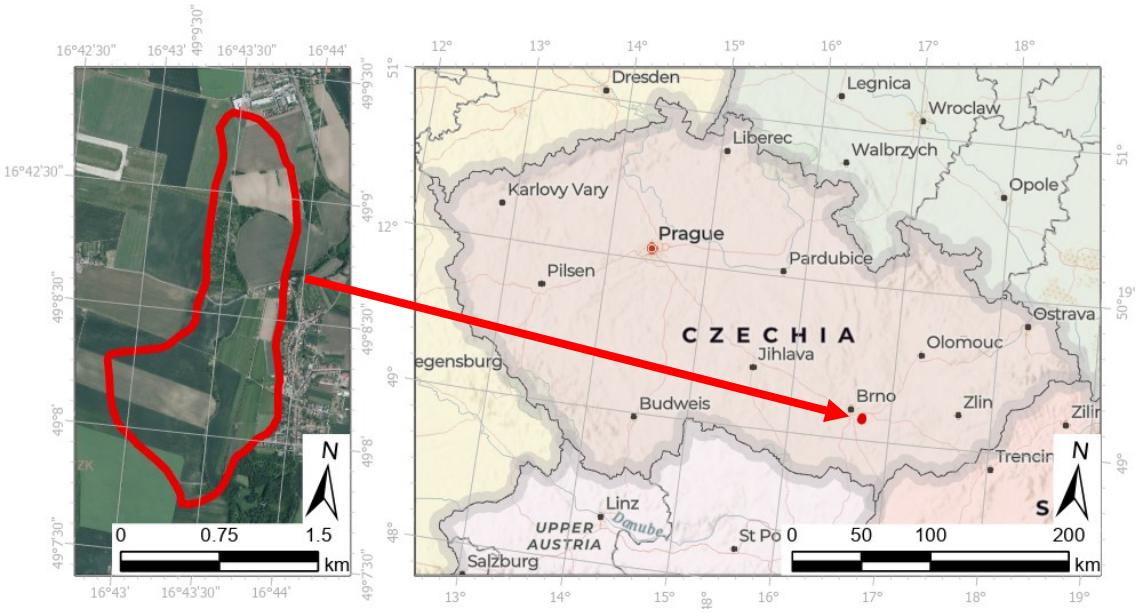

Fig. 1 Location of the area of interest.

Fig. 2 Watercourse (main drainage facility) in the area of interest; location of water samples [own source].

Fig. 3 Sod farm in the area of interest [own source].

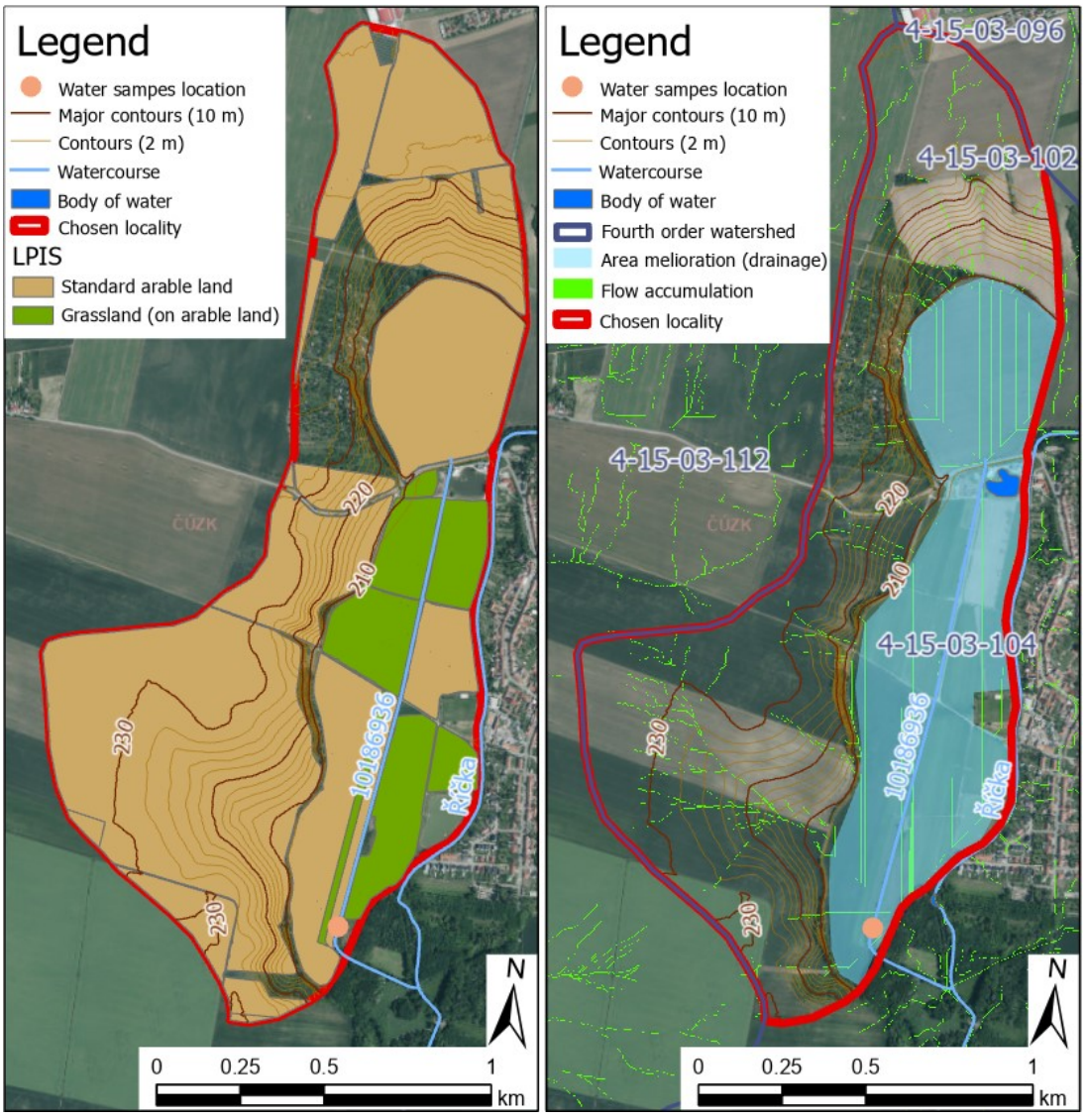

Fig. 4) Land-use (LPIS) – left, b) Area melioration (drainage system) – right.

The area of interest is located at an altitude of 207 to 238 meters above sea level. The highest peak is at the northernmost point of the territory. There is a noticeable place in the territory where there used to be a pond which can be seen as an approximately flat area.

In the locality, the predominant soil type is chernica fluvial (CCf). Different types of chernozems (CEm, CEl, CEx, CEp, and CEr) are here as well.

The territory is partially drained and an area melioration (drainage system) is built there – see Fig. 4 b). In the area of interest, a watercourse (ID 10186936) can be found that is a main drainage facility (Fig. 2) from which water flows into the watercourse Říčka that is outside the locality.

According to LPIS (Land Parcel Identification System), most of the area is used for agricultural purposes. There are blocks of standard arable land and grassland (on arable land). As already mentioned, part of the locality is used as the sod farm (see Fig. 3).

Description of Method Used for Calculation of Soil Loss and Sampling Method

The Universal Soil Loss Equation (abbreviated USLE) is the most widely used soil loss estimation equation in the world. It predicts the long-term average annual soil loss using six factors that are associated with climate, soil, topography, vegetation, and management. The USLE is often given as [9]:

$$G = R \cdot K \cdot L \cdot S \cdot C \cdot P \quad (1)$$

where G is average long-term soil loss in tons per hectare per year, R is rain erodibility factor, K is soil erodibility factor, L is slope length factor, S is slope steepness factor, C is cover-management factor, and P is support practice factor (factor of anti-erosion measures) [9]. Factors L and S are usually together as LS factor.

Water samples were taken from a drain that can be found in the locality, from which water flows into the watercourse Říčka (see Fig. 4 – Water samples location). Sampling took place during the period of May 2023 to September 2023. The dates on which these were taken are following: May 4, May 15, June 7, June 14, July 3, July 18, August 28, September 14, and September 25. The sampling was carried out in both dry and wet conditions (after rains).

One litre PET bottles were used for the samples and the samples were transferred immediately in a cooling box for analyses. Moreover, selected parameters were measured *in-situ* immediately, such as pH or O_2 (with use of a multiparameter Hach sonde). Other parameters were obtained from the chemical analyses in the laboratory which were focused on, for example, phosphorus or nitrogen content. $N\text{-}NO_3$ was determined indirectly by difference between $N\text{-}NO_x$ (with use of a multiunit Hach sonde) and $N\text{-}NO_2$ (spectrophotometric determination of NO_2^- by 1-naphthol/sulphanilic acid reagent). $N\text{-}NH_3$ was determined by spectrophotometric determination using Nessler reagent. An outflow from one of the drains was chosen as a water samples location – see Fig. 2 and Fig. 4.

RESULTS

Average Soil Loss in Chosen Locality

The result of the analysis of the chosen locality in terms of runoff and erosion conditions can be seen in Fig. 5. The average soil loss (G), which is in tons per hectares per year, is classified here into six categories: 0–4 t·ha^{-1}·year^{-1}, 4–8 t·ha^{-1}·year^{-1},8–12 t·ha^{-1}·year^{-1}, 12–16 t·ha^{-1}·year^{-1}, 16–20 t·ha^{-1}·year^{-1}, and 20 and more t·ha^{-1}·year^{-1}.

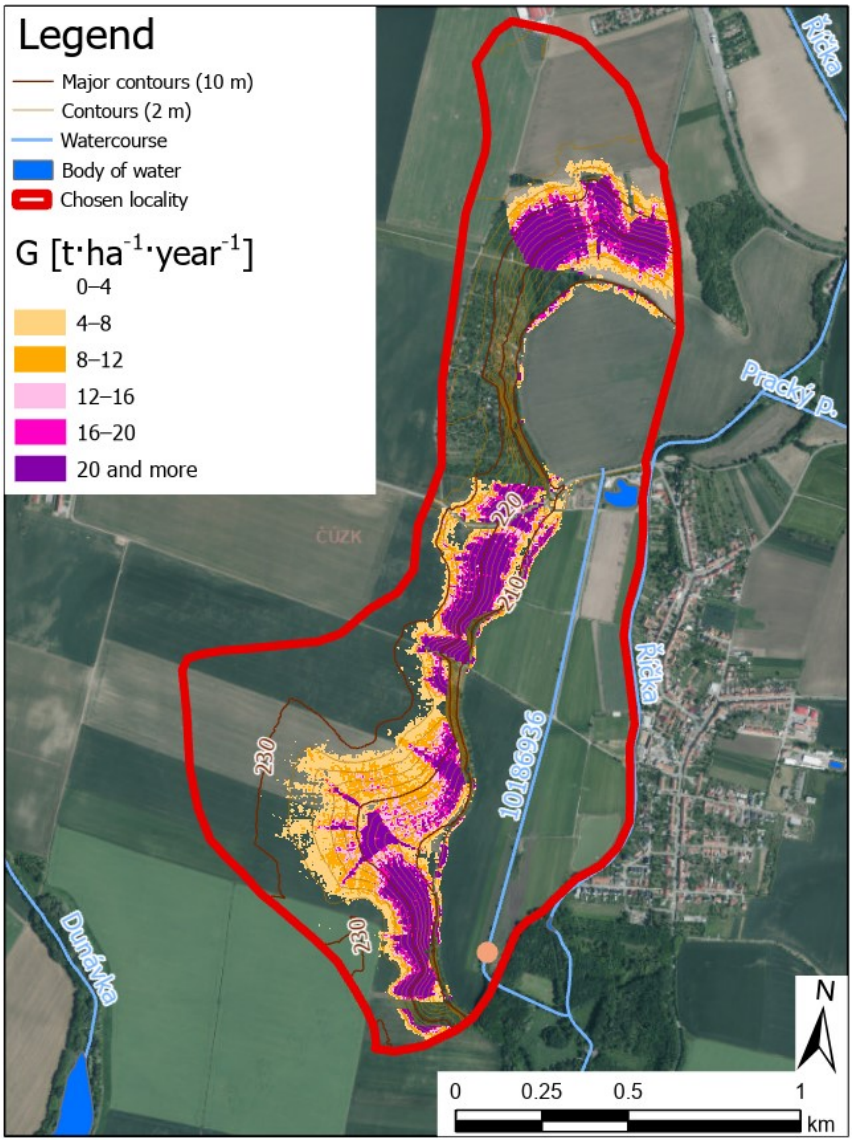

Fig. 5 Average soil loss (G) in tons per hectare per year in the chosen locality.

Analysis of Surface Water in Chosen Locality

As already mentioned, some parameters were measured *in-situ*. Now, for instance, in Fig. 6 it is possible to observe the oxygen (O_2) concentration in the samples and pH of the water samples.

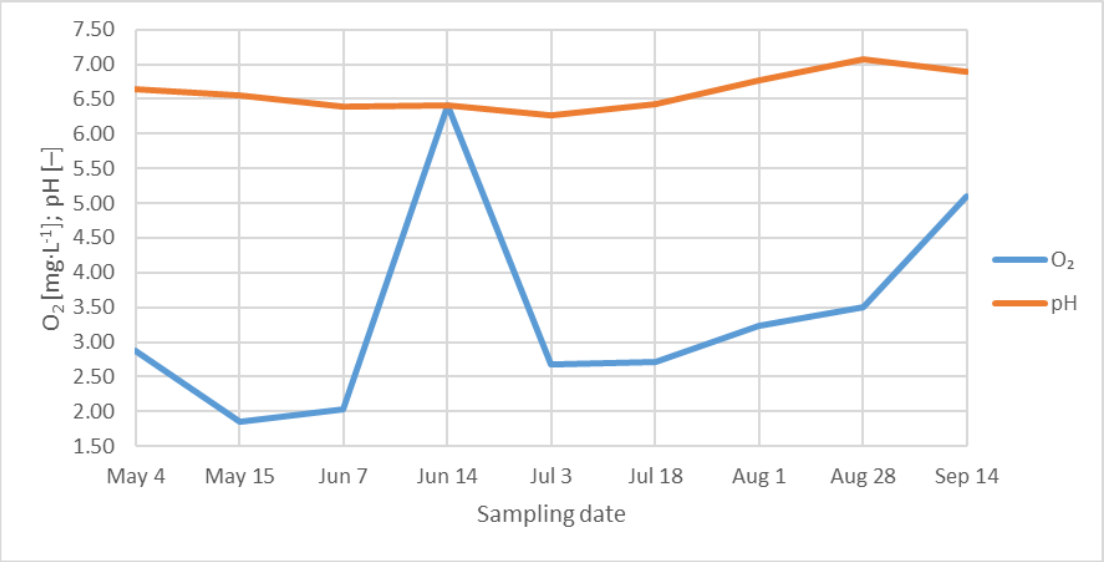

Fig. 6 Oxygen concentration in the samples and pH of the samples taken from the drain.

In the chemical laboratory, values of several parameters were obtained. Fig. 7 shows these selected parameters: nitrate nitrogen (N-NO_3) ammoniacal nitrogen (N-NH_4), and total phosphorus (TP) contents.

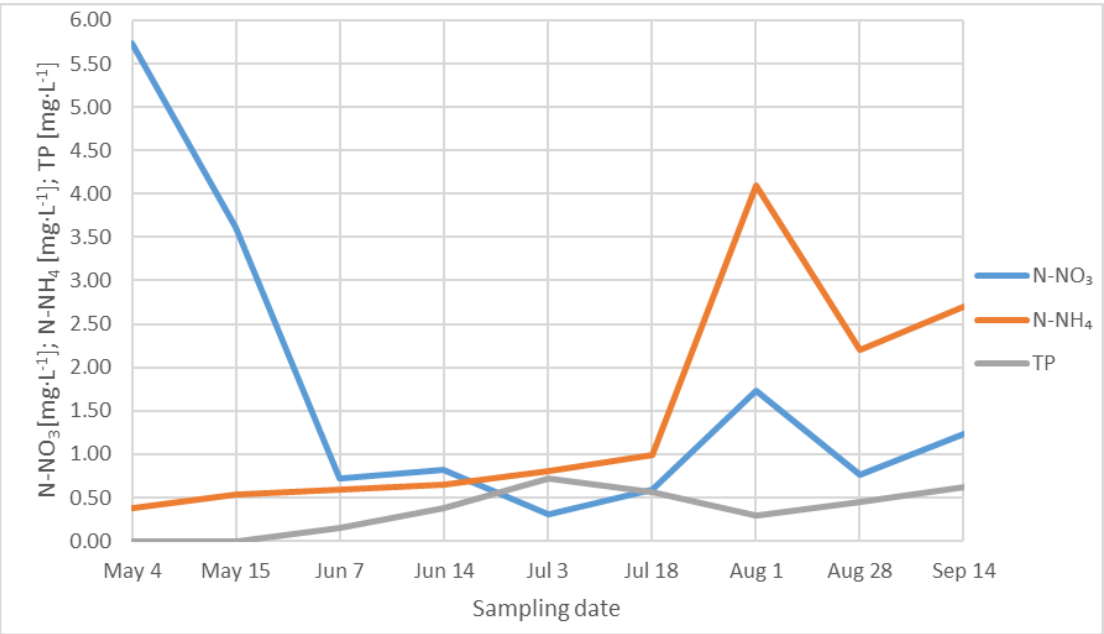

Fig. 7 N-NO3, N-NH4, and total phosphorus (TP) contents in the samples taken from the drain.

DISCUSSION

The results obtained in the part devoted to the analysis of the chosen locality in terms of runoff and erosion conditions show that almost three quarters of soils in the locality fall into the category with average soil loss up to four tons per hectare per year. Considering that a large part of the territory is flat, such a result can be expected. Approximately

nine percent of soils fall into the highest category with average soil loss twenty and more tons per hectare per year.

It is possible to observe that the hydrochemical results show affecting of the monitored area by agricultural pollutants and influence of dry or wet season to water samples (how much water was flowing from the drain).

There are no values of total phosphorus from the first two samplings (May 4 and May 15). Pease [10] stated that nutrient loss in surface runoff tended to be more of an environmental concern. For instance, surface runoff did not typically carry high amounts of nitrogen, but it could carry high amounts of sediment-bound phosphorus into streams and waterways. Excessive phosphorus availability in lakes and streams could result in harmful algal blooms. Total phosphorus values were higher in July and September.

Winter et al. [11] stated that severe droughts, which are predicted to become more frequent across Europe, can reduce the nitrogen retention capacity of catchments, thereby intensifying nitrate pollution and threatening water quality. The first two values of $N\text{-}NO_3^-$ in water samples were higher unlike to others values due to seasonal application of fertilizers. The first sampling data were obtained during the dry season whereas the second sampling data were obtained in the wet season. Later samplings had similar values of $N\text{-}NO_3^-$ in wet or dry season.

Ammoniacal nitrogen is the primary product of the decomposition of organic nitrogenous substances. The values of ammoniacal nitrogen ($N\text{-}NH_4$) were higher during August and September (August 28 – 4,10 $mg \cdot L^{-1}$; September 14 – 2,20 $mg \cdot L^{-1}$; September 25 – 2,70 $mg \cdot L^{-1}$). It is advisable to pay attention for these values due to the presence of aquatic organisms in watercourse - ammoniacal nitrogen can be toxic under certain conditions.

CONCLUSION

This paper was primarily aimed at the analysis of the chosen locality in terms runoff and erosion conditions. The paper also dealt with hydrochemical and chemical parameters in surface water. Nutrients should be produced by an agricultural company that uses part of the area of interest as the sod farm. Because of this, water samples were taken from the drain from which water flows into the watercourse. The samples were afterwards analysed in the chemical laboratory. These analyses were focused, among other parameters, on the nitrogen and phosphorus content.

The Materials and Methods section was first dedicated to method of calculation of soil loss. For the calculation, the Universal Soil Loss Equation was used. In this section, sampling methods and chemical analyses were also briefly described.

The Results section was divided into two parts, the result of the first one is the average soil loss that was classified into six categories. Almost three quarters of the area fall into the category with average soil loss up to four tons per hectare per year. The second part was aimed at analysis of surface water which is influenced by agricultural pollutants. It was found that parameters obtained are influenced by whether the sampling was done during the dry or wet season and by how much water was flowing from the drain. It was found that values of $N\text{-}NH_4$ were extremely high in the samples taken during May (the

first two samplings – May 4 and May 15). Input of ammoniacal nitrogen can be caused by a seepage of fertilizers into soil, underground water, and the drain.

ACKNOWLEDGEMENTS

This paper is a result of an inter-faculty (Faculty of Civil Engineering and Faculty of Chemistry) junior research FAST/FCH-J-23-8283 “Interdisciplinary approach to analysing areas of interest leading to measures for improving ecological state of watershed in terms of erosion and runoff conditions, as well as surface water pollution by pollutants”.

REFERENCES

[1] Ke Q., Zhang K., Patterns of runoff and erosion on bare slopes in different climate zones, Catena, vol. 198, 2021, DOI https://doi.org/10.1016/j.catena.2020.105069

[2] Borrelli P., Robinson D. A. et al., Land use and climate change impacts on global soil erosion by water (2015-2070), PNAS, vol. 117, no. 36, 2020, DOI https://doi.org/10.1073/pnas.2001403117

[3] García-Ruiz J. M., Beguería S. et al., Ongoing and Emerging Questions in Water Erosion Studies, Land Degradation & Development, vol. 28, pp 5-21, 2017, DOI https://doi.org/10.1002/ldr.2641

[4] Panagos P., Ballabio C. et al., Projections of soil loss by water erosion in Europe by 2050, Environmental Science & Policy, vol. 124, pp 380-392, 2021, DOI https://doi.org/10.1016/j.envsci.2021.07.012

[5] Guo Y., Peng C. et al., Modelling the impacts of climate and land use changes on soil water erosion: Model applications, limitations and future challenges, Journal of Environmental Management, vol. 250, 2019, DOI https://doi.org/10.1016/j.jenvman.2019.109403

[6] Du X., Jian J. et al., Conservation management decreases surface runoff and soil erosion, International Soil and Water Conservation Research, vol. 10/issue 2, pp 188-196, 2022, DOI https://doi.org/10.1016/j.iswcr.2021.08.001

[7] Babuji P., Thirumalaisamy S. et al., Human Health Risks due to Exposure to Water Pollution: A Review, MDPI, vol. 15/issue 14, 2023, DOI https://doi.org/10.3390/w15142532

[8] Siedt M., Schäffer A. et al., Comparing straw, compost, and biochar regarding their suitability as agricultural soil amendments to affect soil structure, nutrient leaching, microbial communities, and the fate of pesticides, Science of The Total Environment, vol. 751, 2021, DOI https://doi.org/10.1016/j.scitotenv.2020.141607

[9] Wischmeier W. H., Smith D. D., Predicting Rainfall Erosion Losses: A Guide to Conservation Planning, USDA, 1978.

[10] Pease L., When it rains, it pours, Journal of Nutrient Management, November issue, pp 14-15, 2020.

[11] Winter C., Nguyen T. V., et al., Droughts can reduce the nitrogen retention capacity of catchments, Hydrology and Earth System Sciences, vol. 27, issue 1, pp 303-318, 2023, DOI https://doi.org/10.5194/hess-27-303-2023

APPLICATION OF GAME THEORY IN FLOOD CONTROL USING FLOODPLAIN

Dr. Tomas Kozel[1]

[1] Brno University of Technology, Faculty of Civil Engineering, **Czech Republic**

ABSTRACT

The paper deals with the possibility of applying game theory in the decision of the dispatcher regarding the opening of the gates to the floodplain (construction of flood control measures). When the forecast of the flood course is bur ended with a random error from the normalized normal distribution N (0.1). The forecast itself is in the range of flows are capable of causing significant damage. The experiment tested different options for adjusting the probability of betrayal (error) of the forecast model. The probability of betrayal was assessed from 5% to 95%. Furthermore, different ratios between the damage caused when the gates were opened and the actual damage caused within the city flooding when the gates were not opened were tested. The experimental results clearly show that in the long run it is more beneficial to open the gates to the floodplain in the case of pure Nash equilibrium. In the case of mixed equilibria, opening (not opening) depends on the ratio of damages and the probability of betrayal (error) of the prediction model. The probability of controller betrayal (opposite action to the forecast action) alone is less significant compared to the above conditions.

Keywords: Game theory, flood, floodplain, prisoner's dilemma, random prediction error.

INTRODUCTION

In recent years, Europe has experienced significant floods. One way to reduce the impact of a flood is to perform a flood transformation using reservoir management. In the context of reservoir management for floods, it is generally not a problem to perform flood management using an optimisation algorithm for deterministic forecasting. If the optimisation criterion (loss function) for a given catchment is known. The genetic algorithm method [1] or other optimisation methods such as the lattice method can be used for the optimisation. For the criterion π, the deviation from the harmless flow O_{NE} is usually chosen. The deviation itself can be expressed as the sum of the squared difference between the controlled flow O and the control flow (O_{NE}). Alternatively, a loss function *Zf* can be used to quantify the impact of each flow. Accounting for loss of life is very difficult when using a loss function because the movement of people in a given area often varies greatly over the course of years, months, days and hours. Or an unexpected event (a major cultural or sporting event) may disrupt the movement of people. Development itself also changes, often resulting in the expansion of industrial areas or the modernisation of existing buildings or infrastructure. For these reasons, it is somewhat difficult to work directly with the loss function.

The second reason for the significant complications is the quality of the forecast, which usually changes over time depending on the information (data) available. In many cases, this results in significant deviations from optimised forecast-based control and ideal control. Ideal control is optimised control using realistic inflows (100% forecast). Water dispatchers are therefore often faced with the choice of releasing water from the reservoir and, if the forecast fails, not having enough water for the dry season, or not releasing water in time to cause flood damage. Some tasks are more simply where the controller has to decide whether to flood a particular area to protect another area. The above dilemmas would not need to be resolved by the dispatchers if the forecast was always correct or if the damage caused by flooding the designated area is greatly outweighed by the reduction in damage to the protected area. This is not the case in practice.

The principles of game theory are used in the context of this paper to consider options for decision making [2],[3]. The use of game theory in the field of hydrology begins around 1975 [4]. At that time, various authors used game theory mainly for the reallocation of water rights and water pricing [5],[6],[7]. Alternatively, the allocation of water within rivers or groundwater resources [8],[9],[10]. These models and approaches may also have implications for reservoir management during droughts [11]. In the management framework in general, authors work with a loss function *Zf*, based on which models are taught how to manage the flood while achieving the lowest possible damage. However, this does not address the often more serious problem of forecasting error, which can significantly limit the effectiveness of management. The aim of this paper is therefore to assess the potential impact of forecast error on flood management decision making.

MATERIALS AND METHODS

In the following we will use the Prisoner's Dilemma game [2]. The game in question is quite well known and will therefore only be introduced very briefly. In the game, two players independently make a decision to betray or cooperate. Both players are informed about the possible rewards and behave logically. In the one-round version, it is assumed that they will not meet again. The rewards are as follows: If both players cooperate, they each receive 3 units. If one of them betrays than, the player who cheats gets 5 units and the player who cooperates gets 0 units. If both players betray, each receives 1 unit. The individual payoffs are shown in Table 1.

Table. 1. Individual payoffs.

		Player 2	
		Betrayal	Cooperation
Player 1	Betrayal	2:2	5:0
	Cooperation	0:5	3:3

From Table 1 it is easy to see that the game has two Nash equilibria (stable strategies) [2-3]. Both players betray or both players cooperate. In the case of a one-round game, betrayal is preferable in terms of payoffs because the reward of 2 units is higher than the worst possible payoff of 0 for cooperation.

From a management perspective, consider a relatively simple flood management game available at https://hepex.org.au/[12]. The actual diagram of the game situation is shown in Figure 1. The player has only two options. Open the gates to the floodplain or not open them based on the forecast. If the player opens the gates, he causes X units of damage in the area. If he does not open the gates and the flood comes, he causes Y units of damage. There are only 4 possible variations in the game.

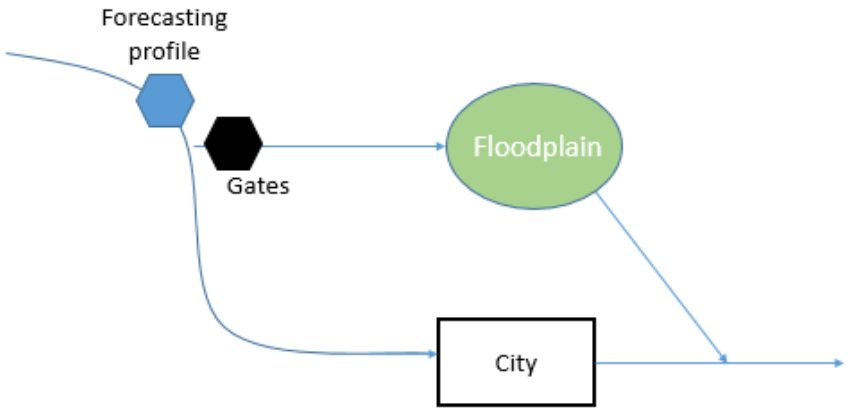

Fig. 1. Schema of game.

1) Prediction is correct and there is inundation relief, total damage X units

2) Prediction is correct, but there is no relief in the floodplain, total damage X units

3) Prediction does not occur and there is inundation relief, total damage Y units

4) Forecast does not occur and there is no relief to the inundation area, total damage is 0 units.

APPLICATION

As part of the application, we will try to link the two games and extract insights from the game that would facilitate the dispatcher's decision making. First, we need to convert the Flood game into a game that corresponds to the Prisoner's Dilemma game. In the Flood game it may seem that there is only one player. This is a nice assumption because the second player is the prediction model (the forecast). So the ideal outcome for both players is cooperation. A state where the dispatcher trusts the model and controls the gate based on its predictions. The problem arises when the prediction is burdened with errors. The prediction model is a p-intelligent player. Without the prediction error, the game would be quite boring.

Let's start by analysing a rather simple situation. In the framework we consider, there is a 1/2 probability that the actual flow will be higher than the prediction and a 1/2 probability that the actual flow will be lower than the prediction.

Let us first analyse a rather simplified situation. We will assume that there is a 1/2 probability that the actual flow will be higher than the forecast and a 1/2 probability that it will be lower. The value of the forecast will be equal to the threshold at which no damage has occurred in the city. This situation is therefore roughly equivalent to a situation where an increase in flow will lead to overtopping and subsequent breaching of the flood barriers designed to protect the city.

If the forecast is 100% accurate, the solution would be to not open the gates and let the water flow harmlessly through the city (Scenario 4). Now set the damage to *X* to -1 and the damage to *Y* to -9. The values have been chosen to demonstrate the calculations. In this example, we do not need to consider the rewards of the prediction model, as it makes the error randomly without any claim to profit (it follows a random strategy). We can therefore simplify the problem to the dispatcher's point of view. We will convert the above information back into a reward matrix (Tab. 2.). The term "betrayal" refers to the situation where the dispatcher performs an action opposite to the situation corresponding to the prediction, or the actual value is higher than that predicted by the model.

Table. 2. Payoffs table for players.

		Player 2 (Forecast)	
		Betrayal (Real flow is higher than forecasted	Cooperation (Real flow is lower than forecasted
Player 1 (Dispatcher)	Betrayal (Opened gates)	-1	-1
	Cooperation (Closed gates)	-9	0

The aim of the game is to get the highest possible reward (i.e. a value of 0). The problem is that the Dispatcher can only trust the prediction ½, so it is risky for him to cooperate, since his reward can be as low as -9. In the case of betrayal, his reward is always -1, which is more than -9 but less than 0. In the case of the one-round version of the game, the Dispatcher's cooperation may seem advantageous, since the 50% chance of nothing happening is still quite high. On the other hand, endangering an entire city and its inhabitants is a rather big gamble for a rational dispatcher, and thus choosing opening gate is a rather irrational choice. In the case of the multi-round version of the game, different strategies can be chosen to solve the above problem:

a) Always open the gate.

b) Never open the gate.

c) Open the gate randomly.

In terms of the long-run solution, strategy *a* offers an average reward of -1, option *b*= -4.5 and option *c*= -2.75 (assuming truly random opening). Of course, the size of the reward (damage) plays a rather large role. Given logical values of *X* and *Y*, strategy *a* can never lose to strategy *b* (assuming that the flood control measure is intended to mitigate the effects of the flood and not the other way around), if game is longer than a few lucky round. In the case of strategy *c*, the results for certain variations of the

weights are already better than for strategy *a*. If the value of *Y* is -2 (lower than -2), strategy *c* can achieve the same (higher) average reward.

Although the above example may seem far from reality. The opposite is true, because in the case of stochastic (ensemble) prediction, it may happen that about ½ of the cases suggest opening the gate and the other half of the cases suggest the opposite. In fact, with stochastic (ensemble) prediction, it may happen that about ½ of the cases suggest opening the gate and the other half suggest the opposite.

RESULTS

We now take a closer look at the case where the model error has a probability of error other than ½. The experiments worked with model error (betrayal) *P* probabilities ranging from 0.05 to 1 on a sample of 1 billion repetitions. In addition, the value of the reward for not opening the gate during a flood (Dispatcher Cooperation; Forecast Betrayal) was varied to values of -9, -5, and -2.5.

Table. 3. Strategy c selected results.

P [-] (Forecast betrayal)	The highest penalty -9	The highest penalty -5	The highest penalty -2.5
0.05	-0.725	-0.625	-0.562
0.1	-0.950	-0.750	-0.625
0.15	-1.175	-0.875	-0.688
0.2	-1.400	-1.000	-0.750
0.25	-1.625	-1.125	-0.813
0.3	-1.850	-1.250	-0.875
0.35	-2.075	-1.375	-0.938
0.4	-2.300	-1.500	-1.000
0.45	-2.525	-1.625	-1.062
0.5	-2.750	-1.750	-1.125
0.6	-3.199	-2.000	-1.250
0.7	-3.650	-2.250	-1.375
0.8	-4.100	-2.500	-1.500
0.9	-4.550	-2.750	-1.625
1	-4.999	-2.999	-1.750

Table 3. shows that when the minimum reward is set to -9, the random strategy *c* is already disadvantaged to strategy *a* at probabilities above 0.1 and worse than strategy *b* at probabilities above 0.9.

If the minimum reward is set to -5.Strategy c is better than strategy *a* up to 0.2 and better than strategy *b* up to 0.8. If the minimum reward is set to -2.5, strategy *c* is advantageous over strategy *a* up to 0.4 and over strategy *b* up to 0.6.

Next we need to test setting the dispatcher's decision ½ as to whether or not to open the gate. If the Dispatcher thinks logically, why should he randomly play ½ his action when the probability of the model's cheating is relatively high (low)? Therefore, we set the

probability of the Dispatcher's decision to be the same as the probability of the model's betrayal (0.05:0.05:1). Selected results of the above experiment are shown in Tab.4.

Table. 4. Strategy c selected results.

P [-] (Dispatcher betrayal)	P [-] (Forecast betrayal)										
	0.050	0.100	0.200	0.300	0.400	0.500	0.600	0.700	0.800	0.900	1.000
0.050	-0.287	-0.325	-0.400	-0.475	-0.550	-0.625	-0.700	-0.775	-0.850	-0.925	-1
0.100	-0.525	-0.550	-0.600	-0.650	-0.700	-0.750	-0.800	-0.850	-0.900	-0.950	-1
0.150	-0.762	-0.775	-0.800	-0.825	-0.850	-0.875	-0.900	-0.925	-0.950	-0.975	-1
0.200	-1.000	-1.000	-1.000	-1.000	-1.000	-1.000	-1.000	-1.000	-1.000	-1.000	-1
0.250	-1.237	-1.225	-1.200	-1.175	-1.150	-1.125	-1.100	-1.075	-1.050	-1.025	-1
0.300	-1.474	-1.449	-1.400	-1.349	-1.300	-1.249	-1.200	-1.150	-1.100	-1.050	-1
0.400	-1.950	-1.900	-1.800	-1.700	-1.600	-1.500	-1.400	-1.300	-1.200	-1.100	-1
0.500	-2.425	-2.350	-2.200	-2.050	-1.900	-1.750	-1.600	-1.450	-1.300	-1.150	-1
0.600	-2.900	-2.799	-2.600	-2.400	-2.200	-2.000	-1.800	-1.600	-1.400	-1.200	-1
0.700	-3.375	-3.249	-3.000	-2.749	-2.500	-2.250	-2.000	-1.750	-1.500	-1.250	-1
0.800	-3.850	-3.699	-3.400	-3.100	-2.800	-2.500	-2.201	-1.901	-1.600	-1.300	-1
0.900	-4.325	-4.150	-3.800	-3.450	-3.100	-2.750	-2.401	-2.051	-1.700	-1.350	-1
1.000	-4.800	-4.600	-4.200	-3.800	-3.400	-3.000	-2.601	-2.201	-1.800	-1.399	-1

Note, however, that the dispatcher's decision has significantly less weight than if he had chosen his action with ½ probability. Of course, his decision has a significant impact on the size of the reward, but it does not push the limits of the strategy's profitability. Again, the limits given in table *x-1* apply.

DISCUSSION

The results of the experiment where the probability of betrayal of both players varies may seem misleading, but we have to accept the fact that strategy *c* is only a transition between strategies *a* and *b*. Thus, according to the results, in the long run strategy *a* cannot be outperformed in the limit settings unless the betrayal of the prediction model can be estimated with sufficient quality. If it is possible to estimate the model's betrayal, a strategy can be constructed that achieves better results. This solution would assume a systematic error (or a combination of both errors) and not just a random error. The results themselves confirm that in the context of flood management, when it is impossible to determine the correct decision due to an uncertain forecast outcome, it is preferable to resist riskier actions and opt for certainty.

The results themselves show that even a relatively small model error rate is quite dangerous for cooperation from the dispatcher's point of view.

The result shows that with a reward ratio of 9:1, a random model error of 10% can already be a significant problem if the forecast is close enough to the thresholds.

Why is strategy *c* preferable even if the forecast error rate increases when we increase the minimum reward?

The answer is quite simple, because by increasing the reward we reduce the potential loss from the risk of cooperation and thus induce the controller to play a possibly disadvantageous action under different conditions. However, it should be emphasised that even with a 2.5:1 ratio, the use of random action only benefits the dispatcher if the model error rate is up to 40%. The model error rate is not directly related to the size of the model error, but to the probability that the model will allow a variant of the hazardous condition (flood).

The paper is mainly concerned with the long-term average reward when the number of trials is limited to a lower values, say 10 (let us assume that this is a very rare phenomenon).

It is, of course, possible to obtain (locally) higher (lower) values for which it is advantageous to play the betrayal (cooperation) game. This is usually a shift of one row (penalty of -9) to two rows (penalty less than -9) with respect to Table 3 and Table 4.

The shift can be in either direction (improvement, deterioration).

An analogy to the long-term series may be the relatively large number of smaller catchments using the same (similar) model with very similar probability distributions of error. Group of p-intelligent player can be replace with one p-intelligent player, if their probability is same or can be replaced by average p-intelligent player.

CONCLUSION

This paper has explored the potential use of theory in flood decision making. The results showed the rather dangerous finding that with a probability of model betrayal of 10% (flood occurs) depending on the damage ratio, it is better to deal with flood information as a real threat than to try to prevent it by not opening the flood gates.

The results showed that the ratio between the reward of each action and the willingness to betray the forecast (random error of the forecast model) plays a very important role. The dispatcher's decision in the situation presented in the paper cannot reverse the marginal values of the mixed strategies, but the dispatcher's decisions are able to significantly improve the results at values lower than the marginal values. The actual application may not be directly limited to direct flood protection, but also to the decision whether or not to start building mobile flood protection. The challenge is the same, as there is a financial cost to building the measures, but not building them can lead to significantly higher repair costs due to flooding. Further research would be beneficial to investigate the behaviour of more complicated strategies than the random ones presented in the paper.

ACKNOWLEDGEMENTS

The article was supported by grant FAST-S-23.

REFERENCES

[1.] Deb, K., Multi-Objective Optimization Using Evolutionary Algorithms. John Wiley and Sons, Chichester, UK. ISBN: 047187339X, 2001.

[2.] Nash, J., "Two-Person Cooperative Games." Econometrica, vol. 21, no. 1, pp. 128–40. JSTOR, 1953. https://doi.org/10.2307/1906951.

[3.] Myerson, R. B., Game Theory: Analysis of Conflict. Harvard University Press, JSTOR, 1991. https://doi.org/10.2307/j.ctvjsf522.

[4.] Bogárdi I, Szidarovszky F., Application of game theory in water management. Applied Mathematical Modelling. 1:16–20. 1976. doi: 10.1016/0307-904X(76)90018-4.

[5.] Thiessen E.M., Loucks D.P., Stedinger J.R., Computer-assisted negotiations of water resources conflicts Group Decision and Negotiation (7), pp. 109-129, 1998.

[6.] Madani K., Game theory and water resources, Journal of Hydrology, Volume 381, Issues 3–4, Pages 225-238, ISSN 0022-1694, 2010. https://doi.org/10.1016/j.jhydrol.2009.11.045.

[7.] Hemati H.,Abrishamchi A., Water allocation using game theory under climate change impact (case study: Zarinehrood). *Journal of Water and Climate Change* 12 (3): 759–771. 2021. doi: https://doi.org/10.2166/wcc.2020.153

[8.] Arnbjerg-Nielsen K. Fleischer H. S., Feasible adaptation strategies for increased risk of flooding in cities due to climate change. Water Science and Technology 60 (2), 273 – 281, 2009. doi:10.2166/wst.2009.298.

[9.] Kicsiny R, Piscopo V, Scarelli A, Varga Z. Game-theoretical model for the sustainable use of thermal water resources: the case of Ischia volcanic Island (Italy). Environ Geochem Health. 2022 Jul;44(7):2021-2035. doi: 10.1007/s10653-021-00871-9.

[10.] Douven, W., Mul, M. L., Alvarez, B. F., Son, L. H., Bakker, N., Radosevich, G., and van der Zaag, P.: Enhancing capacities of riparian professionals to address and resolve transboundary issues in international river basins: experiences from the Lower Mekong River Basin, Hydrol. Earth Syst. Sci., 16, 3183–3197, 2012, doi:10.5194/hess-16-3183-2012,

[11.] Kozel, T., Stary, M., Adaptive Stochastic Management of the Storage Function for a Large, Open Reservoir Using Learned Fuzzy Models. Journal of Hydrology and Hydromechanics 70, no. 2 213–21, 2022. https://doi.org/10.2478/johh-2022-0010.

[12.] https://hepex.org.au/ [1.9. 2023]

ASSESSMENT OF THE CHEPINSKA RIVER WATERS QUALITY (BULGARIA) THROUGH THE COMBINED USE OF DIFFERENT INDICES

Marian Varbanov[1*]
Kristina Gartsiyanova[1]
Stefan Genchev[1]
Gergana Metodieva[1]

[1]National Institute of Geophysics, Geodesy and Geography-Bulgarian Academy of Sciences (NIGGG-BAS), Sofia, **Bulgaria**

ABSTRACT

The article analyzes and evaluates the current status of the water quality of the Chepinska River. It is one of the main right-hand tributaries of the Maritsa River, and large settlements are located in its catchment area and active agricultural activity is carried out. They cause a strong anthropogenic impact and a significant change in water quality. The heterogeneous impact requires the assessment to be carried out by using a complex of indices that includes the Canadian Water Quality Index (CCME WQI), the Bavarian Pollution Index (CJ) and the water oxygen balance index used in the BENILUX countries. The assessment was made according to more than 10 chemical indicators, such as dissolved oxygen, ammonium nitrogen, electrical conductivity, BOD5 and others. The data were obtained from the National Water Monitoring System, at 4 points along the main river and its tributaries, for the period 2015-2022. The reference values for the maximum permissible concentration of polluting substances are in accordance with Regulation N-4 of 2012. Significant water pollution is observed after the settlements, as a result of waste water from urban sewage and agricultural activity. Poor water quality is mainly observed in local sections of the river course. In the lower reaches of the river, the water quality improves significantly.

Keywords: water quality, evaluation indices, water pollution, water quality indicators

INTRODUCTION

In the hydro-ecological studies, considerable attention is paid to the application of various indices to represent the quality state of waters. These are complex evaluations based on a set of physico-chemical indicators used for registrating various types of anthropogenic impact on water. The results are usually presented in the form of a score (or rank), corresponding to a certain interval of change in the indexes value. The obtained score (rank) can be assigned to a corresponding class of water quality (or pollution) status. Depending on the objectives, the adopted research criteria and the selected indicators, the indices can be applied in the evaluation of the condition not only for drinking water, but also river or groundwater used in agriculture, household or industry.

After the acceptance of Bulgaria as a member of the EU in 2007, the country's legislation was harmonized with European norms in the field of the environment as

[*]Corresponding author: varbanov.marian@gmail.com

well.The adoption of the Water Act (2000), developed on the basis of the general European Water Directive (60/2000), necessitated the compilation of an extensive package of normative documents on water quality, tailored to the requirements of various water users, as well as to preserve aquatic ecosystems from harmful human impact. In accordance with the requirements of European legislation, the physicochemical indicators for evaluation the quality of surface water are divided into basic, priority and specific. The reference values developed and approved for Bulgaria for each of the observed indicators for the quality of surface water are listed in Ordinance №4/2012 and the Ordinance on Environmental Quality Standards for Priority Substances and Certain Other Pollutants (2010) [1], [2].

The main goal in the research is the disclosure of the spatio-temporal features generated by the anthropogenic pressure on the waters of the Chepinska River - a direct result of the diverse economic activities carried out in its catchment area.

MATERIALS AND METHODS

The waters of the Chepinska River, were studied. It is one of the large right tributaries of the Maritsa river. The data were obtained from the National Water Monitoring System, at 4 points along the main river and its tributaries, for the period 2015-2022 (Fig. 1), (Table 1). A total of 11 chemical indicators for the quality of surface water, defined in Regulation №-4/2012 (Table 2), were studied. The values for "good" chemical status of the relevant indicators, depending on the type of river, are taken as reference. The reference values for the other two indexes are predetermined by their creators.

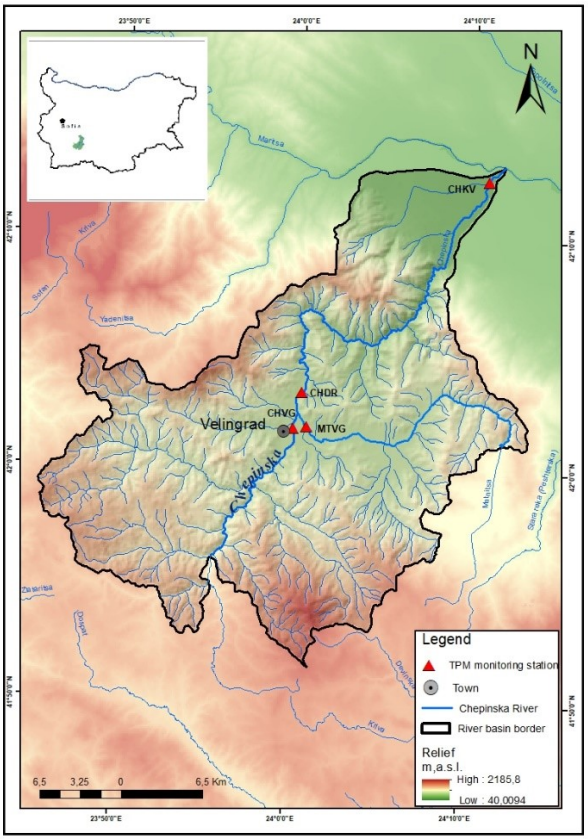

Fig. 1 Location of the monitoring points on the Chepinska River

Table 1 Water quality monitoring points on the Chepinska River

code of the point	point name	water body type	CODE ON THE MAP
BG3MA09235MS1430	Chepinska River - town of Velingrad	R3	CHVG
BG3MA00919MS1390	Chepinska River - before Draginovo village	R3	CHDR
BG3MA09211MS1370	Chepinska River - Kovachevo village	R5	CHKV
BG3MA09221MS1400	Mutnitsa River - town of Velingrad, before the mouth	R3	MTVG

Table 2 Water status indicators in the surveyed water sheds used in the three indices

Indices	WQI – 10	Reference value (according to Ordinance №-4) for river type (R3/R5) (Calculation of WQI)	Water oxygen balance index (WOB)	Chemical index for the quality of river water (CJ)
Water status indicators	OXIG	<6.0	OXIG %	OXIG %
	pH	6.5-8.5		pH
	electrical conductivity	>750		electrical conductivity
	BOD5	>2.5/>3.0	BOD5	BOD5
	N-NH4	0.4	N-NH4	N-NH4
	N-NO3	>0.5/>1.5		N-NO3
	N-NO2	>0.025/>0.03		PO4-P
	PO4-P	>0.02/0.04		T°C
	N-tot	>0.08/>1.5		
	Total P	>0.03/>0.05		

Water oxygen balance (WOB)

The water oxygen balance (WOB) is an express integral assessment of the quality of surface waters through the use of physicochemical indicators, assessing the self-purification ability of water bodies and determining their organic load [1] (table 2). It uses the dissolved oxygen concentration in %, the biochemical oxygen demand (BOD5) and the ammonium nitrogen (N-NO4) content. The evaluation of WOB in the chosen monitoring points is carried out according to each of the listed indicators and by a scale of points depending on its concentration. The developed scale evaluates the condition

through an average annual point value represented in five levels (1- "very good", 15 - "very bad").

Chemical index for the quality of river water (CJ)

The index is calculated according to the following formula:

$$CJ = \prod_{i=1}^{n} q_i^{w_i} = {q_1}^{w_1} q_2^{w_2} q_3^{w_3} \dots q_n^{w_n},$$

where CJ – is the chemical index as a dimensionless value from 0 to 100 (0 – "poor" and up to 100 – "excellent" water quality); n – is the number of indicators – 8 preset by the creator of the index; qi – represents the sub-index for the i-th indicator (a dimensionless value between 0 and 100, representing a function of the i-th indicator); Wi – is for the weight of the i-th indicator (a number between 0 and 1, the sum is equal to 1). The weight is determined depending on the sensitivity of the indicator to contamination. For example, indicators as BOD5, oxygen saturation (in %) and ammonium nitrogen have the highest value of Wi.

The degree of pollution is determined depending on the obtained score [3], [4].

Water Quality Index (WQI)

It includes three components characterizing the anthropogenic impact on water quality:

- Impact range (F1), expressing the range of quality indicators that do not meet the normatively determined maximum permissible concentrations (MPC);
- Frequency (F2), which shows the ratio between the number of so-called "bad samples" (samples where a content of potentially polluting substance with a concentration above the permissible norms) and the total number of samples;
- Amplitude (F3), which indicates the degree or multiplicity of deviation of the values in the "bad sample" from the corresponding reference values of the MPC.

After obtaining the values of the individual components of the integrated formula, proceed to the calculation of the water quality index (WQI), where the value obtained is in the range from 0 to 100, and the status classes are tabulated [5], [6]

RESULTS AND DISCUSSION

According to the adopted reference values (table 2), the river waters of Chepinska River in Velingrad (CHVG) meet the standards for "good" chemical status only for 2018 and 2019. For 2015 and 2016, the river has a "marginal" category, and in 2021, the lowest value (WQI) was calculated - 30.2, placing the river waters into "poor" category. The exceedances of the recorded values were mainly for the indicators - nitrates (N-NO3), nitrites (N-NO2), total N, total P and orthophosphates (P-PO4). The reported deviations from the normative requirements referring to these indicators are evidence for significant organic pollution of the surface waters at this control point. During the entire study period the waters of the Chepinska River before Draginovo village (CHDR) are defined as highly polluted and subjected to intense anthropogenic load. The WQI values do not even reach the upper limit (WQI=44) of the "poor" water quality category (Fig. 2). The highest value of the index was calculated in 2021 – 41.6, and the lowest in 2019 – 31.9. Almost all analyzed physicochemical indicators - dissolved oxygen, ammonium

nitrogen (N-NH4), nitrates (N-NO3), nitrites (N-NO2), total P, total N and orthophosphates (P-PO4), (except for pH and electrical conductivity) show an excess of up to 10 times of the norms. For the indicators orthophosphates (P-PO4) and total P, individual cases of discrepancies between 10 and 25 times of the reference values were registrated.

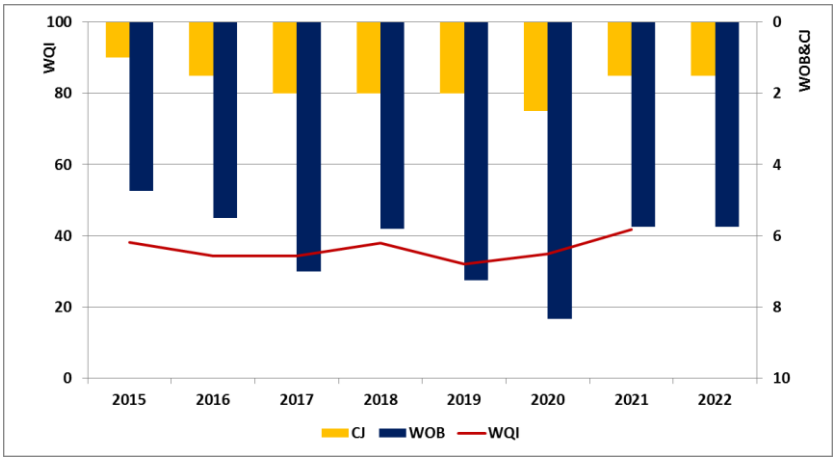

Fig. 2 Assessment of the water quality of Chepinska River before Draginovo (CHDR) for the period 2015-2022.

The WQI values for the Mutnitsa River near Velingrad before its mouth (MTVG) classify the river waters at this section in the categories "marginal" (2015) and "poor" (2016-2021). The waters did not meet the criteria for "good" chemical status during the entire study period. WQI indicates that contaminated or heavily polluted water were significantly and almost always threatened of deterioration due to the anthropogenic impact. In 2019, the lowest value of the complex index was calculated - 29.5 (Fig. 3). Most of the physicochemical indicators do not fulfill the quality indicators (dissolved oxygen, ammonium nitrogen (N-NH4), nitrates (N-NO3), nitrites (N-NO2), total P, total N, orthophosphates (P-PO4) and BOD5. Exceptions were for the values of pH and electrical conductivity, which remained within normal limits during the whole 7-year study period. For indicators that do not meet the normative quality criteria, values exceeding up to 10 times the reference limits are constant, and for the indicators - orthophosphates (P-PO4) and total P, exceedances of more than 25 times are common.

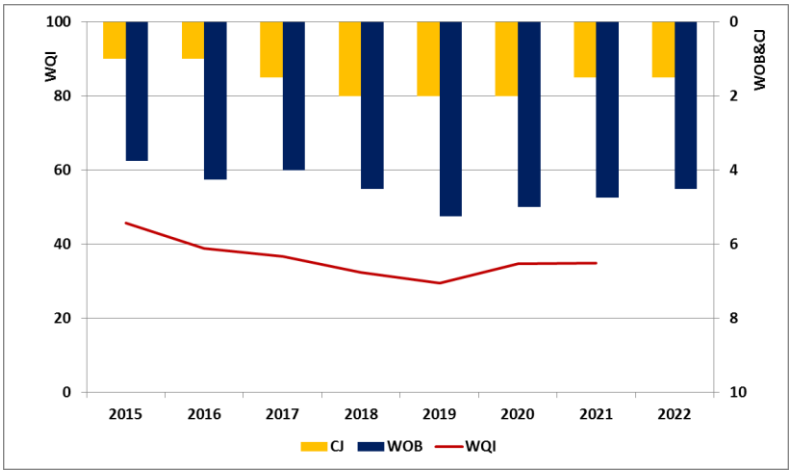

Fig. 3. Assessment of the water quality for the period 2015-2022 of the Mutnitsa River before inflow (CHDR).

https://doi.org/10.5593/sgem2023V/3.2/s12.05

According to the obtained WQI values, the lower reaches of the Chepinska River at the point near the Kovachevo village (CHKV) are in "marginal" (for 2015 and 2019 - 2021) and "fair" (2016-2018) categories. River waters in the first case were threatened or deteriorated by the anthropogenic activity and defined as heavily polluted. In the second category, the water quality status was usually preserved, although a number of cases of anthropogenic pressure have been registered. The best physicochemical status was reported in 2017 when the WQI had a value of 67.8, and the worst one was in 2020 - 48.6. The deteriorated quality of the river during the indicated years is due to the so called "bad" values which exeeded the norms by up to 10 times for almost all studied indicators - dissolved oxygen, nitrate and nitrite nitrogen (N-NO3 and N-NO2), orthophosphates (P-PO4), total N, total P and BOD5. The measured values for the pH and electrical conductivity indicators, were the only exceptions which fulfill the regulated requirements for "good" condition regarding the surface waters.

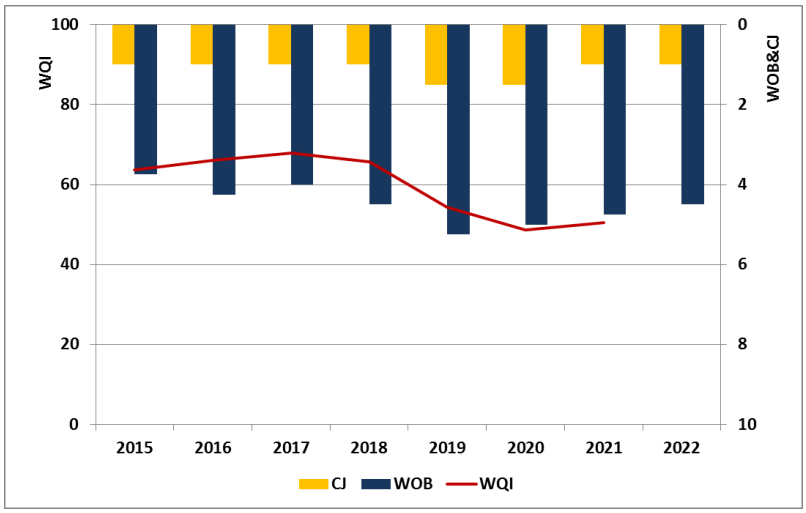

Fig. 4. Assessment of the water quality for the period 2015-2022 of the Chepinska River near Kovachevo (CHKV)

The analysis of the results of the two indexes WOB and CJ show that they are not as sensitive to river water pollution as WQI. For the point of the Chepinska River near Velingrad, they do not account any polution and the water condition is assessed as "very good condition" according to WOB and "absence to slight pollution" according to CJ.The evaluation for the point at Draginovo is significantly worse. At this point, both indices register "average condition" and "moderate to heavy pollution" respectively, especially for 2019 and 2020.

CONCLUSION

As a result of the analysis of the water quality index, carried out in the period 2015-2022 and applied in accordance with the requirements of Ordinance №-4/2012 for the characterization of surface waters, the following generalizations regarding the studied river can be made:

- The point where the worst quality condition of the surface waters was found is the one after Velingrad, near the village of Draginovo. The most favorable quality characteristics were detected in the lower course of the Chepinska River near the village of Kovachevo;

- The analytical results show that in the seven-year studied period no common time interval, characterized by a pronounced good or bad quality condition of the river waters, at the control points has been found;
- The condition of the water quality significantly improves towards the lower reaches of the Chepinska river. The reasons could be sought in the possibilities of self-purification of the river course, as well as in the slightly more liberal norms of the relevant physicochemical indicators for the semi-mountainous type of rivers;
- Previous studies [7] concerning the river basin of the Chepinska River confirm the long-term, critical state of the waters in the point after Velingrad according to the deteriorated physicochemical parameters shown in the present study, especially total P, orthophosphates (P-PO4), ammonium nitrogen (N -NH4) and nitrites (N-NO2);
- The analysis unequivocally shows that the river waters after Velingrad are subjected to significant anthropogenic pressure, which is mainly expressed in the discharge of household sewage. The causes of the recorded pollution can be reffered to the still missing City Wastewater Treatment Plant. Moreover, the fact that, the city is a key resort center leads to a further increase in the discharge of insufficiently treated domestic water. Livestock complexes operating in the city's land, are also a possible diffuse source of water pollution. Unregulated landfills in the catchment area which do not meet ecological requirements also poses a serious danger on the water quality.

ACKNOWLEDGMENTS

This research has been carried out in the frame of the project "Models of anthropogenic impact on the natural environment at river basin scale (ModAiNe)", funded by the National Science Fund, Ministry of Education and Science (Bulgaria), Competition for financial support for basic research projects – 2022 (Contract No КП-06-Н64/6, signed on 15.12.2022).

REFERENCES

[1] MOEW (MINISTRY OF ENVIRONMENT AND WATER) 2013. Regulation N-4/14.09.2012 for characterization of surface waters, Bulgaria. 54 p.(Bg).

[2] Regulation on environmental quality standards for priority substances and other pollutants from 01.11.2010. OG. 88 on 09/11/2010 (Bg)

[3] Environmental Impact Assessment (ed. A. G. Colombo), Vol. 1, 1992, Kluwer Academic Publishers, Netherlands, ISBN 978-94-010-5116-3

[4] European Commission, Directorate-General for Environment, Piavaux, M., Sweeting, R., Newman, P., River water quality – Ecological assessment and control, Publications Office, 1993, ISBN 92-826-2929-5,

[5] UNEP—United Nations Environment Programme. Global Drinking Water Quality Index Development and Sensitivity Analysis Report; UNEP: Toronto, ON, Canada, 2007; ISBN 92-95039-14-9, p. 60.

[6] CCME. 2001. Canadian water quality guidelines for the protection of aquatic life: CCME Water Quality Index 1.0, User's manual. In: Canadian Environmental quality guidelines, 1999, Canadian Council of Ministers of the Environment, Winnipeg, Manitoba (http://www.ccme.ca/assets/pdf/wqi_usermanualfctsht_e.pdf)

[7] Gartsiyanova, K., Georgieva, S. Assessment of the anthropogenic pollution of the Chepinska river. Proceedings of National conference with international participation "Natural Sciences 2017" – Varna (NCNS2017) (2017). University Publishing House "Bishop Konstantin Preslavski", Shumen, ISSN:2603-2937, 141-147 (Bg)

Author Contributions: Conceptualization, MV and KG; methodology, MV and KG; software, MV and KG; validation, MV, KG, GM, SG; resources, MV, KG, GM; data curation, MV, KG, GM; writing—review and editing MV, KG, GM, SG; visualization, GM.; funding acquisition, MV. All authors have read and agreed to the published version of the manuscript.

Conflicts of Interest: The authors declare no conflict of interest. The funders had no role in the design of the study; in the collection, analyses, or interpretation of data; in the writing of the manuscript; or in the decision to publish the results.

BENEFIT-COST ANALYSIS OF SMALL DOMESTIC WASTEWATER TREATMENT PLANTS: A REVIEW

Dr. Reka Wittmanova [1]

Dr. Jaroslav Hrudka [1]

Martin Meliska [1]

Professor Stefan Stanko [1]

Professor Ivona Skultetyova [1]

[1] Slovak University of Technology in Bratislava, Faculty of Civil Engineering, Department of Sanitary and Environmental Engineering, **Slovakia**

ABSTRACT

Due to the historical development of individual regions in Slovakia, there are still areas without access to public water networks. The main reason is the challenging and uneconomical construction of public networks in scattered rural settlements. The small wastewater treatment plants have gained popularity in rural areas of the Slovak Republic. The increasing adoption of decentralized wastewater management is a result of the scattered layout of numerous rural settlements, presenting economic challenges, technical complexities, and inefficiencies in the implementation of a centralized wastewater disposal system. The objective of this paper is to establish a concise methodology for conducting a Benefit-Cost Analysis within the context of the Slovak Republic. This methodology will subsequently serve as an auxiliary decision-making tool when proposing wastewater disposal methods in rural settlements. This study will assess the potential wastewater disposal methods in the specific rural area, while clarifying the proper execution of the benefit-cost analysis.

Keywords: Benefit-Cost Analysis, Small Domestic Wastewater Treatment Plants, Wastewater Treatment.

INTRODUCTION

Public sewer systems are defined as a set of facilities for conveying and disposing of wastewater, playing a significant role in environmental protection. Therefore, high demands are placed on future operation when designing the system. Hence, it is necessary to consider the requirements for optimal functionality, operational stability, appropriate financial considerations for construction and operation, the impact of construction on receiving bodies, groundwater, water resources, the environment, and the long-term sustainability of the entire system. In the design of structures, the entire life cycle of the construction, as well as the return on investment, is currently considered [1].

Based on long-term experience and statistics, the centralized approach to wastewater disposal is the most common method of urban sewage treatment. However, this approach has its limitations. The morphological conditions of the area, the distance to recipients, and the spatial distribution of settlements do not always favor the

construction of public sewer systems. The decentralized approach to wastewater conveyance and treatment is applied in areas with scattered development, locations predominantly used for cottages and recreational purposes, where the investment, operating costs, and long-term sustainability of facilities make centralized solutions impractical [2], [3].

Considering the progress of sewage infrastructure in Slovakia and the fact that not all areas are suitable for the construction of centralized networks, the use of small domestic wastewater treatment plants (up to 50 P.E.) is gaining popularity. Similar situations are found in Scandinavian countries like Sweden and Finland, where 13% and 18% of the population, respectively, live in rural areas without connections to public sewers and central wastewater treatment plants. According to a study by Heinonen-Tanski and Matikka, the number of people utilizing decentralized wastewater treatment methods increases during the summer months and school vacations due to migration to rural and cottage areas. Connecting these residents to public networks is deemed unfeasible due to large distances and the morphology of the terrain [4]. The study by Envalla et al. indicates that approximately one million decentralized wastewater treatment plants are currently operational in Sweden [5]. This trend is also evident in Ireland, where approximately one-third of the population uses decentralized systems [6]. A gradual increase in the number of small domestic wastewater treatment plants is observed in Poland, where 235,685 such plants were registered in 2019, with further growth anticipated in the future [7], [8]. In the Czech Republic, the number of domestic wastewater treatment plants also increased due to state subsidies in 2016, 2017, 2019, and 2021 [9].

In Slovakia, in areas without public sewer systems, the most used method for wastewater disposal is its accumulation in cesspools or septic tanks, followed by its subsequent transport to wastewater treatment plants. However, more conscientious citizens are currently investing in the construction of small domestic wastewater treatment plants, which, if operated improperly, can become a source of environmental pollution.

The aim of the presented contribution is to define the method of Benefit-Cost Analysis for small domestic wastewater treatment plants, intending to use it as a tool in the future decision-making process regarding the method of sewage management in areas with dispersed development.

THE CURRENT STATE OF WASTEWATER DISPOSAL IN SLOVAKIA

Figure 1 illustrates the state of wastewater collection and treatment in the country, reflecting the historical development of the nation, as well as the economic situation and the implementation of new technologies in the construction of sewer networks and wastewater treatment plants (WWTPs). According to the results from the statistics of the Research Institute of Water Management, as of December 31, 2018, 3,724,376 residents were connected to public sewer systems, accounting for 68.40% of the total population.

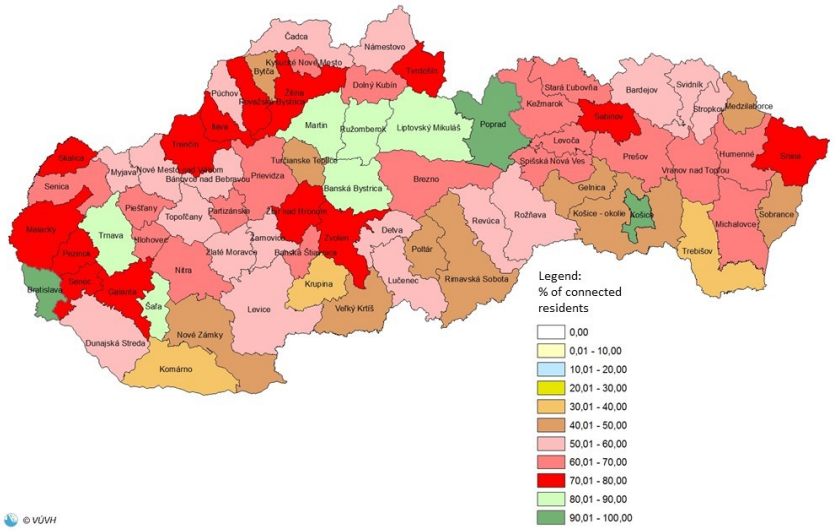

Figure 1: Percentage of residents connected to public sewerage in Slovakia by districts as of December 31, 2018 (Source: Water Research Institute).

In Slovakia, the operation of public sewer systems is predominantly managed by water companies, which are joint-stock companies of cities and municipalities. Out of the total connected population, these water companies handle wastewater discharge for 3,311,717 residents (88.92%). Public sewer systems managed by municipal offices handle the wastewater disposal for 412,659 residents (11.08%). The number of residents connected to sewer systems with wastewater treatment plants (WWTPs) was 3,699,154, representing 67.94% of the total population [1].

BENEFIT-COST ANALYSIS

Benefit – cost analysis (BCA) is an analytical tool used to assess the economic advantages or disadvantages of a product or construction through the assessment of its costs and benefits to evaluate the change in the life standard.

Basic concepts of BCA considered in the evaluation are:

• Opportunity cost.

• Long-term perspective.

• Calculation of economic performance indicators expressed in monetary terms.

• Microeconomic approach.

• Incremental approach.

Opportunity cost is defined as the potential gain that arises from choosing a better alternative. The reason for using BCA is the fact that many investment decisions based on profit assumptions can have negative effects on society. However, if the results and all project effects are positive from an environmental and social perspective, then the project's return is better [10].

The long-term perspective depends on the current sector and ranges from 10 to 30 years, assuming future operating costs and benefits and taking uncertainties into account [10].

The overall contribution of the project is determined based on the monetary value of all positive and negative effects, namely benefits and costs. The overall effectiveness of the project is evaluated through indicators, specifically the Economic Net Present Value (ENPV) and the Economic Rate of Return (ERR), both expressed in monetary terms. These indicators enable comparison and ranking among competing projects or alternatives.

CBA is generally an approach within microeconomics that allows for evaluating a project's impact on society by calculating economic performance indicators, offering an assessment of anticipated changes in welfare. While the direct employment and external environmental effects are considered in the ENPV, indirect effects (such as those on secondary markets) and broader impacts (e.g., on public funds, employment, regional growth) should be excluded. This exclusion is justified for two primary reasons: firstly, most indirect, or broader effects are typically transformed, redistributed, and capitalized forms of direct effects, necessitating the limitation of potential double-counting of benefits. Secondly, there is limited established practice on translating these effects into robust techniques for project appraisal, emphasizing the need to avoid analyses based on assumptions that are challenging to verify for reliability [10].

The Figure 2 illustrates the steps involved in a standard benefit-cost analysis.

BENEFIT-COST ANALYSIS OF SMALL DOMESTIC WASTEWATERTREATMENT PLANT

The BCA of a small domestic wastewater treatment plant can be performed based on the following steps, which result from the European Commission's document "Guide to Cost - Benefit Analysis of investment projects". The process involves five stages: (1) transforming prices from market to accounting, (2) assigning monetary values to non-market impacts, (3) considering additional indirect effects if applicable, and (4) discounting estimated costs and benefits, followed by the computation of economic performance indicators [11].

The overall impact of the project is determined based on the monetary value of all positive and negative effects, i.e., benefits and costs. The evaluation of the project's overall effectiveness involves the use of indicators, specifically the Net Present Value (NPV) and the Economic Rate of Return (ERR). These indicators facilitate the comparison and ranking of competing projects or alternatives [10].

As the EU's water policy is based on the Water Framework Directive, which sets goals for maintaining good water quality, the assessment of small household wastewater treatment systems must consider benefits and costs related to this issue. Therefore, the goal and main motivation of the Benefit-Cost Analysis (BCA) is stated as increasing efficiency in wastewater collection, removal, purification, and elimination, such as through a strategy for the disposal of sludge from urban wastewater treatment.

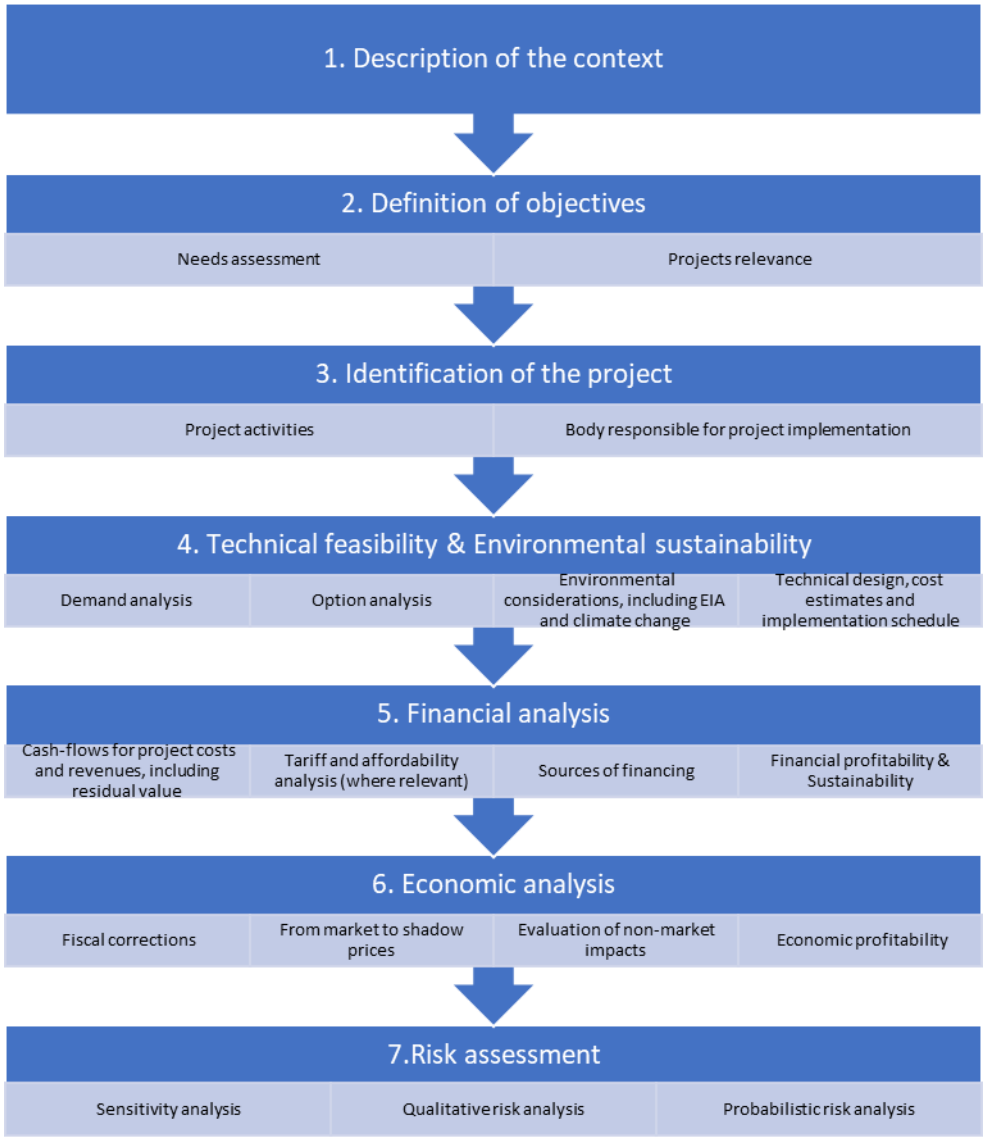

The Figure 2: Appraisal steps of BCA

The first step after defining the analysis goals is to identify the project, describe it, and set its parameters. Subsequently, the project identification is performed, defined as the Renovation/development of infrastructure for wastewater treatment in the case of evaluating small household wastewater treatment systems. The next step involves demand analysis, predicting the water needs' development, considering not only the locality's demographic trends but also anticipated economic development, climate impact, and energy prices. The overall demand is then determined based on two fundamental elements: the number of users and the quality of wastewater over a specified timeframe. The output of this phase includes the estimated volume and concentration of wastewater pollution.

Within the financial analysis, investment and operational costs are quantified, and it is recommended to compare two situations without the project or with the project.

In economic evaluation, indicators such as Net Present Value (NPV) and Economic Rate of Return (ERR) are considered, encompassing the construction and modernization of wastewater treatment processes. Another typical benefit is assumed cost savings in

the construction of small household wastewater treatment systems compared to centralized systems. The final but equally crucial assessment point is risk analysis, performed through sensitivity analysis. Sensitivity analysis for variables in small household wastewater treatment systems may involve demographic trends, wastewater production trends, unit water consumption trends, the number of years required for infrastructure implementation, itemized investment costs, itemized operational and maintenance costs, unit tariff, or estimated wastewater treatment plant for water consumption [10].

The benefits of small domestic wastewater treatment plants are numerous and are based on the key criteria for considering decentralization in municipal wastewater management. The most important benefits of SDWWTP include the benefit from saving the treatment system construction costs, benefit from saving the maintenance and operational costs, benefit from sewage treatment costs, benefits from sewage systems construction costs [11].

DISCUSSION

Currently, many authors are focusing on the economic evaluation of wastewater treatment plants. Djukovic et al. examined the Benefit-Cost analysis and cost-reflective tariff of wastewater treatment plants in Serbia. This study presents a cost-benefit analysis of a tertiary wastewater treatment project with the calculation of full cost recovery. The major economic and environmental benefit of this treatment plant is associated with the removal of nitrogen and phosphorus, as these nutrients are the primary cause of eutrophication. In addition to CBA, a widely used method for economic assessment is the Life Cycle Cost (LCC) method [12].

Pryce et al. also focused on the economic evaluation of a small wastewater treatment plant, assessing various proposals and operational scenarios of the Integrated Fixed Film Activated Sludge (IFAS) system. The scenarios evaluated included tanks made of different materials and various aeration strategies. The evaluation included costs such as tank material, prices of individual components like pipes, valves, pumps, import costs, operating costs, maintenance costs, water prices, costs of qualified and unqualified labor throughout the lifecycle, and costs of renting equipment for maintenance and disposal [12].

CONCLUSION

The use of Benefit-Cost Analysis and Life Cycle Cost Analysis in Central and Eastern European countries will gradually come to the forefront due to increasing demands from the European Union. Given the current state of sewage systems in rural settlements in Slovakia, investors will be interested in alternative and decentralized methods of wastewater disposal and treatment. The aim of the contribution was to gather and consolidate information related to the use of analyses worldwide and tailor them to Slovak conditions, enabling effective utilization of these tools in the future design and assessment processes of small household wastewater treatment systems. This paper aimed to work on a streamlined approach for performing a Benefit-Cost Analysis within the framework of the Slovak Republic. The resulting methodology can be a supplementary decision-making tool for suggesting wastewater disposal techniques in rural communities. The research summarizes various wastewater disposal methods and

its benefit cost analysis in the rural areas and provide guidance on the correct implementation of the benefit-cost analysis in the future. With the help of a literature search, it further offers an overview of the possibility of another method of cost evaluation, using Life cycle cost analysis, and summarizes its use in the research task. The aim of the article was to create a literature search for future research in the field of wastewater disposal in rural areas of Slovakia.

ACKNOWLEDGEMENTS

This work was supported by the Scientific Grant Agency of the Ministry of Education, Youth and Sports of the Slovak Republic and the Slovak Academy of Sciences within the project VEGA 1/0682/23, co-funded by the Slovak Research and Development Agency under contract No. APVV-22- 0564.

REFERENCES

[1] Napojenie obyvateľstva na verejnú kanalizáciu [online] 16.12.2021 © 2022 www.enviroportal.sk [cit.2023-15-11]. Available from: https://www.enviroportal.sk/indicator/detail?id=1276.

[2] Hrudka J., Wittmanová R., Škultétyová I., Stanko Š., Šutúš M, Možnosti čistenia žumpových vôd v medzinárodnom kontexte, Městské vody 2022 = Urban water 2022 [elektronický zdroj] : sborník přednášek konference s mezinárodní účastí. Velké Bílovice, 6. - 7. října 2022. 1. vyd. Brno : ARDEC, 2022, online, s. 157-165. ISBN 978-80-86020-94-5.

[3] Plán rozvoja verejných vodovodov a verejných kanalizácií pre územie SR [online]. [cit.2023-15-11]. Available from: https://www.minzp.sk/voda/verejne-vodovodyverejne-kanalizacie/

[4] Heinonen – Tanski H., Matikka V. Chemical and Microbiological Quality of Effluents from Different On-SiteWastewater Treatment Systems across Finland and Sweden. Water, 9, 47, 2017.

[5] Envall I., Fagerlund F., Westholm L.J., Åberg C., Bring A., Land M., Gustafsson J.P. What evidence exists related to soil retention of phosphorus from on-site wastewater treatment systems in boreal and temperate climate zones? A systematic map protocol. Environ. Evid., 9, 22, 2020.

[6] Dubber D., Gill L. Application of on-site wastewater treatment in Ireland and perspectives on its sustainability. Sustainability, 6, pp. 1623–1642, 2014.

[7] Karczmarczyk A., Bus A., Baryła A. Assessment of the Efficiency, Environmental and Economic Effects of Compact Type On-SiteWastewater Treatment Plants—Results from Random Testing. Sustainability. 13, 982, 2021.

[8] Krzanowski S., Wał˛ega A. New technologies of small domestic sewage volume treatment applied in Poland. Infrastruct. Ecol. Rural Areas, 3, 69–78, 2007Available online: http://www.infraeco.pl/en/art/a_15103.htm (accessed on 13 November 2023).

[9] Váňa M., Kučera J., Rajnyšová R. Zkušenosti z kontroly provozu soustav domovních čistíren odpadních vod v obcích. 12. bienálna konferencia s medzinárodnou účasťou ODPADOVÉ VODY 2022. Štrbské Pleso, 19. – 21. októbra. 1. vyd. Bratislava, online, s. 85-88. ISBN 978-80-973196-3-2. 2022.

[10] European Commission. Guide to cost-benefit analysis of investment projects European Policy – Inforegio, Aviable online: https://ec.europa.eu/regional_policy/sources/studies/cba_guide.pdf (accessed on 13 November 2023).

[11] Bernal D., Restrepo I., Grueso-Casquete S., Key criteria for considering decentralization in municipal wastewater management, Heliyon, 7, e06375, 2021.

[11] Djukic M., Jovanoski I., Ivanovic O.M., Lazic M., Bodroza D., Cost – benefit analysis of an infrastructure project and a cost reflective tariff: A case study for investment in wastewater treatment plant in Serbia, Renewable and Sustainable Energy Reviews, 59, pp. 1419 – 1425, 2006.

[12] Pryce D., Kapelan Z., Memon F.A., Economic evaluation of a small wastewater treatment plant under different design and operation scenarios by life cycle costing. Development Engineering, 7, 100103, 2022.

CLIMATIC AND ANTHROPOGENIC INFLUENCES ON WATER QUALITY IN LAKE BRATES, ROMANIA

Prof. dr. habil. C. Iticescu[1,2],

Prof. dr. eng. P. L. Georgescu[1,2],

PhD. M. Calmuc[1],

PhD V. Calmuc[1],

Lecturer dr. C. Topa[1,2]

[1] Rexdan Research Infrastructure, "Dunarea de Jos" University of Galati, **Romania**
[2] Faculty of Sciences and Environment, "Dunarea de Jos" University of Galati, **Romania**

ABSTRACT

Lake Brates is located near Galati city, in the south-eastern part of Romania being one of the largest lakes in the country. Unfortunately, water quality has greatly decreased in recent years, both due to human actions and to climate change.
The present paper aims at establishing the quality of the water in Lake Brates as resulted from the calculation of the water quality index (WQI) by the weighted arithmetic method. In order to calculate this index, several sampling campaigns were carried out in various points of the lake, followed by the measurement of relevant parameters: pH, conductivity, salinity, oxygen demand (DO), chemical oxygen demand (COD), biochemical oxygen consumption at 5 days (CBO_5), NO_2^-, NO_3^-, N total, Cl^-, SO_4^{2-}, P-PO_4^{3-}, heavy metals (As^{3+}, Cr^{3+}, Cu^{2+}, Ni^{2+}, Zn^{2+}). Both the individual variation of the monitored physicochemical parameters and the variation of the WQI were tracked. Moreover, a correlation of the WQI with the climatic conditions in the region (rainfall and thermal regime) was established.
The determinations were made by applying the standardized methods in force in – situ and ex-situ and by using the following equipment: the UV-Vis-NIR Spectrophotometer, Thermo Scientific Vanquish Flex UHPLC system coupled with the Mass Spectrometer, Thermo Scientific Trace GC coupled with the Quadrupole Mass Spectrometer, the Total Reflection X-Ray Fluorescence (TXRF) Spectrometer and a portable multiparameter.

Keywords: WQI, climate change, anthropogenic influences, physicochemical parameters.

INTRODUCTION

Lake Brateș is one of the largest lakes in Romania, located in the south of Moldova, at the confluence of River Prut and the Danube. According to C14 determinations, Lake Brateș was formed at the end of the 6th millenium BC in the meadow of the lower Prut and the Danube, being fed, mainly, from River Prut. Its initial surface of 30,000 Ha, has reduced to a great extent, in time reaching 7,400 Ha at the beginning of the 20th century.

This phenomenon occurred due to the massive accumulation of sediments as a result of accelerated soil erosion and of the massive deforestation which took place in southern Moldova at the beginning of the 18th century. In the interval 1948 - 1949 and the 60s, the lake was drained in order to obtain agricultural land, and its surface was reduced to a quarter of the initial size, reaching an area of only 2400 ha [1-4] today. Currently, the lake has an average depth of 1.5m. Neverrheless, in recent years, the water depth has reached around 30 cm in some areas of the lake, due to climate change and silting, which has led to a strong eutrophication [3].

Fig. 1. Location of Lake Brates in South East of Romania, near Galati City [2]

Along the years, studies have been carried out to establish the state of the ecosystem, both by means of biological indices [2-4] and by analyzing the physical-chemical parameters [5-10]. Studies have shown that the level of eutrophication is high due to the presence of organic pollutants in the water, and that the low water level in the lake during the dry periods accentuates this phenomenon. The content of nutrients and heavy metals generally falls within the limits of water class 2 or class 3 according to the legal criteria in force [9].

Other studies have focused on the analysis of climatic factors. Average temperatures have increased by 2 degrees Celsius in recent years, and the rainfall regime has been deficient. In addition, the Chineja River which flows into Lake Brateș brings a large amount of sediments in periods of abundant rainfall and potentially polluted water in periods of poor rainfall or as a result of uncontrolled discharges from adjacent localities. These factors have led to the decrease of the water quality in Lake Brateș [3, 6, 7].

In the present study, the Water Quality Index (WQI) was chosen for the water quality analysis and the method of arithmetic averages was applied for calculating this index [11]. The study was completed by the separate analysis of the main parameters which influence the WQI value and the dependence on climatic factors.

MATERIALS & METHODS

1. Sampling areas. The samples were collected from three sampling stations located as follows: S1 at the discharge of River Chineja into the lake; S2 in the middle of the lake; S3 in the beach area where the railway passes, an area with important anthropogenic influence.

2. The methods of analysis of the physico-chemical parameters

17 physico-chemical parameters were measured, their values being determined by applying standardized procedures, thus: pH (SR EN ISO 10523:2012), DO (SR ISO 5814:1984), BOD5 (SR EN 1899-2:2002), COD (SR ISO 15705:2002), NO2- (SR EN 26777:2006), NO3- (SR EN ISO 11905-1:2003), N total (SR EN ISO 11905-1:2003), Cl- (SR ISO 9297/2001), SO42- (STAS 3069-87), P-PO43- (SR EN ISO6878:2005 cap 4), As3+ (ASTM D2972-15 A), Cr3+ (SR ISO 9174-98), Cu2+ (SR ISO 8288:2001), Ni2+ (STAS 8637-79), Zn2+ (STAS 8314-87).
The concentrations of heavy metals were measured by using the inductively coupled plasma mass spectrometry (ICP-MS) technique and the Perkin Elmer NexION 2000 equipment.

3. WQI calculation method

The water quality index (WQI) is a dimensionless number which combines several water quality factors (physical, chemical and biological parameters) into a single number. The WQI provides complex scientific information and indicates any relative change in water quality [11].
There are several ways to calculate the WQI in the scientific literature, but our research team used the **Weighted Arithmetic Water Quality Index Method** with the following equation:

$$WQI = \frac{\sum W_i q_i}{\sum W_i} \qquad (1)$$

where:
- q_i represents a relative water quality score for each parameter, i represents the number of parameters taken into account;
- Wi represents a factor that indicates the weight of that parameter in the WQI calculation (relative weight).

The q_i factor:

$$q_i = 100\frac{V_i - V_0}{S_i - V_0} \qquad (2)$$

where:
- V_i represents the measured (experimentally determined) value of parameter i;
- V_o represents the ideal value of that parameter (it is 0 for all parameters except for pH where it is 7 and DO for which it is 14.6 $mg \cdot L^{-1}$);
- S_i represents the standard value allowed by the legislation in force for water in the quality category in which it was classified.

The Wi factor:

$$W_i = \frac{K}{S_i} \qquad (3)$$

where K is a constant:

$$K = \frac{1}{\sum\left({}^{1}/_{S_i}\right)}$$

The WQI was calculated using the Romanian standards for surface waters [11].
According to the WQI values calculated with this method, water is divided into 5 quality classes [11], as follows:

- Excellent (1): 0 – 25;
- Good (2): 26 – 50;
- Poor (3): 51 – 75;
- Verry poor (4): 76 – 100;

- Unsuitable for drinking (5): >100.

RESULTS

Determinations were made by calculating the water quality indices in the 3 sampling stations, which are relevant for identifying the water quality in Lake Brates.
The variations of the most important parameters in 2023 are presented in Figures 1 and 2.

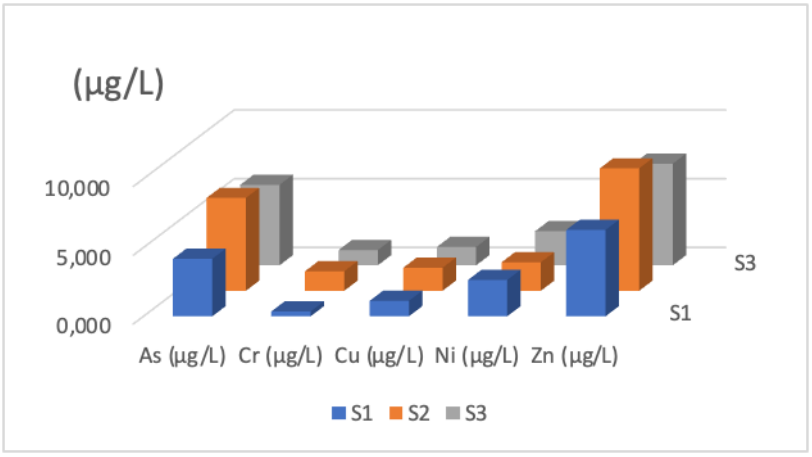

Fig. 1. Variations in heavy metal concentrations in 2023 (annual averages)

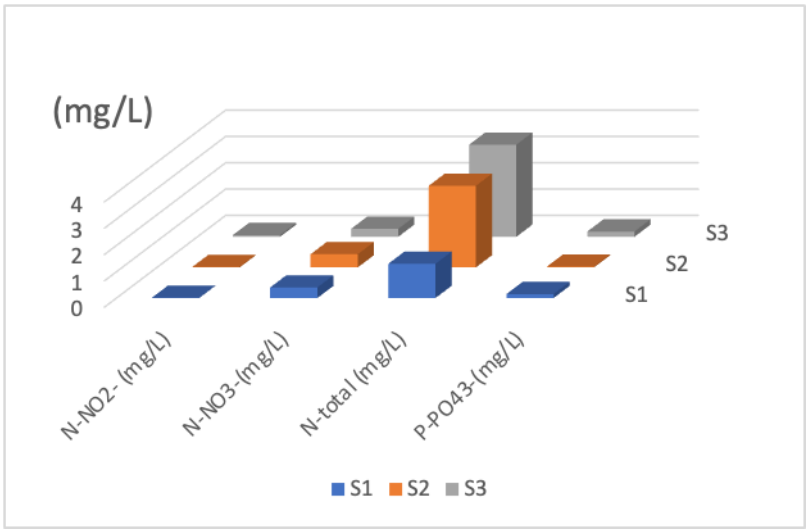

Fig. 2. Variations in nutrient concentrations in 2023 (annual averages)

The WQI variations are shown in Figures 3 and 4.

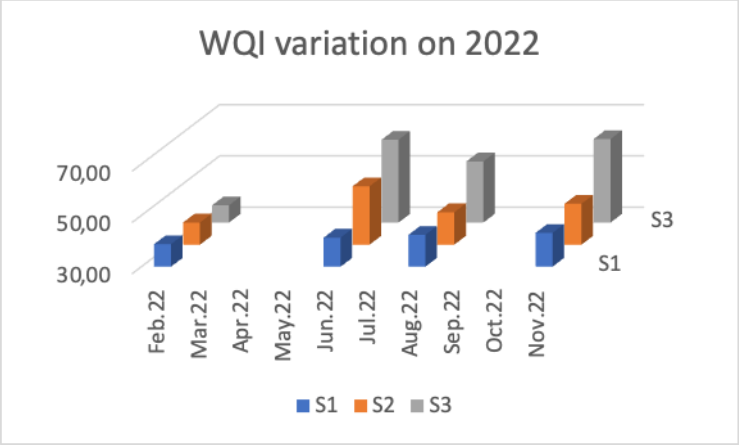

Fig. 3. WQI variation in 2022

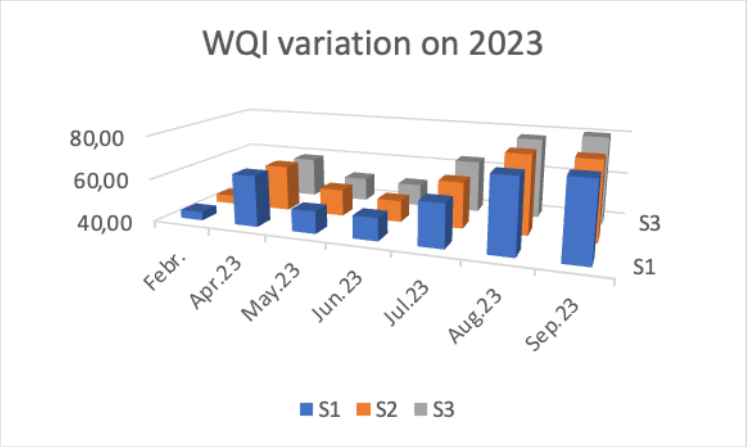

Fig. 4. WQI variation in 2023

The variation of the rainfall regime was analyzed, this having a decisive influence on the water quality (Fig. 5).

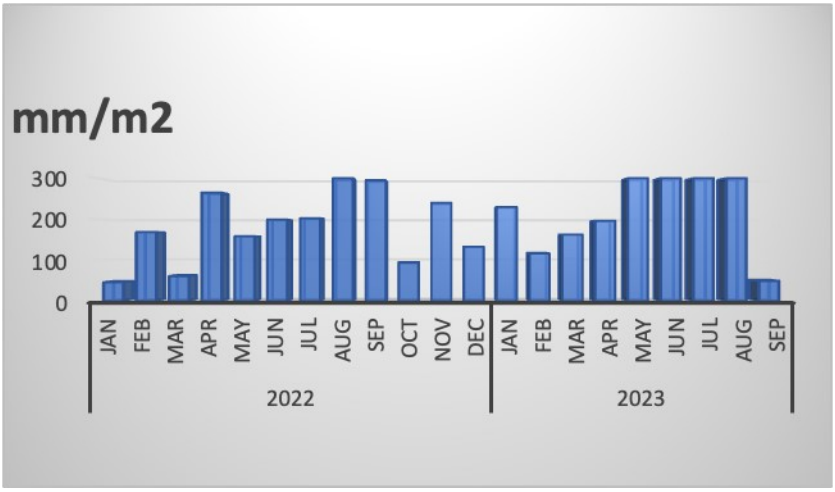

Fig. 5. The amount of monthly average precipitation ($mm \cdot m^{-2}$).

Also, the thermal regime has a special influence (Fig. 6).

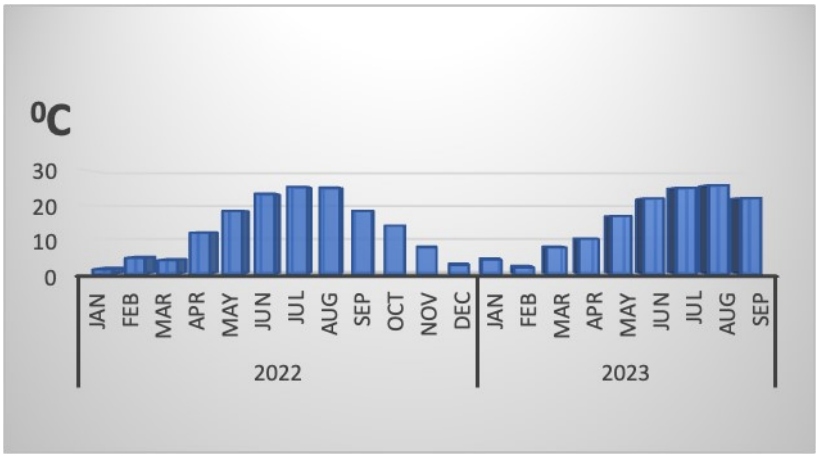

Fig. 6. Average monthly temperature variations during 2022 - 2023.

DISCUSSION

The WQI was calculated based on 17 physical-chemical parameters. In the calculation, some of the parameters have more important weights, decisively determining its value. Thus, the heavy metals which have major importance in the value of the index are: As, Cr, Cu, Ni and Zn. The determined values place the water in the quality class I for Cr, Cu and Zn, in the quality class III for Ni and in the quality class V for As. Regarding the nutrients, the analyses of the parameters values witin the same month revealed that in the case of nitrites, nitrates, N-total and phosphate the water in Lake Brateș corresponds to quality class I for the first 3 parameters, and to quality class III for the last parameter.
Weighting the values of these parameters, the WQI places the water in the selected month (August 2023) in the quality class **poor** (Fig. 4). If the water quality were to be interpreted strictly according to the values of the physico-chemical parameters, it would be impossible to reach a definite conclusion because some of the parameters indicate a very good quality of the water, while others indicate extreme pollution.
Analyzing the WQI values which correspond to the 2 years in which studies were carried out (Fig.3 and Fig.4), the fact may be noticed that the best values were traceable in March, and that the values were higher as the temperature increased and the rainfall regime became poor.
The agricultural activities have a significant influence on the water quality in Lake Brateș, as well, the WQI values increasing in the months of April - May due to the larger amounts of nutrients which result from the use of N and P fertilizers in these months. The increase in WQI values in the following months is closely related to the high values of the ambient temperature and to the dry periods. All these factors lead to a decrease in the water level in the lake, both due to the evaporation and to the fact that River Chineja greatly reduces its flow, the lake no longer receiving enough water, and the concentrations of heavy metals and nutrients obviously increasing.
Comparing the graphs in Figures 3 and 4, a decrease in water quality may be noticed, which is primarily due to the climatic conditions determining the dramatic decrease in the water level in the lake basin, the annual average being below 250 mm/m^2/year, deficit regime in the years studied. In the periods when there was a surplus pluviometric

regime, the water and sediment quality was relatively good, the values of the WQI and, separately, of the physico-chemical parameters falling into quality class II (good).
Analyzing the values obtained for the 3 sampling stations, the best values were obtained at the discharge of River Chineja into the lake, both due to the larger volume of water in the area and to the distance from the inhabited areas. Values were higher in the middle of the lake, the highest WQI values being obtained at station 3, which is near the beach and the railway. Consequently, the anthropic influence speaks for itself again.

CONCLUSION

In the present paper, the WQI was used for the first time to determine the water quality of Lake Brateș. This index is an efficient tool in the characterization of freshwater and it has been used successfully in many studies.
In the 2 years analysed, a decrease in water quality was observed in the summer and autumn months as compared to the winter months and
the first months of spring. Obviously, climate changes have led to a decrease in water quality because excessive heat and the lack of precipitation for long periods of time have favoured the partial clogging of the lake, and implicitly a decrease in its water quality.
Comparing the WQI values obtained in the 2 years, a deterioration of the water quality may be observed in 2023 as compared to the 2022.
Moreover, comparing the values of the physico-chemical parameters measured in the present research with those obtained in previous studies, it may be concluded that the state of the lake is not good at present and that unclogging works should be carried out in the coming period so as to bring both water and sediments values to those identified more than 10 years ago.
Anthropogenic activities had and still have a great impact on the aquatic ecosystem of the lake. The agrotechnical works carried out more than 75 years ago explain the partial destruction of the ecosystem, which has been deteriorated even more in recent yeras due to climatic factors.

ACKNOWLEDGEMENTS

The technical support was provided by the Rexdan Research Infrastructure, the infrastructure created through the project *An Integrated System for the Complex Environmental Research and Monitoring in the Danube River Area, REXDAN,* SMIS code 127065, project co-financed by the European Regional Development Fund through the Competitiveness Operational Programme 2014-2020, contract no. 309/ 10.07.2020

Funding: This research was funded by Fondo Proserpina S.R.L., grant number 2506/2022, ”The impact of heavy metals and microplastics from aquatic organisms on human health”.

REFERENCES

[1.] Tutuianau L., Vespremeanu-Stroe A., Preoteasa L., Rotaru S., Dima A., Dimofte D., Wetlands and lakes formation and evolution on the Lower Danube Floodplain during Middle and Late Holocene, *Quaternary International 602, 2021, 82–91,* https://doi.org/10.1016/j.quaint.2020.12.030

[2.] GEORGIANA BANUC, I. C. STANG, EXPOSURE AND VULNERABILITY TO FLOODS IN URBAN AREAS. CASE STUDY OF GALATI CITY (ROMANIA), RISCURI SI CATASTROFE, NR. XIII, VOL. 14, NR. 1/2014, p. 180 – 191

[3.] Ajeagah Gideon A., Praisler M., Cioroi M.,Constantin O, Palela M., Bahrim G., Biological and Physico-Chemical Evaluation of the Eutrophication Potential of a Highly Rated Temperate Water Body in South – Eastern Romania, http://dx.doi.org/10.5296/jee.v5i2.6512, Journal of Environment and Ecology, Vol. 5, No. 2, 2014, p. 108 – 129, ISSN 2157-6092

[4.] Vartolomei, F., Environment integration of ecological and biological influences in the lakes from lower section of Prut river, Lakes, reservoirs and ponds, vol. 1-2, p. 157-165, December 2008, ISSN 2284-5305

[5.] Cazacu, M., Fish farms as nesting sites for *Chlidonias hybridus* (Aves, Charadriiformes, Sternidae), North-Western Journal of Zoology, 2006, Vol. 2, No. 2, 2006, pp.73-87, ISSN 1843-5629

[6.] Vasile, A., Zara, M., Paltenea, E., The evolution of certain physical-chemical parameters of the water used for the provisioning of the aquatic ecosystem Brates, SCIENTIFIC STUDY & RESEARCH, Vol. X (1), p. 83 – 90, 2009, ISSN 1582-540X,

[7.] Buruiana, D. L., Carp, G. B., Muresan, A. C., Ceoromila, A. M., Obreja, C. D., Ghisman, V., Axente, E. A., Detection of Biomass in Lake Areas using Artificial Intelligence: Applying a Study Case-Brates Lake, Galati, Romania, 42nd MADRID International Conference on "Advances in Science & Technology" (MICAST-2022), p. 100 – 106, 2022, ISBN- 978-989-9121-05-8,

[8.] David, I. G., Matache, M. L., Tudorache, A., Chisamera, G., Rozylowicz, L., Radu, G. L., Food chain biomagnification of heavy metals in samples from the lowe Prut floodplain natural park, Environmental Engineering and Management Journal, , Vol.11, No. 1, 69-73, January 2012, eISSN: 1843-3707

[9.] Ciubotariu, A.C., Istrate, G.G., Physico – chemical parameters of water from Galati area (Romania), 6th International Multidisciplinary Scientific GeoConference SGEM 2016, www.sgem.org, SGEM2016 Conference Proceedings, DOI: 10.5593/SGEM2016/B31/S12.073, ISBN 978-619-7105-61-2 / ISSN 1314-2704, June 28 - July 6, 2016, Book 3, vol. 1, pp.561-568, 2016

[10.] Order 161/2006, The Normative on the Classification of Surface Water Quality in Order to Establish the Ecological Romanian Ministry of Research and Innovation Tatus of Water Bodies; O cial Monitor: Bucharest, Romania, 13 June 2006.

[11.] Georgescu, P. L., Moldovanu, S., Iticescu, C., Calmuc, M., Calmuc, M., Topa, C., Moraru, L., *Assessing and forecasting water quality in the Danube River by using neural network approaches,* Science of the Total Environment 879, 162998, 2023, http://dx.doi.org/10.1016/j.scitotenv.2023.162998

COMPREHENSIVE RISK ASSESSMENT OF FLOODS IN CYPRUS: EVALUATING THE IMPACTS OF CLIMATE CHANGE

Ph.D. Georgios Xekalakis[1]

Assoc. Prof. Dr. Christos Anastasiou[2]

Dr. Evi Riga[3]

Prof. Giulio Zuccaro[4]

Assoc. Prof. Dr. Petros Christou[1, 2]

[1] Frederick Research Center, 1036 Nicosia, **Cyprus**
[2] Frederick University of Cyprus, 1036 Nicosia, **Cyprus**
[3] Aristotle University of Thessaloniki, 54124 Thessaloniki, **Greece**
[4] PLINIVS-LUPT Study Centre, Toledo 402, 80134 Napoli, **Italy**

ABSTRACT

Arid and semi-arid regions, including Cyprus, are increasingly experiencing severe weather events due to climate change. These events, characterized by prolonged droughts and flash floods, pose significant challenges to the environment, economy, and societal well-being. This paper aims to analyze the challenges of Flood Risk Management (FRM) in dry areas, focusing on Cyprus as a case study. It reviews historical data on temperature and rainfall patterns, flood types, and severity to propose effective, nature-based mitigation measures. The study examines temperature and rainfall trends over the last 30 years in Cyprus, categorizes floods since 1859 based on severity, and identifies prevalent flood types. The investigation reveals a decrease in annual rainfall and an increase in average temperatures in Cyprus, leading to heightened flood risks. The study categorizes floods into fluvial, pluvial, flash, and coastal types, with pluvial floods being the most common due to urbanization. The paper underscores the role of community and individual participation in adopting nature-based solutions such as permeable materials, rain gardens, tree planting, and roof gardens. Addressing flood risks in Cyprus requires a combined effort of government initiatives and community engagement. The adoption of sustainable, eco-friendly practices can significantly mitigate the adverse effects of climate change on flood hazards. This holistic approach is imperative for enhancing resilience against future climate-related challenges in Cyprus and similar arid regions.

Keywords: Climate Change, Floods, Hazards, Natural-based Mitigation Measures, Cyprus

INTRODUCTION

Regions with arid and semiarid climates experience both prolonged droughts and flash floods, which affect the economy, people's lives, and the environment [1]. Even in recent years, floods in these arid areas have resulted in many deaths and large economic losses. Recent data from Cyprus, for example, show a decrease in rainfall. Climate change is exacerbating extreme weather events in these areas, like heavy rain, high temperatures, and long droughts and increasing the likelihood of severe flooding in the

future. This problem is made worse by growing populations and human activities like city expansion, wrong land use, economic growth, and lack of awareness.

Besides climate change and human activity, several unique factors make dry areas more prone to severe flooding and unexpected flood damage. The wide variety in climate, geography, rocks, plants, and water systems in these areas makes it hard for local flood managers to do their job [2]. On the other hand, challenges related to humans and systems, such as focusing too much on managing drought and not having the right institutional frameworks, negatively affect Flood Risk Management (FRM).

All these points highlight the need for a better understanding of FRM challenges in dry areas to reduce the negative effects of floods on the environment, economy, and society—now and in the future.

Therefore, this review will first look at the relationship between temperature and rain over the last 30 years in Cyprus, classify floods by how severe they are using data collected since 1859, identify the most common flood types on the island, and suggest some nature-based solutions that can be easily adopted by both the community and individuals.

THE SCENARIO OF CLIMATE CHANGE IN CYPRUS

Cyprus faces several climate risks (Table 1) and the search for efficient, acceptable solutions is a priority [3]. Each risk leads to numerous negative impacts on human well-being and environmental health, ecosystem biodiversity, agriculture, tourism, energy demand and supply, and generally all sectors of society and the economy.

Table 1. Table in relation to climate risks in Cyprus

Type of Climate Risk	Current Level risk	Expected change in Intensity	Expected change in Frequency	Timeline	Indicators relating to the Risks
Extreme Rainfall	Moderated	Increase	Increase	Medium term	Increase of days with intense precipitation (associated with flooding)
Floods	High	Increase	Increase	Medium term	Increase in flooding from rivers and rains
Storms	Moderated	Increase	Increase	Long term	Increase in exceptional phenomena
Coastal Erosion	Mediocre	Increase	Increase	Medium term	Increase in coastal erosion and the resulting salinization of the water table
Heat wave	High	Increase	Increase	Present	Increase in the frequency and duration of heat waves
Drought	High	Increase	Increase	Present	Increase in days without rainfall (2020-2050)
Dust	High	Increase	Increase	Present	Increase in dust levels

Climate in Cyprus is expected to change in the next few years with rising of the local temperatures along with other adverse effects. Geographically located in the Middle East, Cyprus faces a future with high temperatures and less rainfall which will accelerate the island's desertification [4]. These weather conditions will, in the future, probably affect the people and some other sectors such as the food production, the water availability, the tourism and the urban and rural societies because of the great intensity of heat waves.

Average temperatures in Cyprus could rise significantly, by about 1 to 3°C over the next three decades, 3°C to 5°C by mid-century, and 3.5°C to 7°C by the end of the century [5]. This could lead to a two-week increase in the number of hot days in Cyprus exceeding 38°C between 2020 and 2050. In 2019, for example, Nicosia had 12 days with temperatures exceeding 38°C. By 2050, Nicosia could experience about 24 such days, an increase of more than 100%. Cyprus will also experience 30 additional warm tropical nights above 25˚C than is currently the case. In 2019, Nicosia experienced 6 nights where the temperature was above or equal to 25˚C, one month longer than today. By 2050, Nicosia could experience 36 such nights, a 600% increase. Half of these warm tropical nights also had daytime temperatures above 38°C. This means that Nicosia could experience 18 days of incredibly high daytime temperatures in 2050, with no relief at sunset.

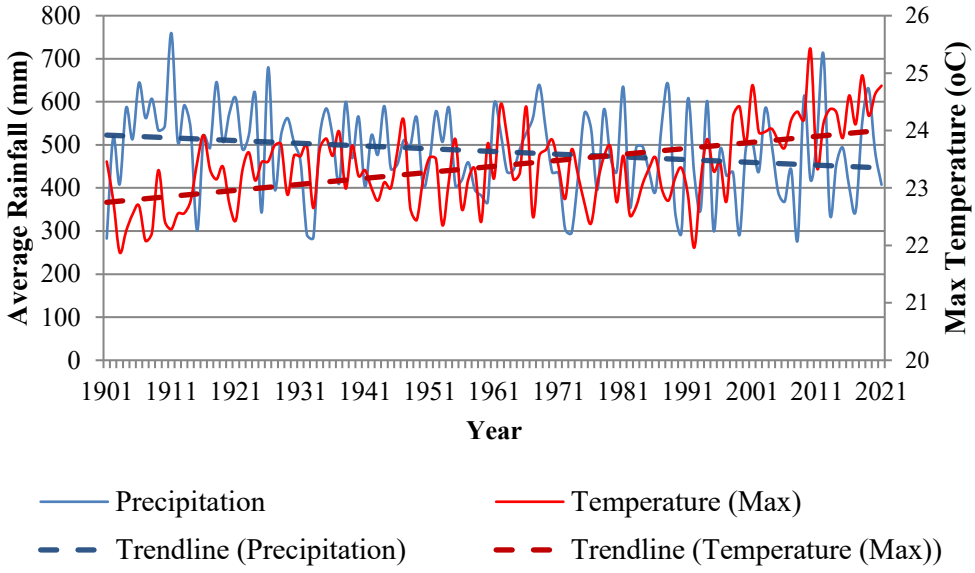

Figure 1. Relationship of Temperature - Precipitation in Cyprus

Figure 1 shows the change in maximum temperature on the island and precipitation from 1901 to 2021. Over the years, the average value of precipitation decreases, while the opposite trend follows that of the maximum temperature per year. According to history.com [6], the early 1980s would mark a sharp rise in global temperatures. Many pundits, such as Nasa scientist James Hansen, point to 1988 as a critical turning point, as turning events brought global warming into the spotlight. Something similar can be observed in the case of Cyprus as shown in the chart below where we have the intersection of the two lines.

The average annual precipitation between 1991 - 2021 (461.71 mm) is about 3% lower than the average annual precipitation between 1961 - 1990 (476.4 mm) and is the lowest in a recorded 30-year period. The average annual precipitation between 1931 - 1960 is 470 mm, and the average annual precipitation between 1901 - 1930 was the highest at 520 mm. The most recent 30-year period was the driest [7], however there were some very extreme events such as the 2012 precipitation of 711 mm and 2019 (Figure 2), the wettest year since 1968, with 631 mm, followed by floods and natural disasters.

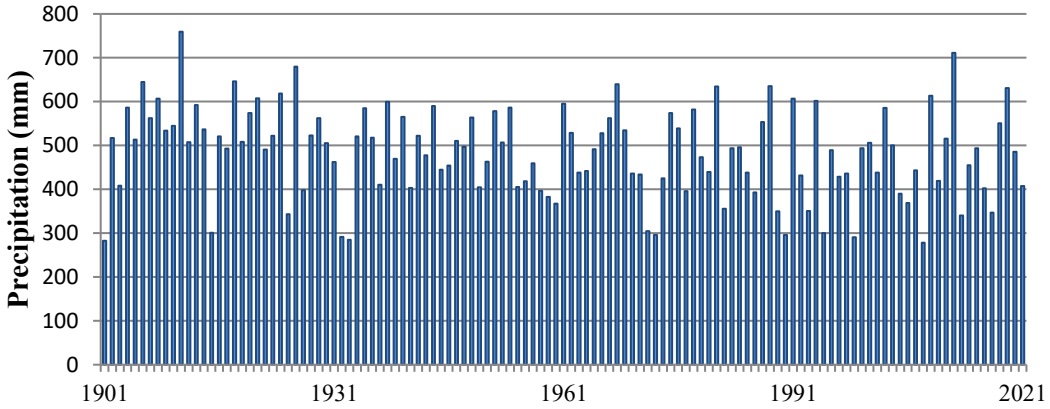

Figure 2. Annual Precipitation in Cyprus

FLOODING IN CYPRUS

Flooding is a natural phenomenon that takes place when the level of a water body begins to rise to the point where it overflows its artificial embankments or natural banks, submerging normally dry areas [8]. The four most common types of floods that someone can encounter in Cyprus are the following;

- Fluvial flood, also known as a river flood, happens when the water level in a river or lake increases and spills over onto the nearby coastlines, banks, and land,
- Pluvial flood, when there is a flood without an overflowing water body, it is called a pluvial or surface water flood,
- Flash flooding, are caused by extreme rainfall events or the sudden release of water over a short period of time and
- Coastal flooding, the flooding of coastal areas by seawater usually caused by high tide, tsunamis, and storm surge.

The following tables provide statistics for all recorded 615 flood events that occurred during the period 1859 - 2021. Most of these events (429) were recorded after 1991. Statistical analysis shows that both the type of floods and their severity are distributed as follows in each 30-year period recorded.

Table 2. Flood rates by severity per 30 year period

Period	**Severity**				
	Very Low	*Low*	*Moderate*	*High*	*Very High*
2021 - 1991	50.3	28.4	19.3	1.9	0.0

1990 - 1961	36.8	43.9	8.8	10.5	0.0
1960 - 1931	37.5	18.8	43.8	0.0	0.0
1930 - 1901	17.9	43.6	28.2	7.7	2.6
1900 - 1859	15.8	57.9	15.8	5.3	5.3

Table 3. Flood types per 30 year period.

Period	**Flood Type**		
	Fluvial	*Pluvial*	*Flash*
2021 - 1991	22.4	58.3	19.3
1990 - 1961	19.3	67.5	13.2
1960 - 1931	25.0	18.8	56.3
1930 - 1901	23.7	0.0	76.3
1900 - 1859	33.3	0.0	66.7

An interesting statistic in Table 2 shows that between 1931 and 1960, most floods (43.8%) were of medium severity. In the 1961-1990 period, the percentage with low severity predominated (43.9%), while it continued to improve in recent years (50.3%).

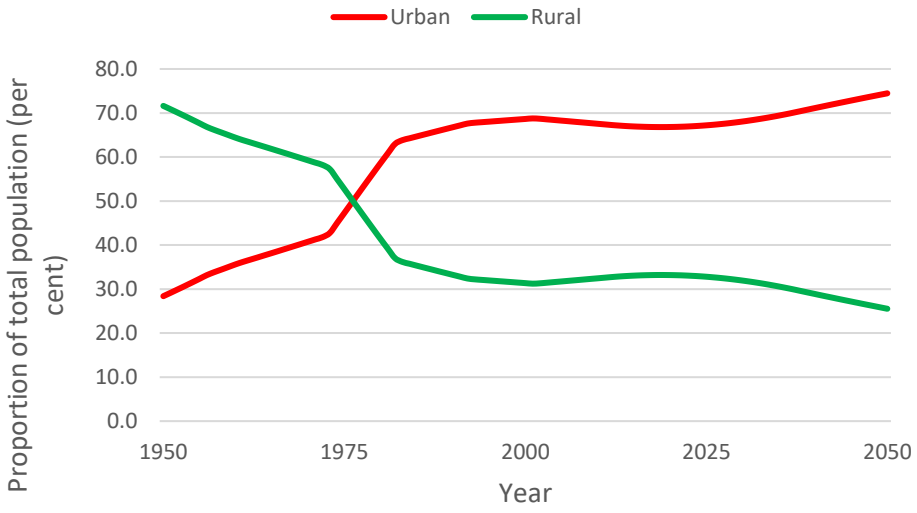

Figure 3. Percentage of population in urban and rural areas

The above percentages (Table 3) are consistent with the fact that floods in the Cypriot region are usually characterized as pluvial floods (58.3%, in the last 30 years), due to extensive urbanization combined with flash floods, which are likely to cause more intense direct damage than other types of floods due to the small size of the watersheds, steepness of the land, low vegetation, high rainfall intensity, and short concentration time (e.g. Fluvial flooding).

The likelihood of flooding from surface water and rivers in urban areas is increasing as a result of urban growth (Figure 3), and lack of effective urban drainage infrastructure.

Until 2014, Cyprus did not have a flood risk plan. Currently, Cyprus has identified 38 (19 areas before 2011 and 19 by 2018) Areas of Potentially Significant Flood Risk (APSFRs) under the Flood Directive. As stated, 5,370 people are currently exposed to significant flood risk at a frequency of 5% (T=20 years) according to the preliminary flood risk management plan [9]. Urbanization will increase this number to 15,170.

The Water Development Department (WDD) of Cyprus has created and posted online Interactive Flood Risk Maps [10] so that every citizen can immediately see the existence or non-existence of a potential flood risk and the possible extent of flooding of their property by entering information such as e.g. the street or parcel number of his property through a GIS platform.

The Flood Hazard Maps (Figure 4) show the area that could be covered by water and the depth of water for 3 different flooding scenarios:

1. A low probability flood (1 in 500).
2. A medium probability flood (1 in 100).
3. A flood with a high probability (1 in 20).

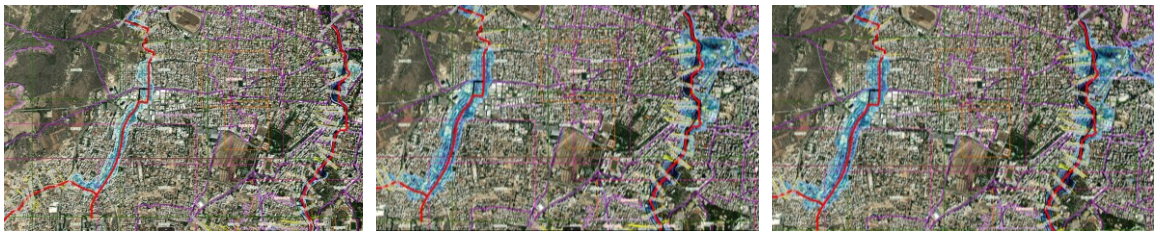

Flooding hazard Map with a high probability (1/20) | Flooding hazard Map with an average probability (1/100) | Flooding hazard Map with low probability (1/500)

Figure 4. Interactive Flood Hazard Maps

NATURAL-BASED MITIGATION MEASURES

In light of escalating climate challenges, societies globally have recognized the imperative need to reassess traditional flood mitigation measures. Historically, flood risk reduction has predominantly focused on hard engineering solutions. However, the unpredictable intensities and patterns of precipitation, as influenced by climate change, necessitate a paradigm shift in our approach to flood management.

The current era of flood mitigation strategies emphasizes to sustainability combined with environmental harmony. The convergence of gray (traditional engineering) and green (nature-based) infrastructure represents this new direction. Presented on table 4 below are a few nature-based measures epitomizing this evolution:

Table 4. Eco-friendly practices against flooding

Measure	Description	Benefits
Permeable Materials	These are non-sealed surfaces designed to allow water absorption. Sealed surfaces often intensify urban flooding, inhibit	Significantly reduce flooding potential by absorbing 80-100% of water during intense rainfall, cutting back on property damage and preventing soil erosion.

	the formation of local ecosystems, and escalate the urban heat island effect.	With increased rainwater infiltration capacity, permeable materials enhance groundwater, helping to save water, especially in times of drought.
Rain Gardens	These specially designed gardens act as natural reservoirs, collecting rainwater and reducing its flow in urban settings.	Mitigate flooding from excessive rainfall and retain pollutants. Control the urban heat island effect.
Tree Planting	An elemental yet potent nature-based solution, increasing vegetation counters several environmental challenges.	Promote water retention and filtration. Aid in soil retention.
Roof Gardens	These are vegetative layers on building rooftops, established over a structured sequence of layers including waterproofing, anti-root protection, moisture retention substrate, drainage, and growth substrate.	Substantially decrease heating expenses due to added thermal insulation provided by the vegetation layer. Reduce summer cooling costs by up to 49% through solar energy reflection and absorption by the plants. Achieve a 40-80% decrease in rainwater runoff into sewers due to the absorption capacity of rooftop plants. Offer an avenue to reintroduce greenery in urban settings.

CONCLUSION

The scope of this paper, centered on reviewing historical data on temperature, rainfall patterns, flood types, and severity, primarily in Cyprus, has provided a comprehensive understanding of the evolving dynamics of flood risks in arid and semi-arid regions. Notably, while the severity of floods has shown a decreasing trend over the years, the increasing prevalence of pluvial floods, particularly in the context of rapid urbanization, poses a significant challenge. This situation underscores the necessity for effective, eco-friendly, and nature-based mitigation measures.

Our findings reveal that although the overall severity of floods may be diminishing, the implications of pluvial flooding, especially in urban areas, cannot be understated. The increased urbanization in recent years has resulted in more impervious surfaces, exacerbating runoff and the potential for flash floods. This trend poses a key area of concern, necessitating targeted mitigation strategies.

In response to these challenges, the paper proposes a range of eco-friendly, nature-based mitigation measures suitable for both individual and community action. These measures include the use of permeable materials in urban construction, which can significantly reduce surface runoff; the establishment of rain gardens to absorb excess rainwater; extensive tree planting to enhance natural water absorption and soil stability; and the development of roof gardens to reduce runoff and improve urban microclimates.

These proposed measures are not just environmentally sustainable but also offer a proactive approach to flood risk management. They emphasize the importance of integrating ecological considerations into urban planning and individual practices. Moreover, these measures highlight the role of community involvement and individual

responsibility in mitigating flood risks. It is through collective action and shared responsibility that the most effective and lasting impact can be achieved.

In conclusion, this paper contributes a valuable perspective to the discourse on flood risk management in arid and semi-arid regions. By combining a thorough analysis of historical data with practical, nature-based solutions, it offers a roadmap for addressing the challenges posed by pluvial floods in the face of rapid urbanization and climate change. The insights and strategies presented here are not only relevant for Cyprus but also applicable to similar regions worldwide, providing a framework for sustainable, community-driven flood risk management.

ACKNOWLEDGEMENTS

This research work was supported by the ISTOS project. This project has received funding from the European Union's Horizon 2020 research and innovation programme (WIDESPREAD-TWINNING) under grant agreement No. 952300.

REFERENCES

[1] Ramadan, E.M. et al. (2022) 'Evaluation and mitigation of flash flood risks in arid regions: a case study of Wadi Sudr in Egypt,' Water, 14(19), p. 2945. https://doi.org/10.3390/w14192945.

[2] IPCC, F.C., 2014. Climate change 2014: impacts, adaptation, and vulnerability. Part A: global and sectoral aspects. Contribution of Working Group II to the fifth assessment report of the Intergovernmental Panel on Climate Change. Clim. Chang.

[3] Cyprus Energy Agency (n.d.). NATURE-BASED SOLUTIONS (NBS) - GUIDE FOR APPLICATION TO HOUSEHOLDS AND PRIVATE PROPERTY. [online] Climate Change, p.11. Available at: https://www.cea.org.cy/wp-content/uploads/2021/06/odigos-efarmogis-lyseon-vasismenon-sti-fysi-nbs-idiotikes-perioysies.pdf [Accessed 20 October 2023].

[4] AVLI |. 2023. Climate Change in Cyprus | Report | AVLI. [ONLINE] Available at: https://avli.org/resources/climate-change-in-cyprus-report/. [Accessed 20 October 2023].

[5] www.cyi.ac.cy. (n.d.). Climate Change and Impact - The Cyprus Institute. [online] Available at: https://www.cyi.ac.cy/index.php/eewrc/eewrc-research-projects/climate-change-and-impact.html [Accessed 9 May 2020].

[6] HISTORY. 2023. Climate Change History - Greenhouse Effect, Treaties | HISTORY. [ONLINE] Available at: https://www.history.com/topics/natural-disasters-and-environment/history-of-climate-change. [Accessed 20 October 2023].

[7] Cyprus - Climatology | Climate Change Knowledge Portal. 2023. Cyprus - Climatology | Climate Change Knowledge Portal. [ONLINE] Available at: https://climateknowledgeportal.worldbank.org/country/cyprus/climate-data-historical. [Accessed 20 October 2023].

[8] www.zurich.com. 2023. No page title. [ONLINE] Available at: https://www.zurich.com/en/knowledge/topics/flood-and-water-damage. [Accessed 20 October 2023].

[9] Πολιτική Άμυνα. 2023. Flood maps – Πολιτική Άμυνα. [ONLINE] Available at: https://civildefence.com.cy/en/floodmaps. [Accessed 20 October 2023].

[10] Ευρωπαϊκή Οδηγία 2007/60/ΕΚ και Κυπριακή Νομοθεσία για τις πλημμύρες | 1ο ΣΔΚΠ 2016-2021. 2023. Ευρωπαϊκή Οδηγία 2007/60/ΕΚ και Κυπριακή Νομοθεσία για τις πλημμύρες | 1ο ΣΔΚΠ 2016-2021. [ONLINE] Available at: https://www.moa.gov.cy/moa/WDD/wfdf.nsf/page08_gr/page08_gr?opendocument. [Accessed 20 October 2023].

DENDROGEOMORPHIC ANALYSIS OF FLASH FLOODS IN A SMALL FOREST CATCHMENT

MSc. Marie Uhrová (Jíchová)[1]

Assoc. Prof. Dr. Josef Křeček[1]

Dr. Eva Pažourková[2]

Dr. Jiří Vrtiška[3]

[1] Czech Technical University in Prague, **Czech Republic**
[2] AON Impact Forecasting, **Czech Republic**
[3] STAVKRAFT, **Czech Republic**

ABSTRACT

Flash floods represent one of the most significant natural hazards in headwater catchments facing the lack of systematic hydrological monitoring. This study focus on the detection of flash floods on growth disturbances detected at trees of European beech (*Fagus sylvatica* L.) located in the torrential channel of the Holubí Potok stream in the Jizera Mountains (North Bohemia, Czech Republic). At the injured stems, flood scars were identified and core samples dated by tree ring analysis; the intensity of the disturbance clearly depends on geomorphology of the stream channel. These data were compared with 40 years of hydrometric measurements at the catchment outlet. The flood injuries were detected in the last 65 years, and those flood signs occurred on average every 12-13 years. All of them correspond with intensive summer rainstorms. Flood waves exceeding the gauging capacity or the period of hydrometric observation were reconstructed by HEC- HMS 4.4 and HEC-RAS 5.0.3 tools. The applied approach contributed to the extrapolation and correction of the standard flood frequency curve at the investigated catchment.

Keywords: headwater catchment, flash flood, stream channel morphology, tree-rings

INTRODUCTION

In the small mountain catchments, intensive rainstorms may trigger flash floods and debris flows according to the local hydrologic, geomorphologic and geotechnical features [1]. Those phenomena represent one of the most significant natural hazards in headwater regions [2], [3]. Headwater streams are the smallest part of rivers but make up the majority of river miles [4]; and the extreme floods, characterised by a return period more than 50 years, have huge destructive potential to devastate landscapes and settlements worldwide [5].

The management of distant headwater catchments often face the lack of long-term (> 30 years) data of precipitation and runoff, and, moreover, stream gauging stations may not record correctly extreme events [2], [3]. Thus, proxy data of growth-ring series of trees affected by past floods can provide an alternative and complementary approach [6], [7]. The aim of this paper is to improve the frequency analysis of floods in the small torrential stream in the Jizera Mts. (Northern Bohemia, Czech Republic) by dating past

events on growth disturbances at affected trees of European beech (*Fagus sylvatica*) located in the stream channel.

MATERIALS AND METHODS

This study was performed in the experimental catchment of the Holubí Potok stream (the Odra river district 2-04-10-014), near the Oldřichov settlement (50°52'14"-50°52'30"N, 15°6'11"- 15°6'21"E), Figure 1, Table 1.

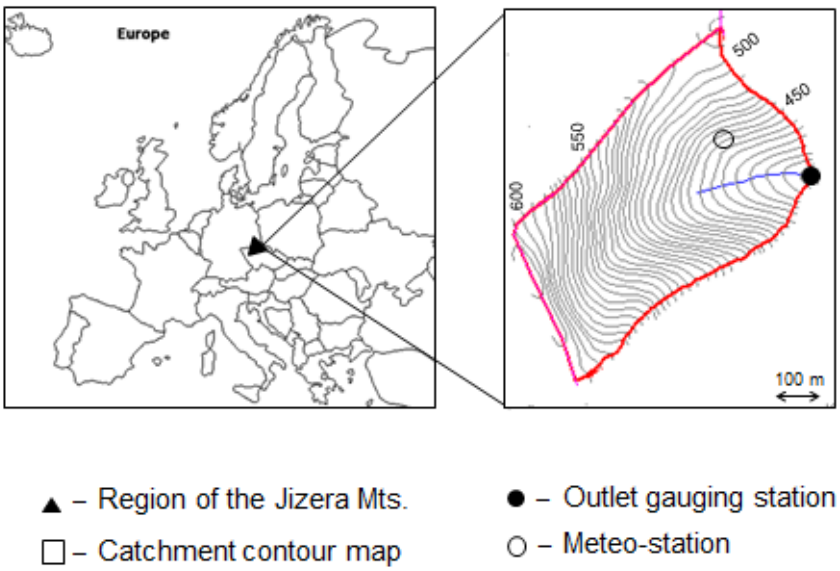

Figure 1. The Holubí Potok experimental catchment.

This area belongs to the humid continental climate (Kőppen's Dfb) with mean annual precipitation 940 mm, mean air temperature 8.3°C, and an average of 86 days with snow cover [8].

Table 1. Catchment morphology.

Parameter	Unit	Value
Area	(km^2)	0.23
Elevation	(m)	518 (409 - 620)
Slope	(%)	34.5 (0.1 - 83.2)
Shape index	(-)	1.56
Length of streams	(m)	405
Drainage density	(km^{-1})	1.76
Slope of the stream	(%)	11.2 (10.1 – 15.3)
Strahler stream order	(-)	1

Low-base-status soils (sand-loamy brown forest soils) developed on porphyritic granite reach depths of 0.7-1.3 m. The stream channel is characterized by steep gradients with step-pools [9] and a water depth below 0.5 m at bank-full discharge. The bed is covered by non-uniform sediments (sand, gravel and boulders) with a predominantly gravel substrate.

The experimental catchment was instrumented in 1982 (and re-instrumented in 1995). The outlet is equipped with a composite sharp-crested weir (Thomson V-notch and Poncelet weirs) and water level is measured by the ALA 4020 compound water pressure and temperature recorder, logging every ten minutes. The capacity of the gauging station (0.39 m^3 s^{-1}) corresponds to a 12 years return period [3]. The cross section geometry along the stream was identified every 10 m from the outlet station to the channel head, and the values of Manning's roughness coefficient n were estimated from the channel configuration using Cowan's composite approach [3]. Flood waves in the stream channel were constructed by HEC – HMS 4.4 [10]; the HEC – RAS 5.0.3 package [11] was used to simulate flow velocities and water depth in the stream channel.

In the stream channel and its wider surroundings, basal parts of trees were inspected for the presence of flood injuries. Scars of doubtful origin (formed by other factors) were not considered. Dendrochronological analysis included 12 beech trees (*Fagus sylvatica*) distributed along the 1 km long section of the stream. Sampling of living trees was restricted to the extraction of wedges from the scars, and, whole cross sections were collected at 2 dead stumps. In addition, 8 undisturbed trees were selected in the valley to obtain a reference chronology representing local growth conditions. The stem cores were sampled by the Pressler borer; preparation of samples included gluing and polishing the surface for a better visibility of tree rings [12]. Ring-width series were measured with a LINTAB measuring table (Rinntech, Heidelberg, Germany) with a precision of 0.01 mm in the Laboratory of Dendrochronology (Faculty of Science, Charles University in Prague). Ring-width series were synchronised, cross-dated and standardised using the PAST software [12]. The years of flood scar detection were confronted with the climate record at the professional meteorological station Liberec (elevation 398 m, record since 1936) located approximately 8 km from the experimental catchment.

RESULTS

In total, 12 detected scars were acceptable for a cross-dating; one samples contained three scars, two samples two scars and nine just one scar. The oldest recorded injury was assigned to the year 1958 and all the identified scars correspond with summer rainstorm events. For the period 1958-2022, five years with stem injuries were detected, therefore, these flood damages occurred on average every 12-13 years. The years with flood scars are 1958 (2 scars), 1983 (2 scars), 1997 (2 scar), 2002 (2 scars) and 2010 (4 scars).

The observed peak-flows in the instrumented period of 1982-2022 originated dominantly by extreme summer rainstorms; the peak flow frequency extrapolated by the Log-normal distribution of the registered annual discharge maxima, are presented in Figure 2.

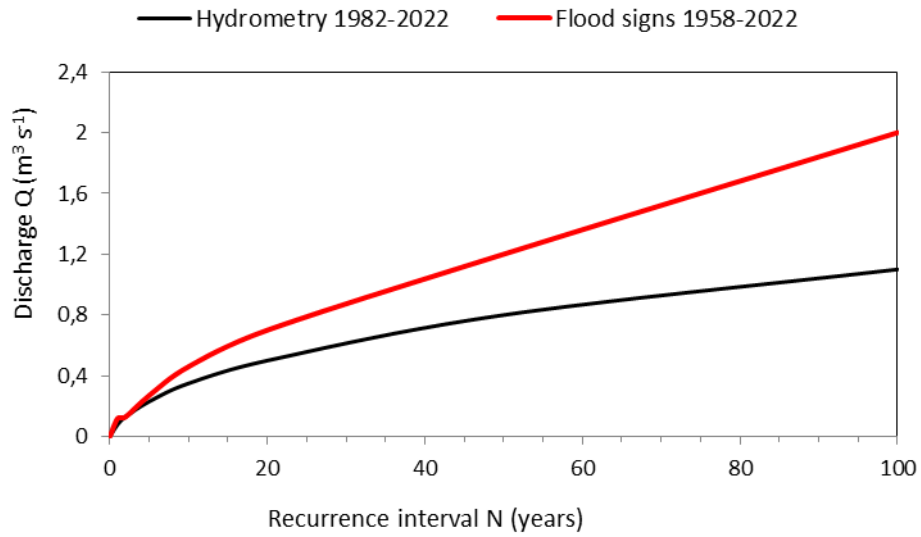

Figure 2. Flood frequency of hydrometric period (1982-2022) and flood scars detection (1958-2022).

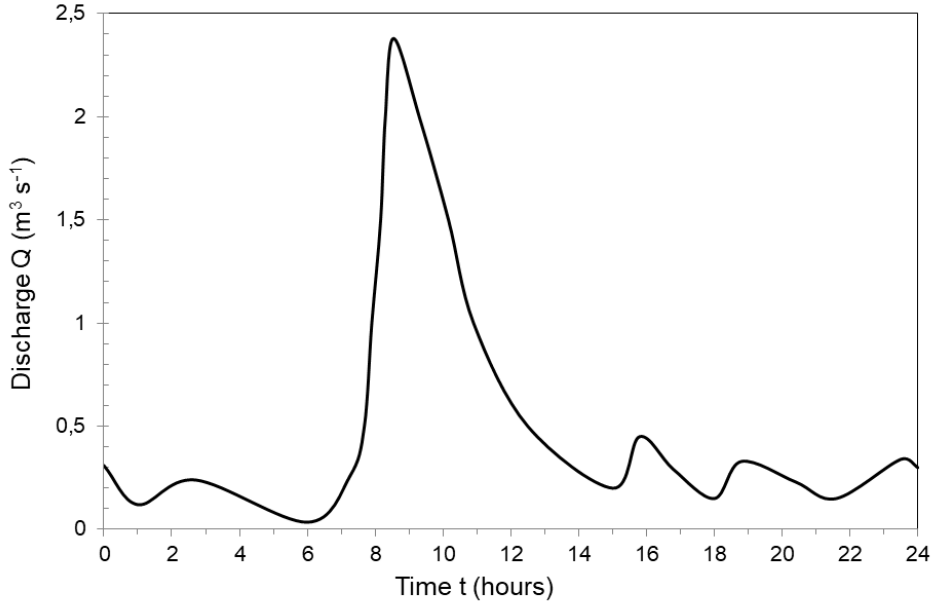

Figure 3. Flash flood of the 7th August 2010: modelled discharge Q (m^3 s^{-1}) at the catchment outlet.

The mean annual discharge Qa = 2.5 10-3 m3 s-1, and the 90% frequency discharge Q330 = 0.53 10-3 m3 s-1 show a perennial streamflow uniformly distributed within the year. The bank-full discharge Qb = 0.1 m3 s-1 corresponds to a return period 1-2 years. In the catchment outlet, flood waves exceeding the capacity of the gauging station (Q > 0.39 m3 s-1) were reconstructed by HEC- HMS 4.4 catchment modelling system [10]

according to the wet perimeter identified by flood scars, Figure 3. Consequently, water depth and currents in the 1 km - section of stream channel (Figure 4) were modelled with HEC-RAS 5.0.3, [11].

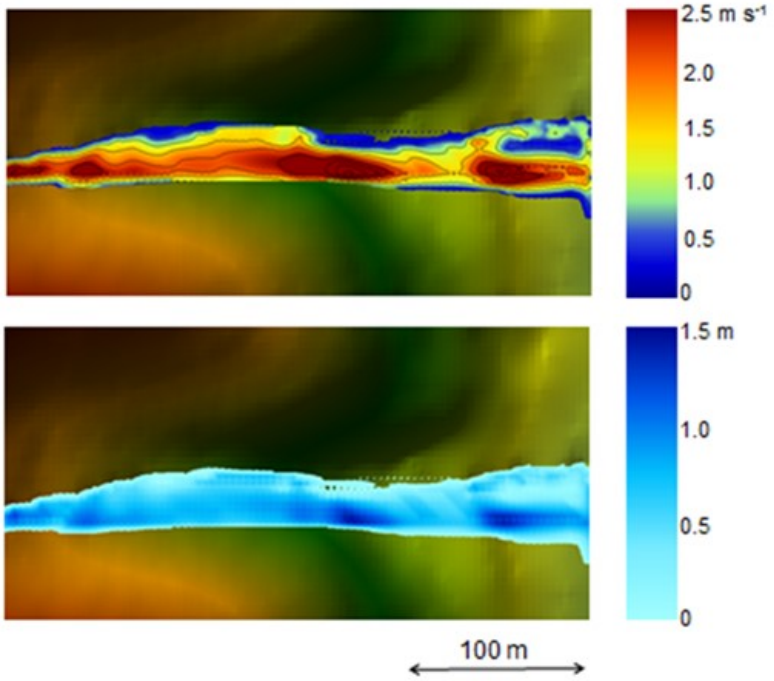

Figure 4. Reconstructed water depth and currents in the studied stream channel by the peak discharge of the 7th August 2010.

Considering the frequency of peak flows analysed for the period 1958-2022 including discharge maxima reconstructed by flood scars dendrochronology, the alternative frequency curve is given in Figure 2. Thus, the alternate flow with frequency of 0.01 (i.e. 100 year return period) Q_{100} = 2 m^3 s^{-1} corresponding to the value of 1.2 m^3 s^{-1} analysed by hydrometric observation in 1982-2022.

DISCUSSION

Generally, dendro-morphology is supposed as the useful and accurate approach for the dating of various geomorphic processes by the determination of incidences with yearly precision [14], [15]. In our study, the method of flood injury detection was used in a small headwater catchment with semi-native beech stands. The frequency of identified flood scars (occurring there every 12-13 years) is lower than those found in upper mountain catchments [13], probably according to relatively milder rainfall phenomena.

Dendrochronological analysis of flood signs at injured stems extended the existing data set of flood events registered by standard hydrological methods for the instrumented period 1982-2022. Therefore, the method of dendrochronology can be used to extrapolate and modify the standard the flood frequency curve according to [6].

CONCLUSION

This study confirmed the dominance of summer rainstorms in flood genesis at a small headwater stream of the Jizera Mts. (Northern Bohemia, Czech Republic). The method of dendrochronology applied in stream channel and its surroundings identified flood injuries at beech trees in the 65 year period (1958-2022); on average, identified flood scars occurred there every 12-13 years. The years with flood scars are 1958 (2 scars), 1983 (2 scars), 1997 (2 scar), 2002 (2 scars) and 2010 (4 scars).

Based on the instrumented period of 1982-2022, peak flow frequency was extrapolated by the Log-normal distribution of the registered annual discharge maxima (Figure 2). The studied stream show a perennial streamflow uniformly distributed within the year, and the bank-full discharge corresponds to the return period 1-2 years, and, the capacity of gauging station with 12 years return period.

According to the stream channel morphology reconstructed by the detected stem scars, HEC- HMS 4.4 and HEC-RAS 5.0.3 modules provided sufficient tools to approximate flood parameters (discharge, velocity and water depth) in the studied 1 km – stream section.

Comparing the frequency of peak flows analyzed for the instrumented period 1982-2022, and discharge maxima reconstructed by flood scars dendrochronology (1958-2022), two alternative frequency curves are provided in Figure 2. Thus, the alternate 100 year flow exceeds the value provided by hydrometric observation by 67 percent.

ACKNOWLEDGEMENTS

This research was funded by the Czech Technical University in Prague (Project SGS2022/093/OHK1/2T/11, 2022-2023).

REFERENCES

[1] Borga M., Stoffel M., Marchi L., Marra F., Jakob M. Hydrogeomorphic response to extreme rainfall in headwater systems: flash floods and debris flows. Journal of Hydrology, vol. 518, pp. 194-205, 2014.

[2] Ruiz-Villanueva V., Díez-Herrero, A., Stoffel M., Bollschweiler, M., Bodoque J.M., Ballesteros J.A. Dendrogeomorphic analysis of flash floods in a small ungauged mountain catchment (Central Spain). Geomorphology, vol. 118, pp. 383–392, 2010.

[3] Pažourková E., Křeček J., Bitušík P., Chvojka P., Kamasová L., Senoo T., Špaček J., Stuchlík E. Impacts of an extreme flood on the ecosystem of a headwater stream. Journal of Limnology, vol. 80(2), DOI 10.4081/jlimnol.2021.1998, 2021.

[4] Richardson J.S. Biological diversity in headwater streams. Water, vol. 11, pp. 1-19, 2019.

[5] Davis D.W. Is the current approach to managing flood threats in the United States sustainable? In: Kabbes K.C. (Ed.), Proceedings of the World Environmental and Water Resources Congress: Restoring our Natural Habitat, American Society of Civil Engineers, Tampa (FL), pp. 1-10, 2007.

[6] St. George S. Tree rings as paleoflood and paleostage indicators. In: Tree Rings and Natural Hazards, Springer, pp. 233-239, 2010.

[7] Vrtiška J., Křeček J., Pažourková E. Flood discharge in a mountain catchment by dendrochronology. SAP Proceedings, Czech Technical University, Prague, pp. 1-6, 2016.

[8] Tolasz R, Míková T, Valeriánová A, Voženílek V. Climate atlas of Czechia. Czech Hydrometeorological Institute, Prague, pp. 254, 2007.

[9] Palucis M.C., Lamb M.P. What controls channel form in steep mountain streams? Geophysical Research Letters, vol. 44, pp. 7245-7255, 2017.

[10] USACE. HEC-HMS technical reference manual. US Army Corps of Engineers, Hydrologic Engineering Center, Davis, pp. 148, 2000.

[11] USACE. HEC-RAS river analysis system. Hydraulic Reference Manual, Version 5.0, US Army Corps of Engineers, Institute for Water Resources, Davis, pp. 538, 2016.

[12] Vrtiška J., Křeček J., Tognetti R. Indication of environmental changes in mountain catchments by dendroclimatology. Soil and Water Research, 13(4), pp. 208–217, 2018.

[13] Zielonka T., Holeksa J., Ciapała S. A 100-Year History of floods determined from tree rings in a small mountain stream in the Tatra Mountains, Poland. Advances in Global Change Research, vol. 41, DOI 10.1007/978-90-481-8736-2_25.

[14] Stoffel M., Bollschweiler M. Tree-ring analysis in natural hazards research: an overview. Natural Hazards and Earth System Sciences, vol. 8, pp. 187–202, 2008.

[15] Reed D.W. Reinforcing flood-risk estimation. Philosophical Transactions of the Royal Society of London, vol. 360, pp. 1373-1387, 2002.

DERIVATION OF FLOOD HYDROGRAPHS IN UNGAUGED BASINS

Santino Spahiu[1]

Andrin Kërpaçi[2]

[1] Department of Hydraulics and Hydrotechnics/Polytechnic University of Tirana, **Albania**
[2] Department of Hydraulics and Hydrotechnics/Polytechnic University of Tirana, **Albania**

ABSTRACT

Estimation of floods is of extreme importance in designing hydraulic structures and systems, as well as in flood management, including ecosystem recovery. Accurate derivation of flood hydrographs in ungauged basins has additional challenges. The aim of this paper is to estimate flood hydrographs with different return periods using a semi-distributed hydrological model, in the ungauged River basin of Bënça, Albania. Bënça River is part of Vjosa River, which is considered the last wild river of Europe. A frequency analysis of annual maximum daily precipitation is conducted for all meteorological stations in the study area. Average precipitation depths are calculated by constructing Thiessen polygons. Storm hyetographs distributions are determined using regional information. For precipitation abstraction, the Curve Number method is applied. Spatial distribution of runoff curve numbers is computed through GIS analysis, based on average antecedent moisture conditions, and hydrological soil-cover complexes. The watershed is modelled via HEC-HMS software, schematized into subbasins, and reaches. For generating hydrographs in each subbasin, the synthetic unit hydrograph recommended by the Natural Resources Conservation Service is used. The stream channel routing methodology applied is the Muskingum method. Subsurface components are also defined. Model results include floods with different return periods, their hourly flow rates, respective volumes, peak discharges, shapes, thus giving a complete representation of flood magnitudes the basin. The findings are relevant to policymakers, researchers, and engineers in the region.

Keywords: Hydrological model, Curve number, Muskingum method, Flood hydrograph

INTRODUCTION

Accurate estimation of floods is significant for infrastructure design and planning, flood management and flood risks assessment [1]. This issue becomes more relevant in areas where there is limited or no available streamflow data. As there is more information available on precipitation then on streamflow, precipitation data are often used to estimate runoff. This paper proposes to use a semi-distributed model, the HEC-HMS model, to simulate floods with various return periods based on precipitation data. The model was built for Bënça River Basin, part of Vjosa River, considered the last wild European river [2]. A precipitation frequency analysis was conducted for all stations in the study area, including the construction of Thiessen polygons. Inputs necessary for the hydrological model were estimated, encompassing loss parameters, unit hydrograph parameters, channel routing parameters, and baseflow components. The generated hydrographs could be useful for policymakers in formulating flood management strategies. Additionally, the

results can be helpful for researchers and engineers involved both in the Bënça River Basin and the broader Vjosa River system.

MATERIALS AND METHODS

Hydrological modelling of Bënça River

The Bënça River is a primary tributary of the Vjosa River, which is the last major river in Europe that has not been dammed and is considered "the last wild European river" [2]. It has a watershed area of 177 km^2, with average basin altitude of 954 m asl. The annual average flow is 7.42 m^3/s, with annual precipitation of 1880 mm. Annual evapotranspiration reaches 560 mm/year. The watershed is characterised by a typical Mediterranean climate, with mild and humid winters succeeded by hot and dry summers. Since 1992, no flow measurements have been recorded in the river basin, thus leaving a significant gap for policymakers and researchers.

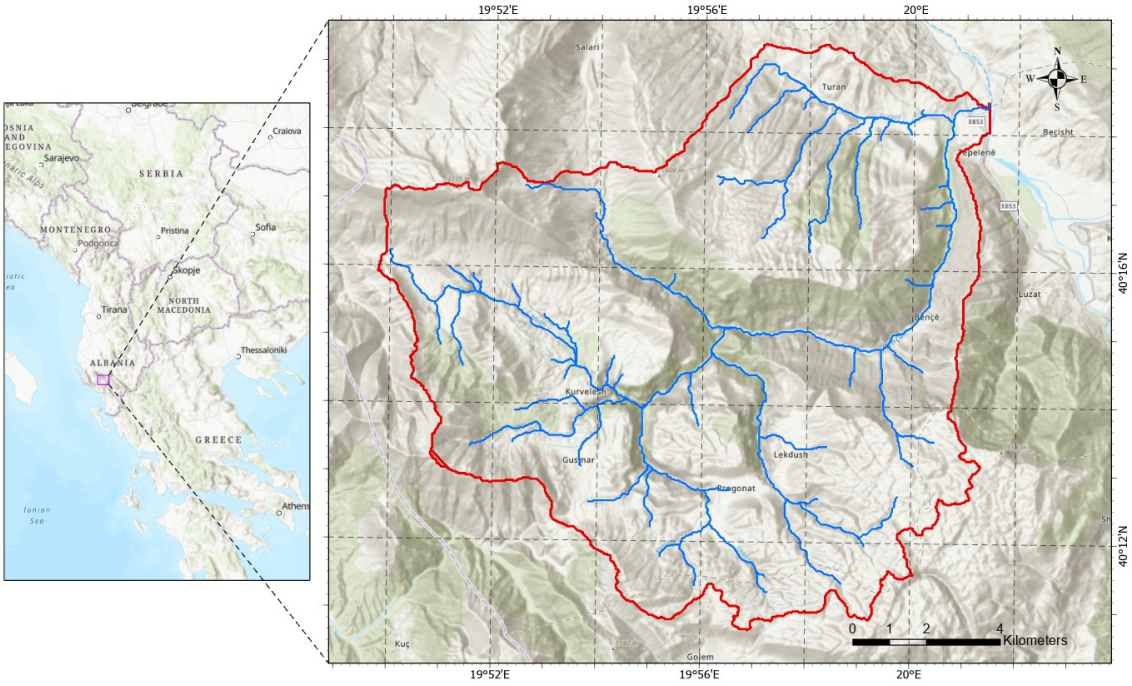

Fig. 1. Geographical location of Bënça River basin.

The terrain data of the watershed was inputted into HEC-HMS software, in the form of a digital elevation model (DEM). The software schematised the watershed into 23 subbasins and 11 river reaches. To construct the hydrological model, we defined the following: meteorology of the study area, loss parameters for each subbasin, transformation parameters of effective precipitation into runoff, how the floods' waves would propagate into the river reaches, as well as baseflow contributions. Using simulation periods longer than rainfall duration, the model generated flood runoff hydrographs with different return periods based on the precipitation scenarios defined.

Precipitation frequency

Historical measurements of precipitation in the study area had been performed through manual gauges. Consequently, records are available only for total daily precipitation depths. For each station inside or near Bënça watershed, a frequency analysis of annual maximum daily precipitation was performed. Sixteen probability distributions were fitted

to the annual maximum series. Using the Kolmogorov-Smirnov statistical test, the probability distribution that best fits the data was selected. The 1%, 2%, 5%, 10%, 20% and 50% quantiles were estimated for each station. These events represent possible meteorological scenarios initiating floods in the watershed.

Each of the 23 subbasins of the model, given their size, has a time of concentration less than 24 hours. This is also the case for the entire Bënça watershed. To find the critical time, when the entire subbasins areas contribute to runoff formation, it was necessary to find precipitation depths for durations less than 24 hours. To find these depths, the following regional formula was used:

$$h_{p,t} = H_{p,24}\left(\frac{t}{24}\right)^{n} \tag{1}$$

where $h_{p,t}$ is the precipitation depth for duration t with frequency p (mm), $H_{p,24}$ is the total daily precipitation with frequency p (mm), n is a reduction parameter that varies from station to station and found based on percentage probability. Depths with durations of 5 minutes, 15 minutes, 1 hour, 2 hours, 3 hours, 6 hours, and 12 hours were determined for each station and for all meteorological scenarios (i.e., with 1%, 2%, 5%, 10%, 20% and 50% exceedance probability).

Bënça watershed area is 177 km^2 and can be classified as a mid-size catchment. Mid-size catchments are defined as catchments with areas larger than 100 km^2. While rainfall intensity in mid-size catchments varies within storm duration, its spatial distribution is uniform over the watershed [3]. As a result, to quantify average precipitation in the watershed for all meteorological scenarios, Thiessen polygons were constructed. Six average depth-duration-frequency curves were determined, each representing a scenario.

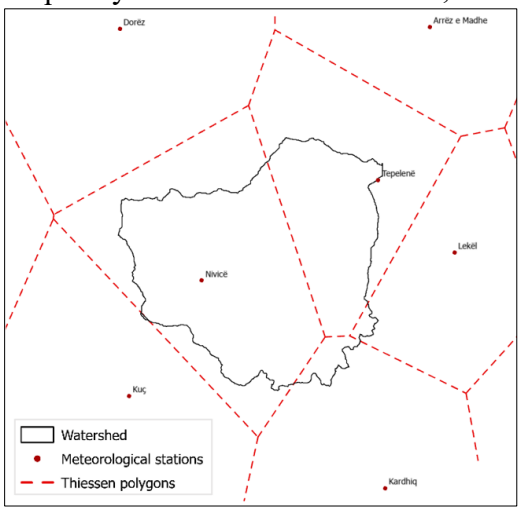

Fig. 2. Thiessen polygons in Bënça River basin.

Station measurements represent precipitation at a point in the watershed. Precipitation depths over an area are less than those measured at a point. For this reason, precipitation depths were reduced using Areal Reduction Factors (ARF) obtained by storm duration and watershed area [4]. In our case, for the watershed area of 177 km^2, an ARF equal to 0.93 was necessary for the 24-hour storm duration.

Depth-duration-frequency curves represent merely statistical results, not real events. Thus, it was necessary to construct frequency-based hypothetical storm events with

consistent exceedance probabilities. To create storm profiles for different return periods, the alternating blocking method [5] was applied through the user interface. This method develops a hyetograph from the incremental precipitation values. In all scenarios, the maximum incremental depth was chosen to be positioned in the middle of the storm event.

Effective precipitation

The method used for storm hyetographs abstraction was the runoff curve number method. It was developed by the U.S. Natural Resources Conservation Service (NRCS) for design applications in ungauged watersheds [3]. The runoff is related to major watershed runoff properties: hydrologic soil type, land use-treatment, and antecedent moisture conditions [6]. The surface runoff equation developed by the NRCS is:

$$Q = \frac{R[CN(P/R + 2) - 200]^2}{CN[CN(P/R - 8) + 800]} \quad (2)$$

where Q is the runoff (cm), P is the total precipitation (cm), CN is the runoff curve number (dimensionless), R is a factor equal to 2.54, present only in the SI formula version. Formula (1) restricts $P \geq R(200/CN) - 2$ to take into consideration initial abstractions happening in the watershed before the runoff begins.

The Curve Number (CN) represents the runoff response of a watershed to precipitation and varies in the range 0-100. For ungauged basins, NRCS has developed tables that provide estimates for runoff curve numbers based on land use, hydrological soil groups and antecedent moisture conditions (AMC) in the watershed. These tables are compiled for urban areas, cultivated agricultural areas, and other agricultural lands, including arid and semiarid rangelands [6].

To derive information about land use and soil types in the watershed, two global datasets were utilised. ESRI's 2022 dataset with 10 meter resolution was employed for land use (Fig.3a), and HYSOG's dataset with 250 meter resolution (Fig.3b) for hydrologic soil groups [7]. Though a GIS analysis, by using data from NRCS tables for average AMC, the land use and soil type maps are combined to generate a CN grid. This grid represents CN spatial distribution throughout Bënça watershed. For each of the 23 subbasins in the hydrological model, an average CN value is found via GIS. These values were then inputted into the model as parameters to estimate loss.

(a) (b)

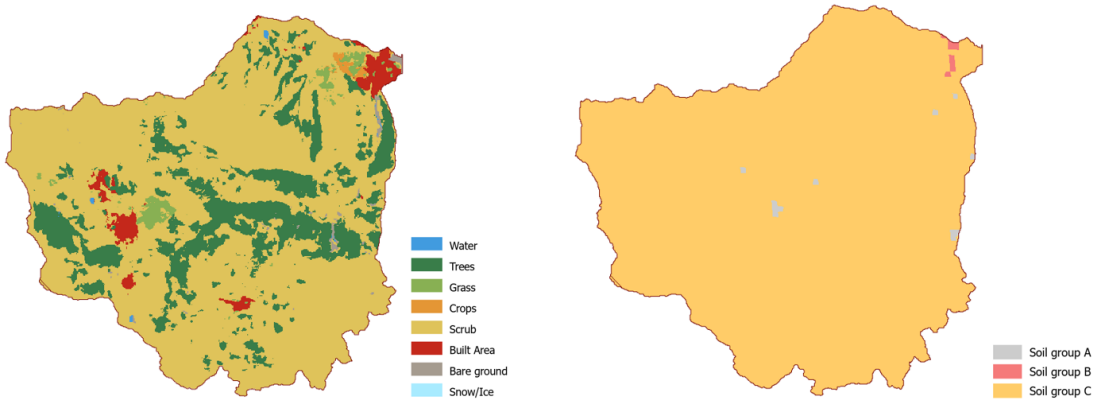

Fig. 3. Spatial distribution of Land Use (a) and Hydrological Soil Groups in Bënça basin (b).

Unit hydrograph

The effective precipitation in each subbasin generates individual flow hydrographs. Bënça watershed is ungauged with no rainfall-runoff data, so no information about the nature of hydrographs in the basin could be directly determined. Thus, hydrograph development was derived by using a synthetic unit hydrograph recommended by NRCS, suitable for ungauged basins of Bënça size i.e., 177 km^2 [8].

The NRCS unit hydrograph is a dimensionless function. Its coordinates are determined by subbasin's time-to-peak and peak flow values. The time-to-peak is a function of basin lag and rainfall duration, whereas the peak flow is determined from basin area and time-to-peak [8]. The basin lag expresses the time lapsed from net precipitation centroid to runoff peak, and takes into consideration the physical runoff properties of the watershed:

$$t_l = \frac{L^{0.8}(2540 - 22.86\,CN)^{0.7}}{14104\,CN^{0.7}Y^{0.5}} \tag{3}$$

where t_l is the watershed lag (hr), L is the hydraulic length (m), CN is the runoff curve number and Y is the average basin slope (m/m). Subbasin characteristics (i.e., length, curve number, slope) were inputted into formula (3), and the resulting time lags for each subbasin were entered into the model as transformation parameters for hydrograph generation. The hydrologic model employs the linearity and superposition principles to then develop surface runoff hydrographs from each subbasin.

Channel routing

The NRCS unit hydrograph method generates flood hydrographs for each subbasin, which are transformed into the stream channels under open channel flow conditions. The method used for channel routing was the Muskingum method. This method is the most used method for channel routing due to its simplicity in application [3]. The Muskingum method is based on the continuity equation, where storage in the channel reach is a linear function of inflow and outflow [9]:

$$S = K[X\,I + (1 - X)\,O] \tag{4}$$

where S is the storage volume, I is the inflow, O is the outflow, K represents the flood wave speed of propagation in the channel reach, X is a dimensionless weighting factor accounting for storage. The routing parameters K and X are related to flow and channel characteristics and are usually determined based on observed inflow and outflow hydrographs at the upstream and downstream end of stream reach, respectively. In our study, as it frequently the case, data on observed hydrographs necessary to directly determine the K and X parameters are lacking.

K values were indirectly determined, by dividing channel reach lengths Δx with wave speed U in the channel, as shown in formula (5). The wave speed was computed from corresponding peak flows Q_p and the typical cross-sectional area of the channel reach, as indicated in formula (6) [10]. Using the relationships provided in the National engineering handbook for peak flow [8], various K values were found for each channel reach, based on their length and typical cross-sectional area.

$$K = \Delta x / U \tag{5}$$

$$U = Q_p / A \tag{6}$$

The estimation of the X parameter is more difficult, as it does not have any direct physical meaning. However, experience has shown that in general its value ranges from 0.2 and 0.3 [10]. In our case, a constant value of X (0.25) was assumed for all channel reaches of the model. Both estimates for K and X, were then inputted into the hydrological model.

Baseflow components

Baseflow is an important process that needs to be considered in flood estimations. In our study, to estimate baseflow the exponential recession method was applied. Based on this method, the recession curve of a hydrograph follows the equation [5]:

$$Q_t = Q_o k^t \tag{7}$$

where Q_t is flow at time t, Q_o is flow at the beginning of the recession curve, k is the exponential decay constant. Three parameters were defined to simulate baseflow: initial discharge, recession constant and the threshold initiating the baseflow recession curve.

Bënça River is classified as an effluent stream with a prolonged duration of constant flows that come from multitudes of springs in the watershed, due to its karstic nature. Historical data showed average annual flows of 7.42 m^3/s. These flow conditions are likely to be present in the river at the start of the floods. Thus, as initial flow the values 7.42 m^3/s was distributed across subbasins, weighted by their respective areas. A recession constant equal to 0.014 was chosen based on relations between recession constants and basin areas for monotonous karstic basins given in [11]. The baseflow initiation threshold was set as ratio to peak, with a value of 0.1, considering the river's perennial nature.

RESULTS

The probability distribution that describes best precipitation depths series, was the General Extreme Value (GEV), with a Kolmogorov-Smirnov test value of 0.051. Using formula (1) with the daily precipitation quantile values, depth-duration frequency curves were determined (Fig.4a). These curves were reduced using appropriate ARFs, chosen automatically by the software. Subsequently, they were converted into hypothetical frequency storms (Fig.4b), which represent six metrological scenarios. For the sake of graphical clarity, only two storm profile events are shown in Fig.4b. Intermediate precipitation events are located between the 1% and 50% storm profile curves.

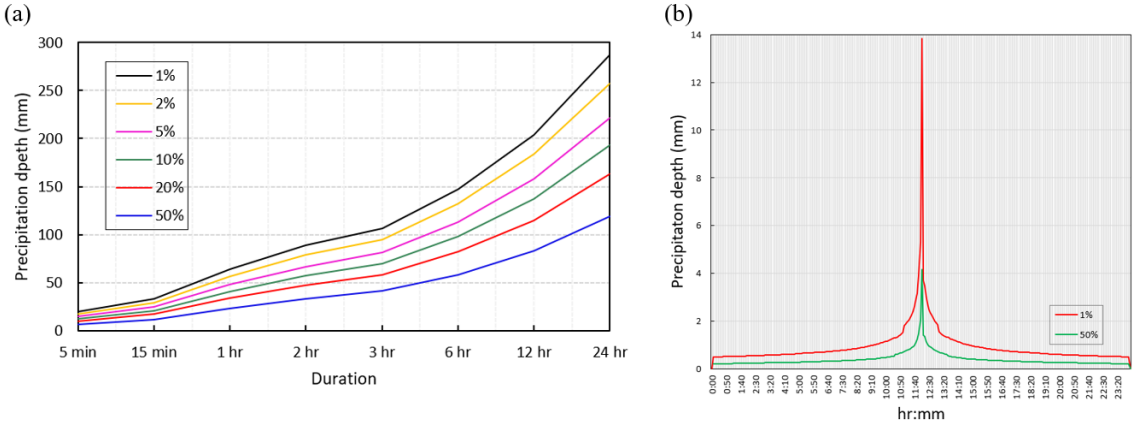

Fig. 4. Depth-duration-frequency curves (a) and the 1% and 50% storm profiles curves (b).

For all scenarios, the simulation duration was set to two consecutive days, in order to observe the full hydrograph development. Outputs of the simulations were the flood hydrographs with 1%, 2%, 5%, 10%, 20%, and 50% exceedance probability (Fig.5). Characteristics for each flood hydrograph, including respective volumes and peak flows are shown in Tab.1.

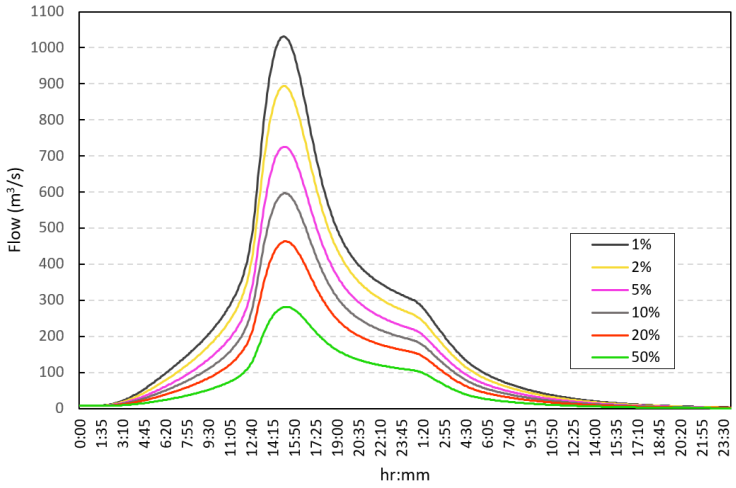

Fig. 5. Flood hydrographs with 1%, 2%, 5%, 10%, 20%, and 50% exceedance probability.

Table 1. Flood hydrographs characteristics for different return periods

	Return period (years)					
	100	**50**	**20**	**10**	**5**	**2**
Volume (Mm³)	208.61	180.72	148.04	123.17	97.4	61.78
Peak discharge (m³/s)	1031.33	893.56	725.88	596.7	463.34	281.94

DISCUSSION

Flood hydrographs with different return periods were simulated assuming the same return period both for both precipitation and floods. This may not be necessarily true, given that actual moisture conditions in the watershed are random and can produce floods with return periods completely unrelated to precipitation's return periods. However, this assumption is a common procedure, which is valuable for design purposes and can provide policymakers an overall context for flood magnitudes in the basin.

All flood hydrographs for different exceedance probability resulted in the same shape, regardless their magnitude. The shape is due to the linear response assumption used in the unit hydrograph method, where discharge is proportional to the increase in effective rainfall. Hydrographs' time to peak was the same for all hydrographs because the storm hyetograph profile is assumed having the maximum intensity value positioned in the centre of the storm. The hydrographs also exhibited what looked like as a second peak near the start of the second day of simulation. This is thanks to shape of the watershed, where some subbasins contributions arrive with a certain lag, producing in the peculiar hydrograph shape. In addition, given the recession constant producing the generated falling limb of the hydrographs, upcoming flow values will likely be unaffected in case another flood hydrographs happens directly after the analysed events.

The Muskingum routing parameters employed in this study exhibit unknown uncertainty. As a rule, routing parameters are found using observed hydrographs. In our study, given the watershed has limited records, using observed hydrographs was not a possibility.

Additionally, even if flow data were available, routing parameters would still retain some uncertainty. They change from even to event. If the aim is to determine the magnitude of floods form design hyetographs, then routing parameters would still be difficult to evaluate. CN values exhibit lower uncertainty compared to other assumed parameters. Their values were selected from NRCS tables, nevertheless, given that they were originally found for small experimental watersheds, their values would still hold some uncertainty. To reduce these uncertainties, there is an urgent necessity to have systematic streamflow measurements in Bënça River basin.

CONCLUSION

In this study, the HEC-HMS semi-distributed model was applied to assess flood hydrographs with 1%, 2%, 5%, 10%, 20% and 50% exceedance probabilities. Depth-duration-frequency curves were determined based on maximum daily precipitation records and served as inputs for the model. For each subbasin, loss and lag-time parameters were calculated to estimate effective precipitation and flow hydrograph generation, respectively. To find how floods propagate in the river network, routing parameters were calculated for each river reach. Also, baseflow components of the model were selected using recommended parameters from literature. The model generated flood hydrographs for return periods of 100 years, 50 years, 20 years, 10 years, and 2 years. Thus, giving a complete outlook on the magnitude of floods in Bënça River basin. Overall, derivation from the assumed parameters can give different time distribution of flood hydrographs, with a possible influence on the peak flow rates. In the context of ungauged basins, these results, while not exact, provide reasonable accurate description of floods in Bënça River basin. The findings highlight the necessity to have systematic streamflow measurements in the river basin. The results can help policymakers in the region to establish flood management strategies and facilitate decision making. In addition, the findings can be relevant for engineers and researchers studying Bënça River and the broader Vjosa River system.

REFERENCES

[1] Maidment D.R., Handbook of hydrology, USA, 1993.

[2] Krenová Z., Int. J. Wilderness 24, pp 86-93, USA, 2018.

[3] Ponce V.M., Engineering hydrology: Principles and practices, USA, 1989.

[4] Feldman A.D., HEC-HMS: Technical reference manual, USA, 2000.

[5] Te Chow V., Maidment D.R., Mays L.W., Applied hydrology, USA, 1988.

[6] Cronshey R.G., Roberts R., Miller N., Urban hydrology for small watersheds (TR-55 Rev.), pp 1268-1273, USA, 1985.

[7] Ross C., Prihodko L., Anchang J., Kumar S., Hanan W. Ji. N., Global hydrologic soil groups (HYSOGs250m) for curve number-based runoff modeling, USA, 2018.

[8] Mockus V., SCS: National Engineering Handbook, USA, 1964.

[9] GT M., The unit hydrograph and flood routing, proceedings of Conference of North Atlantic Division, pp 608-609, USA, 1938.

[10] Musy A., Higy C., Hydrologie appliquée, Edition H* G* A, Rumania, 1998.

[11] Chen X., Zhang Y.-f., Xue X., Zhang Z., Wei L., Estimation of baseflow recession constants and effective hydraulic parameters in the karst basins of southwest China, Hydrology Research, vol.43, pp 102-112, United Kingdom, 2012.

DESTRUCTION OF THE KAKHOVKA RESERVOIR AS A RESULT OF HOSTILITIES: DYNAMICS OF CHANGE AND CONSEQUENCES FOR THE ENVIRONMENT

Prof. Dr. Oleksandr Trofymchuk[1]

PhD Natalia Sheviakina [1]

PhD Olha Tomchenko[2]

[1]Institute of Telecommunications and Global Information Space of the National Academy of Sciences of Ukraine, **Ukraine**

[2]State Institution "Scientific Centre for Aerospace Research of the Earth of the Institute of Geological Sciences of the National Academy of Sciences of Ukraine", **Ukraine**

ABSTRACT

The results of the study of the dynamics of changes in the territory of the Kakhovka reservoir before and after the explosion of the dam on June 6, 2023 are presented. This led to the destruction of the Kakhovka reservoir and the sharp flooding of significant areas downstream of the Dnieper River, including the delta. The analysis was carried out on two indicators: the water surface area and the water level. As a result of the analysis of space images, it was found that the area of the Kakhovka reservoir decreased by 80% from its original. The results of the analysis of the flooded area downstream of the Dnieper River from the dam showed that the water surface area at the peak of flooding increased 3.7 times and the water level has increased from 1 to 7 m above sea level.

The destruction of the Kakhovka reservoir affected the fish population, local bird populations and nesting colonies of migratory birds, the bottom (benthos) and terrestrial fauna, the flora of the reservoir and the flora of the Dnieper River Delta. This disaster affected rare types of biotopes, there was also a decrease in the delta islands and partially their destruction. The lower reaches of the tributaries of the Dnieper River were flooded. The territories of the nature reserve fund, environmental objects and wetlands of international importance and the territories of the Emerald Network were especially affected. Contaminated fresh water came to the Black Sea. All this has disastrous consequences for the environment.

Keywords: war, hydrology, water resources, ecological monitoring, satellite remote sensing.

INTRODUCTION

Since the beginning of the large-scale Russian invasion of Ukraine (24 February 2022), a large number of landscape complexes have been damaged. It can already be said that the negative consequences of military aggression will have a long-term effect and will lead to environmental degradation in the future and the destruction of entire unique ecosystems. The issue of the war's impact on Ukraine's water bodies and water supply is currently extremely relevant. Water security issues are particularly acute in the areas of the war zone in regions with developed critical water infrastructure. Hydroelectric dams,

cooling facilities for nuclear power plants, and reservoirs used for industry, irrigation, and water supply in settlements are at immediate risk.

The impact of hostilities on freshwater resources and water infrastructure during the first three months of the war in Ukraine was analysed in [1]. The results of the study show that the most affected types of infrastructure during the war in Ukraine are dams and reservoirs, underground mines, municipal water supply and wastewater treatment systems. Of particular concern are the large reservoirs along the Dnipro River, which are crucial for energy production, cooling nuclear power plants, supporting agriculture and seasonal flow regulation. Along the Dnipro River, there is a high concentration of settlements at risk of flooding. The flooding of large areas downstream of the dam occurred after the explosion of the Kakhovka hydroelectric power station on 6 June 2023 [2].

The analysis of changes in the water level of the Kakhovka reservoir was carried out by the Hydroweb database [3]. The Hydroweb database studies were conducted mainly using imagery from the Sentinel operational programme since 2016, which allowed for inter-annual comparisons to identify trends and anomalies, such as the destruction of the Kakhovka reservoir and the return of the Dnipro River. Satellite space data, as a tool for conducting observations over a certain area, has long been used for monitoring studies, including these methods and tools that clearly demonstrate the damage to the Kakhovka dam and the flood events of 6 June 2023 [4, 5].

Currently, many scientists pay considerable attention to the study of environmental damage using remote sensing data caused by military operations in different parts of the world. Paper [6] presents the use of remote sensing data to study the environmental consequences of the Russian invasion of Ukraine in 2022. There are many examples [7] of remote sensing application for monitoring the environmental consequences of war in other countries. Paper [8] provides an overview of numerous environmental damages caused by military operations in different parts of the world. The emphasis in the work is on the search and detection of geographical connection, the use of remote sensing sensors and the establishment of the type of environmental degradation.

We present a study on the dynamics of changes in the water level of the Kakhovka Reservoir and flooding of areas along the Dnipro River downstream of the dam, using remote sensing and GIS tools.

MATERIALS AND METHODS

The modern practice of remote sensing of the Earth is based on information obtained by television, optoelectronics, infrared, laser, radio-thermal, and radar systems, as well as traditional photographic systems. Deep learning methods have yielded outstanding results in remote sensing applications [9, 10].

The input data for the satellite monitoring of the water level of the Kakhovka Reservoir were data from the Sentinel-2 spacecraft with a spatial resolution pixel is 10 m and Landsat-8-9 with a spatial resolution pixel is 30 m [11]. The Sentinel-2 satellite image was analysed before the reservoir dam was blown up on 5 June 2023 and the most up-to-date satellite image of 28 September 2023. To analyse the water surface of the Kakhovka Reservoir, the Normalised Difference Water Index (NDWI) was applied, which is used to identify open water bodies and highlight them on a satellite image against the background of soil and vegetation [10, 12]. To monitor the extent of the flooding,

Landsat-8 satellite imagery was used before the reservoir dam was blown up on 1 June 2023 and Landsat-9 at the peak of the Dnipro Delta flooding on 06 June 2023.

The study also used data from hydroweb.theia-land.fr. This resource presents a time series of water levels in rivers and lakes around the world. The Hydroweb database - https://hydroweb.theia-land.fr/ - was designed to monitor changes in water levels over time in large lakes, reservoirs and rivers, based on altimetry measurements. Hydroweb time series of water depths on lakes are obtained by combining data from several profiles of one satellite and/or several satellites, depending on coverage. This significantly improves the accuracy of water heights. The data presented on hydroweb has been available since 2016, allowing for interesting inter-annual comparisons to identify trends and anomalies.

To analyse the situation after the reservoir dam was blown up, the area of the former reservoir and the area of the Dnipro River downstream of the dam before and after the blast were compared. The method of comparative analysis was used in the study to establish the water level and determine the environmental impact. Data for the period from June 2022 to September 2023 were analysed. This range was chosen taking into account the fact that it was from October 2022 that the water level changes in the Kakhovka reservoir showed anomalous behaviour compared to the variations of previous years. Thus, the study took into account two indicators: water surface area and water level.

RESULT

In November 2022, three water gates were raised at the Kakhovka Reservoir dam and water was released. The level of the Kakhovka Reservoir dropped to 13.8 m, compared to the normal level of 16.0-16.5 m. From the end of February 2023, when the floods began, the water level in the reservoir began to rise to 17.3-17.5 m (Fig. 1). This was the water level at the observation point in the central part of the Kakhovka reservoir at the time of the Kakhovka hydroelectric power station destruction. On 6 June 2023, the Kakhovka hydroelectric power station was destroyed.

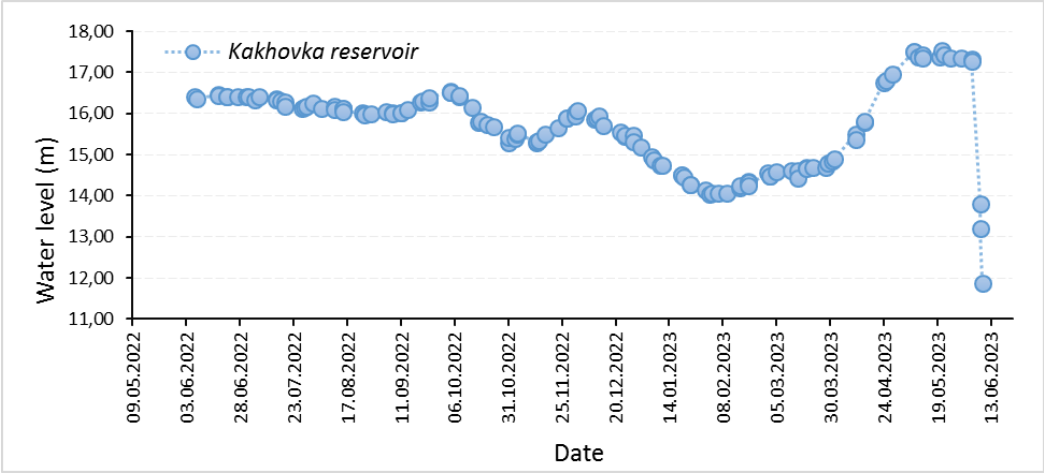

Fig. 1. Water level at the observation point in the central part of the Kakhovka reservoir in the period from June 2022 to June 2013, based on Hydroweb database data.

After the dam of the Kakhovka HPP was blown up, water from the Kakhovka Reservoir rushed downstream of the Dnipro. According to the Hydroweb database - https://hydroweb.theia-land.fr/ - one can see a sharp decrease in the water level in the

reservoir until it was completely dehydrated, so the last point of readings is 09 June. After 09 June 2023, the sensors no longer monitored this area at the observation point in the central part of the Kakhovka reservoir. The results of the study showed the complete destruction of the reservoir (Fig. 1).

Currently, the areas of the destroyed Kakhovka Reservoir, from which water has receded, are undergoing desertification and overgrowth of shrub and meadow vegetation. To analyse and determine the dynamics of changes in the reservoir, we analysed data from the Sentinel-2 spacecraft. The view of the central part of the Kakhovka Reservoir on Sentinel-2 satellite images is shown in Figure 2.

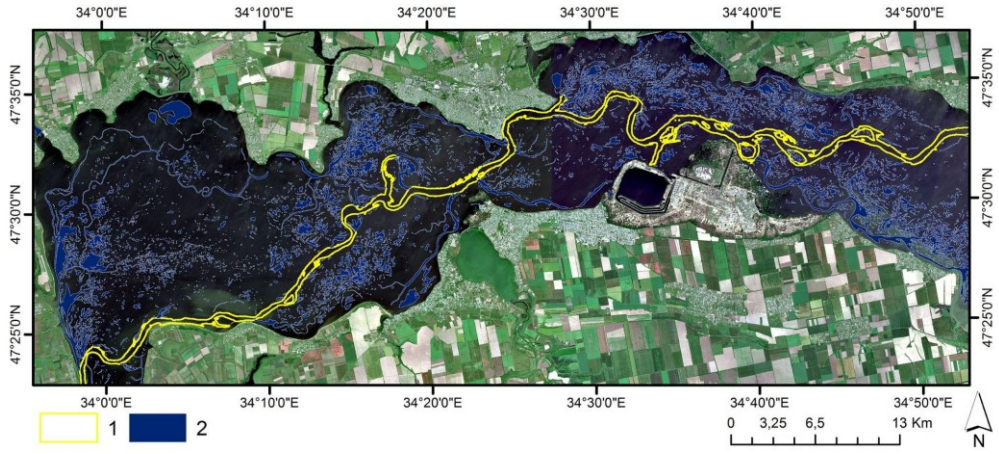

a)

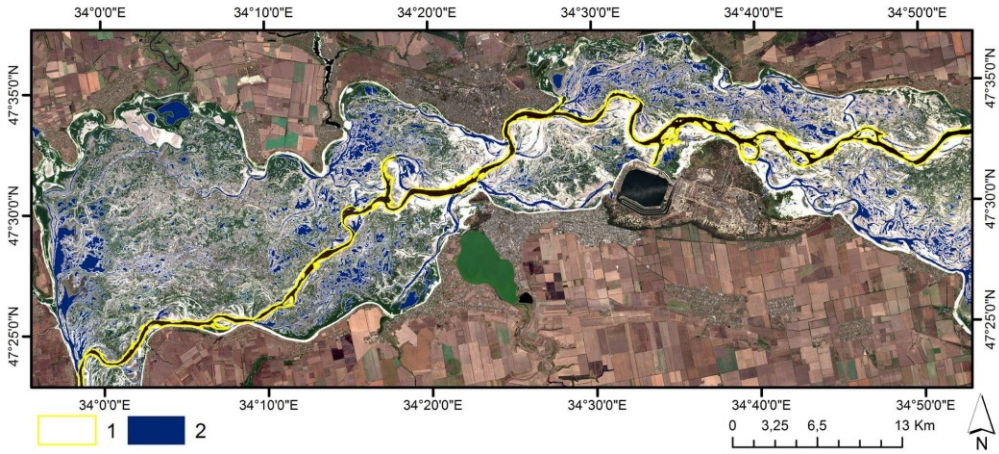

b)

Fig. 2. Central part of the Kakhovka Reservoir on Sentinel-2 satellite images: a) before the dam was destroyed - 5 June 2023; b) after the dam was destroyed - 28 September 2023. Legend: 1) Dnipro riverbed as of 28 September 2023; 2) residual water surface of the reservoir as of 08 September 2023.

The Sentinel-2 satellite image after the dam was destroyed (28 September 2023) shows drained areas covered with bottom sediments and sand fractions. Figure 2 shows the Dnipro River channel as of 28 September 2023, as well as the residual water surface of the reservoir as of 08 September 2023. The analysis revealed that as of 5 June 2023 (Fig. 2 a.), the area of the Kakhovka Reservoir was 2091.48 km2. And on 08 September 2023,

379.742 km2 remained. This shows that 18.2% of the Kakhovka Reservoir's water surface area remained of the original area. A significant part of the reservoir is not only devoid of water, but has physically dried up. According to the analysis of satellite image data (Fig. 2 b.), the Dnipro River channel is being formed or restored at the site of the Kakhovka Reservoir, with a river area of 133.066 km2. As of 08 September 2023, the total area of the water mirror of lakes and shallow waters formed on the site of the reservoir is 246.676 km2. The upper northern part of the former reservoir has undergone the greatest degree of drainage due to the geomorphological structure of the study area.

The destruction of the dam at the Kakhovka hydroelectric power station resulted in uncontrolled water discharge from the reservoir downstream. This led to a critical rise in the water level of the Dnipro River (Figure 3) and flooding of coastal areas. This led to the flooding of at least 80 settlements on both sides of the river. Around 16,000 people in 17 settlements on the right bank of the Dnipro River were in the flood zone. The graph in Figure 3 shows the observed water level of the Dnipro River downstream of the destroyed dam of the Kakhovka hydroelectric power plant between October 2022 and October 2023 at two observation points based on the Hydroweb database. Thus, at observation point № 1, located 17 km downstream of the Dnipro River from the destroyed dam of the Kakhovka hydroelectric power plant, the water level was stable at about 1 metre. On 11 June 2023, there was a peak of flooding at observation point No. 1, where the water level reached 6.8 metres, i.e. increased 7 times.

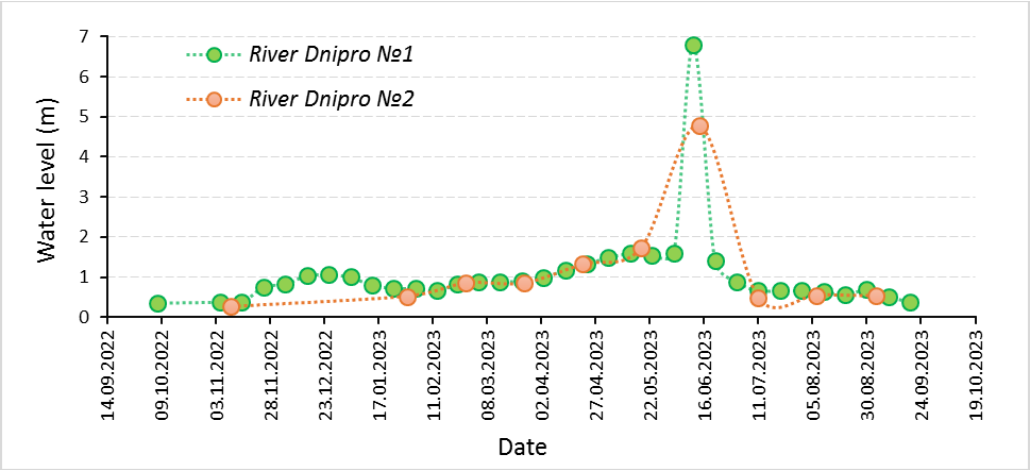

Fig. 3. Water level of the Dnipro River downstream of the Kakhovka hydroelectric power station dam in the period from October 2022 to October 2023 at two observation points: № 1 - 17 km downstream of the Dnipro River from the dam of the Kakhovka hydroelectric power station; № 2 - 10 km downstream of the Dnipro River from the destroyed dam of the Kakhovka hydroelectric power station (Hydroweb database).

The extent of the flooding of the Dnipro River mouth as a result of the destruction of the Kakhovka Reservoir is shown on Landsat-8-9 satellite images (Figure 4). Using the water index, we calculated the water surface area and found that as of 1 June 2023, the water area in the Dnipro River channel and the mouth of the river, shown in Figure 4, was 151 km2. On 11 June 2023, it increased by 3.7 times to 562 km2. This indicates a catastrophic flooding of the coastal area downstream of the Kakhovka hydroelectric power station dam and the Dnipro River mouth.

The extent of the flooding of the Dnipro River estuary as a result of the destruction of the Kakhovka Reservoir is shown on Landsat-8-9 satellite images (Figure 4). Using the water index, we obtained the water surface area. As of 1 June 2023, the water area in the Dnipro River channel and the estuary shown in Figure 4 was 151 km2. On 11 June 2023, it increased by 3.7 times to 562 km2. This indicates catastrophic flooding of the coastal area downstream of the Kakhovka hydroelectric power station dam and the Dnipro River estuary.

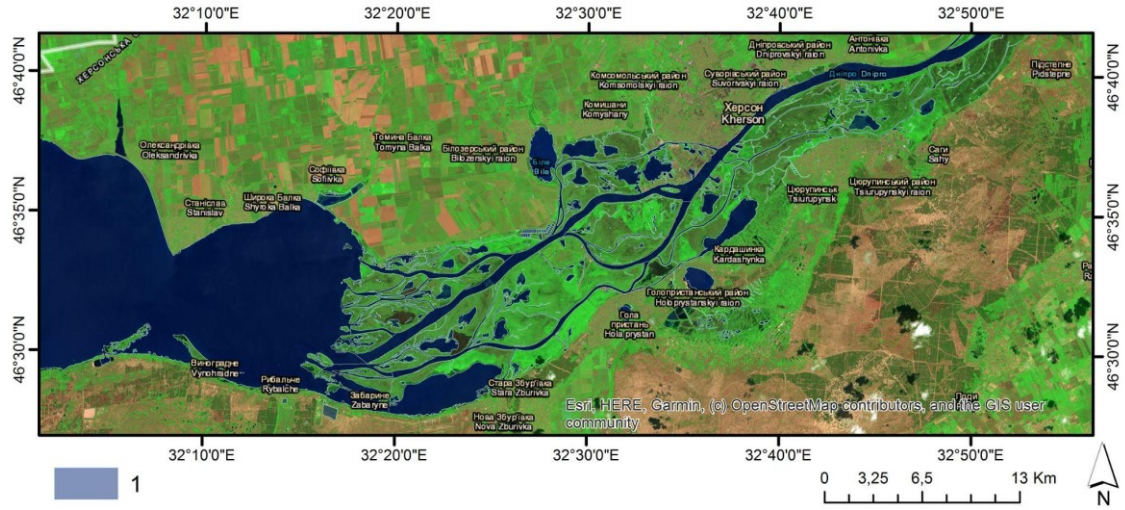

a)

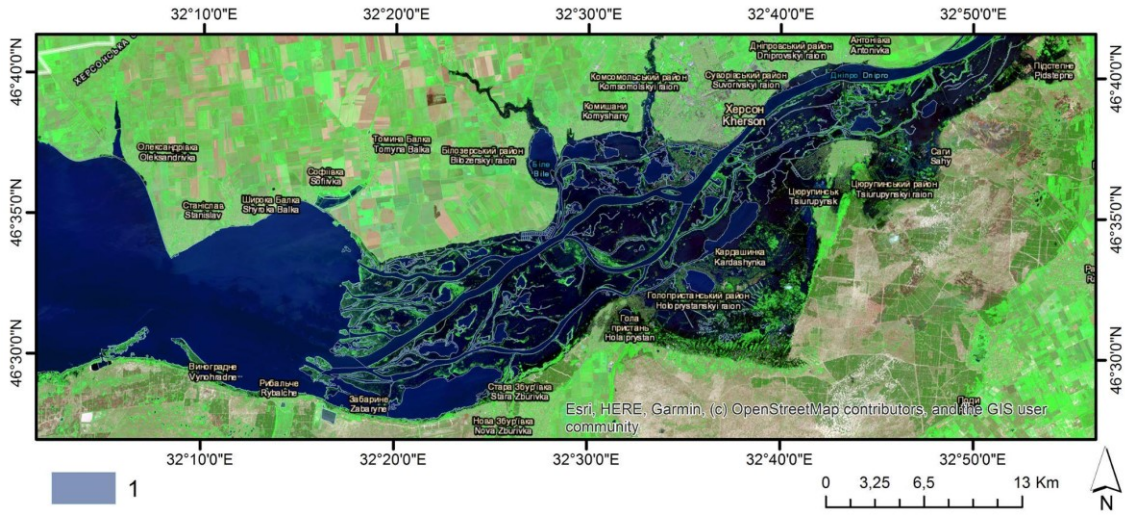

b)

Fig. 4. The Dnipro River estuary on Landsat-8-9 satellite images: a) before the flooding on 01 June 2023; b) after the flooding on 09 June 2023. Legend: 1 - water surface as of 1 June 2023.

The catastrophe affected all living macro- and microorganisms of the ecosystem of the destroyed Kakhovka Reservoir and the Dnipro River downstream of the Kakhovka hydroelectric power station dam, as well as the flora and fauna of the coastal area. In particular, this includes a number of invertebrates that make up the main animal biomass of the reservoir, primarily mollusks, various species of dipterans that serve as food for

fish, birds, amphibians, etc. All fish spawning grounds and the bulk of the water that is the fish habitat have been destroyed. The almost instantaneous rise in water levels in the areas downstream of the Kakhovka dam caused the death of most terrestrial animals (mammals, reptiles, insects, etc.) and colonies of most bird species.

The 48 nature reserve sites will be fully or partially affected by the flooding. The flooded area fully or partially includes 9 sites of the European Emerald Network [13]. The 33630-hectare Dnipro Delta is included in the list of protected areas of international importance under the Ramsar Convention. A number of protected areas, including at least 11 nature reserves, will also be affected upstream of the Kakhovka dam [13].

The flooding of settlements, including cesspools, agricultural land, petrol stations and other sources of pollution, has resulted in an unusually large amount of pollutants entering the Black Sea. Keep in mind the long- term consequences for marine ecosystems: the release of toxic substances from the sea bottom sediments; oil products and other toxic substances will accumulate in biological organisms living in the water and on the seabed; the resilience of the sea's ecosystem, as well as cause the appearance of secondary negative effects, such as loss of biodiversity, landscape changes and destruction of biotopes [14].

CONCLUSION

The use of the spectral water index NDWI is an effective remote tool for studying changes in the state and dynamics of changes in the area of surface water bodies in different periods. It was found that the drainage area of the Kakhovka Reservoir and the intensity of the shallowing process are constantly changing. Based on the results of the study, a map of the dynamics of shallowing of the reservoir was constructed and the current area of the reservoir was obtained. As a result of the analysis of space images, it was found that the area of the Kakhovka Reservoir decreased by 80% from its original. The results of the analysis of the flooded area downstream of the Dnieper River from the dam showed that the water surface area at the peak of flooding increased 3.7 times and the water level has increased from 1 to 7 m above sea level.

This disaster affected rare types of biotopes, there was also a decrease in the delta islands and partially their destruction. The lower reaches of the tributaries of the Dnieper River were flooded. The territories of the nature reserve fund, environmental objects and wetlands of international importance and the territories of the Emerald Network were especially affected. The destruction of the Kakhovka Reservoir affected the fish population, local bird populations and nesting colonies of migratory birds, the bottom (benthos) and terrestrial fauna, the flora of the reservoir and the flora of the Dnieper River Delta. Contaminated fresh water came to the Black Sea.

The presented results of the research allow to conduct continuous monitoring of the Dnieper River; to record crimes against the environment; to evaluate the damage that the Russian army has caused and is still causing as a result of the full-scale war on the territory of Ukraine. And in the future, these data will be necessary for recreational and related additional activities to preserve the environment.

REFERENCES

[1] Shumilova, O., Tockner, K., Sukhodolov, A., Khilchevskyi, V., De Meester, L., Stepanenko, S., Trokhymenko, G., Hernández-Agüero, J. A., & Gleick, P. (2023).

Impact of the Russia–Ukraine armed conflict on water resources and water infrastructure. Nature Sustainability, Vol 6, P. 578–586 (2023). https:// doi.org/10.1038/s41893-023-01068-x
[2] REACH Ukraine: Operational Information Note. The undermining of the Kakhovka hydroelectric station on June 6, 2023 https://repository.impact-initiatives.org/document/impact/ebca9d51/REACH_UKR-Emergency-Brief-Novokakhovka-Dam-06-June_public_UKR.pdf
[3] Hydroweb database https://www.theia-land.fr/en/kakhovka-hydroweb-data-shows-a-reservoir-turned-river/
[4] Chronicles of Destruction: Monitoring the Kakhovka Dam Damage from Space https://www.groundstation.space/chronicles-of-destruction-monitoring-the-kakhovka-dam-damage-from-space/
[5] ReliefWeb (2023) Kakhovska dam damage and flood event monitoring using satellite data, 6 June 2023 https://reliefweb.int/map/ukraine/kakhovska-dam-damage-and-flood-event-monitoring-using-satellite-data-6-june-2023
[6] Shevchuk S., Vyshnevskyi V., Bilous O. (2022) The use of remote sensing data that is studying the environmental consequences of the Russian invasion of Ukraine. Research Square; 2022. DOI:10.21203/rs.3.rs-1770802/v1
[7] Dhari Al Ajmi & Saif ud din. (2009) Remote Sensing: Fundamentals, Types and Monitoring Applications of Environmental Consequences of War. Environmental Consequences of War and Aftermath. Volume 3U. Pages 41-124, 2009 https://doi.org/10.1007/978-3-540-87963-3
[8] Kaplan, G., Rashid, T., Gasparovic, M., Pietrelli, A., & Ferrara, V.. (2022) Monitoring war-generated environmental security using remote sensing: A review. Land Degradation & Development, 33(10), 1513– 1526. 2022 https://doi.org/10.1002/ldr.4249
[9] Kreta D., Klymenko V., Anpilova Y. (2018) Remote sensing and GIS tools for spatial analysis of surface water quality and soil pollution. Ecological safety and nature management. V 4 (28). P. 120-127, 2018. http://es-journal.in.ua/article/download/155960/155403
[10] Zheng Y., Sheviakina N. A., Zagorodnia S. A., Tomchenko O. V., Radchuk I. V. (2022) Remote sensing monitoring of anthropogenic changes in the Desenka river channel (Kyiv, Ukraine). Ukrainian Journal of Remote Sensing, 2022, Vol. 9 (1), P. 8-15. https://doi.org/10/36023/ujrs.2022.9.1.208
[11] Overview. ESA Sentinel Online. https://sentinel.esa.int/web/sentinel/user-guides/sentinel-2- msi/overview
[12] Trofymchuk O., Zahorodnya S., Sheviakina N., Radchuk I., Tomchenko O. Remote Sensing Monitoring of Biotopes Distribution within Nature Reserve Area. Journal of Environmental Research, Engineering and Management. Vol.76. No. 3. p. 109-120, 2020. DOI:10.5755/j01.erem.76.3.25204
[13] UNCG. (2023) What are the consequences of the Russian terrorist attack on the Kakhovka hydroelectric station for wildlife? https://uncg.org.ua/iakymy-ie-naslidky-rosijskoho-teraktu-na-kakhovskij-hes-dlia-dykoi-pryrody/
[14] Vyshnevskyi V., Shevchuk S., Komorin V., Oleynik Yu., Gleick P. (2023) The destruction of the Kakhovka dam and its consequences, Water International, VOL. 48, NO. 5, P. 631–647, DOI: 10.1080/02508060.2023.2247679

DEVELOPMENT OF ADSORPTIVE METHOD FOR REMOVAL OF AZITHROMYCIN FROM WASTEWATER TREATMENT PLANT EFFLUENT USING ACID-MODIFIED NATURAL ZEOLITE

Dr. Imeda Rubashvili[1]

Dr. Ketevan Ebralidze[1]

Dr. Marine Zautashvili[1]

Prof., Dr., Acad. Vladimer Tsitsishvili[1,2]

[1] Petre Melikishvili Institute of Physical and Organic Chemistry, Ivane Javakhishvili Tbilisi State Univeristy, Tbilisi, **Georgia**
[2] Georgian National Academy of Science, **Georgia**

ABSTRACT

The present work is the first case where the adsorptive removal of the most commonly used antibiotic - azithromycin from aqueous solution as a model of wastewater treatment plant effluent by acid-modified natural zeolite - clinoptilolite has been investigated. The adsorption processes were carried out under static and dynamic conditions. The acid-modified form of the above-mentioned natural zeolite were obtained with hydrothermal treatment by using 2M hydrochloric acid solution. In order to investigate the adsorption dynamic process, there was used the specially constructed laboratory dynamic type instrument with a fixed bed adsorption glass column and a high-pressure pump. The effect of the inlet concentration, the flow rate and the pH value of the antibiotic influent solution, also, the contact time of system zeolite/antibiotic solution in the adsorption process were studied. The adsorption was evaluated using the Langmuir adsorption model. In order to determine quantitively azithromycin in influent and effluent solutions, a new effective and specific high performance liquid chromatography method was used.

The results have been shown that the studied acid-modified clinoptilolite were characterized with high dynamic adsorption capacity. The adsorption mechanism was mainly composed of electrostatic interaction between the zeolite surface and adsorbate - azithromycin. This study has been shown and proved that acid-modified natural clinoptilolite could be an efficient, eco-friendly, alternative and competitive adsorbent in terms of cheapness, selectivity and adsorption efficacy for the removal of azithromycin from hospital, pharmaceutical industrial wastewaters and wastewater treatment plant effluents.

Keywords: Adsorption, Natural Zeolite, Azithromycin, Wastewater

INTRODUCTION

Antibiotic residues in the environment, even in very small trace level amounts, cause resistance in bacterial populations and reduce therapeutic effectiveness of antibiotics against infectious diseases. They can be discharged into the environment in several different ways. The excretion of poorly metabolized antibiotics by human and animal is

the primary source of antibiotic residues in the environment. Other sources are the disposal of unused or unwanted antibiotics from pharmaceutical manufacturing and hospital wastewaters. Several studies have reported that antibiotics are detected in wastewater treatment plant influents and effluents, surface waters, groundwater, sediment, and drinking water [1-6].

The aim of the present paper is to describe research study regarding the investigation of adsorption process and the evaluation of the possibility of adsorptive removal of the most commonly used and a semisynthetic macrolide antibiotic with a broad range of antimicrobial activity – azithromycin (AZM) - $C_{38}H_{72}N_2O_{12}$ (>80% of daily dose predominantly unchanged) from aqueous solution as a model of wastewater treatment plant effluent by natural zeolite – clinoptilolite from the local region, Georgia and its acid-modified H-form.

The present study is the first case where adsorptive removal of AZM has been investigated using natural zeolite as a cheap adsorbent with simple treatments and to demonstrate that natural zeolite is a potential adsorbent of antibiotic removal wastewaters. Adsorption is the widely used method for removal of a broad range of antibiotic pollutants due to its simple design, easy operation, and relatively simple regeneration with the principles of "green economy". This approach implies a high degree of minimization of expenses during water purification from toxic and harmful components. Economic aspects of this process play a very relevant role, allowing the purification and additional treatment of wastewater, thus, reducing the anthropogenic load on water bodies. In the field of environmental protection, the most important and perspective direction of use of natural zeolites is their use for conditioning of potable water, treatment of wastewaters and domestic, industrial or agricultural wastes [5, 7-8].

MATERIALS AND METHODS

The local natural zeolite - clinoptilolite (CL) ($(Ca, Na_2, K_2)_3Al_6Si_{30}O_{72}\cdot 24H_2O$) was obtained from Khandaki plot of Tedzami deposit, Eastern Georgia. In order to obtain acid-modified form of CL (H-CL) CL was treated hydrothermally using 2M HCl solution by the appropriate procedure described in papers [5, 7]. In obtained H-CL sample the Si/Al ratio was increased (Si/Al ratio > 4 and Na+K/Ca+Mg ratio < 1).

In order to study of adsorption dynamic process there was used the specially constructed laboratory dynamic type equipment which consists of three parts: 1) a glass adsorption 1.0×8 cm column (packed with 9 g of natural zeolite); 2) influent/effluent collection tanks; 3) a high-pressure pump to control the flow rate of test solution (Figure 1). In dynamic conditions through the prepared zeolite sample placed in a glass adsorption column, the antibiotic test solution at different concentration was passed. The experiment was carried out in the laboratory room with temperature-controlled conditions (20-25°C) and with different liquid flow rates [5, 7-8].

The effluent samples were collected initially, at different time intervals and the end of the adsorption experiment after the saturation state occurred. The effect of working parameters such as the value of pH, the flow rate and the initial concentration of test solution were investigated. The concentration of test adsorbate in influent and effluent stream was determined using HPLC system – Ag 1260 with DAD detector (detection was measured at 215 nm) and a column - Agilent SB-C18 4.6 x 250 mm, 5 μm (USA). The flow rate was 1.0 mL/min; the injection volume was 20 μL; the column temperature

70ºC. A mixture of phosphate buffer solution pH 6.5, acetonitrile and water (10:35:55 v/v) was used as a mobile phase. The test stock solutions (adsorbate influent solution) with 0.2-2.0 mg/mL concentration were prepared by dissolving AZM analytical standard in a few amount (< 2% of total volume) of acetonitrile and then diluted with purified water. For estimation the chromatographic system suitability the resolution check solution was used which was prepared by weighing and transferring accurately 2.0 mg of azithromycin A impurity standard to 20 mL volumetric flask, dissolve in a few amounts of diluent, add 2 mL of azithromycin standard solution (1.0 mg/mL), dilute to volume with diluent, mix well. The quantification was performed by the external standard method. The initial pH value of test solution was adjusted by adding 0.1 N NaOH and HCl solution.

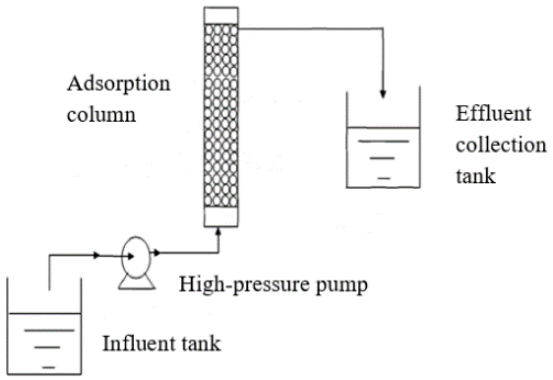

Fig. 1. The laboratory dynamic type equipment for adsorption study.

The concentration of AZM – Cu in an effluent test solution, expressed in mg/mL was calculated by the following formula:

$$C_u = \frac{A_u \times W \times D \times P}{A_s \times 100} \quad (1)$$

Where, Au – the peak area of AZM obtained with an influent/effluent test solution; As – the peak area of AZM obtained with standard solution; W – the weight of AZM analytical standard, mg; D – the combined dilution factor of standard and test solutions; P – the purity of AZM standard, %.

In order to study adsorption by static method, 0.2 g of zeolitic adsorbent with 20 mL of antibiotic test stock solution at 0.2-2.0 mg/mL concentration range was used. Initially, zeolite sample with adsorbate antibiotic solution was left on an orbital shaker at 150 rpm for 15 min, then allowed to stand statically for the determined time interval and then the adsorbent samples were centrifuged at 3000 rpm for 5 min. The taken aliquots from the obtained supernatants at different time intervals during the experiment were analysed using HPLC.

The breakthrough curve for AZM adsorption on zeolite adsorbent in terms of the effluent to influent concentrations ratio, C/C_o, versus the contact time – τ, min was investigated by carrying out a set of fixed bed experiment. The removal efficiency - R, % and the adsorption capacity – q, mg/g were calculated by the following equations [5, 7-8].

The removal efficiency - R, % was calculated by the following formula:

$$R, \% = \frac{(C_0 - C_e) \times 100}{C_0} \quad (2)$$

Where, Ce - the equilibrium concentration of the adsorbate test solution at the fixed time (contact time with adsorbent – τ, hrs), mg/mL; C_0 - the initial concentration in the adsorbate test solution, mg/mL.

The adsorption capacity – q, mg/g was calculated by the followed formula:

$$q = \frac{(C_0 - C_e) \times V}{m} \quad (3)$$

Where, V - the used volume of adsorbate solution, mL; m - the mass of adsorbent, g.

For explanation of the mechanism of adsorptive removal of AZM and the interaction of zeolite adsorbent with antibiotic was studied by the most commonly used Langmuir isotherm model which assumes monolayer adsorption on the surface of the adsorbent. The experiment was carried out with different initial concentrations of antibiotic over a range from 0.5 mg/mL to 2 mg/mL [5, 7-8].

RESULTS

To study adsorption process of the selected adsorbate – AZM with different concentrations – 0.5-2.0 mg/mL and a volume of 20 mL under static conditions, an experiment was carried out using 0.2 g of CL and H-CL at pH 7. Adsorption isotherms constructed on the basis of experimental data are shown in Figure 2.

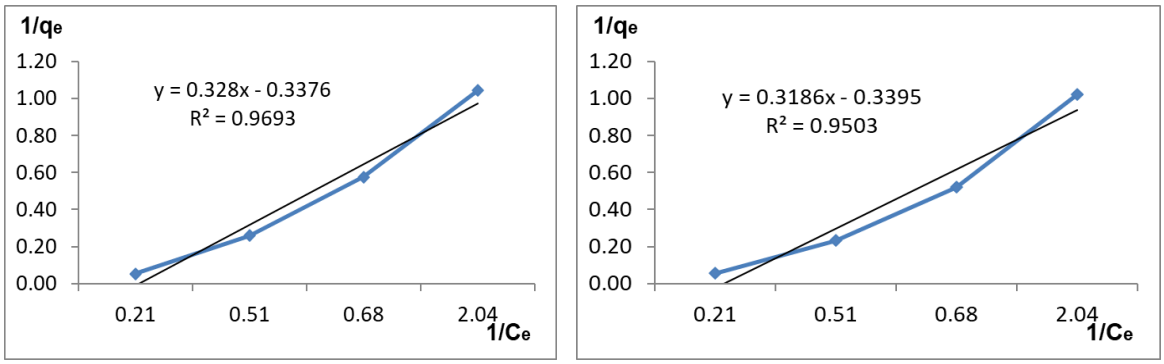

a **b**

Fig. 2. The Langmuir adsorption isotherms of AZM on CL (a) and H-CL (b)

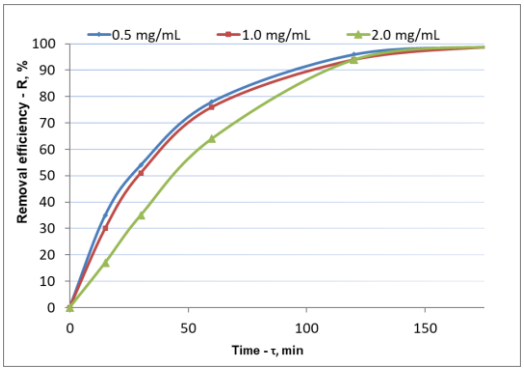

Fig. 3. The graph of the removal efficiency, % versus contact time on CL at three different concentrations of AZM test solution.

The fastest adsorption was observed at the low concentration – 0.5 mg/mL of test antibiotic compound. The removal efficiency (R, %) increased with a decrease of the concentration of adsorbate solution (Figure 3).

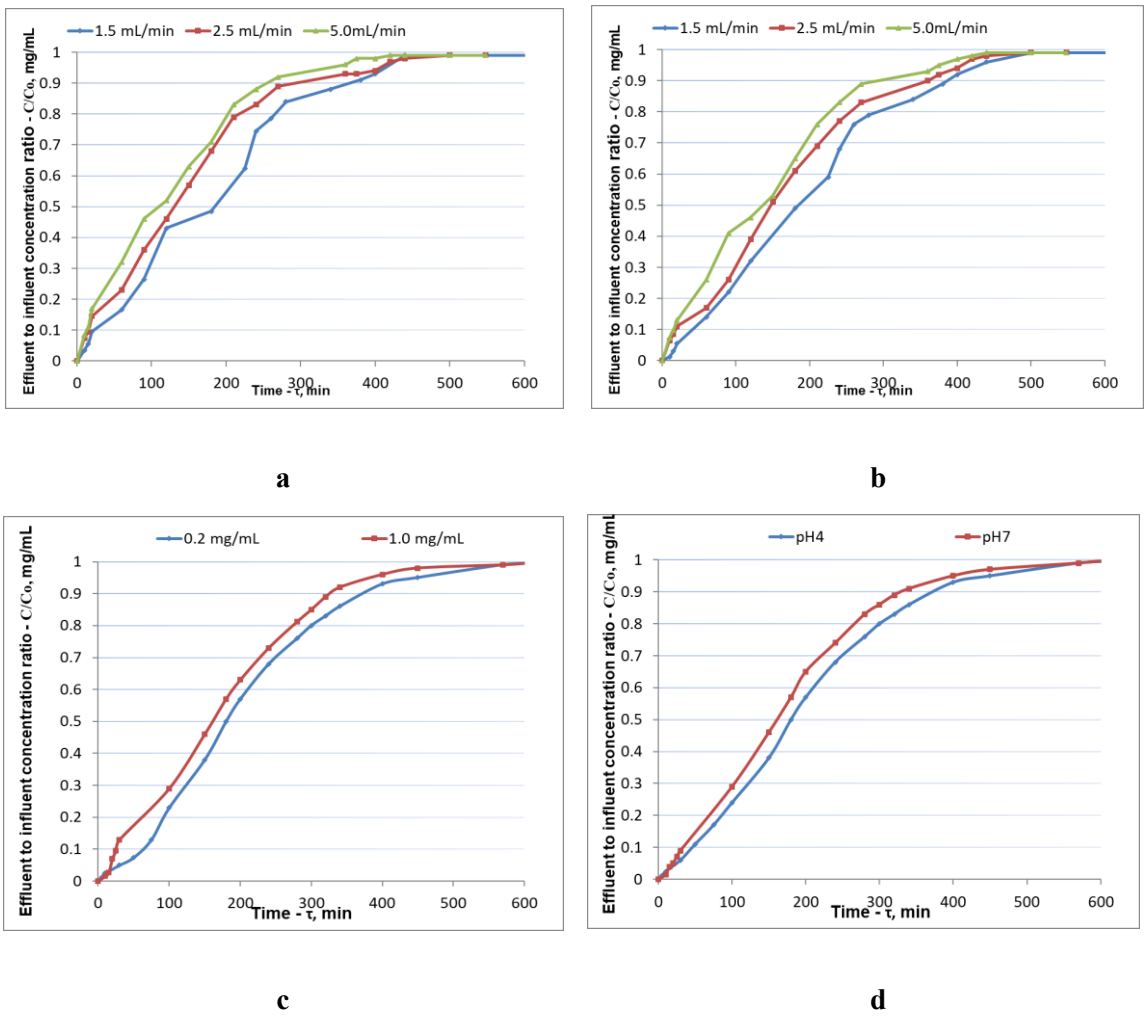

Fig. 4. The breakthrough curves for AZM adsorption on H-CL (a), H-CL (b) at various flow rates – 1.5 mg/mL, 2.5 mg/mL, 5 mg/mL (0.2 mg/mL concentration of influent test solution), on CL at two different concentrations - 0.2 mg/mL and 1.0 mg/mL (1.5 mg/mL flow rate of influent test solution, (c) and on CL at two different pH values – 4 and 7 (1.5 mg/mL flow rate of 0.2 mg/mL concentration of influent test solution (d).

The behaviors of breakthrough curves at different volumetric flow rates (1.5, 2.5 and 5.0 mL/min), inlet concentrations (0.2 mg/mL and 1.0 mg/mL) and pH values (4 and 7) of AZM test solutions were observed in the dynamic adsorption conditions (Figure 4). In case of CL, it can be observed that at volumetric flow rates of 1.5 mL/min and 5.0 mL/min, the breakthrough times at C/C_0=0.42 are reported as 120 and 97 min, respectively (Figure 4a). At time of 60 min the value of C/C_0 at the flow rate of 1.5 mL/min is 2.2 times lower than its value at 5.0 mL/min. According to the breakthrough curve (Figure 4a, b), it can be observed that at the same volumetric flow rate of 1.5 mL/min and at the same breakthrough time of 120 min, the value of ratios C/C_0 are approximately 0.42 and 0.35 for CL and H-CL, respectively. The Figure 4c shows that

at higher inlet concentration, the breakthrough curve is shifted towards the origin. More precisely, the inlet concentration of 0.2 and 1.0 mg/mL, the values of C/C_0 at contact time of 100 min are reported as 0.27, and 0.36, respectively.

The effect of pH value of AZM solution (0.2 mg/mL) on adsorption process was investigated in acidic and neutral conditions at the values of pH 4 and 7, respectively. The results show that the breakthrough curve at the value of pH 4.0 is similar to the experimental data achieved at pH 7. As shown in Figure 4d, along with the pH-dependent speciation, AZM can be more positively charged (cationic). Cationic AZM is the dominant species at the value of pH below 7.

The dynamic adsorption capacities of both studied adsorbents, natural CL and H-CL, were calculated from the data of the adsorption experiment, and the results are given in Table 1.

Table 1. The dynamic adsorption capacities (q_d, mg/g) for CL/AZM and H-CL/AZM systems with minimal and maximal flow rates of AZM solutions with various concentrations - 0.2-1.0 mg/mL at the neutral pH value.

Adsorbent	Azithromycin			
	1.5 mL/min		5.0 mL/min	
	0.2 mg/mL	1.0 mg/mL	0.2 mg/mL	1.0 mg/mL
Natural Clinoptilolite	2.19	1.76	0.91	0.72
Clinoptilolite H-Form	3.66	2.85	1.77	1.03

The typical chromatogram obtained with the effluent test solution during adsorption experiment in dynamic conditions is given in Figure 5.

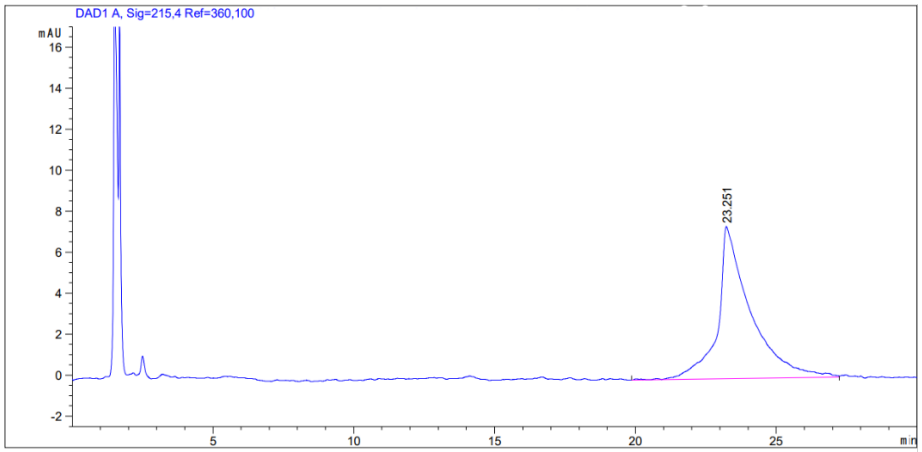

Fig. 5. The typical chromatogram obtained with the test solution.

DISCUSSION

The plotted adsorption isotherms show that isotherms have a good correlation (the square of correlation coefficient - R^2>0.95) and define a monolayer adsorption. The adsorption mechanism mainly composed of electrostatic interaction between the adsorbent surface and adsorbate. As the flow rate drops, the adsorbate has sufficient time to diffuse through pores and produces a higher adsorption capacity. The high flow rate of influent solution reduces the thickness of liquid film around adsorbent particles

leading to low mass transfer resistance and high rate of mass transfer [5, 7]. At the same volumetric flow rate and breakthrough time, the value of ratios C/C_0 are different for CL and H-CL, precisely, the value of ratio C/C_0 for CL is always greater than for H-CL. This can be related to low interaction energy between adsorbates and CL which accelerates breakthrough and saturation. In addition, the earlier breakthrough of adsorbate on CL compared to H-CL is due to relatively low adsorption. The mechanism of interaction between adsorbate and adsorbent can be explained by the fact that CL has a framework, open and stable three-dimensional structure with a negative charge, and antibiotic molecules in aqueous solutions have a positive charge [5, 9]. Consequently, natural CL would be able to retain antibiotic molecules due to the mechanism of electrostatic interaction. As an additional adsorption mechanism, it is proposed that the uptake of the antibiotic on the zeolite surface is due to electron-donor-acceptor interaction with the AZM, caused by the presence of a heterocyclic ring and carbonyl, tertiary amino and hydroxyl groups in adsorbate molecules. The increase in adsorption capacity in the case of H-CL is associated with a modification effect including a change in pore size.

The acid treatment caused a removal of cations and aluminum from initial CL, an increase in the relative content of Si/Al ratio in H-CL framework and pore opening as well. This fact was confirmed by the results of FT-IR and XRD analyses of acid-modified forms of natural zeolites [5, 7-8]. By increasing the flow rate of the influent solution, the amount of adsorbed AZM increases and the inlet concentration changes more rapidly. This can be related to the low interaction between adsorbate and adsorbent at a higher flow rate, which accelerates breakthrough and saturation. The breakthrough curve is shifted towards the origin, becomes steeper, and rapidly reaches saturation. The tendency is found to be exactly the same for both zeolite forms, although for the acid-modified form the adsorption process is slower; therefore, the breakthrough curve is more shifted from the origin, which indicates a higher adsorption capacity of H-CL. As the concentration of the antibiotic influent solution increases, the breakthrough curve is shifted towards the origin. It may be related to the enhancement of the driving force for mass transfer across the liquid film along with the acceleration of the adsorption rate, which leads to an early saturation of the fixed-bed column. The results of the study reveal that the acid-modification of zeolite, the flow rate and the inlet concentration of the antibiotic test solution influence the breakthrough curve. It shows that the fixed bed adsorption conditions affect the value of ratio C/C_0 according to the order: the volumetric flow rate > the inlet concentration > the zeolite's modification. Based on the results of the investigation of the effect of different pH values (pH 4, 7) on dynamic adsorption process, the cationic AZM molecule has more protonated functional groups at pH 4, in acidic condition, which may be the major mechanism of this adsorption. At the value of pH 7, zeolite adsorbent surface would be negatively charged and hence, is the possibility of stronger electrostatic interaction. The AZM molecule become anionic with increasing the value of pH (alkaline condition) which cannot combine with adsorbent surface. The results confirm that the effect of electric charge is a little impact role in the process because AZM molecules and adsorbent surface are same charge at pH 4 and pH 7. The factor of the electron-donor-acceptor interaction in the adsorption process was the most effective at pH 4. Therefore, the observation of the removal efficiency with increasing the value of pH can be explained by lower electrostatic interaction between antibiotic and zeolite adsorbent [5, 7-9].

CONCLUSION

The results show that the decrease in dynamic adsorption capacity of the test antibiotic was caused by increasing the flow rate of inlet solution of adsorbate. The decrease in dynamic adsorption capacity was observed by increasing the inlet concentration of adsorbate. The acid-modified clinoptilolite is characterized with high dynamic adsorption capacity caused by increasing the Si/Al ratio in zeolite framework and pore opening in comparison with natural clinoptilolite. The studied natural zeolites with hydrophilic pores have a greater affinity for adsorbing antibiotic pollutants in aqueous solution. The high volumetric flow rate, the inlet concentration of antibiotic solution and the pH value accelerates breakthrough of adsorbate and correspondingly reduced adsorption capacities. Additionally, this research provides useful information for design of fixed bed adsorption column for removal studies of other antibiotics of different classes or contaminants. Hence, this research confirms that natural zeolite is competitive, eco-friendly and efficient adsorbents in terms of cheapness, shape selectivity and adsorption efficacy.

REFERENCES

[1] Danner M.-C., Robertson A., Behrends V., Reiss J. Antibiotic pollution in surface fresh waters: Occurrence and effects. Science of The Total Environment, vol. 664, pp 793-804, 2019.

[2] Brown K.D., Kulis J., Thomson B., Chapman T.H., Mawhinney D.B. Occurrence of antibiotics in hospital, residential, and dairy effluent, municipal wastewater, and the Rio Grande in New Mexico. Science of The Total Environment, vol. 366/issues 2–3, pp 772-783, 2006.

[3] Watkinson A.J., Murby E.J., Kolpin D.W., Costanzo S.D. The occurrence of antibiotics in an urban watershed: From wastewater to drinking water. Science of The Total Environment, vol. 407/issue 8, pp 2711-2723, 2009

[4] Hernando M., Mezcua M., Fernandezalba A., Barcelo D. Environmental risk assessment of pharmaceutical residues in wastewater effluents, surface waters and sediments. Talanta, vol. 69/issue 2, pp 334-342, 2006

[5] Rubashvili I., Eprikashvili L., Kordzakhia T., Zautashvili M., Pirtskhalava N., Dzagania M. Adsorptive removal study of the frequently used fluoroquinolone antibiotics – moxifloxacin and norfloxacin from wastewaters using natural zeolites. Mediterr. J. Chem., vol. 9/issue 2, pp 142-154, 2019

[6] Sagaseta de Ilurdoz M., Jaime Sadhwani J., Vaswani Reboso J. Antibiotic removal processes from water & wastewater for the protection of the aquatic environment - a review. *J. Water Process Eng.,* vol. 45, 102474, 2022.

[7] Eprikashvili L., Kordzakhia T., Zautashvili M., Rubashvili I., Pirtskhalava N., Dzagania M, Tsintskaladze G., Antia G. Effect of clinoptilolite acid activation on ceftriaxone sorption from wastewaters. *Res. J. Chem. Environ.,* vol. 25/issue 5, pp 80-85. 2021.

[8] Eprikashvili L., Kordzakhia T., Zautashvili M., Rubashvili I., Pirtskhalava N., Dzagania M., Tsintskaladze G. Feasibility study for the use of natural mordenite in purification processes of wastewaters from pharmaceutical pollutants. *International Journal of Advanced Research.*, vol. 9/issue 3, pp 683-691, 2021.

[9] Davoodi, S., Dahrazma B., Goudarzi N., Gorji H. G. Adsorptive removal of azithromycin from aqueous solutions using raw and saponin-modified nano diatomite. Water Sci Technol, vol. 80/issue 5, pp 939–949, 2019.

DIMENSIONAL CHARACTERISTICS OF *NYMPHOIDES PELTATA* (S.G. GMEL.) KUNTZE IN DIFFERENT ECOLOGICAL AND CENOTIC CONDITIONS OF THE BASIN'S WATER BODIES DESNA RIVER (UKRAINE)

Associate professor Iurii Skliar
Prof. Viktoriia Skliar
Associate professor Maryna Sherstiuk
Associate professor Inna Zubtsova

Sumy National Agrarian University, **Ukraine**

ABSTRACT

Nymphoides peltata is a typical representative of higher aquatic plants. Despite its wide geographical distribution, N. peltata is a rather rare species. The development of effective measures to protect a species in any territory is possible only if there is complete information on the status of its populations. Study of the size and morphological structure of plants plays an important role in the system of population studies. The purpose of this publication is to characterise the dimensional values of *N. peltata* plants growing in the waters of the Desna River basin and to assess the impact of the leading ecological and coenotic factors on them. Five *N. peltata* cenopopulations were studied. Morphometric analysis was used, which was accompanied by the recording of 12 static metric morphoparameters. The results of the study showed that *N. peltata* plants respond to changes in ecological and cenotic conditions with a statistically significant change in the values of the leading morphological parameters and total size. As a result, plants of a characteristic habit and morphostructure are formed in each habitat. Based on the results of the study of plant size and the assessment of the influence of the leading ecological and coenotic factors, it was found that the most favourable for the formation, growth and development of *N. peltata* coenopopulations are large floodplain lakes, which are characterised by the following set of indicators: no current, water depth of 30–80 cm, transparency of at least 75–80% of the maximum depth, muddy bottom sediments, and projective coverage of the species of 70–95%. The habitats of the *Nymphoides peltata subpurum* (floodplain lake) and *Nymphoides peltata–Ceratophyllum demersum* (floodplain lake) communities most closely correspond to the parameters of the ecological and cenotic optimum.

Keywords: *Nymphoides peltata*, cenopopulations, morphometric analysis, plant size.

INTRODUCTION

Nymphoides peltata (S.G. Gmel.) Kuntze (*Menyanthaceae*) is a typical representative of higher aquatic plants, whose range covers a large area of Eurasia (Central, Atlantic and Eastern Europe, the Mediterranean, the Caucasus, Western and Eastern Siberia, the Far East (south), Central Asia (north), Western and Central Asia, the Japanese islands) and even reaches North America, where this species is considered to be an adventive [1]. It grows in various regions and natural zones of Ukraine, from Polissya to the Steppe [2]. Despite its wide geographical distribution, N. peltata is a rather rare species. Given its

status as a relict species, ecological and phytocoenotic importance, and decorative value, N. peltata requires protection, which is confirmed by the fact that it is listed in the third edition of the Red Data Book of Ukraine [3].

Sumy region of Ukraine is one of the regions with a well-developed hydrographic network. The largest waterways in Sumy region are the Desna, Seim, Psyol, Vorskla, and Sula rivers. However, populations of *N. peltata* are currently found only in the waters of the Desna floodplain. Since the waters of the Desna basin are constantly subject to direct or indirect anthropogenic pressure, there is a real danger of loss of *N. peltata* populations or significant deterioration of their condition.

The development of effective measures to protect a species in any territory is possible only if there is complete information on the status of its populations. In turn, the study of the size and morphological structure of plants plays an important role in the system of population studies [4–12]. Because the size and shape of plant organisms determine many of their properties, in particular: life span, place in biocenosis, role in food chains [13].

The purpose of this publication is to characterise the dimensional values of *N. peltata* plants growing in the waters of the Desna River basin and to assess the impact of the leading ecological and coenotic factors on them.

MATERIALS AND METHODS OF RESEARCH

Five *N. peltata* cenopopulations were studied. Their habitats differ in terms of water thickness and transparency, bottom sediment composition, total projective cover, and dominant and co-dominant cover (Table 1).

Table 1. Ecological and cenotic characteristics of *Nymphoides peltata* cenopopulations

Association	Average water depth, cm	Flow rate, m/s	Water transparency, cm	Nature of bottom sediments	Projected coverage, %.		
					general	dominant	co-dominant
Nymphoides peltata subpurum (floodplain lake)	40	absent	40	muddy	100	95	-
Nymphoides peltata – Ceratophyllum demersum (floodplain lake)	75	absent	60	muddy	> 100	80	25
Nymphoides peltata subpurum (riverbed)	135	0,01	120	sandy	95	90	-
Nymphoides peltata – Ceratophyllum demersum (bay)	155	absent	120	muddy	95	70	15
Nymphoides peltata – Ceratophyllum demersum (riverbed)	185	0,02	120	sandy	85	55	20

In order to estimate the size parameters of *N. peltata* plants of each of these five cenopopulations, morphometric analysis was used, which was accompanied by the recording of 12 static metric morphoparameters (Table 2).

Table 2. List of static metric morphoparameters used for the population study of attached pterophytes.

Name of the morphoparameter	Symbols and notations	Unit of measurement
Total weight of the accounting unit	W	g
Total phytomass of leaves	WL	g
Total leaf surface area	A	cm^2
Area of one surface leaf	a_{nadv}	cm^2
Area of one underwater leaf	a_{pidv}	cm^2
Total number of leaves	NL	pcs.
Stem length	H^s	cm
Total weight of reproductive organs	Wg	g
Total number of generative organs	Ng	pcs.
Number of buds	Nb	pcs.
Number of flowers	Nf	pcs.
Number of fruits	Np	pcs.

Individual plants (ramets) of generative age were used as phytopopulation accounting units. The plant organs were measured and weighed immediately after their removal from the water.

To determine the presence of a statistically significant influence of the leading ecological and cenotic factors on the state of plants and cenopopulations of N. peltata, we used analysis of variance accompanied by calculations of the strength of influence [14].

RESEARCH RESULTS

The ramet of *N. peltata* consists of two parts: surface and underwater. The surface part includes nodes and internodes. The nodes contain leaves and generative organs (buds, flowers, fruits). The above-water structures of *N. peltata* ramets from different habitats differ statistically significantly ($p < 0.05$) in the degree of branching, number of nodes and internodes (Figure 1), length of the latter, number and weight of leaves and generative organs.

The underwater part of the ramet is a cord-like stem, from which 1-3 leaves on long petioles sometimes extend. They can be located both on the surface and in the water column. The length of the underwater part varies significantly and ranges from 141-184 cm. It is the longest in ramets of the *Nymphoides peltata–Ceratophyllum demersum* (riverbed), *Nymphoides peltata–Ceratophyllum demersum* (bay) and *Nymphoides peltata subpurum* (riverbed) communities.

According to the results of the assessment of morphological parameters (Table 3), it was found that the largest total number of leaves is formed by ramets from the *Nymphoides peltata subpurum* (floodplain lake) group (10.2±1.01 pcs.). Ramets from

the *Nymphoides peltata–Ceratophyllum demersum* community (floodplain lake) are in second place by the number of leaves, where the value of this indicator is 8.3±0.72 pcs. In the *Nymphoides peltata subpurum* (riverbed), *Nymphoides peltata–Ceratophyllum demersum* (bay) and *Nymphoides peltata-Ceratophyllum demersum* (riverbed) communities, this indicator is 1.5-2.3 times lower and ranges from 4.5±0.70 to 5.6±0.64 pcs.

Ramets from the *Nymphoides peltata–Ceratophyllum demersum* group (floodplain lake) have the largest total leaf weight (8.7±1.02 g). A relatively high value of this indicator was also recorded in the *Nymphoides peltata subpurum* community (floodplain lake) (6,3±0.76 g). The lowest leaf mass was observed in ramets from the *Nymphoides peltata subpurum* (riverbed) and *Nymphoides peltata–Ceratophyllum demersum* (riverbed) groups (3.7±0.55 g and 3.7±0.45 g).

The maximum leaf surface area of ramets of the *Nymphoides peltata–Ceratophyllum demersum* (floodplain lake) community (172.0±20.03 cm^2), the minimum – *Nymphoides peltata subpurum* (riverbed) (61.0±9.21 cm^2). In other price populations, the values of this morphoparameter range from 75.7±9.36 cm^2 to 109.5±13.23 cm^2.

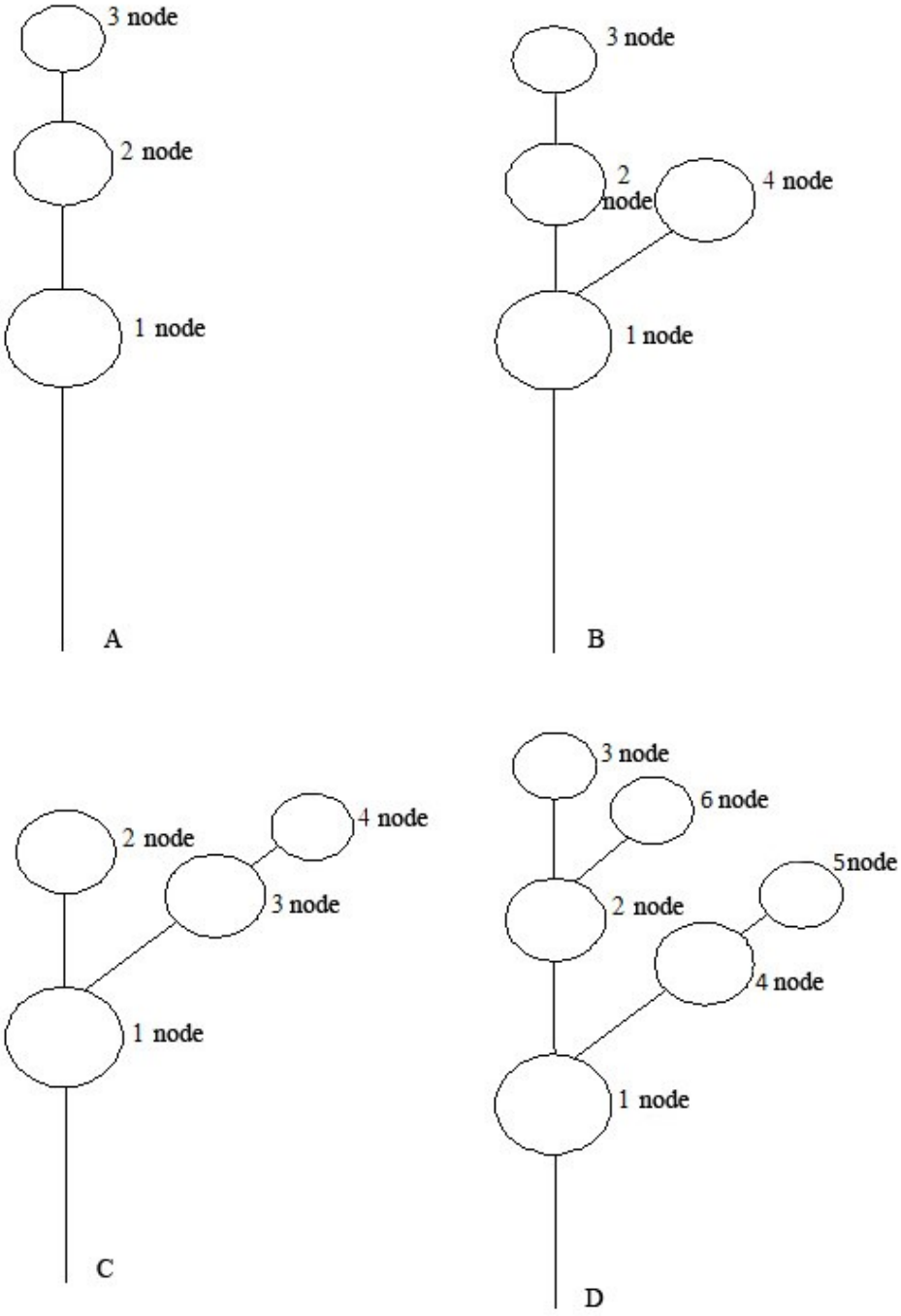

Figure 1. Schemes structure of the surface part of *Nymphoides peltata* ramets in the studied coenopopulations.

A - *Nymphoides peltata–Ceratophyllum demersum* (river bed), B - *Nymphoides peltata–Ceratophyllum demersum* (bay), C - *Nymphoides peltata purum* (river bed), D - *Nymphoides peltata–Ceratophyllum demersum* (floodplain lake) and *Nymphoides peltata subpurum* (floodplain lake)

Table 3. Morphometric parameters of *Nymphoides peltata*

Morphoparameters	Association				
	Nymphoides peltata subpurum (riverbed)	*Nymphoides peltata – Ceratophyllum demersum* (bay)	*Nymphoides peltata – Ceratophyllum demersum* (riverbed)	*Nymphoides peltata subpurum* (floodplain lake)	*Nymphoides peltata – Ceratophyllum demersum* (floodplain lake)
	$\overline{X} \pm S_{\bar{x}}$	$\overline{X} \pm S_{\bar{x}}$	$\overline{X} \pm S_{\bar{x}}$	$\overline{X} \pm S_{\bar{x}}$	$\overline{X} \pm S_{\bar{x}}$
W	18,6 ± 2,44	18,9 ± 1,80	17,5 ± 1,70	36,6 ± 2,62	32,4 ± 3,40
WL	3,7 ± 0,55	4,3 ± 0,51	3,7 ± 0,45	6,3 ± 0,76	8,7 ± 1,02
Wg	1,7 ± 0,24	2,0 ± 0,31	1,7 ± 0,21	6,3 ± 0,71	3,6 ± 0,59
A	61,0 ± 9,21	82,1 ± 9,72	75,7 ± 9,36	109,5 ± 13,23	172,0 ± 20,03
NL	4,8 ± 0,55	5,6 ± 0,64	4,5 ± 0,70	10,2 ± 1,01	8,3 ± 0,72
H^s	149,8 ± 1,61	165,8 ± 12,50	196,7 ± 11,16	88,4 ± 5,15	110,7 ± 7,61
Ng	13,5 ± 1,98	13,2 ± 1,65	10,9 ± 1,29	30,0 ± 1,89	20,4 ± 2,30
Np	3,2 ± 0,92	5,2 ± 1,03	5,2 ± 0,68	13,2 ± 1,70	6,1 ± 1,02
Nf	1,5 ± 0,17	1,2 ± 0,57	1,0 ± 0,21	2,6 ± 0,48	1,8 ± 0,29
Nb	8,8 ± 1,55	6,8 ± 0,76	4,7 ± 0,87	14,2 ± 0,89	12,5 ± 1,42
a_{nadv}	12,5 ± 0,38	15,1 ± 1,52	18,1 ± 1,65	10,7 ± 0,88	21,8 ± 2,56
wl_{nadv}	0,75 ± 0,071	0,79 ± 0,080	0,87 ± 0,081	0,62 ± 0,051	1,11 ± 0,013

The largest mass and area of one leaf are in the ramets of the *Nymphoides peltata–Ceratophyllum* demersum community (floodplain lake) (1.11±0.013 g and 21.8±2.56 cm^2, respectively). The lowest values were recorded in the *Nymphoides peltata subpurum* (floodplain lake) community (0.62±0.051 g and 10.7±0.88 cm^2). In other populations, the weight of one leaf ranges from 0.75±0.071 g to 0.87±0.081 g, and the area - from 12.5±0.38 cm^2 to 18.1±1.65 cm^2.

The largest number and weight of generative organs were recorded in ramets of the cenopopulations of *Nymphoides peltata subpurum* (floodplain lake) (30.0±1.89 pcs., 6.3±0.71 g, respectively) and *Nymphoides peltata–Ceratophyllum demersum* (floodplain lake) (20.4±2.30 pcs. and 3.6±0.59 g, respectively). Ramets of the *Nymphoides peltata–Ceratophyllum demersum* (riverbed) community have the smallest number of generative organs (10.9±1.29 pcs.). In the other two populations, this indicator ranged from 13.2±1.65 to 13.5±1.98. The lowest weight of generative organs in ramets was observed in the *Nymphoides peltata subpurum* (riverbed) (1.7±0.24 g) and *Nymphoides peltata–Ceratophyllum demersum* (riverbed) (1.7±0.21 g) communities.

The largest total weight is observed for ramets of *the Nymphoides peltata subpurum* (floodplain lake) community (36,6±2,62 g). In the *Nymphoides peltata–Ceratophyllum demersum* (floodplain lake) communities, the value of this morphoparameter is 1, 1 times (32.4±3.40 g), Nymphoides peltata subpurum (riverbed) and *Nymphoides peltata–Ceratophyllum demersum* (bay) – 1.9-2.0 times (to 18.6±2.44 g and 18.9±1.80 g, respectively). The smallest weight of ramets was in the *Nymphoides peltata–Ceratophyllum demersum* group (riverbed) (17.5±1.70 g).

DISCUSSION

The results of the study showed that *N. peltata* plants respond to changes in ecological and cenotic conditions with a statistically significant (at $p < 0.05$) change in the values of the leading morphological parameters and total size. As a result, plants of a characteristic habit and morphostructure are formed in each habitat. These general patterns are also inherent in other species of higher aquatic plants. Within the Desna River basin, they are recorded in *Nuphar lutea* (L.) Smith, *Nymphaea candida* J. et C. Presl, *Potamogeton natans* L.) [15–17].

The one-factor analysis of variance showed that among the studied factors, water depth has a statistically significant effect on all static metric morphological parameters of *N. peltata* at the strength of influence of 19.6–62.5%. The projective cover of this species and water transparency have a statistically significant effect on a smaller number of static metric morphoparameters at the strength of influence of 15.1–52.6% and 15.0–52.5%, respectively. The nature of the bottom sediments has an influence strength of 16.2–28.0% and has a statistically significant effect on an even smaller number of morphological parameters. In *N. peltata*, the highest values of most static metric morphological parameters were recorded in cenopopulations growing in water depths from 30 to 80 cm. With increasing water thickness, there is a decrease in the values of these parameters, except for the stem length.

CONCLUSIONS

Based on the results of the study of plant size and the assessment of the influence of the leading ecological and coenotic factors, it was found that the most favourable for the formation, growth and development of *N. peltata* coenopopulations are large floodplain lakes, which are characterised by the following set of indicators: no current, water depth of 30–80 cm, transparency of at least 75–80% of the maximum depth, muddy bottom sediments, and projective coverage of the species of 70–95%. The habitats of the *Nymphoides peltata subpurum* (floodplain lake) and *Nymphoides peltata–Ceratophyllum demersum* (floodplain lake) communities most closely correspond to the parameters of the ecological and cenotic optimum.

In this complex of habitat parameters, it is particularly important to maintain the water column at an optimal level. Therefore, in order to conserve *N. peltata* populations within the Desna basin as a whole, priority should be given to measures aimed at ensuring a stable hydrological regime of water bodies, preserving bays and large floodplain lakes, which are more favourable for this species than river channels. This requires a reduction in deforestation, optimisation of forest cover and the area's maximum natural state with no drainage systems.

REFERENCES

[1.] Macrophytes are indicators of changes in the natural environment, “Макрофиты – индикаторы изменений природной среды” (1993). Отв. ред. С. Гейны & К.М. Сытник. Киев: Наук. думка.

[2.] Dubin D.V., Maroz S.A. (1977). *Nymphoides peltata* (S. Gmel.) Kuntze на Україні. Укр. ботан.журн., 34, 4, 398–402.

[3.] The Red Book of Ukraine. The plant world, “Червона книга України. Рослинний світ” (2009). За ред. Я.П. Дідуха. К.: Глобалконсалтинг. ISBN 978-966-97059-1-4

[4.] Evans G.C. (1972). The Quantitative analysis of plant growth. Oxford.

[5.] Hunt R. (1978). Plant growth analysis. London: Arnold.

[6.] Zlobin Iu. (1989). Principles and methods of studying coenotic plant populations. “Принципы и методы изучения ценотических популяций растений”. Казань: Изд-во Казан. ун-та.

[7.] Hunt R. **(**1990). Basic growth analysis. London: Unwin Hyman.

[8.] Hunt, R., Causton D.R., Shipley B. & Askew A.P. (2002). A Modern Tool for Classical Plant Growth Analysis. Ann Bot., 90 (4), 485–488. doi: 10.1093/aob/mcf214

[9.] Tews J. (2004). Plant population viability analysis in conservation biology: a review. – N.Y.: Elatis Modeling and Consulting Inc., 2004.

[10.] Zlobin Iu. (2009). Population ecology of plants: current state, growth points., “Популяционная экология растений: современное состояние, точки роста”. — Сумы: Университет. книга. ISBN 978-966-680-456-6

[11.] Gibson D. J. (2014). Methods in Comparative Plant Population Ecology (2nd edn). Oxford and New York: Oxford University Press. https://doi.org/10.1093/acprof:oso/9780199671465.001.0001

[12.] Skliar V. & Sherstuk M. (2016). Size structure of phytopopulations and its quantitative evaluation. Eureka: Life Sciences, 1, 9–15. https://doi.org/10.21303/2504-5695.2016.00047

[13.] Marba N., Duarte C.M. & Agusti S. (2007). Allometric scaling of plant life history. Proc. Nation. Acad. Sci. USA, 104 (40), 15777-15780 https://doi.org/10.1073/pnas.0703476104

[14.] Tzarenko O.M., Zlobin Iu, Skliar V.G.. & Panchenko S.M. (2000). Computer methods in agriculture and biology , “Комп’ютерні методи в сільському господарстві та біології”. Суми: Університет. книга. ISBN 966-7550-25-7

[15.] Skliar Iu. (2003). Population structure of Nuphar lutea L. (Nymphaeaceae) in the basin of the Desna River, “Популяційна структура *Nuphar lutea* L. (Nymphaeaceae) басейну р. Десни“. Укр. ботан. журн., 60, 2, 175 – 181.

[16.] Skliar Iu (2017). Ростові ознаки *Potamogeton natans* L. у різних еколого-ценотичних умовах водойм басейну Десни. Науковий вісник Східноєвропейського національного університету імені Лесі Українки, 7 (356), 47–55. DOI: https://doi.org/10.29038/2617-4723-2017-356-7-47-55

[17.] Skliar Iu., Skliar V., Klymenko A., Sherstiuk M. & Zubtsova I. (2020). Growth signs of *Nymphaea candida* in various ecological and cenotic conditions of Desna Basin (Ukraine). AgroLife Scientific Journal., 1, 9, 316–323. ISSN 2285-5718.

EFFICIENCY OF WATER PURIFICATION FROM FOOD PRODUCTION USING BIOCHAR

Dr. Jana Suchánková[1]

Dr. Petra Roupcová[1]

Ing. Jan Slaný[1]

[1] Department of Occupational and Process Safety, Faculty of Safety Engineering, VSB-Technical University of Ostrava, **Czech Republic**

ABSTRACT

Today, more than in the past, water is considered a very valuable resource. Efforts to use it efficiently are growing. One method of using water efficiently is wastewater treatment. Well-treated water minimises negative impacts after discharge into a watercourse, i.e., within or adjacent to aquatic ecosystems, or can be reused, for example, in the form of drinking water. This study focuses on the possibility of treating food industry water using biochar as a sorption medium. Biochar from wood pulp (100%) was used for the experiments. The wastewater collected was a mixture from two production plants, focussing on aspics, fish spreads, or cheese processing. The aim of the experiments was to evaluate the efficiency of the sorption properties of a specific type of biochar in terms of its weighting of different masses for an identical volume of wastewater and also in terms of different sorption times (time dependence). The efficiency was addressed in the context of the determination of the chemical oxygen demand with the oxidising agent potassium dichromate (COD_{Cr} method). The highest efficiency was achieved in the experiment with a load of 2 g of sorption reagent per litre of wastewater. No trend was demonstrated in the efficiency change with respect to the time of contact of the sorbent with the water.

Keywords: Wastewater, Biochar, Water Treatment, Sustainable Development

INTRODUCTION

Pan-European environmental regional priorities – climate change, air quality, biodiversity, chemicals and waste, and freshwater – are all captured in the 2030 Agenda for Sustainable Development including the SDGs and their targets [1], Within the 2030 Agenda, water serves as an (often) unacknowledged but essential connecting factor for reaching the SDGs [2].

Industry, especially the food industry, uses water for several purposes; for example, it is an input raw material, it is a cleaning or cooling medium, but it also leaves the production process as wastewater that is polluted depending on the type of production. The problem is the high content of substances that have a high biochemical and chemical oxygen demand. The search for new solutions to effectively treat water and

return it to the desired quality before discharge into watercourses should be one of the priorities of human activity today.

Fees are paid for the discharge of wastewater into surface waters. Among the indicators subject to charges is the chemical oxygen demand (COD_{Cr}). It is the responsibility of each operator to ensure the quality of the wastewater according to the legal conditions or conditions set by the sewerage network operator. The treatment of industrial wastewater is an important element in the protection of the environment.

Biochar is the product of pyrolysis of waste after the biomass fermentation process. Biomass can come from a variety of sources, e.g. wood waste, corn, straw, dry parts of nuts, fruit peelings, and sewage sludge. Pyrolysis produces a porous carbonaceous material with a compact hydrophobic core of a predominantly aromatic structure encased in a shell with hydrophilic and chemically active properties (surface groups -OH, -C=O, -C-O-C-, -COOH).[3]

Biochar finds its application in many sectors, in agriculture when applied to the soil [4], in electronics, metallurgy, plastics and textile industries, fruit and vegetable storage, and as an economically viable adsorption material for the adsorption of inorganic and organic contaminants [5],[6]. Biochar is also recognised to play an important role in the removal of microbial contaminants present in drinking and used water. The economics of biochar relative to activated carbon (biochar cost 246 USD/tonne compared to 1500 USD/tonne for activated carbon) also speak in its favour. [7].

MATERIALS

Sorption material used

Biochar type 4073 was used for the experiments. Biochar 4073 was prepared by pyrolysis at 470 °C for 25 minutes from a digestate with a composition of 100% wood pulp. The biochar was then ground repeatedly for 2.5 hours on a wheel mill through several passes (5 times VR, VR is type of sieve, for 30 minutes). Pyrolysis was carried out by Bioúhel s.r.o., Zlín. Biochar has a total composition of $C_{14}O$, contains 2% contamination with Si, Al, K, Ca, and Mg salts. The material is described in more detail in Czech patent No. 307022. [8]

Surface structure of biochar by SEM

The surface structure of the porous material was determined using a QUANTA FEG 450 scanning electron microscope, the measured particle sizes were 17.82 μm and 8.63 μm, see Figure 1.

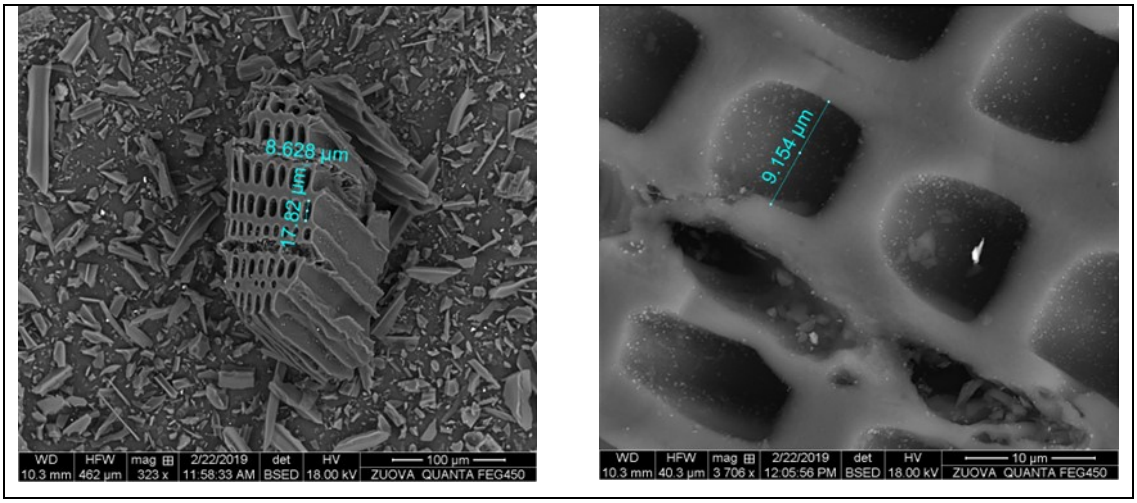

Fig. 1. SEM images of the surface of biochar 4073

Biochar Active Surface Specification (BET)

The size of the total active surface area - the number, size, surface area and pore volume of the material being tested - is also an important indicator of biochar characterization. The test product contains in its structure mainly micropores, mesopores, and macropores, which were not further identified in the testing. The radius of micropores is 0 to 2 nm and of mesopores 2 to 50 nm. The isotherm curve for the analysis performed has a hysteresis shape, which is typical of the mesoporous nature of the material structure. The specific surface area of biochar is determined by BET analysis to be 571.6 ± 9.2 $m^2.g^{-1}$. The volume of the monomolecular layer was found to be 131.3 $cm^3.g^{-1}$, which characterizes the porosity of the tested material. The surface area of the micropore is equal to 325.7 $m^2.g^{-1}$, while mesopores and macropores together form a surface area of 245.9 $m^2.g^{-1}$. The largest distribution of mesopores was 2 and 7 nm, which can be seen in Figure 3, and 1.05 nm for micropores. The total volume of the mesopores was found to be 0.189 $cm^3.g^{-1}$ (see Figure 2), and 0.247 $cm^3.g^{-1}$ for the micropores. From the partial specific surface areas found, we can conclude that the predominant character of biochar 4073 is microporous, containing about 30% more micropores than mesopores. BET analysis was performed using a 3Flex Micromeritics instrument, USA.

https://doi.org/10.5593/sgem2023V/3.2/s12.14

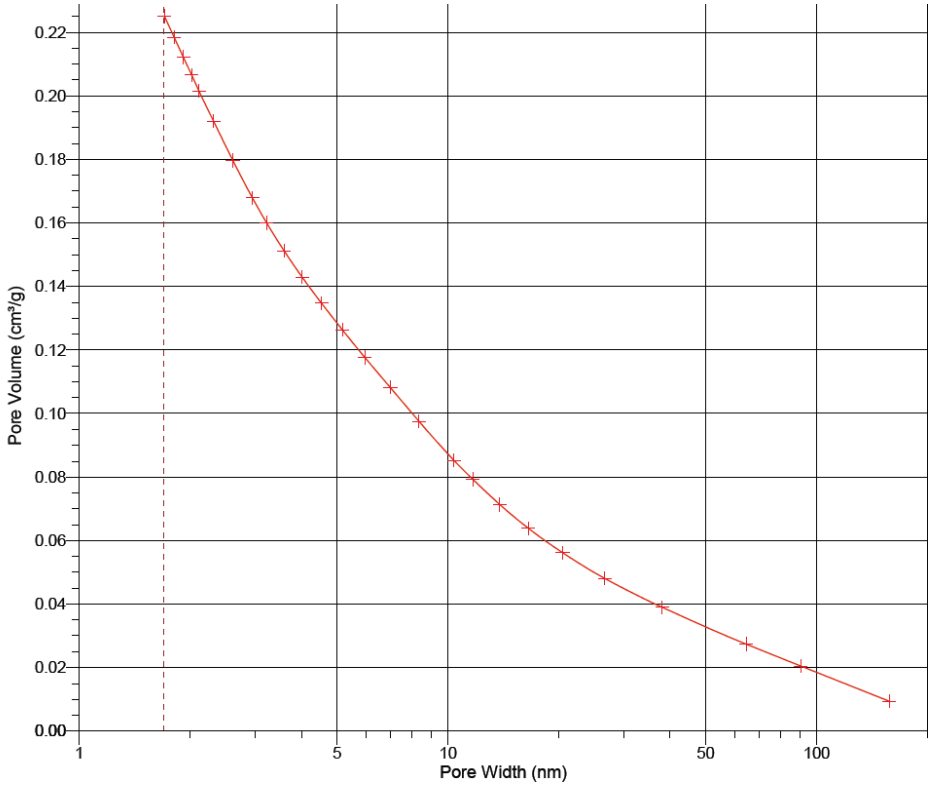

Fig. 2. Total mesopore volume of biochar 4073 [9]

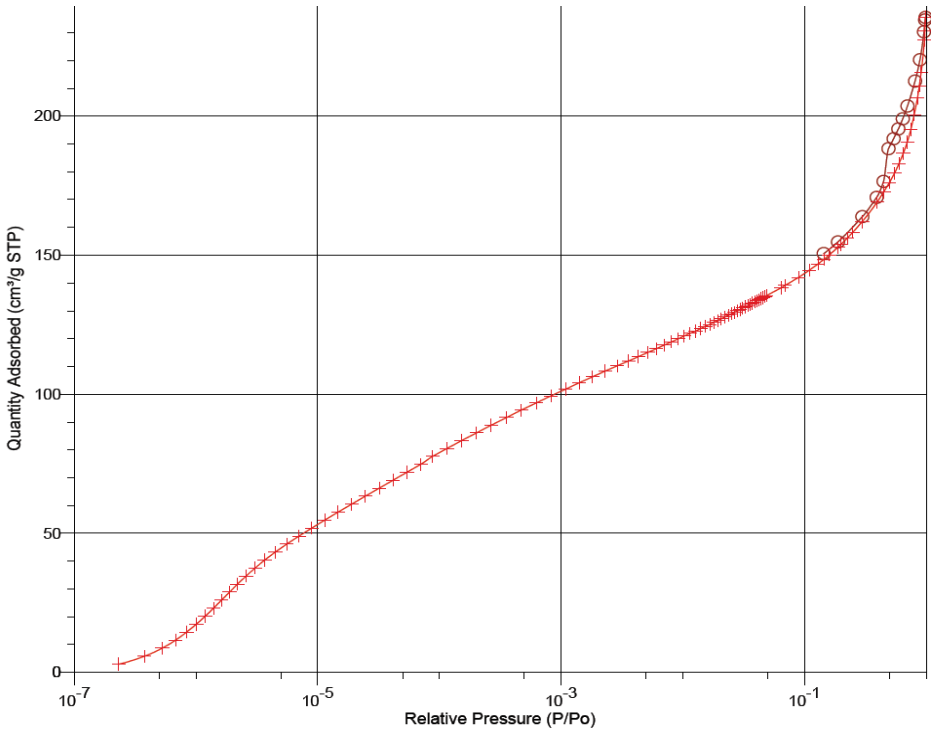

Fig. 3. Largest mesopore distribution of biochar 4073. [9]

Particle size distribution of a batch of biochar

The mean grain size was determined to be 0.09 mm by sieve analysis; see Figure 4.

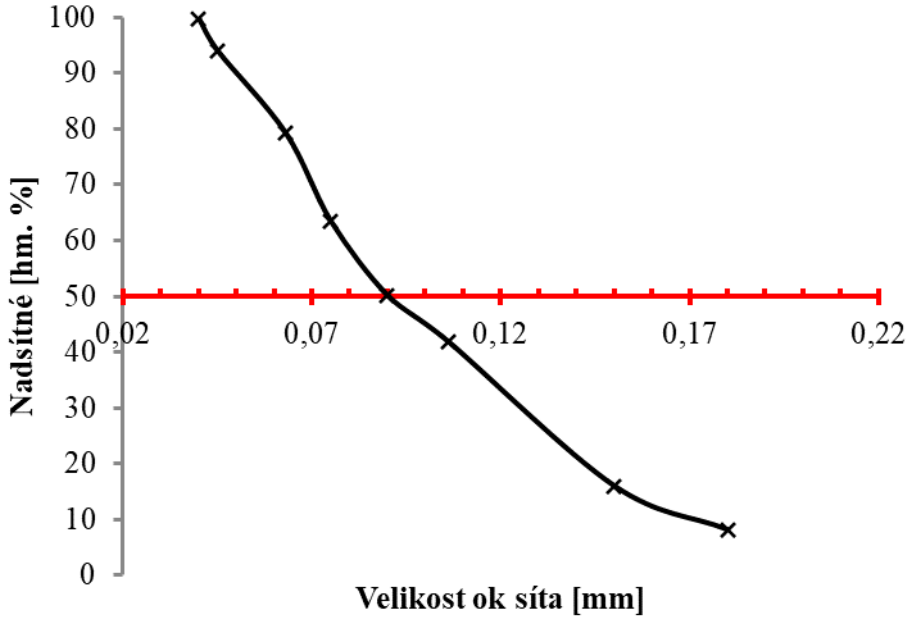

Fig. 4. Particle size distribution of biochar 4073. [9]

Wastewater from food production

The wastewater for the experiment was collected as a mixture of wastewater from two plants. Food production 1: the operation of Gastro - Menu Express a. s. The main activity of the company is the production and subsequent distribution of delicatessen products such as spreads, salads, aspics, and fish products [10]. The wastewater contained mainly vinegar, salt, salami and fish oil, gelatine. Food production 2: MILKEFFEKT s.r.o. establishment, engaged in the production of traditional cheese specialities. The operation focuses mainly on the processing of fresh cheese, of which they process up to 50 tonnes per month. [11]. The wastewater contained mainly salt and milk fat.

Wastewater collection

The wastewater from the sub-plants flows into one pipe where it is mixed and then continues to the lagoons where the grease is separated. Wastewater samples were taken from these lagoons. Water continues to flow through sumps, from which it is then pumped out by a faecal truck and taken to the sewage treatment plant. In total, approximately 10 litres of wastewater was sampled on different dates. The sampling was carried out according to the international standard for wastewater sampling, ČSN ISO 5667-10.

METHODS

Description of the experiment

Three subtests were conducted as part of the experiment. A specific weight of biochar (3 different weights) was added to a one litre sample of wastewater (dairy and

delicatessen wastewater) in the subtests. For test 1 (Z1) 1.5 g of biochar was used, for test 2 (Z2) 2 g of biochar was used and for the third test (Z3) 3 g of biochar was used. For each test, 6 samples were prepared. After placing the biochar in the water, each of the samples was shaken manually several times and then stirred on a magnetic stirrer at 700 rpm for the specified time. Magnetic stirrer IKA, RCT B S000, 220-230 V, 50/60 Hz, 650 W, IP 42 was used. The mixing time for each of the six samples was incremented in intervals of 10 minutes, i.e. the first sample was mixed for 10 minutes, the second for 20 minutes ... the sixth for 60 minutes. The samples were then filtered and sent for COD_{Cr} determination.

Sorption efficiency

For the purpose of the experiments, it was not necessary to know the specific composition of the wastewater. The pollution of wastewater is indicated by a parameter called the chemical oxygen demand. Therefore, to determine the sorption efficiency of Biochar 4073, a method for determining the chemical oxygen demand (using potassium dichromate), called "Test Methods for Chemical Oxygen Demand" was used. The method is based on ISO 6060 Water quality, Determination of Chemical Oxygen Demand. The analysis was carried out by T. G. Masaryk Water Research Institute, a public research institution, Ostrava branch.

RESULTS

The resulting chemical oxygen demand values for each sample are given in Table 1.

Table 1: Chemical oxygen demand values for individual samples

Test number	1		2		3	
Wastewater Quantity (L)	1		1		1	
Weight of biochar (g)	1,5		2		3	
Mixing time (min)	**Sample identification**	**COD_{Cr} (mg/l)**	**Sample identification**	**COD_{Cr} (mg/l)**	**Sample identification**	**COD_{Cr} (mg/l)**
	Blind sample	9906	Blind sample	14850	Blind sample	14850
10	Z1-1	4100	Z2-1	3889	Z3-1	6515
20	Z1-2	3850	Z2-2	3861	Z3-2	6061
30	Z1-3	3900	Z2-3	3861	Z3-3	6162
40	Z1-4	3800	Z2-4	3861	Z3-4	6111
50	Z1-5	4000	Z2-5	3465	Z3-5	6310
60	Z1-6	3900	Z2-6	3861	Z3-6	6212

A raw wastewater sample was set as blank. The results of the wastewater sorption test show that after mixing the water with biochar and subsequent filtration, the magnitude of the chemical oxygen demand decreased in all cases compared to the blank sample, averaging 40% for Z1, 26% for Z2, and 42% for Z3. This means that the biochar sorption efficiency for each test was on average 60 % for Z1, 74 % for Z2 and 58 % for

Z3. It can be seen from the above that the highest efficiency was achieved in the Z2 test when a quantity of biochar of 2 g per 1 litre of wastewater was used.

The sorption efficiency of biochar was also clearly visible visually, the raw wastewater having a yellowish colour, while the water after sorption was clear; see Figure 5.

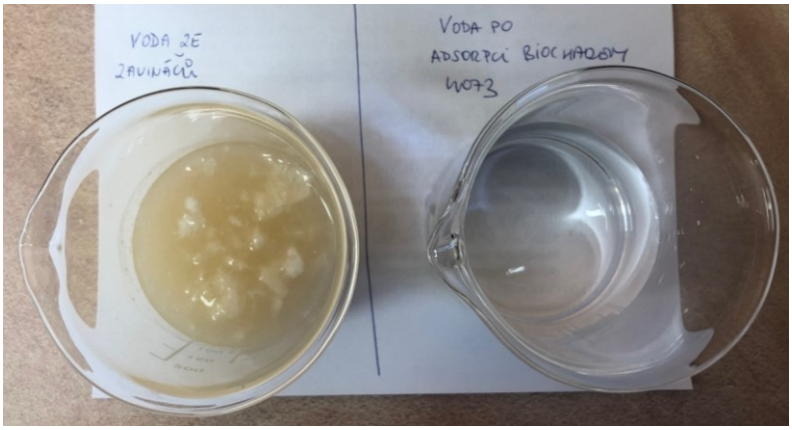

Fig. 5. Visible colour difference between the original wastewater (beaker on the left) and the treated water after sorption (beaker on the right) after 10 min.

DISCUSSION

The experiment was designed to test whether increasing the mixing time of wastewater with the sorbent would result in increased water treatment efficiency. With respect to the time dependence of the magnitude of sorption, it can be concluded that the time of mixing the water with the sorbent did not have a significant effect on the resulting sorption efficiency. The time dependence of the purification efficiency on the length of sorption was not demonstrated.

CONCLUSION

Treating wastewater in an environmentally friendly way is an important step toward meeting sustainability goals in the management of such a valuable resource as water. The study showed that the use of biochar to treat water from the food industry can be a promising route. However, it is possible that the sorption technique alone will not be sufficient.

The COD_{Cr} value of the effluent at the main outlet of the wastewater treatment plant is around 28.3 $mg.l^{-1}$. This value is considerably lower than the values from the experiments described. This leads to the conclusion that in practice, for the purpose of direct discharge of food wastewater to surface waters, a combination of techniques such as sorption and membrane technology will be necessary for more effective treatment of food wastewater.

ACKNOWLEDGEMENTS

T. G. MASARYK Water Research Institute, public research institution, Ostrava branch - analysis of wastewater samples realized. The publication was written within the Norway grants project “Innovative carbon-based sorbents as an efficient way of wastewater treatment” project number 3213200008.

REFERENCES

[1] UNEP a UNECE. *GEO-6 Assessment for the pan-European region*. Nairobi: UNEP, 2016. ISBN 978-92-807-3545-1.

[2] UNESCO and UN-WATER. *United Nations World Water Development Report 2020: Water and Climate Change*. Paris: UNESCO, 2020. ISBN 978-92-3-100371-4.

[3] Tan X., Zeng G., Wang X., Hu X., Gu Y., Yang Z. 2015. Application of biochar for the removal of pollutants from aqueous solutions, *Chemosphere* 125, p. 70-85.

[4] Krishnakumar S., Rajalakshmi A.G., Balaganesh B., Manikandan P., Vinoth C., Rajendran V. 2014. Impact of Biochar on Soil Health, *International Journal of Advanced Research*, vol. 2, p. 933-950.

[5] Xie T., Reddy K. R., Wang Ch., Yargicoglu E., Spokas K. 2015. Characteristics and Applications of Biochar for Environmental Remediation: A Review, *Environmental Science and Technology*, vol. 45, p. 939-969.

[6] Buss W., Masek O. 2014. Mobile organic compounds in biochar – a potential source of contamination – phytotoxic effects on cress seed (Lapidium sativum) germination*, J. Environm. Manag*. vol. 137, p. 111-119.

[7] Inyang, M. a E. Dickenson. The potential role biochar in the removal organic and microbial contaminants from potable and reuse water: A review. *Chemosphere* [online]. 2015, 232-240 [cit. 2023-11-06]. ISSN 0045-6535. Accessed: doi:10.1016/j.chemosphere.2015.03.072

[8] A biochar based material and the method of its preparation. Ing. et Ing. Karel KLOUDA, CSc., Ph.D., M.B.A., Ing. Petra ROUPCOVÁ. Czech Republic. 307022. Application 12.09.2016. Granted 15.11.2017. Accessed: www.upv.cz

[9] Roupcová P. 2018. *Monitoring of the ecotoxicity of the carbon based nanoparticles*. (Disertation Thesis). Ostrava: VSB - Technical University of Ostrava, Faculty of Safety Engineering. 149 p.

[10] GASTRO - MENU EXPRESS a.s. Gastro - Express Menu [online]. [cit. 2023-09-16]. Accessed: https://www.gastromenu.cz/

[11] MILKEFFEKT a.s. Milkeffekt [online]. [cit. 2023-09-16]. Accessed: https://milkeffekt.cz/

FLOOD HAZARD MAPPING TO PROTECT IMPORTANT HABITATS

Dr. Vesela Stoyanova[1]

[1] National Institute of Meteorology and Hydrology, **Bulgaria**

ABSTRACT

Floods are one of the most devastating natural disasters that can lead to significant economic and environmental damage and even loss of lives. Flood hazard mapping is one of the measures of disaster risk reduction and becoming a more important function in conserving biological diversity and protected areas now and future.

Most of the research is focused on determining flood risk in urbanized areas. In this paper, the protected areas affected by potential floods are studied. Protected areas are according to a directive Directive 2009/147/EC of the European Parliament and of the Council of 30 November 2009 on the conservation of wild birds and Council Directive 92/43/EEC of 21 May 1992 on the conservation of natural habitats and of wild fauna and flora. The selected study area is the Batova River catchment. A large part of it is a protected area under both directives and there are recorded a lot of significant floods. The software product HEC-RAS, version 6.0, was used to determine the flooded areas. Flood maps are created for three scenarios: 20-, 100- and 1000-years.

The data used to simulate flash floods are precipitation from monitoring network of the National Institute of Meteorology and Hydrology (NIMH), a Digital terrain model with pixel cell 6/6m from Military Geographical Service at the Ministry of Defense of the Republic of Bulgaria and land cover data from CORINE Land Cover 2018.

As a result of the modeling, the inundated areas during rain with different return period have been determined. An analysis was made of the extent to which they affect the protected areas. This approach can also be applied to other watersheds. Based on these studies, an appropriate set of measures could be drawn up to protect these areas and the endangered species whose habitats fall within them and contribute to the preparation of Flood Risk Management Plans.

By integrating floodplain management and wildlife conservation, such as the protection of habitat communities have the opportunity to reduce flood risk, and protect species and their habitat while enjoying the natural resources.

Keywords: flood hazard map, protected areas, HEC-RAS, habitats

INTRODUCTION

There is no doubt that global climate change has an impact on the frequency and magnitude of flash floods [1]. Most studies related to Flood hazard are focused on urbanized areas. In order to save biodiversity, measures are needed to preserve protected areas from the harmful effects of floods. It is important to define the protected territories under threat of flooding. The adverse impact of this event on flora and fauna includes not only direct losses but also indirect ones due to the lack of food and shelter after flooding as well as possible contamination of water resources and soil in the affected

area. Directive 2000/60/EC of the European Parliament and of the Council establishing a framework for Community action in the field of water policy [2] focuses on this problem. This paper presents an approach for the creation of flood hazard maps in protected areas for three flood scenarios based on 20-, 100- and 1000-year return periods of 24 h max precipitation totals. The pilot watershed chosen for the research is Batova River watershed. A significant territory of the watershed is a protected area under Directive 2009/147/EC of the European Parliament and of the Council of 30 November 2009 on the conservation of wild birds and Council Directive 92/43/EEC of 21 May 1992 on the conservation of natural habitats and of wild fauna and flora. The frequency of historical floods in the watershed is also a factor for selecting this watershed – there are 9 floods recorded for the period 2011-2017.

STUDY AREA

The watershed of Batova River is located in northeastern Bulgaria (Fig. 1). The river is 38.4 km long and the area of the watershed is 443 km^2. The average elevation of the watershed is 236.7 m.

A large part of the watershed is a protected area under two EU directives. The protected area of Directive 2009/147/EC [3] is about 86% of the total watershed area, and according to Council Directive 92/43/EEC [4] it is about 41 % (Fig. 1).

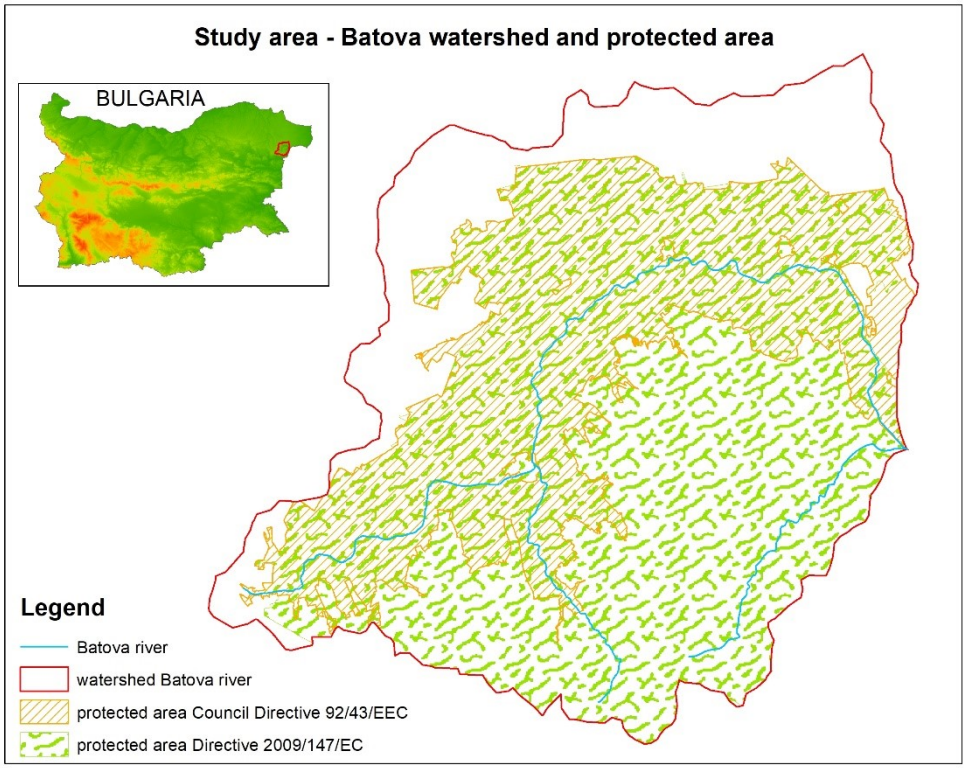

Figure 1 Study area

METHODS AND MATERIALS

The two-dimensional HEC-RAS software version 6.0 [5] is used for modelling the flooded areas. This product is widely used in hydraulic modeling and in recent versions a rainfall-runoff module was added. This is a possibility of using a combined hydrological and hydraulic model for the purposes of the study.

A Digital Elevation Model (DEM) with a pixel size of 6/6 m, developed by the Military Geographical Service at the Ministry of Defense of the Republic of Bulgaria is used for model setup. Manning's 'n' parameter is evaluated using land cover information from Corine Land Cover 2018. Analyzing modeling results and the time of computation several iterations for developing the computational mesh are done. Finally the computational mesh for simulations is 50/50 m cell size. Synthetic hyetographs calculated using the Sokolovsky method [6] are boundary conditions for the 2D flow model (figure 2). One station in the watershed and two more located close to it from NIMH's monitoring network are used in this study (figure 2). Maximum 24-hour rainfall amounts data are used to evaluate the precipitation with 20-, 100- and 1000-year return periods. For the downstream boundary condition normal depth is assumed.

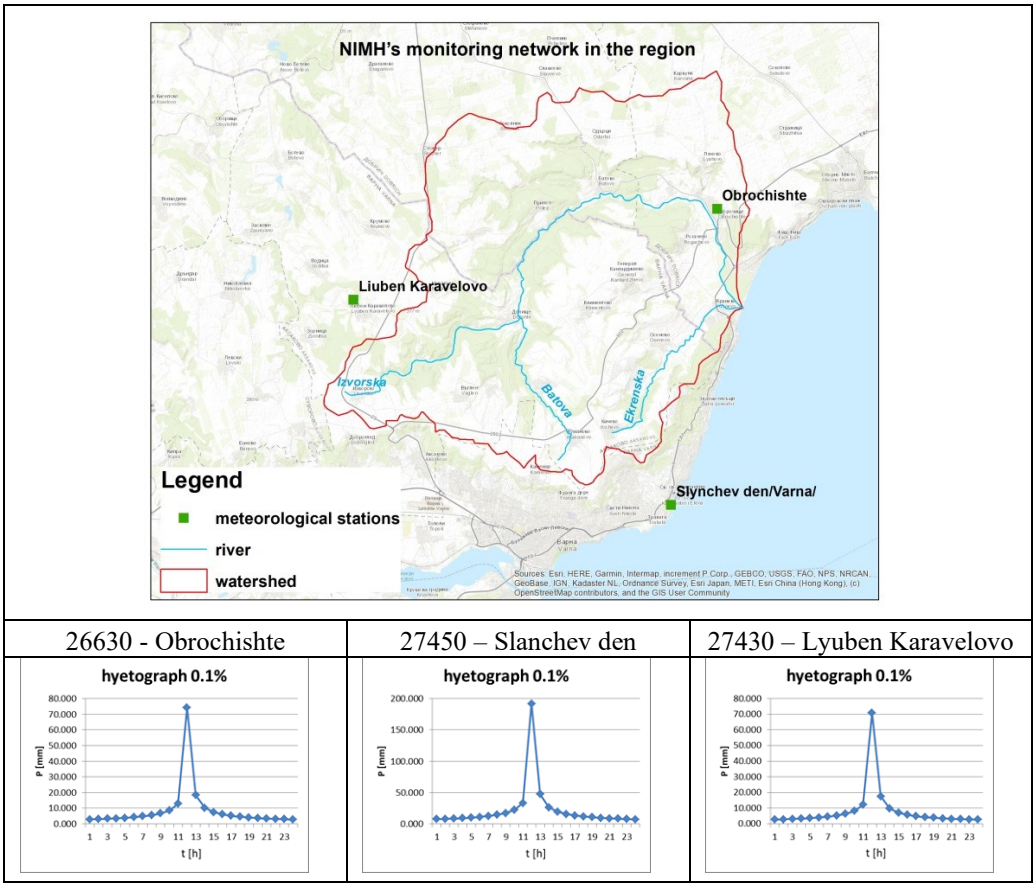

Figure 2 Meteorological stations in the region and synthetic hyetographs with 1000-year return period

The simulation is performed using the equation of the diffusion wave and a time step of 30 s. It is widely accepted by specialist the computational time step (seconds) to be half of the mesh size in meters [7]. Three simulations are performed with hyetographs data for the three scenarios chosen.

RESULTS AND DISCUSSION

The simulation results from the HEC-RAS model are further analyzed and processed using GIS-based environment. Flood hazard maps indicating different characteristics are created.

https://doi.org/10.5593/sgem2023V/3.2/s12.15

Figures 3, 4, and 5 present the flood hazard maps with the flood extent for the different scenarios in the protected area according to the Council Directive 92/43/EEC.

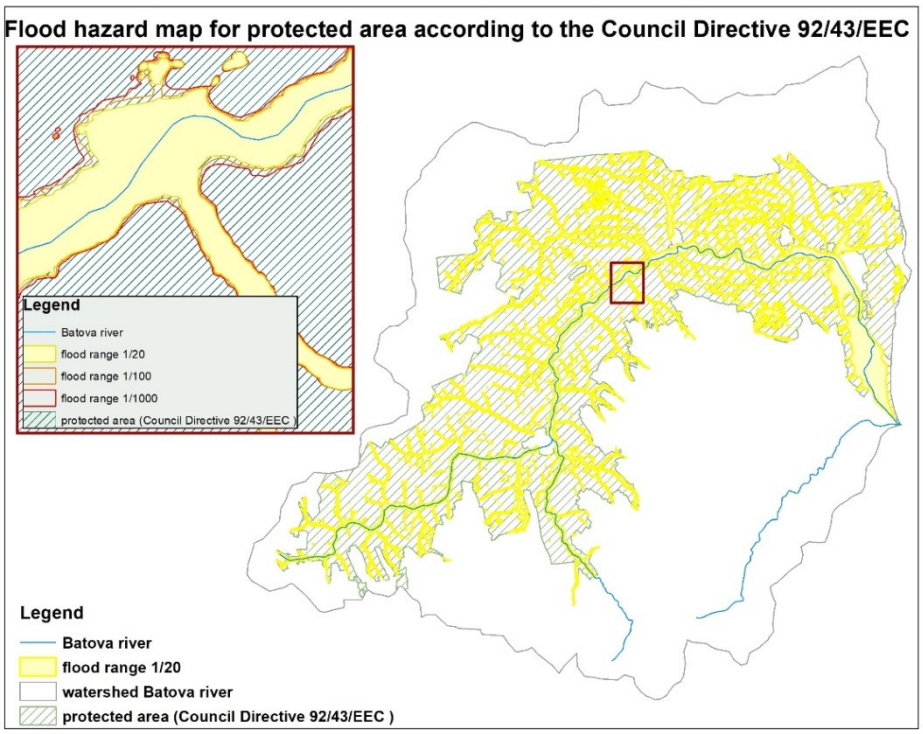

Figure 3 Flood hazard map with flood extent, return period of 1 per 20 years

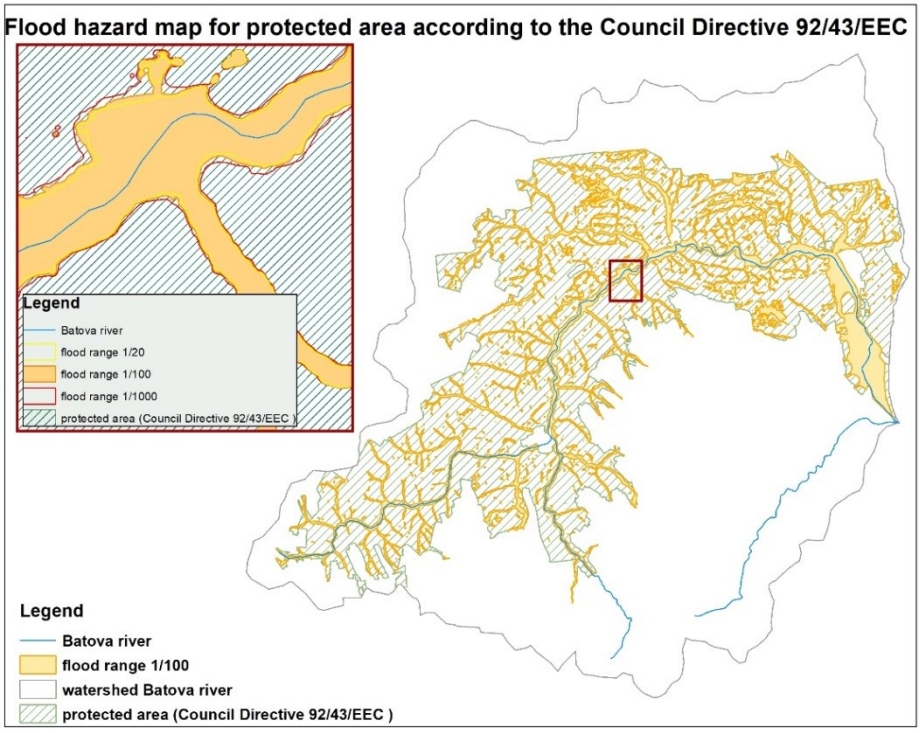

Figure 4 Flood hazard map with flood extent, return period of 1 per 100 years

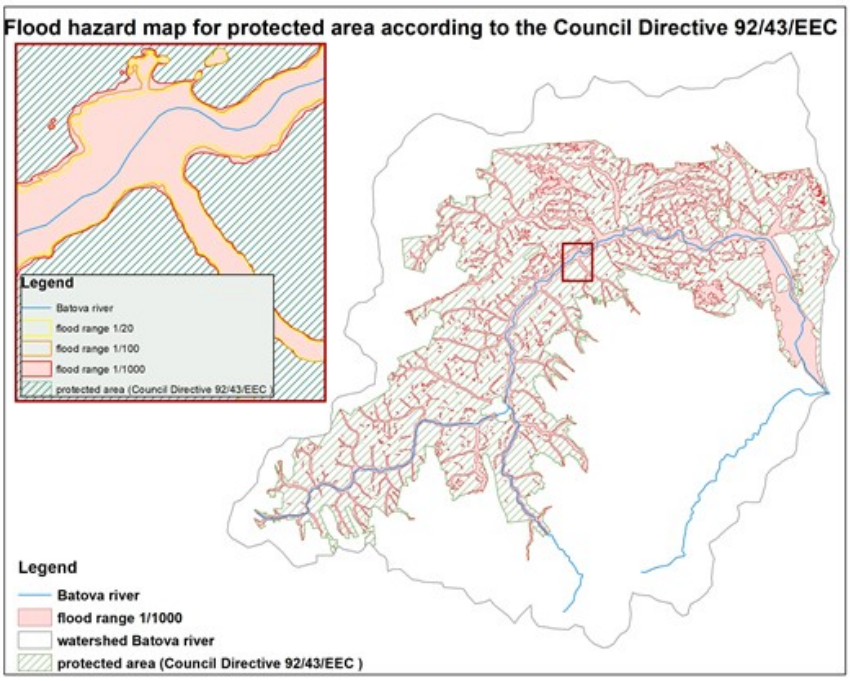

Figure 5 Flood hazard map with flood extent, return period of 1 per 1000 years

Flood hazard maps for the protected areas under Directive 2009/147/EC for the three scenarios are also created. On Figure 6 the scenario with a 1000-year return period is presented. The comparisons of the results of the three scenarios are presented in table 1.

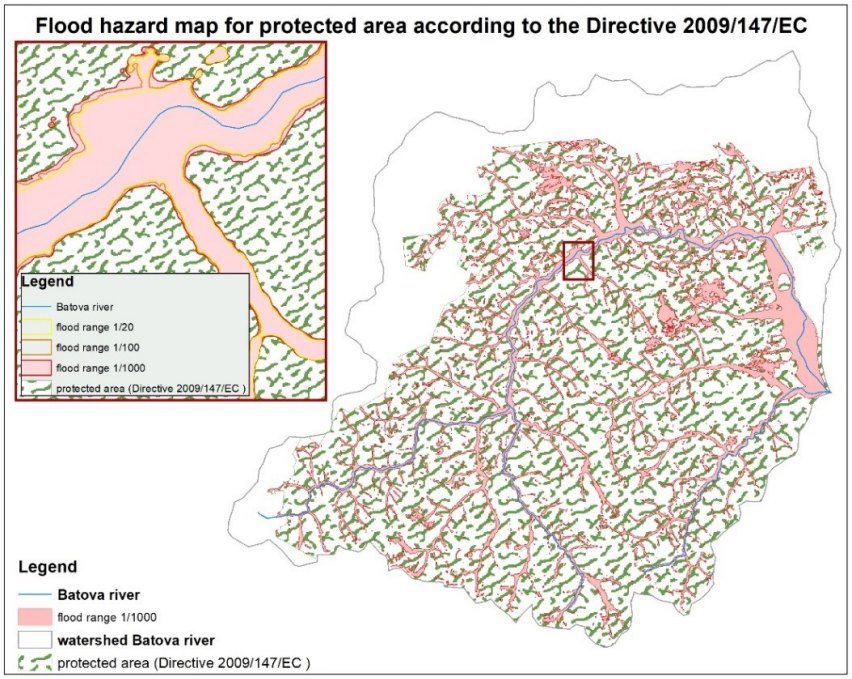

Figure 6 Flood hazard map with flood extent, return period of 1 per 1000 years

The areas of floodplains falling within the protected area have been determined and presented in percentage for each of the scenarios (table 1).

Table 1 Flooded area in protected areas

	Area [m²]	Area [km²]	Area [%]
Protected area according Council Directive 92/43/EEC	184592346.2	184.592	-
Affected area 20-years	30166863.36	30.167	16.34
Affected area 100-years	33596182.78	33.596	18.20
Affected area 1000-years	38649662.12	38.650	20.94
Protected area according Directive 2009/147/EC	381236131.1	381.236	-
Affected area 20-years	44149217.45	44.149	11.58
Affected area 100-years	50092134.9	50.092	13.14
Affected area 1000-years	59019261.55	59.019	15.48

Flood hazard is classified as hazard rank using a combination of the important characteristics of the flood regarding habitats existence [8, 9]. Along with the flood extent another major outputs of the 2D HEC-RAS model are the spatial distribution of water velocities and spatial distribution of water depth. This is the basis for determining the degree of threat depending on water depth and velocity (fig. 7).

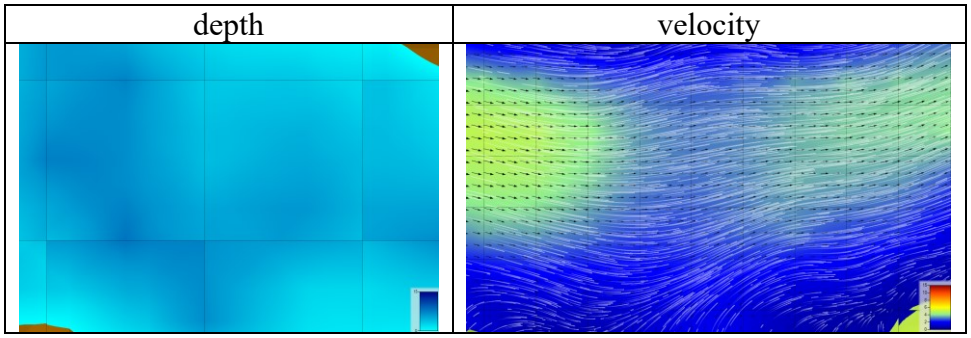

Figure 7 Spatial distribution of water depth and velocity in part of the affected area

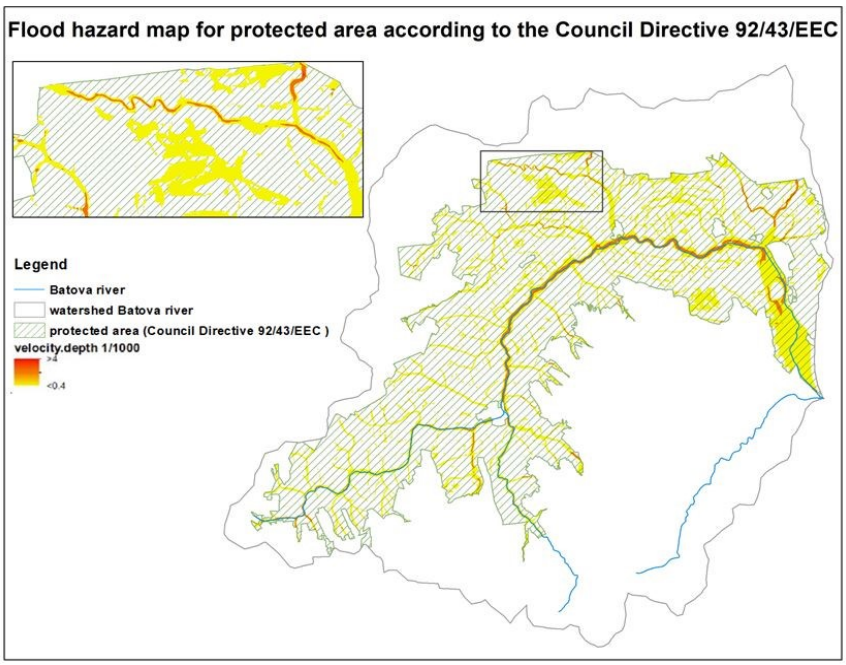

Figure 8 Flood hazard rank map for protected area according Council Directive 92/43/EEC

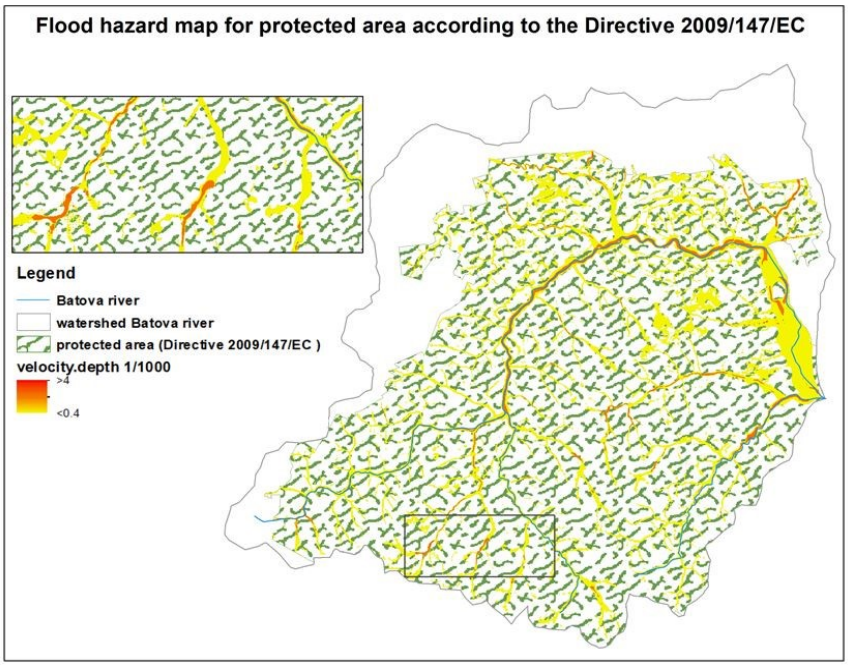

Figure 9 Flood hazard rank map for protected area according Directive 2009/147/EC

Hazard rank is highest in the river bed due to the high depths and high flow velocities. This is expected due to the morphological characteristics of the river bed. It is deep and narrow especially in the upper reaches and mountain tributaries. The map clearly shows that the hazard rank values are higher in the higher parts of the watershed, where the slopes of the terrain are steep therefore the current velocities are also higher.

CONCLUSION

The information from the flood hazard maps with the different characteristics of the flood is the basis for assessing flood risk. Analyzing the spatial distribution of flood characteristics and their combination helps identify the most vulnerable areas prone to flooding as discussed above.

Flood hazard maps are an import tool for the decision makers in preparing prevention and protection against future floods in vulnerable areas.

The results from this study showed that the percentage of flooded areas in protected territories is significant so outlining measures in the Flood Risk Management Plans for protected areas is needed.

The results from this research showed that the proposed approach for studying flood hazard in protected areas could be applied to other areas of interest.

Floodplain management together with wildlife conservation including the protection of habitat communities is a non-structural measure for flood risk mitigation and protection of species and their habitats.

ACKNOWLEDGMENTS

Acknowledgments for the financial support of the National Program "Young scientists and postdoctoral fellows-2" at the Ministry of Education and Science (MES) under the Decision of the Ministry of Education No. 206/07.04.2022.

REFERENCES

[1] Prama, M., Omran, A., Schröder, D., & Abouelmagd, A. (2020). Vulnerability assessment of fash foods in Wadi Dahab Basin, Egypt Environmental Earth Sciences (2020) 79: 114

[2] Directive 2000/60/EC of the European Parliament and of the Council establishing a framework for Community action in the field of water policy

[3] Directive 2009/147/EC of the European Parliament and of the Council of 30 November 2009 on the conservation of wild birds, https://eur-lex.europa.eu/LexUriServ/LexUriServ.do?uri=OJ:L:2010:020:0007:0025:en:PDF

[4] Council Directive 92/43/EEC of 21 May 1992 on the conservation of natural habitats and of wild fauna and flora, https://eur-lex.europa.eu/legal-content/EN/TXT/?uri=celex%3A31992L0043

[5] https://www.hec.usace.army.mil/software/hec-ras/

[6] Соколовски, РЕЧНИЙ СТОК, Гидрометеорологическое издателство, Ленинград, 1959

[7] EA/2/2 Appendix 5- Sun Yan Evans - Environment Agency (2010) Hydraulic Analysis and Design, Practical application of hydraulic modelling. In R.J. Crowder, Fluvial Design Guide

[8] Stoyanova, V., Balabanova, Sn., Yordanova, V. EVALUATION OF THE THRESHOLDS FOR FLOOD FORECASTING AND WARNING. Electronic book with full papers from XXVII Conference of the Danubian Countries on Hydrological Forecasting and Hydrological Bases of Water Management, 2017, ISBN:978-954-90537-2-2, 435-443

[9] METODIKA TVORBY MAP POVODŇOVÉHO NEBEZPEČÍ A POVODŇOVÝCH RIZIK prosinec 2009 poslední aktualizace 13. 3. 2012

FLOODING ASSESSMENT OF SALT MINING AREAS TO REDUCE THE THREAT OF TRANSBOUNDARY SPREAD OF SALINE POLLUTION

PhD Svitlana Stadnichenko

PhD Tetiana Kril

PhD Natalia Siumar

Prof. Dr.Sc. Stella Shekhunova

Institute of Geological Sciences of the NAS of Ukraine, **Ukraine**

ABSTRACT

The former mining of rock and potassium salt deposits in Transcarpathia and Nearcarpathia (western Ukraine) has a potential impact on water resources and the transboundary spread of saline pollution (e.g. Solotvyno rock salt deposit on the banks of the Tisza River on the Ukraine-Romania border; Kalush-Golyn potassium-magnesium salt deposit in the Dniester River basin). The threat of pollution spreading increases during floods, flash floods, and flooding. The aim of the study is to determine the extent of possible flooding based on the analysis of natural and man-made factors and using remote sensing data. The probabilistic, comparative-analytical and statistical methods, mechanical and mathematical bases of engineering geology in a complex with system analysis approaches were used in research. Geological, engineering-geological, hydrogeological and remote sensing data (Sentinel-1A) have been processed using a geoinformation system to the database of indicators of flooding processes. The territory is ranked according to the probability of flooding. The probability of flooding varies from 0.03 to 0.75 within the floodplain of Tisza river, 0.8-1.0 in places with a high groundwater level at settlement. The highlighted areas by GRD processing images (Sentinel-1A mission) according to the data of 2 flash floods indicate the probable places for flooding development in additional abnormal synoptic precipitation. The water mineralisation assessment on the flooding risk zones was based on the data of hydrological stations and wells for the Quaternary aquifer. The mapping shows that the flood zone includes areas of increased mineralisation (up to 13 g/l), but in the conditions of significant water inflow during a flood, the capture of such mineralisation would not lead to chloride concentration increase in the river after the flood. The developed schemes are proposed for use by municipal authorities in risk management programs.

Keywords: Flooding, salt mining area, water pollution, geological hazard, risk, probability, remote sensing data

INTRODUCTION

Potential impact on water resources and transboundary spread of saline pollution are caused by the former mining of rock and potassium salts in the Transcarpathia and Nearcarpathia (western Ukraine), for instance, Solotvyno rock salt deposit, located on the banks of the Tisza River on the Ukraine-Romania border and Kalush-Golyn potassium-magnesium salt deposit in the Dniester River basin. According to the report of the Updated Integrated Tisza River Basin Management Plan “The Tisza River Basin is an

important European resource with a high diversity of landscapes which provides habitats for unique and rich biodiversity of species including endemic ones" [1]. Therefore, assessing the risks of possible pollutant discharges into these water bodies is a crucial task.

The threat of pollution spreading increases during floods, flash floods, and flooding. Rising groundwater levels and persistent disruption of the natural moisture regime cause adverse changes in the geological environment, deterioration of production and living conditions. Especially for the settlement territories, flooding is a significant hazard. It can become a trigger for other hazardous engineering and geological processes, such as landslides and karst, and leads to economic losses. Flooding occurs both in natural conditions and under the influence of man-made factors, such as abnormal synoptic situations, leaks from water supply networks, and in mountainous areas - a consequence of the conservation of mines.

In June 2020, after several days of heavy rainfall and thunderstorms in the Carpathian region, the level of the Tisza River rose, a dam broke, a bridge was destroyed, etc [2], High water levels in the rivers of the region on 20-22 May 2019 due to intense rains caused a flood of dozens of households and farmland, destruction of bridges and bank protection [3].

The area under consideration is located next to Ukraine's state border with Romania, Hungary and Slovakia. The negative impacts of salt mining in Solotvyno have included landscape degradation as a result of uncontrolled salt karst development, and pollution of surface and groundwater, all of which give neighbouring states reason to be concerned about the threat of cross-border deterioration of the environmental pollution parameters of the Tisza River. In 2015 the Ministry of Foreign Affairs of Ukraine and Hungarian governmental organisations initiated an appeal to the EU to send an expert mission to Ukraine. At the end of 2016, the report with the recommendations of the EU expert mission to Ukraine on the situation in Solotvyno was officially handed over to the Ministry of Foreign Affairs of Ukraine and the State Emergency Service. Although the EU expert mission to Ukraine in Solotvyno has not identified a significant level of salt contribution from the assessed area into the Tisza River, since the ending of mining operations in 2010, further investigation and regular monitoring is required.

Previous cross-border research with the participation of scientists from the Institute of Geological Sciences of the National Academy of Sciences of Ukraine (IGS NASU) focused on the identification and description of natural and anthropogenic hazards, their mapping, analysis and ranking within the framework of the project ImProDiReT-783232 (2018-2020) with the support of the European Commission's Directorate-General for Civil Protection and Humanitarian Aid DG ECHO, which resulted in a new risk maps of Solotvyno [4].

The Revital I (HUSKROUA/1702/6.1/0072) grant project under the Hungary-Slovakia-Romania-Ukraine ENI CBC Programme continued research in this area, resulting in the development of a plan for a comprehensive monitoring system for the Solotvyno mining area and surroundings. At the moment, research on these projects has been completed, and Ukraine is currently handling the problem.

Considering the threat of transboundary spread of saline pollution, the aim of this study was to determine the extent of possible flooding based on the analysis of natural and man-made factors and using remote sensing data.

MATERIALS AND METHODS

The GIS database for Solotvyno territory (geological, hydrogeological, engineering-geological, etc.) developed at the IGS NASU and the assessment results of the natural and man-made hazardous processes manifestations were used in current studies [4].

Regarding general geological information, the Solotvyno salt dome is located in the central part of the Solotvyno depression, where the Tortonian and Sarmatian strata are widely developed. The relief of the study area has a structure of steps of floodplain terraces. The salt stack is located within the second and partially the first floodplain terraces. These terraces are separated by ledges 25-30 m high. Hydrological elements are represented by wetlands, lakes, and streams (the largest of which are Izvor, Hlod, Mlynskyi, etc.); their activity intensifies karst, karst-suffosion, and erosion processes. The total surface and near-surface (ground) flow in the Tisza River has changed significantly over the past hundred years and is determined by temporary drainage by mines, drainage shafts, pits, special drainage and other facilities, karstic forms and groundwater backwater by the Tisza River channel flow (primarily during floods).

The risk of flooding, like any risk of disaster, can be characterized by the exposure of vulnerable objects to a hazard, in this case a temporary presence of water [5-7]. These two main factors (vulnerable objects and hazards) are themselves influenced by multiple interconnected factors, such as land use, urbanization and meteorology (Figure 1).

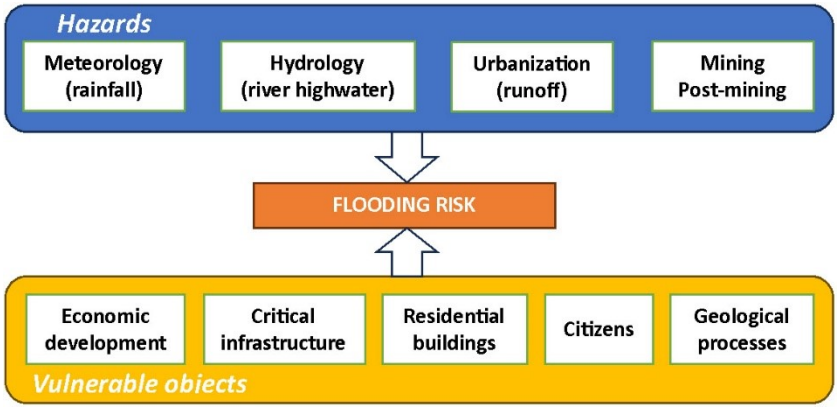

Fig. 1. Flooding risk Components.

Assessment of the degree of hazard and risk from the flooding process requires an evaluation of the susceptibility of the territory to negative processes and the vulnerability of the hazard object to the impact of flooding and other hazardous geological processes caused by it.

1. Vulnerability is characterised by the response of the object to the hazardous impact. The assessment of flood hazard, exposure of the built-up area to hazardous processes, vulnerability of the hazard object and risk from the flooding process at the local level was performed in this order:
2. Zoning by natural conditions of flooding formation. The morphological characteristics of the territory, hydrography, presence of engineering and geological processes, flood areas, hydrogeological conditions (groundwater level) are taken into account.

3. Zoning by anthropogenic factors affecting flooding. Water supply systems whose failures can lead to changes in the groundwater level are taken into account. Separation of the mining industry and technological processes.
4. Zoning by flooding hazard. This takes into account the position of the groundwater level, which causes flooding of the territory; changes in groundwater quality, which leads to groundwater pollution (mineralisation), changes in their aggressiveness towards reinforced concrete and metal structures, salinisation of soils in the aeration zone; changes in the physical and mechanical properties of soils, which leads to additional subsidence, and a decrease in the bearing capacity of soils.
5. Zoning according to the vulnerability of territories to flooding. This zoning takes into account the functional purpose of the territory: industrial, rural, recreational, roads (highways, railways), agricultural, and unused areas. For industrial areas, the division by industry is applied. Residential areas are divided by the number of storeys of buildings, where the presence of basements and underground structures is important.
6. Zoning by risk from flooding processes. The degree of risk of flooding is assessed based on the principle of intersection of the degree of hazard and the degree of vulnerability obtained earlier.

Remote sensing data were used to create a scheme of probable locations of flooding development under additional abnormal synoptic situations. A set of available free images of Sentinel-1A mission during the period of 2019-2020 [8]. They are in the Level-1 Ground Range Detected (GRD) format, VV polarization, spatial resolution – 10×10 m.

In order to determine the flooded area after abnormal meteorological conditions (rainstorms), a pair of satellite images was used in each case, to which the following procedures were applied Calibration, Speckle Filtering, Terrain Correction, Stack Creation, RGB Image. Sigma 0 which is ratio instant to receive backscatter per unit area in ground range is leave default under the Calibration [9-11]. Creation an RGB composite was to distinguish between the flooded areas and the permanent water bodies. The image before flooding was used for the red band, for the green and the blue bands – the image under flooding pike. The flooded areas appear in red as will have a high response in the red channel compared to others. Sentinel Application Platform (SNAP) software was used to perform processing steps.

RESULTS

The flooding of Solotvyno is the result of complex hydrogeological conditions, which have been exacerbated by decades of rock salt mining. Groundwater regime changes caused by economic activity can cause changes in engineering and geological conditions over a large area in a short time, which in turn leads to the intensification of hazardous processes. The floodplain area falls within the flood zone of the Tisza River and requires mapping and risk assessment. During the extremely high floods that were recorded here in October 1926, May 1970, November 1998 and March 2001, May 2019 and July 2020, flooding up to 1.9 m high and covering an area of up to 4 sq. km was recorded within the floodplain; the water level in the Tisza River at the current location of the automatic hydrograph reached 263 m, compared to the annual average of 257.8-261.2 m [12]. Figure 2 shows the results of processing satellite images after the floods in 2019 and 2020 caused by excessive precipitation. In both cases, water spills within the floodplain (marked in red) reached up to 350 m, and agricultural land was also flooded.

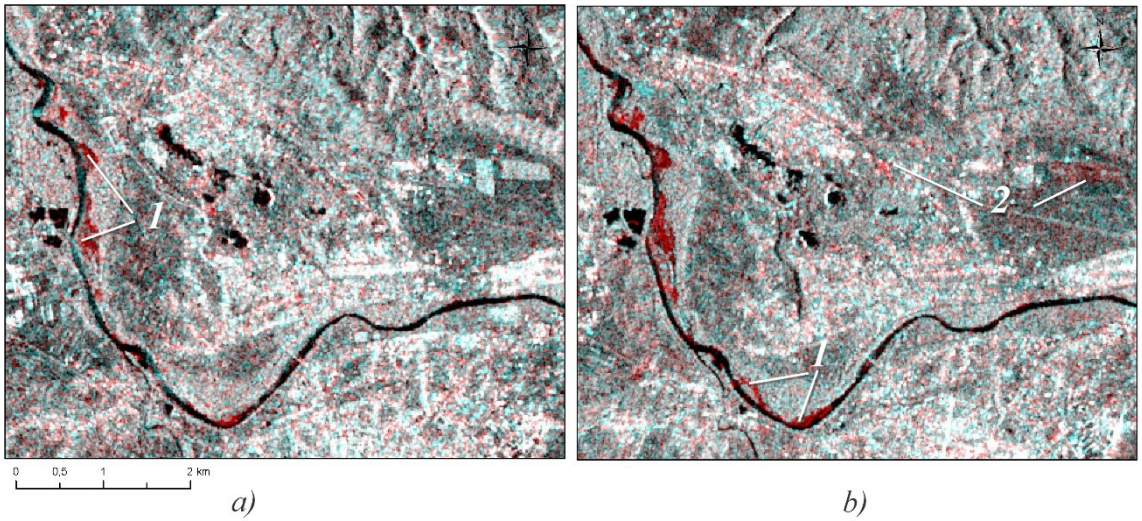

Fig. 2. Flooded areas of floodplains (1) and agricultural fields (2) as a result of the floods of 20 May 2019 (a) and 27 July 2020 (b).

The floodplain area is also characterised by the development of natural flooding. Parameters of the main horizon of alluvial deposits of the floodplain: depth of 0.5-2.5 m, amplitude of water level fluctuations 1.0-1.5 m, thickness 3.5-32 m, confined to boulder and pebble deposits with heterogeneous filtration properties (filtration coefficient 10-1375 m/day).

On the continuation of the salt dome axis downstream, the spread of saline and brackish waters over a distance of 1000 m to the end of the floodplain terrace is noted [13]. In addition, within residential areas, there is an unsatisfactory functioning of the stormwater drainage system (catchment trays are partially destroyed or covered with household waste), and the presence of zones of artificial groundwater backwater near the location of street embankments, highways and railways.

The most intensive flooding occurs in areas adjacent to the river floodplain, streams, canals or mine shafts, etc. The highest probability of flooding was estimated at 1 to 0.8 in sections 1-2 of the Tisa floodplains and along the Hlod stream, with the central flat and slightly sloping sections having a range of probability values of 0.3-0.6, and the sloping part of the second floodplain terrace having a probability of 0.3. Flooding within the built-up area, where there is a persistent violation of the natural environment, moisture and groundwater level rise, leads to a significant deterioration in residential conditions, the functioning of economic facilities and contributes to the occurrence of emergencies. Critical infrastructure facilities are located within the areas with a high probability of flooding: the railway, the section of the national road H09, and the sewage treatment plant system.

Floodplain areas and the first floodplain terrace of the Tisza River have the highest probability of flooding – 0.5-0.75. Therefore, special attention should be paid to the protection of a water supply and wastewater facilities located in flood zones. Based on the analysis of archival materials and expert assessment, the second floodplain terrace is classified as an area with a flood probability of 0.03. However, despite the low value, the presence of residential development in the southern and south-eastern parts increases the magnitude of the possible economic risk.

Analysis of the mapping of surface and groundwater mineralisation isolines on the flooding risk zones as of July 2020 was provided (based on the pre-monitoring data within the framework of the REVITAL 1 project, carried out by partners of the University of Miskolc, Hungary) Fig. 3A. At high water levels in the Tisza River, during floods, pressure gradients in the alluvium at the Solotvyno deposit change. This is particularly relevant for the Tisza River floodplain, which may lead to the mobilisation of mineralised water present in the alluvium). The impact depends on the concentration and time, while likelihood of major floods on the Tisza River is unpredictable due to climate change (flash floods). The obtained plot shows that the flood zone includes areas of increased mineralisation (up to 13 g/l), but in the conditions of significant water inflow during a flood, the capture of such mineralisation would not lead to chloride concentration increase in the river after the flood.

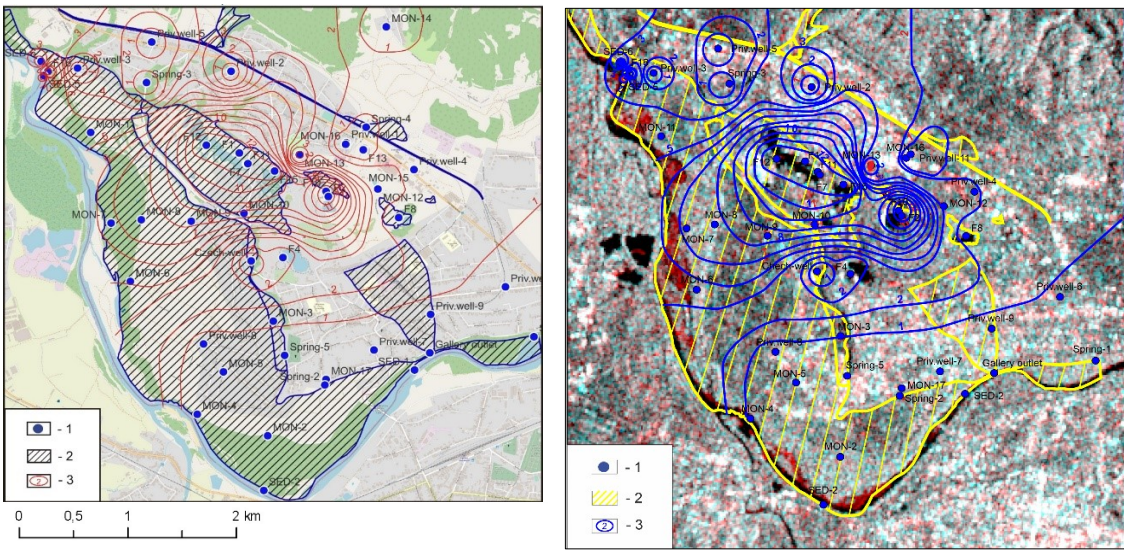

Fig. 3. Visualisation of the assessment of the flooding susceptibility zones of the study area with the water mineralisation isolines (*a*) and comparison of space images processing results with potential flooding zones (*b*). Legend: 1 – wells; 2 – flooding susceptibility zones; 3 – water mineralisation isolines (based on the data of hydrological stations and wells for the Quaternary aquifer) as of July 2020.

To verify obtained results on space images processing compared with potential flooding zones was done (Fig. 3. *b*). It can be seen that obtained flooding areas as of July 2020 fits into previously provided potential flooding zones, confirming the reliability and accuracy of the results of satellite image processing.

DISCUSSION

For more than 230 years, salt-mining companies have been town-forming. The consequence of salt mining became surface subsidence, karst-suffusion processes intensification, the formation of karst-suffusion sinkholes and catastrophic collapses, which have been gradually filling up with water and turning into lakes of various salinity. The main hazard for this area is dissolution (karstification) of the salt, suffusion, sinkholes formation and ground subsidence. Currently, the system "host rocks – salt body – groundwater" and surface water of the Solotvyno study area, according to the results of

field and instrumental studies, as well as the analysis of model constructions, is in a quasi-equilibrium state. This is confirmed by the fact that since 2008 there has been no increase in chlorine content in the Tisza River [14], however, there are many factors that can significantly disrupt this equilibrium, and flooding is one of them. Other factors include active anthropogenic activities and uncontrolled use of brine from karst sinkholes for recreational purposes and/or other anthropogenic activities within the village [15].

The main threat concerns the sudden breakthrough of a large volume of highly mineralised mine water (karst horizon) due to the destruction of the integrity of the salt body and/or the surrounding shielding rocks. There is a possibility that the event will lead to an increase in chloride concentration, that could result in thresholds being exceeded downstream.

It can be concluded that in order to gain a full understanding of the process, including important aspects and consequences of flooding, by integrating remote sensing data with the results of underground and field studies, a significantly improved interpretation and prediction can be achieved, which is also important for risk forecasting, assessment and management.

Monitoring groundwater quality is one of the most important aspects of protecting water resources. This is best achieved by establishing a network of monitoring wells. The most essential action in the given state is the implementation of the proposed comprehensive monitoring system plan, which will allow to control the situation, detect undesirable environmental impacts, record the manifestations of hazardous processes within the studied area at early stage and effectively take appropriate timely measures.

CONCLUSION

Summing up, with SAR data, the flooding after inclement weather can be mapped. As a result, the highest probability of flooding was estimated at 1 to 0.8 in sections 1-2 of the Tisa floodplains and along the Hlod stream. Critical infrastructure facilities are located within the areas with a high probability of flooding: the railway, the section of the national road H09, and the sewage treatment plant system.

According to the analysis of model constructions as well as the results of field and instrumental studies, the system "host rocks – salt body – groundwater – surface water" of the Solotvyno study area is in a quasi-equilibrium state. There are many factors which can significantly disrupt this equilibrium, and flooding is one of them.

The developed schemes are proposed for use by municipal authorities in risk management programs. At the same time, it emphasises the need to implement a monitoring system to protect against the transboundary spread of surface and groundwater pollution.

ACKNOWLEDGEMENTS

The research was carried out under the state budget-financing program CPCEL 6541230 "Support for the development of priority research areas".

REFERENCES

[1] Updated Integrated Tisza River Basin Management Plan (2019). Interreg Danube Transnational Programme – JOINTISZA. 129 p. URL: https://www.icpdr.org/sites/default/files/nodes/documents/updated_itrbmp_2019.pdf

[2] Gavrilenko V. Bukovina is preparing for evacuation due to flooding: a red alert level has been announced. URL: https://24tv.ua/ru/navodnenie-chernovcy-23-ijunja-2020-oblasti-krasnyj-uroven_n1365992

[3] Transcarpathia was covered by heavy water. (2019) Mukachevo.net. URL https://www.mukachevo.net/ua/news/view/504036

[4] Shekhunova S.B., Aleksieienkova M.V., Meijer S., Stadnichenko S.M., Yakovlev E.O. Monitoring of hazardous geological processes as a tool for risks minimization on post-mining areas in Solotvyno (Transcarpathia). EAGE XIII Int. Scient. Conf. "Monitoring of geological processes and ecological condition of the environment", 12-15 November 2019, Kyiv, Ukraine. https://doi.org/10.3997/2214-4609.201903197

[5] Shekhunova S., Kril T. Geological and economic risk assessment for territories of hazardous geological and technogenic processes (exemplified by Solotvyno township). Naukovyi Visnyk Natsionalnoho Hirnychoho Universytetu. 2022, (2): 079 – 085 https://doi.org/10.33271/nvngu/2022-2/079.

[6] UN Sendai Framework for Disaster Risk Reduction 2015-2030. 2017. 36 p. URL: https://www.undrr.org/publication/sendai-framework-disaster-risk-reduction-2015-2030

[7] Rudenko L., Dronova. O. (2014) Evaluation and mapping of state of emergency risk in Ukraine european context. Ukrainian Geographical Journal, 1, Pp. 53-60. https://doi.org/10.15407/ugz (In Ukrainian).

[8] The Copernicus Open Access Hub. (2022). URL: https://scihub.copernicus.eu/dhus/#/home

[9] Flood mapping tutorial SENTINEL-1. 2019. URL: https://step.esa.int/docs/tutorials/tutorial_s1floodmapping.pdf

[10] Wakabayashi, H., Motohashi, K., Kitagami, T.,Tjahjono, B., Dewayani, S., Hidayat, D., Hongo, C. Flooded Area Extraction of Rice Paddy Field in Indonesia Using Sentinel-1 SAR Data. ISPRS International Archives of the Photogrammetry, Remote Sensing and Spatial Information Sciences, Volume XLII-3/W7, 2019, pp. 73-76. https://doi.org/10.5194/isprs-archives-XLII-3-W7-73-2019

[11] Navacchi, C., Cao, S., Bauer-Marschallinger, B., Snoeij P., Small, D., Wagner, W. Utilising Sentinel-1's orbital stability for efficient pre-processing of sigma nought backscatter. ISPRS Journal of Photogrammetry and Remote Sensing, Volume 192, 2022, P. 130-141, ISSN 0924-2716, https://doi.org/10.1016/j.isprsjprs.2022.07.023

[12] Transcarpathian region. Planning Scheme. V. 1. Explanatory note., 2011. 200 p. URL: https://zakarpatoblarch.gov.ua/wp-content/uploads/2019/01/130517_731-I.pdf

[13] Frolov, M.V., 1973. Report. Preliminary exploration of natural brines Solotvyno rock salt deposit in the 1971-1973, Heoinform Ukrainy, inv. No 35329, vol. 1, 83 p.

[14] EUCPT Risk Assessment Report (2016), Advisory Mission to Ukraine "Solotvyno salt mine area", EU–Union Civil Protection Mechanism, 134. URL: https://environmentalrisks.danube-region.eu/mdocs-posts/eucpt_risk-assessment-report-solotvyno-mine-area-final/ .

[15] Gutiérrez F., Parise, M. DeWaele J., Jourde H. A review on natural and human-induced geohazards and impacts in karst (2014) Earth-Science Reviews 138 (2014) 61–88. https://doi.org/10.1016/j.earscirev.2014.08.002

ICE PIER FOR WATER TRANSPORT

Sofiya Andreeva[1,2]

Elena Kudryashova[2]

Viktoriia Saveleva[2]

[1] Admiral Makarov State University of Maritime and Inland Shipping, **Russia**
[2] Peter the Great St.Petersburg Polytechnic University, **Russia**

ABSTRACT

Water transport in icy environments necessitates specialized infrastructure to facilitate safe and efficient movement. Ice piers, vital components in these regions, serve as critical pathways over frozen water bodies, enabling the traversal of ships and vessels. This overview encapsulates the scientific exploration of ice piers, focusing on their design, construction, functionality, and the advancements revolutionizing water transport in challenging icy terrains. The design of ice piers requires a holistic approach that considers various environmental factors, including ice thickness, temperature fluctuations, water currents, and load-bearing capacities. Structural engineers employ advanced modeling techniques and materials to ensure the stability and resilience of these structures under diverse conditions. Construction methodologies, ranging from traditional snow compaction to modern prefabricated modular units, underscore the diverse approaches used to build these piers. Innovative technologies play a pivotal role in the maintenance and sustainability of ice piers. Freezing/heating systems embedded within these structures, coupled monitoring ice conditions and facilitating timely maintenance. The article delves into the environmental impact of ice piers and emphasizes sustainable practices, such as eco-friendly materials and renewable energy sources, to minimize ecological disturbances. Work underlines existing challenges and outlines future research directions, emphasizing the need for materials, predictive models, and smart technologies to enhance the resilience and adaptability of ice piers.

Keywords: Ice Piers, Water Transport, Icy Environments, Structural Design, Construction Techniques, Environmental Impact, Risk Assessment

INTRODUCTION

Water transport in regions characterized by icy conditions presents a unique set of challenges, demanding specialized infrastructure capable of navigating frozen water bodies (figure 1). In these environments, ice piers emerge as crucial components, facilitating the movement of goods, people, and vessels across icy terrains during specific seasons. This introduction aims to elucidate the scientific intricacies and practical implications surrounding ice piers, examining their design, construction, and functionality in enabling efficient water transport in challenging icy environments [1-5]. Icy environments, prevalent in regions like the Arctic, Northern Canada, Scandinavia, and other polar or subpolar areas, pose formidable barriers to conventional transportation methods. Frozen water bodies obstruct the navigation of ships and

vessels, limiting accessibility to remote areas and hindering economic activities. Ice piers, also known as ice roads or ice bridges, play a pivotal role in overcoming these barriers by providing stable pathways across frozen water surfaces, allowing for the continuation of water transport during the ice-bound seasons. The strategic positioning and construction of ice piers contribute significantly to the connectivity and economic development of these regions. They serve as lifelines for communities, enabling the transport of essential supplies, supporting industries such as mining, fishing, and tourism, and facilitating communication between otherwise isolated areas. Therefore, understanding the intricate design principles, construction methodologies, and technological advancements associated with ice piers becomes imperative for enhancing connectivity and sustainability in icy environments [6-10]. The design of ice piers represents a convergence of various scientific disciplines, integrating aspects of structural engineering, environmental science, material science, and geotechnical engineering. Design considerations encompass a range of factors influenced by the dynamic nature of ice and its interaction with environmental conditions. Parameters such as ice thickness, temperature fluctuations, water currents, and load-bearing capacities must be meticulously analyzed and incorporated into the design process. Structural engineers employ advanced modeling techniques, including finite element analysis and computational simulations, to predict and comprehend the behavior of ice under varying conditions. These models aid in determining the optimal pier design that ensures structural integrity, stability, and safety while accommodating the unpredictability of ice dynamics. Furthermore, the choice of materials, such as alloys, composite materials, and innovative construction methodologies, enhances the durability and resilience of piers in harsh environments. The construction of ice piers encompasses a diverse array of methodologies influenced by regional conditions, available resources, and technological advancements. Traditional construction techniques involve compacting snow or using ice blocks to create a stable surface capable of supporting vehicular traffic. However, modern construction practices have evolved to incorporate prefabricated modular units and innovative materials, expediting construction while enhancing the overall durability and load-bearing capacities of ice piers. Advancements in autonomous construction vehicles and drones have revolutionized the construction process by offering precise surveying capabilities and aiding in the efficient assembly of ice pier components. The maintenance of ice piers is integral to ensuring their continued functionality and safety. Innovative technologies have been developed to address challenges related to ice accumulation and structural maintenance. Heating systems embedded within ordinary piers prevent excessive ice buildup, ensuring a navigable pathway for vessels. The utilization of self-repairing (ice is self-removing or self-melting) materials and adaptive structures is being researched to enhance the resilience of ice piers against environmental stressors, contributing to their longevity and sustainability. Incorporating renewable energy sources, such as solar or wind power, for freezing/heating systems and other operational requirements aligns with sustainable practices and reduces carbon footprints in these sensitive environments. Post-season restoration efforts, including removing pier components and restoring natural habitats, contribute to environmental conservation and ecological balance in these regions [11-15].

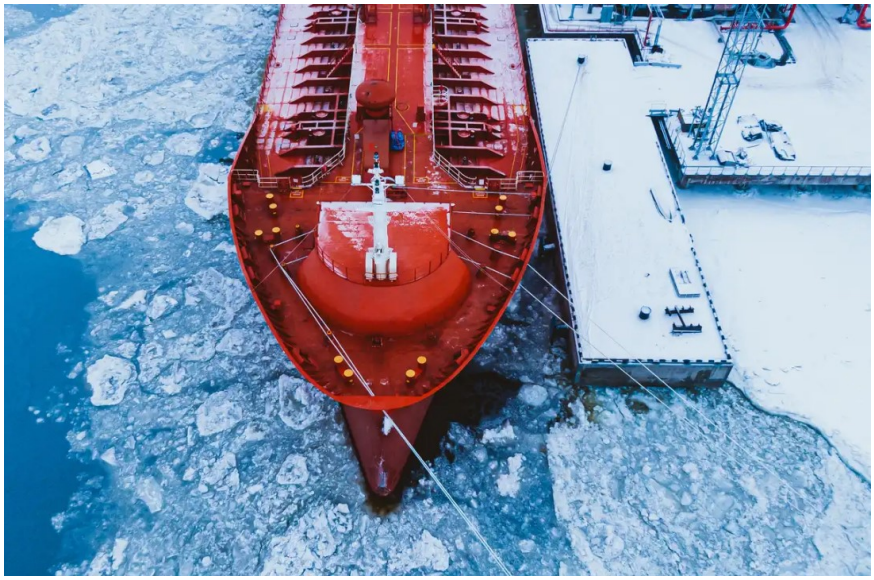

Fig. 1. Example of moorage in arctic conditions

MATERIALS AND METHODS

Designing ice piers demands a comprehensive understanding of the complex interactions between the built structure and the surrounding icy environment. Engineers and designers must account for various factors intrinsic to the nature of ice and the dynamic conditions prevalent in icy regions to ensure the stability, safety, and functionality of these critical infrastructures. Understanding the local climate patterns, ice formation dynamics, and variations in temperature and precipitation is fundamental. Factors such as ice thickness, ice layering, and the presence of snow cover on the water surface profoundly impact the load-bearing capacity and behavior of ice. This analysis forms the basis for predicting and modeling ice behavior under different conditions. Structural engineers employ sophisticated modeling techniques, such as finite element analysis and computational simulations, to evaluate the response of ice piers to various loads and stressors. The design must ensure adequate structural integrity, considering factors like the weight of vehicles and vessels, live loads, impact loads from shifting ice, and potential dynamic forces caused by winds or water currents. The choice of construction materials significantly influences the durability and resilience of ice piers. Alloys, reinforced concrete, and composite materials are often utilized to withstand the harsh environmental conditions. These materials are selected based on their ability to endure freezing temperatures, resist corrosion caused by exposure to water, and maintain mechanical strength despite temperature fluctuations. Ice is not a static material; it responds to environmental changes and external forces. Designing for this dynamic nature involves considering the flexibility and adaptability of the structure. Engineers incorporate allowances for ice deformation, expansion, and contraction to prevent structural damage and ensure stability during varying ice conditions. Proper load distribution across the ice pier surface is crucial to prevent localized stress concentrations that could weaken the structure. Additionally, the foundation design plays a vital role in distributing loads safely onto the ice without compromising its integrity. Techniques like spreading the load over a larger area and utilizing innovative foundation designs enhance the stability and reduce the risk of ice pier failure.

https://doi.org/10.5593/sgem2023V/3.2/s12.17

Incorporating safety measures, such as providing emergency exits, installing warning systems for changing ice conditions, and implementing load restrictions during uncertain periods, mitigates risks and enhances the overall safety of the ice pier for both users and the environment.

The construction of ice piers involves a blend of traditional methodologies adapted to modern innovations, aiming to create robust structures capable of withstanding harsh icy conditions while facilitating safe and efficient water transport. In regions where natural ice formations are abundant, traditional techniques often involve compacting snow or using blocks of ice to construct a stable surface. This method capitalizes on the existing ice and snow, compacting it to form a secure pathway. However, these methods are labor-intensive and highly dependent on favorable natural conditions for their success. Modern construction techniques have introduced prefabricated modular units that expedite the construction process and enhance the overall structural integrity of ice piers. These pre-manufactured components, often made of durable materials like reinforced concrete or composite materials, are designed to interlock and create a stable surface quickly. This approach reduces construction time, increases efficiency, and ensures consistency in the quality of the constructed ice pier. Advancements in construction materials have led to the development of innovative solutions specifically tailored for icy environments. Alloys, advanced composites are used to create durable components resistant to extreme temperatures and corrosive effects of ice and water. Additionally, the integration of smart technologies for surveying and autonomous vehicles for construction, streamlines the construction process, allowing for precise assembly and minimizing human exposure to hazardous conditions. The dynamic nature of ice and the unpredictability of environmental conditions necessitate adaptive construction techniques. Engineers and construction teams must continuously adapt their methodologies to changing conditions, altering construction approaches based on real-time assessments of ice stability and load-bearing capacity. This adaptability ensures the safety and longevity of the ice pier structure. Rigorous quality control measures during construction, such as adherence to design specifications, load testing, and comprehensive safety protocols, are crucial to ensure the reliability and safety of the constructed ice piers. Monitoring systems are often employed to assess the structural integrity and provide early warnings of potential issues, enabling timely interventions to prevent structural failures.

Despite significant advancements in ice pier technologies, several challenges persist, necessitating continuous innovation and research to address emerging issues and enhance the resilience of these critical infrastructures in icy environments. One of the foremost challenges faced by ice pier construction and maintenance is the impact of climate change on ice formation and stability. Rising temperatures and altered weather patterns contribute to unpredictable ice behavior, affecting the structural integrity of ice piers. Future research must focus on understanding the ramifications of climate change on ice dynamics and developing adaptive strategies to mitigate these effects. Increasing occurrences of extreme weather events, such as sudden thaws, storms, and rapid temperature fluctuations, pose significant threats to ice pier stability. Designing ice piers capable of withstanding these extreme conditions while maintaining structural integrity remains a critical challenge. Future directions involve exploring innovative materials and construction methodologies resilient to such extreme events. Developing accurate predictive models that forecast ice behavior and assess risks associated with varying

environmental conditions is crucial. Advanced modeling techniques incorporating data from sensors, satellite imagery, and real-time monitoring systems can aid in predicting ice formation, movement, and potential structural vulnerabilities. Integrating these models into the design and maintenance processes enhances preparedness and risk mitigation strategies. Balancing the construction and operation of ice piers with environmental sustainability remains a challenge. The ecological impact of constructing these structures on fragile ecosystems requires careful consideration. Future directions involve employing eco-friendly construction materials, adopting renewable energy sources for operational needs, and implementing effective environmental restoration measures post-season to minimize disturbances to local habitats. Continuing advancements in technologies, adaptive structures, and artificial intelligence for predictive maintenance, are crucial for enhancing the resilience and longevity of ice piers. Future research may focus on developing materials that dynamically adapt to changing ice conditions or integrating AI-driven monitoring systems for real-time structural health assessments.

CONCLUSION

Ice piers stand as indispensable lifelines in regions characterized by icy environments, enabling crucial water transport during seasons when frozen water bodies pose significant obstacles. The scientific exploration encompassing design, construction techniques, technological innovations, and the challenges surrounding ice pier development underscores their pivotal role in supporting connectivity, economic activities, and community livelihoods in these challenging terrains. The intricate design considerations for ice piers, integrating factors such as environmental conditions, structural integrity, material selection, and load-bearing capacities, underscore the complexity of creating resilient infrastructures capable of withstanding dynamic ice dynamics. Advancements in construction techniques, from traditional methodologies to modern prefabricated units and innovative materials, reflect the evolving strategies to enhance the durability, efficiency, and safety of ice piers. Challenges persist, notably stemming from climate change impacts, extreme weather events, predictive modeling limitations, and the need for sustainability in construction and operation. Addressing these challenges requires concerted efforts in research and development, encompassing adaptive strategies, predictive modeling advancements, and sustainable practices to ensure the viability and resilience of ice piers in changing environments. Future integration of cutting-edge technologies, monitoring systems, new materials, and predictive maintenance tools, holds promise in enhancing ice pier resilience and adaptability. Collaborative interdisciplinary research endeavors aimed at advancing predictive modeling accuracy, understanding ecological impacts, and developing eco-conscious construction methodologies will pave the way for sustainable ice pier development. Ice piers serve as vital links, fostering economic growth, supporting local communities, and connecting remote regions. Embracing innovation, sustainable practices, and robust infrastructure planning will be pivotal in overcoming challenges and ensuring the continued reliability and safety of ice piers for efficient water transport in icy environments. By addressing these challenges and charting innovative pathways, ice piers will continue to play a crucial role in enabling connectivity and fostering economic development in regions characterized by icy conditions.

ACKNOWLEDGEMENTS

This work was done as a part of Project « Study of statistical patterns of ice loads on engineering structures and development of a new method for their stochastic modeling (FSEG-2020-0021)", No. 0784-2020-0021» supported by the Ministry of Science and Higher Education of the Russian Federation.

REFERENCES

[1] Sharapov D., Shkhinek K., Numerical calculation of the ice grow and empirical calculation results, Research in materials and manufacturing technologies, PTS 1-3 Book Series: Advanced Materials Research Volume: 835-836 Pages: 1448-1454, Published: 2013.

[2] Andreeva, S.A., Sharapov, D. Hoek–Brown model for ice breaking simulation. Magazine of Civil Engineering. 2023. 123(7). Article no. 12303. DOI: 10.34910/MCE.123.3

[3] Sharapov D., Shkhinek K., DelValls T.Á., An estimation of the amount of the thermal energy for the moorage wall heating in the Arctic harbours to avoid ice accumulation, OCEAN ENGINEERING, Volume: 100 Pages: 90-96, Elsevier Published: MAY 2015. DOI:10.1016/j.oceaneng.2015.03.016

[4] Shi Y. A numerical investigation of ice-structure interaction using a discrete element model // Ocean Engineering. – 2016. – T. 118. – C. 274-287.

[5] Sharapov D., Shkhinek K., DelValls T.Á., ICE COLLARS, DEVELOPMENT AND EFFECTS, Ocean Engineering, Volume 115, Pages 189-195, Elsevier Published: March 2016. DOI:10.1016/j.oceaneng.2016.02.026

[6] Liferov P, Shkhinek KN, Vitali L, Serre N (2007) Ice gouging study - actions and action effects. Recent Development of Offshore Engineering in Cold Regions 1 and 2: 774-786.

[7] Sharapov D., Klochkov Y., Improving quality of 2D ice load estimation on freezed piles, International Journal for Quality Research v17, n4, 2023, DOI: 10.24874/IJQR17.04-11

[8] Sharapov D., BRIEF ON DEVELOPMENT OF ICE LOAD ESTIMATION FOR HYDROTECHNICAL ENGINEERING, Proceedings of 23rd International Multidisciplinary Scientific GeoConference SGEM 2023, Volume 23, Issue 2.1, ISBN 978-619-7603-57-6 DOI: 10.5593/sgem2023/2.1/s08.18.

[9] Keyang Liu, Baoping Cai, Qibing Wu, Mingxin Chen, Chao Yang, Javed Akbar Khan, Chenyushu Wang, Hasini Vidumini Weerawarna Pattiyakumbura, Weifeng Ge, Yonghong Liu, Risk identification and assessment methods of offshore platform equipment and operations, Process Safety and Environmental Protection, Volume 177, 2023, Pages 1415-1430, ISSN 0957-5820, https://doi.org/10.1016/j.psep.2023.07.081.

[10] Sharapov D (2023) Evolution of ice load prediction tools for hydrotechnical construction. E3S Web of Conf 402:05023. DOI: https://doi.org/10.1051/e3sconf/202340205023.

[11] Emma C. Edwards, Anna Holcombe, Scott Brown, Edward Ransley, Martyn Hann, Deborah Greaves, Evolution of floating offshore wind platforms: A review of at-sea devices, Renewable and Sustainable Energy Reviews, Volume 183, 2023, 113416, ISSN 1364-0321, https://doi.org/10.1016/j.rser.2023.113416.

[12] Sharapov D (2023) Ice adhesion to hydrotechnical structures. E3S Web of Conf 431:03006. DOI: https://doi.org/10.1051/e3sconf/202343103006.
[13] Sharapov D (2023) Structure freezing in the ice. E3S Web of Conf 431:06010. DOI: https://doi.org/10.1051/e3sconf/202343106010.
[14] Victoria Sykes, Maurizio Collu, Andrea Coraddu, A review and analysis of optimisation techniques applied to floating offshore wind platforms, Ocean Engineering, Volume 285, Part 1, 2023, 115247, ISSN 0029-8018, https://doi.org/10.1016/j.oceaneng.2023.115247.
[15] Sharapov D., Andreeva S., Ice reinforcement, E3S Web of Conferences, Volume 431, 06009, 2023, DOI: 10.1051/e3sconf/202343106009.

KAKHOVSKA HYDROELECTRIC POWER PLANT DAM EXPLOSION: IMPACT ON WATER RESOURCES AND ACTIVATION OF HAZARDOUS EXOGENOUS GEOLOGICAL PROCESSES

Prof. DSc. Stella Shekhunova

Iryna Sanina

PhD Tetiana Kril

PhD Nataliia Syumar

Institute of Geological Sciences of the NAS of Ukraine, **Ukraine**

ABSTRACT

Russia's armed aggression against Ukraine has had a catastrophic impact on the natural environment, with hydrology and water resources being among the most vulnerable. The explosion of the Kakhovka hydroelectric power plant dam on 6 June 2023 and the rapid discharge of more than 18 cubic kilometres of water caused an environmental disaster with flooding of large areas, huge human, environmental, economic losses, environmental pollution, significant changes in the hydrology, hydrogeological conditions, activation of hazardous exogenous geological processes along the lower Dnipro River, as well as the Black Sea. Using the methods of satellite image interpretation and hydrogeological modelling, hydrogeological conditions and the development of hazardous exogenous geological processes were assessed. Two areas were distinguished based on the type of changes in hydrogeological conditions relative to the location of the Kakhovka HPP. Upstream of the destroyed dam, in particular, a gradual increase in the depth of the groundwater level up to 10.3-16.1 m is expected. In areas downstream of the dam, on the contrary, the water table will rise to a depth of 0.5-2.5 m in a strip up to 10 km wide on the right bank and 15-20 km on the left bank, with a gradual subsequent increase in the water table depth over time to 2.5-7 m. Draining the largest by water volume in Ukraine Kakhovka Reservoir, and changing the erosion base will predictably lead to increased mass wasting. Changes in the hydrodynamic conditions of groundwater (rise / fall of the level, change in the direction of movement) will intensify karstification, suffosion, subsidence of loess, increase in flooded areas, trigger the intensification of landslide processes, which are widespread along the Dnipro Valley.

Keywords: hazardous exogenous geological processes, water resources, groundwater level, remote sensing data

INTRODUCTION

Russia's armed aggression against Ukraine has had a catastrophic impact on the natural environment, with hydrology and water resources being among the most vulnerable. Since the beginning of hostilities on the territory of Ukraine, there have been a number of cases of dams blown up and shelled, including the Kozarovytska Irpinska Dam (26 February 2022; Irpin River, Kyiv region), the Karachunivsk reservoir Dam (14 September 2022; Ingulets River, Kryvyi Rih region), the Pechenizsk reservoir Dam (21 September

2022; Siverskyi Donets River, Kharkiv), Karlivka reservoir Dam (25 May 2023; Vovcha River, Donetsk region), etc. These events had an impact on the surrounding areas, resulting in flooding of various degrees, changes in the hydrological regime, hydrogeological conditions, intensification of hazardous exogenous geological processes. However, the consequences of the collapse of the dam at the Kakhovka reservoir were extraordinary, far exceeding the impact on the civilian population and infrastructure of any of the previous emergencies mentioned above. The explosion of the Kakhovka hydroelectric dam on 6 June 2023 and the rapid release of more than 18,0 cubic kilometres of water caused an environmental disaster with flooding of large areas, huge human, ecological and economic losses, environmental pollution, significant changes in hydrology, hydrogeological conditions, activation of dangerous exogenous geological processes along the lower Dnipro River and the Black Sea.

Built in 1952-1959, the Kakhovka Reservoir and Dam is one of six large reservoirs in the Dnipro River cascade. The Kakhovka HPP and Kakhovka Reservoir provided annual regulation of the Dnipro River flow to supply electricity, irrigation and water supply to arid areas of southern Ukraine and navigation from Kherson to Zaporizhzhya. The Kakhovka also fed three artificial hydrological systems: the Kakhovka, North Crimean and Dnipro-Kryvyi Rih canals.

Following the destruction of the dam, up to 80 downstream settlements (Nova Kakhovka, Kherson, Oleshky, etc.) were flooded, large areas of agricultural land were inundated, a potential threat to the cooling of the Zaporizhzhia NPP arose, and residents of Kryvyi Rih, Marhanets, Pokrov and Nikopol, located in the area of the reservoir's emptying upstream of the blown-up dam, quickly began to face water supply problems.

Therefore, the research aims to interpret changes in hydrological and hydrogeological conditions, as well as the activation of hazardous exogenous geological processes provoked by them. The results of this work could be used in projects to restore the environment to a level safe for human life and water resource loss assessment.

MATERIALS AND METHODS

For forecasting hydrological and hydrogeological conditions and development of hazardous exogenous geological processes, GIS integrated databases of manifestations of hazardous exogenous geological processes, relief maps, Landsat-8 satellite images, etc. were used [1-6, etc.], and methods of satellite image interpretation, spatial data processing were applied.

Satellite image water surface interpretation methods. Water bodies and objects with a positive degree of moisture in general (vegetation, rivers, lakes, moist soils) are determined on multispectral images consists in calculating different indexes such as NDWI, NDMI, MNDWI, WRI [7-10].

In our research, the assessment of the flooded area according to remote sensing data was carried out indirectly by calculating the Normalized Difference Water Index (NDWI), by Landsat 8 data. The NDWI is used to monitor changes related to water content in water bodies or identify potential water bodies [7, 8]. It was calculated as the ratio between the values of near-infrared radiation (NIR – band 5, Landsat 8) and shortwave infrared reflection (GREEN – band 3, Landsat 8) [9]:

$$\mathrm{NDWI} = \frac{\mathrm{GREEN}-\mathrm{NIR}}{\mathrm{GREEN}+\mathrm{NIR}}.$$

The index can take values from -1 to +1. A raster pixel with a positive index value was classified as a water surface.

To create a view of the study area, three satellite images were used for each point in time. They were downloaded from the USGS Earth Remote Sensing Catalog. Cloudiness of images varies from 10 % to 65 %, spatial resolution – 30×30 m. The removing clouds were using a quality assurance (QA) band [11].

RESULTS

The processing of Landsat-8 images visualised the movement of large volumes of water after the dam was destroyed over a period of 2 months, as shown in Fig. 1. The peak of flooding was observed in the first five days. By early July, the reservoir was completely drained (see Fig. 1, c). At the beginning of August, the Dnipro riverbed that existed before the creation of the Kakhovka reservoir was clearly visible (see Fig. 1, d).

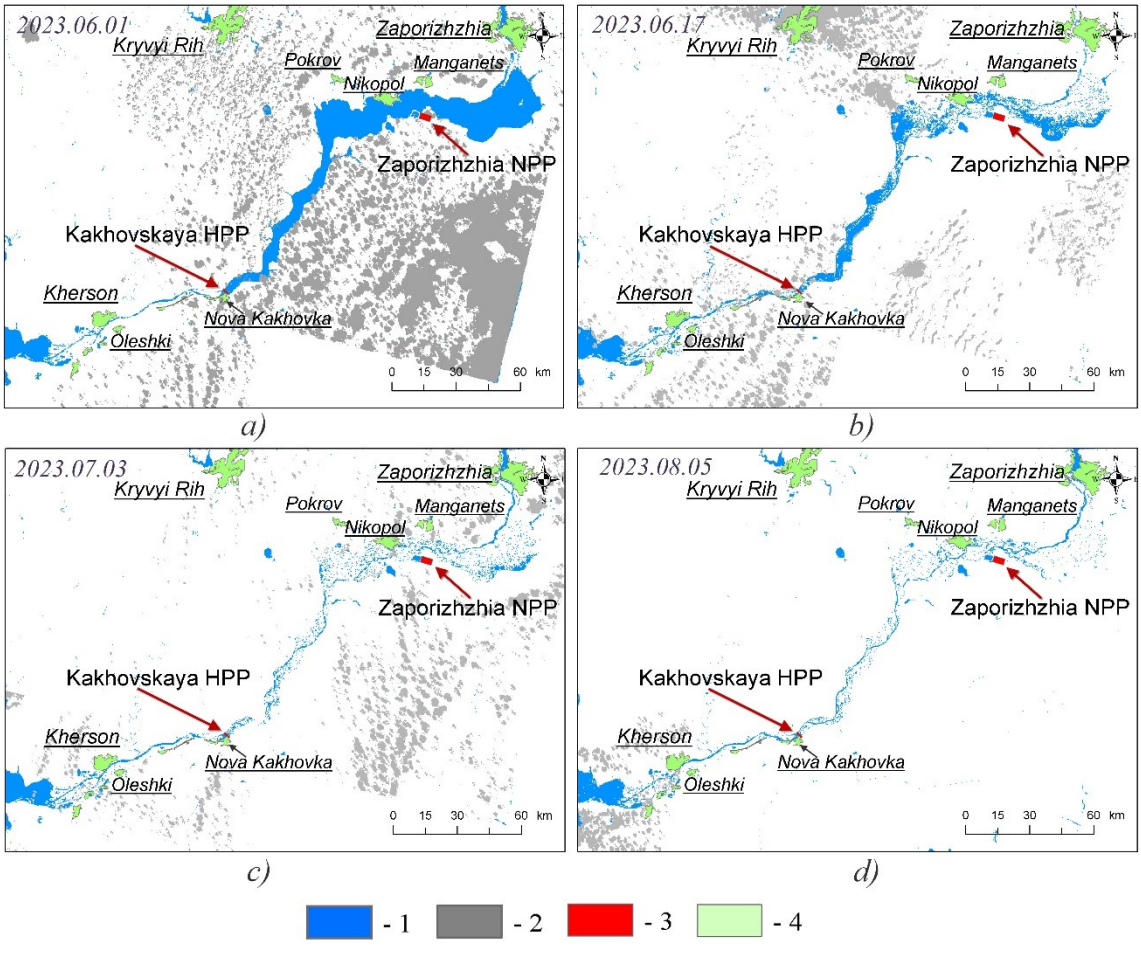

Fig. 1. Analysis of the flooding and drainage of the study area after the dam explosion: the state of the reservoir before the dam destruction on 01 June (a) and after - 17 June (b), 03 July (c), 05 August (d). Legend: 1 – water surface; 2 – cloud mask and shadows from them; 3 – main critical facilities; 4 – individual settlements.

The upper part of the Dnipro Valley is under "drought", the lower part is under flooding. At the same time, in the upper part, an average distributed load of 83526.68 MPa was removed from the geological base of the reservoir.
The morphometric characteristics of the area near/around the Dnipro riverbed play an important role in assessing the process of water release from the reservoir, its spreading below the dam and the development of other hazardous processes under its influence. The relief in the northern right bank of the area is more fragmented than in the southern part. The region has drainless depressions, large in area, and closed depressions – pods. On the left bank, in the Dnipro estuary, there is a dune relief with a height difference of several metres. The surface is characterised by heights of 150-160 m in the north and 2-3 m in the south. Low areas are confined to the sea coast and the Dnipro delta, where absolute elevations do not vary more than 4-1.5 m. The network of gullies and ravines is well developed. The depth of groundwater is 0-5 m in river valleys, 3-10 m in interfluves, 2-5 m in some places, and 10-20 m and more than 20 m on watershed slopes. The depth of the groundwater table is significantly affected by irrigation reclamation, which leads to waterlogging processes and activation of landslides.
Karst, erosion, landslides, dam erosion, waterlogging, land salinisation and loess subsidence are common in the study area (Fig. 2) [1-6, etc.]. Overlaying the data obtained on the movement of large volumes of water after the dam was breached with maps of hazardous geological processes, relief and groundwater levels made it possible to predict areas at risk for the development of hazardous geological processes.

Fig. 2. A map of previously recorded hazardous geological processes :1 – the area of occurrence of loess rocks; 2 – subsidence area; 3 – landslides area; 4 – karst area; 5 – Kakhovka reservoir; 6 – Kakhovka Dam

As a result of the catastrophic discharge of surface water from the reservoir, groundwater hydraulically connected to surface water has also undergone significant changes. First of

all, this affects the hydrogeodynamic indicators of the first aquifers from the surface, which in turn causes changes not only in the quantitative (levels, pressures, flow rates) but also in the qualitative (chemical composition) characteristics of the groundwater.

Two areas can be distinguished based on the type of changes in hydrogeological conditions relative to the location of the Kakhovka HPP. Upstream of the destroyed dam, in particular, a gradual increase in the depth of the groundwater level to the levels observed 70 years ago before the reservoir was filled is predicted: on the right bank of the Dnipro River to 10.3-16.1 m (Prydniprovske, Pokrovske, Vyshetarasivka villages), on the left bank – to 10.5-12.2 m (Tavriysk, Malakhivka village). In areas downstream of the dam, on the contrary, the water table will rise to a depth of 0.5-2.5 m in a strip up to 10 km wide on the right bank and 15-20 km on the left bank, with a gradual subsequent increase in the water table depth over time to 2.5-7 m.

Analysis of changes in surface water levels and monitoring of events confirms the pattern of destruction of the surface water supply system in the Kherson, Zaporizhia and Dnipro regions. In the flooded area, the system for supplying drinking water to the rural population has been destroyed, and irrigation of agricultural land in the southern part of the country has been dried up. The Kakhovka Reservoir was the source of supply for the main Neogene aquifer on the left bank of the Dnipro River. The lowering of the water level in the aquifer will continue to cause:

i) a change in the regional direction of groundwater flow and a lowering of the groundwater level in the horizon;

ii) an artificial increase in the depth of the aeration zone;

iii) a change from reducing to oxidative processes (the hydrogeochemical situation will change and the quality of groundwater in carbonate deposits of the Neogene will deteriorate).

In some areas, the negative impact will be caused by overflows from the Quaternary aquifers, in which in the south of Ukraine under the influence of climatic factors water of increased mineralisation is formed. As a result, groundwater quality indicators and water supply conditions for the population are expected to deteriorate. In the study area, 31 groundwater deposits have been explored, which can be usefully exploited to mitigate the impact on the population.

DISCUSSION

Taking into account the different development durations of individual dangerous geological processes, as well as requiring confirmation of their activation, we classify further statements as debatable and those that require the organization of monitoring using remote sensing analysis methods.

The overwhelming majority of exogenous geological processes are caused by the action of surface (erosion, rock washout on slopes, abrasion, reworking of reservoir banks) and groundwater (karst and sufosion, flooding, waterlogging, salinisation, and forest subsidence). Therefore, anthropogenic activation of exogenous geological processes will be a predictable expected consequence of changes in hydrological and hydrogeological conditions in the area affected by the Kakhovka hydroelectric power plant dam explosion.

Draining the Kakhovka Reservoir and changing the erosion base will predictably lead to increased rock washout and gully formation. Within the significant areas of land flooding in the lower reaches of the Dnipro, a rise in the groundwater level will lead to an increase in flooded areas. Excessive waterlogging of rocks due to surface and groundwater may also trigger the intensification of landslide processes, which are widespread along the Dnipro Valley.

Changes in the hydrodynamic conditions of groundwater (rise or fall of the level, change in the direction of movement) will intensify subsidence of loess rocks, leaching of carbonate rocks, karst and sufosion. Their development is favoured by natural conditions: the thickness of Neogene rocks prone to karst formation ranges from 4-10 m in the north of the study area to 120-140 m in the south, with a simultaneous increase in the thickness of carbonate strata in the section. In the Kherson region, which was most affected by the hydroelectric dam explosion, 94 karst manifestations were recorded [1]. In the 1950s and 1960s, as a result of intensive hydraulic and land reclamation construction in southern Ukraine, karst and sufosic processes were already intensified. In modern conditions, the resumption of karst activation is predicted as a result of changes in the level, direction and speed of groundwater movement due to changes in the erosion base. The processes are expected to intensify at all stages - covered, semi-covered, and open karst. The lower reaches of the Dnipro River are areas with a thick cover (up to 15-30 metres in watersheds) of loess soils, which are prone to subsidence (Fig. 2). The low degree of lithification of these soils results in their increased sensitivity to anthropogenic inputs of water, heat and chemical compounds. Changes in groundwater levels in flooded and inundated areas can lead to a dynamic decrease in the engineering stability of loess soils, the occurrence of subsidence deformations and complications in the operation of engineering structures in built-up areas. The risks of these processes are increased by structural and tectonic heterogeneities, seismic events (Vrancea zone, Carpathian and Crimean foci, “local” earthquakes Kryvyi Rih 5-6 points), neotectonic activity, explosions, and hostilities. An assessment of environmental changes should be carried out taking into account a multi-risk approach for the geological environment, the provision of drinking water resources to the population, and their life safety [12, 13].

CONCLUSION

The explosion of the Kakhovka hydroelectric power station disrupted the balance of groundwater and surface water; significant changes in the groundwater level regime are predicted both below and above the damaged hydroelectric power station dam.

Two types of changes in hydrogeological conditions after the dam explosion have been identified. Upstream of the destroyed dam, in particular, a gradual increase in the depth of the groundwater level up to 10.3-16.1 m is expected. In areas downstream of the dam, on the contrary, the water table will rise to a depth of 0.5-2.5 m in a strip up to 10 km wide on the right bank and 15-20 km on the left bank, with a gradual subsequent increase in the water table depth over time to 2.5-7 m.

This has led to a deterioration in the water supply system in Kherson, Zaporizhzhia and Dnipro regions, making irrigation reclamation of land in southern Ukraine impossible.

Significant hydrogeodynamic changes and changes in chemical transformation processes in the rocks of the artificially created and natural aeration zone are predicted in the main Neogene aquifer on the left bank of the Dnipro.

Artificial changes in the water regime, in particular, the draining of the Kakhovka reservoir and changes in the erosion base, are expected to lead to increased erosion, gully formation, and intensification of landslide processes. It is also expected to change the dynamics of carbonate karst processes, sufosion and subsidence of loess soils, considering that in the upper part, the average distributed load of 83526.68 MPa was removed from the geological base of the reservoir.

To effectively address the problems of intensification of hazardous exogenous geological processes in the context of armed conflict and natural disasters, it is necessary to develop and implement programme activities (with funding), including the restoration of the system for monitoring exogenous geological processes using remote sensing, spatial and hydrogeological modelling.

This is particularly relevant at present, given the significant socio-economic and environmental damage associated with the intensification of hazardous exogenous geological processes as a dynamic and influential factor in the development of changes in engineering and geological conditions. The results of the risk assessment of exogenous geological hazards are necessary for the post-war reconstruction and economic development of the regions of Ukraine affected by the Russian military aggression.

ACKNOWLEDGEMENTS

The research was carried out under the state budget-financing program CPCEL 6541050 project “Development and implementation of new technologies and methods of geological study of the territory of Ukraine and use of mineral resources" (state registration No. 0121U109879).

REFERENCES

[1] National Report on the State of the Environment in Ukraine in 2021. (In Ukrainian). Access mode: https://mepr.gov.ua/wp-content/uploads/2023/01/Natsdopovid-2021-n.pdf.

[2] State geological map of Ukraine of scale 1:200 000 (1975). Explanatory Notes. Prychornomorska series. Sheets L-36-X (Nova Kakhovka). (In Russian). Authors Pasechnyi G.V., Fishman I.L. Chief editor Marchenko Ya.A. Ministry of Geology of USSR, Ministry of Geology of Ukrainian SSR, Trust “Ukrpivdengeologiya”, 1975. 93 p.

[3] State geological map of Ukraine of scale 1:200 000 (1976). Explanatory Notes. Prychornomorska series. Sheets L-36-IX (Mykolaiv). (In Russian). Authors Nasad A.G., Nasad N.P. Chief editor Moliavka G.I. Ministry of Geology of USSR, Ministry of Geology of Ukrainian SSR, Trust “Ukrpivdengeologiya”, 1976. 85 p.

[4] Map of the distribution of exogenous geological processes on the territory of Ukraine. Scale 1:500 000. (In Ukrainian). Authors E.I. Kolot et al. Chief editor N.M. Gavrilenko.

State Geological Enterprise “Geoprognoz”, State Geological Information Fund of Ukraine, 1995.

[5] Map of the assessment of the probability of the risk of the development of the karst process on the territory of Ukraine. Scale 1:1 000 000. (In Ukrainian). Authors Klymchuk L.M., Krasnook L.M., Sergienko A.A. SRDE “Geoinform Ukraine”, Kyiv, 2008.

[6] Map of the assessment of the probability of the risk of developing landslides in the territory of Ukraine. Scale 1:1 000 000. (In Ukrainian). Authors Klymchuk L.M., Drapikovska I.S., Sergienko A.A. SRDE “Geoinform Ukraine”, Kyiv, 2008.

[7] Index DataBase. A database for remote sensing indices URL: https://www.indexdatabase.de.

[8] Liu, S.; Wu, Y.; Zhang, G.; Lin, N.; Liu, Z. Comparing Water Indices for Landsat Data for Automated Surface Water Body Extraction under Complex Ground Background: A Case Study in Jilin Province. Remote Sens. 2023, 15, 1678. https://doi.org/10.3390/rs15061678.

[9] Space solutions for Earth problems. URL: https://eos.com/make-an-analysis/ndwi.

[10] Babichev S., Kril T.V., Shekhunova S.B., Wójcik W. (2021). Geo-informational approach to risk analysis of slope mass movement. CITRisk'2021: 2nd International Workshop on Computational & Information Technologies for Risk-Informed Systems, September 16–17, Kherson, Ukraine. http://ceur-ws.org/Vol-3101/Short23.pdf.

[11] Yang Shen, Yong Wang, Haitao Lv, Hong Li. Removal of Thin Clouds Using Cirrus andQA Bands of Landsat-8. Photogrammetric Engineering & Remote Sensing, 2015. 81(9):721-731 DOI: 10.14358/PERS.81.9.721.

[12] Shekhunova S., Kril T. Geological and economic risk assessment for territories of hazardous geological and technogenic processes (exemplified by Solotvyno township). Naukovyi Visnyk Natsionalnoho Hirnychoho Universytetu. 2022, (2): 079 – 085 https://doi.org/10.33271/nvngu/2022-2/079.

[13] Serkan Girgin, Amos Necci, Elisabeth Krausmann. (2019). Dealing with cascading multi-hazard risks in national risk assessment: The case of Natech accidents. International Journal of Disaster Risk Reduction, vol. 35. DOI: https://doi.org/10.1016/j.ijdrr.2019.101072.

ICE RELATED CHALENGES FOR WATER TRANSPORT

Sofiya Andreeva[1,2]

Viktoriia Saveleva[2]

Elena Kudryashova[2]

[1] Admiral Makarov State University of Maritime and Inland Shipping, **Russia**
[2] Peter the Great St.Petersburg Polytechnic University, **Russia**

ABSTRACT

Water transport in icy conditions presents intricate challenges that significantly impact navigability, safety, and operational efficiency. This article delves into the complexities of navigating icy waters, focusing on the diverse forms and compositions of ice that pose formidable obstacles to maritime operations. Pack ice, icebergs, and frazil ice represent distinct challenges, restricting access, threatening safety, and impeding the fluidity of water transport routes. The challenges for water transport in icy conditions encompass reduced navigability, safety concerns arising from potential collisions, economic implications affecting shipping schedules and trade, and environmental impacts stemming from ice management strategies. However, innovative technologies and strategic approaches have emerged to address these challenges. Advanced ice detection systems, specialized icebreaker vessels, thermal de-icing techniques, and innovative hull designs offer promising solutions to mitigate the impact of ice accumulation on vessels. The overview article explores these technological advancements and strategic measures employed in ice management, emphasizing their role in enhancing safety and efficiency in navigating icy waters. Furthermore, the integration of remote sensing, autonomous technologies, and weather forecasting models enhances situational awareness, aiding in the development of safer navigation routes through ice-prone areas. Understanding and effectively addressing the complexities of ice-related challenges in water transport are essential for devising comprehensive strategies that prioritize safety, operational efficiency, and environmental sustainability. This exploration seeks to offer insights into the multifaceted nature of ice navigation challenges, emphasizing the importance of innovative solutions to ensure the continuity and safety of maritime operations in icy conditions.

Keywords: Ice Navigation, Water Transport, Ice Management, Ice Types, Safety Concerns, Icebreaker Vessels, Technology

INTRODUCTION

Water transport plays a pivotal role in global trade, connecting distant regions and facilitating the movement of goods and people across oceans, rivers, and lakes. However, in regions characterized by icy conditions, such as polar environments or cold-weather climates, water transport encounters formidable challenges that significantly impact its efficiency, safety, and operational capabilities. Understanding

and addressing these challenges related to ice navigation are paramount for ensuring the continuity and safety of maritime operations. The introduction of this article aims to shed light on the complexities inherent in navigating icy waters and the diverse range of challenges faced by water transport in such environments [1-6]. Ice, in its varied forms and compositions, poses significant obstacles that demand innovative solutions and strategic approaches to maintain smooth and secure navigation routes. The diverse forms of ice – pack ice, icebergs, and frazil ice, among others – present unique challenges to water transport. Pack ice, massive floating ice sheets that drift on oceans or polar seas, can hinder vessel movement, leading to increased transit times and potential damage to ships. Icebergs, colossal chunks originating from glaciers or ice shelves, pose severe safety risks due to their size and submerged mass, necessitating careful navigation to avoid collisions [7-11]. Meanwhile, frazil ice, composed of tiny ice crystals formed in supercooled water, can hinder navigation in rivers, estuaries, and turbulent seas. The reduced navigability caused by ice accumulation is a primary challenge, as it restricts access to critical maritime routes and ports. Safety concerns arise from potential collisions with ice formations, endangering both vessels and crew members. The economic implications are significant, leading to delays in shipping schedules, increased maintenance costs, and disruptions in supply chains, affecting regional trade and commerce. Moreover, the environmental impact of ice management strategies, coupled with the ongoing effects of climate change, exacerbates the complexities faced by water transport in icy conditions. In response to these challenges, various technological advancements and strategies have been developed to manage ice in water transport. These include sophisticated ice detection systems, specialized icebreaker vessels, thermal de-icing techniques, and innovative hull designs aimed at minimizing ice accumulation. Additionally, strategic route planning, weather forecasting, and emerging autonomous technologies contribute to safer navigation through icy waters. In essence, this article seeks to explore the multifaceted dimensions of ice-related challenges in water transport, examining the types of ice formations, the challenges they pose, and the diverse array of technologies and strategies employed to mitigate these challenges. Understanding these complexities is vital in developing comprehensive and effective approaches to ensure the safety, efficiency, and sustainability of water transport in icy conditions [12-15].

MATERIALS AND METHODS

Ice, a fundamental element in Earth's hydrosphere, takes on various forms and structures across different water bodies. Its diversity in appearance and composition arises from distinct environmental conditions and the interplay of temperature, currents, and salinity. Understanding the types and formations of ice is crucial, especially in regions where water transport contends with icy challenges.

Pack Ice form comprises large masses of floating ice that accumulate and drift on the surface of oceans or polar seas. Pack ice can vary significantly in thickness and coverage, creating formidable barriers for ships navigating through icy waters. It poses substantial challenges for water transport, requiring specialized vessels or icebreaker assistance to create passages.

Icebergs originate from glaciers or ice shelves and can drift into shipping lanes. Icebergs present severe hazards to maritime traffic due to their substantial size beneath the water surface, necessitating careful monitoring and navigation to avoid collisions.

Frazil Ice is comprising tiny ice crystals formed in supercooled water, frazil ice appears as slush or fine particles floating on the water's surface. It commonly occurs in rivers, estuaries, or turbulent seas, potentially impeding vessel movement and navigation.

Ice formation involves intricate processes influenced by temperature, water movement, and salt content. When water temperature drops below its freezing point, ice crystals begin to form. The process can occur in various ways, including direct freezing of liquid water or deposition of water vapor into ice crystals (known as deposition ice). In oceans, sea ice forms when seawater freezes due to low temperatures. This process results in the creation of various types of sea ice, such as fast ice (ice attached to the shoreline), drift ice (floating sea ice), and multi-year ice (which survives more than one melting season). Currents, wind patterns, and salinity levels significantly impact ice formation. For instance, saltwater freezes at lower temperatures than freshwater, affecting the type and structure of ice formations in different regions. Understanding these diverse types and formation processes of ice is pivotal for developing effective strategies and technologies to mitigate challenges for water transport operating in icy conditions.

Water transport encounters a myriad of challenges, especially in regions prone to icy conditions, which significantly impact navigability, safety, and operational efficiency. In icy conditions, waterways become less navigable due to the presence of ice formations like pack ice, icebergs, or even frazil ice. These obstacles obstruct routes, narrowing navigable channels and creating barriers that impede the movement of vessels. This reduction in navigability often leads to delays in transportation schedules and increased transit times. Ice-related challenges pose significant safety hazards for vessels and crew members. Collisions with ice formations can damage hulls, propellers, or rudders, endangering the structural integrity of ships. Additionally, the unpredictability of ice movement and changes in weather conditions can increase the risk of accidents, threatening the safety of maritime operations. The impact of ice-related challenges extends to economic consequences. Delays in shipping schedules, increased maintenance costs due to ice-related damages, and the need for specialized equipment or icebreaker assistance escalate operational expenses. Moreover, these challenges can disrupt supply chains, affecting trade and commerce in regions heavily reliant on water transport. Ice management strategies, such as using icebreakers, can have environmental repercussions. Noise pollution from icebreaking activities can disturb marine wildlife, affecting their habitats and behaviors. Additionally, the melting of ice due to climate change not only affects navigability but also contributes to rising sea levels and alters ecosystems in polar regions, impacting biodiversity. In regions where icy conditions prevail for a significant part of the year, accessibility to remote or isolated areas becomes a challenge. Transporting goods, supplies, or providing essential services to these areas becomes more difficult due to limited or unreliable water transport routes. Water transport in icy conditions demands compliance with stringent regulations and safety standards to ensure the protection of life, property, and the environment. Meeting these regulatory requirements often involves additional costs and complexities, impacting insurance premiums for vessels operating in icy waters.

Ice management in water transport involves the utilization of various technologies and strategies aimed at mitigating the challenges posed by ice accumulation. These innovative approaches play a crucial role in ensuring safe and efficient navigation through icy waters. Advanced technologies, including radar, sonar, LiDAR, and satellite imagery, enable the detection and monitoring of ice formations. These systems provide real-time data on ice distribution, thickness, and movement, aiding vessels in navigating through ice-prone areas by identifying safe passages. Icebreakers are specialized vessels designed to navigate through ice-covered waters. They use reinforced hulls and powerful propulsion systems to break and clear paths for other ships. These vessels are instrumental in maintaining navigable channels, enabling smoother transit for cargo and passenger vessels. Thermal de-icing involves the application of heat to prevent or remove ice accumulation on vessel surfaces (figure 1).

Fig. 1. Example of a vessel icing

Systems like heated hulls, propellers, and de-icing sprays help prevent ice formation or remove ice buildup, reducing the risk of damage to ship components. Vessel design advancements focus on creating hulls resistant to ice accumulation. Some designs incorporate sloped or curved surfaces to deflect ice, while others use special coatings that minimize ice adhesion. These innovations reduce the surface area where ice can form and enhance a vessel's ability to navigate through icy conditions. Emerging technologies, such as autonomous underwater vehicles (AUVs) and drones equipped with sensors, aid in collecting data on ice conditions in remote or inaccessible areas. These technologies enable a more comprehensive understanding of ice formations and enhance situational awareness for efficient navigation. Utilizing weather forecasting models helps in planning safer routes by anticipating changes in ice conditions and weather patterns. Ship routing software and services provide information on the most favorable paths, optimizing navigation while avoiding hazardous ice-prone areas. These technological advancements and strategic approaches in ice management contribute significantly to enhancing the safety, efficiency, and reliability of water transport in icy conditions, ensuring smoother operations and reducing risks for vessels navigating through challenging environments.

CONCLUSION

The challenges posed by ice in water transport necessitate a multi-faceted approach that combines technological innovation, strategic planning, environmental considerations, and sustainable practices. Ice-related obstacles significantly impact navigability, safety, economics, and the environment, particularly in regions prone to icy conditions. The types and formations of ice, including pack ice, icebergs, and frazil ice, present formidable barriers to water transport. Understanding their dynamics and behaviors is crucial for devising effective strategies to overcome these obstacles. Reduced navigability due to ice accumulation, safety concerns stemming from collisions and unpredictable weather, economic implications in terms of increased operational costs, and environmental impacts highlight the complexities faced by maritime operations in icy waters. However, advancements in ice management technologies offer promising solutions. Cutting-edge detection and monitoring systems provide real-time data on ice distribution, aiding vessels in identifying safe passages. The deployment of specialized icebreaker ships remains instrumental in clearing navigable channels, ensuring smoother transit for other vessels. Thermal de-icing techniques, ice-resistant hull designs, and anti-icing coatings contribute to reducing ice accumulation on vessels, enhancing their ability to navigate through icy conditions. Moreover, the integration of remote sensing, autonomous technologies, and strategic route planning based on weather forecasting models elevates situational awareness and facilitates safer navigation through ice-prone areas. These innovations not only improve the efficiency of water transport but also prioritize safety and environmental considerations. Nevertheless, the impact of ice-related challenges extends beyond technical aspects. It involves adapting to evolving environmental conditions, particularly with the ongoing effects of climate change leading to ice melting and altering waterway conditions. Balancing economic needs with sustainable practices is imperative to minimize the environmental footprint of ice management strategies. The journey toward effective ice management in water transport demands collaboration among stakeholders, including maritime industries, researchers, policymakers, and environmental advocates. In essence, while ice-related challenges persist, continuous innovation, informed decision-making, and a holistic approach are essential to navigating these obstacles effectively, ensuring safe, efficient, and environmentally conscious water transport operations in icy environments.

ACKNOWLEDGEMENTS

This work was done as a part of Project « Study of statistical patterns of ice loads on engineering structures and development of a new method for their stochastic modeling (FSEG-2020-0021)", No. 0784-2020-0021» supported by the Ministry of Science and Higher Education of the Russian Federation.

REFERENCES

[1] Sharapov D., Shkhinek K., DelValls T.Á., An estimation of the amount of the thermal energy for the moorage wall heating in the Arctic harbours to avoid ice accumulation, OCEAN ENGINEERING, Volume: 100 Pages: 90-96, Elsevier Published: MAY 2015. DOI:10.1016/j.oceaneng.2015.03.016

[2] Shi Y. A numerical investigation of ice-structure interaction using a discrete element model // Ocean Engineering. – 2016. – T. 118. – C. 274-287.

[3] Sharapov D., Shkhinek K., DelValls T.Á., ICE COLLARS, DEVELOPMENT AND EFFECTS, Ocean Engineering, Volume 115, Pages 189-195, Elsevier Published: March 2016. DOI:10.1016/j.oceaneng.2016.02.026

[4] Liferov P, Shkhinek KN, Vitali L, Serre N (2007) Ice gouging study - actions and action effects. Recent Development of Offshore Engineering in Cold Regions 1 and 2: 774-786.

[5] Sharapov D., Shkhinek K., Numerical calculation of the ice grow and empirical calculation results, Research in materials and manufacturing technologies, PTS 1-3 Book Series: Advanced Materials Research Volume: 835-836 Pages: 1448-1454, Published: 2013.

[6] Andreeva, S.A., Sharapov, D. Hoek–Brown model for ice breaking simulation. Magazine of Civil Engineering. 2023. 123(7). Article no. 12303. DOI: 10.34910/MCE.123.3

[7] Sharapov D., Klochkov Y., Improving quality of 2D ice load estimation on freezed piles, International Journal for Quality Research v17, n4, 2023, DOI: 10.24874/IJQR17.04-11

[8] Sharapov D., BRIEF ON DEVELOPMENT OF ICE LOAD ESTIMATION FOR HYDROTECHNICAL ENGINEERING, Proceedings of 23rd International Multidisciplinary Scientific GeoConference SGEM 2023, Volume 23, Issue 2.1, ISBN 978-619-7603-57-6 DOI: 10.5593/sgem2023/2.1/s08.18.

[9] Keyang Liu, Baoping Cai, Qibing Wu, Mingxin Chen, Chao Yang, Javed Akbar Khan, Chenyushu Wang, Hasini Vidumini Weerawarna Pattiyakumbura, Weifeng Ge, Yonghong Liu, Risk identification and assessment methods of offshore platform equipment and operations, Process Safety and Environmental Protection, Volume 177, 2023, Pages 1415-1430, ISSN 0957-5820, https://doi.org/10.1016/j.psep.2023.07.081.

[10] Sharapov D (2023) Evolution of ice load prediction tools for hydrotechnical construction. E3S Web of Conf 402:05023. DOI: https://doi.org/10.1051/e3sconf/202340205023.

[11] Sharapov D (2023) Ice adhesion to hydrotechnical structures. E3S Web of Conf 431:03006. DOI: https://doi.org/10.1051/e3sconf/202343103006.

[12] Victoria Sykes, Maurizio Collu, Andrea Coraddu, A review and analysis of optimisation techniques applied to floating offshore wind platforms, Ocean Engineering, Volume 285, Part 1, 2023, 115247, ISSN 0029-8018, https://doi.org/10.1016/j.oceaneng.2023.115247.

[13] Sharapov D., Andreeva S., Ice reinforcement, E3S Web of Conferences, Volume 431, 06009, 2023, DOI: 10.1051/e3sconf/202343106009.

[14] Emma C. Edwards, Anna Holcombe, Scott Brown, Edward Ransley, Martyn Hann, Deborah Greaves, Evolution of floating offshore wind platforms: A review of at-sea devices, Renewable and Sustainable Energy Reviews, Volume 183, 2023, 113416, ISSN 1364-0321, https://doi.org/10.1016/j.rser.2023.113416.

[15] Sharapov D (2023) Structure freezing in the ice. E3S Web of Conf 431:06010. DOI: https://doi.org/10.1051/e3sconf/202343106010.

METHODOLOGY OF TOTAL PHOSPHORUS AND NITROGEN OUTFLOW UNIT DISCHARGES EVALUATION FOR WATERSHEDS WITHOUT MONITORING POINTS

Assoc. Prof. Dr. Victor Tretyakov[1, 2]

Postgraduate Stepan Klubov[2]

Student Anna Nikulina[1]

Prof. Dr. Vasiliy Dmitriev[1]

[1] Saint Petersburg State University, **Russia**
[2] Russian State Hydrometeorological University, **Russia**

ABSTRACT

Anthropogenic eutrophication is the main ecological problem of the Baltic Sea. However, there are many rivers entering the sea without monitoring points. The paper presents methodology for evaluation of the total phosphorus and nitrogen discharges outflow unit discharges from catchment areas of such rivers. As example, we consider Russian part of the Finnish Gulf catchment area. The first stage of the methodology consists in determination of partial catchment areas of rivers with water runoff and the biogenic elements concentrations monitoring points. We must determine the watersheds upstream the monitoring points. The next stage of the exploration is determination of the watersheds spatial landscape structure and the relief features. The stages are processed by GIS-technologies. The same processing must be applied to catchment areas of the rivers without monitoring points. Thus, it is necessary comparison of the watersheds parameters of both the above-mentioned types by means of cluster analysis. As the result, we must determine analogue watersheds of the rivers with the monitoring points for the catchment areas without the points. Of course, the watersheds must have similar landscape structures and relief parameters. At the exploration next stage, we calculate the unit discharges from the analogue watersheds on the base of the monitoring data. The final exploration stage consists in evaluation of the biogenic elements outflow from the watersheds of the rivers without the monitoring points. The research results can be used for planning of actions for marine ecosystems biodiversity keeping and the water resources maintenance for fishery and recreation.

Keywords: total nitrogen and phosphorus outflow

INTRODUCTION

Anthropogenic sources of nitrogen and phosphorus play the predominant role in the biogenic elements inflow into aquatic ecosystems. Many natural and anthropogenic factors have influence with total phosphorus and nitrogen outflow unit discharges. The factors are the catchment area landscape structure, the land-use pattern, the watershed geological structure, the relief degree of dissection, the average and maximum slope of the surface, the river network density, edaphic factors such as the soil types, the acid-base and redox conditions, biotic processes, the catchment area climate and so on [1, 2].

Light soil texture, significant degree of soil erosion promotes high values of the biogenic element outflow unit discharges. Clay soils retain the nitrogen and phosphorus, preventing them outflow from catchment areas into aquatics ecosystems. Vegetation is a natural biogeochemical barrier that traps the phosphorus and nitrogen. Coastal wetlands and macrophytes have high capability of the biogenic elements absorption. It is necessary to stress that plants contain significantly more the biogenic elements than organogenic horizons of soils. When the plant organic matter decomposes, the biogenic elements are involved in circuit of substance. The nitrogen and phosphorus compounds can be washed out from litter, needles, leaves, flowers, fruits, as well as from living matter [3, 4, 5]. As important reservoir of the biogenic elements, we can consider the surface organogenic horizon of soils. There is the biogenic elements accumulation due to precipitation infiltration, surface runoff, leaching from plants and dead organic matter, and nitrogen fixation from the atmosphere by microorganisms. Under anthropogenic load, there is accumulation of various pollutants from detergents, waste, and fertilizer components. The pollutants contain the nitrogen and phosphorus [4]. Soils with high level of organic matter can strengthen the biogenic load on aquatic ecosystems [3, 2]. There are various types of the vegetation influence on the biogenic elements outflow. For example, woodlands are usually characterized by minimal values of the unit discharges, but the snow at the beginning of spring flood often contains the nitrogen and phosphorus in concentrations, which are higher ones in the open countryside [4]. Various compounds of the nitrogen and phosphorus have different capability of mobility within soil. Thus, nitrates move more freely within the soil due to their higher solubility compared with phosphates, which are often absorbed by soil particles. The phosphates tend to move with the particles. The phosphorus outflow has the maximum speed during hurricanes. Groundwater outflow prevails in the nitrogen migration, whereas the phosphorus outflows from the watershed mainly with surface runoff and meltwater [6, 7]. Atmospheric precipitation incomes the nitrogen and phosphorus into the soil. Increase of the precipitation and the runoff leads to the nitrogen and phosphorus outflow. The maximal values of the nitrogen and phosphorus outflow unit discharges take place during period of maximal precipitation [2]. The concentrations dynamics are characterized by pronounced annual course with a maximum during spring high water and gradual decrease in summer. The phosphorus minimal concentrations are observed in winter, and the maximum ones – in spring during the period of the temperature increasing in the soil, which increases the phosphorus mineralization [3]. There is usually some increase of the phosphorus concentrations in the second half of summer. One of the possible increase causes consists in the phosphorus income from the bottom silt that is secondary pollution of the water body. In wetter years, extreme precipitation can increase the nutrients outflow from the watershed. In this case, the nitrogen is mainly transported in dissolved inorganic form, and the phosphorus is transferred in suspended form. The last feature indicates that the transferred phosphorus is mainly the result of the soil erosion. Morphometry of catchment areas plays important role. Thus, the phosphorus is retained in bowl-shaped depressions; the nitrogen is accumulated within wide plains with numerous shallow water areas [6]. Wetlands connected to river drainages play important role in the nitrogen and phosphorus retaining within the catchment areas [1, 8]. Climatic factors have significant influence on the biogenic elements outflow. Thus, temperature increase from 1°C to 35°C leads to increase of the mineralization and the nitrate concentration in the soil water up to two times [4]. High values of the nitrogen and

phosphorus unit discharges within urban areas are connected with storm water from impermeable surfaces and/or sewage effluent and consumer waste [1]. Besides, reasons of the nitrogen and phosphorus income into surface and soil water are usage of fertilizers, feed, detergents, and extraction of minerals containing the nitrogen and phosphorus [3, 9].

MATERIALS AND METHODS

Determination of the catchment areas can be processed by usage of special hydrological functions of GIS-technologies. The functions must be applied to digital terrain models of the watersheds surfaces. The models can be produced on the base of global terrain models SRTM or ASTER GDEM, but the global terrain models have too many mistakes within urban areas and timberlands due to the satellite emission reflection from roofs, anthropogenic objects, vegetation, and so on. Therefore, we carried out digitization of hypsographic curves in image of the topographic map of St. Petersburg and Leningrad Region issued in 2001 with scale 1:200000. The digital terrain model of the all above-mentioned river-drainage systems region was produced in ArcGIS by method of the «Universal kriging». The result consisted in the raster matrix of the height values with the cells dimension equals to 100 per 100 meters. Then the matrix of altitude values was modified. There were prepared 100 meters wide buffer zones around the watercourses. The raster altitude values within the buffer zones were lessened by 10 meters for easement of the rivers catchment areas ascertainment in ArcGIS. The ascertainment of the catchment areas boundaries was carried out by tool «Watershed» of ArcGIS. At the first stage of the ascertainment, the runoff directions were created by tool «Flow Direction». There were manually located nodes in points of the rivers outlets. For the rivers with points of monitoring, the outlets coincide with the points of monitoring, and for rivers without ones with the rivers outfalls. The all rivers watersheds were produced by «Watershed» tool up-stream the nodes. The tool creates new matrices, which contain information of belonging the cells to partial watersheds. Then the matrices cells belonged the same partial watershed are converted into vector area polygon by tool «Conversion tools». At the next stage of the processing, the polygons of the watersheds were aggregated into the entire catchment areas of the river-drainage systems. Figure 1 presents location of the river-drainage systems catchment areas and the monitoring points. Watersheds of the Shingarka River and the Strelka River are joined due to the rivers drainage systems junction. There is nonpoint discharge from the catchment area adjoined the Neva Bay. The catchment area is included into the joined watershed of the Shingarka and the Strelka Rivers. Then it is necessary to determine surface types within the watersheds. As the information source, we used electronic maps from site of GIS-Lab — informal community of Russian-speaking GIS/RS specialists (gis-lab.info). There was processed intersection of the watersheds layer with the layers produced on the base of the GIS-Lab maps. Then there were calculated the watersheds areas and the areas which are occupied by various types of surface within the watersheds. Thus, there were calculated shares of the each type of the surface within the watersheds. Table 1 demonstrates the shares of the surface types. In addition, figure 2 presents forest cover and farming land within the watersheds. The researched catchment areas of the watercourses and water reservoirs in the figures are designated by the following numbers: 1) the Privetnaya River, 2) the Smolyachkov Stream, 3) the Chyornaya River, 4) the Ushkovskiy Stream, 5) the Vosmoy Stream, 6)

the Bystraya River, 7) the Zelenogorskiy Stream, 8) the Shestoy Stream, 9) the Tretiy Stream, 10) the Sestroretskiy Razliv, 11) the Chyornaya Lakhta River, 12) the Lahtinskij Razliv, 13) the Ligovskij Channel and the Krasnenkaya River, 14) the Dudergofka River and the Dudergofskiy Channel, 15) the Strelka Stream, 16) the Kikenka River, 17) the Shingarka and Strelka Rivers, 18) the Troitskiy Stream, 19) the Kristatelka River, 20) the Karasta River watersheds. The analogous watercourses watersheds are designated by the numbers: 1) the Mga River, 2) the Tosna River, 3) the Izhora River, 4) the Oredezh River, 5) the Vruda River, 6) the Volchya River ones. The catchment areas parameters, which we have to take into account at the cluster analysis, are shares of the following types of the surface: forests, wetlands, farmland areas, residential constructions, and industrial zones.

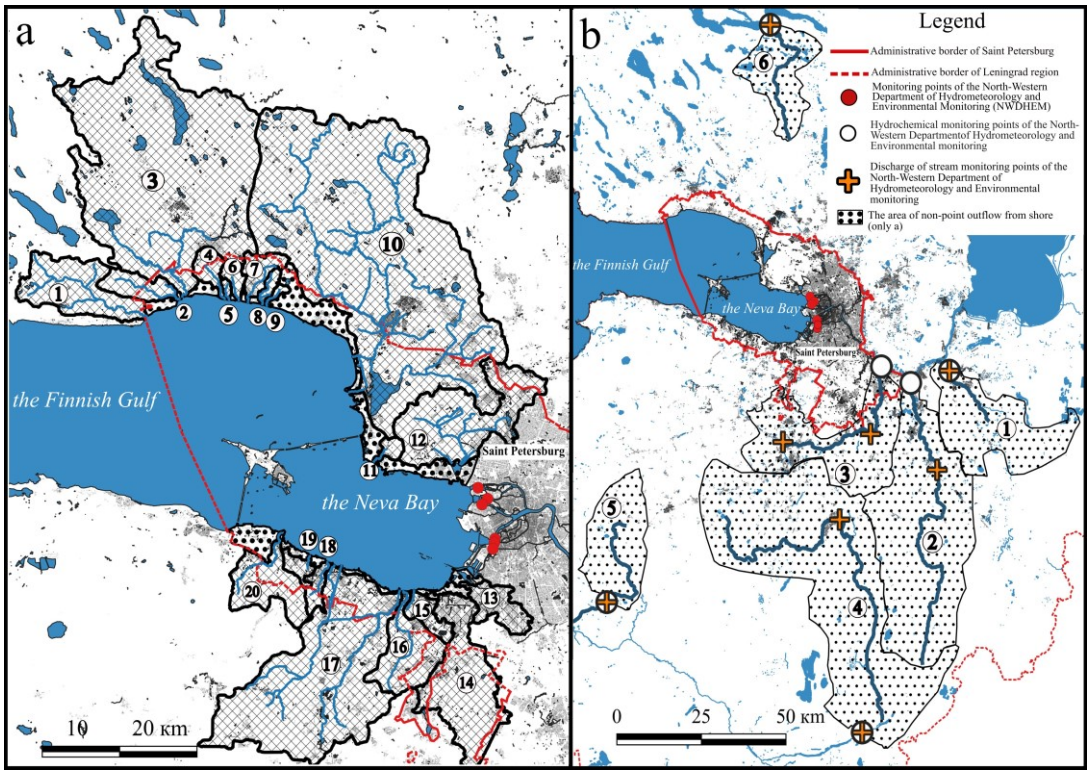

Fig. 1. Location of the river-drainage systems watersheds and the monitoring points

In addition, we include in the list of the parameters drainage network density, and average slope of the watersheds. The last parameter ascertainment can be produced by two manners. The first of them demands digital terrain model and usage of special GIS tools. Another way proposes usage of topographic maps with creation strict lines between adjacent hypsographic curves. Thus, we can determine length of a line and altitude difference between the line end points. Of course, we must produce many the lines for precise ascertainment of the parameter. The above-mentioned parameters are used for calculation of distances between the watersheds in many-dimensional space of the features. The calculation is stage of the cluster analysis. Because the Neva Bay has very short residence time equal to 7 days, it is necessary to ascertain annual dynamics of the biogenic elements daily unit discharges. For the purpose, we used data of Northern-Western Department of Hydrometeorology and Environmental monitoring. There are data of the analogue rivers runoff for each day throughout a year, but there are only few

days of sampling for determination of the total nitrogen and phosphorus concentrations in the rivers. Therefore, we have to apply interpolation for ascertainment of the concentrations at each day throughout a year. The interpolation was processed by specially designed program of Mathcad. We used results of the linear interpolation because the results do not exceed the limits of the monitoring data. Calculation of the average daily unit discharges was processed in tables of Microsoft Excel. The initial values of the rivers runoff in each day have dimension in cubic meters per second. The values are recalculated in cubic meters per day (24-hour), and the results are multiplied by the total phosphorus and nitrogen concentrations. Thus, we obtain the substance flow through water abstraction point per day (24-hours). Then the result is divided by the watershed area in square kilometers. Consequently, we have annual dynamic of the substance unit discharge from the catchment area for a year. Processing of analogous data of the same watershed for series of years allows to determine generalized annual dynamics of the substance unit discharge with confidential interval. Revealing of similarities and dissimilarities among the generalized annual dynamics can be processed by the modified Nash–Sutcliffe criteria. The total annual and daily unit discharge can be applied for evaluation of ones for catchment areas without the monitoring data of the substances outflow.

RESULTS

Figure 2 and Table 1 demonstrates spatial structures of the watersheds.

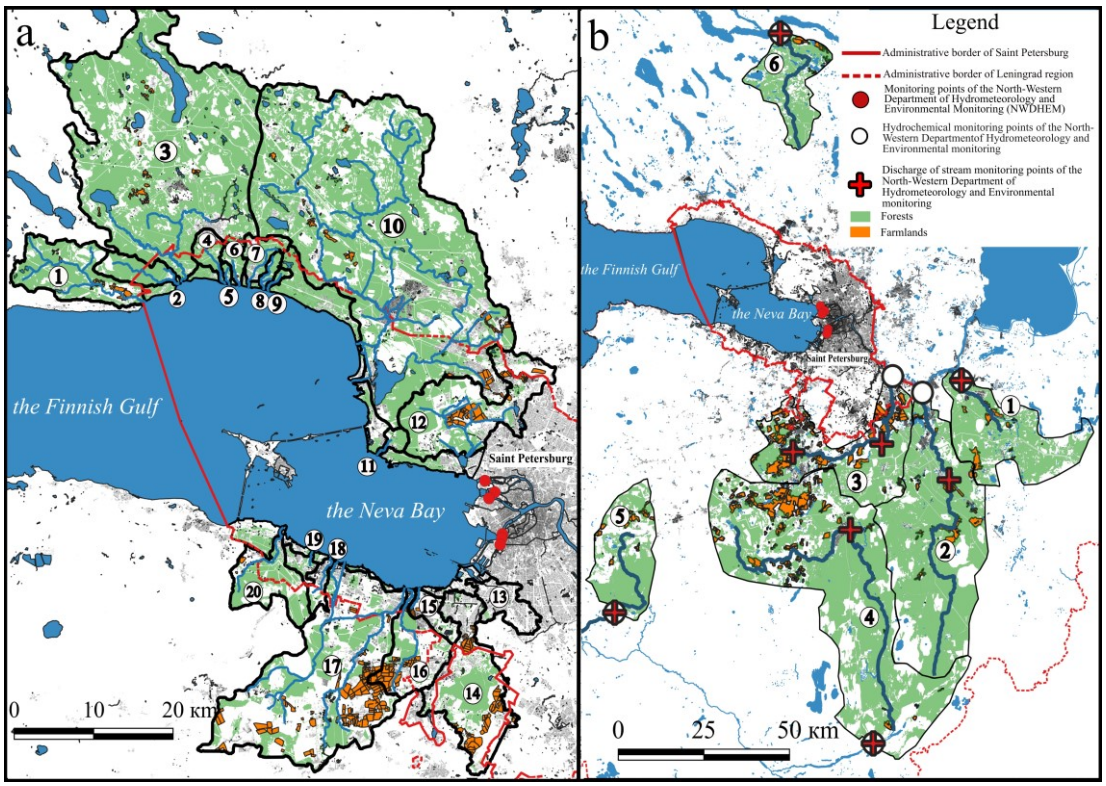

Fig. 2. Spatial structure of the catchment areas

The watersheds are clustered up in the following groups: the Bystraya, Chyornaya, Karasta, and Privetnaya Rivers, Shestoy, Tretiy, Ushkovskiy, and Vosmoy Streams, and **Volchya** River; the Sestroretskiy Razliv, the Smolyachkov Stream, the **Mga**, **Oredezh**,

Tosna, and **Vruda** Rivers; the Chyornaya Lakhta, Kikenka, Kristatelka Rivers, the Shingarka and Strelka Rivers, the Dudergofka River and Dudergofskiy Channel, the Ligovskij Channel and Krasnenkaya River, the Lahtinskij Razliv, the Strelka, Troitskiy, Zelenogorskiy Streams, Northern shore of the Finnish Gulf, Northern shore of the Neva Bay, Southern shore of the Neva Bay, and the **Izhora** River ones. Names of the analogous watercourses are highlighted in bold.

Table 1. Spatial structure of the catchment areas (1 – forests, 2 – wetlands, 3 – farmland area, 4 – residential construction, 5 – industrial zones)

Catchment area	Area, km^2	Share of the total watershed area, %				
		1	2	3	4	5
The researched watersheds						
Bystraya River	9.8	75.6	0.3	0.5	3.5	0.2
Chyornaya River	544.1	68.2	5.5	0.7	2.5	0.2
Chyornaya Lakhta River	7.6	61.7	0.0	0.0	17.6	0.7
Dudergofka River and Dudergofskiy Channel	126.7	27.7	0.1	10.0	10.7	4.7
Karasta River	59.6	60.6	3.2	0.8	3.4	0.7
Kikenka River	65.4	22.5	0.5	14.8	11.3	3.1
Kristatelka River	10.1	38.7	0.1		16.4	6.0
Lahtinskij Razliv	135.7	37.5	5.5	7.6	10.3	4.2
Ligovskij Channel and Krasnenkaya River	31.6	2.6	<0.1	0.0	27.9	14.6
Privetnaya River	83.6	68.6	5.8	3.4	4.1	<0.1
Sestroretskiy Razliv	766.1	60.7	9.7	1.2	4.8	0.4
Shestoy Stream	6.2	79.7	0.5	0.0	0.9	0.4
Shingarka and Strelka Rivers	324.7	27.8	3.4	9.1	9.5	2.1
Smolyachkov Stream	26.5	84.6	11.2	<0.1	0.2	0.1
Strelka Stream	19.0	11.6	0.9	6.1	16.0	5.8
Tretiy Stream	3.1	90.6	3.1	0.0	0.0	0.0
Troitskiy Stream	12.7	20.3	0.9	0.5	17.3	1.3
Ushkovskiy Stream	15.6	68.3	1.5	0.0	8.6	0.1
Vosmoy Stream	2.6	72.9	0.3	0.0	2.7	0.0
Zelenogorskiy Stream	19.9	62.3	0.7	0.0	21.1	1.8
Northern shore of the Finnish Gulf	68.7	63.3	1.6	0.0	14.6	2.0
Northern shore of the Neva Bay	22.3	33.2	5.8	0.1	21.5	0.7
Southern shore of the Neva Bay	40.1	25.3	9.2	0.0	7.9	17.2
The analogous watercourses watersheds						
Izhora River	864.7	36.9	3.1	13.9	7.0	2.8
Mga River	709.4	67.6	15.5	2.8	1.9	0.2
Oredezh River	2485.8	58.4	9.9	5.2	3.1	0.3
Tosna River	1637.7	69.5	17.5	2.8	1.9	0.4
Volchya River	417.3	71.1	3.5	3.0	4.0	0.1
Vruda River	537.3	62.2	7.9	3.3	1.1	<0.1

The analogous rivers watersheds are characterized by the following annual values of the total nitrogen and phosphorus unit discharges: one of the Volchya River – 130.6

kgN/km^2 and 11.7 kgP/km^2, the Vruda River – 1376.1 kgN/km^2 and 8.8 kgP/km^2, the Izhora River – 2416.0 kgN/km^2 and 141.4 kgP/km^2, the Mga River – 578.8 kgN/km^2 and 132.0 kgP/km^2, the Oredezh River – 812.8 kgN/km^2 and 11.5 kgP/km^2, and the Tosna River – 186.3 kgN/km^2 and 21.7 kgP/km^2. The total area of the first group of the researched watersheds is equal to 724.6 km^2, the second group – 792.6 km^2, and the third one – 884.5 km^2. For evaluation of the biogenic elements outflow from the researched watersheds of the groups, we used the unit discharges of the analogous rivers watersheds of the same groups. Therefore, the total nitrogen and phosphorus annual outflow from the first group of the researched watersheds is equal to 94.6 metric tons N and 8.5 metric tons P, from the second group – 585.3 tons N and 34.5 tons P, and from the third group – 2137.0 tons N and 125.1 tons P. Thus, the average annual outflow of the total nitrogen and phosphorus from the researched watersheds into the Neva Bay and the Finnish Gulf is equal to 2816.9 metric tons N and 168.1 metric tons P.

DISCUSSION

The research results add new knowledge to results of the biogenic elements outflow simulation from the Finnish Gulf catchment area according to the ILHM and ILLM computer models of Institute of Limnology of the Russian Academy of Sciences [10]. We research smaller watersheds within St. Petersburg and its outskirts.

CONCLUSION

Average annual income of the total nitrogen and phosphorus into the Neva Bay with the Neva River and its spill streams runoff for 1979-2019 was equal to 56860 metric tons of the nitrogen and 1716 tons of phosphorus [11]. Thus, the nonmetered income of the biogenic elements into the Neva Bay and the eastern part of the Finnish Gulf from the researched catchment areas is equal to about 5% of the nitrogen and about 9.8% of the phosphorus income with the Neva River and its spill streams runoff. The values do not include the biogenic elements income from some St. Petersburg areas, adjoining the Neva Bay, for example, the Vasilyevsky Island, and from the Kotlin Island. The authors plan to do evaluation of the income. It is evident, that urbanization of the researched watersheds and residential construction area increase within the watersheds can lead to increase of the total nitrogen and phosphorus income from St. Petersburg administrative area into the Neva Bay and the eastern part of the Finnish Gulf. Assessment of the ecologically reasonable rate of the anthropogenic impact on the Neva Bay and the Finnish Gulf ecosystems demands taking into account all sources of the nitrogen and phosphorus income into the ecosystems and wide appliance of computer simulation methodology.

ACKNOWLEDGEMENTS

The research was funded by Russian Science Fund, grant No 23-27-10011, and by Saint Petersburg Science Fund.

REFERENCES

[1] Boardman E., Danesh-Yazdi M., Foufoula-Georgiou E., Dolph C., Finlay J.C. Fertilizer, landscape features and climate regulate phosphorus retention and river export in diverse Midwestern watersheds, Biogeochemistry, vol. 146, pp 293–309, 2019. DOI: 10.1007/s10533-019-00623-z

[2] Jun D., Zhou Y., Chu L., Wei Y., Li Z., Wang T., Dai C. Spatiotemporal variations and determinants of stream nitrogen and phosphorus concentrations from a watershed in the Three Gorges Reservoir Area, China, International Soil and Water Conservation Research, vol. 11/issue 3, pp 507-517, 2023. DOI: 10.1016/j.iswcr.2022.09.004

[3] Verheyen D., Gaelen N. V., Ronchi B.J., Batelaan O., Struyf E., Govers G., Merckx R., Diels J. Dissolved phosphorus transport from soil to surface water in catchments with different land use. AMBIO A Journal of the Human Environment, vol. 44/issue 2, pp 228–240, 2015. DOI: 10.1007/s13280-014-0617-5

[4] Dolgov S.V., Koronkevich N.I. Current Features and Dynamics of Nutrient Balance in the Kud'ma River Basin. 2. Seasonal Removal of Nitrogen and Phosphorus, Water Resources, vol. 48/issue 5, pp 794-803, 2021. DOI: 10.1134/S0097807821050092

[5] Ulen B., Geranmayeh P., Blomberg M., Bieroza M. Seasonal variation in nutrient retention in a free water surface constructed wetland monitored with flow-proportional sampling and optical sensors, Ecological Engineering, vol. 139, 2019. DOI: 10.1016/j.ecoleng.2019.105588

[6] Goyette J.O., Bennett E.M., Maranger R. Differential influence of landscape features and climate on nitrogen and phosphorus transport throughout the watershed, Biogeochemistry, vol. 142, pp 155–174, 2019. DOI: 10.1007/s10533-018-0526-y

[7] Law J.Y., Brendel C., Long L.A., Helmers M., Kaleita A., Soupir M. Impact ofstacked conservation practices on phosphorus andsediment export at the catchment scale, Journal of Environmental Quality, vol. 49/issue 6, pp 1552–1563, 2020. DOI: 10.1002/jeq2.20140

[8] Hansen A.T., Dolph C.L., Foufoula-Georgiou E., Finlay J.C. Contribution of wetlands to nitrate removal at the watershed scale, Nature Geoscience, vol. 11/issue 2, pp 127–132, 2018. DOI: 10.1038/s41561-017-0056-6

[9] Yang J., Li M., Liu L., Zhao H., Luo W., Guo Y., Ji X., Hu W. Dynamic characteristics of net anthropogenic phosphorus input to the upper Yangtze River Basin from 1989 to 2019: Focus on the phosphate ore rich area in China, Journal of Environmental Management, vol. 347, 2023. DOI: 10.1016/j.jenvman.2023.119140

[10] Kondratyev S.A., Ignatyeva N.V., Shmakova M.V., Ershova A.A., Minakova E.A., Terekhov A.V. Model-based assessment of nutrient load into water bodies from different landscape types, Landscape Modelling and Decision Support, Springer Nature Switzerland AG, pp 299-310, 2020. DOI: 10.1007/978-3-030-37421-1_15

[11] Serebritskiy I.A., Grigoryev I.A. Environment protection, natural management, and ecological safety supporting in St. Petersburg. Russia, Sezam-Print, 2019, 448 pp (In Russian)

MICROPOLLUTANTS IN WATER FROM SURFACE RUNOFF AND THEIR IMPACT ON THE ENVIRONMENT

Ing. Jaroslav Hrudka, PhD.[1]

Ing. Reka Wittmanova, PhD.[1]

prof. RNDr. Ivona Skultetyova, PhD.[1]

Ing. Adam Kollar[1]

prof. Ing. Stefan Stanko, PhD.[1]

[1] Slovak University of Technology in Bratislava, Faculty of Civil Engineering, Department of sanitary and environmental engineering, **Slovakia**

ABSTRACT

Changing climatic conditions in urbanized areas have an enormous impact on the quality of life in urbanized areas. Persistent long-term dry periods, extreme downpours with large quantities or long-lasting rains are an extreme problem for efficient water management in cities. Extreme changes in the weather also result in a risk to the environment when soaking in or relieving highly contaminated water from the first flush. These wastewaters are a potential source of groundwater and surface water pollution, in which various types of pollutants are concentrated. In our research, we focus on the evaluation of water quality from surface runoff with an emphasis on concentrations of micropollutants on a global scale. The article is focused on research in the subject area and is a summary of the current view on the issue of micropollutants in water from surface runoff. Research in the field of pollution focuses on the evaluation of heavy metals, polycyclic aromatic hydrocarbons, non-polar extractable substances, halogen organic compounds or nitrogenous pollution.

Keywords: stormwater, sewer network, domestic water, micropollutants

INTRODUCTION

The nature of substances that enter the environment and threaten ecosystems based on contamination from rain runoff from paved areas can be divided into primary pollution sources - by the composition of rain water itself, which absorbs gases and solid substances found in the air, and sources of contact pollution, which occurs after contact of rain with a reinforced surface [1]. From the point of view of rainwater management (reuse) in urbanized basins, secondary pollution is a primary factor that can significantly degrade the quality of rainwater. The chemical composition of the rain itself is influenced by natural factors such as: the chemical composition of the air (nitrogen and oxygen content), the morphology of the territory and the like. The quality of atmospheric precipitation is largely conditioned by the intensity of development of urbanized areas, transport infrastructure and industry [2] [3]. Intensification of the creation of reinforced surfaces, suppression of permeable so-called vegetation areas was caused by the presence of undesirable and environmentally dangerous substances in the rainwater runoff, which are considered to be the main source of pollution of water bodies (rivers, lakes) [4].

Environmentally hazardous substances occurring in surface runoff can be of organic or inorganic origin from paved surfaces, e.g. from the road, parking lot, roof of buildings. Pollutants can be in soluble and insoluble form. Inorganic substances present in surface runoff include: particles of dust, sand, heavy metals (Cd, Cu, Ni, Pb, Zn), sulfates, chlorides, compounds of nitrogen, phosphorus and others. Organic substances mainly consist of petroleum substances, chlorinated hydrocarbons, PAHs, PBCs, pesticides, dioxides, various microbial substances such as coliform bacteria, mesophilic bacteria, etc. [3].

The variability of pollutants in surface runoff is determined by several parameters, but mainly depends on the use of the territory, the material used, internal and external factors such as: characteristics of pollutants and soil, and last but not least, the intensity and duration of precipitation. The dependence between the characteristics of rain and the concentration of pollutants has been described by many scientists in their studies. Lee et al. (2011) claims that this dependence can be conditioned by the intensity and duration of rain and the length of the dry season [5]. While Soller et al. (2005) in turn describes that the concentration of pollutants does not depend on the use of the territory and the duration of the rain, but on the intensity of the rain itself [6]. Other studies, on the other hand, claim that the largest amount of pollutants in surface runoff is after a long rainless period [7]. From the conclusions of the study, it can be concluded that the greatest concentration of pollutants accumulates in the initial phase of surface runoff, i.e. at the beginning of a precipitation event, and primarily depends on the intensity of rain and the length of the rain-free period. If, in the event of a precipitation event, surface runoff occurs, these substances will be moved, and they can be transported to the sewer system and subsequently transported to the nearest recipient. Over the years, many studies have been devoted to the analysis of the qualitative parameters of rainwater due to the manifestation of climate change and thus the risk of a crisis due to the lack of high-quality groundwater, an increase in air temperature, etc. The simultaneous use of a large amount of high-quality water and the removal of heavily polluted water causes significant damage to the aquatic ecosystem.

MATERIALS AND METHODS

As a rule, rainwater before hitting the earth's surface contains harmless concentrations of foreign substances, such as various gases, dust particles, aerosols, etc.. After contact with a paved surface, the number and diversity of these substances increases significantly, while their concentrations can exceed the limit values by several times , which establish the possibility of reusing these waters and thereby causing serious environmental damage. Due to the increasing trend of building paved areas, rainwater from surface runoff results in a number of environmental problems that can leave acute or cumulative effects caused by pollution. According to Slovak standards, acute sources of pollution can be considered to be their one-time effects that manifest themselves within 48 hours of contact with water, while cumulatively they have long-term effects that manifest themselves after months or years. The chemical composition of surface runoff from paved areas is determined by a number of factors, while its impact on the environment depends on the way it is handled in the urbanized area. Many studies consider rainwater runoff from roads as a direct source of pollution due to the increased content of dust particles and mixtures of toxic substances such as: heavy metals (Ba, Cr, Cu, Fe, Mn, Ni, Pb and Zn). The toxicity of these substances is variable, but mostly at a

high level and can represent potential ecological risks that differ according to the type, amount, toxicity and mobility of pollutants. Many studies indicate that heavy metals and polyaromatic hydrocarbons (PAHs) are the most dangerous contaminants due to their high toxicity and carcinogenic effects. While it is clear that the presence of a single type of heavy metal does not represent a significant risk, while the presence of several types of heavy metals can cause health problems. As part of the level of toxicity, it can also be stated that mercury, cadmium, copper and zinc can be identified as the most dangerous metals, while their risk to human health is significantly influenced by the volume of traffic and the industrial activity of the given area, given that the risk associated with rainwater from industrial areas is higher than from residential areas.
Uneconomic management of surface runoff has become a significant problem not only at the regional but also at the global level, which requires a better understanding due to the diversity of pollutants in surface runoff and their impact on water bodies. Direct removal of urban surface runoff to the nearest recipient, without any modifications, is considered a potential source of environmental pollution. Given the ever-increasing demand for water in the future, this could pose a serious environmental problem.

RESULT AND DISCUSSION

Výskum zameraný na kvlaitu povrchového odtoku z urbanizovanýc území môže byť zameraný na veľké množstvo polutantov. Priámrnymi ukazovateľmi sú ale anorganické ukazovatele, na ktoré sa zameriavame aj v našom výskume. Kvalita vody z povrchového odtoku je priamo ovplyvnená úrovňou urbanizácie sledovaného územia.

Table. 1 Characteristics of the event mean concentration (EMC) from rainfall runoff on an urban highway [8].

Parameter	Unit	Wooden shingle	Concrete tile	Ceramic covering	Sheet metal tile
pH	[-]	6,0 – 9,0			
TSS		213,9	309	219,3	285,8
TOC	[$mg.l^{-1}$]	49,7	32,9	35,6	31,8
SO_4^{2-}		5,57	3,64	3,1	2,87
Al		227	535	243	622
Cu		34	58	37	59
Fe	[$\mu g.l^{-1}$]	154	160	155	302
Pb		10	14	11	12
Zn		135	196	131	428

The material of the surface on which precipitation falls has a primary effect on water contamination. In table no. 1 shows the monitored footmeters that they monitored in their research in a highly urbanized area [8]. The research is also focused on the quality of water from different surfaces, such as a wooden or concrete roof. Of the monitored

surfaces, it appears to be the most suitable for is a wooden surface from which heavy metals are released or accumulate with it to the smallest extent.

Table. 2 Pollutant concentrations and pollution loads in stormwater runoff from different land uses [9].

Parameter	Concentration [mg.l^{-1}]	Parameter	Concentration [mg.l^{-1}]
TSS	631 ± 608	Zn	0,69 ± 0,43
CHSK	418 ± 311	Cu	0,13 ± 0,07
N_{total}	8,1 ± 5,0	Pb	0,58 ± 0,08
P_{total}	1,2 ± 1,4	Cd	0,051 ±0,009
N-NH_3	4,3 ± 2,3	Fe	11,8 ± 5,6

It is also important to observe real samples from different types of surfaces and from different types of urbanized areas. In table no. 2 shows the results from the research [9], where the basic parameters from the surface runoff were monitored. From these results, it is clear that the highest concentration in the monitored samples of the parameter zinc and lead, which represents localities with very intensive traffic.

Table. 3 Effect of Roofing Material on the Quality of Harvested Rainwater [10].

Rainwater samples	Heavy metals concentrations [mg/l]		
	Zinc	Cooper	Lead
Vegetated roof	0,5441	0,0156	0,1010
Gravel roof	0,696	0,0138	0,1104
Bituminous	2,7182	0,0122	0,109
Corrugated galvanized	2,6097	0,0101	0,0855
Colourbond steel	3,2081	0,0114	0,0532
Concrete tile	0,7283	0,0136	0,0814

Regarding the water from the surface runoff from the roof and the possibility of its use, it is necessary to take into account the material used on the surface of the roof. In research [10], the authors dealt with the quality of water from six types of materials used for roofs. They focused on the possibility of accumulating such water and reusing it. From the results of the research, which are shown in table no. 3, it is obvious that concrete tiles are the most suitable material in terms of the quality of retained water, while the most unsuitable material is bituminous tiles.

CONCLUSION

In the territory of the Slovak Republic, rainwater management in urbanized areas is not yet dealt with in detail by legal regulations and technical standards. In our research, we deal with this topic in detail. And we propose measures for efficient management of water from surface runoff in the territory of the Slovak Republic. On the territory of the Slovak Republic, this topic is partly dealt with in the legislation of the Water Plan of Slovakia in accordance with Article 4.7 letter d), Framework Directive on Water (2000/60/EC), which unreservedly supports measures to build water retention facilities in urbanized areas. Part of the content of NV SR no. 269/2010 in § 9, points 1–3, the requirements for the discharge of water from surface runoff into surface and underground waters are set, which define that in the event of the assumption of the content of hazardous substances in the surface runoff before indirect discharge, the necessary measures must be taken. According to Slovak regulations, surface runoff from paved areas means runoff from decommissioned and assembly areas, from areas of industrial areas and other areas where there is a risk of accumulation of pollutants, and monitoring of its quality is not considered for other waters from urban areas. The lack of Slovak regulations covering the area of water management is the precise definition of limit indicators of pollution when discharging/draining rainwater from surface drainage (communications, parking lots, roofs of buildings) into underground and surface waters.

ACKNOWLEDGEMENTS

This work was supported by the Scientific Grant Agency of the Ministry of Education, Youth and Sports of the Slovak Republic and the Slovak Academy of Sciences within the project VEGA 1/0682/23, co-funded by the Slovak Research and Development Agency under con-tract No. APVV-22- 0564.

REFERENCES

[1.] YANNOPOULOS, S., ANTONIOU, G., KAIAFA-SAROPOULOU, M., ANGELAKIS, N.A. Historical development of rainwater harvesting and use in Hellas: A preliminary review. Water Science & Technology: Water Supply, 2017. Volume 17. Issue 4. 1022–1034. © IWA Publishing 2017. ISSN 1606-9749.Thomas K.V., et al.: Comparing illicit drug use in 19 European cities through sewage analysis. Sci. Total Env.432, pp.432-439 (2012).

[2.] LI, CH., LIU, M., HU, Y., SHI, T., QU, X., TODD WALTER, M. Effects of urbanization on direct runoff characteristics in urban functional zones. Science of the Total Environment. 2018, Volume 643. Pages 301-311. ISSN 0048-9697.

[3.] PITTER, P. Hydrochémie, 4. VŠCHT Praha. 2009. 580 s. ISBN 978-80-7080-701-9.

[4.] LEE, J.Y., BAK, G., HAN, M. Quality of roof-harvested rainwater - Comparison of different roofing materials. Environmental Pollution, 2012. Volume 162. Pages 422-429. ISSN 0269-7491.

[5.] LEE, J.Y., KIM, H., KIM, Y., HAN, M.Y. Characteristics of the eventmean concentration (EMC) from rainfall runoff on an urban highway. Environmental Pollution, 2011. Volume 159. Issue 4 Pages 884-888. ISSN 0269-7491.

[6.] SOLLER, J., STEPHENSON, J., OLIVIERI, K., DOWNING, J., OLIVIERI, A.W. Evaluation of sesonal scale first flush pollutant loading and implications for urban runoff management. Journal of Environmental Management, 2005. Volume 76. Issue 4. Pages 309-318. ISSN 0301-4797.

[7.] QIAN, W., QIONGAHUA, Z., XIAOCHANG, C.W., JIEGUANG, H., YUAN, G. Impact of key factors on heavy metal accumulation in urban road-deposited sediments (rds): Implications for RDS management. Chemosphere, 2020. Volume 261. Article No. 127786. ISSN 0045-6535.

[8.] LEE, J.Y., KIM, H., KIM, Y., HAN, M.Y. Characteristics of the event mean concentration (EMC) from rainfall runoff on an urban highway. Environmental Pollution, 2011. Volume 159. Issue 4 Pages 884-888. ISSN 0269-7491.

[9.] WANG, S., HE, Q., AI, H., WANG, Z., ZHANG, Q. Pollutant concentrations and pollution loads in stormwater runoff from different land uses in Chongqing. Journal of Environmental Sciences, 2013. Volume 25. Issue 3. Pages 502-510. ISSN 1001-0742.

[10.] Ahmad, N., Faiz, M., Suif, Z., Othman, M., Che O., Siti K. (2022). Effect of Roofing Material on the Quality of Harvested Rainwater. 10.1007/978-981-16-7924-7_87.

MODERN TECHNOLOGIES IN THE FIELD OF HYDROLOGY TO PREVENT CRISIS PHENOMENA AND EXTRAORDINARY EVENTS

Ing. Boris Kollár[1]

Ing. Bronislava Halúsková[1]

Ing. Karin Nováková[1]

prof. Ing. Jozef Ristvej, PhD. EMBA[1]

[1] University of Žilina, **Slovak Republic**

ABSTRACT

Climate change brings a number of risks. Increasing numbers of weather fluctuations, floods, extreme heat and droughts have potential to endanger people's lives, health and property. The paper presents modern technologies and possible use in the field of hydrology connected to disaster management. Main attention is paid to the use of innovative technologies for the needs of protecting and prevent population from hydrological risks. Currently, the trend of introducing new technologies is clear, due to adapting to the challenges of today's digital age, thanks to their versatile usability and intelligent technological solutions. Tools for monitoring, analysing and evaluating extraordinary events caused by climate change are a basic prerequisite for their management and successful management. It primarily involves use of various sensors and radars for data collection, geographic information systems that enable spatial analysis and visualization, but also information systems and application software for creating models and simulations. Thanks to progress in development in the field of information technology, today it is also possible to use the Internet of Things, artificial intelligence or a DT to make predictions and create models. The mentioned tools represent an effective means of managing risks, planning and the necessary response of the responsible entities in the area of population and environmental protection, but also in the adoption of adaptation measures against the manifestations of climate change. It is important to minimize risks and damages to society and the ecosystem, always looking for innovative solutions in improvement that would contribute to environmental sustainability and progress, which is also the intention of this contribution.

Keywords: Disaster Management, New Technologies, Hydrology, Risk, Prevention, Climate Change.

INTRODUCTION

Climate-related extreme events, as manifested in hydrology, are major, increasingly frequent and intense events, particularly as a result of climate change. Threats associated with climate change impacts on hydrology affect different areas of life. These are mostly events of a contradictory nature, where water is in surplus or, on the contrary, in short supply. Both of these extreme situations are equally important for crisis management because they have a negative impact on humanity and require measures to protect lives,

property and sustainable management of water resources. Both phenomena are currently being studied by scientists as they affect processes and phenomena across the globe. Their impact is felt at different levels, from local and regional to the global sphere. In recent years, this has been particularly the case for events associated with the growing threat of drought, as evidenced by annual reports and statistics from domestic and international sources. The aim of this paper is to identify new opportunities for the use of modern technologies in building prevention and preparation against drought and water scarcity.

LACK OF WATER RESOURCES AS A CURRENT CHALLENGE IN THE FIELD OF HYDROLOGY

Drought is currently receiving considerable attention in various sectors. This is mainly due to its adverse impacts on people and society. However, drought is a relative term. This is due to differences in the world's understanding of the concept. In one part of the world, drought may not be considered as what it is in another [1]. In general, however, we can say that it is a lack of water for a particular activity, group of people, or environment due to a lack of rainfall over an extended period of time [2]. This drought can be manifested in the soil, plants or in the atmosphere [1]. Therefore, we can divide drought into categories. According to the area affected by the drought we distinguish:

- Meteorological drought,
- Soil drought,
- Hydrological drought
- Socio-economic drought [3].

A meteorological drought is a negative rainfall deficit from the long-term average for a given area. In terms of time, we can talk about one to two months. Meteorological drought, together with other factors such as soil characteristics or management practices, can lead to soil drought. This type of drought is characterised in particular by low soil moisture, which is important for plants. Soil drought can therefore cause problems for farmers in particular. Longer-term persistence of meteorological drought in conjunction with other climatic factors can lead to hydrological drought. This is characterised by a decline in watercourse levels and groundwater levels [3]. Mishra and Singh (2010) state in their publication that groundwater drought could be classified as a new type of drought [4-5]. The above mentioned types of drought considering mainly hydrological drought can lead up to socio-economic drought. This type of drought is characterised by an increased population demand for water that cannot be adequately met. In this case, water consumption exceeds naturally renewable and existing supplies [3].

These categories of drought have different impacts on the landscape and society, but are interrelated. There are dependencies between the drought categories. Lack of rainfall is the first cause of meteorological drought. Absence of rainfall leads to loss of soil moisture, thus creating soil drought. Insufficient runoff then leads to hydrological drought, which can result in socio-economic drought [6]. This link is illustrated in Fig. 1.

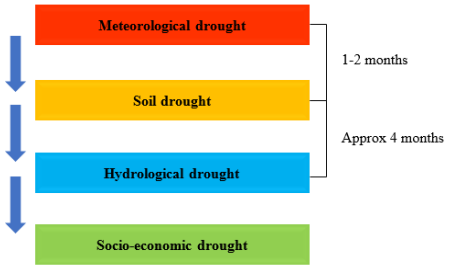

Figure 1 Connectivity of the different drought categories

We will refer to socio-economic drought in the next section as 'drinking water scarcity'. In the conditions of the Slovak Republic, drinking water scarcity was not specified as an extraordinary event (EE) or an emergency situation (ES) until at least September 2018. From 2013 until September 2018, a drinking water supply interruption or shortage was categorised as other. Therefore, it is not possible to assess the frequency of occurrence and the areas where this EE or ES occurred. In 2018, a separate category of EE and ES called drinking water shortage was created. In most cases, the individual data on drinking water scarcity lacks specification as to whether drought was the cause. In 2019, this EE was caused by a water main break. The cause 'adverse weather conditions' was specified for only one EE in 2018. The remaining EEs and ESs were not specified [6]. The annual reports on declared emergencies in the country record more frequent occurrences of drinking water shortages due to drought from year to year. The record year in the number of recorded events in our territory was recently the year 2022, when 25 cases were recorded [7-8]. The year 2022 was characterized by extreme heat events, when the highest temperature record in Europe fell multiple times. Drought and the associated scarcity of water resources and potable water have been a global problem for humanity in several parts of the world in many cases [9]. An example is Africa, where 88.9 million people have been affected by drought. In China, the drought affected 6.1 million people and caused financial losses of USD 7.6 billion, in the USA (USD 22 billion) and in Brazil (USD 4 billion). In Uganda, drought-induced famine caused 2 465 deaths [10].

IMPORTANT FACTORS INFLUENCING DROUGHT IN GROUNDWATER

Hydrological drought, or groundwater drought, which can lead to a shortage of drinking water for an area's population, is influenced by several factors. These factors include:

- precipitation activity,
- evapotranspiration,
- soil moisture,
- geology (hydrological properties of bedrock),
- the orographic structure of the territory,
- abstraction [4], [11].

The different factors influencing hydrological drought as well as other drought categories enter into the assessment of drought or its identification in a given area. This assessment is carried out through drought indices. They are used to quantitatively assess individual parameters that determine the extent, duration, intensity and magnitude of drought. The individual variables should be able to quantify drought according to different time periods. For this, long time series data are needed. For population water supply and groundwater abstractions, monthly time periods for monitoring the effects of drought

seem to be the most appropriate. These indices use rainfall as the main variable. However, in many cases they also include other hydro meteorological variables such as air temperature or evaporation [4]. Table 1 below shows some selected indices to assess the effects of drought or its characteristics in a particular area. The table also includes the necessary input data for the calculation of each index.

Table 1 Selected indices for assessing effects of different drought categories [1; 12-14].

Drought index	**Required input data**
Standardised precipitation index (SPI)	• total precipitation
Effective Drought Index (EDI)	• total precipitation
Standardised groundwater level index (SGI)	• total precipitation • groundwater level
Standardised precipitation and evapotranspiration index (SPEI)	• total precipitation • air temperature
Soil moisture index (SMI)	• soil moisture

As mentioned, hydrological drought or groundwater drought is influenced by other drought categories [6]. Table 1 shows only some of the indices identifying drought, and the indices used for different drought categories are listed here. The table also includes the necessary input data required for the calculations. The drought characteristics computed using the indices can further input into various models used for drought prediction [15].

MODERN TECHNOLOGICAL SOLUTIONS IN THE FIELD OF HYDROLOGY

Current meteorological information can be used for real-time weather assessment. Information on current and future possible rainfall totals, surface and subsurface water level heights, evaporation or air temperature can provide us with warning signals of crisis phenomena [16-17]. From a prevention perspective, it is important to collect and record this information. The collected and processed data can serve as input data for the calculation of indices and the creation of models or simulations of droughts that can lead to drinking water shortages.

In general, two modern approaches can be used to collect meteorological or hydrological data. These include digital data collection using satellites or drones, and in the second case, the Internet of Things (IoT) involving various smart meters and sensors [18]. The CIMA Research Foundation focuses on exploiting the potential of satellites and using satellite data to cover larger areas, filling in the gaps for hard-to-reach environments where sensors cannot be installed [19]. IoT is a network infrastructure whose objects are equipped with computing and communication capabilities and enable the collection and transmission of data to central servers. The structure of the IoT consists of several layers, with the first two being crucial for the collection of meteorological and climate data. The first layer represents physical objects, i.e., sensors that can measure soil moisture, air temperature, evaporation, precipitation, and other factors affecting hydrological drought. The second layer consists of transmitting the data to the system for its processing. This

transmission is provided by, for example, Wi-Fi, Bluetooth, 3G or other forms of network technologies [18].

The EU's new climate change adaptation strategy also addresses digital transformation and the use of new technologies and climate services. It highlights the use of digital twin (DT) technology to support decision-making on crucial topics, taking into account the considerable uncertainties of future climate impacts [20].

THE DIGITAL TWIN IN HYDROLOGY

The DT concept was developed as a priority for industries, for a comprehensive record of the operation of factories and the effect of proposed changes in a plant or process [21]. Gradually, however, the concept began to expand into more areas and domains. Over time, technology has been implemented in many industries and areas of social life, hence there is no standardized definition of the concept of DT [22].

One of the earliest of the DT definitions can be considered to be that of the National Aeronautics and Space Administration (NASA). DT stands for: "an integrated, multiphysics, multidimensional, probabilistic simulation of a vehicle or system as-built that uses the best available physical models, sensor updates, fleet history, etc. to mirror the life of its corresponding flying twin"[23]. DT represents in virtual form a replica of physical systems and their processes. The replication is based on artificial intelligence and machine learning, which is where IoT comes in. The main components of DT are: the physical object, the virtual object and their interconnections [24]. Both physical and virtual elements exchange information in order to monitor, simulate, predict, diagnose, and control the state and behaviour of the physical object in the virtual space" [25]. The principle is the use of real-world data, simulations and machine learning models combined with data analysis. The main goal is to enable and support understanding, learning, and reasoning about "what if" questions in the specific conditions under study, with an emphasis on predicting the possible direction of events [22].

Concerns about drought, drinking water scarcity and the overall management of water resources are justified by the impact of climate change. In the field of hydrology, DT can support adaptation to climate change in several ways:

- Predicting periods with potential drought and extreme weather events,
- identification of potentially vulnerable locations,
- testing hydrological adaptation strategies,
- Virtual modelling of buildings, places, systems, environments,
- modelling and simulation of water flows, catchments, groundwater systems,
- increasing knowledge of hydrological risks,
- assessing potential risks and impacts of climate change on hydrology, etc. [26].

A realistic implementation of the DT concept would represent a significant advance in hydrology and would keep the technological pace with countries in the world:

- The DT would contain databases that would provide the user with a range of information about events where the monitored area has historically experienced extreme drought. The information would cover the affected population, their numbers and age structure at the time of EE as well as current demographic trends for the purpose of providing potable water supplies when needed.

- A digital replica of the physical environment, supported by maps, 3D visualization, would provide an overview of the monitored area (rock composition and soil structures, surface and groundwater flows, flow diversion possibilities, soil moisture and potentially drought-prone areas.
- Real environment would transmit real-time data to the DT using monitoring sensors for prediction purposes for areas that are susceptible to drying out. Using indices, models, machine learning AI, IoT, exploratory thresholds would be defined and set in DT to predict water balance, highlight opportunities and threats taking into account current and future climate change.
- DT can be a valuable tool to reduce and manage disaster risk through updated data and regular forecasts, strengthen early warning systems, minimize the impact of detected extreme events, and build societal hydrological resilience.
- Using implemented simulation and forecasting models to test adaptation options, strategies in a safe environment in parallel with potential risks and impacts of climate change.
- Decision support [26], and further reading in this domain.

CONCLUSION

Knowing the level of risk of crisis phenomena, their causes and consequences, and the areas of occurrence are a prerequisite for taking preventive measures. Prevention is the basic idea of crisis management, and the knowledge gained in this phase is further fed into the phase of preparation and preparedness for emergencies. The implementation of preventive measures also enables the creation of conditions for the preparation of all forces and resources for the effective management of EE. This is nowadays aided by technologies such as the increasingly popular (DT).

A major prerequisite for the development and implementation of DT in hydrology is the availability of data from a variety of sources, in particular sensors, monitoring systems and other sources of good quality information. Once collected, the data need to be cleaned, standardized and integrated into a DT, for the purpose of creating the necessary models. The DT should include other advanced computing technologies and resources capable of evaluating, predicting, and combining data from the real environment in real time for the purpose of early warning and transmission of information about potential change and deviation from standard processes (e.g.: reaching thresholds of monitored water level, reduction of soil moisture of the study area due to absence of precipitation, soil drought caused by extreme temperatures, etc.). When implementing, it is important to define, among other things, the goals, plans and objectives for the use of DT as well as the opportunities for the use of the technology. Collaboration with stakeholders from different sectors, industry, government and academia is key in identifying potential application areas.

The complexity and difficulty of creating and implementing technology, whether at regional or national level, requires the necessary financial resources, expertise, and staffing and technical support. However, it can be assumed that any investment made will be leveraged for the benefit of decision support, adaptation to change and risk reduction. In hydrology, this could support decision-making in water resources management, climate change adaptation and disaster risk reduction and overall crisis management

support during ES. DT could strengthen sustainable water resources management, water security, planning and the implementation of early action on potentially vulnerable areas.

ACKNOWLEDGEMENTS

The contribution was created as part of the KEGA project no. 043ŽU-4/2022 "Implementation of knowledge from social, behavioural and humanitarian scientific disciplines in the preparation of students of the study field of security science."

Publication of this paper was supported by the Scientific Grant Agency of the Ministry of Education, Science, Research and Sport of the Slovak Republic – VEGA No. 1/0459/21: "Proposal of adaptation measures to reduce the risks arising from climate change in terms of the occurrence of the disasters and the extreme weather events."

REFERENCES

[1] Jarošová M., Igaz D., Identification of the occurrence of drought according to different indices at stations in western SR, Meteorological journal, vol. 20/ issue 2, pp 73-82, 2017. ISSN 1335-339X

[2] Wilhite, D. A. (ed.). Drought and Water Crises: Science, Technology and Management Issues. CRC Press, Boca Raton, FL, 2005, 432 p.

[3] Cutter, S. L. [ed.]. American Hazardscapes: The Regionalization of Hazards and Disasters. – Natural Hazards and Disasters Series, 2001, 211 p.

[4] Ashok K. Mishra, Vijay P. Singh, A review of drought concepts, Journal of Hydrology, Volume 391, Issues 1–2, Pages 202-216, 2010. ISSN 0022-1694.

[5] Rehak, D., et al. (2020): T. Personnel Threats in an Electric Power Critical Infrastructure Sector and Their Impacts on Dependent Sectors. Safety Science, 2020, 127: 104698. DOI: 10.1016/j.ssci.2020.104698.

[6] Ministry of the Interior of the Slovak Republic. Monthly situational reports on reported emergencies and other events on the territory of the Slovak Republic and abroad and annual reports. Available at: https://www.minv.sk/?mesacna_situacna_sprava

[7] Emergency statistics for 2020. 2021 [online]. Ministry of the Interior of the SR. Available at: https://www.minv.sk/swift_data/source/images/skr-mimoriadne-udalosti-2020-prehlad.pdf

[8] In 2022, Slovakia faced 222 emergencies, emergency situations were declared in 102 cases, 2023 [online]. Ministry of the Interior of the Slovak Republic. Available at: https://www.minv.sk/?tlacove-spravy-7&sprava=v-roku-2022-slovensko-celilo-222-mimoriadnym-udalostiam-mimoriadna-situacia-bola-vyhlasena-v-102-pripadoch

[9] Rehak, D. et. al. (2017) Indication of Critical Infrastructure Resilience Failure. In Safety and Reliability - Theory and Applications - Proceedings of the 27th European Safety and Reliability Conference (ESREL 2017), 2017, pp. 963-970.

[10] CRED. 2022 Disasters in numbers. Brussels: CRED; 2023. Available from: https://cred.be/sites/default/files/2022_EMDAT_report.pdf

[11] Nejedlík P., Minďaš J. (ed.), Impacts of climate change and possible adaptation measures in different sectors. Final report–summary, SHMU, Bratislava, 2011. Available at:

https://www.shmu.sk/File/projekty/Zhrnutie%20projektu%20Klim.%20zmena%20a%20Adaptacie%202012.pdf

[12] Surda P., Tárník A., Roncak P., Vítková J., Regional drought assessment based on the meteorological indices for locality Nitra, Acta hydrologica slovaca, vol. 20, issue 1, pp. 63-73, 2019, DOI: 10.31577/ahs-2019-0020.01.0007.

[13] Halder, S., Roy, M.B. & Roy, P.K. Analysis of groundwater level trend and groundwater drought using Standard Groundwater Level Index: a case study of an eastern river basin of West Bengal, India. SN Appl. Sci. 2, 507 (2020). DOI:10.1007/s42452-020-2302-6

[14] Vido, J., Šustek, Z. Drought and biodiversity. Prievidza, Zvolen: Oikos, (2021). 110 p.

[15] Fung, K. F., Huang, Y. F., Koo, C. H., & Soh, Y. W. Drought forecasting: A review of modelling approaches 2007–2017. Journal of Water and Climate Change, vol. 11, issue 3, pp. 771-799. (2020). DOI:10.2166/wcc.2019.236

[16] Jánošíková M., Ristvej J., Zábovská K., Lacinák M., Use of constructive simulation in preparation of crisis management personnel for solving crisis events, 34th Annual European Simulation and Modelling Conference, ESM, Toulouse, pp. 92-97. (2020).

[17] Lacinák M., Ristvej J., Jánošíková M., Sensors and Simulations for Transport Resilience, Journal: EAI Endorsed Transactions on Energy Web, vol. 9, issue 40, (2022), ISSN 2032944X.

[18] Hsu A., Khoo W., Goyal N., Wainstein M., Next-Generation Digital Ecosystem for Climate Data Mining and Knowledge Discovery: A Review of Digital Data Collection Technologies, Journal: Frontiers in Big Data, vol. 3, (2020), ISSN 2624-909X, DOI: 10.3389/fdata.2020.00029

[19] Hydrological Digital Twin: the water cycle in a virtual reality. CIMA Research Foundation. 2023. Available at: https://www.cimafoundation.org/en/news/hydrological-digital-twin-the-water-cycle-in-a-virtual-reality/

[20] EC 2021. EU Strategy on Adaptation to Climate Change. COM/2021/82 Final. Available at: https://eur-lex.europa.eu/legal-content/EN/TXT/?uri=COM:2021:82:FIN

[21] Milner, G., South Korean City Uses a Digital Twin to Meet Challenges. In: ArcUser. Summer 2021. Esri. 21-23, 2021. Available at: https://www.esri.com/about/newsroom/arcuser/south-korean-city-uses-a-digital-twin-to-meet-challenges/

[22] Halúsková B., Digital Twin in Smart City. TRANSCOM 2023: 15th International Scientific Conference on Sustainable, Modern and Safe Transport.

[23] Glaessgen EH, Stargel DS. (2012) The Digital Twin Paradigm for Future NASA and U.S. Air Force Vehicles. 53rd. AIAA/ASME/ASCE/AHS/ASC Structures, Structural Dynamics and Materials Conference 20th AI 23-26. April 2013, Honolulu, Hawaii.

[24] Grieves M., Digital twin: manufacturing excellence through virtual factory replication. *White paper* 2014; 1: pp. 1-7.

[25] Segovia, M.; Garcia-Alfaro, J., (2022) Design, Modeling and Implementation of Digital Twins. In: Sensors 2022, 22, 5396. DOI: 10.3390/s22145396

[26] Henriksen H.J. at al. A New Digital Twin for Climate Change Adaptation, Water Management, and Disaster Risk Reduction (HIP Digital Twin). In Water 2023, vol. 15, issue 1, 25, 2023. DOI: 10.3390/w15010025.

MULTI-CRITERIA ANALYSIS OF THE DYJE BASIN AND COMPARISON WITH ANALYZES IN THE PARDUBICE REGION

Ing. Miroslava Plevková

Prof. Ing. Miroslav Dumbrovský

CSc., Ing. Martina Kulihová

Brno University of Technology, Faculty of Civil Engineering, Institute of Landscape Water Management, **Czech Republic**

ABSTRACT

Adaptation strategies are highly desirable documents based on more frequently occurring hydrological extremes. These strategic documents are prepared at different levels, the state level on one side and the regional or city level on the other side. The complex approach that was chosen for the Pardubice and Pilsen regions was also applied to the territory of the Dyje basin. Specifically, a multi-criteria analysis was used as a means of selecting priority model areas. Based on the analyses developed from the available geospatial landscape data, an evaluation scheme was created, divided into three categories: problems, potential, and needs. This simply means that geospatial information about the area under consideration was combined and evaluated in various ways. The result is the regionalization of the territory based on the given preferences. All categories contain additional subtopics and problem indicators. These include subtopics such as climatic drought, drought in waterways, soil, floods, and land cover. The continuation of this analysis will include the social aspect, namely the consent of the owners regarding the implementation. The outcome will be a summary table of all IV. basins in a specific order with individual evaluation parameters, as well as the creation of a geospatial database that can be utilized in the framework of proposals for adaptation measures.

Keywords: multi-criteria analysis, Dyje basin, floods, land cover, erosion

INTRODUCTION

The topic of adaptation measures has come to the fore in response to climatic and hydrological extremes such as floods and droughts. Different views on finding optimal solutions result from a lack of effective communication not only between the academic community and investors implementing these measures, but also with the wider public. Regarding the significantly changed landscape of the Czech Republic due to historical human activity associated with limitations of resources and workforce capacity, the primary goal is to identify areas where adaptation measures will bring the most significant effectiveness.

Although there is a need for comprehensive solutions for adaptation measures, their implementation in a shorter time interval and at the same time on a larger spatial scale is not realistic. For this reason, the territory needs to be regionalized in terms of the need to implement adaptation measures and to define the most priority areas. Adaptation measures will be designed and implemented in these priority areas, and they will

proceed to less priority regions. For this purpose, a procedure was established for the selection of priority (most problematic) areas, which will be as objective as possible and will reflect the actual state of the area. In this way, basins in the Pardubice [1] and Pilsen [2] Regions have already been selected and processed. The presented article compares some indicators of the Pardubice region with the developed analysis for the Dyje basin, in terms of partial overlap in the northern part of the area of interest.

MATERIALS AND METHODS

Multi-criteria analysis (MCA) involves systematic procedures for formulating, evaluating, and selecting alternatives, usually relying on conflicting criteria. Its application is used in various areas of decision-making in environmental topics [3].

The Dyje basin (Figure 1.) was chosen as the area of interest, which extends into eleven basins of the third order. The selection of the project is linked to the scope of the state enterprise Povodí Moravy, which has been making continuous efforts to enhance conditions, not only along watercourses but also within the basin area.

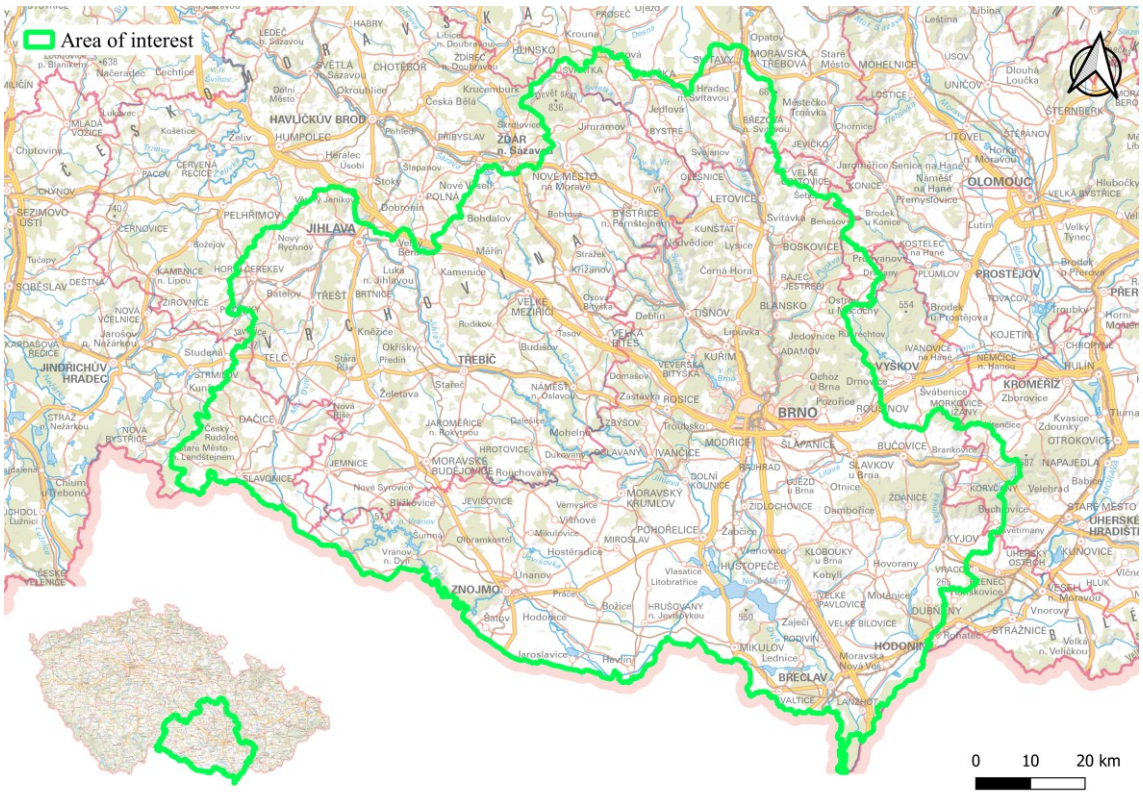

Fig. 1: Area of interest.

The territorial unit for carrying out the multicriteria analysis was basin IV. order. These basins were defined by the Digital base of water management data [4]. A revision of the watersheds defined in this way was carried out for the area under consideration, and the smallest watershed (with a size of units under 0.1 km^2) was associated with neighboring larger watersheds. Also, basin IV. order, which extended more than 50 % of its area beyond the borders of the Czech Republic, was not assessed. Main reason was that the data used in MKA are only available for the territory of the Czech Republic, so there would be an error when converting parameter to the area of the basins. In the result, a

total of 1001 watersheds with a size from 0.11 km^2 to 64.5 km^2 were defined in the area of interest.

The multicriteria analysis was divided into three main themes. Each theme had a sub-theme, and the sub-theme was expressed by indicators. Three main themes were problem (expresses the problem of the given territory), potential (expresses the natural and social prerequisites for improvement) and need (expresses the needs of the socio-economic sphere in the territory. The logic of the solution is that, although the territory may be very problematic, it is expedient to propose measures here only if there is potential for improvement. At the same time, it is expedient to propose measures where the requirements (needs) for the territory are clearly given, and without the implementation of the measures, the territory could cease to fulfill its functions.

Since the presented paper is part of a complete multi-criteria analysis, the indicators listed below are put into context, but the resulting priority areas are not selected. This will be part of the overall MCA for the Dyje basin.

For purposes of MCA, individual indicators were given points, expressing the area or the total length of the catchment area. Specifically, by overlaying the layers in the ArcMap program (using the “Intersect” command), it was determined which area is in a specific IV order basin. The given indicator was subsequently divided into categories on a scale of 0 to 5 points, where 0 = the indicator does not occur here either at all or only negligibly, and 5 = significant influence and occurrence of the indicator. The second group of indicators was whether the given phenomenon is located in the territory or not, i.e. a value of one or zero.

The following data were used for the analyses:

- Digital base of water management data [4], specifically A01 - Watercourse shapefile, A05 - Water dams, A07 - fourth order basins, A08 - third order basins, C09 - CHOPAV (Protected area of natural water accumulation), C10 - OPVZ (Protection zones of water resources), D01 to D05 Flooded areas,
- LPIS (Land parcel identification system) [5], information about arable land, permanent grass vegetation, heavily and slightly erosion-prone areas,
- Land reclamation data (vector shapefile format), acquired by the former Agricultural Water Administration under the administration of the Ministry of Agriculture [6],
- Critical points and their contributing area [7],
- Dyje sub-basin plan 2021-2027 [8], specifically areas with a significant risk of flooding,
- Data Monitored erosion events 2022 [9].

The result of this paper is a preliminary representation of the ten most problematic catchments of the fourth order. The resulting value in the individual basins was determined as the sum of the indicators in the topic "problem". The following parameters were included: 1. Extent of surface drainage, 4. Extent of arable land, 5. Extent of slightly eroded soil blocks (MEO) according to LPIS, 6. Extent of highly eroded soil blocks (SEO) according to LPIS, 7. Occurrence of erosion events, 8. Land parcel over 30 ha in the basin, 9. Areas with a significant risk of flooding, 10. Occurrence of critical points, and 11. Critical points – contributing area.

Other categories (2. Total length of melioration drainage channels in the basin and 3. Total length of water regulation) are only described through the results and will be included in further evaluations within the overall MKA.

RESULTS AND DISCUSSION

Since the presented article is part of a complete multi-criteria analysis, the indicators listed below are put into context, but the resulting priority areas are not selected. This will be part of the overall MCA for the Dyje basin. As already mentioned, only 11 indicators will be evaluated below. The total number of indicators in the Pilsen region reached 135 (but just 64 indicators were used in MCA) and in the Pardubice region 97 indicators and all of them were used in MCA.

Specific indicators:

1. Extent of surface drainage

Land reclamation data were used, the result is the percentage of drained areas from the total area of the basin. In the area of interest there are catchments without surface drainage, the highest value was 100 %. This indicator will be valuated into 6 categories. According to the results in the MCA of the Pardubice Region, the values ranged from 0 to 83 %. As the territory of the Pardubice region and the Dyje basin overlap, we can check the categorization here. Within the Pardubice region, a distinction was made into 5 categories (0 = there is no drainage and 4 = the largest proportion of drained areas. The correct setting of categories and intervals in individual parameters will be the most important step for comparing data within the Czech Republic (see table for basic differences).

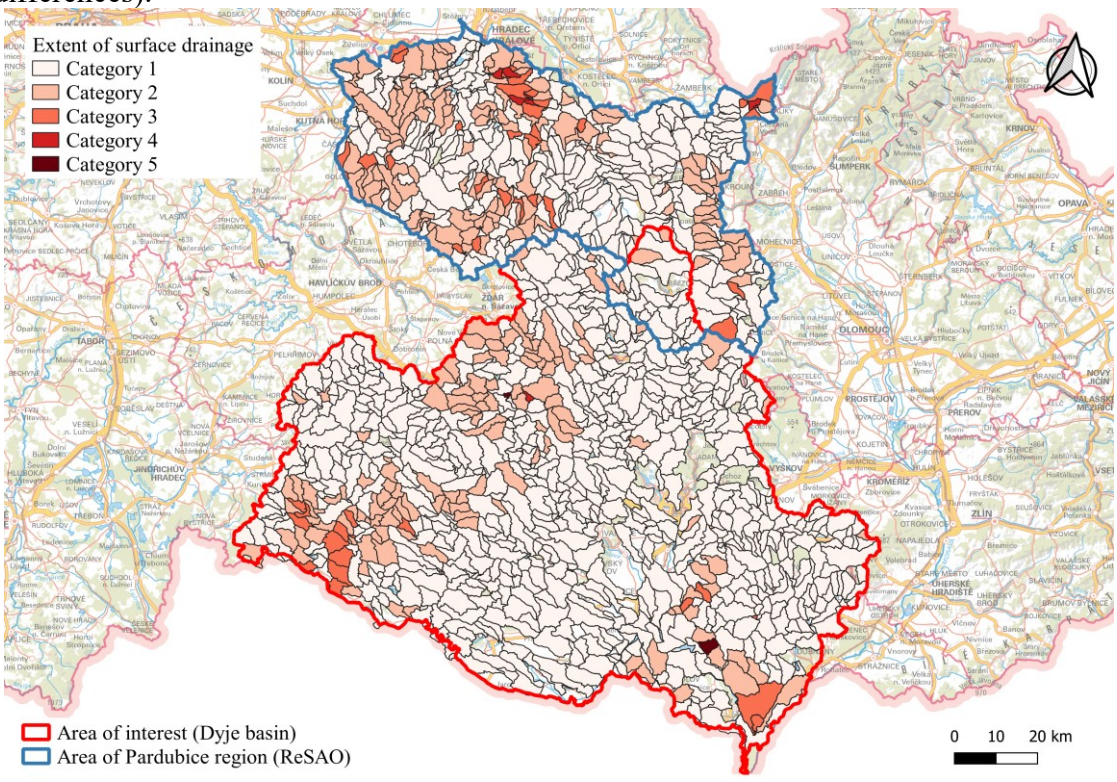

Fig. 2: Comparison of indicator “Extent of surface drainage” in Pardubice region and in area of interest, we can see a partial overlap (category 0 is transparent).

Table number 1: Indicator categories and results:

Category	Value	Sum of basins (Dyje basin)	Basin percentage (Dyje basin)	Sum of basins (Pardubice region)	Basin percentage (Pardubice region)
0	Null	125	12,5	52	10,4
1	1 - 20 %	718	71,7	292	58,6
2	21 - 40 %	137	13,7	143	28,7
3	41 - 60 %	17	1,7	3	0,6
4	61 - 80 %	2	0,2	7	1,4
5	81 - 100 %	2	0,2	1	0,2

2. Total length of melioration drainage channels in the basin (not included to final representation - potential)

Land reclamation data were used, the result is in the kilometres of melioration drainage ZV110 (main drainage facility), ZV300 (main melioration facility open), and ZV310 (main melioration facility piped) was included. This indicator was valuated into 6 categories. Total length of melioration drainage in the Dyje basin is 710 km, mostly watershed in in the open countryside. Higher value of total length was 20 km per basin.

3. Total length of water regulation (not included to final representation - potential)

Land reclamation data were used, the result is in the kilometres of watercourse regulation ZV 200 (watercourse adjustment) and ZV210 (watercourse adjustment by piping) was included in this category. Total length in the Dyje basin is 2324 km of watercourses. It is almost 20 % of the whole length of all watercourses.

4. Extent of arable land

LPIS data were used, the result is in the percentage of arable land areas from the total area of the basin. Same categorization as in indicator 1. In the area of interest there are basins without arable land, the highest value was 92 %. This indicator will be valuated into 6 categories. Here the question of categorization arises. If we use the same categorization as in the first indicator, up to 86 % of the basins are in category 1. For this reason, it is possible to consider division into categories using a different distribution. Below is a table of the various breakdowns into categories. This indicator was not assessed in the Pardubice region.

Table number 2: Different distribution of the same indicator:

Category	Value	Sum of basins and percentage	Value	Sum of basins and percentage
	Original values		Natural breaks	
0	Null	19 (1.9 %)	Null	19 (1.9 %)
1	1 - 20 %	192 (19.2 %)	0,1 - 16,2	146 (14.6 %)
2	21 - 40 %	265 (26.5 %)	16,3 - 33,9	217 (21.7 %)
3	41 - 60 %	299 (29.9 %)	34,0 - 50,8	263 (26.3 %)
4	61 - 80 %	183 (18.3 %)	50,9 - 67,1	201 (20.1 %)
5	81 - 100 %	43 (4.3 %)	67,2 - 92	155 (15.5 %)

Table number 3: Different distribution of the same indicator:

Category	Value	Sum of basins and percentage	Value	Sum of basins and percentage
	Quantile		Geometrical interval	
0	Null	19 (1.9 %)	Null	19 (1.9 %)
1	0,1 - 22,4	225 (22.5 %)	0,1 - 24,9	248 (24.8 %)
2	22,5 - 37,5	180 (18.0 %)	25,0 - 40,9	218 (21.8 %)
3	37,6 - 48,4	181 (18.1 %)	41,0 - 51,1	164 (16.4 %)
4	48,5 - 63,2	202 (20.2 %)	51,2 - 67,0	197 (19.7 %)
5	63,3 - 92	194 (19.4 %)	67,1 - 92	155 (15.5 %)

5. Extent of slightly eroded soil blocks (MEO) on arable land according to LPIS
6. Extent of highly eroded soil blocks (SEO) on arable land according to LPIS

In both indicator above LPIS data were used, the result is in the percentage of MEO and SEO on arable land from the total area of the basin. Parcels marked as slightly eroded soil blocks (MEO) in the LPIS, farmers are obliged to ensure that erosion-prone crops: corn, potatoes, beets, soybeans, soybeans, sunflowers and sorghum will be established only with the use of soil protection technologies. Parcels marked as highly eroded soil blocks (SEO) in the LPIS, farmers are obliged to ensure that erosion-dangerous crops are not grown on them: maize, potatoes, beets, soybean, soybean, sunflower and sorghum; stands of other cereals and oilseed rape on so marked areas will be established using soil protection technologies; in case of cultivation of others of cereals, the condition of applying soil protection technologies during establishment does not have to be met stands only if they are grown with an underseeding of clover, grass or clover fodder mixtures.

7. Occurrence of erosion events

Erosion events data were used, from the point of evaluation is the second group of indicators whether the given phenomenon is located in the territory or not, i.e. a value of one or zero. According to the provided documents, 662 erosion events have been recorded in the area of interest. Since this is data that is recorded at the initiative of citizens or a responsible worker, there may be an error in the underlying data, when more significant and extensive erosion events may not be recorded.

8. Land parcel over 30 ha in the basin

LPIS data were used, from the point of evaluation is the second group of indicators whether the given phenomenon is located in the territory or not, i.e. a value of one or zero.

9. Areas with a significant risk of flooding

Areas with significant risk of flooding were used, from the point of evaluation is the second group of indicators whether the given phenomenon is located in the territory or not, i.e. a value of one or zero.

10. Occurrence of critical points

Critical points data were used, from the point of evaluation is the second group of indicators whether the given phenomenon is located in the territory or not, i.e. a value of one or zero.

11. Critical points (contributing area)

Critical points data, specifically their contributing area were used. The result is in the percentage of contributing area to basin area.

Preliminary representation of the ten most problematic catchments of the fourth order. The maximum value achieved by the above sum was 19 and this was reached in one basin (ID 415030420). All the listed parameters are located in this basin, and the territory was potentially selected as a priority area. After all indicators will be included, the evaluation will be supplemented and closed. On the figure below we can see ten priority areas after evaluating ten indicators in the theme problem. The ten most priority basins are still highlighted in the picture below.

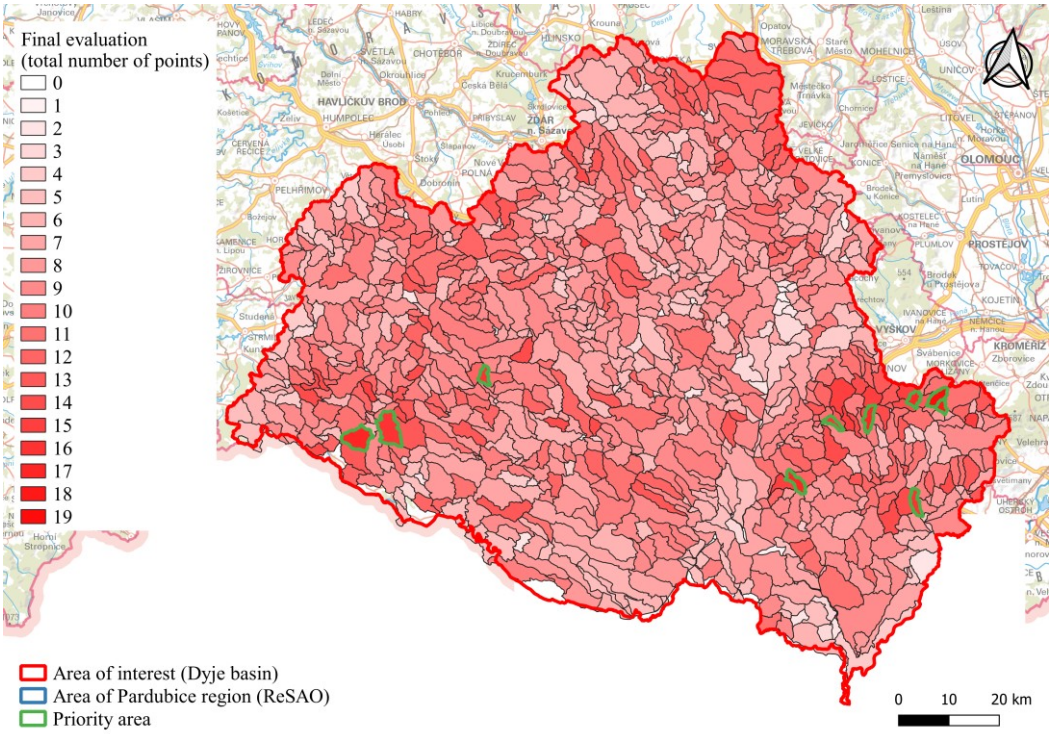

Fig. 3: Final evaluation.

CONCLUSION

If we look at the above results, we can see that the landscape of the Dyje basin is significantly modified by man. The length of the treated waterways is almost 20% of the total length of all the streams, a significant part of the territory is used as arable land, even in places with a significant slope of the territory. The total summary of identifiers in the topic problem, they show us which watersheds IV. of the order are the most threatened from different views of the landscape (see figure no. 3). This preliminary statement of problematic basins will be further supplemented with other themes and categories.

From the point of view of division into categories, based on the evaluation of all parameters, it will be necessary to check statistically whether any indicator is undervalued or, on the other hand, overvalued. The possibilities of division are, for example "natural breaks", "quantile" "geometrical interval" or "standard deviation", as main distribution models in ArcGIS.

The application of MCA (Multi-criteria analysis proves to be effective in the Czech Republic. As part of digitalization, more and more information and data are freely available which can be used for geospatial analysis. On the other hand, the processing of separate multi-criteria analyses by region introduces errors into the evaluation and comparison, both in terms of the number of evaluated criteria, but also the inclusion of more and more information. From a planning point of view, an appropriate step would be to create an MCA for the entire Czech Republic, considering the uniqueness of some territories. It is therefore expedient to create a comprehensive methodology that would form supporting material for reproducing this analysis, including from the point of view of evaluating individual indicators. On the other hand, it is also important to realize that the selection of priority areas can contribute to better realizability, on the other hand, it is not expedient to prioritize only these basins, but to strive for the widespread implementation of adaptation measures. However, the solution of integrated watersheds can help to evaluate the effect of even small measures in the landscape to protect residents and improve the ecological value of the area. As already mentioned, the presented article is part of a complete multi-criteria analysis, with the intention of selecting the most priority watersheds in which the design of specific adaptation measures and their evaluation will continue. The output will be a summary of overview maps of individual indicators, but also the creation of an overview of freely available data that can be used in the design of measures and take into account their limitations.

ACKNOWLEDGEMENTS

Supported by specific research FAST-S-23-8222 "Modeling and optimalization of rainfall-runoff and erosion processes in the landscape."

REFERENCES

[1] Envicons, s.r.o., Regionální strategie adaptačních opatření (ReSAO), 2019, Online: https://www.ieva.cz/resao;

[2] Vodohospodářský rozvoj a výstavba a.s., Regionální strategie adaptačních opatření Plzeňského kraje pro zadržení vody v krajině, 2021;

[3] Kiker, G. A., Bridges, T. S., et al., Application of multicriteria decision analysis in environmental decision making, Integrated Environmental Assessment and Management, 2009;

[4] Fojtík, T., Jašíková, L., Kurfiřtová, J., at al. GIS a kartografie ve VÚV TGM. Vodohospodářské technicko-ekonomické informace. 2022, 64(1), s. 47–52. ISSN 0322-8916, Online: https://www.dibavod.cz;

[5] Ministry of Agriculture of the Czech Republic, Data Land Parcel Identification System, 2022, Online: https://eagri.cz/public/web/mze/farmar/data-ke-stazeni/;

[6] Land reclamation data (vector shapefile format), acquired by the former Agricultural Water Administration (ZVHS) under the administration of the Ministry of Agriculture, 2023, Online: https://eagri.cz/public/portal/mze/farmar/LPIS/data-melioraci;

[7] Drbal, K., Dumbrovský, M. et al., Metodický návod pro identifikaci KB, Ministerstvo životního prostředí ČR, Praha, (2009);

[8] Department of water management planning, Dyje sub-basin plan 2021-2027, Online: http://pop.pmo.cz/cz/stranka/schvalene-plany-povodi-2021-2027/;

[9] Data Monitored erosion events 2022 © VÚMOP, SPÚ;

POPULATION ANALYSIS OF MEDICINAL PLANTS OF THE FLOODPLAIN OF THE SEIM RIVER (SUMY REGION, UKRAINE)

Assoc. Prof. Inna Zubtsova [1]

Prof. Dr. Viktoriia Skliar [2]

[1, 2] Sumy National Agrarian University, **Ukraine**

ABSTRACT

The article presents the results of population studies conducted in the floodplain of the Seim River within Sumy region, Ukraine. The ontogenetic and vitality structures populations of *Potentilla erecta* and *Althaea officinalis*. During the study, the following methods were used: the geobotanical method, morphometric analysis, complex vitality analysis.

In general, for the region of research on *P. erecta* priority is the introduction of active protection measures aimed at increasing the distribution centers and the formation of high-quality (with a significant area of the population field, population density, severity of invasive processes and belonging to the category of prosperous) populations capable of sustainable existence and self-maintenance. Based on the results of ontogenetic and vitality structures, the *A. officinalis* population, three populations can be considered as potential as potential cells of regulated procurement of medicinal raw materials: from the associations *Scirpetum (sylvatici) ranunculosum (acris), Scirpetum (sylvatici) lycoposum (europaei), Caricetum (acutae) agrostidosum (stoloniferae)*. They are distinguished not only by belonging to the category of prosperous, but also by high values of population density, significant values of recovery indices.

Keywords: population analysis, vitality analysis, ontogenetic structure floodplain of river, *Potentilla erecta* (L.) Raeusch., *Althaea officinalis* L.

INTRODUCTION

The meadow ecosystems are extremely important from the point of view of preserving biodiversity, maintaining the ecological balance of adjacent territories, and the floodplain meadows have always been considered stabilizers of the hydrological regime. The meadows have existed for a long time under conditions of active economic use. In the floodplain meadows of the forest-steppe zone of Eurasia, taking into account the high population density and the significant plowing of the fallow lands, the anthropogenic influence is particularly intense.

The medicinal plants (Plantae medicinales) are the plants, the organs or parts of which are raw materials for obtaining means used in folk, medical, or veterinary practice with curative, prophylactic purposes and are an important component of research and development in the pharmaceutical, food, and cosmetic industries. About 70,000 species of plants are used in traditional and modern medicine around the world. About 1,500 types of medicinal plants are used in Europe, including 1200-1300 species

from the natural environment (in situ). It is reasonable to mention that 2219 out of 6086 types of vascular plants of Ukraine contain biologically active substances, the raw material of which is used or can be used for medical purposes.

Plant raw materials used in the manufacture of medicinal products in Ukraine are mostly obtained by collecting wild medicinal plants. In general, official medicine widely uses 210 species of flora of Ukraine. In significant volumes (over 10 tons), 20-30 types of wild medicinal plants are harvested annually, and 44 species are cultivated. Compared to other European countries, Ukraine is in the leading positions in terms of these indicators. As a result of uncontrolled harvesting of medicinal plants, their number has significantly decreased, and some species have disappeared completely [1].

Traditional ecology deals with plant species, while populations are the real form of existence of plant species. The stability of existence, the preservation of sustainable productivity and the dynamics of meadow communities are largely determined by the structure of populations of plant species that make up the grassland. Plant populations are structural units of phytocenoses. They are individually distributed along ecological and kenotic gradients, differ in life strategies [2] and determine dynamic and successional processes in vegetation. In ecological studies, the ontogenetic and vitality structures of populations are primarily analysed [3]. The age structure of populations is determined by the ratio of plant individuals of different ontogenetic states [4] and the vitality structure is determined by the ratio of plants of different vitality, which is a morphostructural expression of the life state of plants [5]. An objective assessment of the vitality of individuals is determined, as a rule, by three diagnostic signs, the set of which depends on the life form and the age of the plants [6].

Therefore, it becomes expedient to conduct the study of medicinal plants within individual regions, especially those that are distinguished by significant species and kenotic diversity and are considered promising in the aspect of expanding the exploitation of medicinal plant resources.

MATERIALS AND METHODS

The presented work is based on the materials of field research conducted on the territory of the Seim River floodplain within Sumy region, Ukraine.

The populations of medicinal plants, which were covered by the study, are part of various phytocenoses. In order to establish the state and structure of plant communities, generally accepted geobotanical approaches were used.

The study of the state of medicinal plants in each of the selected habitats was carried out on the basis of a comprehensive analysis, which included the assessment of indicators of the area of the population field, population density, ontogenetic and vitality structures of the populations.

The correspondence of plants to one or another ontogenetic state was established on the basis of methods covered in scientific works under the general editorship of L.O. Zhukova. At the same time, 3 periods of development and 5-8 ontogenetic states were distinguished in the plants of the studied species.

Statistical processing and generalization of data on the ontogenetic structure of populations of studied species of medicinal plants was carried out using the special computer program ANONS6, developed by Yu. Zlobin [7].

At the final stage of the study of the ontogenetic structure, it was established that the population belonged to a certain category. According to it, populations were assigned to one of three categories: invasive, which is characterized by the predominance of individuals of pre-generative states, generative (normal) – characterized by the predominance of generative individuals, regressive – distinguished by the predominance of post-generative individuals.

The calculation of static metric indicators was carried out using a ruler and scales of the AXIS model with a weighing accuracy of up to 0.01 g. The area of the assimilation surface in plants was determined by the upper surface of the leaves. It was assessed using the Petiole mobile application.

Vitality parameters of populations were determined according to the method of Yu. Zlobin [5]. First of all, the vitality analysis involves the determination of key morphoparameters, that is, those indicators that are an objective quantitative reflection of the level of vitality of plants. Because of this, the following algorithm of actions was implemented: 1) an assessment of the level and nature of correlation relationships between all dimensional quantities and the formation of correlation constellations was carried out; 2) factor analysis was applied to morphoparameters; 3) a comparison of the results of factor and correlation analyses was made; 4) interpreted the obtained data based on biological and ecological rules and regularities.

At the final stage of calculations of vitality analysis based on key morphoparameters in the composition of the population, the share of plants of different levels of vitality (lowest (class «c»), intermediate (class «b») and highest (class «a»)) was estimated and the value of the quality index Q was determined:

$$Q = 1/2\ (a+b)$$

where a is the share of plants with the highest level of vitality (in fractions of a unit),

b is the share of plants of an intermediate level of vitality (in fractions of a unit).

As a result, the population was determined to belong to one of the qualitative types: a) depressed ($Q < 0{,}16667$), b) balanced (Q from 0,16667 to 0,3333), c) prosperous ($Q > 0{,}3333$). Vitality analysis was implemented using the VITAL computer program, where the procedure for assessing the level of plant vitality and the vitality structure of populations is automated.

The use of a complex of the specified methods allowed objective and comprehensive information about the parameters of local growth of the populations of the studied species of medicinal plants, about the state of their populations, as well as about the peculiarities and regularities of their functioning.

RESULTS

The population analysis covered five populations of *Althaea officinalis* L. They formed in groups with dominance and co-dominance of such species as *Lycopus*

europaeus L., *Phragmites australis* (Cav.) Trin. ex Steud., *Agrostis stolonifera* L., *Scirpus sylvaticus* L., *Carex acuta* L., *Carex acutiformis* Ehrh., *Ranunculus acris* L., *Elytrigia repens* (L.) Nevski, *Urtica dioica* L .

In the populations covered by the study, the area of the population field varies from 486 to 932 m^2. At the same time, the average indicators of population density vary within the range of 5,5–7,5 individuals/m^2. In the driest habitats (in the group of associations *Elytrigietum (repentis) urticosum (dioicae)*) the density of populations was somewhat lower than in wetter ones (5,5 plants/m^2 versus 6,6–7,0% individuals/m^2) (Table 1).

Table 1. Population density of *Althaea officinalis*

Population	**Group of associations**	**Population density, individuals/m^2**
1	*Elytrigietum (repentis) urticosum (dioicae)*	5,5 ± 1,17
2	*Scirpetum (sylvatici) ranunculosum (acris)*	6,6 ± 1,51
3	*Scirpetum (sylvatici) lycoposum (europaei)*	7,4 ± 1,94
4	*Caricetum (acutae) agrostidosum (stoloniferae)*	7,5 ± 2,08
5	*Phragmitetum (australis)glyceriosum (arundinaceae)*	7,0 ± 2,14

Based on the results of the study of the ontogenetic structure, it was established that all studied populations have incomplete ontogenetic spectra: in which plants of 5–7 ontogenetic states out of 9 covered by the study are represented. Seedlings and senile plants are absent in all populations. In one population (from the *Phragmitetum (australis) glyceriosum (arundinaceae)* group) even subsenile plants are absent. In the group of associations *Elytrigietum (repentis) urticosum (dioicae)*, in addition to seedlings and subsenile individuals, there are also no juveniles and immatures. That is, among the studied populations of *Althaea officinalis*, those growing in the wettest and, especially, the driest areas were the least complete in terms of ontogenetic structure.

All studied populations include virginal, as well as young generative and medium generative ones. In the population from the *Elytrigietum (repentis) urticosum (dioicae)* group of associations, the most important (31,82%) is the share of young generative individuals, in three others (from the group of associations *Scirpetum (sylvatici) ranunculosum (acris), Scirpetum (sylvatici) lycoposum (europaei), Caricetum (acutae) agrostidosum (stoloniferae)* – virgin plants (at the level of 27,27–32,43%). In another population (from the *Phragmitetum (australis) glyceriosum (arundinaceae)*) juvenile plants make up the largest share (26,67%). In general, the ontogenetic spectra of the studied populations are monomodal centered (for example, in the group of associations *Elytrigietum (repentis) urticosum (dioicae)*) or left-sided (for example, in the group of associations *Phragmitetum (australis) glyceriosum (arundinaceae)*). In general, there is a tendency to increase the severity of left-sidedness as increase in the degree of wetting of the territory.

The results of the vitality analysis showed that two of the studied populations of *Althaea officinalis* belong to the depressed category and three to the prosperous

category. The values of the quality index Q in the studied populations vary from 0,0334 to 0,4667.

It was established that the functioning of *Althaea officinalis* populations is accompanied by their realization of both vitality variability and vitality plasticity. However, the vitality variability is somewhat more pronounced: three populations (from the group of associations *Scirpetum (sylvatici) ranunculosum (acris), Scirpetum (sylvatici) lycoposum (europaei)* and *Caricetum (acutiformis) agrostidosum (stoloniferae)*) have exactly the same values of the Q index (0,4667), at the same time, they differ reliably in their vital structure.

This is manifested in a different proportion of plants of high (class «a») and intermediate vitality (class «b»). In the *Scirpetum (sylvatici) ranunculosum (acris)* group of associations, this ratio is 0,9333 : 0,0 in *Scirpetum (sylvatici) lycoposum (europaei)* – 0,5333 : 0,4000 in *Caricetum (acutiformis) agrostidosum (stoloniferae)* – 0,0 : 0.0667.

The population analysis covered four populations of *Potentilla erecta (L.)* Raeusch. They formed in groups with dominance and co-dominance of such species as *Trifolium pratense* L.*, Comarum palustre* L.*, Elytrigia repens* L.*, Typha latifolia* L. [8].

In the populations covered by the study, the area of the population field varies from 12 to 87 m^2. At the same time, the average indicators of population density vary within the range of 5,5–10,9 individuals/m^2. Population density indicators increase from population №1 to population №5, which generally corresponds to the gradient of increasing soil moisture (Table 2).

Table 2. Population density of *Potentilla erecta*

Population	**Group of associations**	**Population density, individuals/m^2**
1	*Elytrigietum (repentis) hypericosum (perforati)*	5,5±1,19
2	*Elytrigietum (repentis) trifoliosum (repentis)*	7,9±2,26
3	*Deschampsietum (cespitosae) festucosum (pratensis)*	7,5±2,11
4	*Deschampsietum (cespitosae) potentilliosum (anserini)*	9,3±2,11
5	*Deschampsietum (cespitosae) arostidosum (stoloniferea)*	10,9±3,75

According to the results of the study of the ontogenetic structure, it was established that all studied populations have incomplete ontogenetic spectra in which plants of 5–6 ontogenetic states out of 9 covered by the study are represented. Juvenile, senile plants and seedlings are absent in all populations.

In one population (from the *Deschampsietum (cespitosae) rotentilliosum (anserini)* group of associations) even subsenile plants are absent. The ontogenetic spectra of all populations are monomodal and centered. Although the populations from the groups *Elytrigietum (repentis) trifolietosum (pratensis)* and *Elytrigietum (repentis) hypericosum (perforati)* show a tendency to pronounced «left-sidedness»: against the

background of the general predominance of the share of generative plants (in the range of 49,99–53,85%), the largest indicators regarding the representation of plants of certain ontogenetic states correspond to virgin plants (30,77–31,48%).

The results of the vitality analysis showed that two of the studied populations of *Potentilla erecta* belong to the depressed category, one to the balanced category, and two to the prosperous category. The values of the quality index Q in the studied populations vary from 0,0333 to 0,4667.

For the studied populations, the quality index Q increases in the following sequence of phytocenoses: *Elytrigietum (repentis) hypericosum (perforati)→Elytrigietum (repentis) trifoliosum (repentis)→Deschampsietum (cespitosae) festucosum (pratensis)→Deschampsietum (cespitosae) potentilliosum (anserini)→Deschampsietum (cespitosae) arostidosum (stoloniferea).*

DISCUSSION

Based on the use of a complex of generalizing ontogenetic indices, it was established that in the population of *Althaea officinalis* from the *Elytrigietum (repentis) urticosum (dioicae)* group of associations, the indicators of the aging index are slightly higher than the values of the renewable index (27,27 – 22,73%). It is characterized by the highest values of the generativity index (68,18%) and the general dominance of degradation processes. A characteristic feature of all other populations is that the values of the renewability index are greater than those of the aging index (45,45–62,16% versus 10,81–17,4%).

In addition, these populations are characterized by fairly high values of the generativity index (at the level of 32,43–51,2%) with the predominance of invasive processes.

The analysis of changes in the values of the index of vitality dynamics (IVD) of *Althaea officinalis* populations according to the studied groups and soil moisture gradient showed that in two cases (at the transition between the group of associations *Scirpetum (sylvatici) ranunculosum (acris), Scirpetum (sylvatici) lycoposum (europaei)* and *Caricetum (acutiformis) agrostidosum (stoloniferae)*) they are naturally equal to zero and, accordingly, the constancy of the qualitative type of population is manifested. In two other cases, the values of the index of vitality dynamics (IVD) represent the category of «significant» values (they exceed 2 units by modulus), the transition of populations is accompanied by a change in their qualitative type.

Therefore, the populations of *Althaea officinalis* formed in the floodplains of the Seim River have incomplete and monomodal ontogenetic spectra that are constant within the population fields. Populations are mostly in a state of active formation and development and are distinguished by the predominance of invasive processes.

Potentilla erecta populations have incomplete and monomodal ontogenetic spectra, which are constant within population fields. Populations are mostly in a state of fairly active formation and development and are distinguished by the predominance of invasive processes.

Thus, the adaptation of plants and populations of *Potentilla erecta* to the conditions of local growth is accompanied by their differentiation according to the level of vitality and, as a result, an active manifestation of vitality variability and plasticity.

CONCLUSION

According to the results of a comprehensive study, it was established that the populations of *Potentilla erecta* and *Althaea officinalis* have significant differences in both quantitative and qualitative characteristics.

The positive thing about *Potentilla erecta* populations is that they are characterized by the predominance of invasive processes, with most of them belonging to maturing and all three qualitative types in terms of vitality structure. At the same time, in the absolute majority of cases, populations of *Potentilla erecta* have insignificant indicators of the area of the population field. This, in particular, is one of the consequences of long-term unregulated use of resources of this species in the region. Taking into account the identified features of the state of the populations of *Potentilla erecta*, we consider it impossible today to consider them as centres of active harvesting of medicinal raw materials in the floodplain of the Seim River within Sumy region. A certain exception may be populations from the group of associations *Deschampsietum (cespitosae), rotentilliosum (anserini)* and *Deschampsietum (cespitosae) arostidosum (stoloniferea)*. They have a relatively large area of the population field (within 69-87 m^2), fairly high indicators of population density (at the level of 9,3-10,9 individuals/m^2), a significant share of pre-generative ones (36.51-38.03%) and generative plants (61,90-61,07%), while belonging to the category of prosperous ones. It is in them that it is potentially possible to procure small amounts of medicinal raw materials.

In general, the priority for the research region regarding *Potentilla erecta* is the implementation of active protection measures aimed at increasing the centres of distribution and forming high-quality (with a significant area of the population field, population density, severity of invasive processes and belonging to the category of prosperous) populations capable of sustainable existence and self-maintenance. When implementing active protection measures, the source of planting material can be the populations of the *Deschampsietum (cespitosae) rotentilliosum (anserini)* and *Deschampsietum (cespitosae) arostidosum (stoloniferea)* group of associations, and peat meadows should primarily be used as foci of the formation of new populations.

In *Althaea officinalis*, three populations can be considered as potential foci of regulated harvesting of medicinal raw materials: from the *Scirpetum (sylvatici) ranunculosum (acris), Scirpetum (sylvatici) lycoposum (europaei)* and *Caricetum (acutiformis) agrostidosum (stoloniferae)* group of associations. They are distinguished not only by belonging to the category of prosperous (Q=0,4667), but also by fairly high values of population density (about 7−8 individuals /m^2), significant values of renewable indices (within 45,45−62,16%) and relatively high values of the generativity index (32,43−51,52%) and, as a result, belonging to the category of young people with a general predominance of invasive processes.

REFERENCES

[1] Minarchenko V. N. Medicinal plant resources in Ukraine. Melbourne: Bayda Books, 2000. P. 3-7.

[2] Grime J. P. Plant strategies and vegetation procesess. Chichester. N.Y.: Wiley, 1979. 222 p

[3] Skliar V., Kovalenko I., Skliar Iu, Sherstiuk M. Vitality structure and its dynamics in the process of natural reforestation of Quercus robur L. AgroLife Scientific Journal, 2019. 8 (1). P. 233-241.

[4] Скляр В. Г. Динаміка віталітетних параметрів лісоутворювальних видів Новгород-Сіверського Полісся: теоретичні засади та способи оцінки. Український ботанічний журнал, 2013. Т. 70, № 5. С. 624–629.

[5] Злобин Ю. А. Популяционная экология растений: современное состояние, точки роста. Сумы: Университетская книга, 2009. 263 с

[6] Злобин Ю. А. Компьютерные программы для анализа популяций. Вісник Сумського національного аграрного університету. Серія «Агрономія і біологія». 2012. Вип. 2 (23). С. 3–6.

[7] Злобін Ю. А., Скляр В. Г., Бондарєва Л. М., Кирильчук К. С. Концепція морфометрії у сучасній ботаніці. Чорноморск. ботан. журн. 2009. Т. 5, № 1. С. 5–22.

[8] Зубцова І. В. Віталітетна структура ценопопуляцій *Potentilla erecta* (L.) Raeusch. на заплавних луках Кролевецько-Глухівського геоботанічного району. Вісник Львівського університету. Серія біологічна. Львів, 2017. №76. С. 112-119.

STUDY OF THE HYDROLOGICAL, TERRAIN AND ANTHROPOGENIC FACTORS FOR THE DEVASTATING FLOOD AT THE SOUTHERN BLACK SEA COAST OF BULGARIA ON 4-6 SEPTEMBER 2023

Assoc. Prof. Dr. Olga Nitcheva[1,2]

Research Assist. Eng. Donka Shopova[2]

Dr. Eng. Albena Vatralova[2]

Assoc. Prof. DSci Vesselin Koutev[3]

Assoc. Prof. Dr. Polya Dobreva[1,2]

[1] Institute of Mechanics - Bulgarian Academy of Sciences (BAS), Sofia, **Bulgaria**
[2] Climate, Atmosphere and Water Research Institute - (BAS), Sofia, **Bulgaria**
[3] University of Forestry, Sofia, **Bulgaria**

ABSTRACT

Heavy rainfall in the summer have become more frequent, and when they occur over the coastal region, the cumulative hazardous pressure leads to floods, loss of physical life and socio-economic impact. Such is the disaster due to the floods in Tsarevo at the end of summer 2023. The paper contains a conceptual analysis of hydrological and meteorological conditions, land cover and use, and institutional preparedness to deal with dangerous floods. It is prepared on the basis of the data from Copernicus Land Monitoring Service, NCEP Reanalysis, EFAS–EC (European Flood Awareness System), IMERG–NASA (Integrated Multi-Satellite Retrievals for GPM), national hydro-meteorological measurements and CLM model study. The results of the research show that in addition to severe weather conditions, the human factor has contributed to the disaster situation - inadequate information to the population, problems with the dams around Tsarevo, over urbanization, failures in critical infrastructure maintenance, unavailable public information for surface and groundwater monitoring.

Keywords: flood, Tsarevo, CLM model, Copernicus, NCEP, EFAS, IMERG

1. INTRODUCTION

Storm Daniel considered as the deadliest and costliest Mediterranean tropical-like cyclone in recorded history appeared on 4 September and lasted until 12 September 2023 affecting Greece, Bulgaria and Turkey with extensive flooding, then moving toward the coast of Libya, where it caused catastrophic flooding. Such extreme event is not an exception nowadays – the heavy rains in summer have become more frequent. Coastal flooding is one of the most common and destructive natural disasters that affects many onshore areas. Coastal urban areas are floodplains with low-lying terrains that face the influence of many natural factors such as storms, rainfalls, river runoff, etc., each of which can directly lead to flooding.

The combination of heavy rains, upstream flooding and sea turbulence from cyclones greatly worsens the severity of the flooding. Such is the case with the consequences of

Storm Daniel, which dramatically affected with extensive flooding the Bulgarian Black Sea coast near the southern town of Tsarevo on 4-6 September 2023 (Fig.1).

The storm river runoff is an essential characteristic of the water regime. The latter is defined as short-term periodic high waters formed by storm (torrential) rainfall or by intense snowmelt [1]. The precipitation amounts ≥ 100 mm/24 h, measured in a certain station, is not by all means connected with similar amounts in neighbouring stations [2]. Zyapkov [1] proposes a classification of storm runoff based on the calculation of indicators for evaluating the degree of turbidity They determine five classes thus making possible to distinguish rivers of lowest, low, moderate, intense and most intense storm runoff. The rivers of intense and most intense storm runoff are prevailing in Bulgaria. As early as 1988 the areas of the country vulnerable to torrential rainfall were mapped, the Southern Bulgarian Black Sea Coast classified in 4th degree of danger category of total 5 degrees [1].

Contrary to many mid- to upper latitude regions where positive trends in precipitation amounts were reported, the investigations of some authors show that in Bulgaria the measured precipitation totals generally decrease in the last decades but extreme daily rainfall increase is observed in the same period. An increase of mean annual number of days with torrential precipitation with about 50% is obtained for the period 1991–2007 versus those for 1950–1990 [2]. However, for the East Bulgaria and the Black Sea coast (where 200mm/24 hours is considered) the observed increase of mean annual heavy precipitation days during the period 1991–2007 versus the previous one is 6 time bigger than those for the whole country. As to the seasonal distribution, for the period 1961–1990 the greatest number of heavy rain days is observed in December and June, but in 1991–2007 such type of precipitation more frequently occurred in July and September, when their increase is about 75–100%. The study of Nojarov for the period 1950–2014 states that significant increase in September precipitation amounts is observed since 1995 in Bulgaria [4]. This trend continues to be valid in the recent years. For instance, after 10 hours of continuous rain on 2nd September 2022 the rivers in Karlovo, Kaloyanovo and Maritsa municipalities (South Central part of the Bulgarian Balkan Mountain) came out of their river beds, flooded agricultural lands and pumping stations, broke river dykes, took away bridges, cut the electricity and water supply, roads were damaged.

The prerequisites for the development of rainfall stem from the impact of complex natural and anthropogenic factors. The geological-geomorphological factors (lithological basis, slopes and exposure of the relief, etc.) have the greatest impact. Atmospheric circulation processes also create prerequisites for an increase in the frequency of torrential rainfall. [1]. In addition to the natural environment and climate change, human intervention and socio-economic development also have an impact on the spatial and temporal changes of flooding in coastal regions. Various anthropogenic factors affect the development of rainfall – e.g. construction works, urbanization, agriculture, forestry, industry, etc. When in a small watershed roughness of the cover is reduced by cutting down trees beforehand, it increases the risk of such a disaster to occur. The removal of a certain number of trees from the catchment reduces the obstacles to the water, which flows unhindered and quickly into the main bed of the river and raises the wave. The disturbed water-regulating and anti-erosion properties of the soil-vegetation cover on a significant territory and the expansion of urbanized areas, technical infrastructure and waterproof covers (concrete, asphalt, stone, etc.) activate the

surface runoff of rainwater and the development of water erosion [1]. Soil sealing being the permanent covering of the land surface by buildings, infrastructures or any impermeable artificial material strongly modifies the hydrological cycle, reducing infiltration, evapotranspiration and groundwater recharge. The reduction of infiltration capacity is the main cause of the increased runoff, which increases flooding risk. The latter may be enhanced by the increased vulnerability of the urbanized and settled land [3]. The flood protection measures may also lead to additional hazards in the event of extreme flooding, such as dam wall failure, culvert blockage, etc. Therefore, evaluating the positive and negative contributions of human influence becomes a long-standing issue that needs to be addressed.

The paper contains a conceptual analysis of hydrological and meteorological conditions, land cover and use and hydrological modeling study, as well as human interventions and institutional preparedness to deal with extreme events.

The results of the study show that in addition to severe weather conditions, other crucial factors for the disastrous situation are inappropriate human interventions, inadequate information to the population, problems with the dams around Tsarevo, over urbanization, failures in critical infrastructure maintenance, lack of public information from surface and groundwater monitoring.

2. MATERIALS AND METHODS

2.1. Description of the studied area

The studied area - Southern Bulgarian Black Sea watershed (Fig. 1), also known as Eastern Strandja region has an area of 1900 sq.km. Regardless of the fact that the Southern Bulgarian Black Sea region is located in close proximity to the sea, due to its small size and the prevailing zonal circulation throughout the year, the region belongs to the Continental-Mediterranean climate. The region borders on the north with the Burgas region, on the south with the Turkish border, on the east with the Black Sea, on the west with the slopes of the eastern part of the Strandja mountain, from which springs many short independent rivers with small catchment basins that flow into the Black Sea.

Surface water. The main rivers are Ropotamo (springs from the mountain at an altitude of 400 m), Dyavolska (springs from the mountain at an altitude of 440 m), Kitenska River (originates from at an altitude of 331 m), Veleka (originates in Turkish territory at an altitude of 664 m) and Rezovska (originates in Turkish territory at an altitude of 666 m and almost its entire length serving as a border between Bulgaria and Turkey).

The area around the town of Tsarevo (Fig.2b, c), being heavily affected by Storm Daniel, includes several small rivers and ravines as follows: the Poturnashka river flowing into the Oasis beach; the Arap ravine flowing into the sea at the "Arapya" campsite; Popska River flowing into Popska Bay near Tsarevo; Cherna River flowing into the regulated territory of the town of Tsarevo; Lisovo (Izgrevsko) ravine flowing into the bay of "Nestinarka" campsite (Fig.2c). Their watersheds are distinguished by specific geography, which combined with the intense rainfall caused the disaster.

The designation of the catchments of Poturnashka River, Arap ravine, Popska River, Cherna River and Lisovo ravine in the Bulgarian River Basin Management Plans (RBMPs) and Bulgarian Flood Risk Management Plans (FRMPs) as "rivers", "ravines" and "surface water bodies“ is unclear. The flood showed that the five water bodies had

"coastal floodplains". In the RBMP for 2010-2015 only Lisovo ravine -BG2IU800R015 is identified as a river, and it is indicated as Lisovo ravine/Cherna River, thus mixing the two water bodies. In the RBMP for 2016 – 2021 Lisovo ravine is indicated as an area with a significant potential risk of floods. It is in good ecological condition and its preservation is a management objective. In the 2022 Interim Review Report of Significant Issues in Water Management Lisovo ravine continues to be the only body of water reported as a "river".

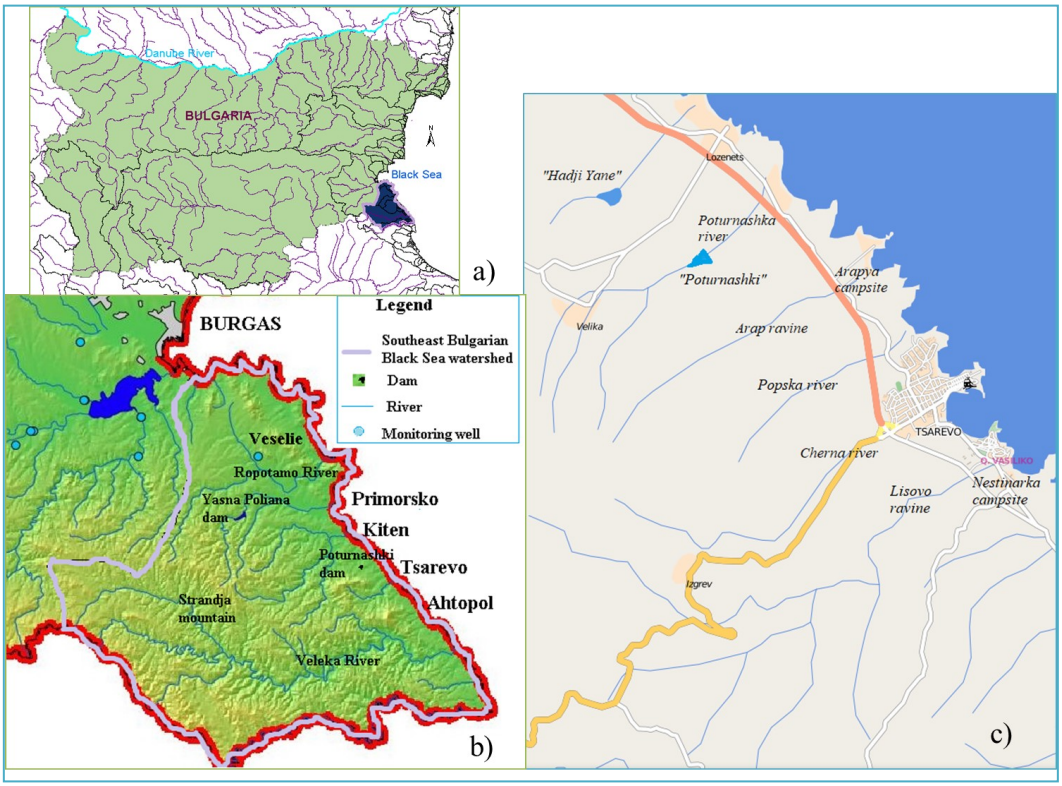

Fig.1. *Hydrological information of the Southeast Bulgarian Black Sea Watershed*

In the 1970-s years of the last century, the "Poturnashki" and "Hadji Yane" dam reservoirs were built on the Poturnashka River with the main purpose of irrigation (Fig.2b, c). The volume of the "Poturnashki" dam reservoir is 552,103 m^3, the water surface area is 14.5 ha and the catchment area is 8.50 km^2. The dam wall is an earthen embankment type, with a crest length of 210 m; height from the crest 11 m; dimensional water quantity Q_{max}=17.5 m^3/s; bottom outlet with Q_{max}=0.74 m^3/s. The volume of the Hadji Yane dam reservoir is 65,103 m^3, the water surface area is 2.7 ha and the catchment area is 1.80 km^2. The dam wall is an earthen embankment type, with a crest length of 135m; height from the crest 9 m; dimensional water quantity Q_{max}=21.5 m^3/s, bottom outlet with Q_{max}=0.375 m^3/s. The dams are classified in the first high degree of potential danger by a commission under Article 138a, paragraph 3 of the Bulgarian Water Act. Over the past 10 years, repairs and inspections by control bodies have been carried out, where it has been found out that the dam walls are in good technical condition and can fulfill their purpose.

Groundwater. In the area studied, the upper aquifer is unconfined only in the northern part and there is a hydraulic connection with the rivers, while in the south the aquifers are confined, in some places there are open recharge areas but in general there is no

hydraulic connection with the rivers. In the western part of the Ropotamo river the aquifer is unconfined; in the eastern part of the river after the village of Veselie up to its confluence into the Black Sea, the aquifer is unconfined with a length of 10 km, a width of 0.5-1 km and a thickness of 12 m, composed of alluvial sands and gravels [5]. There groundwater flow is hydraulically connected to the river. At low water the river drains the groundwater and at high water it is recharged the groundwater flow. To the south of the Ropotamo River the Dyavolska River is situated, being with confined gravel aquifer of about 3 m thickness and covered by a clay layer with a thickness of 1 to 45 m in the west-east direction. In the catchment of the Veleka River the alluvial aquifer represented by sands and gravels is confined with a thickness of 3.5 m covered by clay aquitard with a thickness of 7 m. To the south of the Ropotamo river the precipitation almost does not infiltrate but mostly transforms into surface runoff. The deforestation of the area, the reduction of the soil layer favours conditions for severe flooding.

2.2. Data sets

1. Public data from the monitoring national meteorological and hydrological network of the National Institute of Meteorology and Hydrology of Bulgaria were used.
2. In order to clarify the nature of the catastrophic flood, international databases were also examined.
    - The European Flood Awareness System (EFAS) https://www.efas.eu/efas_frontend/#/home , developed by the European Commission and the European Centre for Medium-Range Weather Forecasts (ECMWF). The EFAS research contribute to adequate preparedness measures for flood prevention, as well as to provide information for national and transnational river basins and across Europe as a whole.
    - The Integrated Multi-satellitE Retrievals for GPM (IMERG) algorithm https://gpm.nasa.gov/data/imerg , that gives information from the GPM (Global Presipitation Measurements Mission) satellite constellation for estimated precipitation over the majority of the Earth's surface.
    - The Copernicus Land Monitoring Service – Corine land cover https://land.copernicus.eu/en/products/corine-land-cover. Land cover and land cover changes in Tsarevo municipality (Southeast Bulgarian Black Sea Watershed (SBBSW)) in 2000-2018 as changes in riparian zones are studied.

2.3. CLM Model

The Community Land Model version 3.0 (CLM3) used is the land surface module of the Community Earth System Model and the Community Atmosphere Model (http://www.cgd.ucar.edu/tss/clm/). It is a spatially distributed deterministic model developed in the USA National Center for Atmospheric Research [6]. The model simulates snow, water and soil water hydrology in the soil column up to 3.43 m at any regional level. Atmospheric forcing is set through the time dependent parameters of the wind, specific humidity, pressure, air temperature, solar radiation and precipitation. Soil and plant information is imposed by information of soil texture (% of sand and % of clay), soil color and vegetation parameters (monthly leaf LAI and stem SAI indices). The model meteorological input is prepared from the data supply by the NCEP/NCAR Reanalyses 1 product (https://psl.noaa.gov/data/gridded/data.ncep.reanalysis.html).

3. RESULTS AND DISCUSSION

In order to clarify the meteorological and hydrological conditions during the period of the flood, 4-6 Sep 2023, national and international databases were examined for the Southern Bulgarian Black Sea watershed. The national monitoring network for surface and groundwater bodies for the area studied include 2 hydrometric stations – one on the Ropotamo river (Veselie village, Fig.1a) and the other is at the beginning of the Veleka river - in the most western part. There is only one point for monitoring the groundwater level (Veselie village, Fig.1a). The information is not public.

In conditions of intense rainfall, information on the groundwater level is essential for a realistic assessment of the hydrological situation and for planning activities to deal with the critical conditions of potential or actual flooding. The insufficient national monitoring information on water bodies put the necessity to search in the world databases. The databases of EFAS - EC (European Flood Awareness System) and IMERG - NASA (Integrated Multi-Satellite Retrievals for GPM) are used (Fig.2).

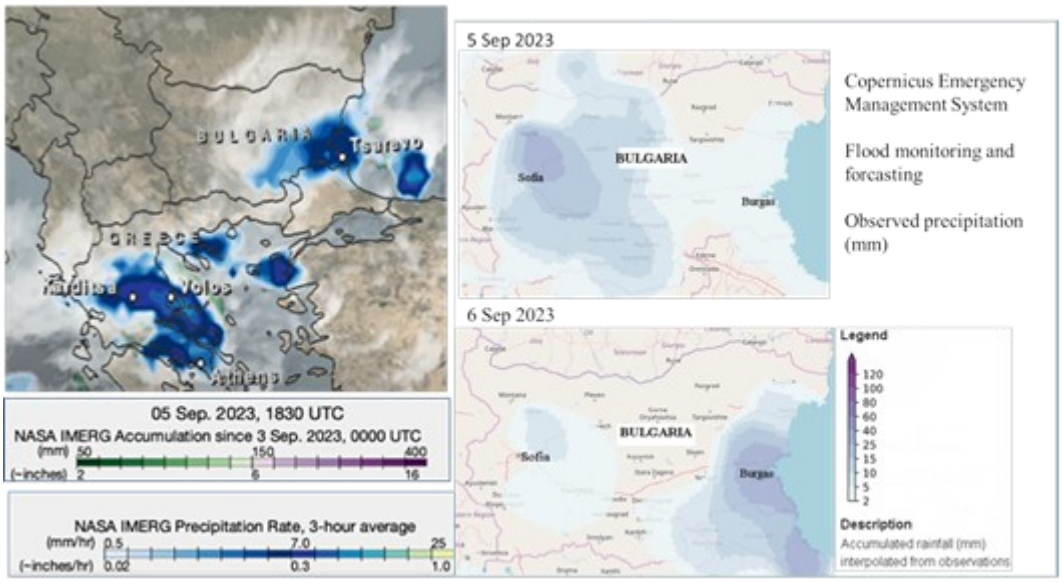

a) Source: IMERG-NASA *b) Source: EU Copernicus EFAS*

***Fig. 2**. Observed precipitation on the territory of Bulgaria on 5-6 Sep2023*

There was no forecast information for intense amounts of rainfall on 4-6 September and the responsible authorities were surprised. Only in the monthly bulletin of National Institute of Meteorology and Hydrology of Bulgaria (NIMH) for September 2023 [7] there is information about the rainfall during the disaster, where the rain is over 200 mm/day. Figure 2b shows the precipitation amounts on 5-6 September 2023 for the Southern Black Sea watershed. These are observed data from national synoptic stations, interpolated and visualized by EFAS. On 5 September the precipitation is 60 mm, on 6 September the precipitation is over 100 mm. The NASA IMERG database (Fig.2a) information shows over 7 mm/hour of precipitation for 05.09.2023 for the Southern Black Sea watershed. Precipitation data from EFAS and IMERG NASA are available days after the event and there is a discrepancy in the amount of precipitation. EFAS information from measurements of precipitation is provided by NIMH also but the values are two times lower than those in the NIMH bulletin.

CLM simulation results. A study was conducted to calculate the monthly values of the hydrological parameters with the CLM mathematical model. The water balance processes were simulated for the Southern Bulgarian Black Sea watershed, for a normal, wet and dry year – 2013, 2018 and 2019, respectively. The summer months – June, July, August and September – were considered with calculated monthly values of precipitation, surface runoff, soil infiltration and average monthly air temperature.

The results from CLM simulations are shown in Table 1 together with the precipitation values from the measurements at the synoptic stations in the area [7].

Table 1. *CLM model simulations and field measurements*

Years	2013, CLM model results							2018, CLM model results						
	June	July	Aug	Sep	Summer rainfall, study region (mm)	Annual precip, study region (mm)	Annual precip., country (mm)	June	July	Aug	Sep	Summer rainfall, study region (mm)	Annual precip, study region (mm)	Annual precip., country (mm)
Rain (mm)	**78**	49	25	**55**	**207**	**560**	**702**	39	65	1	**97**	**202**	**759**	**1158**
Soil infiltration (mm)	**31.7**	7.2	7.5	14.3				8.9	2.6	-5.4	**25.52**			
Surface runoff (mm)	**11.2**	7.7	2.3	7.3				2.7	4.4	0	**13.4**			
Average air T(°C)	21.6	23.7	25.1	19				23	24.6	26.5	21.8			
Years	**2019, CLM model results**							**2023, Measured data, NIMH**						
	June	July	Aug	Sep	Summer rainfall, study region (mm)	Annual precip, study region (mm)	Annual precip., country (mm)	June	July	Aug	Sept	Summer rainfall, study region		
Rain (mm)	27	45	25	**24**	**121**	**439**	**793**	51	42	2	**245**	**340**		
Soil infiltration (mm)	-1.22	4.33	-0.31	1.35										
Surface runoff (mm)	1	3	1.5	1.6										
Average air T(°C)	24	24.7	25.3	21.8										

The CLM simulations show that normal summer precipitation for the period June-September is 210 mm (2013, 2018), in a dry year it is 120 mm (2019), and in a year with extreme precipitation (2023) it is 340 mm. Heavy rainfall turns to be a normal phenomenon for September at the southern Black Sea coast, for which the flood management authorities should be prepared.

The results of the CLM model for surface runoff and soil infiltration show that with a monthly summer rainfall of 78 mm (June 2013) and 97 mm (Sep 2018) the amount of runoff is almost half of the rainfall, which means that with rainfall values above 100 mm the runoff can reach up to 100% of the fallen precipitation.

A comparison between the annual precipitation values for the Southern Black Sea watershed and for the whole country (Table 1) shows that on the Southern Black Sea coast the precipitation is 30% less than the average annual precipitation of the country. Water supply is limited in the coastal area, which necessitates the search for additional onshore and offshore water sources. On the other hand the intense rain waters are pouring into the sea during a flood and put at risk the conventional water sources. A research is being carried out by some of the authors under the COST 21112 project ("Offshore freshened groundwater: An unconventional water resource in coastal regions?) to search for offshore water sources in the fresh submarine aquifers. With the present trends in climate change the need for new and reliable water sources will increase in the future that makes this offshore exploration relevant and necessary.

Anthropogenic factors for the severe consequences of the flood

The research shows that the anthropogenic factor has a significant contribution to the disaster that occurred in the five watersheds (Poturnashka river, Arab valley, Pop river, Cherna river, Lisovo valley, Fig.1c) that are subject of the analysis. This is related to the location and character of the hydrotechnical and bridge facilities and the construction of the flood terraces. The boundaries of the water bodies that are public state property are determined by the director of the Basin Directorate, together with the technical services of the municipalities and the services of geodesy, cartography and cadaster (Article 155, Paragraph 1 of the Bulgarian Water Act). One of the many problems is that the Law does not specify who defines the boundaries of water bodies that are not public state property. The illegal construction along the riverbeds and ravines in the area of Tsarevo and illegally placed objects also played a crucial role. According to Article 134 of the Water Act, the construction of commercial and residential buildings is prohibited on the coastal floodplains and the lands belonging to the reservoirs. It is prohibited to place residential and villa buildings and farm buildings on the flooded terraces of the rivers. According to Art. 146 the basin directorates notify the authorities issuing permits for the construction of residential, villa and farm buildings about the location and extent of the coastal floodplains of the rivers.

In the first Bulgarian Flood Risk Management Plans (FRMP) Black Sea - Tsarevo was identified as an area with a significant potential risk of river floods. For this sub-district there have been identified a risk of flooding from the Black Sea along the coast and a risk of river flooding from Lisovo ravine. In the FRMP for 2016-2021 as flood prevention measure for the land of Tsarevo it is recommended cleaning a section of the river Lisovo ravine, and for the land of Lozenets - cleaning and widening the narrow riverbeds of the Poturnashka River. In the draft FRMP for 2022-2027 the region is marked with *a significant potential risk of floods* but with a change, namely – river flood for Lisovo ravine and rain flash (torrent) flood for Cherna and Popska Rivers, but the flood risk maps indicate *a low risk of river flooding*. According to the analyses, the considered areas with a significant potential risk of floods do not exceed the threshold for a negative impact of climate change regarding any of the considered indicators, which turned out to be extremely wrong.

The situation with increased rates of deforestation is analyzed. Sealed surface in Bulgaria accounted 1213 km^2 in 2018 (1.09% of the total country area). Sealed surface in Southern Bulgarian Black Sea watershed accounted for 73.48 km^2 in 2018 (0.95% of total area) which is slowly less at national level.. For 2012-2018 the forest and semi natural areas change in Southern Bulgarian Black Sea watershed accounted for - 0.11% which is with 60% more than in national level for 2000-2018 period - 0.069%. Larger sealed areas are observed on North from Tsarevo in Lozenets – two places with 19.6 ha and 20.83 ha.

LIDAR survey has determined that the infrastructure in the flood concerned area near Tsarevo is not adequate of the catchment observed. The survey permit to observe with high precision in details the area surface characteristics and two bridges constructed without adequate planning of possible water amounts possibly collected in the catchment. From satellite imagery it is seen that for the past 10 years some patches of deforestation exist that are not only not filled, but they continue to expand. That is, if we have a catchment with a small area (7 km^2) and a specific shape and cut down 10% of

the forests in it some disaster could happened. The characteristic feature of oblong catchments is that the flow of the individual tributaries reaches the bed of the main river at the same time, and this leads to a greater peak of the water quantity. In this small catchment the total area of clearings is 85.8 hectares - exactly 12% of the area of the entire catchment is cut down and 28.6% of the area of the forest areas in it.

In such extreme natural conditions, every tree counts, and every squared meter is a powerful collector of rain waters.

Consequences of the disaster. In the period 4–6 September 2023, prolonged heavy rains cause rivers overflow, floods, much material damage and even human casualties in the south-eastern regions of the country. The whole southern region of Bulgaria's Black Sea coast is affected by the disaster. Most of the rivers in the region overflow their banks. The walls of two dams are compromised, 13 bridges are completely or partially destroyed causing serious transporting and rescue problems to over 4000 inhabitants and tourists. The storm causes floods in the country's southern resort town of Tsarevo on the Black Sea coast where authorities declared a state of emergency. The extreme water wave drags cars and caravans into the sea, floods streets and hotels, activates landslides. The villages of Lozenets and Kosti, the town of Tsarevo and the Arapya and Nestinarka campsites are evacuated. Villages, mainly in Tsarevo and Malko Tarnovo municipalities, are left without electricity and water, roads are closed. Ahtopol, Varvara, Sinemorets and Rezovo are completely isolated due to destroyed bridges after the water disaster. In the upper and narrowest part of the watershed the wave had considerable force seriously damaging the bridge after the village of Izgrev. There is no publicly available information about the damages regarding the flooding level of the Popska river, Arap ravine and Poturnashka river watersheds.

In the most affected section of the flood area, between Kiten and Ahtopol, there is the Poturnashki dam, for which there is no information on quantitative monitoring. After the rain that fell on September 5, 2023 a number of checks have been made and it has been found out that the "Poturnashki" and "Hadji Yane" dam reservoirs have an open main spillway and waters are flowing over the crown of the dam wall thus the process of collapsing the crown and airstrip has begun. The overflow has prevented wall failure and further damages and thanks to the retention function of the dams the inflow to the gullies has been reduced.

CONCLUSIONS

The evolving climate changes negatively affect the hydrological regime, leading to extreme summer rainfall. This necessitates the establishment of a mechanism and policies for the management of water resources in flood-vulnerable areas. For this purpose, the hydrological conditions for the summer months of June-September were studied with observed and modeled parameters for the Southern Black Sea catchment area. The results show that heavy rainfall is becoming a normal occurrence for September along the Southern Black Sea coast, and that after a dry August, heavy rains should be expected in September, for which flood management services should be prepared.

The definitions of "river", "ravine" and "surface water body" in the Bulgarian Water Act should be clarified, as well as the boundaries of all water bodies, regardless of their ownership, should be defined. In the Bulgarian River Basin Management Plans

(RBMPs) and Bulgarian Flood Risk Management Plans (FRMPs), all water bodies with a catchment that flows directly into the Black Sea in populated areas must be considered rivers. In the FRMPs, measures for the adaptive capacity of the infrastructure located on the water bodies, and especially of this infrastructure that limits the passage of large quantities of water, must be foreseen. Also implement and evaluate the effectiveness of the "cleaning the riverbeds" measure. Absolute ban on logging and strict compliance with construction and geological norms in coastal areas.

Creation of an adequate network for quantitative monitoring of surface and groundwater bodies in the Southern Black Sea. Publicity of the data, so that at every level - local, regional and national, there is a program prepared by the experts in the water sector and by other institutions, municipalities, citizens, etc. for flood prevention and management.

ACKNOWLEDGEMENTS

This publication is based upon work within the National Science Programme "Environmental Protection and Reduction of Risks of Adverse Events and Natural Disasters", approved by the Resolution of the Council of Ministers № 577/17.08.2018 and supported by the Ministry of Education and Science (MES) of Bulgaria (Agreement № Д01-271/09.12.2022) as well as within the COST Action CA21112 “Offshore freshened groundwater: An unconventional water resource in coastal regions? (OFF-SOURCE)”, supported by COST (European Cooperation in Science and Technology).

REFERENCES

[1] Zyapkov L., Storm runoff intensity of the rivers in Bulgaria, Problems of Geography, vol. 3, 1988, pp 35-42, *(In Bulgarian*).

[2] Bocheva L., Simeonov P., Gospodinov I., Marinova T., Torrential Precipitation Events in Bulgaria: A Comparative Analysis for East Bulgaria. Paper presented at the international conference “BALWOIS 2008”, Republic of Macedonia, 2008, 7 p.

[3] Ungaro F., Calzolari C., Pistocchi A., Malucelli, F. Modelling the impact of increasing soil sealing on runoff coefficients at regional scale: a hydropedological approach. - J. Hydrol. Hydromech., vol. 62, Issue 1, 2014, 33-42.

[4] Nojarov, P. The increase in September precipitation in the Mediterranean region as a result of changes in atmospheric circulation. - Meteorology and Atmospheric Physics. Springer, vol. 129, 2017, 145–156.

[5] Antonov H., Danchev D., Ground waters in Bulgaria, Tehnika, Bulgaria, 360 p. 1980, (in Bulgarian).

[6] Oleson K., Dai Y., Bonan G. B., Bosilovichm M., Dickinson R., Dirmeyer P., Hoffman F., Houser P., Levis S., Niu G.-Y., Thornton P., Vertenstein M., Yang Z.-L., Zeng, X. Technical Description of the Community Land Model (CLM). NCAR/TN-461+STR. National Center for Atmospheric Research, Boulder, Colorado, 2004, 174p.

[7] NIMH. Monthly hydrometeorological bulletin. National Institute of Meteorology and Hydrology of Bulgaria, September 2023, Sofia.

SUSTAINABLE TREATMENT OF WASTEWATER FROM SOURCES WITH SEASONAL VARIATION

Dr. Costel Bumbac

Dr. Elena Elisabeta Manea

Dr. Valeriu Robert Badescu

National Research and Development Institute for Industrial Ecology - ECOIND, **Romania**

ABSTRACT

Compliance with EU environmental regulations and directives regarding effluent water quality discharged is seen as the main driver for the development of wastewater treatment technologies. The Water Framework Directive, the UWWT Directive, and the Nitrates Directive require the reduction of eutrophication caused by nitrogen and phosphorus emissions. In Romania, only approx. 54% of the population is connected to centralized sewage and wastewater treatment systems, meaning that approximately 8 million inhabitants are not connected to centralized sewage and wastewater treatment systems. However, while larger municipalities are getting closer to meeting EU standards and the sustainable development goal of Sanitation for all (SDG6), smaller communities especially in rural areas are lagging behind considerably. The discrepancy is explained by the high proportion and very low density of the rural population compared to the rest of the European countries (in Romania connecting a household from the rural area costs much more due to the large distances between properties). This does not necessarily mean that the rural population has no access to sanitation services as they switched to individual wastewater management solutions such as septic tanks or open pits, meaning that there is an urgent need for adequate solutions for wastewater treatment. Moreover, for the touristic accommodation facilities in regions with seasonal variability of occupancy (e.g. seaside/Danube Delta area) built in remote location, proper wastewater treatment solutions capable of dealing with peak flows and long rest period needs to be developed.

The paper emphasizes on the design of a vermifiltration system installed for the treatment of the wastewater generated by a touristic building in Romania and the adequate treatment performances achieved in terms of organic and nutrient loads

Keywords: decentralized wastewater treatment, seasonal variation

INTRODUCTION

In remote locations or rural areas that are not connected to centralized sewage systems, touristic buildings face unique challenges when it comes to wastewater treatment [1].

The fluctuation in tourist occupancy throughout the year leads to significant variations in wastewater quantity and quality. During peak seasons, these wastewater treatment systems are often overloaded, leading to the discharge of untreated or partially treated wastewater into the environment. This can have a serious impact on water quality and aquatic ecosystems.

In recent years, there has been a growing interest in the development of sustainable wastewater treatment technologies that can effectively treat wastewater from sources with seasonal variation. These technologies should be able to meet the following criteria: ensure effective treatment of wastewater, regardless of the influent load; should be sustainable in terms of energy consumption, resource use, and environmental impact and, last but not least, should be cost-effective to implement and operate.

Several promising sustainable wastewater treatment technologies have been developed in recent years. These technologies include: membrane bioreactors (MBRs), anaerobic treatment or nature based sollutions (NBS such as constructed wetlands or vermifiltration). MBRs are a type of biological wastewater treatment system that uses a membrane to separate treated wastewater from the biomass. This technology is effective at treating wastewater from sources with seasonal variation, as it can be easily adapted to changes in influent load. Anaerobic digestion is a process that uses microorganisms to break down organic matter in wastewater. Anaerobic digestion is an effective and sustainable way to treat wastewater from sources with seasonal variation but as a stand-alone technology offers poor-quality effluents. Constructed wetlands are artificial wetlands that are designed to treat wastewater. Constructed wetlands are effective at removing pollutants from wastewater, and they are also a sustainable treatment option however requires large footprint. The choice of sustainable wastewater treatment technology will depend on the specific needs of the application. Factors to consider include the volume and quality of wastewater, the available space, and the budget.

To address these challenges, vermifilter based wastewater treatment solutions offer a sustainable and efficient approach. These vermifilters not only provide a low-cost and environmentally friendly alternative for wastewater treatment but are also capable of withstanding peak flows and long periods of no influent, such as during the off-season periods of three months or more. The use of vermifilters for wastewater treatment has been extensively studied in various contexts such as swine and municipal wastewater [2]. These studies have shown that vermifilters are highly effective in treating wastewater, with favorable performance in terms of pollutant removal .

Additionally, vermifilters promote the synergistic activities of earthworms and microbes, making them more robust and potent in handling a wide range of wastewater including both industrial and domestic wastewater. This earthworms-assisted vermifilter system not only provides a cost-effective solution but also ensures the efficient removal of nitrogen, ammonia, and other impurities present in the wastewater [3]. Furthermore, vermifilters also have the ability to immobilize and remove suspended solids, chemicals like heavy metals, and pathogens from treated wastewater [4]. The introduction of earthworms to the vermifilter system enhances the treatment process by breaking down organics and promoting synchronous treatment of wastewater and stabilization of sludge [5]. Moreover, the treated water from vermifilters becomes fit for reuse, particularly in the irrigation of parks or other green spaces. The use of vermifilters for wastewater treatment in remote touristic buildings offers a sustainable and efficient solution to the challenges posed by seasonal variations in wastewater sources. By implementing vermifilter based wastewater treatment solutions, these touristic buildings can effectively manage their wastewater without relying on centralized sewage systems.

Overall, the implementation of vermifilter based wastewater treatment solutions provides a viable and eco-friendly option for sustainable treatment of wastewater in remote locations or rural areas that are not connected to centralized sewage systems [6].

MATERIALS AND METHODS

Wastewater treatment challenge in Romania

The difficulties related to the implementation of the European directive on wastewater treatment are determined by the low level of provision of water supply, sewage and wastewater treatment services, the physical and moral wear and tear of the related infrastructure and the particularly high costs required for the investments needed to comply with European requirements. The connection rate of the Romanian population to sewerage services is 55.8%, being the lowest among EU countries (fig.1). Although progress has been made at the national level in the implementation of Directive 91/271/EEC on wastewater treatment, in the period 2009-2021 the increase in the level of wastewater collection and treatment was registered especially in urban areas at rates above 90%. The differences between urban and rural areas are very large: while larger municipalities are getting closer to meeting EU standards, smaller communities (especially in rural areas) are lagging behind considerably.

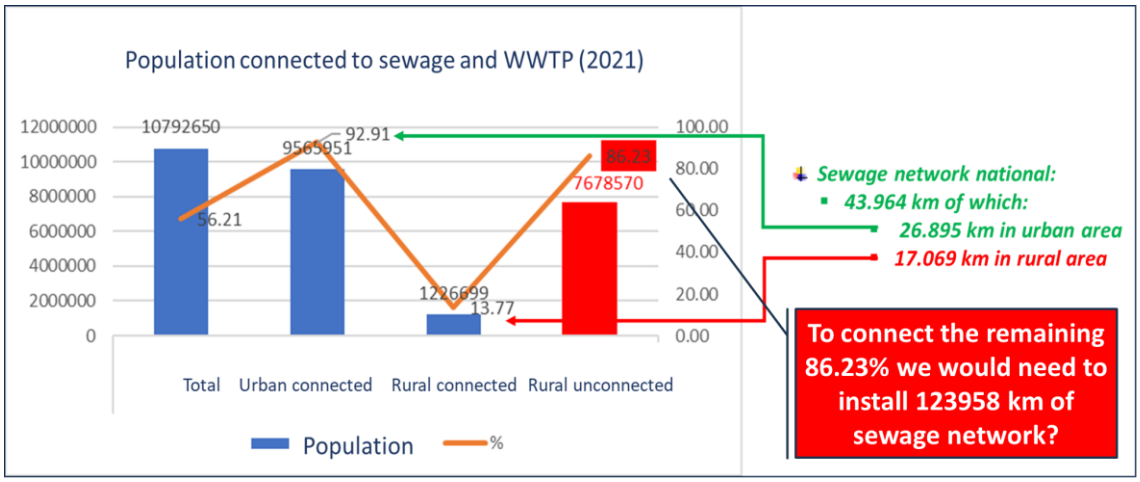

Fig.1. Population connected to sewage and WWTP (2021)

The low degree of connection is explained by the high proportion and very low density of the rural population compared to the rest of the European countries (in Romania connecting a household in the rural area costs much more due to the large distances between properties). A rough estimation based on existing sewage infrastructure in rural area used to connect 13.77% of the rural population shows the need to install at least 123958 km of sewage network to reach 100% coverage of rural population. (fig.2).

Romania is the country in the EU with the highest percentage of the population, which in 2015 did not have access to a bathroom, a shower and a toilet in the house, respectively 30.5% compared to the EU average of only 2.0% 47. In 2021, although progress has been made in this regard, Romania is still in last place, being reported that 21.2% of the population, approximately 4 million inhabitants, do not have access to civilized sanitation conditions.

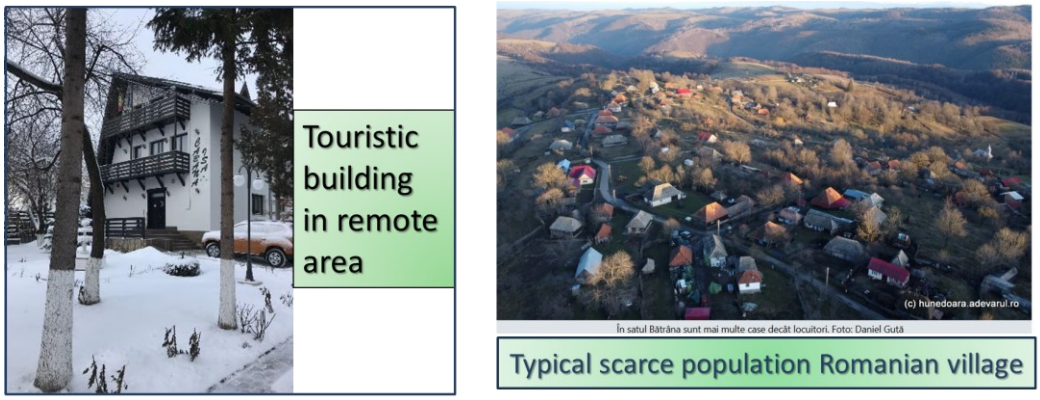

Fig.2. Touristic building in remote rural area and scarce population Romanian Village

Touristic building seasonal occupancy variation

In the last 20 years, agro-touristic activities have bloomed considerably as the number of touristic accommodations increased as a result of the market increase and non-refundable funds allocation by different national and European support programs. Moreover, the recent pandemic boosted the idea of spending holidays in remote locations, or smaller accommodation facilities. The frequency and seasonality of occupancy of such touristic buildings can have a significant impact on wastewater flows. Thus, during the tourist season, when the guesthouse is full of tourists, the wastewater flows can be higher and more regular. In the off-season, when the accommodation capacity of the guesthouse is reduced or when the guesthouse is temporarily closed, sewage flows may be lower or even absent. At the level of Romania, in 2022, there were 5,128 accommodation units of the type of guesthouses and agro-tourism guesthouses with an accommodation capacity of approximately 91,000 tourists. Their degree of occupancy varies depending on several factors, especially seasonality, thus, in the coastal area the guesthouses are active approximately 5 months a year (May-September), those in the delta area are active approximately 8 months (March-October) and those in the mountain areas are active all year round with peaks of occupancy in the holidays and school vacation seasons (fig. 3).

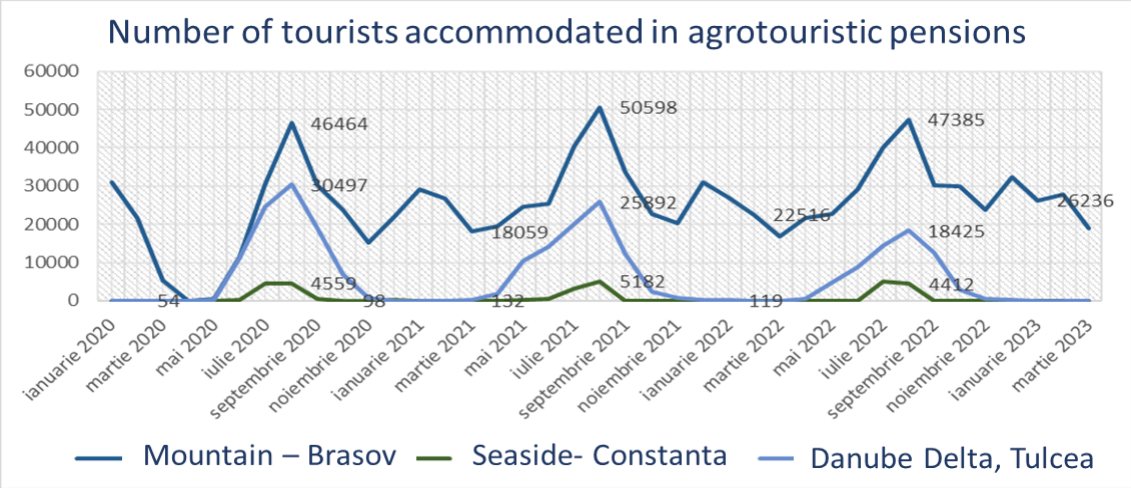

Fig.3. Tourists accommodated in agrotouristic pensions in 3 highly touristic areas

The quality of wastewater can vary depending on the number of people served, the type and number of sanitary facilities available, as well as the share of water from the kitchen/restaurant. Wastewater may contain organic substances from toilets, showers, fats and oils from the kitchen, detergents used for washing clothes, dishes, or sanitizing surfaces as well as other chemicals and solid particles. The ranges of variation of the main quality parameters of wastewater from a touristic building are represented in table 1.

Table 1. Influent concentrations (mg/L)

Conc. (mg/L)	TSS	COD	BOD	NH_4	$N\text{-}NO_3^-$	Total N	Total P
average	355	922	421	40.5	0.68	103	9
min	77	449	125	19	<0.01	53	3.54
max	1045	1540	681	98	1.6	207	13.5

Thus, it is important to correctly design, assess and size the treatment system in order to properly manage the wastewater flows in the tourist guesthouse. An adequate treatment system can ensure efficient and safe processing of wastewater, protecting the environment and complying with the rules and regulations in force in Romania

RESULTS AND DISCUSSIONS

To address these challenges, a vermifilter based wastewater treatment solution was used to assess the adaptability of the system and long-term treatment performances in conditions of seasonal wastewater flow variability. These vermifilters not only provide a low-cost and environmentally friendly alternative for wastewater treatment but are also capable of withstanding peak flows and long periods of no influent, such as during the off-season periods of three months or more.

Vermifilter technology

Vermifiltration relies on the “power of earthworms” in an engineered trickling filter to treat wastewater. Able to perform primary and secondary treatment, TSS and organic load removal, but also nitrification and partial denitrification have been identified with consistency during operation;

The reactor is filled with successive layers of materials with different functions: from bottom to top: river pebbles (in two size ranges) as draining support, wood chips as an active layer for microbial biofilm, and home for earthworms.

The influent is sprayed on top of the active layer and passes through the active layer where bacteria remove dissolved nutrients while earthworms provide the service of consuming the TSS and regulating the microbial biomass (biofilm).

The results of the present study are correlated to literature data, suggesting that vermifilters may effectively treat municipal wastewater by reducing various pollutants including chemical and biological oxygen demand, and turbidity to adequate levels that meet most environmental and irrigation water standards. However, the residual amounts of nutrients (ammonium, nitrate and phosphate) make the system suitable to use the

effluent as irrigation water after proper microbial load assessment and eventual reduction.

Table2. Average removal rates of main wastewater contaminants

Removal rate	TSS	BOD_5	COD	NH_4-N	TP	PO_4-P	Turb.	TN
Average (%)	**64.05**	**77.17**	**70.91**	**65.95**	**35.83**	**25.41**	**73.43**	**55.38**
St. dev. (σ)	**±20.5**	**±15.17**	**±13.86**	**±18.47**	**±15.9**	**±15.59**	**±14.92**	**±20.38**
Median	**69.32**	**83.42**	**73.1**	**70.22**	**32.94**	**23.07**	**78.33**	**61.94**

CONCLUSION

In conclusion, vermifilter based wastewater treatment solutions offer a sustainable and efficient approach for remote touristic buildings or rural areas that are not connected to centralized sewage systems. By harnessing the power of earthworms and microbes, vermifilters provide a cost-effective and environmentally friendly alternative for treating wastewater. In addition to their ability to adequately treat wastewater, vermifilters also have the advantage of being able to withstand peak flows and long periods of no influent, making them ideal for seasonal variations in wastewater sources.

Moreover, the use of vermifilter-based wastewater treatment solutions offers a sustainable and efficient approach to addressing the challenges posed by seasonal variations in wastewater sources such as touristic buildings in remote locations or rural areas. These solutions not only effectively remove impurities and promote synchronous stabilization of wastewater and sludge, but also can immobilize and remove suspended solids and nutrients from influent wastewater.

ACKNOWLEDGEMENTS

This work was carried out through the “Nucleu” Program within the National Research Development and Innovation Plan 2022-2027 with the support of Romanian Ministry of Research, Innovation and Digitalization, contract no. 3N/2022, Project code PN 23 22 03 02.

REFERENCES

[1] Calheiros, C. S. C., Bessa, V. S., Mesquita, R. B. R., Brix, H., Rangel, A. O., and Castro, P. M. L., "Constructed wetland with a polyculture of ornamental plants for wastewater treatment at a rural tourism facility". Ecological Engineering, Volume 79, Pages 1-7, 2015, https://doi.org/10.1016/j.ecoleng.2015.03.001.

[2] Xing, M., Li, X. and Yang, J.. "Treatment performance of small-scale vermifilter for domestic wastewater and its relationship to earthworm growth, reproduction and enzymatic activity", African Journal of Biotechnology Vol. 9(44), pp. 7513-7520, 2010.

[3] K. H. Suhaib and P. Bhunia. "Clogging index: A tool to quantify filter bed clogging in horizontal subsurface flow macrophyte-assisted vermifilter", Water Environment Research, vol. 95 (1), 2023.

[4] Sinha, R.K., Herat, S., and Valani, D.(2010) ‘Earthworms - The Environmental Engineers: Review of Vermiculture Technologiesfor Environmental Management &

Resource Development ‘, Int. J. of Environmental Engineering, Special Issue Special Issue on ‘Vermiculture Technology for Environmental Management and Resource Development, Vol. X, No. Y., pp. 000 000.

[5] Samer M (2015) Biological and Chemical Wastewater Treatment Processes. Wastewater Treatment Engineering. InTech. Available at: http://dx.doi.org/10.5772/61250

[6] René van der Velden, Warde da Fonseca-Zang, Joachim Zang, Dominic Clyde-Smith, Wilson M. Leandro, Priti Parikh, Aiduan Borrion & Luiza C. Campos (2022) Closed-loop organic waste management systems for family farmers in Brazil, Environmental Technology, 43:15, 2252-2269, DOI: 10.1080/09593330.2021.1871660

THE INTERCONNECTION BETWEEN PREVENTING WATER POLLUTION AND ADDRESSING CLIMATE CHANGE

Assoc. Prof. Dr. Laura Șmuleac[1]

Lecturer Dr. Raul Pașcalău[1]

Assoc. Prof. Dr. Adrian Șmuleac[1]

Prof. Dr. Florin Imbrea[1]

Lecturer Dr. Alina Lațo[1]

[1] University of Life Sciences ”King Mihai I” from Timișoara, **Romania**

ABSTRACT

Water pollution and climate change are two of the most pressing environmental challenges of our time, and their interconnection is increasingly evident.
Water pollution and climate change are interconnected in various ways. The release of greenhouse gases, primarily carbon dioxide, methane, and nitrous oxide, is a significant driver of global warming. These gases contribute to the greenhouse effect, leading to rising global temperatures, which, in turn, affect water resources. Warmer temperatures exacerbate water pollution by increasing the prevalence of harmful algal blooms, the degradation of water quality, and disruptions in aquatic ecosystems. Additionally, climate change-induced extreme weather events like floods and droughts can intensify water pollution by causing the runoff of pollutants into water bodies.
Preventing water pollution is an essential component of mitigating climate change.
Furthermore, the preservation of healthy ecosystems plays a vital role in both preventing water pollution and addressing climate change. Wetlands and forests act as carbon sinks, sequestering carbon dioxide, while also filtering pollutants from runoff. Protecting and restoring these ecosystems is a win-win strategy for combatting both issues simultaneously.
These global challenges require integrated strategies that recognize the symbiotic relationship between them. By implementing effective pollution control measures, reducing carbon emissions, and protecting vital ecosystems, we can make significant strides in combating these urgent issues and ensuring a sustainable future for our planet.

Keywords: water pollution, climate changes, interconnection, measures, impact, influence, environment

INTRODUCTION

Water pollution and climate change are two paramount environmental issues confronting humanity in the 21st century. While they are often discussed as separate challenges, a closer examination reveals a profound and intricate interconnection between the two. This introduction sets the stage for a comprehensive exploration of the relationship between preventing water pollution and addressing climate change, highlighting the pressing need for integrated solutions to combat these global crises [1].

Climate change, driven primarily by the emission of greenhouse gases, has emerged as one of the most formidable threats to the planet's ecological balance. The rise in global temperatures, extreme weather events, and altered precipitation patterns are all manifestations of this global transformation. Beyond the more obvious consequences of climate change, such as rising sea levels and more frequent heatwaves, its influence on water resources is increasingly evident [2].

The impact of climate change on water systems is multifaceted. Warmer temperatures can intensify water pollution by fostering the proliferation of harmful algal blooms, impairing water quality, and disrupting aquatic ecosystems [3]. Extreme weather events, such as floods and droughts, amplify the problem by causing runoff of pollutants into rivers, lakes, and oceans. These interconnected phenomena underscore the urgent need to address water pollution in the context of climate change mitigation.

Conversely, mitigating climate change is pivotal for preventing water pollution. Many sources of water contamination, including industrial discharges, agricultural runoff, and untreated sewage, emit greenhouse gases. Such pollutants, when released into water bodies, contribute to the greenhouse effect [4] Consequently, implementing effective pollution control measures, investing in sustainable agriculture practices, and enhancing wastewater treatment can reduce the release of potent greenhouse gases like methane and nitrous oxide, thus playing a significant role in climate change mitigation.

Furthermore, safeguarding water resources and ecosystems is indispensable for addressing both water pollution and climate change. Wetlands and forests, for instance, act as vital carbon sinks, sequestering carbon dioxide and mitigating climate change while also serving as natural filters that purify water. Protecting and restoring these ecosystems can have a double positive impact on our environment.

This interconnectedness between water pollution and climate change emphasizes the necessity of a holistic approach that recognizes the mutual dependence of these two crises. As we delve deeper into this subject, we will explore the various facets of this complex relationship, analyse the potential solutions, and consider the broader implications for our environment and society. By adopting integrated strategies that simultaneously tackle water pollution and climate change, we can strive for a more sustainable and resilient future for our planet.

MATERIALS AND METHODS

For this scientific paper we have used the analysis and the comparative method.

The use of analysis and comparative methods is crucial. Here's how these methods can be applied:

Analysis:

Environmental Data Analysis: This involves the examination of environmental data related to water quality, temperature trends, greenhouse gas emissions, and extreme weather events. Statistical and analytical tools were used to identify patterns, correlations, and causative relationships. For instance, how changes in temperature and precipitation patterns correlate with alterations in water quality or the frequency of pollution events.

Policy Analysis: In this context, we analysed existing environmental policies and regulations related to both water pollution control and climate change mitigation. We considered factors like policy effectiveness, enforcement, and areas where improvements may be needed.

Economic Analysis: We evaluated the economic implications of strategies to prevent water pollution and address climate change. This analysis included cost-benefit assessments of various pollution control measures, as well as the economic impact of climate change on water resources, agriculture, and infrastructure.

Case Study Analysis: we examined specific case studies or real-world examples to gain deeper insights into the relationship between water pollution and climate change. We also analysed how extreme weather events have affected water quality, or how specific pollution control measures have influenced greenhouse gas emissions.

Comparative Method:

Comparative Policy Analysis: We tried to compare environmental policies and regulations from different regions or countries to identify best practices and lessons learned, and also to understand how different approaches to pollution control and climate change mitigation have succeeded or failed in various contexts.

Comparative Case Studies: There were examined multiple case studies to identify commonalities and differences in how different regions or ecosystems are impacted by the interconnection of water pollution and climate change.

Temporal Comparisons: we analysed data and information over time to track changes in the interconnection between water pollution and climate change.

Comparative Economic Analysis: We compared the economic impacts of different pollution control and climate change adaptation strategies.

By employing analysis and comparative methods, we reached to a deeper understanding of the complex relationship between water pollution and climate change. These methods allow for the identification of effective strategies, the evaluation of policy outcomes, and the adaptation of practices that can help address these critical environmental challenges in a more integrated and holistic manner.

RESULTS

We presented the key findings from the analysis of environmental data, including trends in water quality, temperature, and greenhouse gas emissions. We used all the gathered info and data to make significant patterns and correlations. For example, we might highlight how rising temperatures correspond with an increase in harmful algal blooms or the correlation between extreme weather events and water pollution incidents.

Here are a few examples of how addressing water pollution and mitigating the impacts of climate change can have positive impacts:

1.Promoting sustainable agriculture practices: Implementing sustainable agriculture practices, such as reducing the use of chemical fertilizers and pesticides, can help prevent water pollution and reduce the carbon footprint of agricultural operations. This can include the use of cover crops, conservation tillage, and integrated pest management to reduce the amount of chemicals entering waterways [5].

2.Restoring wetlands and other natural habitats: Restoring wetlands, marshes, and other natural habitats can help to absorb pollutants and improve water quality. These ecosystems also play an important role in mitigating the impacts of climate change by sequestering carbon and reducing greenhouse gas emissions.

3.Investing in green infrastructure: Investing in green infrastructure, such as green roofs, rain gardens, and permeable pavements, can help to reduce the amount of runoff

entering waterways and improve water quality. These infrastructure solutions also provide co-benefits such as reducing energy consumption and improving air quality.

4.Improving wastewater treatment: Improving wastewater treatment can help reduce the amount of pollutants entering waterways and improve water quality. This can include the use of advanced treatment technologies, such as constructed wetlands, to remove pollutants and improve water quality.

5.Promoting the use of clean energy: Promoting the use of clean energy, such as wind, solar, and hydropower, can help reduce greenhouse gas emissions and improve water quality.

By reducing the use of fossil fuels, we can reduce the amount of pollutants entering waterways and improve the health of our ecosystems.

These are just a few examples of how addressing water pollution and mitigating the impacts of climate change can have positive impacts. By taking a multi-disciplinary and collaborative approach, we can work towards a more sustainable future for our water resources and the environment [6].

There are several measures that could be undertaken to address water pollution and mitigate the impacts of climate change:

1.Implementing regulations and policies: Governments can implement regulations and policies to reduce the amount of pollutants entering waterways, such as regulations on the use of chemicals in agriculture and industry. Additionally, governments can implement policies to reduce greenhouse gas emissions, such as carbon pricing and renewable energy mandates.

2.Promoting public education and outreach: Education and outreach programs can help raise awareness of the importance of preventing water pollution and mitigating the impacts of climate change. This can include educating individuals about the sources of water pollution, such as runoff from agricultural lands, and encouraging them to reduce water usage and waste.

3.Investing in research and development: Investing in research and development can help to improve our understanding of water pollution and the impacts of climate change, and lead to the development of new and innovative solutions. This can include investing in new technologies, such as advanced water treatment systems, and in the development of more sustainable practices, such as agroforestry [7].

4.Encouraging private sector innovation: The private sector can play an important role in addressing water pollution and mitigating the impacts of climate change. This can include encouraging the development of new technologies and solutions, such as the use of sustainable materials in products, and supporting the development of clean energy and water management practices.

5.Supporting community-based initiatives: Community-based initiatives, such as watershed management programs, can help to reduce the amount of pollutants entering waterways and improve water quality. These initiatives can include community-led efforts to reduce runoff, improve waste management practices, and implement sustainable agriculture practices.

These are just a few of the measures that could be undertaken to address water pollution and mitigate the impacts of climate change. By working together and taking a multi-

disciplinary approach, we can make a positive difference for our water resources and the environment.

There are several strategies that can be adopted to address water pollution and mitigate the impacts of climate change:

1.Integrated Watershed Management: This approach involves coordinating efforts across multiple stakeholders, including government agencies, local communities, and the private sector, to develop a comprehensive strategy for managing water resources within a watershed.

2.Green Infrastructure: This approach involves incorporating natural features, such as forests, wetlands, and green roofs, into the built environment to reduce runoff, improve water quality, and provide other benefits, such as reducing the urban heat island effect.

3.Sustainable Agricultural Practices: Implementing sustainable agricultural practices, such as reduced tillage, cover cropping, and the use of integrated pest management, can reduce runoff and improve water quality.

4.Water Reuse and Recycling: This approach involves treating and reusing wastewater and stormwater for non-potable purposes, such as irrigation and industrial processes, to reduce the amount of water withdrawn from natural resources.

5.Clean Energy and Energy Efficiency: Adopting clean energy sources, such as solar and wind power, and implementing energy efficiency measures can reduce greenhouse gas emissions, which contribute to climate change, and reduce the demand for water used in energy production.

6.Public Education and Outreach: Education and outreach programs can help raise awareness of the importance of preventing water pollution and mitigating the impacts of climate change, and encourage individuals to adopt more sustainable practices [8].

These are just a few of the strategies that can be adopted to address water pollution and mitigate the impacts of climate change. By taking a multi-disciplinary and integrated approach, we can develop effective and sustainable solutions for managing our water resources and protecting the environment.

We analysed the influence of water on soil and climate.

Water is a critical component of the Earth's climate system and plays a key role in regulating soil moisture and temperature.

1.Soil Moisture: Water is essential for maintaining soil moisture, which is critical for plant growth and soil health. Excess water can lead to soil saturation and decreased oxygen levels, which can damage roots and reduce plant growth. On the other hand, too little water can cause drought conditions and limit plant growth.

2.Climate: Water also plays a critical role in regulating the Earth's climate. The water cycle, also known as the hydrologic cycle, involves the movement of water from the ocean, to the atmosphere, to the land, and back to the ocean. This cycle helps regulate the Earth's temperature by transferring heat from the ocean to the atmosphere [9].

3.Evapotranspiration: Another important aspect of the water cycle is evapotranspiration, which is the process by which water is taken up by plants and then released into the atmosphere through transpiration. This process helps regulate the Earth's temperature and also contributes to atmospheric humidity [10].

4.Soil Erosion: The water cycle also affects soil erosion, which can impact soil health and lead to decreased crop productivity. Soil erosion can be caused by heavy rainfall and runoff, which can remove valuable topsoil and decrease the fertility of the soil.
In conclusion, water plays a critical role in regulating soil moisture, temperature, and the Earth's climate, and has a significant impact on soil health, plant growth, and crop productivity.
Understanding the influence of water on soil and climate is important for developing sustainable agricultural practices and managing our water resources effectively [11].
Rivers, seas, and lakes play a critical role in the Earth's climate system, as well as in maintaining regional and local ecosystems[12]. Some of the ways these bodies of water impact the climate include:

1.Regulating Climate: Water bodies store and release heat, which helps regulate the Earth's climate. For example, oceans absorb and store heat from the sun, helping to regulate temperatures around the world [13].

2.Humidity and Precipitation: Water bodies also play a critical role in the formation of clouds and precipitation. Water evaporates from the surface of the oceans and other bodies of water into the atmosphere, where it can form clouds and precipitation.

3.Currents: The ocean's currents also play a role in regulating the Earth's climate by transporting heat and water from one place to another. For example, the Gulf Stream is a warm ocean current that transports heat from the tropics to northern Europe, helping to regulate temperatures in the region.

4.Biodiversity: Rivers, seas, and lakes provide critical habitats for many species of plants and animals, and support complex ecosystems that are critical for maintaining the planet's biodiversity [14].
In conclusion, rivers, seas, and lakes are important components of the Earth's climate system, and play a critical role in regulating temperature, humidity, and precipitation, as well as supporting biodiversity and maintaining regional and local ecosystems [15].

CONCLUSION

Toward Integrated Solutions
The intricate interconnection between preventing water pollution and addressing climate change underscores the urgent need for integrated solutions in environmental management and policy. Through an in-depth exploration of environmental data, policy analysis, economic considerations, and case study insights, this study has shed light on the multifaceted relationship between these two pressing global challenges.

1. Interconnection as a Core Challenge:

Our analysis reveals that water pollution and climate change are not isolated issues; rather, they are mutually reinforcing challenges. Rising global temperatures and extreme weather events exacerbate water pollution, impacting the health of aquatic ecosystems and water quality. Simultaneously, pollution contributes to climate change by releasing greenhouse gases into the atmosphere. Recognizing this interdependence is pivotal in developing effective strategies for a sustainable future.

2. Policy Synergies and Implications:

The examination of environmental policies at various levels of governance reveals both promising synergies and areas for improvement. Policymakers have an opportunity to

develop integrated approaches that harness the interconnection between these challenges. Strategies that simultaneously reduce pollution and mitigate climate change, such as green infrastructure and sustainable land-use planning, should be prioritized. Additionally, international collaboration is imperative to address these global issues effectively.

3. Economic Feasibility and Incentives:

Economic considerations are central to the successful implementation of integrated solutions. Our analysis underscores the importance of considering the economic implications of policies and measures to prevent water pollution and address climate change. It is evident that upfront investments in pollution control, wastewater treatment, and sustainable agriculture can yield long-term benefits, both in terms of environmental protection and cost savings. Additionally, carbon pricing and other economic incentives should be leveraged to drive environmentally responsible practices.

4. Lessons from Real-World Examples:

Case studies provide valuable insights into the practical challenges and successes in addressing the interconnection between water pollution and climate change. These real-world examples underscore the importance of adaptive management and resilient infrastructure. It is essential to learn from these experiences and adapt strategies to the specific needs and vulnerabilities of different regions and ecosystems.

5. A Call for Future Research and Action:

This study serves as a call to action for the research community and policymakers. Future research should focus on expanding our understanding of the complex dynamics at the intersection of water pollution and climate change. Further studies are needed to assess the effectiveness of integrated policy approaches and to develop innovative technologies and practices.

In conclusion, addressing the interconnection between preventing water pollution and addressing climate change requires a holistic and multidisciplinary approach. It demands the collaboration of governments, scientists, environmentalists, and industries to create integrated strategies that effectively combat these global crises. By recognizing the symbiotic relationship between water pollution and climate change, we can forge a path towards a sustainable future, safeguarding water resources and ecosystems while mitigating the impacts of a changing climate. The time to act is now, as our planet's health and the well-being of future generations hang in the balance.

ACKNOWLEDGEMENTS

Support was also received by the project Horizon Europe (HORIZON) 101071300 - Sustainable Horizons -European Universities designing the horizons of sustainability (SHEs)

REFERENCES

[1] Taylor R. W., Watershed Management for Climate Resilience and Water Quality. Springer Nature, pp 32-45, 2019.

[2] Adams J. M., International Collaboration on Water Pollution and Climate Change: Achievements and Challenges. International Policy Press, pp 23-34, 2020.

[3] Brown O. R., Water Pollution, Climate Change, and Human Health: An Integrated Approach. Environmental Health Publications, pp 15-21, 2019.

[4] Șmuleac, L., Rădulescu H., Imbrea F., Șmuleac A., Pașcalău R., Water management to reduce floods in the hydrographic Basin Bega-Timiș, International Multidisciplinary Scientific GeoConference Surveying Geology and Mining Ecology Management, SGEM, 22(3.2), pp. 247–254, 2022.

[5] Pașcalău R., Stanciu S., Șmuleac L., Șmuleac A., Ahmadi Khoe M., Danci M, Feher A., Iosim I., Sălășan C., Bakli M., Amara M., The importance of English language in attracting foreign tourists in the mures valley region, namely in the wine road area, county of Arad, Western Romania, Research Journal of Agricultural Science, ISSN: 2668-926X, Vol. 52(2), 2020.

[6] Matti S., Sampo P., Tin-Yu L., Tapio S., Kari H., Crop production, water pollution, or climate change mitigation—Which drives socially optimal fertilization management most?, Agricultural Systems,Volume 186, 102985,ISSN 0308-521X, https://doi.org/10.1016/j.agsy.2020.102985, 2021.

[7] Wilson D. L., Urbanization, Water Pollution, and Climate Change: Challenges and Opportunities. Urban Development Journals, pp 41-56, 2018.

[8] Pașcalău R., Șmuleac L.,. Stanciu S. M, Imbrea F., Șmuleac A., Bakli M., Amara,M., Non- formal education in teaching foreign languages for agriculturists, Research Journal of Agricultural Science, 54 (2), ISSN: 2668-926X, 2022.

[9] Jingling Z., Lili Z., Renming M., Yanfeng J., Fan Y., Hongyang Z., Xiangying C., Influence of soil moisture content and soil and water conservation measures on time to runoff initiation under different rainfall intensities, CATENA, Volume 182, 104172, ISSN 0341-8162, https://doi.org/10.1016/j.catena.2019.104172, 2019.

[10] Turner J. M., Water Pollution Control Technologies for a Changing Climate. Environmental Engineering Books, pp 56-72, 2020.

[11] Pașcalău, R., Șmuleac, L., Stanciu, S., Imbrea, F., Șmuleac, A., Modern translation in climate change nowadays, International Multidisciplinary Scientific GeoConference Surveying Geology and Mining Ecology Management, SGEM, 22(4.2), pp. 351–356, 2022.

[12] Șmuleac, A.; Șmuleac, L.; Popescu, C.A.; Herban, S.; Man, T.E.; Imbrea, F.; Horablaga, A.; Mihai, S.; Pașcalău, R.; Safar, T. Geospatial Technologies Used in the Management of Water Resources in West of Romania. Water, 14, 3729. https://doi.org/10.3390/w14223729, 2022

[13] King M. P., Green Infrastructure Solutions for Water Pollution and Climate Resilience. Urban Planning Publications, pp 26-42, 2018.

[14] Garcia M. R., Protecting Ecosystems: A Key to Combating Climate Change and Water Pollution. Nature Conservation Society, pp 45-67, 2017.

[15] Șmuleac, A., Șmuleac, L., Pașcalau, R., Popescu, G., Horablaga, A., Using ground control points (gcp) and UAV poind cloud processinf in water management, International Multidisciplinary Scientific GeoConference Surveying Geology and Mining Ecology Management, SGEM., 22(3.2), pp. 231–238, 2022.

VOLUMETRIC QUANTIFICATION OF SOIL EROSION AND ANALYSIS OF CHOSEN LOCALITY IN TERMS OF RUNOFF AND EROSION CONDITIONS

Lukáš Buršík[1]

Prof. Dr. Miroslav Dumbrovský[1]

Dr. Veronika Sobotková[1]

Martina Kulihová[1]

[1] Brno University of Technology, **Czech Republic**

ABSTRACT

The purpose of this paper is volumetric quantification of soil erosion using the so-called erosion bridge. For the measurement, a locality in the South Moravian Region of the Czech Republic was chosen. With the erosion bridge, we can measure erosion rills. Rill erosion is caused by concentrated water flow. It occurs when runoff water forms small channels as it concentrates down a slope. The erosion bridge is a very simple device that enables us to accurately measure the shape of the soil surface in a given place. It was designed and created at the Institute of Landscape Water Management, Faculty of Civil Engineering, Brno University of Technology. The erosion bridge consists, besides other parts, of a rectangular steel frame to which needles are attached. These needles are lowered onto the terrain, copying its profile. Using this method, we get photos of the profile of the terrain, which are subsequently evaluated using a software program and exported into a DXF file that can be opened in AutoCAD. It is then possible to calculate soil loss. This paper also deals with the analysis of the chosen locality in terms of runoff and erosion conditions. This analysis was made by using geographic information systems, mainly ArcGIS Pro software program.

Keywords: surface runoff, water erosion, rill erosion, erosion bridge, soil loss

INTRODUCTION

In the Czech Republic soil erosion is a serious degradation process that threatens more than fifty percent (about 1.5 million hectares) of arable land. Soil degradation by water erosion and related impacts can be effectively limited by various types of soil erosion control measures.[1]. Erosion deprives the agricultural soils of the most fertile part which is a humus horizon. It makes degradation of physical, chemical, and biological soil properties and reduces the thickness of the soil and humus content in the soil [2].

Rill erosion is one of the most important types of soil erosion that has caused the destruction of many lands in recent decades, and its management has become an essential issue in world research [3]. It can contribute vastly to the overall erosion rate [4].

Rill erosion is one of the most important causes of land degradation, and it is caused by the flow concentration on the surface of hillslopes. It, therefore, results in several times increase in the amount of soil loss and sediment yield [5].

Rill erosion generally turns into gully erosion with severe environmental impacts. Changes in land use and human activities can have heavy effects in rill formation. Soil morphology plays a significant role in these effects [6].

Rills caused by runoff concentration on erodible hillslopes generally have very irregular longitudinal profiles and cross-section shapes. Rill erosion directly depends on the flow hydraulics within the rills which may differ greatly from that in larger and regular channels such as streams or rivers [7].

MATERIALS AND METHODS

Description of Chosen Locality

The chosen locality can be found in the South Moravian Region (NUTS 3) of the Czech Republic, in the Vyškov District (NUTS 4). It is situated approximately twenty kilometers southwest of the city of Brno (see Fig. 1). It is located in a municipality Otnice (cadastral territory Otnice). The area of the chosen locality covers approximately 2,300 square meters.

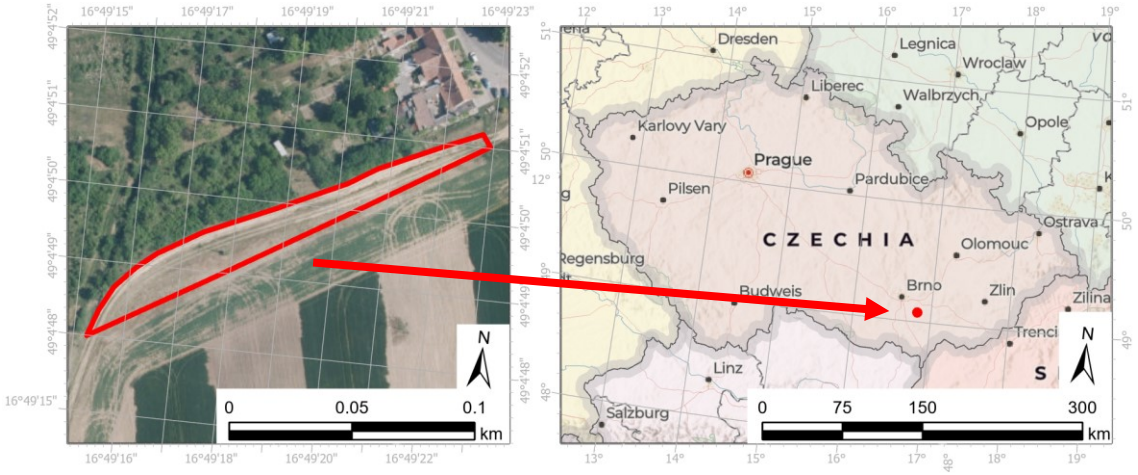

Fig. 1 Location of the area of interest

For the analysis, one block of LPIS (Land Parcel Identification System) was chosen. The reason is that a deep erosion rill was formed here (see Fig. 2). From the erosion rill, soil was eroded and subsequently sedimented in the bottom part of the hillside, outside of the area of interest (see Fig. 3). According to LPIS, land-use of this block is a grassland (on an arable land). The territory is located at an altitude of 219 to 243 meters above sea level.

In the locality, brown soil modal (HNm) can be found. From the point of view of hydrologic soil groups, all the area belongs to a group B. Regarding the soil depth, there are deep soils (soil depth is more than 60 cm).

Fig. 2 Erosion rill [own source]

Fig. 3 Sediment accumulation [own source]

Volumetric Quantification of Erosion and Calculation of Soil Loss

The erosion rill was measured with the use of so-called erosion bridge [8]. It is a very simple device that enables us to accurately measure the shape of the soil surface in a given place. It was designed and created at the Institute of Landscape Water Management, Faculty of Civil Engineering, Brno University of Technology. The erosion bridge consists, besides other parts, of a rectangular steel frame to which needles are attached (see Fig. 4). These needles are lowered onto the terrain, copying its profile. There is also a camera that is used for taking photos of the erosion bridge. In these photos, it is possible to observe the profile of the terrain (see Fig. 5).

Fig. 4 Measuring with the use of the erosion bridge and its main parts [own source]

Lukáš Dobrovolný, a student at Faculty of Mechanical Engineering, Brno University of Technology, as part of his Bachelor's Thesis [9] created with the use of MATLAB a software program "Erosion bridge" that enables us to evaluate photos obtained and export them into DXF files which can be opened in AutoCAD (see Fig 6). It is visible

that the software program rotates and tilts the pictures slightly so that the exported curves are in the same position and dimension.

Fig. 5 Photo of the profile [own source].

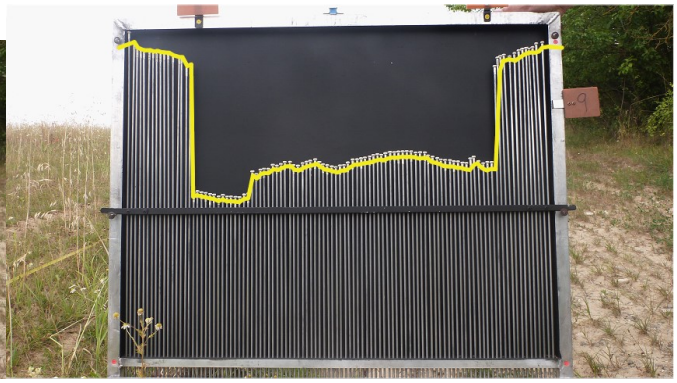

Fig. 6 Exported curve (yellow) and the photo of the profile [own source].

After that, in AutoCAD, parameters of the profiles such as area, width or depth can be measured. Distances between the profiles are known, the volume can be obtained from the area.

The Universal Soil Loss Equation (abbreviated USLE) was used for a calculation of soil loss. Using six factors, it is possible to estimate a long-term average annual soil loss in tons per hectares per year. These factors are associated with climate, soil, topography, vegetation, and management [10].

RESULTS

Volumetric Quantification of Rill Erosion in Chosen Locality

As already mentioned, with the use of AutoCAD, several parameters of the profile measured were obtained. These parameters, seen in Tab. 1, are following: area (A) wetted perimeter (P), width (B), and maximal depth (d_{max}).

Tab. 1 Parameters of the profiles measured

Profile'	A' [m^2]	P' [m]	B'[m]	d'_{max} [m]
1	0.028	0.678	0.639	0.079
2	0.034	0.674	0.590	0.111
3	0.036	0.848	0.757	0.093
4	0.030	0.889	0.762	0.081
5	0.012	0.480	0.426	0.050
6	0.178	1.353	0.730	0.324
7	0.044	0.692	0.182	0.292
8	0.038	0.850	0.459	0.260
9	0.052	1.085	0.636	0.247
10	0.012	0.643	0.598	0.044

Afterwards, profiles between measured ones were computed based on their average values (see Tab. 2). For instance, Profile 1–2 was obtained from values of the first two profiles.

In the table, the areas of the profiles were multiplied by ten (distances between profiles), thereby obtaining partial volumes (V_i). The final volume is their sum. It is visible that the volume eroded (soil loss) in the rill is equal to 4.44 cubic meters.

Tab. 2 Parameters of the profiles computed.

Profile	A [m^2]	P [m]	B [m]	d_{max} [m]	V_i [m^3]
1–2	0.031	0.676	0.615	0.095	0.31
2–3	0.035	0.761	0.674	0.102	0.35
3–4	0.033	0.869	0.760	0.087	0.33
4–5	0.021	0.685	0.594	0.066	0.21
5–6	0.095	0.917	0.578	0.187	0.95
6–7	0.111	1.023	0.456	0.308	1.11
7–8	0.041	0.771	0.321	0.276	0.41
8–9	0.045	0.968	0.548	0.254	0.45
9–10	0.032	0.864	0.617	0.146	0.32
					4.44

Average Soil Loss in Chosen Locality

The result of the analysis of the chosen locality in terms of erosion conditions can be seen in Tab. 3 and Fig. 7. The average soil loss (G), that is in tons per hectares per year, is classified here into six categories which are typically for soil conversation measures design in the Czech Republic. These are following:

1. 0–4 $t \cdot ha^{-1} \cdot year^{-1}$
2. 4–8 $t \cdot ha^{-1} \cdot year^{-1}$
3. 8–12 $t \cdot ha^{-1} \cdot year^{-1}$,
4. 12–16 $t \cdot ha^{-1} \cdot year^{-1}$
5. 16–20 $t \cdot ha^{-1} \cdot year^{-1}$
6. 20 and more $t \cdot ha^{-1} \cdot year^{-1}$

Tab. 3 Categories of average soil loss and their percentages.

G [$t \cdot ha^{-1} \cdot year^{-1}$]	Percentage
0–4	9.6
4–8	15.1
8–12	31.5
12–16	23.3
16–20	15.1
20 and more	5.5

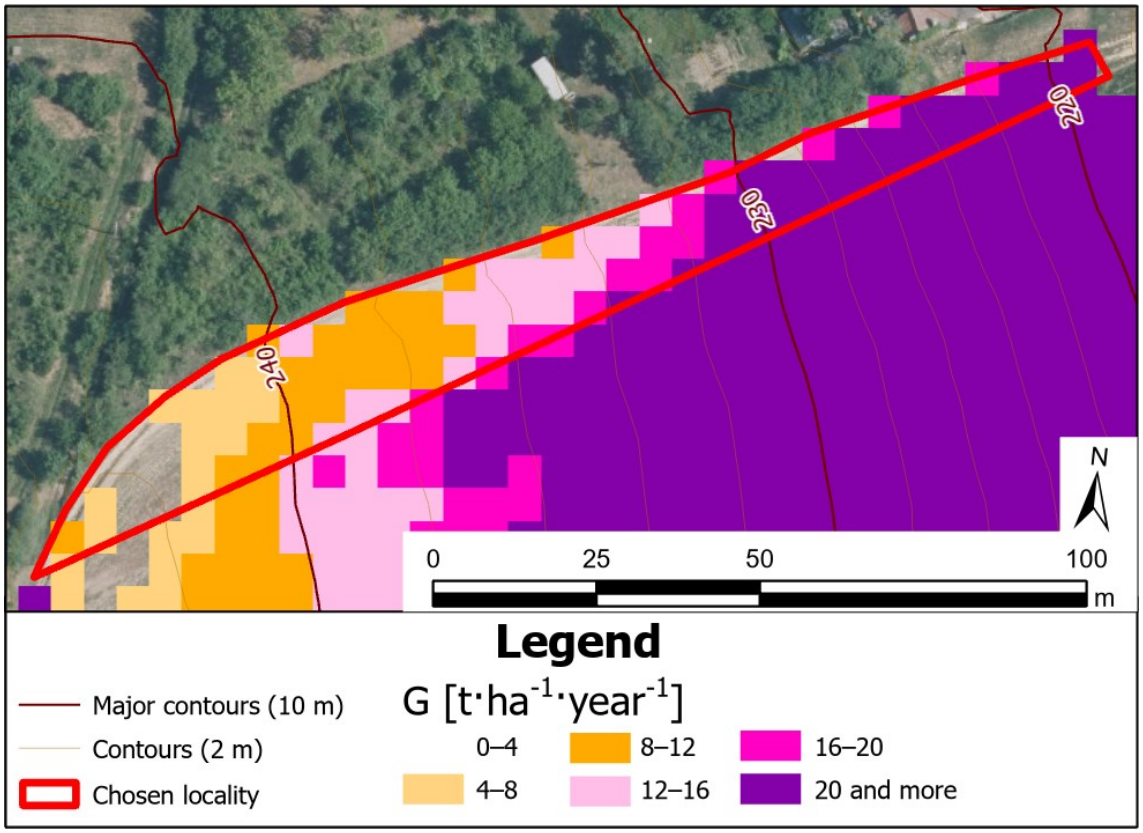

Fig. 7 Average soil loss (G) in tons per hectare per year in the chosen locality

DISCUSSION

The results obtained in the part devoted to the volumetric quantification show that soil loss in the rill is equal to 4.44 m^3. In the locality, the bulk density of the soil is 1.35 $g \cdot cm^{-3}$. Thus, there were eroded six tons of soil.

In the part, which is aimed at soil loss, it is possible to observe that less than 10% of the area fall into category with average soil loss up to four tons per hectare per year. In the Czech Republic, it is considered a permissible soil loss. Approximately 31.5% of the area fall into the category with the average soil loss in range of eight to twelve tons per hectares per year.

It was found that the average soil loss equals 15.61 tons per hectare per year. The area of the locality is 0.23 hectares. Thus, the average soil loss there is equal to 3.59 tons per year.

Regarding similar publications or researches, for instance Sobotková and Dumbrovský [11] dealt with a suitable method for assessment of rill erosion. Their research was primarily aimed at measurement of erosion in the field in municipality Šardice. There were small erosion rills there. The measurement was carried out in two transects in the period from 2007 to 2010. It was discovered that the average soil loss from these transects was in range of 0.060 m^3 (in 2007) to 0.109 m^3 (in 2010). It is understandable

that these values obtained are much lower than in the locality in municipality Otnice. The erosion rill there is large and deep.

CONCLUSION

This paper was primarily aimed at the volumetric quantification of soil erosion using the so-called erosion bridge which was designed and created at the Institute of Landscape Water Management, Faculty of Civil Engineering, Brno University of Technology. For the purposes of the paper, the locality in the municipality Otnice (in the South Moravian Region of the Czech Republic) was chosen. The photos of the terrain there were evaluated with the use of the software program "Erosion bridge" and exported to the DXF files. In AutoCAD, several parameters of the terrain profiles were obtained. These parameters are following: area, wetted perimeter, width, and maximal depth. Finally, the total soil loss in the erosion rill was computed. It was found that there 4.44 cubic meters of soil were eroded.

The paper also dealt with analysis of the locality in terms of erosion conditions. Based on the Universal Soil Loss Equation, the average soil loss was obtained. This soil loss was subsequently classified into six categories.

The results obtained and method used will be the motivation for further scientific research in the field of soil erosion and volumetric quantification of soil loss by water erosion directly in the field.

ACKNOWLEDGEMENTS

This paper is a result of a standard research FAST-S-23-8222 "Modeling and optimalization of rainfall-runoff and erosion processes in the landscape".

REFERENCES

[1] Dumbrovský M., Sobotková V. et al., Cost-effectiveness evaluation of model design variants of broad-base terrace in soil erosion control, Ecological Engineering, vol. 68, 2014, pp 260-269, DOI https://doi.org/10.1016/j.ecoleng.2014.03.082

[2] Sobotková V., Dumbrovský M., Sobotka J., The methods for field assessment of rill erosion in the Czech Republic, Water Resources, Forest, Marine and Ocean Ecosystems, SGEM 2015, vol. II, 2015, pp 371-377, ISBN 978-619-7105-37-7

[3] Ghasemzadeh Z., Parhizkar M., Forest soil inoculation with Bacillus subtilus reduces soil detachment rate to mitigate rill erosion, Rhizosphere, vol. 26, 2023, DOI https://doi.org/10.1016/j.rhisph.2023.100707

[4] Kavka P., Jeřábek J., Landa M., SMODERP2D—Sheet and Rill Runoff Routine Validation at Three Scale Levels, MDPI, Water 2022, vol. 14/issue 3, 2022, DOI https://doi.org/10.3390/w14030327

[5] Jafarpoor A., Sadeghi S. H., Changes in morphologic, hydraulic, and hydrodynamic properties of rill erosion due to surface inoculation of endemic soil cyanobacteria, CATENA, vol. 208, 2022, DOI https://doi.org/10.1016/j.catena.2021.105782

[6] Parhizkar M., Shabanpour M. et al., Rill Erosion and Soil Quality in Forest and Deforested Ecosystems with Different Morphological Characteristics, MDPI, Resources 2020 vol. 9/issue 11, 2020, DOI https://doi.org/10.3390/resources9110129

[7] Di Stefano C., Nicosia A. et al., Rill flow velocity and resistance law: A review, Earth-Science Reviews, vol. 231, 2022, DOI https://doi.org/10.1016/j.earscirev.2022.104092

[8] Dumbrovský M., Drbal K. et al., An approach to identifying and evaluating the potential formation of ephemeral gullies in the conditions of the Czech Republic, Soil and Water Research, vol. 15, pp 38-36, 2020, DOI https://doi.org/10.17221/231/2018-SWR

[9] Dobrovolný L. Development of SW for automatic evaluation of photos from measurements using the erosion bridge, Brno University of Technology, Bachelor's Thesis, 2022.

[10] Wischmeier W. H., Smith D. D., Predicting Rainfall Erosion Losses: A Guide to Conservation Planning, USDA, 1978.

[11] Sobotková V., Dumbrovský M., The new volumetric approach for field measurements of rill erosion, Eurasian Journal of Soil Science, 2015, ISSN 2147-4249

WASTEWATER TREATMENT EFFICIENCY IN VERTICAL FLOW CONSTRUCTED WETLANDS USING RECYCLED AGGREGATES

Ondrej Zednik

Assoc. Prof. Dr Michal Kriska Dunajsky

Institute of Landscape Water Management, Faculty of Civil Engineering, Brno University of Technology, **Czech Republic**

ABSTRACT

The article discusses the efficiency of vertical subsurface flow filters in wastewater treatment wetlands, where the main filtration layer is composed of recycled aggregates. To determine the efficiency of the vertical filter using modified recycled aggregates, three test columns were created. The first column contained natural gravels, while the second and third columns used masonry (RMA) and concrete aggregates (RCA). The test filters were loaded with wastewater from a combined sewer system, with non-dissolved substances removed through sedimentation and filtration. The wastewater was intermittently applied to the filter bodies. During the testing period, the RMA filter column achieved an efficiency of up to 99.9% for NH_4^+–N, 83.9% for COD, and 40.1% for TP. The RCA filter column had an efficiency of 99.6% for NH_4^+–N, 77.2% for COD, and 42.3% for TP. These values are comparable to the efficiencies of filter columns filled with natural aggregates (NA). These results suggest there is a potential for RMA or RCA to replace NA. This would lead to the conservation of natural resources and a reduction in the initial cost of vertical filters.

Keywords: vertical subsurface flow filters, constructed wetlands, filter material, recycled aggregates, semi-operational testing

INTRODUCTION

Constructed treatment wetlands (CW) are a suitable alternative to conventional wastewater treatment methods. Compared to long-established intensive methods, which concentrate treatment processes in small buildings, it is a technology that requires an extensive area. Treatment processes in a large wastewater treatment plant take place over a large area, which is usually required to meet the surface area and volume needs of the filter fields. This is the section of the treatment plant that carries out the main treatment. The filter field complex is preceded by a mechanical pre-treatment stage made up of sedimentation tanks. The complete treatment system can be supplemented by tertiary treatment, which can be, for example, waste stabilization ponds [1]. Extensive technologies target small producers with their advantages, such as a long retention time or the ability to cope with irregular influent volumes. CWs have been successfully applied to municipalities up to 1,000 inhabitants in size, where significant inflow fluctuations can be encountered, both from a hydraulic and organic point of view [2].

Currently, filtration fields used as the main treatment stage are often designed with a vertical wastewater flow. However, it is not uncommon to encounter a combination of

filters, both horizontal and vertical. A vertical filter is made up of several structural layers, or filtration materials, through which there is an intermittent flow of wastewater. These layers are primarily made up of drainage, transition, main treatment, and top layers with thicknesses of 10–20 cm, 10 cm, 50 cm, and 5–20 cm, respectively. Typically, coarse-grained aggregates with particle sizes of 16–32 mm or 8–16 mm are used for the drainage, top, and transition layers. In contrast, the main layer is formed from fine-grained aggregates with a particle size of no more than 0–4 mm [3]. All the NAs that are used do not contain dust particles, meaning they are washed or extracted from aquatic environments. Water is delivered to the filter bed in several daily doses with a time interval of 3–6 hours to ensure the regular aeration of the filtration medium and the creation of aerobic conditions [2]. Water inflow is facilitated by a distribution pipeline, which is laid on the surface of the filter in a regular square grid pattern to ensure even filling of the filtration layers.

A variety of biochemical processes are responsible for the reduction of pollution within the filter body. Organic substances undergo aerobic decomposition in the presence of biogenic elements, microorganisms, and oxygen [4]. On the other hand, nitrogenous compounds are subjected to processes such as nitrification, denitrification, fixation, the influence of plants, dissimilation, assimilation, or ammonification, depending on the prevailing oxygen conditions [5]. Within vertical filters, it is usually possible to observe the progression of nitrification reactions, depending on the availability of oxygen, which diffuses into the filter and is driven by convection [6]. When it comes to phosphorus removal, processes such as sorption, chemical precipitation, and both plant and microbial assimilation may occur [7]. In addition to biochemical reactions, physical processes, such as filtration and sedimentation, also contribute to the reduction of pollution and occur naturally within the porous filter medium [2].

The specific quantity of aggregate required for a vertical filter corresponds to 3.4 tons per equivalent person (PE) [3], this is for a main filtration layer height of 500 mm and a surface area of 4 m^2 per PE. The high consumption of NAs in the construction of vertical filters leads to higher costs in wastewater treatment plant construction. As the amount of non-renewable aggregates diminishes, their price steadily increases. To halt this rise in the initial cost and ensure there will be an adequate supply of non-renewable resources for future generations, it is necessary to explore alternative materials, such as recycled materials created from construction and demolition waste.

Within the Czech Republic, recycled materials made from both brick and concrete can be found, along with combinations of the two. Typically, these materials are manufactured to provide similar particle sizes as NAs, for example, 0–4 mm or 0–5 mm, and they contain a high proportion of particles smaller than 0.063 mm [8]. The low demand for recycled materials without dust particles and limited utilization of the 0–4 mm fractions does not currently create sufficient interest to drive an improvement in the recycling process. Nevertheless, recycled materials prepared abroad, or initial research findings from the Czech Republic, indicate that it is possible to produce RMA and RCA with a dust content of less than 3% [9].

The use of recycled materials for vertical filters is dependent on the initial assessment of grain size requirements and the coefficient of saturated hydraulic conductivity [10]. However, ultimately the usability of these materials is primarily determined by the filter's performance in the removal of the monitored pollution indicators. The fundamental

hypothesis of the contribution revolves around providing an answer to the question of whether a vertical filter with recycled aggregates can achieve similar treatment efficiencies to a filter with NAs.

MATERIALS AND METHODS

To verify treatment efficiency, several test columns were created and subsequently loaded with wastewater. Two recycled materials were evaluated, RMA and RCA. However, to provide a direct comparison of the results, a column filled with NA, commonly used in wastewater filtration, was also prepared.

The recycled materials were obtained from local recycling plants and contained a significant number of particles smaller than 0.063 mm. In the RMA, the dust content was as high as 21.8%, while for RCA, it was 12.0%. Both materials were put through a washing process before use, during which the excess levels of undesirable particles were separated until the values specified in Table 1 were met. The washing process was based on the mechanical agitation of the material under a flow of water [9]. After this treatment, the recycled materials closely resembled the NA 0–4 mm fraction, which was delivered already washed from the sand pit. The treated RMA and RCA were able to meet the maximum dust content criteria, set at 3% [3].

Table 1 Quality of tested materials

Material	d_{10} (mm)	d_{60} (mm)	Uniformity U	Particles < 0.063 mm (%)
RMA	0.30	1.5	3.6	1.5
RCA	0.42	1.8	4.3	0.3
NA	0.25	0.9	3.6	0.6

The hydraulic conductivity of both RMA and RCA was adjusted by washing. The initial values of saturated hydraulic conductivity coefficient (k_s), were 1.8×10^{-5} m s^{-1} for RMA and 1.7×10^{-5} m s^{-1} for RCA. After washing, the coefficient was 2.4×10^{-4} m s^{-1} for RMA and 1.1×10^{-3} m s^{-1} for RCA. The recycled materials under evaluation, and NA, met the hydraulic conductivity requirements for the main filtration layers. No modification of the parameters of NA was required as it had a k_s value of 2.0×10^{-4} m s^{-1} on delivery.

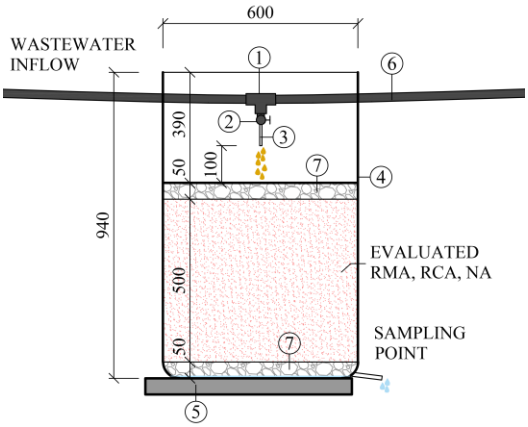

Figure 1 Construction of the filter column

Three test columns made from high-density polyethylene with a diameter of 60 cm and a height of 94 cm (4), were created for testing purposes. Drainage from the column was provided by a drain pipe connection with an inner diameter of 20 mm. The internal space was filled, up to a height of 5 cm, with drainage material (7) prepared from naturally extracted aggregate with a particle size of 4–8 mm. The same aggregate was subsequently used for the top layer (7), which covered the main filtration layer. The columns only differed in the material used for the main filtration layer. One column contained RMA, the second RCA, and the third, the reference column, contained NA with quality parameters as per Table 1. The columns were placed on an extruded polystyrene board (5) to ensure they were on a level surface. The setup of the filtration columns during semi-operational testing is shown in Figure 1.

Wastewater was delivered to the filter columns under test by a sludge pump located in one of the distribution chambers at the municipal WWTP. Polyethylene pipe, with an internal diameter of 25 mm (6), led from the pump to the filtration columns, at the centre of each column a "T" piece (1) was installed along with a valve (2) and silicone hose with a diameter of 5 mm (3). The valve was used as required to adjust the flow rate or hydraulic loading rate (HLR) of the filter under evaluation to simulate different operational conditions.

The semi-operational testing was conducted over a period of 12 weeks. The operational parameters were adjusted every three weeks to assess the influence of increased dosing frequency and HLR. During the first testing period, wastewater was pumped onto the surface of the columns at 3 hour intervals, with an HLR of 123 mm day^{-1}. Over the next three week period, the columns were loaded every 1.5 hours, again with an HLR of 123 mm day^{-1}. The third three week operational period retained a dosing interval of 1.5 hours but increased the loading to 247 mm day^{-1}, surpassing the standard limit of 150 mm day^{-1} (WA-A 262E. 2017)[3]. In the fourth and final three week period, the dosing frequency was maintained at 1.5 hours, but with an HLR of 370 mm day^{-1}, to simulate a significant overload of the columns. The detailed operational settings are listed in Table 2.

Table 2 Operational settings

Week	Loading interval (h)	Doses per day (-)	Duration of single dosing (min)	HLR (mm $dose^{-1}$)	HLR (mm day^{-1})
1-3	3.0	8	2	15.4	123
4-6	1.5	16	1	7.7	123
7-9	1.5	16	2	15.4	247
10-12	1.5	16	3	23.2	370

Throughout the trial, precipitation totals were also recorded and used to adjust the value of HLR for each test period. The maximum weekly precipitation total, 38.9 mm, was recorded in the first week of the trial. Consequently, this increased the HLR by almost 32%. In the other weeks, precipitation did not exceed 18 mm, in most weeks it was below 5 mm, which caused no significant increase in HLR. The weekly precipitation totals are shown in Figure 2.

The columns were loaded using wastewater that arrived at the WWTP, from the village of Dražovice, via a combined sewer system, as per the operational settings listed in Table

2. Prior to loading the test columns, insoluble substances were removed by mechanical pretreatment facilities, including screens, sand traps, and settling tanks. After mechanical filtration, the water passed through a horizontal filter operated in an anaerobic mode. This pre-treated wastewater was subsequently pumped to the individual test columns. The composition of the wastewater used for semi-operational testing is provided in Table 3.

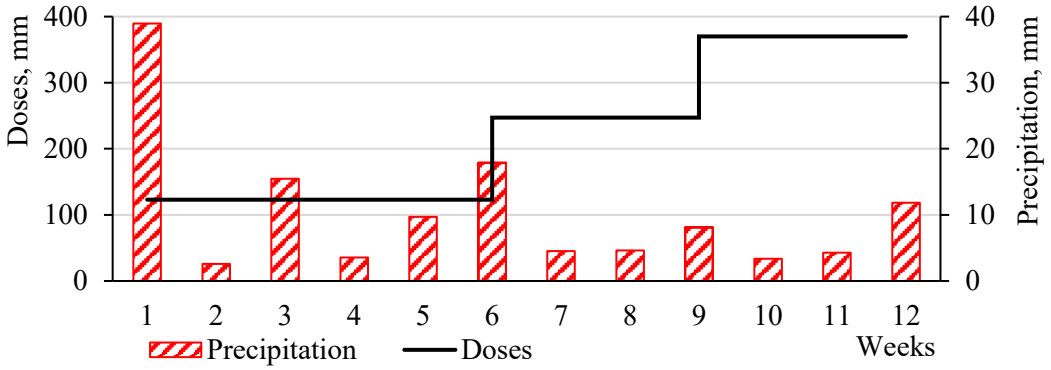

Figure 2 HLR with weekly rainfall totals

Table 3 Influent wastewater quality

Week	COD (mg l^{-1})	NH_4^+-N (mg l^{-1})	NO_3^--N (mg l^{-1})	TP (mg l^{-1})
1–3	102.2±28.7	15.6±2.6	4.8±7.4	2.2±1.2
4–6	110.4±47.6	16.6±5.2	1.1±0.6	2.3±1.3
7–9	153.6±90.2	18.6±4.7	1.3±1.1	2.9±1.5
10–12	107.6±32.7	25.9±4.1	1.0±0.2	4.1±1.6

In the combined sewer system leading to the WWTP, the wastewater was subject to dilution through precipitation. As a consequence, fluctuations in the pollution concentrations were recorded at the inlet of the test columns. Table 3 shows the changes in concentration during different operational periods using average values and standard deviations.

Throughout the trial period, water samples were collected from the inlet and outlet of each column on a weekly basis. After collection, the water was immediately cooled to a temperature of 5 °C and transported to the laboratory for evaluation. Concentrations of NH_4^+-N, NO_3^--N, TP, and COD were subsequently determined using spectrophotometry. A HACH DR 3900 spectrophotometer was utilized for the analyses. The test columns were loaded with wastewater three weeks before the commencement of sampling, and the actual testing took place from April to July, when the water temperature did not fall below 12 °C.

RESULTS

The tests provided a comprehensive view of the development of effluent concentrations in relation to the HLR and changes in daily dosing. The test column with the NA fill achieved the best outflow COD levels during the first three weeks of the trial with an average of 15.4 mg l^{-1}. In terms of COD, the RMA column provided the closest

performance to the NA column and it's best average concentration was recorded in weeks four to six, with a level of 15.6 mg l^{-1}. Conversely, during the same period the RCA column provided a higher average concentration of 22.8 mg l^{-1}. A similar trend was observed for NH_4^+-N, where the lowest average effluent concentration of 0.1 mg l^{-1} was achieved by the RCA column in the second of the three-week trial periods. For the RMA and NA filled columns, the NH_4^+-N remained almost constant. Both materials were capable of producing concentrations close to zero.

Increased effluent concentrations, in comparison with the inflow was measured for NO_3^--N for all the trial filter columns. The lowest average value, 17.1 mg l^{-1}, came from the RCA column during the third test phase. An increase in NO_3^--N concentration after passing through the filtration material is a common occurrence in vertical filters and is an indication of the progress of nitrification reactions. The TP levels in the effluent from the RMA and RCA columns was lower in all of the evaluation periods than that from the NA column. The lowest average effluent value of 1.4 mg l^{-1} was recorded for both the RMA and RCA filled columns in the second three-week period of operation, the fourth to sixth weeks. The development of the effluent concentrations for all the monitored indicators is further documented by the graphs in Figure 3.

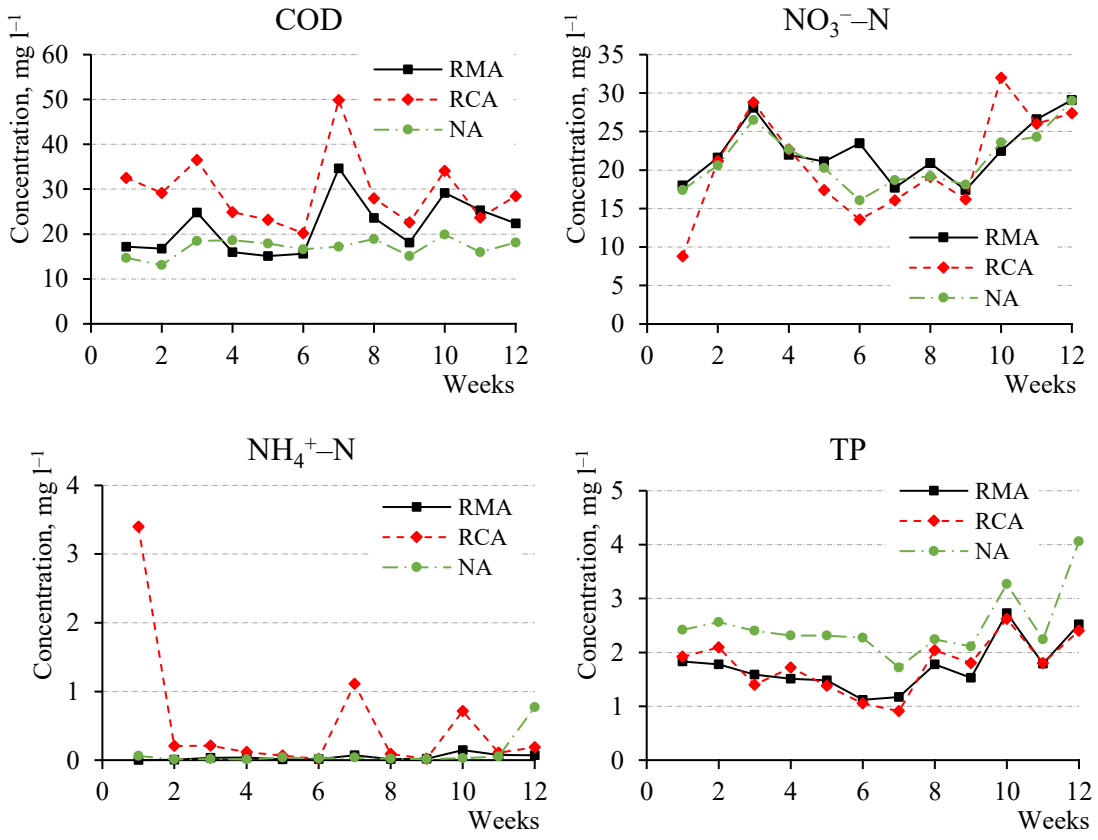

Figure 3 Outflow concentrations

The experimental data shows that the increase in hydraulic loading did not have a significant negative effect on the effluent concentrations of any of the monitored indicators. However, the best results were obtained when the number of daily doses was changed from 8 to 16, while the total HLR remained constant. The initial high effluent concentration of NH_4^+-N at 3.4 mg l^{-1} for the RCA column was the result of a lack of

biofilm development and nitrifying bacteria. Over the following weeks the system stabilized and the effluent concentration only intermittently exceeded 1 mg l^{-1}. The increase in the TP values during the last phase of testing was not a result of a reduction in efficiency (Table 4), but to an increase in the influent concentrations, which were as high as 4.1 mg l^{-1}.

Table 4 Efficiency of the individual materials

Weeks	RMA			RCA			NA		
	COD	NH_4^+-N	TP	COD	NH_4^+-N	TP	COD	NH_4^+-N	TP
1–3	80.4	99.9	0.0	66.4	90.6	2.5	84.3	99.8	0.0
4–6	83.9	99.9	27.0	77.2	99.6	29.1	82.0	99.8	0.0
7–9	81.4	99.8	40.1	76.2	97.1	42.3	86.2	99.9	16.5
10–12	74.4	99.6	40.1	71.9	98.7	41.7	82.4	99.0	21.3

The low concentrations found in the effluent were also reflected in the overall pollution removal efficiency of all the test columns. The RMA and RCA test columns generally had lower levels of efficiency than the NA test column for removal of COD, and in the case of RCA, also for NH_4^+-N. In contrast, higher efficiencies were achieved for the removal of TP, with both the RMA and RCA test columns able to remove up to 40% during the final two three-week test periods.

DISCUSSION

High treatment efficiencies (Table 4) were achieved for both the COD and NH_4^+-N parameters during testing. All the test materials met the limits for effluent required for a WWTP of the size category 500–2000 PE. The effluent COD did not exceed the Czech national limit of 75 mg l^{-1} for either material. Similarly, in the case of NH_4^+-N, all the effluent concentrations were below 12 mg l^{-1} [11]. The requirements of the European Directive, which has set 125 1 mg l^{-1} as the high limit was also met for COD [12].

However, for COD removal the test columns generally achieved lower efficiency levels than vertical filters are normally able to achieve. This could be a consequence of the low concentration of COD in the influent. Most of the easily degradable organic substances had already degraded in the horizontal filter or were deposited in the sedimentation beds. Thus, the residual concentration that loaded the surface of the test columns may only have been composed of more difficult-to-degrade organics. Consequently, the vertical filter environment was not able to provide suitable conditions for the complete degradation of COD to take place. The same phenomenon can be observed for the residual concentrations of effluent from vertical filters used for municipal water treatment.

All the limits set for WWTPs of the size category up to 2000 PE were met, even when the HLR limit was significantly exceeded. Neither the efficiency nor the effluent concentrations were adversely affected by an increase in the number of daily doses, which affects the amount of oxygen delivered to the filter media. In contrast, for RMA and RCA filled columns, the highest efficiencies for COD and NH_4^+-N removal were observed during the period when the dosing frequency was 16 doses per day. The effect of HLR on all the columns was only associated with a decrease in COD efficiency during the final test phase, when the HLR was 370 mm day^{-1}, more than twice the limit reported in other

studies [3]. However, even in this case, the decrease was only 9.5% for RMA and 5.3% for RCA. The efficiency of NH_4^+-N removal was maintained at high HLR levels by all columns. The lower efficiency levels of the RMA and RCA test columns, compared to the NA column, for COD removal could be influenced by the higher degree of granularity of the recycled materials, where a sufficiently long water retention time in the filter body was not achieved, as it was for the NA column. The lower retention time consequently led to the water being in contact with the biofilm for a shorter length of time and a potential reduction in efficiency.

Both the RMA and RCA columns showed higher levels of efficiency for TP removal over almost all of the studied periods. The higher degree of removal, or retention, of phosphorus in the filter media than in the NA column may have been a result of the higher levels of ferrous, aluminous, or calcareous compounds in the recycled materials that reacted with the phosphates in the influent. However, the quantity of these elements in the recycled materials is limited, as is the sorption capacity of NA. For this reason, it is not possible to assume that the long-term removal of TP will be at the level achieved during these tests.

From the test results, it is evident that both RMA and RCA columns can achieve comparable treatment efficiencies to NA columns for the parameters evaluated. However, more attention must be paid to the initial quality and grain composition. RMA and RCA appear to be viable alternatives that can provide both financial and environmental savings, provided that the basic requirements of grain size and hydraulic conductivity are met. However, the results obtained only represent a single initial evaluation, which needs to be supplemented by a number of further tests. In order to accurately describe the biochemical reactions taking place in the filter body, it is necessary to monitor a number of other indicators such as ORP, oxygen saturation, the progress of pollution by height, the influence of effluent through leaching of hazardous substances, pH, freezability of the material, etc. Closer monitoring and evaluation of both RMA and RCA should be the subject of further research.

CONCLUSION

Vertical filters are an indispensable component of extensive WWTPs, mainly due to their potential to create aerobic conditions for subsequent treatment processes. The potential to replace NA as the material used to form the main filter layer with RMA or RCA was verified by testing. Both of the alternative materials achieved comparable results to NA under normal HLR levels and during the subsequent overloads. When compared to NA, they were able to show a higher cleaning efficiency for TP. Thus, their high treatment efficiencies predispose both RMA and RCA for future use. However, careful attention to the grain composition is required in any application. Both materials are generally supplied with a high level of dust particles, which subsequently reduces their hydraulic conductivity. On the other hand, the removal of an excessive amount of the fine-grained components can also have a negative effect, resulting in lower retention times, which was resulted in higher outflow concentrations of COD, as was observed for RCA. The research carried out provides a basic comparison of NA, RCA and RMA in the common operational situations faced by vertical filters. However, this is quite a limited amount of information that needs to be supplemented by a range of further tests and assessments to ensure that the use of these recycled materials is truly safe.

ACKNOWLEDGEMENTS

This article was supported by an internal grant from Brno University of Technology FAST-S-23-8222: Modelling and Optimization of Precipitation-Runoff and Erosion Processes in the Landscape.

REFERENCES

[1] Kadlec R. H., Wallace S. D., Treatment wetlands, United States of America, 2009.

[2] Dotro G. et al., Biological Wastewater Treatment Series: Volume 7: Treatment Wetlands, IWA Publishing, United Kingdom, 2017.

[3] DWA-A 262E, Grundsätze für Bemessung, Bau und Betrieb von Kläranlagen mit bepflanzten und unbepflanzten Filtern zur Reinigung häuslichen und kommunalen Abwassers. Hennef: Deutsche Vereinigung für Wasserwirtschaft, Abwasser und Abfall, Germany, 2017.

[4] Saeed T., Sun G., A review on nitrogen and organics removal mechanisms in subsurface flow constructed wetlands: Dependency on environmental parameters, operating conditions and supporting media, Journal of Environmental Management, vol. 112, pp 429-448, 2012.

[5] Abou-Elela S. I. et al., Municipal wastewater treatment in horizontal and vertical flows constructed wetlands. Ecological Engineering, pp 460-468, 2013.

[6] Platzer C., Design recommendations for subsurface flow constructed wetlands for nitrification and denitrification, Water Science and Technology, vol. 40/issue 3, pp 257-263, 1999.

[7] Ilyas H., Masih I., The effects of different aeration strategies on the performance of constructed wetlands for phosphorus removal, Environmental Science and Pollution Research, vol. 25/issue 6, pp 5318-5335, 2018.

[8] Pavlů T., Zkoušení a vlastnosti recyklovaného kameniva pro použití do betonu, TZB-info, vol. 15/issue 35, 2013.

[9] Zedník O., Kriška Dunajský M., Modification by washing of recycled aggregates from construction and demolition waste for vertical subsurface flow constructed wetlands, International Multidisciplinary Scientific GeoConference Surveying Geology and Mining Ecology Management, vol. 22/issue 42, pp 75-82, 2022.

[10] Langergraber G. et al., Removal efficiency of subsurface vertical flow constructed wetlands for different organic loads, Water Science and Technology, vol. 56/issue 3, pp 75-84, 2007.

[11] Nařízení vlády č. 401/2015 Sb., o ukazatelích a hodnotách přípustného znečištění povrchových vod a odpadních vod, náležitostech povolení k vypouštění odpadních vod do vod povrchových a do kanalizací a o citlivých oblastech, Sbírka zákonů, Czech republic, 2015.

[12] Council Directive 91/271/EEC of 21 May 1991 concerning urban waste-water treatment.

WATER SUSTAINABILITY OPPORTUNITIES ARISING FROM THE SDGs AND THE RECOVERY AND RESILIENCE PLAN

Dipl. Ing. Ivana Majerníková[1]

Assoc. Prof. Dr. Denisa Čiderová[1]

Dipl. Ing. Simona Sakáčová[1]

Dipl. Ing. Jozef Čerňák[1]

[1] University of Economics in Bratislava, **Slovak Republic**

ABSTRACT

Water is one of the basic necessities of life. However, water crises have become more frequent around the world as billions of people continue to suffer from a lack of access to clean water, sanitation and hygiene. Water is a limited resource that has been in growing demand – with the world's population increasing and water-intensive economic development continuing, infrastructure of many countries is not fit to meet accelerating demand. With climate change and its variability fluctuations in rainfall and extreme temperatures occur, causing shorter rain seasons and longer dry periods – making water and its availability more unpredictable. These changes have a serious impact on lives and livelihoods.

Water is essential in all sectors for the production of food, energy, goods, and services. Over the past century, global water consumption has increased at more than twice the rate of population growth. Many water sources are drying up, more polluted, or both.

The European Environment Agency (EEA) defines water stress as a situation where there is not enough water of sufficient quality to meet the needs of the people and of the environment. Lack of water is a relative term, the amount of water that is physically available changes as supply and demand change. Water scarcity intensifies when demand increases and/or when water supply is affected by declining quantity or quality.

Water, energy and food security are key to sustainable long-term economic development and human well-being. The water, energy and food nexus focuses on decision-making in the complex linkages between systems that produce, supply and use goods and resources. The purpose of assessing such linkages is to identify untapped potential of synergies, such as in the case of water- and energy-related measures and the consequent impact of coordinated measures in contrast to uncoordinated measures.

Based on the application of scientific methods in relation to the investigation of sustainability in water resources (the "W" Matrix in the framework of the Water-Energy-Food (WEF) Nexus) on the background of quantitative & qualitative sustainable development and CSR trends, the main aim of our paper is to assess sustainability in water resources in the context of the WEF nexus as well as in the light of the United Nations 2030 Agenda Sustainable Development Goals (SDGs) in order to formulate opportunities arising from the European Union Recovery and Resilience Plans. When documenting quantitative & qualitative sustainable development trends in the context of the WEF Nexus, our paper addressed the United Nations 2030 Agenda (alias *"SDG*

diplomacy") as well as the NextGenerationEU Agenda (alias *"Green Deal diplomacy"*).

Keywords: United Nations 2030 Agenda Sustainable Development Goals (UN SDGs); *CSR-SDG Correspondence Index*; Water-Energy-Food (WEF) Nexus; ICJ *Case Concerning the Gabčíkovo-Nagymaros Project (1997,* ICJ Reports 7*)*; Visegrád (V4) countries.

INTRODUCTION

"In 2022, 2.2 billion people lacked safely managed drinking water. To meet 2030 targets, pace of progress will have to accelerate 6x [with regard to] drinking water."
"1 in 3 people worldwide struggle with moderate to severe food insecurity." [13b], Fig. 2, Fig. 3.

On the one hand, recognition that "ecological interdependence does not respect national boundaries and that issues once considered to be matters of national concern have international implications – at the bilateral, subregional, regional or global levels – that can often only be addressed by international cooperation, including by law and regulation" [14] has contributed to the emergence of international environmental law. On the other hand, economic costs of environmental controls and the number of countries negotiating a treaty mitigate the chances of reaching an agreement.
The 1987 Brundtland Report defining *sustainable development* identified conservation of the resource base; and meeting essential needs for water, energy, and food – *alias* the Water-Energy-Food (WEF) Nexus – among critical objectives conducive to sustainable development. A decade later, in the *Case Concerning the Gabčíkovo-Nagymaros Project* [Gabčíkovo-Nagymaros (Hungary/Slovakia) (1997) ICJ Reports 7], quoted in 14] the International Court of Justice (ICJ) recognised sustainable development as an international legal term. According to the 1977 Treaty Providing for the Construction and Joint Operation of the Gabčíkovo-Nagymaros Barrage System, "Hungary and Czechoslovakia agreed to build the Dunakiliti dam and reservoir, a barrage system including two hydroelectric power stations (one on Czechoslovak territory at Gabčíkovo, and one on Hungarian territory at Nagymaros), and a 25 km bypass canal for diverting the Danube from its original course through a system of locks and then back to its original course". In light of the course of events, diplomatic exchanges and expert negotiations, the ICJ was addressed in July 1993 by Special Agreement "to decide, on the basis of the 1977 Treaty and 'rules and principles of general international law', three questions:

(1) whether Hungary was entitled to suspend and subsequently abandon the works on the project;
(2) whether the Czech and Slovak Federal Republic was entitled to proceed to and put in operation the 'provisional solution'; and
(3) what were the legal effects of the notification on 19 May 1992 of the termination of the 1977 Treaty".

In a nutshell, the ICJ concluded that:

(1) "Hungary's ecological concerns over the project were not sufficient to justify a suspension of works in 1989 on the basis of necessity";

(2) “Czechoslovakia had committed an internationally wrongful act by putting the provisional solution into operation”; and
(3) “it was of 'cardinal importance' that [the ICJ] had found that the 1977 Treaty was still in force and governed the relationship between the parties, although it acknowledged that it could not overlook the factual situation – or the practical possibilities or impossibilities to which it gave rise – in deciding on the legal requirements for the future conduct of the parties. In light of the course of events, the ICJ considered that decisions on the future implementation of the Gabčíkovo-Nagymaros project were, first and foremost, for the parties themselves. The ICJ stressed that in future negotiations between the parties the project’s impact upon, and implications for, the environment, should be a key issue. Evaluation of the environmental risks would need to be undertaken, taking into account current standards.” [14].

Correspondingly, the ICJ ruled that in terms of reparation for the internationally wrongful acts committed by both parties, Hungary as well as Slovakia were under an obligation to settle compensation to the other as specified in **Box 1**.

Box 1 Excerpt from the *Case Concerning the Gabčíkovo-Nagymaros Project* [Gabčíkovo-Nagymaros (Hungary/Slovakia) (1997) ICJ Reports 7]

“Slovakia is … entitled to compensation for the damage suffered by Czechoslovakia as well as by itself as a result of Hungary’s decision to suspend and subsequently abandon the works at Nagymaros and Dunakiliti, as those actions caused the postponement of the putting into operation of the Gabčíkovo power plant, and changes in its mode of operation once in service.
Hungary is entitled to compensation for the damage sustained as a result of the diversion of the Danube, since Czechoslovakia, by putting into operation Variant C, and Slovakia, in maintaining it in service, deprived Hungary of its rightful part in the shared water resources, and exploited those resources essentially for their own benefit.
Given the fact, however, that there have been intersecting wrongs by both Parties, the Court wishes to observe that the issue of compensation could satisfactorily be resolved in the framework of an overall settlement if each of the Parties were to renounce or cancel all financial claims and counter-claims.”

Source: [Gabčíkovo-Nagymaros (Hungary/Slovakia) (1997) ICJ Reports 7, quoted in 14]

The *McGraw-Hill Concise Encyclopedia of Science and Technology* [6] claims that approx. 4000 km^2 of water is withdrawn annually from surface and ground waters, which corresponds with a sixfold increase from the levels withdrawn in 1900 (in contrast with a quadruple rise of population). Agricultural activities are linked to roughly two-thirds of water withdrawals, four-fifths of water consumption, and irrigated cropland doubling globally since 1960. On the one hand, river channels have been subject to adjustments in line with a variety of man-made activities related to irrigation, navigation, or power production; on the other hand, the pace at which a number of ground-water resources was depleted exceeds the rate at which they could be recharged, causing the so-called groundwater overdraft. Overall, water resource development has been of importance for e.g. flood control, agricultural production, industrial just like energy development; all in all, implications for natural hydrologic features, together

with impact in the form of pollution and global climate change are likely to continue to affect the distribution of water. Such linkages bring us to the so-called WEF Nexus Index and its Water pillar, in particular.
Bearing in mind the COVID-19 era between 2019-2022, top scores and bottom scores of the WEF Nexus Index Water pillar correspond with the following intervals in the respective years: between 89.5 (Fiji, rank 1) and 15.8 (Eritrea, rank 173) in 2019; between 88.7 (Fiji, rank 1) and 24.5 (Somalia, rank 173) in 2020; between 85.7 (Colombia, rank 1) and 27.3 (Somalia, rank 166) in 2021; between 81.9 (Malaysia, rank 1) and 28.2 (Somalia, rank 167) in 2022. Trends in the Water pillar in the 2019-2022 period point out convergence among the territories covered, subject to data availability. The Visegrád countries' (*alias* V4: Czechia, Hungary, Poland, the Slovak Republic) 2019-2022 overview is displayed in **Tab. 1**.

Tab. 1 The Water pillar (2019-2022) of the Water-Energy-Food (WEF) Nexus Index from the Visegrád (V4) perspective

Water pillar	CZ	HU	PL	SK
2019 Score	66.8	64.5	60	68.2
2019 Rank	62nd	71st	93rd	49th
2020 Score	66.6	68.2	60.4	69.7
2020 Rank	59th	50th	91st	38th
2021 Score	67.2	65.3	67.7	67.7
2021 Rank	61st	68th	57th	58th
2022 Score	66.3	64.8	67.5	66.1
2022 Rank	53rd	64th	47th	55th

Source: [15]

The score of 68.2 (rank 49) registered by the Slovak Republic in 2019 is the same score of Hungary a year later, just with rank 50 (**Tab. 1**). Next, the identical score of 67.7 for Poland and the Slovak Republic in 2021 reflected in ranks 57 and 58, respectively. Whilst in 2019 Poland recorded the least convenient rank among the V4 countries, the opposite was true in 2022. At a closer look, the WEF Nexus Index Water pillar consists of two sub-pillars: Water access and Water availability, further specified in Part *Materials and Methods*.

Based on the application of scientific methods in relation to the investigation of sustainability in water resources (the "W" Matrix in the framework of the Water-Energy-Food (WEF) Nexus) on the background of quantitative & qualitative sustainable development and CSR trends, the main aim of our paper is to assess sustainability in water resources in the context of the WEF nexus as well as in the light of the United Nations 2030 Agenda Sustainable Development Goals (SDGs) in order to formulate opportunities arising from the European Union Recovery and Resilience Plans [7]. When documenting quantitative & qualitative sustainable development trends in the context of the WEF Nexus, our paper addressed the United Nations 2030 Agenda (alias *"SDG diplomacy"*) as well as the NextGenerationEU Agenda (alias *"Green Deal diplomacy"*).

MATERIALS AND METHODS

"[W]ater is essential for food production but food production can compromise water quality." [4] (for the entire WEF nexus see SDG 2, SDG 6 and SDG 7 in **Fig. 1**)

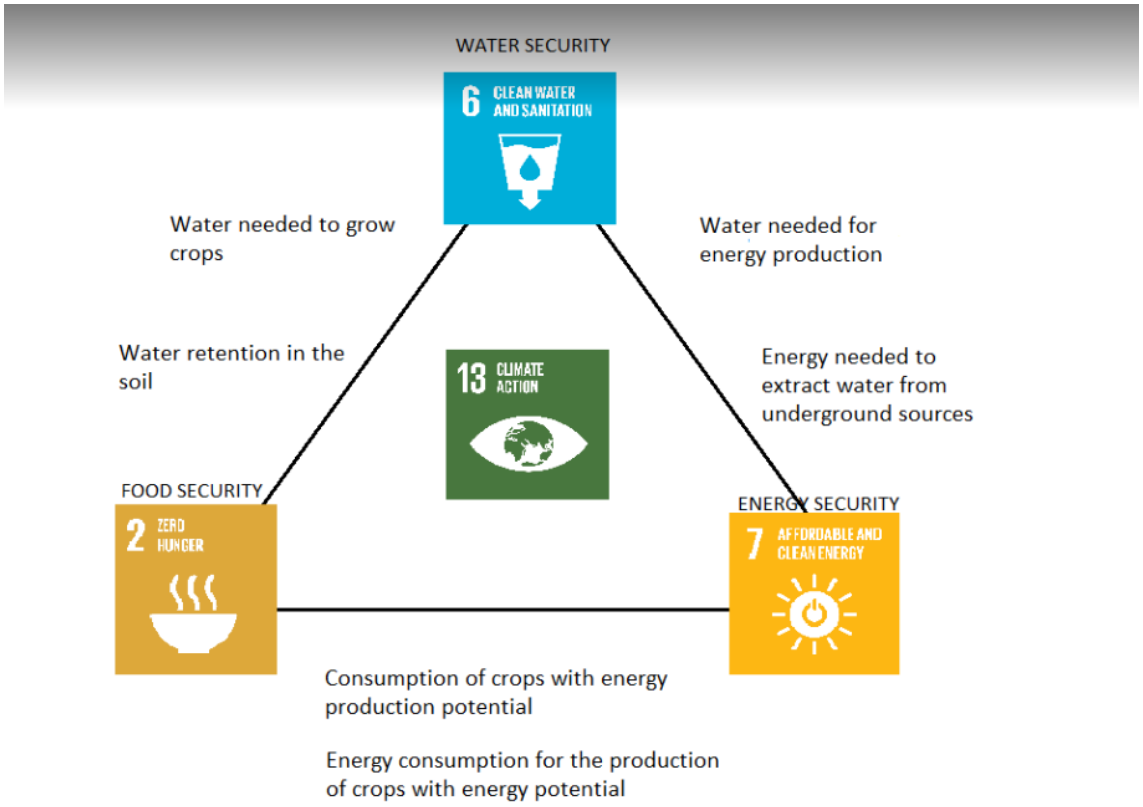

Fig. 1 The Water-Energy-Food (WEF) Nexus in a clockwise constellation
Source: own illustration by authors based on UN SDGs.

The WEF Nexus Index created in response to "a call to move from 'nexus thinking' to 'nexus action'" [15] represents a composite indicator covering 21 relevant indicators measured on the country level across three WEF Nexus pillars of equal weight, with special focus of this paper on its Water pillar (**Tab. 2**).

Tab. 2 Indicators in the Water pillar of the Water-Energy-Food Nexus Index

Water-access sub-pillar indicators:	**Unit**	**Water-availability sub-pillar indicators:**	**Unit**
The percentage of people using at least basic drinking water services	%	Annual freshwater withdrawals, total	% of internal resources
The percentage of people using at least basic sanitation services	%	Renewable internal freshwater resources per capita	m^3
Degree of IWRM implementation	1-100	Environmental flow requirements	10^6 m^3/annum
		Average precipitation in depth	mm/annum

Source: [15]

As highlighted by [15], the WEF Nexus Index "should not be viewed in isolation but as an entry point into the underlying hierarchical dataset. It can also be utilised in parallel with complementary quantitative and qualitative nexus assessments.".

In the form of a cross-impact matrix intended to assess interactions Dzebo & Shawoo [3] addressed in their global analysis existing research gaps "by going beyond regional and sectoral studies of SDG interactions to conduct a global assessment of synergies and trade-offs between key SDG targets from a climate change perspective".

Thus, out of 29 SDG Targets (clustered into 21 categories) on the background of the applicable 5 SDG Targets shortlisted in our paper we consider both the WEF Nexus Index Water pillar (Water-access & Water-availability sub-pillars) [15] and the following SDG targets of the respective matrix [3]:

- SDG Target 2.4 – By 2030, ensure sustainable food production systems and implement resilient agricultural practices that increase productivity and production, that help maintain ecosystems, that strengthen capacity for adaptation to climate change, extreme weather, drought, flooding and other disasters and that progressively improve land and soil quality;
- SDG Target 6.1 – By 2030, achieve universal and equitable access to safe and affordable drinking water for all;
- SDG Target 6.4 – By 2030, substantially increase water-use efficiency across all sectors and ensure sustainable withdrawals and supply of freshwater to address water scarcity and substantially reduce the number of people suffering from water scarcity;
- SDG Target 6.6 – By 2020, protect and restore water-related ecosystems, including mountains, forests, wetlands, rivers, aquifers and lakes;
- SDG Target 14.2 – By 2020, sustainably manage and protect marine and coastal ecosystems to avoid significant adverse impacts, including by strengthening their resilience, and take action for their restoration in order to achieve healthy and productive oceans.

RESULTS

"The European Green Deal (alias "Green Deal diplomacy") is an integral part of the European Commission's "strategy to implement the United Nations 2030 Agenda and the sustainable development goals" (alias ***"SDG diplomacy")****".* [2]

On the basis of a 3-level-impact scale spanning from strong impact to weak impact and vice versa, the respective matrix [3] applied the blue colour to indicate (promoting: "indivisible (+3)"; "reinforcing (+2)"; "enabling (+1)") positive values and the red colour to indicate (restricting: "cancelling (–3)"; "counteracting (–2)"; "constraining (–1)") negative values as shown correspondingly within the "W" Matrix in **Tab. 3**.

Tab. 3 "W" Matrix with reference to SDG Targets 2.4, 6.1, 6.4, 6.6, 14.2

"W" Matrix	2.4	6.4 and 6.1	6.6 and 14.2	Σ out: (down)
2.4	-	Strongly blue "indivisible" (+3)	Moderately blue "reinforcing" (+2)	24
6.4 and 6.1	Moderately blue	-	Weakly blue	18

	"reinforcing" (+2)		"enabling" (+1)	
6.6 and 14.2	Weakly blue "enabling" (+1)		-	2
Σ in: (right)	22	19	12	-

Source: abridged and adapted from [3]

As displayed in **Tab. 3**, the SDG Target 2.4 ranks high in the total score of outward influence, while the combined SDG Targets 6.6 and 14.2 rank low in the 2023 study [3]. The total score of outward influence in the case of the combined SDG Targets 6.6 and 14.2 results from a combination of both "promoting" SDG Targets as well as "restricting" SDG Targets in the WEF context. Among the SDG Target 2.4, the combined SDG Targets 6.4 and 6.1 as well as the combined SDG Targets 6.6 and 14.2 only the "promoting" aspect of these SDG Targets was identified in the 2023 study [3]. In the total score of inward influence the SDG Target 2.4 stands at nearly a double of the combined SDG Targets 6.6 and 14.2; still, all of the SDG Targets identified are characterised by a combination of both "promoting" SDG Targets as well as "restricting" SDG Targets in the WEF context. The 2023 study [3] classified the influence between the combined SDG Targets 6.4 and 6.1 on the one hand, and the combined SDG Targets 6.6 and 14.2 on the other hand, in terms of mutual outward/inward influence as (0), i.e. neither "promoting" (on the positive scale), nor "restricting" (on the negative scale). A spectrum of purely "promoting" linkages is exposed in **Tab. 4**.

Tab. 4 "W" Matrix with reference to SDG Targets 2.4, 6.1, 6.4, 6.6, 14.2 in terms of WEF outward & WEF inward influence

SDG Target	WEF outward ("pull") influence Σ		SDG Target	WEF inward ("push") influence Σ
2.4	24	>	2.4	22
6.1 and 6.4	18	<	6.1 and 6.4	19
6.6 and 14.2	2	<	6.6 and 14.2	12

Source: based on [3]

On the whole (**Tab. 4**), the outward influence in the WEF context of the SDG Target 2.4 is above its inward influence in the WEF context, whereas the opposite relates to the combined SDG Targets 6.4 and 6.1 just like the combined SDG Targets 6.6 and 14.2 in the respective "W" Matrix.

The 17 SDGs of the United Nations 2030 Agenda are at their mid-point in 2023; thus, the time period since 2015 can be considered in two four-year intervals: the pre-COVID (2015-2018) and the COVID (2019-2022) time interval. In **Tab. 5** we show the opening and the closing years of both four-year intervals for the four Visegrád countries based on data attached to the *Sustainable Development Report 2023*, with coverage of the overall SDG Score and the respective particular SDG Score for SDG 2, SDG 6 and SDG 14.

Tab. 5 Overall SDG Score and particular SDG 2, SDG 6 and SDG 14 scores for individual Visegrád countries (pre-COVID interval & COVID interval)

Overall SDG Score	Year	CZ	HU	PL	SK
17 SDGs	2015	80.3	78.0	79.0	78.0
	2018	80.9	78.9	80.2	78.7
	2019	81.1	79.1	80.9	79.1
	2022	81.9	79.4	81.8	79.1
Particular SDG Score	Interval	CZ	HU	PL	SK
SDG 2	Pre-COVID interval (2015-2018)	60.4 – 63.1	70.2 – 73.2	65.3 – 67.8	69.6 – 74.4
	COVID interval (2019-2022)	61.2 – 62.1	70.3 – 71.7	65.8 – 67.7	71.2 – 72.6
SDG 6	Pre-COVID interval (2015-2018)	84.0 – 84.1	86.6	82.7 – 83.8	81.8
	COVID interval (2019-2022)	82.9	86.6	84.4	81.8
SDG 14	Pre-COVID interval (2015-2018)	n.a.	n.a.	67.7 – 70.7	n.a.
	COVID interval (2019-2022)	n.a.	n.a.	72.1 – 72.9	n.a.

Legend: CZ – Czechia; HU – Hungary; PL – Poland; SK – Slovak Republic.
Source: [5; 8; 9; 12; 13a]

The overall SDG Score of the V4 countries indicates a great degree of convergence. A closer look at SDG 2 and SDG 6 applicable to all four Visegrád countries points out score in the interval below 70 in the case of Czechia & Poland in the case of SDG 2; in the interval over 70 in the case of Hungary & the Slovak Republic; and in the interval over 80 in the case of all four Visegrád countries. SDG 14 does not relate to Czechia, Hungary, and the Slovak Republic as landlocked countries.

DISCUSSION

"Europe needs integrated and coordinated interventions in economic, financial, political, and social systems, and along whole value chains, in order to identify an innovative new structure that will be resilient and sustainable. The EGD, the SDGs, and the Paris Agreement are the blueprints to achieve this system innovation." [11b]

In the course of the EU's Lisbon Strategy (2000 – 2010), the Europe 2020 Strategy (2010 – 2020) and the European Green Deal (EGD, since 2019) the so-called European Semester and its Country-Specific Recommendations (CSRs) have been in place to foster co-ordination and convergence among EU member states. Similarly, just like the

Millennium Development Goals (MDGs) have been transformed into the United Nations 2030 Agenda SDGs, their incorporation into EU policy-making can be tracked by means of the so-called *CSR-SDG Correspondence Index*.

All of 17 SDGs mapped across 27 EU member states represent the total of 459 assessments documenting the degree of their achievement. With the exception of 5 missing assessments because of unavailable information, in 45 cases individual SDGs have been already achieved, and 166 challenges remained. Additionally, 84 major challenges and 159 significant challenges (i.e. combined in the total of 243 major or significant challenges) were identified by the respective report [11b] among the 17 SDGs. In summary, 321 out of 459 assessments addressed by CSRs correspond with "an efficiency ratio estimate of 70%, meaning that currently the European Semester Process can capture approximately 7 out of 10 weaknesses identified by the Sustainable Development Report" [11b]. The respective *CSR-SDG Correspondence Index* is even higher in the case of the V4 countries in **Tab. 6-10** below.

Tab. 6 *CSR-SDG Correspondence Index* (major or significant SDG challenges) for the V4 countries

	Total Significant and Major Challenges	Not addressed by CSR	Addressed by CSR	*CSR-SDG Correspondence Index*
CZ	9	2	7	78%
HU	10		10	100%
PL	10	2	8	80%
SK	10	1	9	90%

Source: abridged and adapted from [11b]

Achievement of SDG 6 in Czechia (**Tab. 7**) did not necessitate any CSR reference. In the case of Czechia, out of SDG 2, SDG 6 and SDG 14 only SDG 2 (ranked among bottom-5 according to the SDSN INDEX Dashboard for 2020) was addressed by CSRs (2022).

Tab. 7 Assessment and trends of SDG 2, SDG 6 and SDG 14 in Czechia relevant to CSRs

SDG	SDG (CZ)	SDG assessment (CZ)	SDG trend (CZ)	Trend assessment (CZ)	Addressed by CSRs (CZ)	SDG (CZ)
	SDR2020	SDR2020	SDR2020	SDR2020	SDSN2021	SDR2021
SDG 2		Significant challenges		Moderately improving	NO	
SDG 6		Achieved		On track or maintaining SDG trend	Not required	
SDG 14		Information unavailable		Information unavailable	NO	

Source: [10; 11a; 11b]

In the case of Hungary (**Tab. 8**), SDG 2 (ranked among bottom-5 according to the SDSN INDEX Dashboard for 2020) together with SDG 6 were addressed by CSRs (2019-2020 & 2022).

Tab. 8 Assessment and trends of SDG 2, SDG 6 and SDG 14 in Hungary relevant to CSRs

SDG	SDG (HU)	SDG assessment (HU)	SDG trend (HU)	Trend assessment (HU)	Addressed by CSRs (HU)	SDG (HU)
	SDR2020	SDR2020	SDR2020	SDR2020	SDSN2021	SDR2021
SDG 2		Major challenges		Stagnating	YES	
SDG 6		Challenges remain		On track or maintaining SDG trend	YES	
SDG 14		Information unavailable		Information unavailable	YES	

Source: [10; 11a; 11b]

Although SDG 2 and SDG 14 ranked among bottom-5 according to the SDSN INDEX Dashboard for 2020 in the case of Poland (**Tab. 9**), only SDG 2 was addressed by CSRs (2020 & 2022).

Tab. 9 Assessment and trends of SDG 2, SDG 6 and SDG 14 in Poland relevant to CSRs

SDG	SDG (PL)	SDG assessment (PL)	SDG trend (PL)	Trend assessment (PL)	Addressed by CSRs (PL)	SDG (PL)
	SDR2020	SDR2020	SDR2020	SDR2020	SDSN2021	SDR2021
SDG 2		Significant challenges		Moderately improving	NO	
SDG 6		Challenges remain		On track or maintaining SDG trend	NO	
SDG 14		Major challenges		Moderately improving	NO	

Source: [10; 11a; 11b]

In the case of the Slovak Republic (**Tab. 10**), SDG 2 (ranked among bottom-5 according to the SDSN INDEX Dashboard for 2020) together with SDG 6 were addressed by CSRs (SDG 2: 2019-2020; SDG 6: 2020).

Tab. 10 Assessment and trends of SDG 2, SDG 6 and SDG 14 in the Slovak Republic relevant to CSRs

SDG	SDG (SK)	SDG assessment (SK)	SDG trend (SK)	Trend assessment (SK)	Addressed by CSRs (SK)	SDG (SK)
	SDR2020	SDR2020	SDR2020	SDR2020	SDSN2021	SDR2021
SDG 2		Major challenges		Stagnating	NO	
SDG 6		Challenges remain		Moderately improving	NO	
SDG 14		Information unavailable		Information unavailable	NO	

Source: [10; 11a; 11b]

CONCLUSION

"Many of the proposed measures in the field of green transition are aimed at improving outdated energy infrastructure and energy efficiency, particularly in the residential sector. The national recovery plans typically foresee measures such as investing in water and waste management, inter alia by liquidating illegal landfills, recycling infrastructure, water retention measures and support of biodiversity, renewable energy investments, promoting residential solar panels, replacement of coal-fired burners, integrating renewable electricity production by directly connecting the new photovoltaic parks, investing in innovative decarbonisation technologies in industry, modernisation of district heating distribution networks, increasing the number of smart meters, and implementing electricity-based residential heating systems." [1].

Progress of the V4 countries towards the SDGs in the last 5 years may be summarised as follows:

- CZSDG2, SKSDG2, SKSDG6 have been progressing towards SDG achievement and their status is better than across the EU;
- CZSDG6 has been progressing towards SDG achievement;
- HUSDG2 has been progressing towards SDG achievement, but its status is worse than across the EU;
- PLSDG14 has been moving away from SDG achievement;
- PLSDG2 and PLSDG6 have been moving away from SDGs and their status is worse than across the EU.

Having assessed the 2019-2022 CSRs, the European Commission concluded that at the respective stage of NextGenerationEU implementation of Recovery and Resilience Plans, CSRs on structural issues related to the COVID-19 (2019-2022) interval have registered:

- up to 36% at least 'some progress' & up to 64% 'limited progress' in Czechia;
- up to 20% at least 'some progress' & up to 68% 'limited progress' in Hungary;
- up to 33% at least 'some progress' & up to 50% 'limited progress' in Poland;
- up to 51% at least 'some progress' & up to 44% 'limited progress' in the Slovak Republic.

In view of this, emphasis on priorities (P) in terms of policy focus relates to:

- P4 (Clean Energy), P5 (Sustainable Industry), P6 (Building and Renovation), P8 (Elimination of Pollution), and P9 (Climate Action), followed by P2 (From Farm to Fork), P3 (Sustainable Agriculture) and P1 (Biodiversity) in Czechia;
- P2 (From Farm to Fork), P4 (Clean Energy), P5 (Sustainable Industry), P8 (Elimination of Pollution), and P9 (Climate Action), followed by P3 (Good health & Well-Being) and P6 (Building and Renovation) in Hungary;
- P1 (Biodiversity), P2 (From Farm to Fork), P4 (Clean Energy), P5 (Sustainable Industry), P6 (Building and Renovation), P8 (Elimination of Pollution), and P9 (Climate Action) in Poland;
- P2 (From Farm to Fork), P4 (Clean Energy), P5 (Sustainable Industry), P8 (Elimination of Pollution), and P9 (Climate Action), followed by P6 (Building and Renovation) in the Slovak Republic.

ACKNOWLEDGEMENTS

The authors would like to thank the research projects: "Nová vízia ekonomickej diplomacie SR ako nástroja proexportnej politiky do roku 2023 / New vision of economic diplomacy of the Slovak Republic as a tool of export promotion until 2023" funded by the Foundation of the Ministry of Economy of the Slovak Republic (July 2021 – July 2022); and KEGA project No. 003EU-4-2022 for providing their support.

REFERENCES

[1] Astrov, V., Stehrer, R., Zavarská, Z., Recovery and Resilience Facility funding in the Visegrád countries and its impact on Austria, Policy Notes and Reports, No. 56, The Vienna Institute for International Economic Studies (wiiw), Austria, 2022.

[2] Čerňák, J., Čiderová, D., Benashvili, G., Sustainable Economic Development From Global Perspective: Transregional European Union Economic Diplomacy and "Green Deal Diplomacy". In SGEM 2022: 22nd International Multidisciplinary Scientific GeoConference, pp. 205-214, 2022.

[3] Dzebo, A., Shawoo, Z., Sustainable Development Goal interactions through a climate lens: a global analysis, Stockholm Environment Institute, Sweden, 2023.

[4] Holmatov, B., Lautze, J., Uhlenbrook, S., The nexus across water, energy and food (WEF): Learning from research, building on evidence, strengthening practice. Natural Resources Forum, 47(4), pp 817–841, 2023.

[5] Kroll, Ch., Sustainable Development Goals: Are the rich countries ready?, SDSN, Bertelsmann Stiftung, 2015.

[6] McGraw-Hill Concise Encyclopedia of Science and Technology, 5th ed., McGraw-Hill, USA, 2005.

[7] Official website of the European Union (https://european-union.europa.eu/index_en) and of its European Commission, Country Pages, https://commission.europa.eu/business-economy-euro/economic-recovery/recovery-and-resilience-facility/country-pages_en, Belgium.

[8] Sachs, J., Schmidt-Traub, G., Kroll, C., Lafortune, G., Fuller, G., SDG Index and Dashboards Report 2018, Bertelsmann Stiftung and SDSN, USA, 2018.

[9] Sachs, J., Schmidt-Traub, G., Kroll, C., Lafortune, G., Fuller, G., Sustainable Development Report 2019, Bertelsmann Stiftung and SDSN, USA, 2019.

[10] Sachs, J., Schmidt-Traub, G., Kroll, C., Lafortune, G., Fuller, G., Woelm, F., The Sustainable Development Goals and COVID-19. Sustainable Development Report 2020, Cambridge University Press, United Kingdom of Great Britain and Northern Ireland, 2020.

[11a] Sachs, J., Kroll, C., Lafortune, G., Fuller, G., Woelm, F., The Decade of Action for the Sustainable Development Goals: Sustainable Development Report 2021, Cambridge University Press, United Kingdom of Great Britain and Northern Ireland, 2021.

[11b] SDSN. Transformations for the Joint Implementation of Agenda 2030 for Sustainable Development and the European Green Deal – A Green and Digital, Job-Based and Inclusive Recovery from the COVID-19 Pandemic, 2021.

[12] Sachs, J., Lafortune, G., Kroll, Ch., Fuller, G., Woelm, F., From Crisis to Sustainable Development: the SDGs as Roadmap to 2030 and Beyond. Sustainable Development Report 2022, Bertelsmann Stiftung, SDSN, Cambridge University Press, United Kingdom of Great Britain and Northern Ireland and USA, 2022.

[13a] Sachs, J. D., Lafortune, G., Fuller, G., Drumm, E., Implementing the SDG Stimulus. Sustainable Development Report 2023, SDSN, Dublin University Press, France and Ireland, 2023.

[13b] United Nations, The Sustainable Development Goals Report 2023 – Special Edition, USA, 2023.

[14] Sands, Ph., Peel, J., Fabra, A., MacKenzie, R., Principles of International Environmental Law, 4th ed., Cambridge University Press, United Kingdom of Great Britain and Northern Ireland, 2018.

[15] Simpson, G. B., Jewitt, G. P. W., Becker, W., Badenhorst, J., Masia, S., Neves, A. R., Rovira, P., Pascual, V., The Water-Energy-Food Nexus Index: A Tool to Support Integrated Resource Planning, Management and Security. Front. Water 4(825854), 2022. Retrieved from: https://www.wefnexusindex.org

ANNEX

Fig. 2 Status quo of SDG 6 on the global level (2023) Source: [13b]

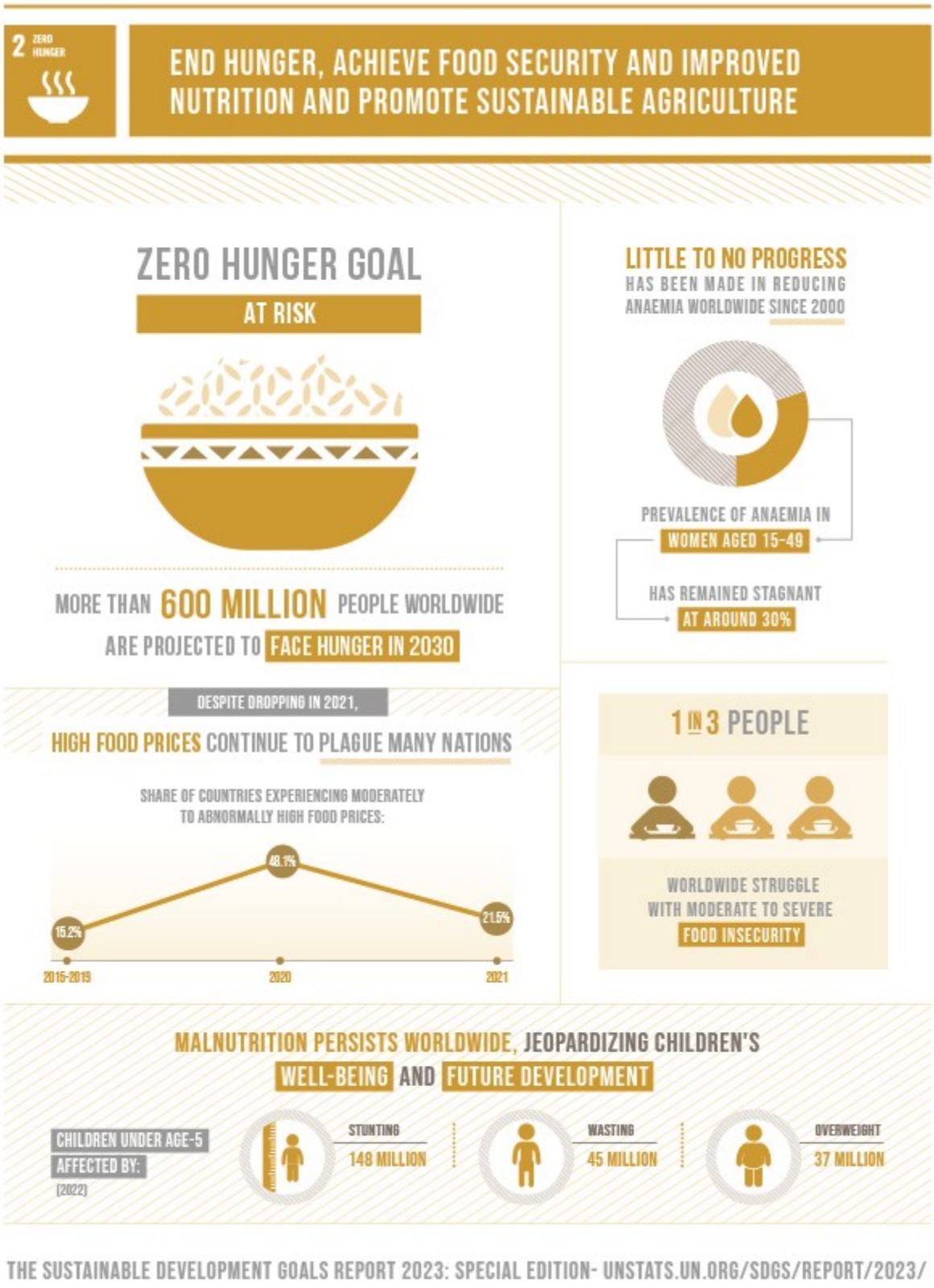

Fig. 3 Status quo of SDG 2 on the global level (2023) Source: [13b]

SECTION

OIL AND GAS EXPLORATION

ICE MODELS FOR ARCTIC OFFSHORE STRUCTURES

Assoc. Prof. Dr. Dmitry Sharapov[1]

[1] Peter the Great St.Petersburg Polytechnic University, **Russia**

ABSTRACT

The Arctic region's extreme climatic conditions, characterized by freezing temperatures, sea ice, and challenging weather patterns, present formidable challenges for offshore structures. These structures, vital for energy exploration, transportation, and scientific research, encounter significant difficulties due to the dynamic and unpredictable nature of ice loads. The article provides an overview of the impact of ice loads on offshore structures in the Arctic, focusing on engineering challenges, technological advancements, and environmental considerations. Ice loads exert immense pressure on offshore structures, posing threats to their integrity and stability. Understanding the complexities of ice behavior, such as thickness variations, ice movements, and load dynamics, is critical for accurately predicting and mitigating ice-induced stresses. Engineering solutions involve specialized design considerations, including robust structural configurations, innovative materials, and mitigation strategies to withstand the diverse forces exerted by ice. Advanced numerical modeling, physical testing, and field observations contribute to a deeper comprehension of ice-structure interactions, aiding in the development of predictive models and guidelines for safer and more resilient offshore installations. However, the unpredictability of ice behavior and the need for continuous improvements in design and operational practices remain ongoing challenges. Balancing industrial progress with environmental sustainability in the Arctic requires stringent regulations, environmental impact assessments, and a commitment to ecologically responsible practices.

Keywords: Arctic, Offshore Structures, Ice Loads, Ice-Structure Interaction, Numerical Modeling, Sustainability, Risk Mitigation

INTRODUCTION

The Arctic region, with its extreme climate and unique environmental conditions, poses significant challenges for offshore industries and infrastructure. As the effects of climate change continue to transform this pristine but fragile ecosystem, the exploration and development of its vast resources have gained increasing attention. However, the formidable presence of ice, with its dynamic and unpredictable nature, creates substantial hurdles for the design, construction, and operation of offshore structures in these remote and harsh environments. The Arctic, characterized by its frigid temperatures, extensive sea ice, and permafrost, encompasses a complex ecosystem that is highly sensitive to environmental changes. The region's Arctic Ocean is covered by ice for a significant portion of the year, with seasonal fluctuations in ice extent and thickness. These conditions, coupled with extreme cold, harsh storms, and limited daylight, create a challenging setting for any industrial activity, especially for offshore installations. Offshore structures play a pivotal role in supporting various industries

operating in the Arctic, primarily focusing on oil and gas exploration, transportation, and scientific research [1-6]. Calculation of ice loads on such structures is complicated. Special norms for ice loads on Arctic offshore structures were developed [7]. These structures serve as drilling platforms, production facilities, and logistical hubs for extracting and transporting hydrocarbons from the region's vast reserves. Additionally, they facilitate scientific endeavors, providing platforms for research and environmental monitoring crucial for understanding climate change impacts in the Arctic. Ice loads, stemming from various forms of ice interaction including pressure ridges, drifting icebergs, and pack ice, pose substantial challenges for offshore structures. Ice loads can exert immense pressure on these installations, leading to structural deformation, damage, and potential failure. The dynamic nature of ice movements and the unpredictability of ice-related phenomena make it inherently challenging to accurately predict and design structures capable of withstanding these forces. Designing offshore structures capable of enduring ice loads requires specialized engineering approaches [8-12]. Engineers must consider various factors such as ice characteristics (thickness, strength, and behavior), environmental conditions, structural integrity, and safety protocols. Innovations in materials, construction techniques, and mitigation strategies are continually sought to improve the resilience of these structures against ice-induced stresses. Advancements in research and technology have played a crucial role in addressing the challenges posed by ice loads on offshore structures. Numerical modeling, physical experiments, and field observations contribute to a deeper understanding of ice-structure interactions, aiding in the development of more accurate predictive models and design guidelines. Ongoing research efforts focus on improving material resilience, enhancing structural designs, and devising efficient operational strategies to mitigate the impact of ice loads [13-15]. The fragility of the Arctic ecosystem necessitates a delicate balance between industrial activities and environmental preservation. The potential risks associated with offshore operations, including oil spills and disturbances to marine ecosystems, underscore the importance of stringent regulations, environmental impact assessments, and sustainable practices to ensure the protection of this sensitive region.

MATERIALS AND METHODS

The vast energy resources and increasing economic opportunities in Arctic region have led to a surge in interest in offshore structures (figure 1). The Arctic poses unique challenges owing to its extreme climate characterized by sub-zero temperatures, ice formation, permafrost, and harsh weather conditions. The presence of icebergs and sea ice, along with the potential for ice loading, presents formidable challenges for offshore operations. Structures in the Arctic must withstand these dynamic and severe conditions, necessitating specialized design and engineering approaches.

Offshore structures are crucial for energy exploration and resource extraction in the Arctic. They facilitate the drilling of oil and gas wells in offshore locations, enabling access to the region's abundant hydrocarbon reserves. However, these structures must contend with ice loads, ice scouring, and the risk of icebergs, demanding robust design strategies and materials capable of enduring extreme conditions.

Offshore structures in the Arctic also serve as essential hubs for transportation and logistics. They support the transfer of extracted resources, enabling their transportation

through ice-covered waters. These structures play a pivotal role in facilitating the movement of goods and materials, as well as providing docking and mooring facilities for vessels navigating in icy conditions.

Fig. 1. Arctic offshore platform Prirazlomnaya

Beyond resource extraction, offshore structures serve as platforms for scientific research and environmental monitoring in the Arctic. These platforms host various scientific instruments and sensors that collect data crucial for understanding the region's changing climate, ecosystem dynamics, and environmental impact assessment. They offer unique vantage points for studying marine life, ice formation, and other ecological processes.

Ice loads present significant challenges for offshore structures operating in Arctic and cold-temperate regions. These structures face several problems due to the impact of ice loads:

- Ice loads exert immense pressure on offshore structures. The impact can lead to structural damage or even failure, compromising the stability and integrity of the platforms. The force exerted by moving ice masses can cause bending, deformation, or buckling of the structure's components, potentially leading to catastrophic consequences.
- Continuous exposure to cyclic loading from ice can induce fatigue in the materials of the structure. This repetitive stress can weaken the structural components over time, leading to cracks, fractures, or material degradation. Such weaknesses can compromise the overall strength and safety of the offshore platforms.
- Ice loads are not static; they fluctuate due to various factors such as changes in ice thickness, drift, and collisions. These dynamic forces induce vibrations and impacts on the structure, potentially causing resonance issues or amplification of stress. Prolonged exposure to these dynamic loads can accelerate wear and tear on the structure's elements.
- Offshore structures face the risk of direct impact from moving ice sheets or icebergs. The collision of these massive ice masses with the platforms can result in significant damage, including crushing or puncturing of the structural components. The

localized impact forces can exceed the design capacity of the structure, leading to severe structural damage.

- Ice loads can interrupt regular operations of offshore structures. Accumulation of ice around the platforms or on critical components such as support structures, risers, or pipelines can hinder access, maintenance, or transportation, leading to operational disruptions and increased downtime.
- The harsh conditions and frequent exposure to ice loads necessitate extensive maintenance and repair activities on offshore structures. Repairing damages caused by ice loads requires specialized techniques and materials, which often result in elevated operational costs.

Addressing these problems requires advanced engineering designs, materials, and operational strategies specifically tailored to withstand ice loads. Incorporating innovative technologies, such as ice-resistant materials, de-icing systems, and dynamic positioning, plays a crucial role in enhancing the resilience of offshore structures in ice-prone environments. Additionally, ongoing research and development efforts focus on improving predictive models and methodologies to better understand and mitigate the impact of ice loads on these structures. Calculating ice loads on offshore structures involves a comprehensive understanding of ice mechanics, environmental conditions, and structural response. Several methods and approaches are used to estimate and calculate ice loads on these structures:

Empirical formulations are based on historical data and observations. These formulas typically relate ice load to ice thickness, velocity, and other relevant environmental factors. They provide a simplified estimation of ice loads but may lack accuracy due to variations in ice behavior and environmental conditions.

Physical model tests involve creating scaled-down models of offshore structures and subjecting them to simulated ice loading conditions in laboratory settings. These experiments provide valuable data to understand how different ice conditions affect structures and help in calibrating and validating numerical models.

Numerical modeling utilizes mathematical and computational simulations to predict ice loads. Finite Element Analysis (FEA) and Computational Fluid Dynamics (CFD) methods are commonly employed. These models consider factors such as ice properties, structural geometry, ice-structure interaction, and environmental conditions to estimate ice loads on different parts of the structure.

Understanding the mechanical behavior and rheology of ice is crucial for accurately predicting ice loads. Models incorporating ice properties like strength, density, thermal conductivity, and deformation characteristics under various loading conditions aid in determining the forces exerted by ice on structures.

Given the variability and uncertainties in ice conditions, probabilistic approaches assess the probability of extreme ice loads. Statistical methods and data analysis techniques help in estimating the likelihood of different ice load scenarios, considering variations in environmental parameters.

Installing instrumentation on existing structures or in ice-covered regions provides real-time data on ice loads. These measurements help validate models and improve

understanding of local ice conditions, contributing to more accurate predictions and risk assessments.

Combining multiple methods and approaches often yields more reliable estimations of ice loads on offshore structures. However, due to the complex nature of ice-structure interaction and environmental variability, predicting ice loads with absolute precision remains a challenging task. Therefore, a multidisciplinary approach integrating theoretical models, empirical data, and field observations is typically adopted to ensure offshore structures are designed and operated safely in ice-prone environments.

Ice models used in numerical calculations offer several advantages in estimating ice loads on offshore structures:

Ice models provide a more accurate representation of ice behavior and interaction with structures compared to empirical methods. They consider various factors such as ice thickness, geometry, rheology, and structural properties, leading to a more precise estimation of ice loads.

Numerical ice models offer flexibility in simulating different ice conditions and structural configurations. They can be adjusted to account for variations in ice properties, environmental parameters, and complex geometries of offshore structures, allowing for versatile and adaptable simulations.

These models enable a deeper understanding of the interaction between ice and offshore structures. By simulating the dynamic response of ice impacting the structure, they provide insights into load distribution, stress concentration areas, and potential failure points, aiding in optimizing structural design and safety measures.

Numerical ice models can simulate extreme ice loading scenarios, including ice ridge collisions, ice jams, and ice-induced vibrations. By predicting these extreme conditions, they help in assessing the structural integrity and resilience of offshore installations under severe ice loads.

While physical model tests can be expensive and time-consuming, numerical ice models offer a cost-effective and efficient alternative. They allow for multiple simulations and parametric studies at a fraction of the cost and time required for physical experiments, facilitating a more extensive exploration of design options.

Ice models can be validated and calibrated using available field data or physical model test results. This process enhances the reliability and accuracy of the numerical predictions by ensuring that the model accurately represents real-world ice-structure interactions.

These models assist in risk assessment by quantifying the probabilities associated with different ice load scenarios. They enable engineers to identify potential risks and vulnerabilities in offshore structures, facilitating the development of appropriate mitigation strategies to enhance safety and reliability.

Several ice models are employed for calculating ice loads on offshore structures, each with its specific focus, assumptions, and applicability.

Finite Element Models simulates the ice-structure interaction by discretizing the structure and ice into finite elements and solving mathematical equations describing

their behavior. It provides detailed stress and deformation analysis, allowing for the assessment of localized responses and potential failure points.

Discrete Element Models models ice as a collection of discrete elements or particles interacting with each other and the structure. These models are suitable for studying ice fragmentation, ice-structure interaction at small scales, and ice rubble generation.

Boundary Element Models focuses on the interaction between the structure and ice by discretizing the structure's boundary. It calculates the response of the structure to external loads, including ice forces, accounting for wave-ice-structure interactions and their effects on load distribution.

Coupled Ice-Structure Interaction Models consider the dynamic interaction between ice, structure, and the surrounding environment. They incorporate fluid-structure interaction and ice-structure interaction, considering the effects of waves, currents, and ice forces on offshore structures.

Probabilistic and Statistical Models assess the probability of ice loads exceeding certain thresholds. They rely on statistical analysis of historical data and stochastic modeling to estimate the likelihood of extreme ice loads and their impact on structures.

These models vary in complexity, computational requirements, and the level of detail they provide. Engineers often select models based on the specific characteristics of the ice regime, the structural design requirements, and the intended application. Combining multiple models or using a hybrid approach can sometimes yield more comprehensive and accurate predictions of ice loads on offshore structures.

DISCUSSION

Ice loads exert substantial pressure on offshore structures, posing significant challenges to their integrity and stability. Structural components are susceptible to damage, deformation, and fracture due to the dynamic and unpredictable nature of ice-induced forces. The risk of structural failure increases when confronted with icebergs, ice ridges, and dynamic ice movement, highlighting the need for robust design strategies.

Various methodologies, including empirical formulations, physical model tests, and numerical modeling, are employed to calculate ice loads on offshore structures. Numerical models, such as Finite Element Analysis and Discrete Element Models, provide detailed insights into ice-structure interaction and stress distribution. However, challenges persist in accurately predicting extreme ice load scenarios due to uncertainties in ice behavior and environmental factors.

Ice loads necessitate extensive maintenance and repair activities, increasing operational costs and downtime for offshore installations. Fatigue induced by cyclic loading from ice and the risk of structural damage require ongoing monitoring and maintenance to ensure the structural integrity and safety of these installations.

Safety measures and risk mitigation strategies are crucial to mitigate the impact of ice loads on offshore structures. Innovative designs, specialized materials, and de-icing systems are employed to enhance structural resilience. Moreover, risk assessments and probabilistic approaches aid in identifying potential vulnerabilities and developing contingency plans.

CONCLUSION

The influence of ice loads on offshore structures in Arctic environments presents multifaceted challenges that demand sophisticated engineering solutions and risk management strategies. The accurate estimation of ice loads remains an ongoing challenge due to the complexity and variability of ice behavior. Numerical models offer valuable insights into ice-structure interaction, enabling engineers to design structures capable of withstanding ice-induced forces.

Efforts towards enhancing structural resilience through innovative designs, materials, and operational strategies are essential. The integration of advanced technologies, continuous monitoring, and ongoing research are imperative to address the evolving demands of operating offshore structures in ice-prone regions. While uncertainties persist, a multidisciplinary approach and a commitment to safety and environmental preservation remain paramount for the sustainable development of offshore structures in Arctic environments.

ACKNOWLEDGEMENTS

This work was done as a part of Project « Study of statistical patterns of ice loads on engineering structures and development of a new method for their stochastic modeling (FSEG-2020-0021)", No. 0784-2020-0021» supported by the Ministry of Science and Higher Education of the Russian Federation.

REFERENCES

[1] Shkhinek KN, Blanchet D, Croasdale K. et al (1994) Comparison of the Russian and foreign codes and methods for global load estimation. Paper presented at the 13th ISOPE Conference, vol 4, pp 75-81.

[2] Andreeva, S.A., Sharapov, D. Hoek–Brown model for ice breaking simulation. Magazine of Civil Engineering. 2023. 123(7). Article no. 12303. DOI: 10.34910/MCE.123.3

[3] Sharapov D., Klochkov Y., Improving quality of 2D ice load estimation on freezed piles, International Journal for Quality Research v17, n4, 2023, DOI: 10.24874/IJQR17.04-11

[4] Shi Y. A numerical investigation of ice-structure interaction using a discrete element model // Ocean Engineering. – 2016. – T. 118. – C. 274-287.

[5] Sharapov D., BRIEF ON DEVELOPMENT OF ICE LOAD ESTIMATION FOR HYDROTECHNICAL ENGINEERING, Proceedings of 23rd International Multidisciplinary Scientific GeoConference SGEM 2023, Volume 23, Issue 2.1, ISBN 978-619-7603-57-6 DOI: 10.5593/sgem2023/2.1/s08.18.

[6] Sharapov D (2023) Evolution of ice load prediction tools for hydrotechnical construction. E3S Web of Conf 402:05023. DOI: https://doi.org/10.1051/e3sconf/202340205023.

[7] DS/ISO 19906-2019 Petroleum and natural gas industries – Arctic offshore structures. International Organization for Standardization, 2010.

[8] Liferov P, Shkhinek KN, Vitali L, Serre N (2007) Ice gouging study - actions and action effects. Recent Development of Offshore Engineering in Cold Regions 1 and 2: 774-786.

[9] Sharapov D (2023) Ice adhesion to hydrotechnical structures. E3S Web of Conf 431:03006. DOI: https://doi.org/10.1051/e3sconf/202343103006.

[10] Loset S, Shkhinek K, Gudmestad OT, Hoyland K. (2006) Actions from ice on Arctic offshore and coastal structures: student's book for institutes of higher education. Publisher "LAN", St. Petersburg, p 272.

[11] Sharapov D (2023) Structure freezing in the ice. E3S Web of Conf 431:06010. DOI: https://doi.org/10.1051/e3sconf/202343106010.

[12] Sharapov D., Andreeva S., Ice reinforcement, E3S Web of Conferences, Volume 431, 06009, 2023, DOI: 10.1051/e3sconf/202343106009.

[13] Keyang Liu, Baoping Cai, Qibing Wu, Mingxin Chen, Chao Yang, Javed Akbar Khan, Chenyushu Wang, Hasini Vidumini Weerawarna Pattiyakumbura, Weifeng Ge, Yonghong Liu, Risk identification and assessment methods of offshore platform equipment and operations, Process Safety and Environmental Protection, Volume 177, 2023, Pages 1415-1430, ISSN 0957-5820, https://doi.org/10.1016/j.psep.2023.07.081.

[14] Victoria Sykes, Maurizio Collu, Andrea Coraddu, A review and analysis of optimisation techniques applied to floating offshore wind platforms, Ocean Engineering, Volume 285, Part 1, 2023, 115247, ISSN 0029-8018, https://doi.org/10.1016/j.oceaneng.2023.115247.

[15] Emma C. Edwards, Anna Holcombe, Scott Brown, Edward Ransley, Martyn Hann, Deborah Greaves, Evolution of floating offshore wind platforms: A review of at-sea devices, Renewable and Sustainable Energy Reviews, Volume 183, 2023, 113416, ISSN 1364-0321, https://doi.org/10.1016/j.rser.2023.113416.

SEISMIC SIGNALS, ACQUISITION AND INTERPRETATION METHODS

Prof. Dr. Mariana Jurian

Mr. Enis Muslim

[1] University of Pitesti, **Romania**

[2] University of Pitesti, **Romania**

ABSTRACT

In this article, we will present the types of seismic waves, how their collection is performed and their preparation for analysis and processing. Understanding these aspects can help improve in future any stage of the process, by using new hardware and/or software equipment, in continuous development around the world. There are three steps in seismic exploration of the ground. The first one is seismic data acquisition which is done in a specific location, ground or water, using a seismic source. The seismic wave generated by the source travels thru the layers of rock or sediments and is registered with the use of wave receivers also known as geophones or hydrophones. Data collected by this receivers is made in digital form, making it easier to be stored and analyzed on PC. After acquisition data needs to be processed, that means we need to identify and enhance the desired signal. A good system for processing the collected data will help to interpret the information and have a good image of the distribution of material proprieties of the subsurface.

Keywords: seismic-signals-acquisition-interpretation

INTRODUCTION

The seismic wave received by the geophone represents the ground motion in time, and a complete seismic wave is made up of various distinct waves.

The seismic signals, initiated by the natural seismic source or induced and received by the geophones, shows the variation in time of the seismic movement, to identify amplitude, duration and aspect of the same. These are produced by different waveforms - P (primary), S (secondary) and Rayleigh (surface wave), but also by the structure of the ground layers and of the propagation methods – direct, reflected, refracted.

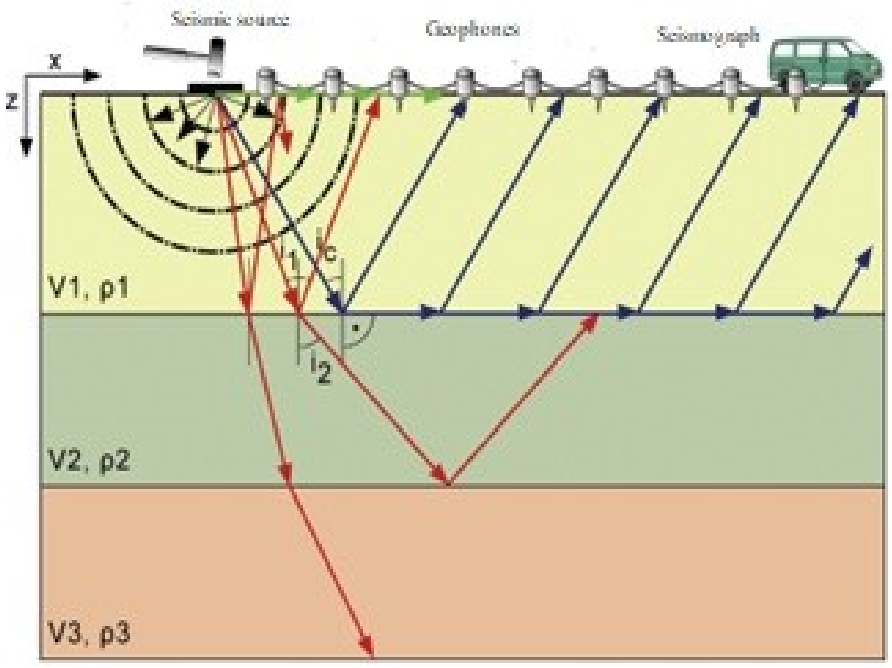

Fig. 1 – Wave acquisition [4]

The seismic signals collected in the geophone network are not continuous. These accompany the short duration events, such as earthquakes, the natural or induced seismic movements.

When graphicly recording the seismic motion, the wavelets are easily recognized as short oscillations around an isoelectric line. Marking them by filling in the peaks helps to identify the propagation of movement in the subsurface and thus to highlight the layers.

As a mathematical instrument, the wavelets can be used for extracting data from various types of seismic data. The wave sets are, generally, necessary for the complex data analysis. A set of complementary waves will decompose the data without gaps or overlaps, so that the decomposition process is mathematically reversible. Thus, complementary wavelet sets are useful in wavelet-based compression/decompression algorithms, where it is desirable to recover the original information with minimum loss.

The following graphic describes (Fig. 2) the seismic wave collected on the geophone.

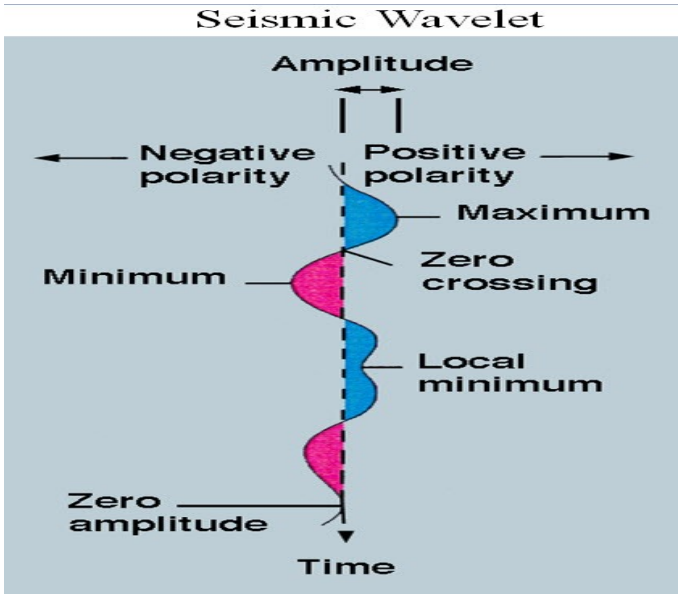

Fig. 2 – Seismic wave [5]

For an intuitive presentation of the waves, we recommend the youtube video: https://www.youtube.com/watch?v=F7Lg-nFYooU

The seismic waves are generally asymmetric. In order to better represent the seismic signals, the asymmetrical waves are defined as fractional derivatives of the Gaussian function. Ricker defines the seismic waves in the frequency domain corresponding to the relation:

$$(1)\quad g(\tau) = \sqrt{\pi}\omega_0 e^{-\frac{\omega^2}{4}(\tau-\tau_0)^2}$$

where τ represents the position in time of the symmetrical center and represents the reference frequency.

The seismic waves are usually represented in the time domain as fractional derivatives of the Gaussian function, described by the equation:

$$(2)\ g^{(u)}(\tau) = \frac{1}{\Gamma(m-u)}\int_0^{\tau}(\tau-\xi)^{m-u-1}\, g^{(m)} d\xi$$

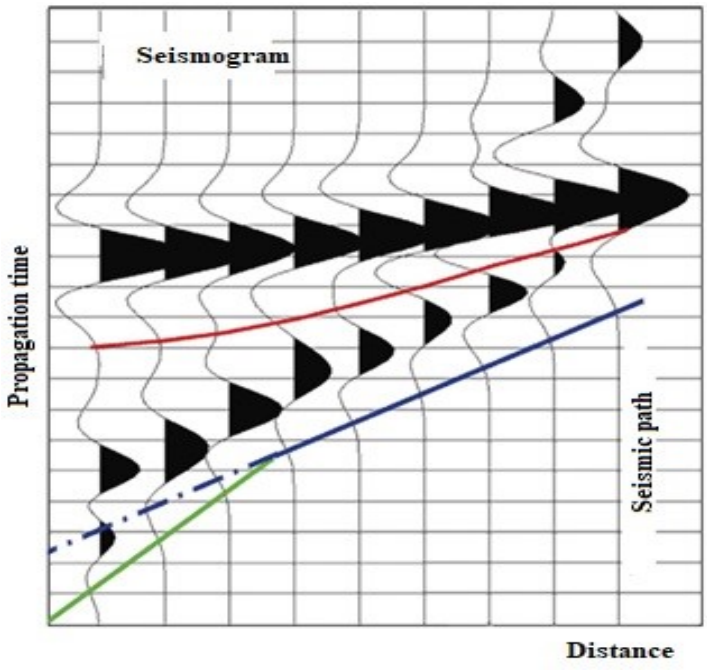

Fig. 3 – Seismic waves [4]

The diagram of fig. 3 presents the evolution throughout time of the seismographic signals, in which the waves' peaks are highlighted in black starting from the isoelectric line to distinctively and suggestively mark the progress of the same and facilitate their interpretation.

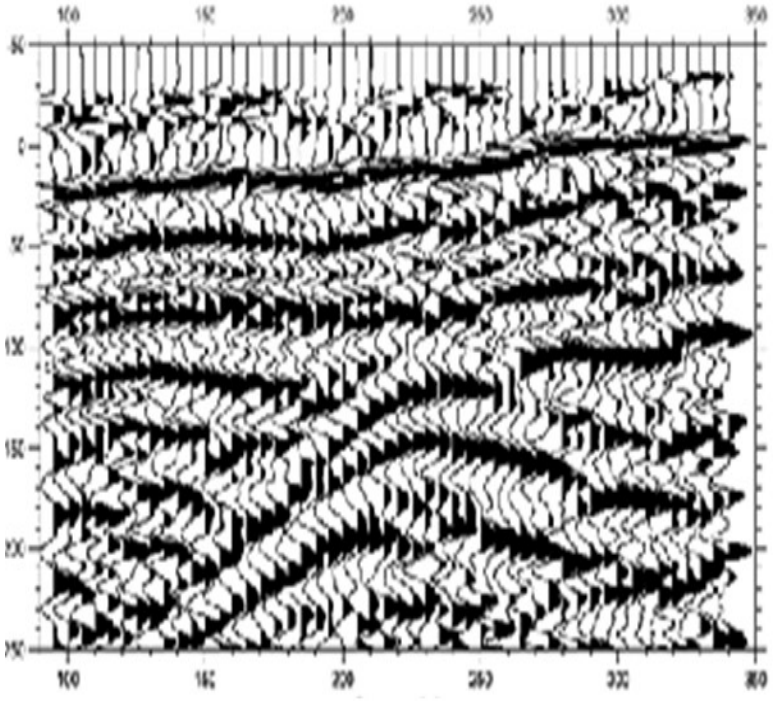

Fig. 4 – Signal evolution [1]

At a larger scale representation of the seismic signals the advantage of the waveform representation becomes obvious, marking distinctly the arrangement of layers and how they respond to seismic motions

Each seismic peak is represented by a wave (short oscillation of a wave around the isoelectric line), composed of sampled numerical data and their temporal location.

In the image above, we notice each individual location on the surface is represented by a wave. This wave is in fact made up of the digital data that have been sampled throughout time, processed and then graphically recomposed under the form of a seismic wave.

A key aspect for processing the signal applied to these waves, or time series, is that they not be aligned. Alignment takes place when the signal is resampled, in such a manner is the output of data appear as much different as the input data. This phenomenon is shown in the example in the fig. 5 below. [3]

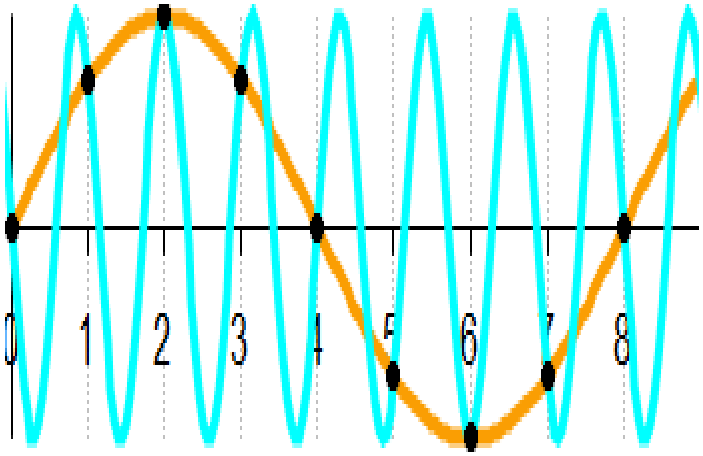

Fig. 5 – Sample alignment [2]

The blue line shows the original wave, while the orange line shows the resulting wave, if the same input the data are assembled at a lower sampling rate, as indicated by the individual dots marked in black. If the sampling rate is lower, it does not preserve all the details existing in the original, resulting an aligned data version, which is of no useful interest.

When processing the geophysical signal, the alignment is avoided by applying an anti- alignment filter, which is used before the digital sampling to restrict the bandwidth of the input signal. In fact, any mathematical operation applied on a sequence of numbers can be used in applying the filters to the data that have been collected. A filter simply takes an input data flow and either filters them, or manipulates them in the desired manner to create a new set of output data. For instance, the mere elimination of the random noise from the input signal can be considered an output signal and use for subsequent processing, in such a manner as to offer a clearer visualization of the subsurface.

In processing the geophysical signal, various transformations are often used to change the data from one mathematical representation to another. For instance, a Fourier transform is used on time-varying signals, such as those collected from seismic surveys, to transfer them into the frequency domain. This processing can focus on discrete portions of the signal.

CONCLUSION

The article offers an overview of the seismic waves, the instrument used for the acquisition and interpretation of the obtained results. Using this information, we can develop new methods and equipment, using the new technologies developed during the latest years. The transmission of the data to be interpreted can be improved using the latest technologies, just as new software can be developed for data analysis. Having a better image of the distribution of material in the subsurface will help with better and more economical decision for mining and drilling for raw materials. Better data will also help to fully understand the evolution of sedimentary basins.

REFERENCES

[1] Li Ming1, Yuan Zi2, Jiang Chunlan1, Design of seismic data acquisition system, ICSP Proceeding 2010

[2] Ozkan Kafadar, A geophone-based and low-cost data acquisition and analysis system designed to microtremor measurements, Preprint. Discussion started: 26 May 2020

[3] Shell Brasil Petroleo Ltda , Fully Autonomous Marine Seismic Acquisition Systems for Reservoir Monitoring, Conference Paper · January 2019

[4] Santoso, Didik R. & Maryanto, Sukir & Nadhir, Ahmad & Sugiharto, T.. (2017). A simple and low-cost data acquisition system with multi-nodes facility for geophone array sensors. International Journal of Applied Engineering Research. 12. 2109-2114. Philip Kearey et al (2002), An Introduction to Geophysical Exploration, 3rdEd, Blackwell Science Ltd

[5] Rana, S. & Burley, Stuart & Chowdhury, S.. (2006). The application of hierarchical seismic attribute combination to high precision infill well planning in the South Tapti Field, offshore Western India. Geohorizons. 11. 32-38.

STOCHASTIC DEM ICE MODELS PERSPECTIVE

Assoc. Prof. Dr. Dmitry Sharapov[1]

[1] Peter the Great St.Petersburg Polytechnic University, **Russia**

ABSTRACT

The Discrete Element Method (DEM) serves as a crucial computational tool in studying ice-structure interactions pertinent to offshore marine constructions. The article highlights the significance of DEM in simulating and comprehending the complex dynamics of ice loads on offshore structures. Offshore marine constructions face challenges associated with ice loads, especially in regions prone to icy conditions. DEM, adapted to model ice behavior, offers a micro-scale perspective, representing individual ice particles to capture their interactions with offshore structures. This approach enables the assessment of ice-induced forces, structural responses, and failure mechanisms critical for designing resilient offshore installations. We underscore DEM's role in simulating ice-structure interactions, encompassing phenomena such as ice crushing, fracturing, and the dynamic response of offshore structures subjected to varying ice loads. These simulations aid in evaluating the structural integrity and performance of offshore installations, contributing to the design and optimization of platforms, rigs, and offshore wind structures in ice-prone environments. Challenges in DEM modeling for ice calculations for offshore marine constructions include the accurate representation of ice properties, validation against experimental data, and computational demands for simulating large-scale systems. However, ongoing advancements in computational capabilities, refinements in ice modeling techniques, and integration with experimental observations continue to enhance the accuracy and reliability of DEM simulations for offshore structures in icy environments.

Keywords: Discrete Element Method, DEM, Ice-Structure Interactions, Offshore Marine Constructions, Ice Loads, Ice Modeling, Computational Simulations

INTRODUCTION

The Discrete Element Method (DEM) represents a powerful computational tool used to investigate and comprehend the intricate behavior of ice and its interactions with structures or other materials. As an extension of its applications in granular materials, DEM has been adapted to study the complex dynamics of ice, offering a micro-scale perspective crucial for understanding ice-related phenomena across various domains [1-6]. Ice, despite its seemingly homogeneous appearance, exhibits a multitude of intricate behaviors and properties, such as fracturing, brittleness, anisotropy, and sensitivity to environmental conditions. There are many regulations on calculation of ice loads on the structures [7-11]. Understanding and predicting these characteristics are vital in numerous industries and disciplines, including civil engineering, maritime operations, environmental sciences, and climate change studies. The application of DEM in ice simulations involves representing individual ice particles or discrete elements, allowing for a granular-level representation of ice structures. This approach enables the modeling

of ice interactions at a micro-scale, considering factors like ice crystal shapes, sizes, orientations, and material properties, thus capturing the nuances of ice behavior. DEM simulations of ice encompass a range of phenomena, including ice-structure interactions, ice formation, fracturing due to mechanical loading or temperature changes, ice flow dynamics, and the influence of external forces on ice behavior. By tracking the movement, collisions, and forces between these discrete ice particles, DEM provides insights into the mechanical response of ice under different loading conditions, aiding in the assessment of structural integrity and resilience against ice loads. The applications of DEM in ice-related studies are diverse and impactful. In maritime engineering, DEM facilitates the analysis of ship-ice interactions, aiding in the design of ice-going vessels and offshore structures. In civil engineering, it assists in evaluating the structural response of infrastructure subjected to ice loads, such as bridges, dams, and coastal structures. Moreover, DEM finds applications in glaciology and climate sciences, enabling the study of ice flow, glacier dynamics, and the impact of climate change on ice formations. Despite its potential, DEM simulations of ice come with challenges. Accurately representing the complex nature of ice, including its anisotropic behavior, material properties, and intricate interactions, demands meticulous calibration and validation against experimental or observational data. Additionally, computational demands remain a challenge, particularly for large-scale ice simulations involving numerous ice particles or complex geometries. However, ongoing advancements in computational resources, refinement of ice models, and integration with experimental data continue to enhance the accuracy and reliability of DEM simulations of ice. These developments pave the way for improved understanding and predictive capabilities regarding ice behavior, contributing to safer designs and better-informed decision-making in ice-related applications [12-15].

MATERIALS AND METHODS

Discrete Element Method (figure 1) is a numerical technique used for simulating the behavior of granular materials, particles, or objects at a micro-scale level. This method is particularly useful for studying the behavior of systems where individual particles interact with each other, such as in granular flow, powder mechanics, rock mechanics, and various industrial processes involving particulate materials.

The DEM model represents individual particles or discrete elements as distinct entities that interact with each other based on prescribed rules and physical properties such as size, shape, density, and material properties. These particles can have various shapes and sizes, and their interactions include forces like contact forces, friction, cohesion, and other relevant physical interactions.

The simulation using DEM involves tracking the motion, interaction, and collisions between these individual particles over time to understand the collective behavior and properties of the entire system. By simulating the behavior of each individual particle, the DEM model can provide insights into phenomena such as particle flow, segregation, mixing, compaction, and other complex behaviors exhibited by granular materials.

DEM simulations are widely used in industries like pharmaceuticals, mining, agriculture, civil engineering, and many others where the understanding of particulate behavior is crucial for optimizing processes and improving designs.

The primary difference between Discrete Element Method and continuous models for ice lies in their approach to representing and simulating ice behavior.

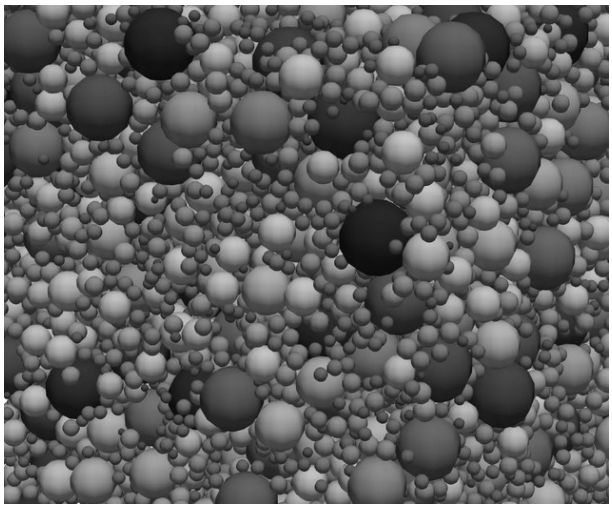

Fig. 1. Example of DEM material model

Continuous Models:

- **Continuum Approach:** Continuous models represent ice as a continuous medium, describing its behavior using mathematical equations based on continuum mechanics. These models treat ice as a homogeneous material with averaged properties.
- **Macroscopic Description:** They focus on describing ice behavior at a larger scale, considering bulk properties such as stress, strain, temperature, and phase changes.
- **Simpler Interactions:** Continuous models may not capture the detailed interactions between individual ice particles. Instead, they rely on constitutive equations and simplified assumptions about ice behavior and its interaction with structures.
- **Lower Computational Demand:** Generally, continuous models are less computationally demanding than DEM as they involve solving partial differential equations governing the behavior of ice as a continuous medium.

Discrete Element Method (DEM):

- **Particle-Based Approach:** DEM models ice as a collection of discrete particles or elements that interact individually. Each ice particle is represented separately, and interactions between these particles are simulated based on defined physical laws and contact mechanics.
- **Microscale Detail:** It offers a high-resolution, granular-level representation of ice, enabling the simulation of individual particle interactions, fracturing, and the behavior of ice masses under various conditions.
- **Complex Interactions:** DEM is capable of capturing complex interactions between ice particles and structures, including ice-structure impacts, fracturing, and micro-scale ice behavior.

- **Computational Intensity:** It can be computationally intensive, especially for simulations involving a large number of discrete ice particles, making it more resource-demanding in terms of computation time and resources.

DEM provides a more detailed, particle-level representation of ice behavior, while continuous models offer a more macroscopic view, treating ice as a continuous medium. Both approaches have their advantages and limitations, and the choice between them depends on the specific requirements of the simulation, the level of detail needed, and the computational resources available. Often, a combination of both approaches or hybrid models might be employed to leverage their respective strengths for accurate ice simulations.

The Discrete Element Method (DEM) has been used in various simulations, including those related to ice load calculations; some advantages and disadvantages of using DEM for ice load calculations:

Advantages: DEM provides a granular, particle-level representation of the ice structure, allowing for a more detailed analysis of interactions between individual ice particles and structures. It allows for the representation of different types of ice structures, including various shapes, sizes, and material properties, providing flexibility in modeling different ice conditions. DEM can simulate complex interactions between ice and structures, such as ice-structure impacts, fracturing, and ice-structure interaction dynamics, offering insights into structural response. DEM can be applied to both micro and macro scales, making it adaptable for different scenarios, from small-scale laboratory experiments to large-scale real-world applications. It can model failure mechanisms of ice, enabling the study of ice breakage, crack propagation, and structural damage due to ice loads.

Disadvantages: DEM simulations involving a large number of particles can be computationally intensive, requiring significant computational resources and time, especially for complex scenarios or large-scale simulations. Modeling interactions between numerous particles accurately requires sophisticated algorithms and computations, which can be challenging and prone to numerical errors. DEM simulations often involve various parameters related to particle properties, contact models, and material behaviors. Sensitivity to these parameters can affect simulation accuracy, requiring careful calibration and validation. Real-time simulations of large-scale ice loads using DEM may not always be feasible due to computational constraints, limiting its immediate application in certain real-time monitoring or control systems. Obtaining experimental data for validation of DEM simulations, especially for complex ice-structure interactions, can be difficult, limiting the accuracy and reliability of the model.

While DEM offers a detailed approach for studying ice-structure interactions, its use in ice load calculations requires consideration of these advantages and limitations to ensure accurate and reliable simulations. Combining DEM with other modeling techniques or experimental data can help mitigate some of these limitations and improve the accuracy of ice load calculations. Stochastic models within the context of Discrete Element Method (DEM) simulations can be beneficial for several reasons:

Stochastic models account for inherent uncertainties and variability present in real-world systems. In DEM simulations, these uncertainties can arise from various sources such as particle properties, contact parameters, external forces, or initial conditions. By

incorporating stochasticity, these models can provide insights into the range of potential outcomes due to these uncertainties.

Systems involving granular materials or particle interactions often exhibit stochastic behavior in their interactions. Stochastic models allow for a more realistic representation of such systems by introducing randomness or probabilistic elements into the simulation.

Stochastic simulations help in assessing the robustness and reliability of the modeled systems. They allow for the evaluation of how variations or uncertainties in parameters affect the overall behavior of the system, providing insights into the system's sensitivity to these uncertainties.

Stochastic DEM models enable statistical analysis of simulation results. They can provide probability distributions, variance, or other statistical measures characterizing the system behavior, allowing for a more comprehensive understanding of the system's response.

Stochastic models are useful for conducting sensitivity studies by systematically varying parameters within certain probability distributions. This helps in identifying which parameters have the most significant impact on the system's behavior and which ones are less influential.

Stochastic models can aid in the validation and calibration of simulation results against experimental data or real-world observations. By considering stochastic variations, these models can potentially better match the variability seen in empirical data.

In fields where DEM is used to analyze structures or systems under uncertain loading conditions, stochastic DEM models can help in assessing risk by considering uncertainties in loads, material properties, or environmental conditions.

In DEM simulations, energy dissipation plays a crucial role in accurately modeling the behavior of granular materials or particle systems. Energy dissipation refers to the conversion of mechanical energy into other forms, such as heat, during interactions between particles or with surrounding structures. Several reasons highlight the importance of considering energy dissipation in DEM models:

Energy dissipation is inherent in the interactions between particles, such as during collisions, sliding, rolling, or deformation. Realistic simulations of granular systems should consider these dissipative effects to accurately represent the behavior observed in physical systems.

Neglecting energy dissipation can lead to unrealistic simulations that do not accurately reflect the behavior of granular materials. Including dissipation mechanisms helps in obtaining simulation results that align better with experimental observations and real-world behavior.

Energy dissipation can significantly impact the stability of DEM simulations. It helps in damping excessive energy that might otherwise accumulate in the system, preventing unrealistic behaviors like perpetual motion or unbounded energy increase.

Energy dissipation leads to heat generation within the system. In certain applications, such as in materials processing or geological studies, considering thermal effects due to

energy dissipation becomes crucial for understanding temperature changes and their influence on material behavior.

Energy dissipation affects force transmission between particles during interactions. Accurate modeling of these dissipative forces is essential for correctly predicting the overall behavior and forces within the granular assembly.

Energy dissipation mechanisms can provide insights into the deformation, flow, compaction, and failure of granular materials. By considering dissipation, DEM models can better capture phenomena such as energy loss during compaction or the formation of force chains in granular systems.

Energy dissipation mechanisms in DEM models is crucial for accurately simulating the behavior of granular materials and particle systems. It helps in achieving more realistic and reliable simulations that align with experimental observations and real-world behavior, enabling a better understanding of the complex dynamics exhibited by these systems.

DISCUSSION

Continued advancements in computational capabilities and modeling techniques offer opportunities to address several challenges associated with DEM simulations. Efforts in developing parallel computing algorithms and leveraging high-performance computing resources aim to mitigate computational demands, allowing for more extensive and faster simulations. Refinements in contact models and material characterization contribute to enhancing the accuracy of DEM predictions, facilitating better correlation with experimental data.

Hybrid modeling approaches combining DEM with other numerical methods, such as Finite Element Method (FEM) or Computational Fluid Dynamics (CFD), offer promising avenues to expand the scope of DEM applications. These hybrid models enable the simulation of coupled systems, incorporating fluid-particle interactions or structural responses, thereby enhancing the realism of simulations in scenarios involving complex environments.

Moreover, the integration of machine learning and data-driven techniques with DEM holds potential for improving model calibration, predicting material behaviors, and optimizing simulations. Data-driven approaches can aid in parameter estimation, uncertainty quantification, and reducing computational expenses by leveraging available experimental or observational data.

Looking ahead, the future of DEM in granular material simulations involves addressing existing challenges while exploring new frontiers. This includes advancing multiscale modeling techniques to bridge the gap between micro- and macro-scale simulations, enhancing predictive capabilities, and expanding applications in emerging fields like biomedicine, renewable energy, and smart materials.

CONCLUSION

The Discrete Element Method (DEM) has emerged as a powerful numerical technique for simulating the behavior of granular materials, offering invaluable insights into

complex interactions between individual particles and structures. Its applications span across various industries, including pharmaceuticals, mining, agriculture, civil engineering, and more, where understanding granular behavior is critical for optimizing processes and designs. DEM's ability to model granular systems at a micro-scale level provides a detailed understanding of particle interactions, enabling simulations of phenomena such as particle flow, segregation, compaction, and structural response to external forces. This methodology's granular representation offers advantages in capturing intricate behaviors, including particle-particle and particle-structure interactions, failure mechanisms, and energy dissipation. Computational intensity remains a significant hurdle, especially for large-scale simulations involving a vast number of particles. The accuracy of DEM simulations heavily depends on appropriately defining parameters such as contact laws, material properties, and the handling of energy dissipation, which can pose challenges in model calibration and validation. Furthermore, the complexity of real-world granular systems often necessitates a balance between model accuracy and computational efficiency.

ACKNOWLEDGEMENTS

This work was done as a part of Project « Study of statistical patterns of ice loads on engineering structures and development of a new method for their stochastic modeling (FSEG-2020-0021)", No. 0784-2020-0021» supported by the Ministry of Science and Higher Education of the Russian Federation.

REFERENCES

[1] Shi Y. A numerical investigation of ice-structure interaction using a discrete element model // Ocean Engineering. – 2016. – T. 118. – C. 274-287.

[2] Andreeva, S.A., Sharapov, D. Hoek–Brown model for ice breaking simulation. Magazine of Civil Engineering. 2023. 123(7). Article no. 12303. DOI: 10.34910/MCE.123.3

[3] Sharapov D., Klochkov Y., Improving quality of 2D ice load estimation on freezed piles, International Journal for Quality Research v17, n4, 2023, DOI: 10.24874/IJQR17.04-11

[4] Shkhinek KN, Blanchet D, Croasdale K. et al (1994) Comparison of the Russian and foreign codes and methods for global load estimation. Paper presented at the 13th ISOPE Conference, vol 4, pp 75-81.

[5] Sharapov D., BRIEF ON DEVELOPMENT OF ICE LOAD ESTIMATION FOR HYDROTECHNICAL ENGINEERING, Proceedings of 23rd International Multidisciplinary Scientific GeoConference SGEM 2023, Volume 23, Issue 2.1, ISBN 978-619-7603-57-6 DOI: 10.5593/sgem2023/2.1/s08.18.

[6] Sharapov D (2023) Evolution of ice load prediction tools for hydrotechnical construction. E3S Web of Conf 402:05023. DOI: https://doi.org/10.1051/e3sconf/202340205023.

[7] DS/ISO 19906-2019 Petroleum and natural gas industries – Arctic offshore structures. International Organization for Standardization, 2010.

[8] Liferov P, Shkhinek KN, Vitali L, Serre N (2007) Ice gouging study - actions and action effects. Recent Development of Offshore Engineering in Cold Regions 1 and 2: 774-786.

[9] Loset S, Shkhinek K, Gudmestad OT, Hoyland K. (2006) Actions from ice on Arctic offshore and coastal structures: student's book for institutes of higher education. Publisher "LAN", St. Petersburg, p 272.

[10] Sharapov D (2023) Ice adhesion to hydrotechnical structures. E3S Web of Conf 431:03006. DOI: https://doi.org/10.1051/e3sconf/202343103006.

[11] Sharapov D (2023) Structure freezing in the ice. E3S Web of Conf 431:06010. DOI: https://doi.org/10.1051/e3sconf/202343106010.

[12] Sharapov D., Andreeva S., Ice reinforcement, E3S Web of Conferences, Volume 431, 06009, 2023, DOI: 10.1051/e3sconf/202343106009.

[13] Emma C. Edwards, Anna Holcombe, Scott Brown, Edward Ransley, Martyn Hann, Deborah Greaves, Evolution of floating offshore wind platforms: A review of at-sea devices, Renewable and Sustainable Energy Reviews, Volume 183, 2023, 113416, ISSN 1364-0321, https://doi.org/10.1016/j.rser.2023.113416.

[14] Victoria Sykes, Maurizio Collu, Andrea Coraddu, A review and analysis of optimisation techniques applied to floating offshore wind platforms, Ocean Engineering, Volume 285, Part 1, 2023, 115247, ISSN 0029-8018, https://doi.org/10.1016/j.oceaneng.2023.115247.

[15] Keyang Liu, Baoping Cai, Qibing Wu, Mingxin Chen, Chao Yang, Javed Akbar Khan, Chenyushu Wang, Hasini Vidumini Weerawarna Pattiyakumbura, Weifeng Ge, Yonghong Liu, Risk identification and assessment methods of offshore platform equipment and operations, Process Safety and Environmental Protection, Volume 177, 2023, Pages 1415-1430, ISSN 0957-5820, https://doi.org/10.1016/j.psep.2023.07.081.

SECTION

FOREST ECOSYSTEMS

AMAZON DEFORESTATION, CLIMATE LAW AND THE PRINCIPLE OF ECOLOGICAL SOLIDARITY: A COMMON BRAZILIAN AGENDA

Ph.D. candidate Ari Rogério Ferra Júnior[1]

[1] University of Camerino in *cotutela* with University of São Paulo – **Italy/Brazil**

ABSTRACT

Climate change is a topic of worldwide relevance, not only because of the recent heat waves affecting the globe as a whole but also because of the importance of conserving the ecologically balanced environment itself. Climate is a vital aspect of human survival and ecological balance. With this in mind, the world is turning its attention to Brazil and the Amazon rainforest, the target of recurrent attacks that have resulted in high percentages of deforestation. It is known that since the signing of the Amazon Cooperation Treaty by the eight countries of the Amazon biome, many new challenges have arisen; however, the main commitment signed in the treaty of July 1978 remains a common commitment (and agenda) for the preservation and conservation of the environment and the rational use of the Amazon's natural resources. In addition to preserving the Amazon territory, the development of the Amazon territory is prioritized in order to achieve sustainable development. As a result, deforestation liabilities must be tackled and combated through reforestation and ecological restoration. According to preliminary government data from the Space Research Institute, deforestation alerts in the Amazon may have fallen by 39 percent in the first half of 2023. What emerges within the topics of climate change and consequent climate litigation is climate law as a means of resisting and confronting the climate crisis. Nevertheless, the Brazilian government itself was ordered by the Supreme Court to take action because of omissions by the Brazilian government responsible for the increase in deforestation in the Amazon in relation to the Climate Fund and the paralyzing of the Amazon Fund. As a response to climate litigation, what is assumed to be necessary is an understanding of the so-called ecological Constitution and the duty to sustainable development, and ecological solidarity in a broad normative perspective, in its governmental actions and not being silent on environmental positions; in addition, Brazil's commitment to its own normative order, to international treaties and agendas, such as Agenda 2030, must be part of the Brazilian agenda in order to regain environmental prominence. To achieve the expected goals, the methodology used is bibliographical, documentary, and exploratory, using the deductive method.

Keywords: Brazilian Amazon, climate litigation, ecological solidarity, ecological human dignity, ecological agenda.

INTRODUCTION

Brazil aims to regain international prestige and position itself on the world stage as one of the protagonists in the fight against climate change. Examples of this stance include the speeches made by Brazilian diplomats and the President of the Federative Republic of Brazil himself at the 2023 United Nations conference, the successive statements combating climate denialism and the candidacy of the Brazilian state to host

the 30th UN Conference on Climate Change (COP-30) in November 2025 in Belém (Pará).

The moment is unique, attracting global attention to Brazil and at the same time demanding a reorientation in the path the country has taken as a defender of sustainable development and the preservation of the Amazon, which has been so threatened in recent years.

The article is structured as follows: introduction, materials and methods, tables and graphs, results, discussion, conclusion, etc.

MATERIALS AND METHODS

To achieve the expected goals, the methodology used is bibliographical, documentary, and exploratory, using the deductive method. Judicial decisions from the Brazilian Supreme Court, technical data from the Brazilian government and independent bodies, as well as specialized articles written by researchers in the field, are used as examples.

TABLES AND GRAPHS

In Brazil, to understand how impacts and damage have affected the Amazon in recent years, *MapBiomas* presents data on the area (ha) of land cover and land use in the legal Amazon from 1985 to 2022 [1].

Table 1

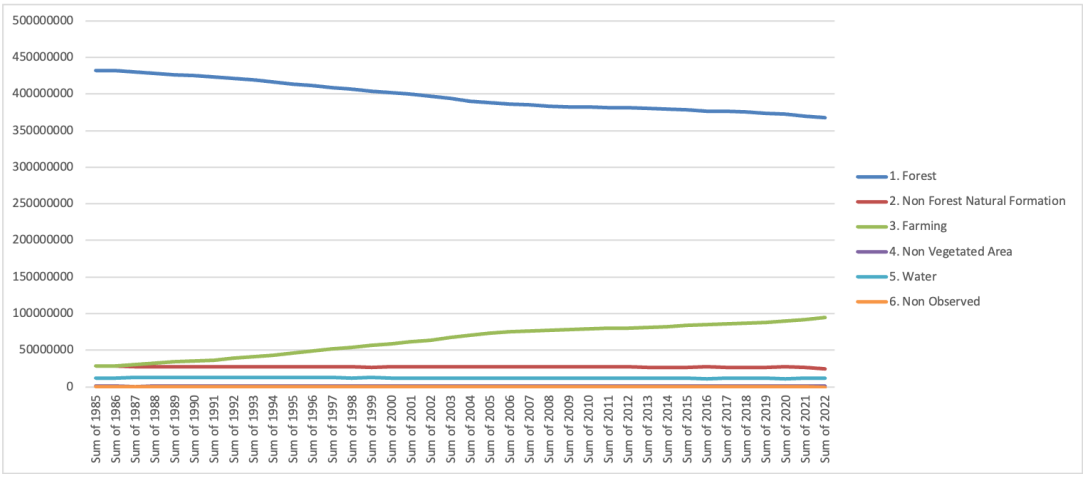

Source: *MapBiomas*

The table above shows the areas (ha) of transition between land cover and land use classes for the Legal Amazon region since 1985. In 1985 the total area of forest represented 431761553.3 ha, while in 2022 it represented 367385096.1 ha.

Mapbiomas is a collaborative network, made up of non-governmental organizations, universities, and technology start-ups, responsible for producing annual mapping of land cover and use, and we monitor water surface and fire scars on a monthly basis with data from 1985 onwards.

The Amazon Fund has 105 projects throughout Brazil, involving municipalities, states, the Federal District, and the Union (federal government), as well as the third sector, universities, and international projects [2].

Table 2

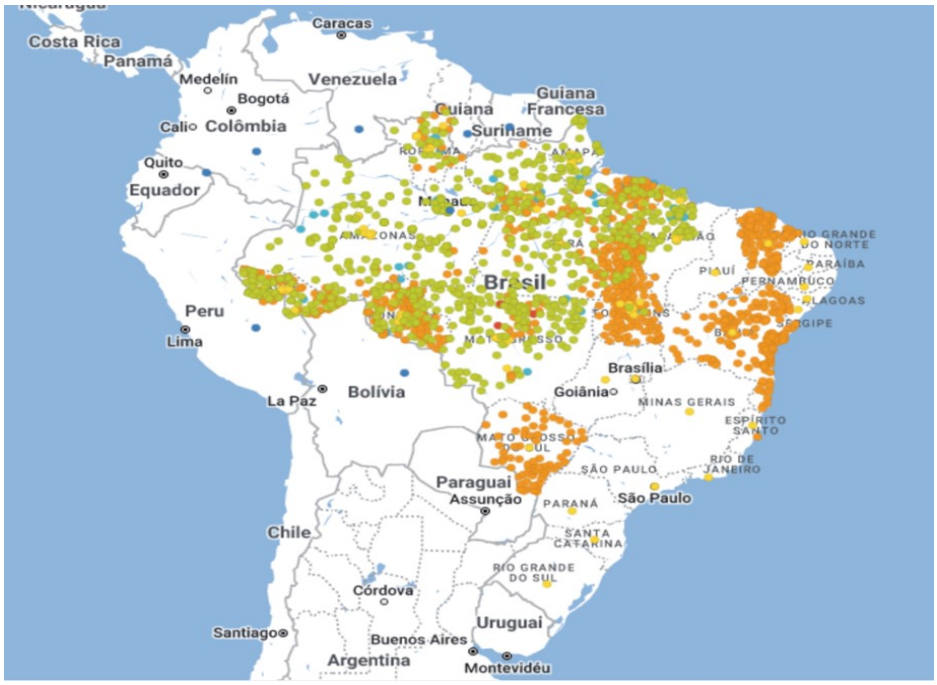

Source: Amazon Fund

RESULT

This research seeks to demonstrate that government inertia represents a serious threat to the planetary challenges caused by climate change. In this case, the government's neglect of the Amazon Fund has led to the paralysis of projects developed in the region and, as a consequence, there has been a vertiginous increase in deforestation in the Amazon.

DISCUSSION

AMAZON CO-OPERATION TREATY

The Amazon Cooperation Treaty, signed in Brasilia on 3 July 1978, is made up of the eight Amazonian countries: Bolivia, Brazil, Colombia, Ecuador, Guyana, Peru, Suriname, and Venezuela, and aims to promote the harmonious and integrated development of the Amazon basin, through regional economic development with the rational use of natural resources and in favor of improving the quality of life of the region's inhabitants.

It is not a recent claim that there is a shortage of natural resources and that the world is turning its eyes to the Amazon, arguing even that in the medium and long term exploiting natural resources in the Amazon would be natural. In fact, the same countries that have neglected the development of their "Amazonian hinterland" for centuries continue to do so, despite the treaty whose main objective is to create awareness for the development of the area through harmonious strategies [3].

Since 1978, therefore, the countries of the Amazon region have aimed to promote the region in search of a common agenda, capable of involving: scientific and technological research; information exchange; and rational utilization of natural

resources; among others. Pragmatism made it possible for the eight contracting parties to the Cooperation Treaty to harmonize their political and other differences in order to lay the foundations for future joint efforts, both bilateral and multilateral, aimed at the integrated and balanced development of the Amazon.

What can be seen more than 40 years later is that the Amazon Cooperation Treaty seems to have been forgotten by the signatory countries. There was a clear divergence between the countries at the summit that took place in Belém, Pará, in 2023, when Brazil defended, for example, oil exploration at the mouth of the Amazon River, while Colombia strongly opposed it, alleging greenwashing by the signatory countries of the Amazon Cooperation Treaty.

The treaty members, however, came together to reaffirm the principles of the Rio Declaration on the Environment and Sustainable Development and the 1992 Declaration of Principles on Forests, the United Nations Framework Convention on Climate Change (UNFCCC), and its Paris Agreement, among others. Indeed, apart from the differences, the Amazon continued to suffer from the neglect of significant countries. This has given rise to climate litigation, especially in Brazil. This is not in keeping with the objectives set out by the signatories to the Treaty.

CLIMATE LITIGATION

Brazil really wants to regain international prestige and respect in order to make up for lost time and reconcile itself with the values expressed in its Constitution with the objectives of the Republic, as well as, of course, the ecologically balanced environment, a good for the common use of the people and essential to a healthy quality of life, protection imposed on the Public Power and the community as a duty to defend and preserve it for present and future generations (art. 225, CRFB 1988).

In addition, the Constitution also recognizes the Brazilian Amazon Forest, Atlantic Rainforest, Serra do Mar, Mato Grosso Pantanal, and Coastal Zone as national heritage, and their use will be made, in the form of the law, within conditions that ensure the preservation of the environment, including the use of natural resources (art. 225, paragraph 4, CRFB 1988).

In recent years Brazil has received negative attention on the environmental agenda. An example of how little proactive action the Brazilian state has taken to protect and preserve the environment can be seen in the number of climate disputes the country has faced in recent years [4].

The Brazilian judiciary is known, and not without criticism, for its strong performance in environmental matters. Brazilian jurisprudence has moved in this direction, such as when the Federal Supreme Court (STF) judged a paradigmatic case in which it recognized the government's inertia in complying with its legal duty to preserve the environment. Some judgments are considered a benchmark in the environmental area, with the Brazilian Federal Supreme Court having already recognized the "unconstitutional state of affairs" developed by the Colombian Constitutional Court in environmental matters, due to the widespread violation of fundamental rights and guarantees, whether by action and/or omission of public bodies, which are responsible for protecting them.

In 2022, the Federal Supreme Court organized a "green agenda" to concentrate the judgment of cases that were awaiting a decision by the Brazilian court. To outline just a few paradigmatic judgements on environmental issues, we have the following cases: Argument for Non-Compliance with Fundamental Precept (ADPF) 760, an action against alleged omissive and commissive acts by the Federal Government in relation to the implementation of an effective plan to prevent deforestation in the Amazon; Direct Action of Unconstitutionality by Omission (ADO) 54, an action against the unconstitutional omission of the President of the Republic and the Minister of the Environment to curb the advance of deforestation in the Amazon, under the terms of articles 23 (items VI and VII) and 225 (caput and paragraph 1, items VI and VII) of the Federal Constitution; Argument for Non-Compliance with Fundamental Precept (ADPF) 708, an action to demand the government's constitutional duty to operate and allocate the Climate Fund's resources annually, for the purpose of mitigating climate change, with its contingency being prohibited, due to the constitutional duty to protect the environment (CF, art. 225) and the international rights and commitments assumed by Brazil (CF, art. 5, paragraph 2); and the Direct Action for Unconstitutionality by Omission (ADO) 59, which aimed to recognize the government's omission in relation to the paralysis of the Amazon Fund and the National Climate Change Fund (Climate Fund) to finance preservation projects in the Legal Amazon [5].

As a paradigm for this work, in 2022, there was a Direct Action of Unconstitutionality by Omission (ADO) 59, when the Plenary of the Federal Supreme Court (STF) ordered the Brazilians' federal government to adopt, within 60 days, the administrative measures necessary to reactivate the Amazon Fund, without further paralyzes. Directly related to this decision are SDG 15 (life on land), SDG 16 (peace, justice, and effective institutions), and SDG 17 (partnerships and means of implementation).

The Court judged that the changes made to the fund's format since 2019, with the unilateral extinction of committees and without the creation of another administrative body, prevented the financing of new projects, which constitutes an omission by the government in its duty to preserve the Amazon. This is a clear example of a serious climate dispute, given the importance of the Amazon Fund [6].

The Amazon Fund is a practical example of how the goals of the Amazon Co-operation Treaty, such as scientific and technological research, can be understood in practice, as the fund aims to raise donations for investments in efforts to prevent, monitor, and combat deforestation, and to promote the conservation and sustainable use of the Legal Amazon. Also, the Amazon Fund is a REDD+ mechanism.

The Amazon Fund's axes of action are (i) sustainable production (activities that keep the forest standing are economically attractive); (ii) monitoring and control (government actions ensure that anthropogenic activities comply with environmental legislation); (iii) territorial planning (the area of the Legal Amazon is territorially organized); and (iv) science, innovation, and economic instruments (economic instruments and science, technology and innovation activities contribute to the recovery, conservation and sustainable use of biodiversity).

The Amazon Fund has already supported 105 projects. Citing specific cases from its areas of activity: in sustainable production, 653 institutions are or have already been supported directly or through partners, R$ 294 million in revenue obtained from

the commercialization of products, 241,000 people benefiting from sustainable production activities and 75 million hectares of forest area with sustainable management; in monitoring and control, 1.1 million rural properties have been registered in the Rural Environmental Registry and 1. 896 environmental inspection missions carried out; in land-use planning, there are 196 conservation units supported, 101 indigenous lands in the Amazon supported and protected areas with strengthened management, 74 million hectares of protected areas with strengthened management and 61,000 indigenous people directly benefiting; and finally, in science, innovation and economic instruments, there are 603 scientific or informative publications produced and 2,159 researchers and technicians involved in CT&I activities supported [7].

Therefore, what can be seen is that government action is essential to maintain the preservation of the Amazon. Recently, the Amazon Fund received donations from other countries, such as The USA and Switzerland that joined Norway, Germany, and Petrobras in the Amazon Fund, currently the largest instrument for reducing emissions from deforestation and forest degradation (REDD+) in the world. The contributions are in addition to around R$3.4 billion already received by the Fund over the years [8].

An example of an ongoing project within the Amazon Fund is Profisc I - B (Brazilian Institute for the Environment and Renewable Natural Resources), with a total project value of R$140,264,000.00. The project's objectives are to support IBAMA's environmental inspection and deforestation control activities in the Legal Amazon. An example of the activities carried out are actions to inspect and combat illegal deforestation in the Legal Amazon, with more than 9,893 hours of helicopter flights and 955 missions carried out by the Brazilian Institute for the Environment and Renewable Natural Resources, with 279,010 civil servants employed in environmental inspection actions. The agency issued 12,074 infraction notices against flora, totaling R$8.9 billion [9].

CLIMATE LAW AND THE 2030 AGENDA

In fact, deforestation in the Amazon has decreased in the last year. The National Institute for Space Research (INPE), linked to the Ministry of Science, Technology and Innovation (MCTI), has finalized its estimate of the rate of deforestation in the Brazilian Legal Amazon (ALB). The estimated deforestation from 1 August 2022 to 31 July 2023 was 9,001 km². This figure represents a reduction of 22.37 percent in relation to the deforestation rate consolidated by PRODES 2022, which was 11,594 km² for the nine states of the ALB. This estimate is the result of the Brazilian Amazon Forest Satellite Monitoring Programme (PRODES) [10].

In the first seven months of 2023, deforestation in the Amazon fell by 42.5 percent compared to the same period last year. The state of Amazonas recorded the biggest reduction from January to July. The 62 percent drop goes against the 158 percent increase in the period from August to December 2022 [11].

The issue demonstrates that Brazil is a highly advanced country when it comes to climate legislation. The country has long been developing the issue in national legislation and through international treaties and agreements. Therefore, what is presented internally as "Climate Law" is a strong legal current for climate protection.

This requires harmony between the social minimum, the guarantee of a dignified existence, good governance, and an ecologically balanced environment. Development

that does not respect the principle of human dignity, which has an ecological dimension, cannot be considered sustainable [12].

In this respect, the dignity of the human person has an ecological dimension, which is not limited to a biological or physical extension, but encompasses the quality of the environment in which life develops. There is an interaction between the natural dimension and the ecological dimension (broader than environmental), with the aim of increasing the standard of safety and quality of life, but not exclusively, of the human person [13]

Brazil has tried to publicize its commitment to sustainable development, the 2030 Agenda, and the Paris Agreement. Nevertheless, the global goals cannot be empty formulas, at the risk of becoming greenwashing in reverse, i.e., greenwashing by countries and international organizations, which should, in the first analysis, be more reliable in consistent practices. Brazil is seeking to play a leading role in realizing the goals of the 2030 Agenda, as demonstrated by the report on the proposal to adapt the global goals of the 2030 Agenda for Sustainable Development to the Brazilian reality [14].

CONCLUSION

The 40 years of apparent lethargy in the countries' actions in favor of Amazonian cooperation show that the essential role in favor of regional development in the Amazon began not just recently, but decades ago. It is from this perspective that the importance of a common agenda is demonstrated, especially by the Brazilian government, given its desired role in favor of a new climate and ecological agenda. First and foremost, then, he needs to do his homework and fulfill environmental protection and climate preservation within Brazilian territory.

In fact, by failing to comply with its environmental legislation, Brazil has been the target of numerous climate litigations, as demonstrated by the paradigmatic constitutional action challenging the paralyzing of the Amazon Fund.

Climate law and climate litigation are becoming increasingly common in the world and Brazil has realized this in practice. Brazil has built a strong regulatory framework based on strict environmental legislation. Therefore, when the country fails to comply with its own legislation, it is the target of so-called climate litigation and serves as a negative global example, an agenda that the country does not want at all.

What is new is Brazil's commitment to international treaties and agendas, such as the 2030 Agenda and the Paris Agreement, which are general guidelines for combating climate change and in favor of sustainable development. Consequently, they also serve as guidelines for Amazon protection and must be understood in line with the Amazon Cooperation Treaty.

Brazil cannot deliberately choose silence through omission as an environmental position. So, Brazil must be guided by ecological solidarity within its common agenda. Even because the government's disregard for the Amazon Fund was capable of paralyzing projects developed in the region and causing an increase in deforestation in the Amazon.

REFERENCES

[1] *MapBiomas Brasil*. (2023). [Dados de área (ha) de cobertura e uso da terra na Amazônia legal de 1985 a 2022.]. https://brasil.mapbiomas.org/estatisticas/

[2] *Amazon fund*. (2023). Brazilian Development Bank. https://www.fundoamazonia.gov.br/en/home/

[3] Landau, G. (1980). The Treaty for Amazonian Cooperation: A Bold New Instrument for Development. *Georgia Journal of International & Comparative Law*, *10*(3), 463–489, p. 486-87.

[4] Wedy, G. (2023). *Litígios Climáticos: De acordo com o direito brasileiro, norte-americano e alemão*. Fórum.

[5] Julgamento da 'Pauta Verde' no STF é marco de avanços ambientais em 2022. (2022). *WWF Brasil*. https://www.wwf.org.br/?84500/Julgamento-da-Pauta-Verde-no-STF-e-marco-de-avancos-ambientais-em-2022

[6] Ação Direta de Inconstitucionalidade por Omissão n. 59, Rosa Weber (Supremo Tribunal Federal 2023). https://portal.stf.jus.br/processos/detalhe.asp?incidente=5930766

[7] *Amazon Fund in Numbers*. (2023). Brazilian Development Bank. https://www.fundoamazonia.gov.br/en/monitoring-evaluation/fundo-amazonia-em-numeros/index.html

[8] Fundo Amazônia recebe doações de Suíça e EUA. (2023). *Brazilian Development Bank.* http://www.bndes.gov.br/wps/portal/site/home/imprensa/noticias/conteudo/fundo-amazonia-recebe-doacoes-de-suica-e-eua

[9] *Profisc I - B - Instituto Brasileiro do Meio Ambiente e dos Recursos Naturais Renováveis*. (2023). Amazon fund. https://www.fundoamazonia.gov.br/pt/projeto/Profisc-I-B/

[10] *Nota Técnica PRODES Amazônia 2023*. (2023). Instituto Nacional de Pesquisas Espaciais. https://www.gov.br/inpe/pt-br/assuntos/ultimas-noticias/estimativa-de-desmatamento-na-amazonia-legal-para-2023-e-de-9-001-km2

[11] Desmatamento na Amazônia tem queda histórica de 66% em julho. (2023). *Serviços e Informações do Brasil*. https://www.gov.br/pt-br/noticias/meio-ambiente-e-clima/2023/08/desmatamento-na-amazonia-tem-queda-historica-de-66-em-julho

[12] Wedy, G. (2018). *Desenvolvimento Sustentável na Era das Mudanças Climáticas: Um direito fundamental*. Saraiva Educação S.A.

[13] Fensterseifer, T. (2008). *Direitos Fundamentais E Proteção Do Ambiente: A Dimensão Ecológica Da Dignidade Humana*. Livraria do Advogado Editora.

[14] Andrade da Silva, E. R. (2018). *Repositório do Conhecimento do Ipea: Agenda 2030—ODS - Metas nacionais dos objetivos de desenvolvimento sustentável: Proposta de adequação*. Instituto de Pesquisa Econômica Aplicada (Ipea). https://repositorio.ipea.gov.br/handle/11058/8636

ANALYSIS OF IMPACTS OF WAR ON ECOSYSTEMS OF PROTECTED AREAS UKRAINE

Prof. Oleksandr Trofymchuk

PhD Vyacheslav Vishnyakov

PhD Natalia Sheviakina

PhD Viktoriia Klymenko

PhD Snizhana Zahorodnia

Institute of Telecommunications and Global Information Space of the National Academy of Sciences of Ukraine, **Ukraine**

ABSTRACT

The article presents the results of satellite remote sensing to assess the consequences of hostilities in nature protected areas. Since February 24, 2022, 20% of the nature reserve fund of Ukraine has suffered from the war. The real level of damage to the objects of the nature reserve fund as a result of the war cannot be estimated. After all, active hostilities continue, and restrictions are created for environmental activities in the temporarily occupied territories. Therefore, remote monitoring is the only tool for studying changes in the occupied protected areas and territories on the front line.

To analyze satellite data, advanced image processing methods were used, including algorithms for detecting changes and classification based on a series of satellite images of the Sentinel-2A, SkySat and WorldView 01-03 missions, with a spatial resolution of 10 to 0.5 meters. It was found in places of violation of the surface layer of soil by vents, numerous fortifications (trenches, trenches, dugouts), burned out, the tracks were formed due to the active movement of military equipment. The obtained result makes it possible to understand which territories are most affected by hostilities, including the destruction of vegetation, changes in soil cover. The results of the study contribute to understanding the environmental consequences of hostilities and are a valuable tool for managing the environment for post-war recovery in Ukraine.

Keywords: war, satellite remote sensing, protected areas, land cover changes, environmental consequences.

INTRODUCTION

The ongoing war in Ukraine has led to significant damage and destruction of critical environmental sites. Deforestation, outbreaks of forest fires, and increased pollution of wildlife with heavy chemicals [1]. Protected areas play a crucial role in conserving biodiversity and maintaining ecosystem services [2]. More than 20% of protected areas in our country are under occupation or in the war zone. Studies of previous armed conflicts show that the environmental impact of war can be profound and long-lasting, manifesting environmental degradation and loss. Studies such as Negret et al. (2019) have documented significant loss of forest cover as a result of military operations. The loss of

forest habitats, exacerbated by the disruption of natural ecological processes, negatively affects the diversity and abundance of plant and animal species. In addition, Solomon et al. (2018) emphasize the increase in pollution during active armed conflicts. Military operations involve the use of equipment, weapons, and explosives that emit toxic substances, which leads to environmental pollution [3]. Such pollution can have significant and long-term effects, affecting various organisms and ecosystems, leading to reduced biodiversity and disruption of ecosystem functioning. Direct damage to wildlife is another aspect of armed conflict that has been thoroughly studied, with Coppock and Dzivenka (2020) and Braga-Pereira et al. (2020) highlighting injuries and deaths of wildlife as a result of military operations. Collateral damage, disruption of migratory routes and destruction of critical habitats all contribute to the decline of biodiversity in conflict zones. However, it is important to note that biodiversity can also demonstrate the potential for recovery in demilitarized zones characterized by minimal human activity. Such examples can be seen in areas such as the Korean Demilitarized Zone (DMZ). Brady (2021) discusses the regrowth of vegetation and subsequent increase in biodiversity observed in these areas where military restrictions indirectly protect habitats [4].

Satellite remote sensing, with its ability to capture images from space, has proven to be a valuable tool for monitoring and analyzing changes in these conflict-affected areas. The Gulf War between Iraq and Kuwait was one of the first large-scale environmental disasters to be closely monitored using remote sensing technologies such as NOAA, Landsat and SPOT data to assess the impact of urban development, vegetation, and coastal wetlands. In recent years, various satellite missions have provided high-resolution optical and radar data for remote sensing analysis. This includes optical data from satellites such as Sentinel-2A, SkySat, and WorldView 01-03, with spatial resolutions ranging from 10 to 0.5 meters. Additionally, radar data from satellites such as Sentinel-1A, Capella, CSM, RCM1, and ICEYE have provided valuable information due to their ability to penetrate clouds and provide consistent observations regardless of weather conditions. Using these diverse remote sensing datasets, it is possible to assess the extent and nature of damage to protected areas caused by military operations [5, 6]. Satellite image analysis can provide valuable information on various aspects, including changes in land cover, habitat loss, deforestation, and landscape fragmentation [7]. The high spatial resolution of some satellite sensors allows for the identification and mapping of specific objects, such as trenches, craters, and infrastructure damage. Additionally, temporal analysis of remote sensing data allows the progression and intensity of damage to be tracked over time, providing valuable information for current and future conservation efforts. By comparing images before and after military operations, it is possible to quantify impacts, describe the nature of environmental damage, and assess the potential for natural recovery [8]. The purpose of this paper is to present the results of a large-scale satellite remote sensing analysis conducted in the protected areas that are occupied and affected by military operations in Ukraine. The study uses optical and radar data from various satellites to assess and document the extent of damage, formulate effective strategies for restoration and environmental protection.

MATERIALS AND METHODS

According to the State Cadastre of the Nature Reserve Fund, as of the beginning of 2023, there were 8,633 territories and objects of the nature reserve fund. According to the Ministry of Environmental Protection and Natural Resources of Ukraine, the war has

affected 900 protected areas with a total area of 1.2 million hectares. This is about a third of the total area of the nature reserve fund of Ukraine. There are currently 20 nature reserves and national parks in the temporarily occupied territory [9]. Askania-Nova is one of the largest, most famous, and oldest nature reserves in Ukraine [10]. Since the beginning of March 2022 and until now, the Ivory Coast of Sviatoslav National Nature Park located in the Mykolaiv region has been in the zone of active hostilities [11]. It is an object of the Nature Reserve Fund of Ukraine for the protection, popularization and restoration of a part of the Kinburn Peninsula.

This publication presents a study of the occupied territory of the Kinburn Peninsula, which is located in the Kherson and Mykolaiv regions. The Kinburn Peninsula separates the Dnipro-Bug estuary from the Black Sea. Dolphins often swim in the coastal waters here and stingrays bask in the sun. Long-legged stilts and kittiwakes, galagos and puffins, terns and gulls, and dozens of other bird species are also common here [12, 13]. They are the rightful owners here, because it is here that they nest and raise their chicks, and pink pelicans come with their young in search of food. The area under study remained important for the conservation of the white-tailed eagles (Haliaeetus albicilla) before the war. Up to 3 pairs of the white-tailed eagles bred on the Kinburn Peninsula, although several dozen to 300 birds gather here for wintering every year. The threat to the white-tailed eagle can also be a direct hit (rupture) of cluster munitions in the place of traditional concentration of the bird (up to 60% of the winter concentration), as well as damage to wintering places and the factor of disturbance that will force the bird to look for new feeding places during the critical winter period. The white-tailed eagle is listed in the Red Data Book of Ukraine, the Red List of the International Union for Conservation of Nature, the European Red List, and is protected by the Bonn and Bern Conventions.

Among the most common problems faced by protected areas (PAs) under occupation are loss of control, damage to the territories by military equipment, construction of trenches and fortifications, intimidation of animals, mining of territories, shelling, poaching, and humanitarian crisis.

In the course of the research, a series of satellite images from the Sentinel-2A, SkySat and WorldView 01-03 missions were processed with a spatial resolution of 10 to 0.5 meters, as well as radar data from such satellites as Sentinel-1A, Capella, CSM, RCM1 and ICEYE. The following processing methods were used to decipher the satellite images:

- Preliminary image processing was performed to correct and enhance satellite images to ensure accurate interpretation. This included processes such as radiometric and geometric correction, atmospheric correction and noise reduction.
- Satellite images were classified into different classes based on their spectral characteristics. The methods of controlled, unsupervised and object classification were used to identify trenches, potholes, and craters formed as a result of shell explosions and the presence of military equipment on the territory.
- Change detection methods were used to identify and analyze changes that have occurred over time in protected areas by comparing several satellite images taken at different time intervals. Image differentiation, normalized difference vegetation index (NDVI) differentiation, and image correlation.
- Feature extraction - extracts certain features from satellite images, such as roads, buildings, and other military features.

- Combining multiple satellite images with different spectral or spatial resolutions to create a composite image with enhanced spatial and spectral information.
- Geospatial analysis is performed.

The use of these methods made it possible to obtain up-to-date and objective information on the state of the studied territory of the nature reserve complex.

RESULT

The authors used FIRMS data for the period from February 24, 2022, for the study according to the methodology described above. Satellite monitoring was carried out using optical remote sensing data of high and ultra-high spatial resolution - Sentinel-2A (10 m), SkySat (0.5 m), WorldView 01-03 (0.5 m), radar remote sensing data - Sentinel-1A, Capella, CSM, RCM1, ICEYE. The space images were analyzed to detect the presence of enemy military equipment, construction of various fortifications (trenches, trenches, shelters for equipment), presence of firing positions, location and movement of automobile and other large vehicles, as well as surface and submerged watercraft to establish evidence of the impact of military operations on the protected area As a result of the work, 2 thematic maps and 38 situational maps were created. The availability of such a large number of situational maps makes it possible to conduct high-quality monitoring and determine the state of these areas, while proving the facts of ecosystem disruption as a result of military operations. The analysis of situational maps in the observation areas showed that satellite monitoring of the Kinburn Peninsula was carried out 13 times in 2022 and 26 times in 2023.

An analysis of satellite imagery data from the WorldView 03 spacecraft as of 14:41 (Kyiv time) on June 3, 2022, was carried out on the territory of the Kinburn Peninsula. More than 2,100 hectares of the destroyed surface of the nature reserve area were identified in the survey area as a result of the construction of various fortifications (trenches, trenches, shelters for equipment), firing positions, craters, destroyed buildings and burned areas. The processing of remote sensing data revealed the presence of military (499 units) and automotive (45 units) equipment and numerous signs of its movement over rough terrain.

To determine the dynamics of military influence and identify changes in the study area, satellite images taken in March 2023 were analyzed. According to satellite imagery from the WorldView 03 spacecraft, as of 10:58 a.m. (Kyiv time) on 13.03.2023, 22.2 km of trenches, 21 km2 of burned areas, 159 shell craters with a total area of 6,406 m2 and 60 military vehicles were identified in the survey area. In general, according to the available satellite imagery data, the location of 1751 units of various military objects was identified near the land territory of the Kinburn Peninsula, including: samples of weapons and military equipment - 499 units, fortifications of terrain equipment - 1189 units, vehicles and large equipment - 45 units, firing positions of weapons and military equipment, including MLRS - 11 units.

The consequences of ecosystem disturbance in protected areas lead to the suspension of nesting of rare bird species, disruption of their habitats, destruction of Black Sea landscapes and, as a result, the food supply for rare and endangered species of animals, insects, arachnids, etc. The territory of the Kinburn Peninsulais an important element of the ecosystem, especially for the population of the white-tailed eagle. Regular explosions

and fires scare the eagles away from the Kinburn Peninsula, as well as other waterfowl that are the basis of this predator's winter feeding.

The deployment of a significant number of military equipment and personnel in nature reserves leads to the suspension of nesting of rare bird species, disruption of their habitats, destruction of Black Sea landscapes and, as a result, the food supply for rare and endangered species of animals, insects, arachnids, etc.

All this will negatively affect all living organisms in the Black Sea region, changing ecosystems and disrupting food chains. Downstream, there are territories and water areas that are protected at the national level and are areas of international importance: The Dnipro-Bug Estuary, Kinburn Peninsula, Ivory Coast of Sviatoslav National Nature Park, Oleshky Sands National Nature Park, and other national parks.

Based on the results obtained in this article, the authors have proved the effectiveness of using remote sensing methods to conduct monitoring studies to identify areas of soil surface disturbance as a result of military operations. Such studies indicate the need to increase the frequency of research of these areas. Continuous monitoring will facilitate a qualitative analysis of the impact of hostilities and prove the presence of enemy military equipment, construction of various fortifications, presence of firing positions, location and movement of automobile and other large vehicles. This publication pays special attention to the study of nature reserve complexes, taking into account the value of the protected area.

CONCLUSION

The findings will improve our understanding of the impact of armed conflict on the natural environment and will inform future monitoring and conservation efforts in conflict-affected areas around the world. The integration of satellite remote sensing with environmental data and conservation planning can provide decision makers with important information for the sustainable management and restoration of protected areas affected by military operations.

The impact of the ongoing war in Ukraine on valuable protected areas raises serious concerns about the ability to preserve nature and biodiversity. According to the results of satellite monitoring of protected areas, the location of 1751 units of various military objects was established, including: samples of weapons and military equipment - 499 units, fortifications of local equipment - 1189 units, transport and large-sized equipment - 45 units, firing positions of weapons and military equipment and, in particular, MLRS - 11 units. It is proved that the war unleashed by Russia causes great damage to the nature-protected areas of Ukraine. The study confirms the need to take urgent measures to protect protected areas from hostilities. Monitoring the state of natural areas and biodiversity, establishing pollution control measures, and reconstructing damaged ecosystems are important. Satellite observations indicate that the situation on these issues is changing for the worse. As the war continues in Ukraine, space monitoring to detect violations of the ecosystem of protected areas as a result of military operations is extremely relevant and necessary. It is extremely important to assess the damage that the Russian army has caused and continues to cause as a result of a full-scale war on the territory of Ukraine.

The results of the study contribute to the effective planning of appropriate measures to assess changes in the environment and make decisions on its protection and restoration. In the future, these data will be necessary for recreational and related additional environmental conservation activities.

ACKNOWLEDGMENTS The author S. Zahorodnia, express their gratitude to the Department of Geography of the University of Cambridge for their support in continuing research with the aim of improving academic qualifications.

REFERENCES

[1] Serhii, A. Shevchuk, Viktor I. Vyshnevskyi, and P. Bilous Olena (2022) The Use of Remote Sensing Data for Investigation of Environmental Consequences of Russia-Ukraine War. Journal of Landscape Ecology (Berlin, Germany). 15.3 (2022): 36-53. DOI:10.21203/rs.3.rs-1770802/v1

[2] Lawrence, Michael J, Holly L.J Stemberger, Aaron J Zolderdo, Daniel P Struthers, and Steven J Cooke (2015) The Effects of Modern War and Military Activities on Biodiversity and the Environment. Environmental Reviews 23.4 (2015): 443-60. DOI: 10.1139/er-2015-0039

[3] Pereira, P., Bašić, F., Bogunovic, I., and D. Barcelo (2022). Russian-Ukrainian War Impacts the Total Environment. The Science of the Total Environment 837: DOI: 10.1016/j.scitotenv.2022.155865.

[4] Brady, Lisa M. (2021). From War Zone to Biosphere Reserve: The Korean DMZ as a Scientific Landscape. Notes and Records: The Royal Society Journal of the History of Science, 75(2), 189-205. https://doi.org/10.1098/rsnr.2020.0023

[5] Yelistratova, L.O., Apostolov O.A., A.Ya Khodorovskyi, A.V. Khyzhniak, O.V. Tomchenko, and V.I. Lialko (2022) Use of satellite information for evaluation of socio-economic consequences of the war in Ukraine. Ukrainian Geographical Journal 2022.2 (2022): 11-18. DOI: 10.15407/ugz2022.02.011

[6] Yelistratova, L., Apostolov, A., Movchan, D. (2022). Using night illumination images based on remote sensing data for the socio-economic assessment of a besieged city (Mariupol City, (Ukraine) as an example). Publishing House “Baltija Publishing”, 2022, P 82-85 DOI https://doi.org/10.30525/978-9934-26-235-7-19

[7] Oleksandr Trofymchuk, Vyacheslav Vishnyakov, Natalia Sheviakina, Viktoriia Klymenko, Serhii Slastin (2022) Monitoring of fires and assessment of changes in the state of nature-protected territories of Ukraine as a result of military operations. International Multidisciplinary Scientific GeoConference – SGEM, 2022 (2), pp. 369 – 377. DOI 10.5593/sgem2022V/3.2/s14.43

[8] Tomchenko, O., Khyzhniak, A., Sheviakina, N., Zahorodnia, S., Yelistratova, L., Yakovenko, M. & Stakhiv, I.(2023).Assessment and monitoring of fires caused by the War in Ukraine on Landscape scale. Journal of Landscape Ecology,16(2) 76-97. DOI: 10.2478/jlecol-2023-0011

[9] Blazheevska Y. (2023) War and the environment: protected areas affected. www.checkregion-ua.info . https://www.checkregion-ua.info/viina-ta-dovkillia-pryrodookhoronni-terytorii-iaki-postrazhdaly/

[10] Ministry of Environment and Natural Resources of Ukraine (2023) Due to the actions of the occupiers, about 300 hectares of protected steppe in "Askania-Nova" https://mepr.gov.ua/cherez-diyi-okupantiv-zgorilo-blyzko-300-ga-zapovidnogo-stepu-u-askaniyi-novij/

[11] Ivory Coast of Sviatoslav National Nature Park https://wownature.in.ua/parky-i-zapovidnyky/natsionalnyy-pryrodnyy-park-biloberezhzhia-sviatoslava/
[12] Havryliuk M. (2022) How russia's war against Ukraine can affect birds. Ukrainian Nature Conservation Group. https://uncg.org.ua/en/how-russias-war-against-ukraine-can-affect-birds/
[13] Dudkin O. (2022) The impact of the Russian invasion of Ukraine on wild birds and their habitats. BirdLife International. https://www.birdlife.org/news/2022/08/23/impact-russian-invasion-ukraine-wild-birds-habitats/

CARBON DYNAMICS IN DECIDIOUS FORESTS ON ORGANIC SOILS: ASSESING FOREST OFFSET IN RESPONSE TO DRAINAGE DISRUPTION

Mg. silv. Kārlis Bičkovskis[1,2]

Mg. silv. Valters Samariks[1,2]**,**

Dr. silv. Āris Jansons[1,2]

[1] Latvian State Forest Research Institute "Silava", **Latvia**
[2] Latvia University of Life Sciences and Technology, **Latvia**

ABSTRACT

Forest ecosystems are essential when dealing with climate change mitigation goals. Carbon stock of forest stand can hold substantial amounts of carbon as well products made from wood provide substitution effect, reducing reliance on fossil fuels. Silvicultural practices, such as drainage, have proven to be highly efficient of enhancing tree volume, aligning with climate change mitigation goals. As forest drainage disruption for rewetting of drained areas gains momentum with appealing goals such as enhancing biological diversity and restoring natural ecosystems, it becomes imperative to account for the consequential trade-offs. While these efforts hold promise for achieving ecological objectives, it is crucial to recognize that carbon sequestration dynamics within these areas may undergo significant alterations. Notably, the years required to offset carbon losses resulting from deadwood formation may no longer align with climate change mitigation targets, necessitating a comprehensive understanding of the interplay between drainage disruption, carbon dynamics, and climate goals.

Aim of the study was to quantify carbon dynamics in tree carbon pool 15 years after drainage disruption. Our central research question revolves around understanding when newly established forest can offset carbon losses resulting from deadwood formation and decay in their predecessors. Our findings suggest that, on average, the new forest stand is poised to offset these losses in approximately 12-15 years. These insights are critical for forest management strategies aimed at maximizing carbon sequestration and mitigating climate change impacts.

Keywords: Carbon dynamics, drainage disruption, organic soils, stand replacement

INTRODUCTION

Forests play a pivotal role in climate regulation, acting as substantial carbon (C) sinks through the absorption of carbon dioxide in tree biomass. The C sequestration rates and total C stock that a forest stand can attain during one rotation are contingent upon growth conditions, species composition and silvicultural practises. Growth potential for particular forest stand more commonly is expressed through site index, indicating the attainment of species-specific height in relation to stand age. Silvicultural practises such as forest drainage can increase site index as this intervention directly enhance site productivity. Drainage system ensure lower groundwater level so that soil is more aerated, thus creating more favourable growth conditions. In Latvia forest drainage systems were actively established during 1960-1990 in total draining 700

thousand hectares of forested land. Studies show that this intervention has resulted in obtaining higher site index as stand productivity can increase 3-4 times compared to non-drained conditions[1]. This, in turn, amplifies C sequestration within the wood biomass, and thus providing substitution effect which reduces reliance on fossil fuels[2].

Disruption of drainage system has adverse effects, resembling those of natural disturbances like flooding of forest stand. Over time, drainage ditches become overgrown, lose their designed profiles, and are often obstructed by sedimentation or beaver dams. Research in Latvia indicates a significant decline in drainage system functionality after 25 years without maintenance [3]. Beaver dams disrupting drainage can revert the groundwater level to pre-drained conditions, potentially leading to stand replacement. Consequently, the potential for C storage in tree biomass diminishes with declining site productivity following such transformations.

C dynamics after a stand replacement disturbance can be significantly altered. After a natural disturbances forest ecosystem can be short term C source [3], however after a time (10-40 years) as new tree cohort develop, forest ecosystem turns to C sink [4][5]. Regenerated tree cohort can show increased forest growth when fast growing early-serial species occupy area post-disturbance. This can be attributed to reduced competition with previous generation trees and released nutrient availability due to deadwood decay[4]. C dynamics after stand replacement disturbance is affected by decomposition rates of deadwood. The decomposition rate of deadwood is primarily influenced by microbial activity, a process tightly regulated by temperature and moisture conditions. Generally, in warm and wet conditions deadwood decomposes faster. Moreover, wood traits and the physical position of dead wood, whether as a standing snag or a downed log, significantly influence decay rates, with lying deadwood acting as a short-term C reservoir [6].

This study aims to analyze C dynamics in a tree biomass 15 years after drainage disruption. Our specific objectives include understanding the accumulation dynamics of C in tree biomass, determining the duration required for the living tree biomass to offset C losses, and quantifying the emissions resulting from these stand transformations.

MATERIALS AND METHODS

A drained peatland site, located in hemi-boreal forest zone in the Eastern Baltic region (56° 55’ 07.7”, 23° 33’ 58.6”) was studied. The study was conducted within the territory of Kemeri National Park. Drainage system was established around the 1960s. The area initially was designated for commercial use of timber production. However, in 1997, it was incorporated into the status of a national park, leading to the cessation of management activities and initiating a natural process-driven forest development. The drainage system within this area has remained unmanaged for the past 30 years, significantly reducing its functionality.

Due to beaver damming activities, site remained in a prolonged flooded state, initiating a rapid decline of the overstory trees. Orthophoto images obtained every three years illustrates the developmental trajectory of forest stand (Fig. 1). This allows the tracking of stages of development and providing insights into the approximate year of disturbance initiation (2007) as well as observation of following regeneration of advanced growth.

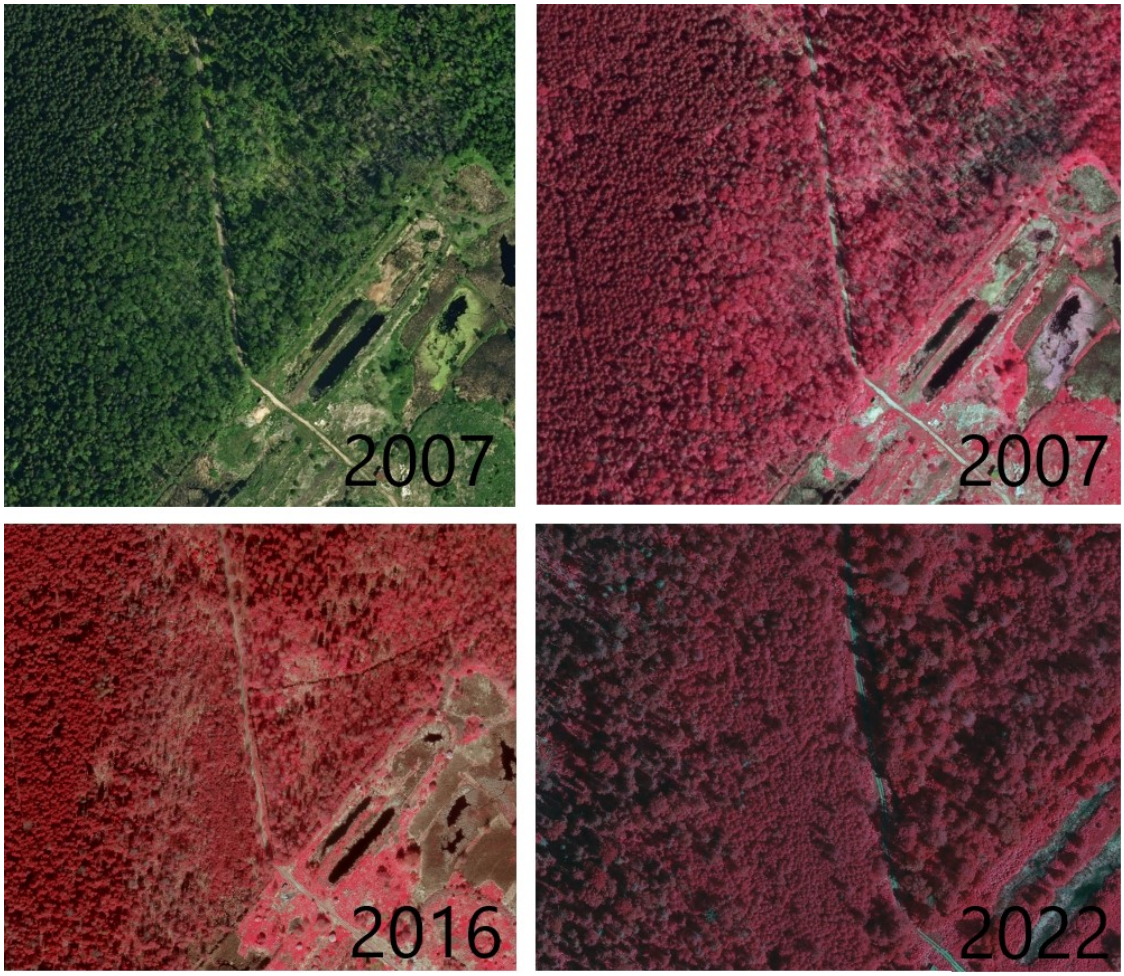

Fig. 1. **Orthophotos (2007 – 2022) of studied object**

For this study, inventory data from two stands with dominating deciduous trees were utilized. The previous stand overstory tree layer consisted predominantly of silver birch (*Betula pendula*) with an average age exceeding 100 years (Table 1). Admixture of conifer species – Norway spruce (*Picea abies*) and other deciduous species such as black alder (*Alnus incana*), ash (*Fraxinus excelsior*) and European aspen *(Populus tremula*) were present.

Table 1. **Inventory data of studied object before drainage disruption**

Stand nr.	Site index	H, m	DBH, cm	Age	Basal area, m^2 ha^{-1}	Standing volume, m^3 ha^{-1}
11	II	28	34	111	33	478
13	III	24	29	101	26	276

In each stand, two circular sample plots of 500 m² were established. All tree diameters at breast height (DBH) larger than 6.1 cm were measured within each circular sample plot. Additionally, smaller subplots of 25 m^2 were created for advanced growth (DBH 2.1 - 6.1 cm. Heights of living trees were measured for 5-7 trees of each species for each

canopy layer. Similarly, tree core samples were collected for all species of all canopy layers. All height measurements were taken for standing dead trees with DBH larger than 6.1 cm. For dead lying trees diameters at both ends were measured for any sections within sample plot that reached diameter 6.1 cm and length of 1 meter. The decay class of each deadwood was recorded using the "knife" method, categorized into five decay stages according to Köster et al.[7].

Heights of living trees and dead standing trees with tops were estimated using Gaffrey's models [8]. The C stock of living tree biomass of the previous stand was calculated based on the forest inventory data using local equations developed by Liepiņš[9]. Stand volume and composition index was used as factors to estimate the C stock of the stand. The C stock was obtained by calculating both aboveground and belowground using (1) equation:

$$Y_{sc} = a * GS_s^{b1} * CI_s^{b2},$$

Where Y is stand biomass (t), GS is growing stock (m^3), CI is species composition index and a, b1, b2 are species specific coefficients.

Due to the unavailability of data on the quantity of deadwood before disturbance, an average 6 t C ha^{-1} was adopted for this study based on local studies by Šēnhofa [10].

C stock of tree biomass post disturbance was calculated by individual tree biomass and C concentration calculations specific to each tree species, following equations developed by Liepiņš [11]. A truncated cone formula was used to determine the volume of the lying deadwood and dead standing trees with broken tops. The deadwood C pool was calculated as a product of deadwood volume estimates, decay class-specific densities and species specific C content [7].

The change in C stock due to stand replacement is determined by subtracting the C stock of the previous stand from the C stock of the remaining trees from the first generation that are still present in the new stand at the time of measurement. Emission rate were estimated based on the C stock generated from the difference in previous generation trees, divided by the duration since disturbance (15 years). The average age of the new generation trees was determined from wood core samples. The course of C accumulation by decades for the black alder was taken from NFI data for undrained site types.

We used anova (α=0.05) to test decay class effect on C stock in deadwood. Data analysis were performed using R [12].

RESULTS

Forest stand has undergone significant changes in dominant forest floor, with black alder regeneration replacing previously dominating birch stand. Standing volume of first-generation canopy layer has decreased more than 8 times during 15-year period (table 2).

Table 2. **Stand parameters 15 years after disturbance.**

Stand component	Dominant Species	H, m	DBH, cm	Age	Standing volume, m^3 ha^{-1}	Stand density, trees ha^{-1}
Advanced growth	Black alder	5.7±0.2	3.02±0.2	8.6±0.7	3.6±1.8	1300±295
New trees	Black alder	12.4±0.1	11±0.2	12,7±0.7	53.8±26.9	1330±240
Old trees	Birch	17.1±1.7	23.7±2	84.2±6.8	44.9±19.6	75±37

The total C stock of tree biomass before disturbance is estimated at an average of 149.6 ±23.5 t C ha^{-1} (Fig. 2). Following disturbance, the C stock in living trees of the previous generation averaged 16.8 ±7.8 t C ha-1, while deadwood exhibited an average of 24.4 ±0.2 t C ha-1. Specifically, average C stock in dead lying trees, dead standing trees, and snags were estimates are 11.29 ±0.99, 4.38 ±3.49, and 8.70 ±1.66 C t ha^{-1} respectively. Results show that decay class has a significant effect on C stock in deadwood (p-value = 0.00332).

The new generation of trees displayed substantial regrowth, averaging 37.4 ±14.9 t C ha^{-1}, with a stocking density averaging 1330 trees ha^{-1}. The estimated C loss from the previous generation of trees accounts for 102.4 ±15.8 t C ha-1, resulting in an average annual emission of 6.8 ±1 t C ha^{-1} over a 15-year period.

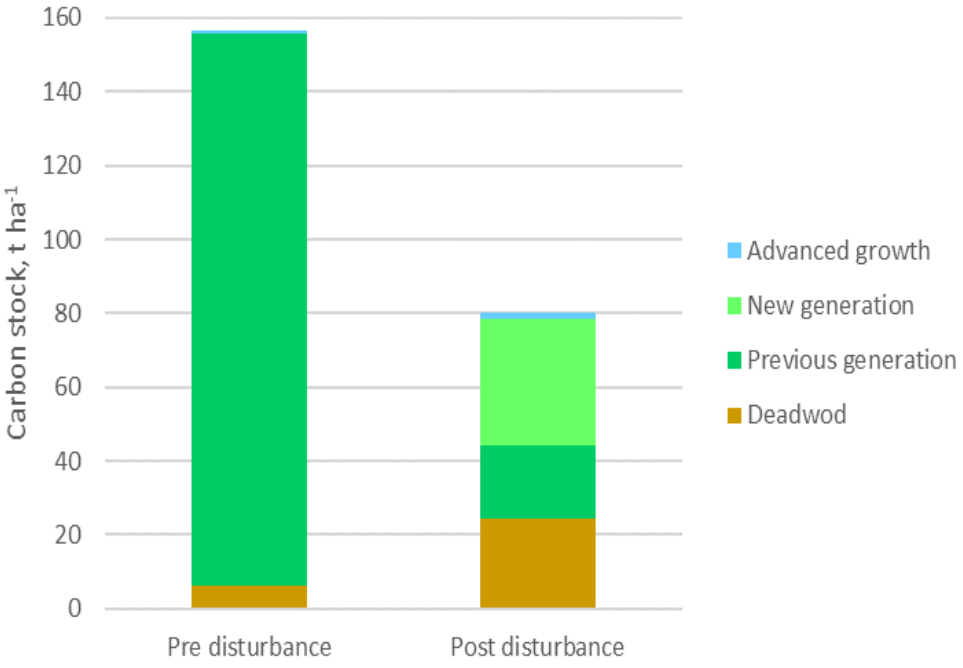

Fig. 2. Carbon stock of tree biomass before and after drainage disruption

Over the stand replacement period, there is a noticeable decline in the average C stock. Our findings reveal that, following a 15-year interval, the prevailing trend of diminishing C stock in living trees undergoes a significant shift, indicating a noteworthy

alteration in C dynamics, averaging 78.7 ±7.3 t C ha^{-1} of total C pool in tree biomass including deadwood. National Forest Inventory (NFI) data shows that the black alder's yearly growth rate on organic wet soils averages 1.4 t C ha^{-1} and potentially reaches its peak within 61-70 years at 129 ±13.10 t C ha^{-1} (Fig.3). Our estimations indicate a transition in the forest stand from being a C source to a C sink in the second decade, with the new generation's C stock offsetting C losses from deadwood.

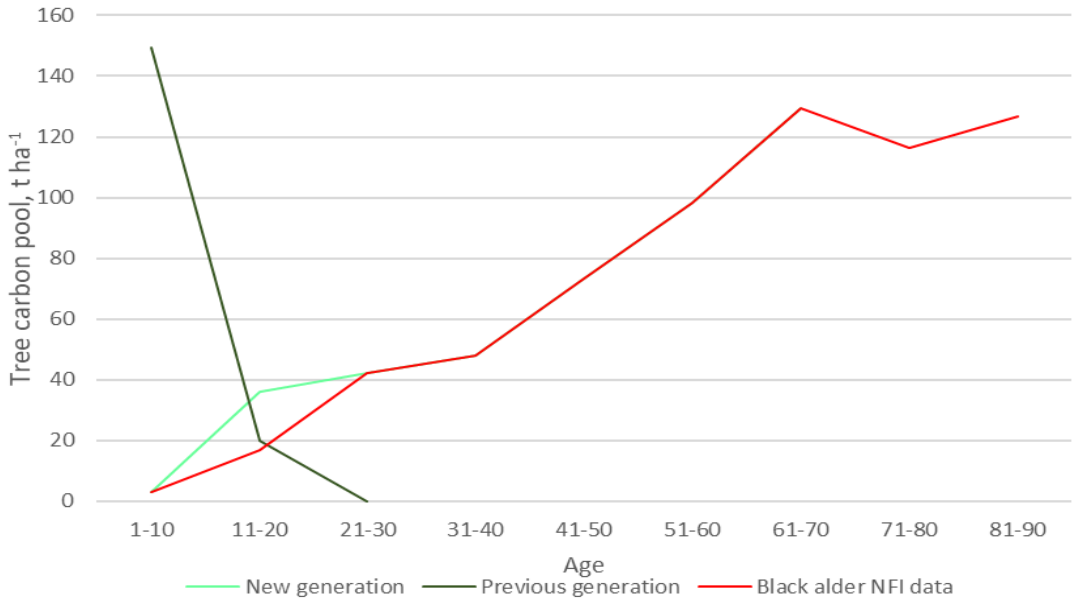

Fig. 3. **Projected carbon dynamics after stand replacement**

DISCUSSION

Prior studies have demonstrated that disturbances can lead to diverse trajectories in forest C dynamics and may require decades to recover from disturbance related C losses. Our case study indicates that a severe disturbance has the potential to transform a forest landscape into a net C source, with a compensatory period of around two decades to recover from the C loss induced by the disturbance. The birch, reaching its biological age, demonstrated diminished resilience to disturbance, leading to rapid stand collapse and thus emissions of 6.8 tons ha^{-1} during 15-year period. The combined effect of altered moisture conditions and the inherent decay characteristics of birch softwood contributes to the observed high rates of deadwood decomposition in our study.

The reduction of 72% in the C stock of the previous generation of trees has resulted in an average decline of 52% in the total C stock of tree biomass in a forest stand 15 years after the disturbance. However, compensatory regrowth from the new generation of trees appears to offset these C losses within 12-15 years which is consistent with findings from other studies indicating a short-term C source after stand replacement disturbances [9]. Regenerated tree cohort show on average 45% higher C stock at this age than it is on average in according to NFI data. Thus, our results align with other studies, that shows prosperous regrowth after stand replacement disturbances [10]. It is crucial to highlight that black alder stands demonstrate robust growth in wet conditions,

potentially accumulating 129 t C ha^{-1} within the 61-70-year range. However, this accumulation level falls short of what was observed for birch in drained soil conditions. This observation underscores a notable decrease in site index in this area after stand replacement, emphasizing the discernible difference between drained and undrained forests. Future growth of the stand is not easily predictable. With the dense regeneration, some trees may succumb to competition and follow a trajectory similar to the NFI results.

This study highlights that, without management interventions post-disturbance, most deadwood contributes to emissions through decay. A selective harvest approach could reduce emissions, offering a substitution effect. It is advisable to contemplate a moderate harvest, preserving some standing stock to foster biodiversity through retained deadwood. Additionally, the utilization of part of harvested timber products would prolong captured C in this reservoir.

CONCLUSION

Stand-replacement disturbances significantly alter C dynamics in forest ecosystems. This study offers insights into the stand's development following natural stand replacement resulting from drainage disruption. Deciduous forest stand attaining its biological age experiences rapid collapse after disturbance and following quick deadwood decomposition, resulting in annual emissions averaging 6.8 tons. Despite the swift decomposition of the previous generation's trees, rapid regeneration turns the stand into a C sink with 37.4 t C ha^{-1} after 12-15 years.

The extensive establishment of forest drainage systems has implications for ongoing debates in Europe regarding the future management of drained forests. Our findings emphasize the necessity of a holistic approach that considers the interplay between silvicultural practices, natural disturbances, and C dynamics. Although re-wetting drained areas may seem beneficial for other ecosystem values, trade-offs should be accounted for when deciding on management strategies. Therefore, further research would be necessary to investigate C dynamics after drainage disruption incorporating also other tree species and different management intensities in order to improve management strategies for acquiring different goals.

ACKNOWLEDGEMENTS

This research was funded by project “Tool for assessment of C turnover and greenhouse gas fluxes in broadleaved tree stands with consideration of internal stem decay (Nr. 1.1.1.1/21/A/063)""

REFERENCES

[1.] Zālītis, P. *Mežs Un Ūdens*; 2012; ISBN 9789934801662.

[2.] Leskinen, P.; Cardellini, G.; González-García, S.; Hurmekoski, E.; Sathre, R.; Seppälä, J.; Smyth, C.; Stern, T.; Verkerk, P.J.; Johannes, P. Substitution Effects

of Wood-Based Products in Climate Change Mitigation., doi:10.36333/fs07.

[3.] Peters, E.B.; Wythers, K.R.; Bradford, J.B.; Reich, P.B. Influence of Disturbance on Temperate Forest Productivity. *Ecosystems* **2013**, *16*, 95–110, doi:10.1007/S10021-012-9599-Y.

[4.] Zhou, T.; Shi, P.; Jia, G.; Dai, Y.; Zhao, X.; Shangguan3, W.; Du, L.; Wu, H.; Luo, and Y. Age-Dependent Forest Carbon Sink: Estimation via Inverse Modeling. *J. Geophys. Res. Biogeosciences* **2015**, doi:doi:10.1002/2015JG002943.

[5.] Luyssaert S, Inglima I, Jung M, Richardson AD, Reichstein M, Papape D, Piao SL, Schulze E-D, Wingate L, Matteucci G, Aragao L, et al. Age-Dependent Forest Carbon Sink: Estimation via Inverse Modeling. *Glob. Chang. Biol.* **2007**, doi:10.1111/j.1365-2486.2007.01439.x.

[6.] Hararuk, O.; Shaw, C.; Kurz, W.A. Constraining the Organic Matter Decay Parameters in the CBM-CFS3 Using Canadian National Forest Inventory Data and a Bayesian Inversion Technique. *Ecol. Modell.* **2017**, *364*, 1–12, doi:10.1016/J.ECOLMODEL.2017.09.008.

[7.] Köster, K.; Metslaid, M.; Engelhart, J.; Köster, E. Dead Wood Basic Density, and the Concentration of Carbon and Nitrogen for Main Tree Species in Managed Hemiboreal Forests. *For. Ecol. Manage.* **2015**, *354*, 35–42, doi:10.1016/J.FORECO.2015.06.039.

[8.] Sharma, R.P.; Vacek, Z.; Vacek, S. Nonlinear Mixed Effect Height-Diameter Model for Mixed Species Forests in the Central Part of the Czech Republic. *J. For. Sci.* **2016**, *62*, 470–484, doi:10.17221/41/2016-JFS.

[9.] Liepiņš, J.; Lazdiņš, A.; Kalēja, S.; Liepiņš, K. Species Composition Affects the Accuracy of Stand-Level Biomass Models in Hemiboreal Forests. *Land* **2022**, *11*, 1108, doi:10.3390/LAND11071108/S1.

[10.] Šenhofa, S.; Jaunslaviete, I.; Šņepsts, G.; Jansons, J.; Liepa, L.; Jansons, A. Deadwood Characteristics in Mature and Old-Growth Birch Stands and Their Implications for Carbon Storage. *For. 2020, Vol. 11, Page 536* **2020**, *11*, 536, doi:10.3390/F11050536.

[11.] Liepiņš, J.; Lazdiņš, A.; Liepiņš, K. Equations for Estimating Above- and Belowground Biomass of Norway Spruce, Scots Pine, Birch Spp. and European Aspen in Latvia. *https://doi.org/10.1080/02827581.2017.1337923* **2017**, *33*, 58–70, doi:10.1080/02827581.2017.1337923.

[12.] TEAM, R.D.C. R: A Language and Environment for Statistical Computing. 2008.

DEMOGRAPHIC STRUCTURE OF *QUERCUS CANARIENSIS* FROM THE OULED BECHIH FOREST OF ALGERIA

Prof. RACHED-KANOUNI Malika[1]
Assoc. Prof. KARA Karima[2]
Assoc. Prof. REDJAIMIA Lilia[1]
Dr. TOUAFCHIA Boutheyna[1]
Dr. ZERROUKI Alia[1]

[1]Laboratory of natural substances, biomolecules and biotechnological applications, Department of Natural and Life Sciences, Faculty of Exact Sciences and Natural and Life Sciences, Larbi Ben M'Hidi University, Oum El Bouaghi, **Algeria**
[2]Department of Biology and Plant Ecology, Mentouri Brothers University, Constantine1 **Algeria**

ABSTRACT

The main objective of this study is to analyze the demographic structure and spatial distribution of *Quercus canariensis* populations in the Ouled Bechih forest in northeastern Algeria. Knowledge of these parameters is an essential step in their sustainable management. Sample inventory plots measuring 30m x 30m (900m^2) were identified by random sampling. Tree diameter at 1.30 m above the ground and total height of *Q. canariensis* were measured for each tree in four inventory plots. The demographic structures were established according to the classes of diameter and height and adjusted to the theoretical distribution of Weibull. The results show that the highest values of density (178 individuals/ha) and basal area (37.87 m^2/ha) were respectively obtained in plots P2 and P1; while the highest values of Lorey's average height (18.56 m) and quadratic diameter (73.67 cm) were obtained in plot 1. The diameter and height structures show a concentration of adult individuals throughout the stands of this forest. The demographic analysis shows that the diameter structure of plots 1 and 3 present a left asymmetrical distribution, characteristic of monospecific stands with a predominance of old individuals with values of the coefficient c of 4.782 and 5.352 respectively. The values of c for plots 2 and 4 are less than 3.6; these values are of the order of 2.427 (P2) and 3.227 (P4). The distribution according to the diameter of these plots shows a right asymmetrical, characteristic of monospecific stands with a predominance of young individuals. Analysis of the height structure of these stands shows that plot 3 has a "c" value of less than 3.6 while the values of the other plots are greater than 3.6; this result attests to a predominance of tall individuals (10 to 15 m). In the perspective of rehabilitation and sustainable management of forest ecosystems, this study provides additional information on the current state of *Quercus canariensis* stands in the Ouled Bechih forest.

Keywords: Ouled Bechih, *Q. canariensis*, dendrometric parameters, demographic structure.

INTRODUCTION

The Mediterranean character of the Algerian forest is not to be demonstrated given its geographical location and the physiognomy that it presents. This set of trees is in perpetual struggle against man, fire, herds. An adaptation is thus carried out insofar as the tree becoming frugal takes root. This state of uncertain equilibrium is conditioned by the influences of the physical and human environment. These pressures on the forest and the unsustainable exploitation of its resources cause negative impacts on its genetic resources [1]. It is therefore important to find mechanisms for the sustainable management of forest ecosystems. Sustainable forest management requires a better understanding of the ecological and physiognomic aspects of vegetation.

Sustainable use of these important forest ecosystem services requires sustainable forest planning and management. In-depth knowledge of the structural and ecological characteristics of forests is indispensable for this purpose. Indeed, characterizing the structure of a stand comes down to characterizing all of its structural attributes: tree density; basal area; species richness; spatial structure [2] and spatial distribution [3].

The spatial distribution of forest species provides information on the mode of seed dispersal, the evolution of seedlings, their survival and mortality during their life cycle [4]. The study of the spatial distribution of a species makes it possible to understand its dynamics, the ecological processes that influence it, the community life of species, and determines reproduction, dispersion, the use of resources and the distances between individuals [5; 6].

The spatial structure of an ecosystem, ie the way in which the individuals that compose it are organized in space, often plays an essential role in its functioning [7]. It relates to both the vertical and horizontal use of space by the elements of an ecosystem. The population structure of a forest species is generally defined by the diameter distribution of these [8]. The latter can be considered at two levels: the tree stand as a whole or the populations of species. They reflect the dynamic state of the population as a whole, the temperaments of the species, the particular situations and the ecological preferences of the species [8; 9].

Research on the structural and ecological characteristics of forests is therefore essential for sustainable management and constitutes a prerequisite for all planning decisions. It is in this logic that our study on the forest of Ouled Bechih, north-eastern Algeria, is inscribed. The choice of this forest is justified by the fact that it is a favorite area for the valuable species targeted. In the context of sustainable management of natural forest ecosystems, the present study is necessary to determine the dendrometric parameters of *Quercus canariensis* (Willd.), to analyse their demographic structure and to assess the status of natural regeneration of Ouled Bechih forest.

MATERIALS AND METHODS

Presentation of the study area

The Ouled Bechih forest is located in northeastern Algeria. It is recognized for its ecological richness and its biodiversity. It covers a considerable area of 3915.52 hectares; it is located between the geographical coordinates 36° 21′ 26″ N and 7° 50′ 08″ E. The climate of the region is sub-humid characterized by an average annual temperature of 16°C, average annual rainfall of 700 to 900 mm and high atmospheric humidity of 70% [10].

Data collection

Four plots of *Q. canariensis* were randomly chosen, with an equivalent area of 900m² (30m x 30m) [11]. It is preferable to carry out an exhaustive inventory. This consists of counting all the stems by diameter class. This type of inventory is the most commonly used. The description of the populations was carried out on the basis of data on individuals of dbh ≥ 10 cm. The parameters taken into account are:

- Basal area: It is the sum of the basal sections of all the trees of dbh ≥ 10 cm found in the plot, it is expressed in m²/ha:

$$G = \frac{\pi}{4s}\sum_{i=1}^{n} d_i^2$$

With n: total number of trees of dbh ≥ 10 cm in the plot, di: diameter of the tree i (m), s: area of the plot.

- Mean basal area tree diameter: It is the diameter of the tree having a basal area equal to the average basal area, it is expressed in cm

$$Dg = \sqrt{4G/\Pi n}$$

n: total number of trees with dbh ≥ 10 cm in the plot, G: basal area of the plot (m²/ha).

- Average height of Lorey: This is the average height of all the trees present in the plot weighted at their respective basal areas, it is expressed in m:

$$HL = \sum_{i=1}^{n} gihi / \sum_{i=1}^{n} gi$$

n: total number of trees with dbh ≥ 10 cm in the plot, gi: basal area of tree i (m²/ha), hi: total height of tree i (m).

- Demographic structure

The diameter and height structures of the population of *Q. canariensis* were established for the two forests. These structures were fitted to the theoretical Weibull distribution based on the maximum likelihood method [12]. The Weibull distribution with three parameters (a, b and c) is characterized by a probability density function, f(x), which takes the following form [13]:

$$f(x) = \frac{c}{b}(x - a/b)^{c-1} \quad exp\left[-\left(\frac{x-a}{b}\right)^{c}\right]$$

Where "x" is the diameter or height of the trees, "a" is the position parameter, "b" is the scale or size parameter, and "c is the shape parameter related to the observed structure (Table 1). To test the adjustment of the observed structure to the theoretical Weibull

distribution, a log-linear analysis, method of analysis of variance carried out on the logarithm of the densities of the classes, was carried out using the MiniTab 19 software [14]. Adjustment tests were then carried out to check the adequacy between the observed structure and the theoretical distribution.

Table 1. Shape of the Weibull distribution according to the values of the parameter "c".

« c »	Shape of the Weibull distribution
c< 1	Inverted "J" distribution, characteristic of multi-species or uneven-aged stand.
c = 1	Exponentially decreasing distribution, characteristic of populations in extinction.
1 < c < 3.6	Positive asymmetric or right asymmetric distribution, characteristic of monospecific stands with a predominance of young or small diameter individuals.
c = 3.6	Symmetrical distribution; normal structure, characteristic of even-aged or monospecific stands even-aged or monospecific stands of the same cohort.
c > 3.6	Negative or left-skewed distribution, characteristic of monospecific stands with a predominance of older individuals.

RESULTS

Table 2 presents the dendrometric characteristics of *Q. canariensis* in the Ouled Bechih forest. It emerges from the analysis of this table that the values of the different parameters obtained vary between the plots.

Table 1. Dendrometric parameters.

Plots	N (ha)	H_L (m)	D_q (cm)	G (m^2/ha)
P1	89	18.56	73.67	37.87
P2	178	6.81	47.59	32.75
P3	144	16.74	43.68	21.63
P4	144	15.47	44.98	22.94
Average	138.75	14.395	52.48	28.7975

The comparison of the dendrometric parameters of this species reveals a significantly higher average density in plot 2 compared to the others (178 individuals/ha). The basal area also varies according to the plots. The lowest basal area value is obtained for *Q. canariensis* in plot 3 (21.63 m^2/ha), while the highest is obtained in plot 1 (37.87 m^2/ha). The quadratic diameter values and Lorey's mean height are higher in plot 1; they are respectively 73.67 cm and 18.56 m.

The diameter structures of *Q. canariensis* trees in the plots of the Ouled Bechih forest are illustrated in figure 1. The analysis of the latter shows that the diameter structure of

plots 1 and 3 present an asymmetrical distribution with the values of the coefficient c which are 5.083 and 4.015 respectively. The diameter structure of *Q. canariensis* trees in plots 2 and 4 shows values of c between 1 and 3.6; these values vary from 3.227 and 2.427 respectively.

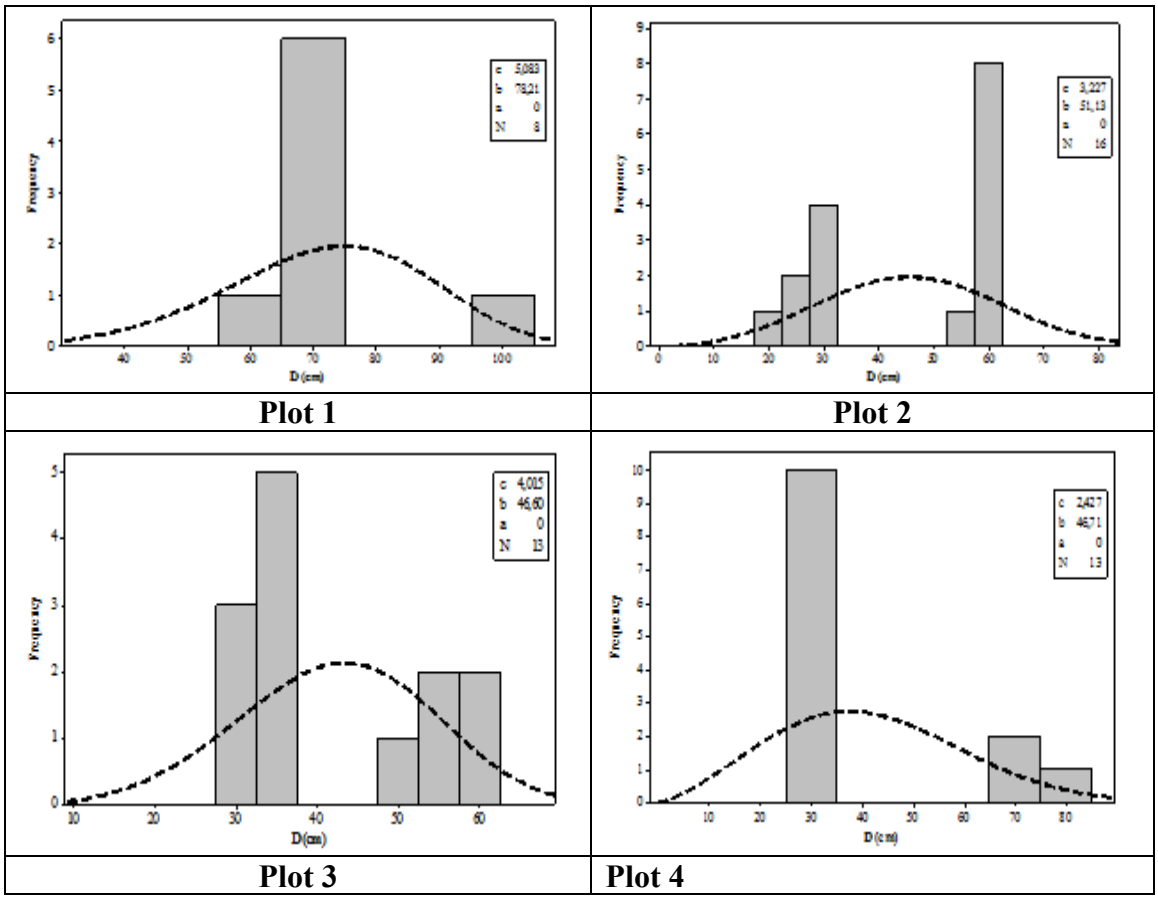

Figure 1. Diameter structure of the Ouled Bechih forest.

The results of the structures in natural stand heights of *Q. canariensis* in the forest are given in figure 2. With the exception of plot 3, this has a "c" value of less than 3.6; analysis of the height structure of these stands shows that the values of the other plots are greater than 3.6; this result attests to a predominance of tall individuals (10 to 20 m). Individuals taller than 20 m are poorly represented in the Ouled Bechih forest.

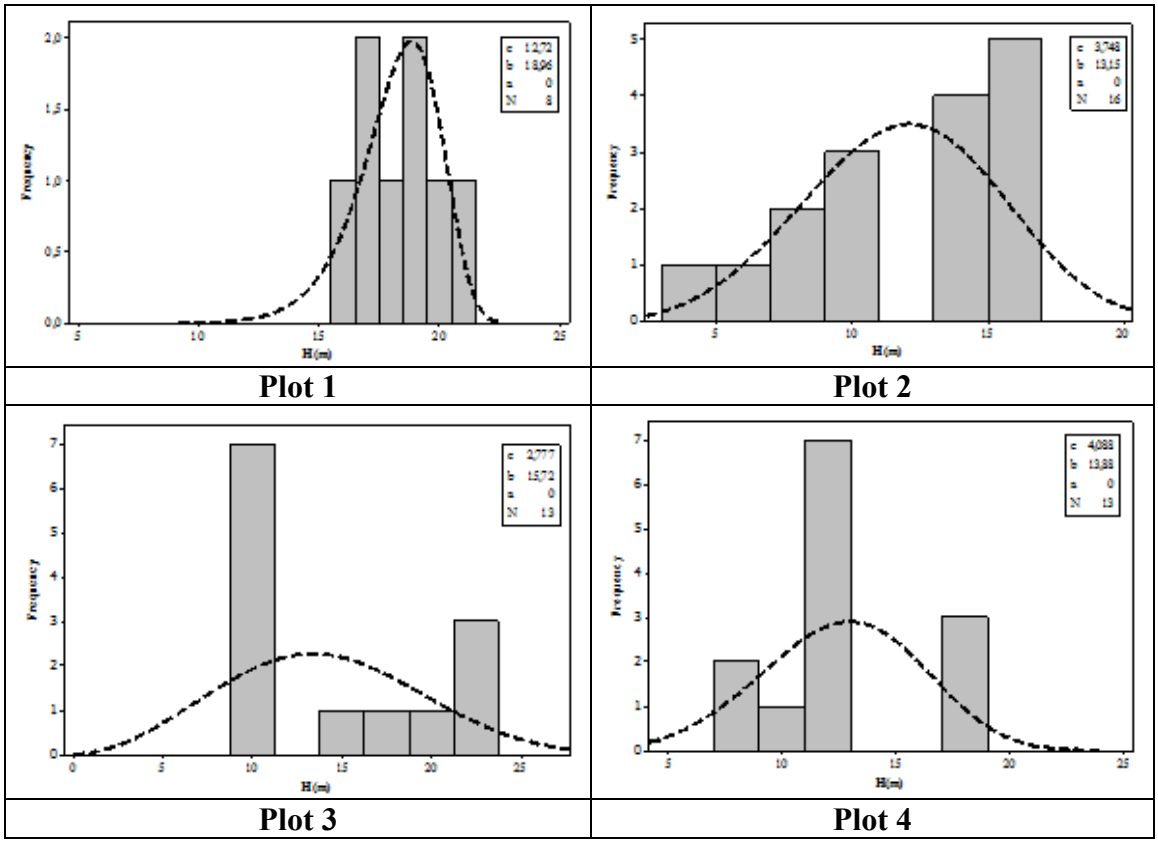

Figure 2. Height structure of the Ouled Bechih forest.

DISCUSSION

Forest stands, depending on whether they are natural or planted, monospecific or multispecific, even-aged or uneven-aged, young or old, have typical structures (characteristics). It is known that the diameter structures of these types of forest stands fit known theoretical distributions [15; 16; 17]. Thus the use of theoretical models is necessary to be aware of any deviations from the standard structures of the stands and thus to deduce the state of life of the stands and to be able to define adequate management options. Also, the parameters of the theoretical distributions considered are useful for better characterizing the structure of the stands.

The distribution by diameter and height classes shows variations according to ecological parameters. According to the literature, adaptations to ecological conditions, competition for resources, anthropozoic activities and exploitation are the basis of this structural variability. The diameter and height structure of the natural stands of *Q. canariensis* in the Ouled Bechih forest reveals the predominance of large-diameter individuals with more or less significant heights. This structure globally reveals a high representativeness of large-diameter old individuals, and predicts a risk for the future of their populations. In natural stands, when the frequency of small-diameter stems (young individuals) is lower than that of large-diameter individuals (old individuals), the future of the stand cannot be guaranteed [18]. This high representativeness of large-diameter individuals can be explained by anthropogenic factors such as overgrazing or repeated fires that are likely to hinder the survival of young plants and make natural regeneration very weak, or even non-existent [19]. Indeed, the potential for regeneration exists, but

the seedlings are unable to cross the seedling stage to the adult stage. The main obstacles are, among others, vegetation fires, pressure from herbivores and reduced rainfall patterns.

CONCLUSION

This study made it possible to characterize the Ouled Bechih forest in terms of demographic structure. This structure tends towards a monospecification, because the majority of individuals participating in the recovery belong to a single species. This study also revealed the existence of weak natural regeneration of *Q. canariensis*. However, it remains subject to strong anthropogenic pressure which contributes to the continuous degradation of this forest ecosystem. This study constitutes on the one hand a reliable scientific database and on the other hand a state of reference for restoration works. It is also important to continue the investigations on the characterization of the herbaceous layer for a global knowledge of the current state of this forest formation.

REFERENCES

[1] Fonton N. H., Atindogbe G., Fandohan B., Lejeune P., Ligot G., Structure spatiale des arbres des savanes boisées et forêts claires soudaniennes : implication pour les enrichissements forestiers, Biotechnologie, Agronomie, Société et Environnement, vol. 16 (4), pp 429-440, 2012.

[2] Pélissier R., Goreaud F., A practical approach to studying the spatial structure in simple cases of heterogeneous vegetation stands, Journal of Vegetation Science, pp 99-108, 2001. https://doi.org/10.1111/j.1654-1103.2001.tb02621.

[3] Condit R., Ashton P. S., Baker P., Bunyavejchewin S., Gunatilleke S., Gunatilleke N., Hubbell S. P., Foster R. B., Itoh A., LaFrankie J. V., Lee H. S., Losos E., Manokaran N., Sukumar R., Yamakura T., Spatial Patterns in the Distribution of Tropical Tree Species, Sciences, Vol. 288, pp 1414-1417, 2000.

[4] Comita L. S., Condit R., Hubbell S. P., Developmental changes in habitat associations of tropical trees, Journal of Ecology, vol. 95, pp 482-492, 2007.

[5] Nishimura S., Yoneda T., Fujii S., Mukhtar E., Kanzaki M., Spatial patterns and habitat associations of Fagaceae in a hill dipterocarp forest in Ulu Gadut, West Sumatra, Journal of Tropical Ecology, vol. 24, pp 535-550, 2008.

[6] Wiegand T., Gunatilleke S., Gunatilleke N. et Okuda T., Analyzing the spatial structure of a Sri Lankan tree species with multiple scales of clustering, Ecology, vol. 88, pp 3088-3102, 2007.

[7] Herrero-Jáuregui C., García-Fernández C., Sist P.L., Casado M.A., Recruitment dynamics of two low-density neotropical multiple-use tree species, Plant Ecology, vol. 212 (9), pp 1501-1512, 2012.

[8] Yêhouénou Tessi R. D., Akouèhou S. G., Ganglo C. J., Caractéristiques structurales et écologiques des populations de *Antiaris toxicaria* (Pers.) Lesch et de *Ceiba pentandra* (L.) Gaertn dans les forêts reliques du Sud-Benin, International Journal of Biological and Chemical Sciences, vol. 6 (6), pp 5056-5067, 2012.

[9] Pastorella F., Paletto A., Stand structure indices as tools to support forest management: an application in Trentino forests (Italy), Journal of forest science, vol. 59(4), pp 159-168, 2013.

[10] Touafchia B., Beldjazia A., Redjaimia L., Missaoui K., Zerrouki A., Rached-Kanouni M., Viability of Ouled Bechih forest (Algeria), Asia Life Science, vol. 12 (11), pp 1617-1624, 2022.

[11] Rached-Kanouni M., Zerrouki A., Lahmar M., Beldjazia A., Kara K., Ababsa L., Assessment of the health status of the Sidi R'Ghies forest, Oum El Bouaghi, north-east Algerian. Biodiversitas, vol. 21, pp1980-1988, 2020.

[12] Rabiou H., Inoussa M. M., Bakasso Y., Diouf A., Mamoudou M. B., Mahamane A., Structure de la population de *Boscia senegalensis* (Pers.) Lam. ex Poir. suivant la toposéquence dans la commune de Simiri (Niger). Journal of Animal & Plant Sciences, vol. 23 (3), pp 3657-3669, 2014.

[13] Rondeux J., La mesure des arbres et des peuplements forestiers. Gembloux, Belgique, Presses agronomiques de Gembloux, 522 p., 1999.

[14] Glèlè Kakaï R. L., Sinsin B., Palm R., Étude dendrométrique de *Pterocarpus erinaceus* Poir. des formations naturelles de la zone soudanienne au Bénin, Agronomie Africaine, vol. 20 (3), pp 233-335, 2008. doi.org/10.4314/aga.v20i3.46233.

[15] Husch B., Beers T., Kershaw J.R., Forest Mensuration, John Wiley, New York, 2003.

[16] Kudus K.A., Ahmad M.I., Lapongan J., Nonlinear regression approach toestimating Johnson SB parameters for diameter data, Can. J. For. Res., vol. 29 (3), pp 310-314, 1999.

[17] Rennolls K., Wang M., A new parameterization of Johnson's SB distribution with application to fitting forest tree diameter data, Can. J. For. Res., vol. 35 (3), pp 575-579, 2005.

[18] Douma S., Rabi C., Mahamane A., N'da H. D., Saadou M., État actuel de dégradation des populations de quatre espèces ligneuses fruitières en zone sahélo-soudanienne du Niger : réserve totale de faune de Tamou, Revue Ivoirienne des Sciences et Technologies, **vol.** 16, pp 191-210, 2009.

[19]Fandohan B., Glèlè Kakaï R., Sinsin B., Pelz D., Caractérisation dendrométrique et spatiale de trois essences ligneuses médicinales dans la forêt classée de Wari-Maro au Bénin, Revue Ivoirienne des Sciences et Technologies, vol. 12, pp 173-186, 2008.

DYNAMICS OF PINE FOREST STRUCTURE ON A PEATBOG REVEALS HALF-CENTENNIAL FOREST DECAY AND ONGOING SUCCESSION (DARWIN BIOSPHERE RESERVE, NW RUSSIA)

Andrej Mukhin[1]

Dr. Dmitrii Sadokov[2, 3]

Lera Akhmetshina[3]

Elena Bykovskaia[3]

Olga Koniaeva[3]

[1] Darwin Nature Biosphere Reserve, **Russia**
[2] Shenzhen MSU-BIT University, **China**
[3] ITMO University, **Russia**

ABSTRACT

Bogs of Darwin Biosphere reserve (southern NW Russia) represent sustain ecosystem balance on an outstandingly large scale. Dynamics of the bog metabolism and structure should be estimated both under the influence of the Rybinsk reservoir and beyond it (in terms of natural evolution), although these cannot always be distinguished clearly. Forested bog areas are most sensible ecosystems to trace decadal or centennial dynamics of the landcover.

Longstanding observations of the geobotanical and forest structure have been continuously performed in Darwin Nature Biosphere reserve from 1947 to 2012 within a series of the model grounds. Changes of parameters of sphagnous pinewood through 65 years are overviewed, based on the on-site censuses and, partially, remote sensing data.

During the first decades of observations (1947-1991) the accounted forest stand gained maturity, and ultimately tree died off numerously. Pinewood shrinkage was noticed in 1990-s, due to the reached tree age limits (in bog conditions), and the durative drought to have affected those years. At present mature and undergrowth pine stand covers almost 1.7 times less of the surrounding 500-area around the model ground, than 40-50 years ago, mainly due to the tree dying off in 1990-2000. A 20-year forest regrowth brings repopulation of pine on the site, which gradually spreads over the bog around the model ground.

The assessed changes of qualitative and quantitative properties of the microlandscape enable to trace ecosystem function transformation on the local level, i.e., enhancement of peat soil humidity, hygrophytic vegetation appearance, and reformation of habitats suitable for bog-nesting birds, as the pine forest decayed.

Keywords: bogs, ecosystem transformation, forest dynamics

INTRODUCTION

Proximity of the large artificial Rybinsk reservoir is one of the key natural factors of evolution of the Darwin Nature Biosphere Reserve natural complexes. Since its creation in 1945, its northwestern shores have been designated for strict nature protection, with a pursue to trace changes of the environment under the reservoir influence. Many forest massifs were flooded and eventually died off during the first decades after the water raise. Vast inundation zone was formed along 102 m a.s.l. (headwater elevation) [5]. Forest land along the coast has been being affected by the permanent or seasonal raise of underground water table (UWT).

In the context of indirect human impact, centennial dynamics of the peatland natural complexes represents a matter of individual investigation. Changes in vegetation (in particular, tree stand) is one of the most vivid transformation processes on and around the boggy landscapes in Darwin Biosphere reserve. Long-term centennial bog formation is considered the main driver to alter forest structure in the peatland marginal zone [7]. This has been particularly well described for "low ridges" in the bog center, which are island sites composed of well-sorted fine sand. Medium- and high-class pine forests overgrow the most elevated of these ridges (over 0.5-1.0 meters above the surrounding peatland surface), where underground and bog water do not cause any marked effect. On flat ridges peat thickness is notable, and different stages of bogging process can be observed. Low-class pine woods typically die off on such sites.

Dynamics of forest phytocoenoses confined to the peatlands has been studied in Darwin Biosphere Reserve on the long-term regular basis. A network of forest stations (model grounds) was launched by A.M. Leontyev in 1947, and embraced various forest types. Here we present an analytical overview of the accumulated data on the tree and shrub cover on the model ground (MG) No. 18 from 1947 to 2012.

MATERIALS AND METHODS

Archive records on vegetation changes on the MG 18 were used during the work. Tree census was performed 7 times, from 1947 to 2012 (table 1). The following parameters were measured and evaluated during the surveys: species diversity, thickness of stand, average tree diameter, average tree height, maximum age of the prime pine generation, relative canopy density (RCD), forest class, condition of living and dead-standing trees, timber volume (living trees – L, dead-standing trees – D, fallen deadwood – F).

Species composition was assessed with the use of 10-point scale, where 10 is single-species tree stand (e.g., 10 Pinus) and 1 is equal to 10% of all mature tree species of the site.

Relative canopy density (RCD) was calculated as a ratio of the standing trees sum of section squares over 1 hectare ($\sum G_d$) and the sum of section squares of the complete stand (with the highest density value in the given forest growth conditions) ($\sum G_n$).

Forest class was evaluated using the standard method and 6-point scale, after M.M. Orlov. Living tree stand condition was evaluated visually by signs of diseases, retarded growth or die-back. Shrubs and herbs abundance was estimated according to the Drude scale, after A.P. Shennikov (1964), and later corresponded to Braun-Blanquet classification (1964) in order to be reliably represented. Names of the plant associations are given with reference to the relevant All-Russian nomenclature [9].

Aerial imagery of the Darwin Biosphere reserve territory (28.07.1978) and satellite ESRI imagery (24.06.2018) were used for work and processed with the use of QGIS software.

STUDY SITE

Darwin Nature Biosphere Reserve is situated in the south-west of Vologda region (NW Russia). Here, in the center of the Mologa-Sheksna Lowland, the major landscape type is peatlands. Vegetation of the research area belongs to the southern taiga zone, Valdai-Onego subprovince of the North-European province of the European taiga region [2]. Most of the nature reserve territory is in some way waterlogged or bogged. Sphagnum raised bogs and wet peatland forests (primarily pinewoods) represent up to 80% of the protected area. Shrubs and herbs species diversity is poor, with the most abundant species are leatherleaf, bog-rosemary, wild rosemary, bog bilberry, cranberry, cottongrass, cloudberry, pod grass, bog-sedge [4].
Model ground 18 (N 58,552133°, E 37,564817°, square 0.5 hectares) is located in the central part of the bog “Bolshoj Mokh” in the west of the Darwin Biosphere reserve (Fig. 1), which belongs to the river Mologa watershed. The raised bog surface lies at 105 m a.s.l. Peat thickness at the research site (as of 1947) varies between 1.7 and 3.5 meters, underlain by sandy sediments with silt. Soil was classified by A.M. Leontyev in 1947 as peaty podzol-gleysol.

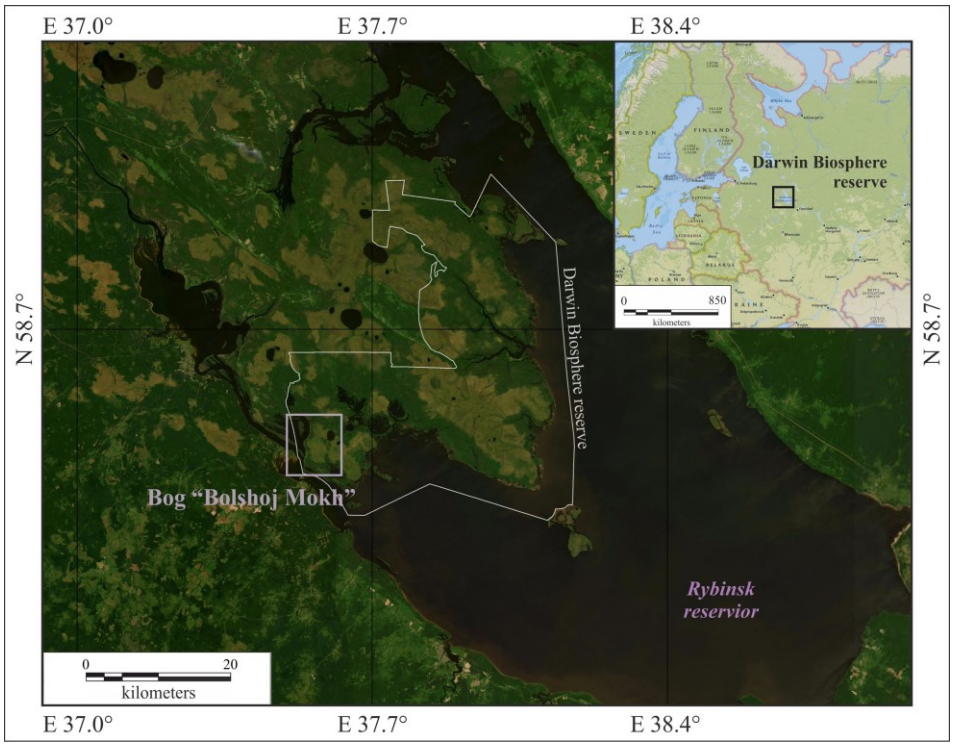

Figure 1. Geographical position of the research site (bog “Bolshoj Mokh” in Darwin Biosphere Reserve)

RESULTS

First census held up at the MG 18 in 1947 showed the tree stand to had been overmature (127 years), single-species pinewood (10 *Pinus*) of low class (Vb). The growing stock was small (89 m^3/hectare), RCD was moderate (0.71), the trees were thin (diameter 12.5 cm) and short (height 8.1 m) (table 1). Forest reproduction was represented by *Pinus sylvestris* L., both due to seedfall and minor undergrowth. The latter was restricted to the places of scattered *Ledum palustre* L. and *Chamaedaphne calyculata* (L.) Moench abundance (up to 200 seedlings per 1 m^2). *Ledum palustre* and *Chamaedaphne calyculata* were the most common shrub species (abundance scored 5-6 and 4-5 of the Drude scale respectively, plant cover 50% and 30%) (Fig. 2). Among other bog plant species, the following were recorded abundant: *Eriophorum vaginatum* L. (4 score (s.)) suppressed, *Oxycoccus palustris* Pers. (4-5 s.), *Rubus chamaemorus* L. (3 s.), *Andromeda polifolia* L. (2 s.). *Sphagnum magellanicum* Brid. (5-6 s., 40% cover), *Sph. Angustifolium* (Russ) G. lens (4-5 s., 40% cover), *Sph. Fuscum* (Schimp) Klinger (5 s.) and *Sph. Centrale* C.E.O.Jensen (4 s.) predominated in moss layer. Small patches of *Dicranum unndulatum* Schrad. Ex Brid (2 s.), *Pleurozium schreberi* (Willd. Ex Brid.) Mitt. (1 s.), *Polytrichum commune* Hedw. (2 s.) were recorded on the hummocks.
During the first 20 years of monitoring (until the late-1960-s), the stand was presented by healthy trees aged 150 years, wielded high RCD (0.75) and stock around 100 m3/hectare (Fig. 3A). Although, stepwise tree die-back was recorded in 1971, along with RCD reduced to 0.40 and stock to 50 m^3/hectare.

Table 1. Taxational specifications of growing stock of the model ground 18. Legend: d – diameter, h – height, A – age, L – living trees, D – dead-standing trees, F – fallen deadwood

Year of survey	Tree species composition	Average		A, years	Relative canopy density	Tree class	Condition, %		Growing stock, m^3/hectare		
		d, cm	h, m				Living trees	Dead-standing trees	L	D	F
1947	10 *Pinus*	12,5	8,1	127	0,71	Vb	92,0	0,2	89	0,2	0
1960	10 *Pinus*	12,7	8,2	141	0,75	Vb	94,0	7,5	95	8	0
1971	10 *Pinus*	12,7	8,2	152	0,39	Vb	94,0	53,3	49	56	5
1981	10 *Pinus*	13,2	8,3	162	0,40	Vb	94,2	48,4	52	48	19
1991	10 *Pinus*	12,6	8,3	172	0,11	Vb	91,1	85,3	14	79	29
2001	10 *Pinus*	11,5	7,9	182	0,03	Vb	87,0	95,6	3	65	59

2012	10 *Pinus*	11,6	5,3	193	0,03	Vb	100	94,9	0,5	22	100
2012	10 *Pinus*	8,5	4,5	50	0,01	V	100	-	0,6	-	-

During the next decade (until 1981) the stagnation was observed in the tree stand dynamics, with major taxational parameters had not been changing. Although, the ongoing loss of the remaining living trees was recorded after the 1991 survey. At the same time, new undergrowth was abundant (1200 trees/hectare), in good condition, equally distributed, with its predominant height near 1.0-2.0 m. Undergrowth trees were considered within the height range between 0.1-0.2 m (seedling level) and 4.0 m. *Chamaedaphne calyculata* and *Eriophorum vaginatum* predominated in among shrubs and herbs (4 s., 20% cover for each species), while abundance of other species decreased: *Ledum palustre* (3-5 s., 10% cover), *Oxycoccus palustris* (4 s., 10% cover), *Rubus chamaemorus* (3 s.) and *Andromeda polifolia* (2 s.). *Sphagnum magellanicum* (5 s., 40% cover) and *Sph. angustifolium* (5-6 s., 60% cover) remained the major moss species.

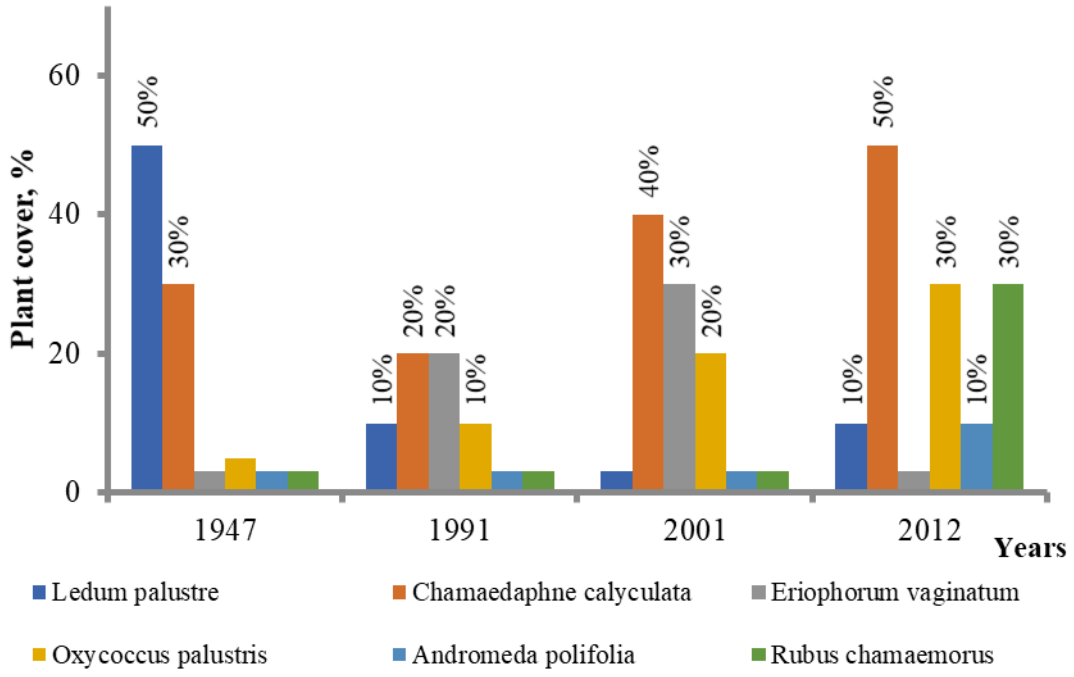

Figure 2. Shrubs and herbs abundance dynamics on the model ground 18 from 1947 to 2012.

Aerial imagery from 1978 reveals distinctive grain texture of the surface, color tone was dark-grey. Overall color gradient changed for the brighter tone and less grainy texture westward of the model ground 18, while more coarse-grained image appearance was

traced northward and eastward. Both these gradients intersected on the MG 18, from the western and eastern sides of the ground respectively.
Tree stand loss that had started in 1990-s, turned it into a sparse stand. RCD declined to 0.03, growing stock was 3 m^3/hectare and overall number of undergrowth trees increased to 2500 trees/hectare, as it was recorded in 2001. *Chamaedaphne calyculata* (4 s., 40% cover), *Eriophorum vaginatum* (4 s., 30 %) and *Oxycoccus palustris* (4 s., 20%) remained the most abundant species of the plant cover (Fig. 2). Share of *Ledum palustre* decreased notably (3 s.); abundance of *Rubus chamaemorus* and *Andromeda polifolia* maintained on the same level as decade before. Structure of moss cover did not change.

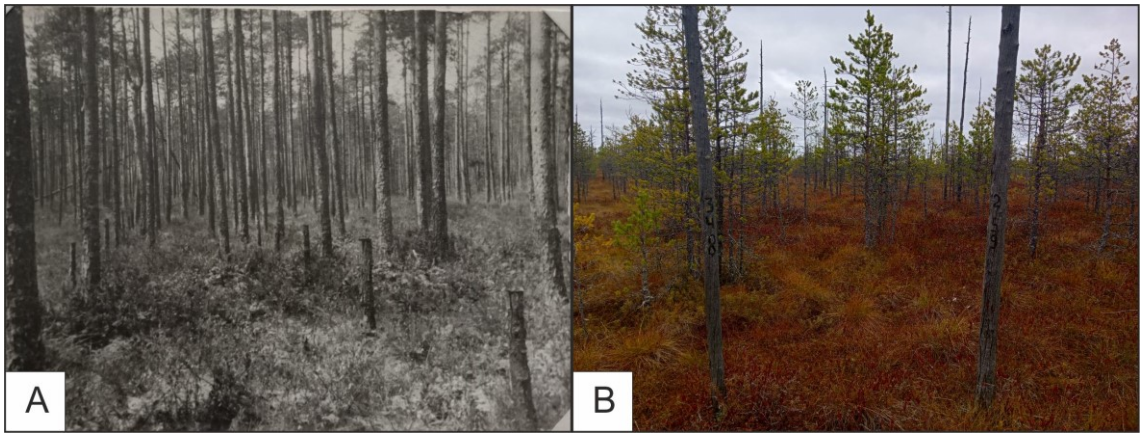

Figure 3. Appearance of the forested peatbog microlandscape on the model ground 18. A – Mature Pinetus sphagnosum (1961-1963). B – Open pine undergrowth with dwarf shrubs and cottongrass.

During the last performed census in 2012 it was shown that mature trees (aged 193) has died off almost completely, growing stock of living trees declined to 0.5 m^3/hectare. New generation of an undergrowth (pines of 40-60 years) appeared among the sparse old trees, with RCD near 0.01 and the stock near 0.6 m^3/hectare. Some young trees had reached stem strength value of 6 cm by 2012 and was accounted as mature trees. Considering this, the number of 1.0-3.5 meters high underwood (Fig. 3B) was estimated near 2000 young trees/hectare. As previously, *Chamaedaphne calyculata* predominated among dwarf shrubs (5 s., 50% cover) (Fig. 2), *Ledum palustre* grew more abundantly than during the previous survey (3-4 s., 10% cover). Abundance of *Eriophorum vaginatum* declined (2-3 s.). *Rubus chamaemorus* (4 s., 30% cover), *Andromeda polifolia* (3-4 s., 10% cover) and *Oxycoccus palustris* (4 s., 30% cover) were more frequent in 2012. *Sphagnum angustifolium* (6 s., 90% cover) remained the only massive moss species to be represented in the community by 2012, as *Sph. magellanicum* and *Polytrichum commune* were recorded very sparsely (2-3 s. and 1 s. respectively).
General tone gradients of the landcover surface of the 2018 imagery are smoother and lighter (Fig. 4), grain texture is less expressed than on the aerial imagery in 1978. Within the 500-meter range around the model ground 18 overall appearance becomes less grainy, object contours turn smoother and tones are distributed evenly. The increased of light gray-brown patches amplifies overall mosaic texture to the east from the model ground 18 (in the direction of the bog center). The tones change to more equal green with fine-grained texture to the west in the direction of the bog margin.

DISCUSSION

Principles of dynamic typology [6] and analysis of 65-year changes of vegetation cover allow to outline four stages of the over-mature forest (*Pinetum fruticuloso-sphagnosum*), namely:

1. *Pinetum fruticuloso-sphagnosum* (*Ledum palustre*, *Chamaedaphne calyculata*), was described in 1947 and remained near 40 years. Durational maintenance of RCD around 0.40 – 0.75 on the MG 18 can be ascribed as due to natural maturity of the tree stand, in accordance to the concept of cyclicity of forest cover dynamics in bog ecosystems [3]. During this period, intensive loss of the pine stand that had reached natural maturity, was observed.
2. *Pinetum cassandroso-sphagnosum* subass. *eriophorum vaginatum* was recorded during the survey in 1991. The tree stand continued to degrade which contributed into accumulation of dead-standing trees and fallen deadwood.
3. *Pinetum fruticuloso-sphagnosum* (*Oxycoccus palustris*, *Chamaedaphne calyculata*) subass. *eriophorum vaginatum* was the predominant association recorded in 2001. At this stage mature tree stand has degraded almost completely, meanwhile pine undergrowth of good condition started spreading over the MG 18.

The ongoing dying-off of the living tree stand, which had been recorded in 1991 and 2001, could be influenced by the contemporary climatic effects, i.e., by very humid climate of late 1980-s and extremely dry summer in 1992. Slight increment of the remaining mature forest stand was recorded after the draught in 1990-s.

4. *Pinetum fruticuloso-sphagnosum* (*Oxycoccus palustris*, *Rubus chamaemorus*, *Chamaedaphne calyculata*) was the community recorded in 2012. The underwood was abundant and partially turned into the general tree stand, forming its young generation.

At present young pine tree stand and undergrowth reproduces effectively on the area previously covered with mature trees. New young generation of *Pinetum fruticuloso-sphagnosum* is expected to form during the nearest decade.

Aerial and satellite imagery data (1978 and 2018) (Fig. 4) reveal that the visible spatial tree stand dynamics correspond decadal taxation data. Several polygons of tree and shrub vegetation were delineated on and around the MG 18 (see the squares presented in table 2). Greater crown density was observed in 1978 compared to 2018. Many unforested light-brown spots are visible on the image to the east of the MG 18 in 2018, most likely covered with cottongrass. Dense *Pinetum sphagnosum* massif of medium canopy with mature and premature trees decreased by 1.7 times from 1978 to 2018. Decline of crown size and shades indicate changes in tree height, thickness and canopy, and, consequently, age, which confirms observations of mature tree stand die-off and gradual renewal by the undergrowth.

The mentioned quantitative and qualitative changes of landcover enable to trace ecosystem functions transformation within the peatland microlandscape. Peat soil moisture raise is indicated by an increase of the area occupied by open *Pinetum fruticulilosum* or *Pinetum eriophorosum* by 1.4 and 1.9 times correspondingly by 2018 (table 2). Hygrophytic vegetation cover (particular the presence of *Eriophorum vaginatum*) supports this observation particularly.

As of 2018, hummocky bog was recorded to be altered by smoother landforms was recorded, which corresponds to the landscape dynamics trend towards tree stand die-off without its synchronous renewal. Vegetation cover response reveals transition from *Ledum palustre* and *Chamaedaphne calyculata* (typical for hummocks) to *Oxycoccus palustris* and *Rubus chamaemorus* (covering plain bogs).

At present phytocenosis of the MG 18 starts to develop into a “complex stage” of boggy forest vegetation dynamics, that is characteristic for ecosystems with unfavorable conditions restricting mature wood increment or seedlings growth [3]. Old tree stand degradation, ongoing growth of the upcoming generations and appearance of regular undergrowth trees are observed during such complex stage simultaneously.
Boggy landscapes transformation duration is greater than that of margin parts, due to the larger energetic balance rate and ecosystem sustainability and maturity of the former [10]. Along the bog edges trees die off more intensively due to hydrological or climatic conditions changes (wind influence and increased inundation).

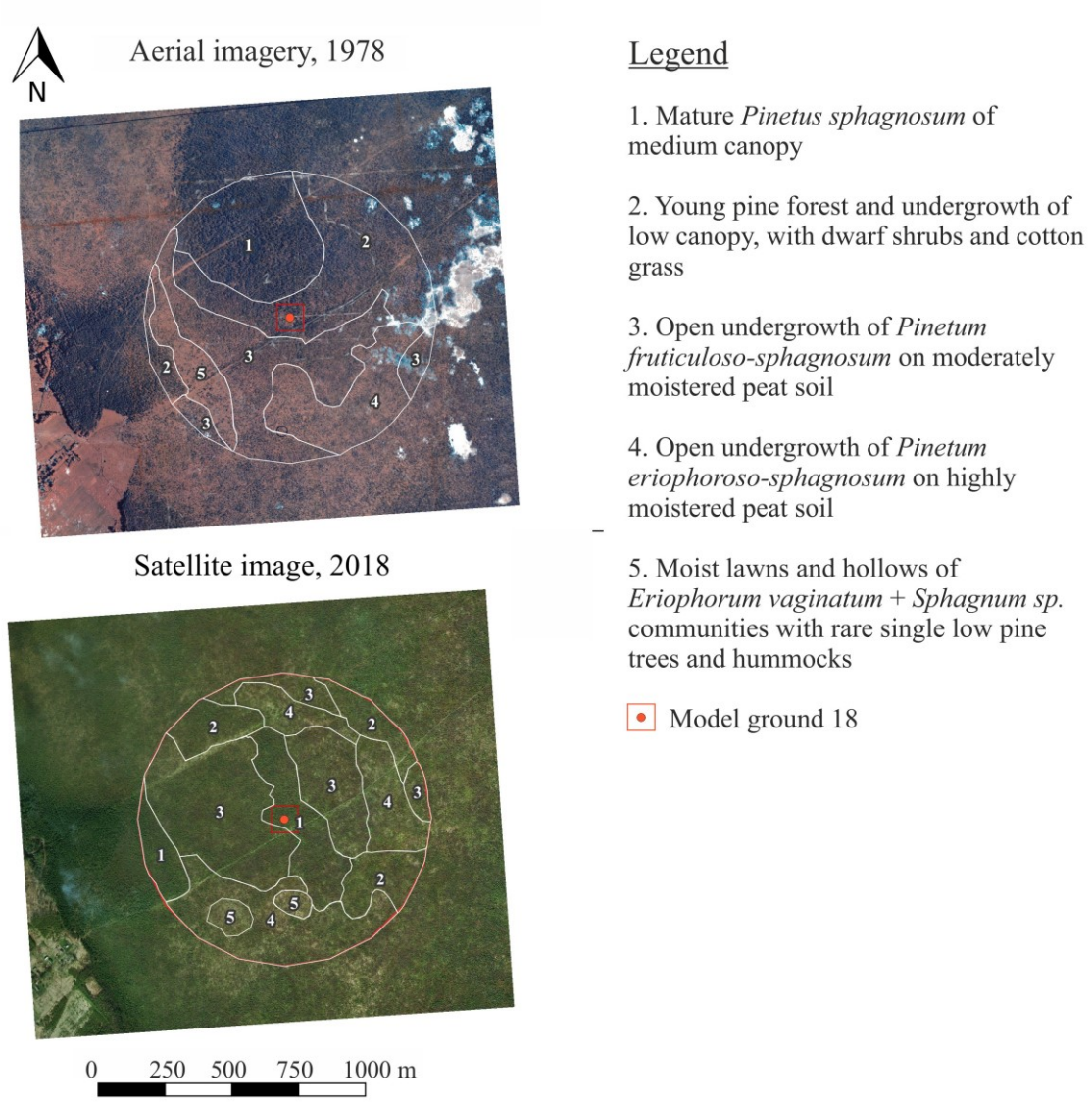

Figure 4. Results of vegetation cover delineation on the site of 500 range around the model ground 18 on the bog “Bolshoj Mokh”, Darwin Biosphere Reserve. Aerial imagery of 1978 and satellite imagery of 2018 were used as raw source data.

The observed RCD changes can correspond to loss of the tree stand that had covered “low ridges” of the bogs in the north of the “Bolshoj Mokh”. Forested area of the low ridges decreased from 10-30% to 60-80% for 70 years, according to the field and

remote sensing estimates [1]. Tree stand degradation on and around MG 18 could be as well triggered by the increased stress (due to enhanced moisture of soil) that had been imposed on the overmature pines. Although, nevertheless similar trend was noticed for both general bog tree stand degradation and that of pinewoods of low ridges, the specifics of the long-term dynamics on MG 18 is determined by the low-class pinewood. Thus, ecosystem transformation has been mainly expressed on the level of low thin mature trees and undergrowth, and on the level of bog dwarf shrub species evenness and abundance (in the long-term perspective). In turn, vegetation change on the low ridges is more visually evident than on the plain bog, due to the presence of medium- and high-class trees. For such communities tree stand loss leads to greater structural contrast on its margins, which is accompanied by progressive soil moisture gain. Geobotanic structure changes of the phytocoenoses similar to those of MG 18 likely occur in the course of the natural ongoing bogging of pine forests, though extended investigation is necessary, with support of the multi-year landscape monitoring data.

Table 2. Area covered by different geobotanic units (for numbers in the left column see legend on Fig. 4) in 500-meter range zone around the MG 18, in 1978 and 2018.

Plant association index (according to the legend given for Figure 4)	**Area covered in 1978 (hectares)**	**Area covered in 2018 (hectares)**
1	18.97	13.87
2	28.48	14.05
3	25.01	34.34
4	14.00	27.45
5	6.21	2.69

Many ecosystem functions of bogs are dependent on tree stand dynamics, which contributes to biodiversity maintenance, in particular avifauna species diversity. One of the key ecosystem functions of Darwin Biosphere reserve, which is influenced by the pine sphagnum tree stand degradation, is reproduction and dispersal of upland fowl birds (partridges, blackcocks, capercaillies) over the boggy terrain. Capercaillies mostly prefer forest margins, lawns, branch trails and bogs alternated by pine forest with bilberry, redberry or cranberry. Especially high pines on bogs are used by capercaillie males during lekking [8]. Old overmature trees die-off, appearance of thin suppressed undergrowth and spread of *Eriophorum vaginatum* groups (loss of berry-bearing plants) at sites similar to MG 18 can possibly alter capercaillie habitats in unfavorable way. Die-off of high pine trees is also likely to deteriorate structure of habitats used by ospreys, since they basically nest on trees towering within the landscape.

CONCLUSION

Multi-year records of dynamics of the virtually undisturbed forest ecosystems dynamics enable to trace recent changes of vegetation cover, which cannot be reconstructed via single or short-term surveys. Interpretation of aerial imagery of different time-slices help to specialize spatial changes both for the model grounds and for the surrounding area. Several significant structural changes of the bog pinewood have been outlined

during 65 years of continuous monitoring in Darwin Biosphere reserve, starting from its earliest years.

During the first decades (1947-1981) mature and dense tree stand was recorded on the site, undergoing intensive natural die-off. Degradation of this overmature tree stand strengthened by the 1990-s, which is associated with the age limit reach for the trees within bog conditions, and partially due to the pronounced draught of 1992. From that time abundance of cottongrass increased, mostly on the spots that had been transiting from low-class tree cover to sparse stand. At present *Pinetum fruticuloso-sphagnosum* (with *Oxycoccus palustris*, *Rubus chamaemorus* and *Chamaedaphne calyculata* as major predominant species) wields much less canopy density than previously, due to the pinewood degradation in 1990-2000-s. The tree stand renewal has been contributed by the undergrowth.

It is undoubtful that the general bog evolution trends have been alternated since the formation of Rybinsk reservoir, in accordance to its impact on the hydroclimatic conditions of the region. Enhancement of winter air humidity, thickness of snow cover, frequency of cyclones, reduction of number of clear sunny days and greater weather instability create conditions which generally facilitate excessive moistening of soil, longer residence time of precipitated water within moss and peat layers. Ultimate consequences of these hydroclimatic changes include, among other, inundation of the bog-forest transition zone and, thus, pine massifs degradation accelerates.

Expanded analysis of the long-term forest dynamics monitoring data is essential for assessment of forested bogs sustainability under the ongoing climatic change and alterations of moisture distribution. Variability potential of different peatland landscape facies can be investigated, meeting the key objective of Darwin Biosphere reserve, i.e., tracing ecosystem response to the environmental changes on the regional-to-global scales, as part of baseline monitoring.

ACKNOWLEDGEMENTS

The study was performed in frames of basic scientific research topic of Darwin State Nature Biosphere Reserve “Investigation of natural processes occurrences and long-term dynamics of ecosystems of Darwin Nature Reserve and the adjacent area under the influence of natural and anthropogenic factors” (2024-2026), No. 122061700061-4.

REFERENCES

[1] Galanina O.V., Petrova E.A., Sadokov D.O., Tyusov G.A., Vegetation dynamics of the forested mineral islands on the bog of Darwin Nature Reserve (Vologda region), Natural Heritage of Russia, International scientific conference, Russia, 2017, pp. 125-128 (In Russian)

[2] Gribov S.A., Isachenko T.I., Lavrenko E.M., Vegetation of the European USSR, Russia, 1980, 429 p. (In Russian)

[3] Kudinov K.A., Pisanov V.S., Stages and cycles of the development of forested bog ecosystems in the Mologa-Sheksna interfluve, Transactions of Darwin State Nature Reserve, issue 15, 1979, pp. 59-62 (In Russian)

[4] Kuznetsov A.V., Zelenetskiy N.M., Rybnikova I.A., Nemtseva N.D., Kalutskova N.N., Essay of the natural conditions of Darwin Nature Reserve, Transactions of Darwin State Nature Biosphere Reserve, issue 16, 2006, pp. 5-21 (In Russian)

[5] Kuznetsov A.V., Rybnikova I.A., Some methodic approaches to analysis of the Rybinsk reservoir water level regime being a factor of the biotic complex development in the zone of periodical inundation, Transactions of Darwin State Nature Biosphere Reserve, issue 17, 2015, pp. 9-37 (In Russian)

[6] Melekhov I.S., Typology of forests, Russia, 1976, 73 p. (In Russian)

[7] Mukhin A.K., Long-Term Dynamics of Waterlogging Pine Forests under the Reservoir Influence, Lesnoy Zhurnal (Russian Forestry Journal), issue 3, 2019, pp. 17-31 (In Russian)

[8] Nemtsev V.V., Fauna of Darwin Nature Reserve. Birds, Russia, 1988, pp. 29-57 (In Russian)

[9] Neshatayev V.Yu., The Project of the All-Russian code of phyrocoenological nomenclature, Vegetation of Russia, vol. 1, 2001, pp. 62-70

[10] Smolyanitskiy L.Ya., Bog metabolism in the context of their interrelations with forest ecosystems, 1979, Transactions of Darwin State Nature Reserve, issue 15, 1979, pp. 21-31 (In Russian).

EVALUATION OF ONTOGENETIC AND VITAL STRUCTURES OF STELLIARIA HOLOSTEA L. IN BEECH FORESTS IN THE SOUTH OF LOW SAXONY, GERMANY

MSc. Nataliia Yaroshenko[1,2]

Dr. Viktoriia Skliar[1]

Dr. Gert Rosenthal[2]

[1] Sumy National Agrarian University, **Ukraine**
[2] University of Kassel, **Germany**

ABSTRACT

In this study, we conducted the plant population investigations in the Goettingen forest, located in Low Saxony, Germany, from 2022 to 2023. Our research focused on six distinct populations of *Stellaria holostea L.* across six plots within the forest. These plots encompassed varying tree species and forest management conditions, including a young beech managed forest (Plot #1), a virgin beech forest (Plot #2), and four managed old beech forest plots (Plots #3-6) subjected to different anthropogenic influences.

To assess these coenopopulations' ontogenetic and vitality structures, we employed a range of scientific methodologies, including geobotanical description, morphometry analysis, complex vitality assessment, and statistical data analysis.

Morphometric analyses allowed us to discern the characteristic size parameters of *S. holostea* plants within each specific habitat. Notably, our findings revealed that the ontogenetic spectra of *S. holostea* in areas varying in the intensity of anthropogenic influence exhibited incompleteness, except in the virgin forest plot, where all ontogenetic stages were observed.

We conducted a factor analysis to gauge vitality, identifying critical morphological parameters unique to each population. Our results indicated a pronounced level of resilience in coenopopulations residing in areas devoid of forestry activities. Specifically, five of the six *S. holostea populations* were classified as having low vitality (class c). In contrast, the highest vitality class (class a) was predominantly observed among the populations residing in the virgin forest.

This study, utilizing *S. holostea* as an exemplar species, highlights the considerable disruption that forestry management imparts upon the herbaceous layer of forest ecosystems and underscores the resultant degradation in population quality.

Keywords: beech forest, population analysis, plant communities, morphometric analysis, Stellaria holostea.

INTRODUCTION

Forest ecosystems have the widest distribution and the highest value among all terrestrial ecosystems. The total area of forest land is over 4 billion hectares, accounting for about

31% of the Earth's land surface. The area covered by forest vegetation is approximately 3 billion hectares, and industrial wood reserves reach 527 billion cubic meters. [1, 2]

Forest ecosystems are significantly affected by forestry activities and require the implementation of measures to ensure their recovery and enhancement of protective, sanitary-hygienic, health, and other functions. [2, 3, 4]

The forest flora serves as an extremely sensitive barometer, indicating the condition of the plantation, particularly the state of its internal environment. [3] When clearing the plantation, the most abrupt changes occur in the composition and character of the herbaceous flora due to alterations in biometeorological conditions and partially in the soil environment. The most common change is the replacement of shade-tolerant flora with light-loving elements, represented by representatives of onions and weeds. [4, 5-7]

For our research, the representative of forest herbaceous vegetation was selected, which is among the most widespread in beech forests in Germany, has notable medicinal properties, and is affected by anthropogenic influence - *Stellaria holostea L.* [2, 6, 7]

Stellaria holostea - medicinal, decorative, honey-bearing plant. The sugar concentration in the nectar is 62.6%. The maximum nectar productivity in broad-leaved forests is 0.4 kg/ha (with a plant density of 25 per 1 m^2). The leaves and stems contain 80 mg% of ascorbic acid. In folk medicine, a decoction of *Stellaria holostea* is used to treat coughs, colds, and stomach ailments. Widely distributed in broad-leaved and mixed forests of Europe, the Caucasus, Asia, North Africa, and Western Siberia. [1, 2] Nevertheless, investigations into the ontogenetic and vitality structure of *S. holostea* utilizing population analysis methods in forest ecosystems under the context of forestry utilization have not been undertaken previously.

MATERIALS AND METHODS

In Germany, the research was conducted in the southern part of Lower Saxony in the Goettingen Forest. The study covered beech forests of various ages, differing in the degree of management influence. Among the studied phytocenoses was also a virgin forest, within which a nature conservation regime was established, excluding direct anthropogenic impacts.

The plots are the following:

Plot #1 – young beech forest (approximate age – 55 years) with an anthropogenic impact;

Plot #2 – virgin forest without anthropogenic impact;

Plot #3-6 – old beech forest (age varies from 120 to 165 years old) with with an anthropogenic impact.

Information about the condition of the studied phytocenoses was obtained based on the application of widely accepted geobotanical methods. [6, 8-10] Fifty-four populations were examined, nine per each plot. The analysis was accompanied by an assessment of 10 static morphological parameters in plants (seven metric and three allometric).

To assess the statistical significance of the obtained quantitative data and their generalization, point estimation and analysis of variance were employed. [8]

TABLES, GRAPHS & FIGURES

Table 1

The proportion of plant samples in different ontogenetic stages (%)

Ontogenetic stages	Plots					
	№2	№3	№4	№6	№7	№9
p	0,00	2,27	0,00	0,00	0,00	0,00
j	0,00	4,55	0,00	0,00	0,00	0,00
im	0,00	6,82	4,26	0,00	5,33	0,00
v	40,00	31,81	14,89	65,80	5,33	0,00
g^1	60,00	15,91	21,28	7,89	41,34	11,11
g^2	0,00	9,09	53,18	17,54	32,00	59,26
g^3	0,00	15,91	0,00	8,77	0,00	5,56
ss	0,00	9,09	2,13	0,00	0,00	24,07
s	0,00	4,55	4,26	0,00	16,00	0,00
Total	100	100	100	100	100	100

https://doi.org/10.5593/sgem2023V/3.2/s14.40

Table 2

The meaning of ontogenetic indices in populations of S. holostea

Ontogenetic indexes		**Measurement units**	**Plots**					
			№1	**№2**	**№3**	**№4**	**№5**	**№6**
By I. M. Kovalenko	Recovery index	%	40,00	45,45	19,15	65,79	10,67	0,00
	Aging index	%	0,00	29,55	6,38	8,77	16,00	29,63
	Generativity index	%	60,00	40,91	74,47	34,21	73,33	75,93
	Age index	amount	0,00	0,65	0,33	0,13	1,50	29629,63
By L.O. Zhukova and M. Glotova	Recovery index	amount	0,40	0,51	0,20	0,66	0,13	0,00
	Aging index	amount	0,00	0,14	0,06	0,00	0,16	0,24
	Substitution index	amount	0,67	0,79	0,24	1,92	0,12	0,00
By L.I. Vorontsova	Recovery index	%	66,67	105,56	25,71	192,31	14,55	0,00
By A.O. Uranov	Age index	Δ	0,21	0,37	0,40	0,25	0,43	0,58
By L.A. Zhivotovsky	Efficiency index	ω	0,64	0,54	0,79	0,58	0,71	0,82

Table 3

The vitality structure of Stellaria holostea L. populations in different phytocenoses

Plots	Share of individuals of different classes			Quality Index (Q)	Vitality class	Statistical validity of the evaluation (%)
	High class (A)	Intermediate class (B)	Low class (C)			
№ 2	0,3333	0,1667	0,5000	0,2500	equilibrium	80
№ 3	0,4333	0,1000	0,4667	0,2667	equilibrium	92,5
№ 4	0,2667	0,1667	0,5667	0,2167	equilibrium	70
№ 6	0,3000	0,1667	0,5333	0,2333	equilibrium	80
№ 7	0,4000	0,2000	0,4000	0,3000	equilibrium	97
№ 9	0,3333	0,1667	0,5000	0,2500	equilibrium	80

RESULTS

In the population of *Stellaria holostea*, all morphometric parameters vary in size across all surveyed plots, indicating different growth conditions. Regarding the change in average size values across the plots, the following trend was observed: the highest values for eight morphometric parameters (i.e., half of them) are found on plot #4. Plots #1 and #2 have three highest indicators each, while plots #3 and #6 have one each.

As for the lowest values of morphometric parameters, plots #3 and #6 have the highest number of lowest indicators – six each. Plot #2 has three lowest indicators, plot #1 has two, and plot #4 has one. On plot #5, all dimensional values of morphometric parameters are at an average level.

Based on the analysis of ontogenetic structure, it is established that populations of *S. holostea* on all plots, except plot #2, have incomplete ontogenetic spectrums (Table #1). For example, on plot #1, only virgin and young generative plants are present, on plot #3, there are no seedlings and juvenile plants, as well as old generative plants, on plot #4, only virgin and generative plants are found, on plot #5 – immature, virgin, young, and middle-aged generative plants, as well as senile ones, and on plot #6 – generative and sub-senile individuals.

On plot #2, the proportion of degenerative individuals is 45.5%, exceeding the proportion of generative ones, which is 40.9%, indicating a left-sided ontogenetic spectrum. Plot #4 also has a left-sided ontogenetic spectrum, with the highest proportion of virgin

individuals (65.8%) and a predominance of degenerative plants. This suggests favorable conditions for the regenerative process on plots #2 and #4.

The other four plots have centered spectrums with a high proportion of generative individuals: plot #1 – 60.0%, plot #3 – 74.5%, plot #5 – 73.3%, and plot #6 – 75.9%. These plots are characterized by weakly pronounced regenerative processes (Table #1).

General ontogenetic indices show that plots #2 and #4 have the highest regeneration indices (45.45% and 65.79%, respectively), exceeding generativity indices (according to I.M. Kovalenko) by 1.1 and 1.9 times, respectively. These plots also have the highest regeneration indices according to L.O. Zhukova – M.V. Glotova (coefficients of 0.51 and 0.66, respectively) and according to L.I. Vorontsova (105.6% and 192.3%, respectively) (Table #2).

The lowest regeneration indices (according to I.M. Kovalenko) belong to *S. holostea* populations on plots #3 – 19.15%, #5 – 10.67%, and #6 – 0.00%, which are much lower than generativity indices. These plots also have the lowest regeneration indices according to L.O. Zhukova – M.V. Glotova and according to L.I. Vorontsova.

It was also investigated that on plot #2, the *S. holostea* population is transitional, on plot #4 – young, on plot #1 – maturing, on plots #3 and #5 – mature, and on plot #6 – aging (according to L.A. Zhivotovsky). It is established that plots #5 and #6 are dominated by degradation processes, while on all other plots, invasive processes prevail (according to I.M. Kovalenko).

Vitality analysis showed that all plots are represented by populations of equilibrium type with a quality index (Q) ranging from 0.2167 to 0.3000 (Table #3).

From the table, we can see that despite the high proportion of generative individuals and low regeneration indices, the highest population quality index of *Stellaria holostea* is found on plot #5 (Q = 0.3000). This plot has the highest proportion of individuals in the intermediate vitality class and the lowest proportion of individuals in the lower class compared to other plots.

In second place is plot #2 with a population quality index Q = 0.2667, which has the highest proportion of plants in the higher vitality class compared to other plots.

DISCUSSION

The acquired data unequivocally demonstrate that *Stellaria holostea*, akin to numerous arboreal species, manifests heightened sensitivity in responding to alterations in eco-cenotic conditions within habitats, eliciting concomitant shifts in size-morphometric indicators.

In the course of the factor analysis deployed for scrutinizing population vitality, it was ascertained that each population manifests discrete critical morphoparameters, underscored by noteworthy Pearson pairwise correlation coefficients. Consequently,

dedicated investigations were conducted for each population, facilitating a comprehensive elucidation of inter-trait relationships.

The conducted research underscores a substantial correlation between the degree of forestry management and the age of trees. This robustly reinforces the hypothesis positing a correlation between forestry management intensity and the ontogenetic and vitality structures of plant populations. Population analyses assume a pivotal role in affording a nuanced comprehension of the repercussions of forestry management on the studied species.

CONCLUSION

The outcomes of the investigation conducted across six distinct plots within the Goettingen forest, spanning the distribution range of *Stellaria holostea*, elucidate the role of size-morphostructural indicators as vivid and informative proxies for assessing the plant's physiological status in diverse forest vegetation contexts. These indicators not only integrate but also elucidate eco-cenotic interactions within specific phytocoenotic realms at the regional level. The acquired dataset substantiates the illustrative capacity of these indicators to depict the ecological-cenotic dynamics operational within both specific phytocoenoses and broader regional frameworks.

Within this context, plot #2, situated in the virgin forest, emerges as noteworthy in ontogenetic analyses, manifesting representation across all ontogenetic stages—a singular characteristic among the selected plots. Concurrent vitality analyses reveal the virgin forest's distinguished status, marked by the minimal presence of b-class representatives, reaching a nadir at 0.1.

Contrastingly, plot #1, characterizing a juvenile forest, exclusively features virginal and generative-1 stages, signifying distinct ecological nuances inherent to this specific plot.

In synthesis, for a comprehensive delineation of the idiosyncrasies and patterns governing Stellaria holostea populations across varied sectors of the distribution range, prospective scientific inquiry should encompass an exhaustive analysis. This analysis should extend beyond the scrutiny of size-morphostructural attributes to encompass the nuanced examination of structural facets (ontogenetic, vitality, spatial) and the characteristics of population fields.

ACKNOWLEDGEMENTS

We are thankful to the Deutshe Bundesstiftung Umwelt (DBU) support which allowed this scientific cooperation to start.

REFERENCES

[1] Wodkiewicz, M., Gruszczynska B., Genetic diversity and spatial genetic structure of Stellaria holostea populations from urban forest islands. Acta Biologica Cracoviensia. Series Botanica, Poland, 56.1, pp 42-53, 2014.

[2] Werner P., Rebele F., Bornkamm R., Wirkung von Lichtintensität und Lichtqualität auf die Entwicklung der Schattenpflanze Lamium galeobdolon (L.) Crantz und der Halbschattenpflanze Stellaria holostea L., Flora, vol. 172/issue 3, 1982, pp 235-249, 1982.

[3] Salk, C. F., Chazdon, R., Kamp; Waiswa, R., Thinking Outside the Plot: Monitoring Forest Biodiversity for Social-Ecological Research. Ecology and Society, 25(1), vol. 7, 2020.

[4] Peringer, A., Rosenthal, G., Establishment patterns in a secondary tree line ecotone. Ecological Modelling - ECOL MODEL, Germany, p. 222, 2011.

[5] Dierschke, H., Goedecke, F. Forty years of symphenological research in a submontane calcareous beech forest under the influence of climate change. Fl. Medit., vol. 31 (Special Issue), pp 257-270, 2021.

[6] Yakubenko, B. Ye., Popovych, S. Yu., Ustymenko, P. M., Dubyna, D. V., Churilov, A. M., Heobotanika: metodychni aspekty doslidzhen [Geobotany: methodological aspects of research], p. 316, 2020.

[7] Skliar, V., Sherstuk, M., Size Structure of PhytPopulations and Its Quantitative Evaluation. EUREKA: Life Sciences, (1), pp 9-15, 2016.

[8] Kovalenko, I. M., The formation and structure of clones of forest herbs in ecosystem of north-eastern Ukraine. Geomatics, Landmanagement and Landscape, vol. 2, pp. 61-76, 2016.

[9] Zlobin, Yu. A., Skliar, V. G., Klymenko, G. O., Biologiia ta ekologiia fitopopuliatsii [Biology and ecology of phytopopulations] Sumy, Universytetska knyga, p. 512, 2022.

[10] Yaroshenko, N., Skliar, V., Ontogenetic and Vitality Structure Evaluation of Asarum europaeum L. in Göttinger Wald, Lower Saxony, Germany. Bulletin of Sumy National Agrarian University. The Series: Agronomy and Biology, 49(3), pp 76-81, 2023.

GENETIC VARIABILITY AND DEGRADATION DRIVERS FOR CONSERVING AND MANAGING OAK POPULATIONS AT THE LANDSCAPE OF OUTSTANDING FEATURES "KOSMAJ" (SERBIA)

Prof. Dr. Mirjana Šijačić-Nikolić[1]

Assoc. Prof. Dr. Marina Nonić[1]

Ivona Kerkez Janković[1]

Prof. Dr. Jelena Milovanović[2]

Marija Jovanović[2]

[1]University of Belgrade – Faculty of Forestry, Belgrade, **Serbia**
[2]Singidunum University – Environment and Sustainable Development, Belgrade, **Serbia**

ABSTRACT

Identification and quantification of the factors that influence genetic diversity is particularly important for the representatives of the genus *Quercus* L. In this genus, the characterization of the genetic diversity correlations can serve as a basis for predictive models of its distribution. The adaptive and neutral genetic variability of four autochthonous oak species (*Quercus petraea* (Matt.) Liebl. – sessile oak, *Q. pubescens* Willd. – pubescent oak, *Q. frainetto* Ten. – Hungarian oak, *Q. cerris* L. – Turkey oak) was studied at the Landscape of Outstanding Features (LOF) "Kosmaj" in Serbia. This study aimed to test to which degree the inter- and intraspecific genetic variability of oaks is the result of the genotype influence, local habitat conditions, environmental factors, population management practices, and the historical processes that the analyzed populations have gone through. In total, 247 individuals of the four selected oak species were investigated. Adaptive variability was studied using geometric morphometric methods (landmarks and outlines), and neutral variability using nuclear microsatellites (nSSRs). The results showed that the adaptive variability of oaks at the LOF "Kosmaj" is related to habitat characteristics, environmental conditions, and oak population management practices, while neutral variability analysis showed relatively high genetic diversity levels of all studied oak species. The consistency of the results obtained using adaptive and neutral genetic markers, and the consistency of the obtained results with previously published data on genetic variability of oaks was also observed. The results suggest that the effective conservation of oak genetic resources at the LOF "Kosmaj" requires coordinated efforts of the forestry, environmental and nature protection sectors. An important goal is the determination of priority species, populations and areas for the conservation of oak genetic resources in the form of *in situ* conservation units and *ex situ* methods, within a coherent program and in accordance with national policies and the biological capabilities of each species.

Keywords: gene pool conservation, protected area, oaks, variability

INTRODUCTION

Genetic diversity is a key resource for the survival of species during environmental changes. The conservation and sustainable use of genetic resources requires an understanding of the distribution and the degree of genetic diversity (*in situ* and *ex situ*) in a large number of species. Identification and quantification of factors that influence genetic diversity are particularly important in the genus *Quercus* L., and the characterization of genetic diversity correlations in well-studied oak species can serve as a basis for predictive models of its distribution [1]. Patterns of distribution of genetic variability reflect species' responses to evolutionary pressures operating in current or past environments and can provide information about how species adapt over time. Most research on patterns of genetic variation in forest woody species has been driven by the attempts to understand the biodiversity at the intraspecific level or evolutionary dynamics within plant species during the early stages of domestication [2, 3]. However, forest trees possess numerous valuable aspects to be investigated, which can be accomplished using both morphological and molecular markers, to make recommendations for the conservation of their genetic resources [4].

In this paper, we investigated four oak species at the Landscape of Outstanding Features (LOF) "Kosmaj" in Serbia, by analysing adaptive variability using leaf geometric morphometrics and neutral variability using molecular markers (nSSRs). Kosmaj is a low mountain of volcanic origin, located about 40 km south of Serbia's capital (Belgrade) [5, 6]. In 2005, the area of mountain Kosmaj was placed under protection as a Landscape of Outstanding Features (Official Gazette of the City of Belgrade, no. 29/2005). Here, four autochthonous oak species occur (*Quercus petraea* (Matt.) Liebl. – sessile oak, *Q. pubescens* Willd. – pubescent oak, *Q. frainetto* Ten. – Hungarian oak, *Q. cerris* L. – Turkey oak), distributed throughout the mountain.

The hypothesis was tested that the degree of inter- and intraspecific genetic variability of oaks can be the result of the genotype influence, local habitat conditions, environmental factors, population management practices, and the historical processes which the analysed populations have gone through. By measuring genetic variability at different levels, we aimed to characterize the ecological and conservation status of four oak species at the LOF "Kosmaj" and to define specific conservation measures, as well as ecological and conservation principles of managing oak populations.

MATERIALS AND METHODS

In 2022, 247 individuals of four different oak species were sampled: Turkey oak – 60 individuals, sessile oak – 60 individuals, pubescent oak – 65 individuals, and Hungarian oak – 62 individuals (Figure 1).

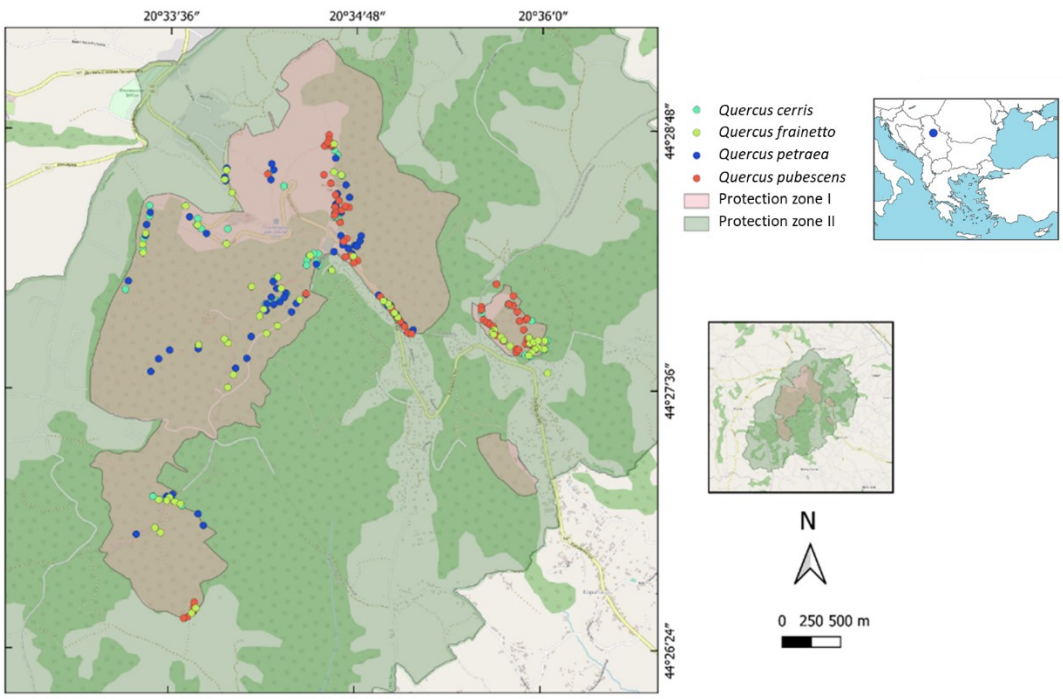

Figure 1. Distribution of investigated oak individuals at the LOF "Kosmaj".

Adaptive variability was investigated using leaf geometric morphometrics. For geometric morphometric analyses, 100 fully developed leaves were sampled from each selected individual. On each of the collected leaves, 13 landmarks were marked, according to the methodology proposed by Viscosi [7], capturing the entire leaf shape. Inter- and intraspecific variability of leaf size and shape was studied using morphological analysis of size and shape – MASS [8] and landmarks, previously described in detail [9-11].

Neutral variability was analyzed using nuclear microsatellites. Ten normally developed young leaves were collected from each selected individual. The molecular analysis included: selection of individuals of four oak species, collection and preparation of plant material (leaves), selection of microsatellites for genotyping, homogenization of plant material, extraction of total genomic DNA, verification of the yield of DNA isolates, parallel multiplication of nuclear microsatellites by polymerase chain reaction (PCR), assessment of the success of PCR amplification on agarose gel, determination of the length of PCR amplification products (scoring), and determination of the level of genetic diversity of the analyzed species and their genetic differentiation. Twenty nuclear microsatellites were selected for genotyping, 14 of which proved to be highly informative and reliable after testing [12, 13]. Detailed methods and results of these analyses are presented in Šijačić-Nikolić et al. [12, 13].

The main negative factors that influence oak genetic resources at the LOF "Kosmaj" were identified, and the patterns of genetic variability of oaks in this area, presented in recent publications [9-13], were used to define specific conservation priorities, as well as environmental and conservation principles of managing oak populations.

RESULTS

Based on the results of our previous studies [9-11], the analyses of adaptive variability of oaks at the LOF "Kosmaj" showed the presence of significant differences in leaf size and shape of sessile, pubescent, Hungarian, and Turkey oak (Figure 2). At intraspecific levels, both size and shape influenced morphological variability in each species. Also, clear patterns of interspecific variability were observed – Hungarian oak had a narrow lower and wider upper part of the leaf blade and a short petiole, Turkey oak had a narrow and pointed leaf blade, while pubescent and sessile oak had a longer petiole and low difference in the width of the upper and the lower part of the leaf blade.

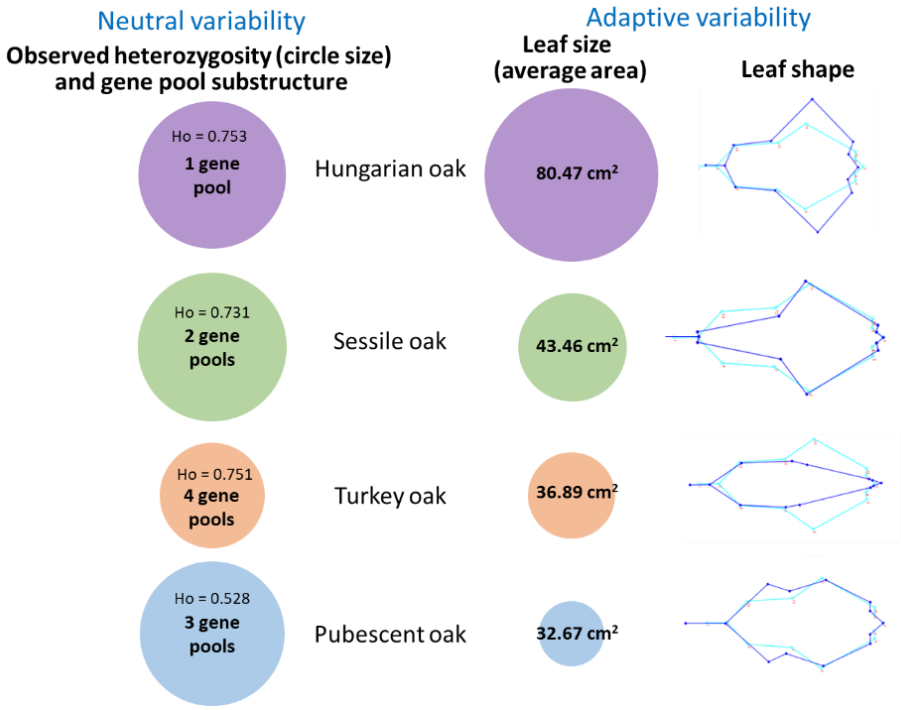

Figure 2. Summarized results of the adaptive and neutral genetic diversity analyses of oaks from the LOF "Kosmaj". Oak species are represented by different colors (purple – Hungarian oak, green – sessile oak, orange – Turkey oak, blue – pubescent oak). Results of nuclear microsatellite analyses (i.e., neutral variability) are represented by the observed heterozygosity values (Ho) and the number of gene pools obtained for each species (for full results see references 12 and 13). Geometric morphometrics results (i.e., adaptive variability) are represented as leaf size values (average area) and shape differences among species (wireframe graphs) (for full results see references 9-11).

The results of neutral variability of oaks from mountain Kosmaj, presented in Šijačić-Nikolić et al. [12, 13], showed that the four analyzed oak species were characterized by high levels of genetic diversity (Figure 2). Interspecific differentiation was the lowest among pubescent and sessile oak, and the highest among sessile and Hungarian oak. At the intraspecific level, population substructuring was observed in all species except the Hungarian oak, which represented a coherent and distinct genetic group. The populations of Turkey, sessile and pubescent oak, on the other hand, belonged to separate gene pools.

The main degradation drivers and their impact on oak genetic resources at the LOF "Kosmaj" were identified and presented in detail in Figure 3. These drivers corresponded to the commonly accepted "HIPPO" acronym [14], which describes habitat destruction, invasive species, pollution, population size, and overexploitation.

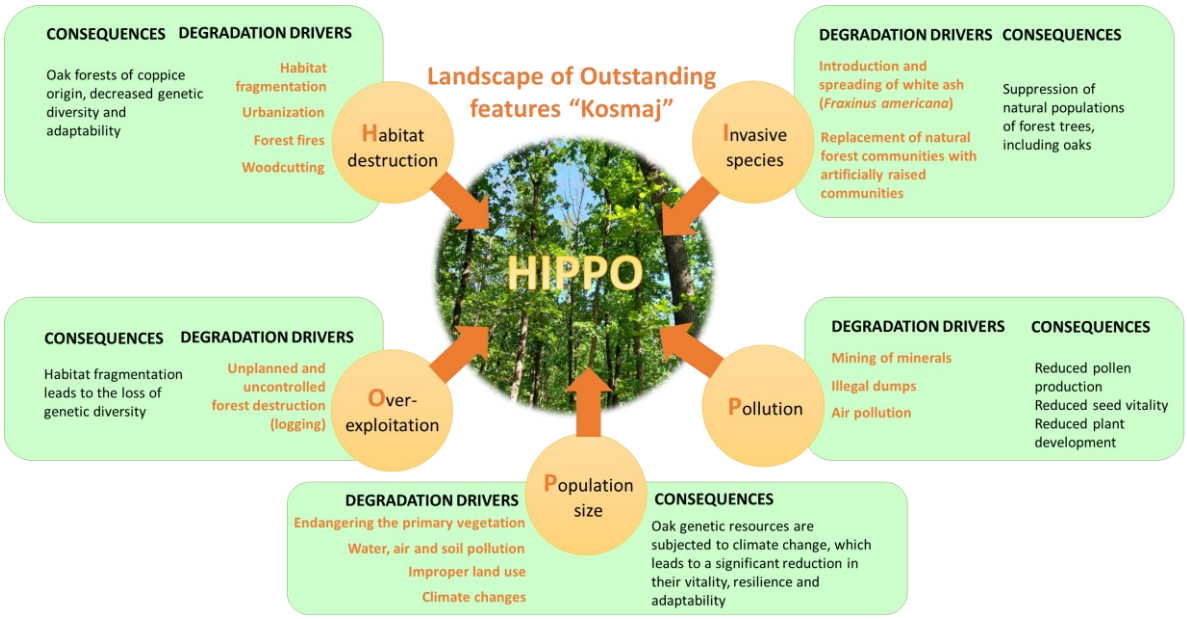

Figure 3. Major degradation drivers and consequences for oak genetic resources at mountain Kosmaj.

Based on the obtained information on the genetic variability of oaks at the LOF "Kosmaj", the general goals of oak genetic resources conservation were represented as follows:

(1) research and education in the field of conservation,
(2) strategic, legal, and program frameworks of conservation,
(3) international and intersectoral cooperation in the conservation,
(4) capacity building and dissemination of information on the conservation,
(5) monitoring and integration of conservation principles into the forest management system.

The main priorities of the oak genetic resources conservation are shown in Figure 4.

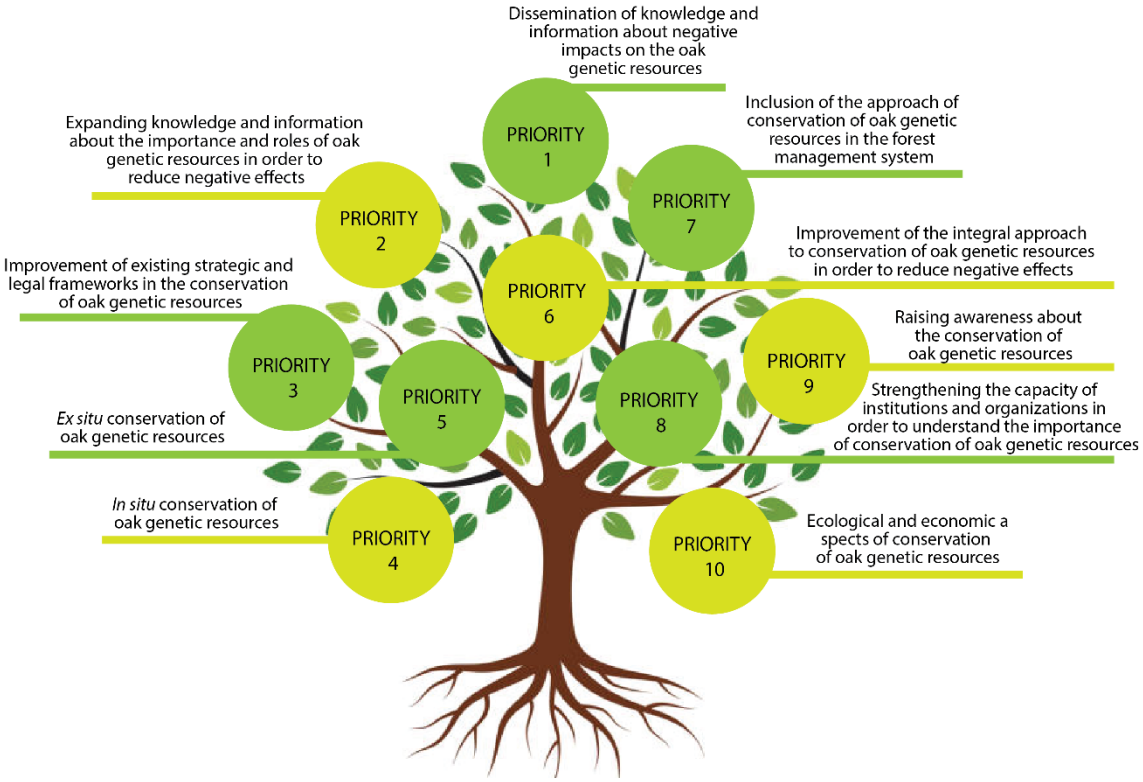

Figure 4. The main priorities of oak genetic resources conservation at the LOF "Kosmaj".

DISCUSSION

The study of adaptive and neutral variability at the inter- and intraspecific levels can be used for the assessment of the influence of local habitat conditions and species population management on survival, especially in widespread species, such as oaks. The Balkan Peninsula represents one of the most significant areas of Europe in terms of the phylogeny of the genus *Quercus*, an area where the postglacial, and generally posttertiary and tertiary evolution of European oak species took place, thanks to its refugial character, specific climate and relief. The significant diversity of the forest vegetation at mountain Kosmaj, and the specific geological, pedological and orographic characteristics, make this area very favorable for the comparative analysis of their genetic characteristics in a relatively small area, which enables the data to be interpreted following the local habitat conditions and to incorporate the obtained information into the wider frame of oak genetic variability in Europe.

Adaptive genetic variability, represented by morphological features, is closely related to adaptability and reflects survival strategies. Analyses of leaf size and shape are very helpful for studying functional features at different scales, to gain a better insight into how morphology adapts to environmental changes. Based on the presented results, the populations of sessile, pubescent, Hungarian, and Turkey oak at the LOF "Kosmaj" were characterized by different, but high levels of genetic diversity, which are a prerequisite for their long-term survival. Also, despite the presence of sympatry, all four species of oaks have retained their genetic integrity, which resulted in a pronounced genetic structure. This was also reflected in the existence of a substructure

of the populations of the most of studied species. Therefore, it can be concluded that the survival of the investigated populations is not threatened. When considering that the study area is located at the European oak phylogenetic hot spot (Balkan Peninsula) with significant degradation drivers that trigger genetic erosion at the mountain Kosmaj (e.g., habitat destruction, climate change, pollution, poor management practices), it can be suggested that the degrees of inter- and intraspecific genetic variability of oaks can be the result of the influence of genotype, local habitat and environmental conditions, population management practices, and the historical processes which the investigated populations have gone through.

The consistency of the results obtained using adaptive and neutral genetic markers and their correspondence with previously published data on genetic variability of oaks was observed. Based on a review of literature data published for different oak species [9-13], it can be noted that the patterns of morphological variability, as well as the levels of genetic diversity in general, fit into the levels observed by other authors on the territory of Europe and wider.

Adaptive and neutral genetic variability are related to the conservation of oak species and supported by the studies of morphology, evolution and classification. New technological advances offer efficient and powerful tools to deepen knowledge and provide better support for planning and conservation. A key step in the conservation of oak genetic diversity, in addition to following modern research trends, is the incorporation of the existing patterns of variability observed at the local level into those observed at the regional and/or global level.

Based on the defined ten priorities for the conservation of the oak genetic resources, it is suggested that the forest management at the LOF "Kosmaj" must be combined with good planning and coordination of activities at the local, national and regional levels. Conservation of the biological diversity of forests, which includes oak genetic resources, is essential for maintaining the productive value of forests, as well as for maintaining the health and vitality of forest ecosystems, and thus for sustaining their protective, ecological and cultural functions. A major threat to forest ecosystems on the mountain Kosmaj is the use of forest land for other purposes, which is why land use changes should be carefully planned to ensure that the complementary goals of conservation and development are achieved. This can be implemented by intensifying conservation at the LOF "Kosmaj", as a main component of land use planning and resource management strategies.

Conservation decisions related to oak genetic resources should not be made in isolation, but as an integral component of management plans for protected areas and forest management. The key to success is to develop programs that balance the conservation and sustainable use of oak biological diversity and genetic resources within a "mosaic" of land use options. Also, the effective conservation of oak genetic resources requires coordinated efforts of the forestry, environmental, and nature protection sectors. An important goal is the determination of priority species, populations and areas for the conservation of oak genetic resources in the form of *in situ* conservation units and *ex situ* methods, within a coherent program that is in accordance with national policies and the biological capabilities of each species.

There are no fundamental technical barriers to achieving conservation goals. In recent years, numerous activities have been initiated to conserve and sustainably use the

genetic resources of oaks. However, the practical experiences of many activities are insufficiently documented, and the acquired knowledge receives little attention and is rarely applied on a larger scale. Experience shows that careful and timely measures and programs based on the best available knowledge can make a vital contribution to the conservation of oak genetic resources. It is therefore of the utmost importance that this experience, together with current knowledge of conservation theoretical principles, be made widely available in the form of generalized guidelines and procedures.

CONCLUSION

To determine the general patterns of variability of oaks, the use of adaptive and neutral markers in the oak genetic variability assessment at the LOF "Kosmaj" allowed the comparison of the obtained results with data published in other studies. Also, the obtained results enabled a deeper understanding of the connections between morphometric and molecular characteristics of oaks, as a response to the influence of environmental conditions, population management and historical processes. The contribution of this research is primarily reflected in setting the ground for the conservation of oak populations in the studied area.

Based on the obtained results, the main goal of the study, which included the characterization of the environmental and conservation status of four oak species at the LOF "Kosmaj" was fulfilled, and the definition of specific conservation measures, as well as environmental and conservation principles of managing their populations, was successfully performed. Relying on the clear recognition of different species and their limitations in the area of mountain Kosmaj, the conservation of species in this area goes far beyond the provision of genetic diversity of populations and ecosystems. However, the study of genetic diversity is the first and crucial step for establishing successful conservation strategies, because without a true understanding of overall biodiversity, conservation procedures and attempts remain incomplete and fragmented.

ACKNOWLEDGEMENTS

The research was funded by the Secretariat for Environmental Protection of the city of Belgrade (Grant No. 401.1-119/21), and the Ministry of Education, Science and Technological Development of the Republic of Serbia (Grant No. 451-03-47/2023-01/200169 and Agreement No. 0801-417/1).

REFERENCES

[[1] Suzuki Spence E., Fant J.B., Gailing O., Griffith M.P., Havens K., Hipp A.L., Kadav P., Kramer A., Thompson P., Toppila R. Comparing Genetic Diversity in Three Threatened Oaks. Forests, vol. 12/issue 5, no 561, 2021.

[2] Krutovsky K.V., Neale D.B. Nucleotide diversity and linkage disequilibrium in cold-hardiness- and quality-related candidate genes in Douglas fir. Genetics, vol.171/issue 4, pp 2029-2041, 2005.

[3] Finkeldey R, Ziehe M. Genetic implications of silvicultural regimes. Forest Ecology and Management, vol. 197/issue 1-3, pp 231-244, 2004.

[4] Barrandeguy M.E., Garcia M.V. Microsatellites as a tool for the study of microevolutionary process in native forest trees. In: Abdurakhmonov, I.Y. (ed.) Microsatellite Markers. InTech Open, 2016.

[5] Sredojev, S. Pavković, D., Miljić, M. Possibilities of application of GIS in assessment and protection of natural values of Region of outstanding features "Kosmaj". Collection of Papers – Faculty of Geography, University of Belgrade, vol. 59, pp 235-246, 2011.

[6] Stajić S.A. Determination of forest phytocoenoses of mt. Kosmaj by combining the standard phytosociological method with photointerpretation. PhD Thesis, Faculty of Forestry, University of Belgrade, Serbia, 2016.

[7] Viscosi, V. Geometric morphometrics and leaf phenotypic plasticity: assessing fluctuating asymmetry and allometry in European white oaks (*Quercus*). Botanical Journal of the Linnean Society, vol. 179/issue 2, pp 335-348, 2015.

[8] Chuanromanee T.S., Cohen J.I., Ryan G.L. Morphological Analysis of Size and Shape (MASS): An integrative software program for morphometric analyses of leaves. Applications in Plant Sciences, vol. 7/issue 9, no e11288, 2019.

[9] Jovanović M. Characterization of ecological and conservation status of oaks (*Quercus* L.) from the Region of outstanding features “Kosmaj”. PhD Thesis, Singidunum University, Belgrade, Serbia, 2023 (*accepted for defense*)

[10] Jovanović M., Kerkez Janković I., Milovanović J., Nonić M., Šijačić-Nikolić M. Intraspecific variability of the sessile oak (*Quercus petraea* Matt. Liebl.) leaf traits from the Mount Kosmaj (Serbia). Biology Bulletin, https://doi.org/10.1134/S1062359023602471, 2023a.

[11] Jovanović M., Kerkez Janković I., Milovanović J., Nonić M., Šijačić-Nikolić, M. Intraspecific variability of *Quercus pubescens* Willd. leaves from the Outstanding Natural Landscape „Kosmaj” in Serbia. Biology Bulletin, in press, 2023b.

[12] Šijačić-Nikolić M., Vilotić D., Aleksić J., Milovanović J., Nonić M., Kerkez Janković I., Jovanović M. Identification, monitoring and conservation of the gene pool of endemic, rare and endangered woody species in the area of the Region of outstanding features "Kosmaj" - the monograph. Faculty of Forestry, University of Belgrade, Serbia, 2023.

[13] Šijačić-Nikolić M., Kerkez Janković I., Jovanović M., Milovanović J., Aleksić J. M. Genetic diversity and genetic structure of three sympatric oak species in the Serbian Outstanding Natural Landscape "Kosmaj" assessed by nuclear microsatellites. South-east European Forestry, in press, 2023

[14] Wilson, O. E. The diversity of life. Harvard University Press, pp. 424, 1992

TREE LITTER PRODUCTION IN GREY ALDER (*ALNUS INCANA*) STANDS ON DRY AND WET MINERAL SOILS

Mg. silv. Kārlis Bičkovskis[1 2]

Mg. silv. Valters Samariks[12],

Dr. silv. Āris Jansons[1 2]

[1] Latvian State Forest Research Institute "Silava", **Latvia**
[2] Latvia University of Life Sciences and Technology, **Latvia**

ABSTRACT

Forests play an important role in carbon storage and global carbon cycling. The processes of litter decomposition, movement within the soil, and incorporation into different soil layers play a crucial role in the functioning of forest ecosystems. These activities are important in regulating the cycling of soil organic matter and the storage and release of carbon into the atmosphere. Soil carbon and carbon input via litter has been well-recognized, however studied relatively less compared to other carbon pools, but local estimates are necessary to reduce uncertainties and due to climate change mitigation goals. The aim of the study is to evaluate differences in tree litter production in different age classes and forest types in grey alder (*Alnus incana*) dominated forests.

In total 12 grey alder stands were selected to represent each age class (10-year interval) in two different soil moisture regimes (dry and wet mineral soils). In each stand 4 litter collectors were placed in a transect and samples collected every month for a full year. Each sample was air dried until constant weight and weighted afterwards to determine litter dry-weight.

Our study results indicate seasonal differences in litter production, however significant differences between average litter production of grey alder stands in dry and wet mineral soils was not observed. Moreover, litter production amount is lower for younger stands and increases with age, as study results indicate that main factor determining litter production is stand basal area.

Keywords: carbon, hemiboreal, litterfall, litter flux

INTRODUCTION

Forests of boreal and hemiboreal region are essential for carbon storage and global carbon cycle, as they are large carbon (C) and nitrogen (N) store, thus play an important role in climate change mitigation. One of parameters in estimating soil organic carbon stock and its changes is tree litter production, however relatively less studied carbon pool [1] [2]. Tree canopy litterfall plays an important role in aboveground litter flux in forest ecosystems, affecting soil carbon and nutrient cycles, and soil fertility [1]. Annual litterfall depends on several stand characteristics such as tree species composition, stand age, basal area and site fertility [3]. In Nordic region to estimate soil carbon stock and its changes, the Yasso model has been developed for forest on mineral soils [4] [5]. The model allows to estimate soil C stock and changes in soil C pool using different climatic

conditions and soil C input data, including aboveground litter data. Therefore, to provide reliable estimates of soil C input via tree aboveground litter, it is essential to obtain regional specific data.

It has been reported, that the annual litter production in deciduous stands is higher than in coniferous stands, for example, in Europe, an average litterfall in deciduous forests was 1.5-2.1 C t ha^{-1} yr^{-1}, but in conifer forests 1.7-1.8 C t ha^{-1} yr^{-1} [2] [6] [7]. Despite the significant role, the dynamics of litterfall are not thoroughly studied in the hemiboreal region for all most common tree species. Recent studies have focued on Scots Pine (*Pinus sylvestris*), Norway spruce (*Picea abies*), silver birch (*Betula pendula*) and black alder (*Alnus glutinosa*) [6] [7], however information about grey alder (*Alnus incana*) is lacking. Therefore, the aim of the study is to evaluate differences in tree litter production in different age classes and forest types in grey alder dominated stands, as well as to develop regional litter models for estimating the annual litter flux. We hypothesize that annual litterfall will not differ between grey alder stands on dry and wet mineral soils.

MATERIALS AND METHODS

The study was conducted in the hemiboreal vegetation zone in Latvia [8]. The climate is described as temperate, but strongly affected by the Baltic Sea and the North Atlantic. The mean annual sum of precipitation is 692 mm, and the mean annual air temperature is +6.4 ℃. The coldest month is February, with the average air temperature around -3.7 ℃, and the warmest month is July with the average air temperature +17.4 ℃ as described by Latvian Environment Geology and Meteorology Centre.

Study objects are 12 Grey alder stands on dry and wet mineral soils (Table 1). Stand selection was based on occurrence of target soil type (mineral soil) with two differing soil moisture regimes (dry and wet). Grey alder as dominant tree species (> 60% of stand composition) and stands with different age classes (from 10 to 70 years old).

Table 1. Study site description

Dominant tree species	Soil type	Moisture regime	Age class	Mean height, m	Mean diameter, cm	Basal area, m^2
Grey alder	Mineral soil	Dry	10	7	7	2
Grey alder	Mineral soil	Dry	20	12	8	16
Grey alder	Mineral soil	Dry	30	16	13	24
Grey alder	Mineral soil	Dry	40	18	20	7
Grey alder	Mineral soil	Dry	50	20	20	18
Grey alder	Mineral soil	Dry	60	24	26	19
Grey alder	Mineral soil	Dry	70	22	22	26

Grey alder	Mineral soil	Wet	10	4	4	3
Grey alder	Mineral soil	Wet	20	9	8	13
Grey alder	Mineral soil	Wet	30	19	17	9
Grey alder	Mineral soil	Wet	40	17	17	16
Grey alder	Mineral soil	Wet	50	22	24	21
Grey alder	Mineral soil	Wet	60	18	18	13

In each stand four litter collectors (D=110 cm, Area=0.95 m^2) were placed at the height of 1.3 m above ground in a transect. On the bottom of each litter collector a litter bag was placed to collect all aboveground litter. Samples were collected once a month in a snow free season and once after the end of winter season for a full calendar year. Collected samples were delivered to the laboratory and air dried at 75°C until constant weight to assess biomass dry weight. Litter C content was calculated using estimate of 52.1% of C content in litter obtained in hemiboreal region for deciduous tree species [7].

Statistical analysis

Study data were checked for normal distribution with Shapiro-Wilk test. Prior to model development, correlation matrix was developed for assessment of stand characteristic relationship with litter production. Average values and 95% confidence intervals were calculated for each parameter. Significant differences between analysed parameters were assessed using t-test for parametric variables and Wilcoxon test for non-parametric variables. Logarithmic model was developed to describe annual litter production relationship with stand basal area for stands on dry and wet mineral soils. All data analysis were performed using MS Excel.

RESULTS

Aboveground litter shows seasonal differences in litter production (Figure 1.). Highest litter production has been observed in autumn with an average litter up to 8.39±1.02 t ha^{-1} yr^{-1} (average ± 95% confidence interval) and 7.36±0.74 t ha^{-1} yr^{-1} in stands with dry and wet soils, respectively. Second highest seasonal litter production has been observed in summer with an average of 2.95±0.32 t ha^{-1} yr^{-1} and 3.69±0.45 t ha^{-1} yr^{-1} in stands with dry and wet soils, respectively. Winter season litter production makes up to 1.41±0.23 t ha^{-1} yr^{-1} and 1.55±0.28 t ha^{-1} yr^{-1} in stands with dry and wet soils, respectively. Lowest litter production was observed in spring season with an average up to 0.68±0.25 t ha^{-1} yr^{-1} and 1.0±0.40 t ha^{-1} yr^{-1} in stands with dry and wet soils, respectively. Differences between seasonal litter in stands with dry and wet soils were not statistically significant, however differences in litter production between seasons were statistically significant in all cases ($p<0.05$), except between spring and winter season in stands with wet mineral soils. On average annual litter in stands with dry mineral soil was 3.36±1.30 t ha^{-1} yr^{-1} and 3.40±1.17 t ha^{-1} yr^{-1} in wet mineral soils.

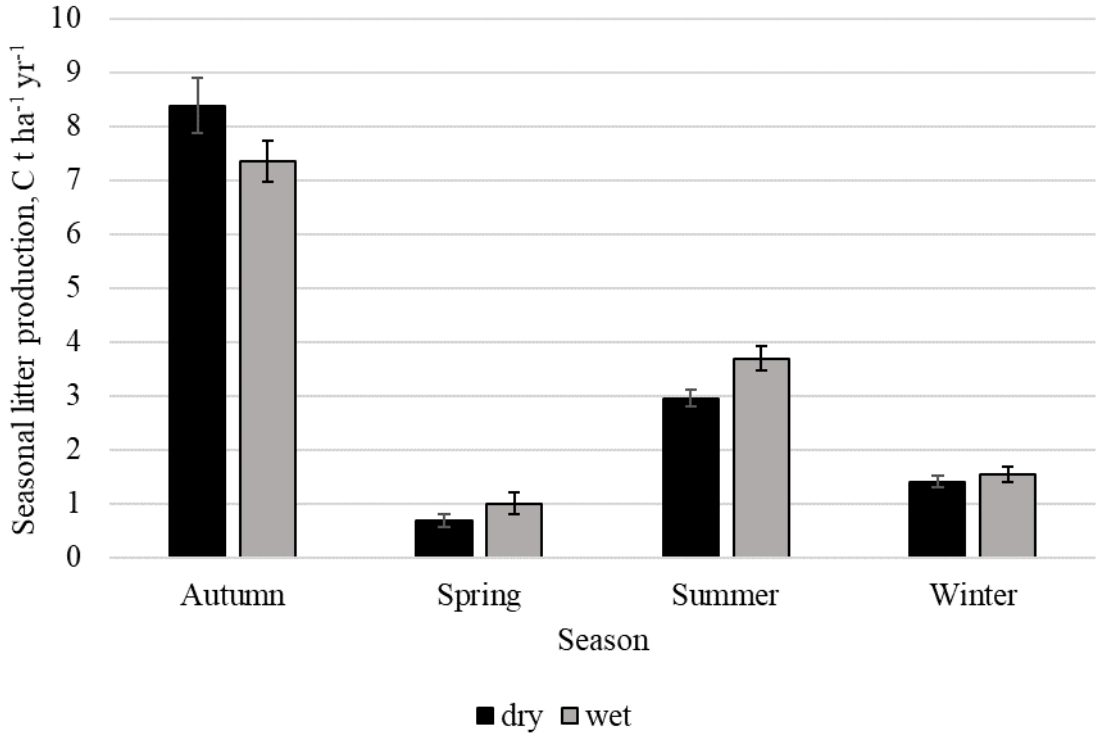

Figure 1. Seasonal soil C input by litter in grey alder stands on dry and wet mineral soils. (Whiskers denote ± 95% confidence interval)

Correlation matrix indicates close relationship of annual litter with stand basal area and growing stock (Table 2), moreover annual litter has moderate correlation with other stand characterizing variables (age, height and diameter at breast height). Based on obtained results further litter production was estimated using basal area as easier measurable variable in forest stands.

Table 2. Correlation matrix of stand characteristics and litter input

	Age, years	Height, m	Diameter, cm	Basal area, m^2	Growing stock, m^3	Litter, t ha^{-1} yr^{-1}
Age, years	X	0.87	0.88	0.64	0.77	0.60
Height, m	0.87	X	0.97	0.68	0.79	0.65
Diameter, cm	0.88	0.97	X	0.57	0.75	0.66
Basal area, m^2	0.64	0.68	0.57	X	0.93	0.78
Growing stock,m^3	0.77	0.79	0.75	0.93	X	0.88
Litter, t ha^{-1} yr^{-1}	0.60	0.65	0.66	0.78	0.88	X

In grey alder stands the data suggest that annual litter and stand basal area was best predicted by logarithmic function (Figure 2). The coefficient of determination for stands on dry mineral soils showed moderate relationship (R^2=0.60), but on wet mineral soils it showed weaker relationship (R^2=0.25), however on average relationship was moderate (R^2=0.47).

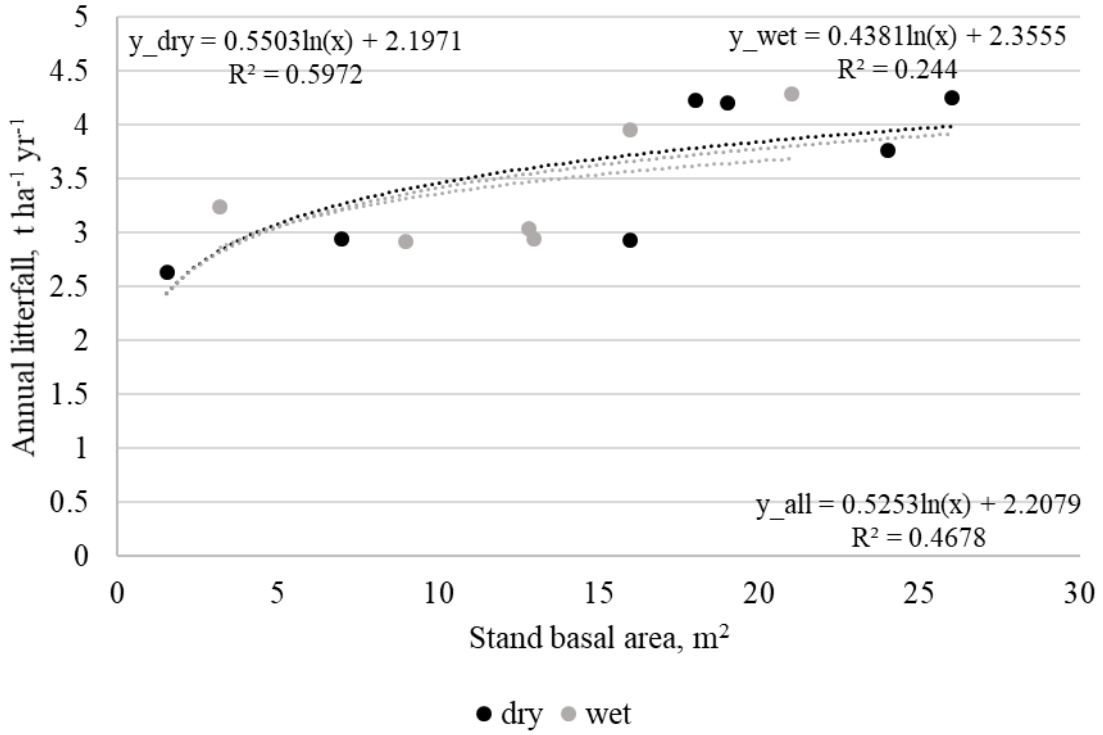

Figure 2. Relationship between annual litter production and stand basal area in dry and wet mineral soils

Annual soil C input by litter was estimated based on annual litter biomass for dry and wet mineral soils and all soil types together due to no significant differences between wet and dry soils (Figure 3). The annual soil C input by litter ranges from 1.37±0.57 to 2.21±0.75 C t ha^{-1} yr^{-1} in dry mineral soils, and from 1.52±0.64 to 2.24±0.81 C t ha^{-1} yr^{-1} in wet mineral soils. On average annual soil C input by litter is 1.75±0.65 C t ha^{-1} yr^{-1} and 1.77±0.54 C t ha^{-1} yr^{-1} in dry and wet mineral soils, respectively.

Model results suggest that young stands have a steeper increase in annual C input by litter at the beginning, but further increase in the basal area have a more gradual impact on annual C input.

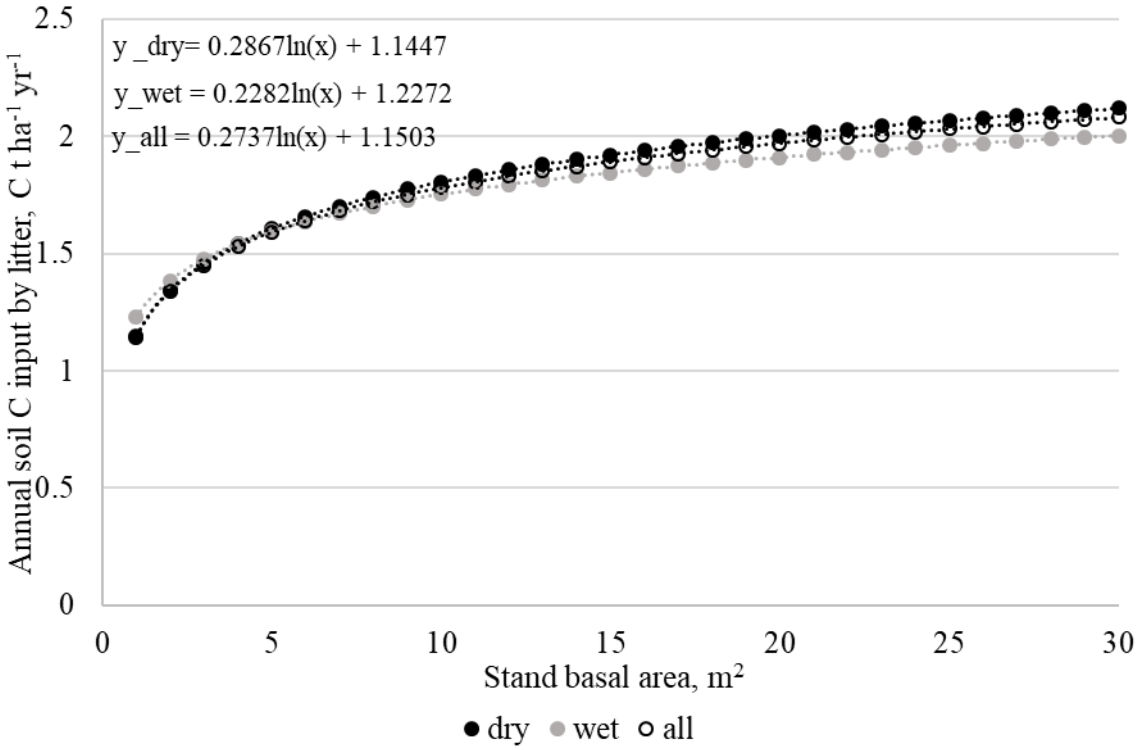

Figure 3. Logarithmic model of annual soil C input with above-ground litter characterized by stand basal area in grey alder stands on dry and wet mineral soils and all analyzed stands together.

DISCUSSION

Studies have highlighted factors affecting annual litter production and results can differ depending on climatic region and factors, precipitation and evapotranspiration that are greatly related to geographical conditions [2] [3] [9]. Study results indicate litter production and C input in soil by litter has moderate relationship with stand age, tree height, diameter at breast height and close relationship with growing stock, as well as stand basal area (Table 2). However there might be additional factors affecting litter production such as tree species composition and site fertility [2] [9].

Study results reveal information about seasonal litterfall of stands on dry and wet mineral soils. The highest amount of litter of deciduous tree species can be observed in autumn, but the lowest in spring season. On average annual soil C input by litter is 1.75±0.65 and 1.77±0.54 C t ha^{-1} yr^{-1} in dry and wet mineral soils, respectively, but the differences are insignificant ($p>0.05$), therefore approving our hypothesis. Study findings on annual soil C input by litter are within the range of uncertainty with findings from Northern Europe (boreal region) where annual litter C input was slightly lower (1.5±1.1 C t ha^{-1} yr^{-1}) for deciduous trees [2]. In addition, similar relationship with stand basal area have been observed in silver birch stands in hemiboreal region, however estimates of average soil C input by litter were higher (2.07±0.03 C t ha^{-1} yr^{-1}) [6]. Differences between observed annual C input by litter could be partially explained by different tree species compared between studies of similar regions, and the variation in

litterfall data acquired in the studies can be explained with the variation of basal area of the forest stands studied.

Incorporating many variables into models can result in more accurate predictions [4]. However, this would also increase the complexity of the models, limiting their practical applicability. Generally, models with fewer and easily accessible independent variables may have reduced precision, but they can be more broadly used for practical purposes. Concerning litterfall modelling, the basal area of a stand is a significant variable, typically correlating with litter biomass and canopy closure. [6] [7] [9]. Also in our study we have moderate relationship of basal area with litter biomass (Figure 2), therefore used it as a predictor for annual C litter models (Figure 3) for practical implications. Model results indicate a steeper increase in annual C input by litter for younger stands, but further increase in the basal area have a more gradual impact on annual C input by litter. Such findings are in accordance with studies conducted in hemiboreal region about birch annual litter flux where a rapid increase in the annual leaf litter flux was observed in birch stands at the early stage of development (10–15 years old) and stabilized thereafter [10]

CONCLUSION

The study reveals novel information about annual C litter input in soil in grey alder stands on dry and wet mineral soils, supplementing existing knowledge and estimates in hemiboreal region. Average annual soil C input by litter is 1.75±0.65 C t ha^{-1} yr^{-1} and 1.77±0.54 C t ha^{-1} yr^{-1} in dry and wet mineral soils however differences are not distinct. Developed model provides reliable estimates for practical application using easily measurable stand parameter. Litter production has strong seasonal variation. Annual litter production changes with stand basal area. During early stages of stand succession a rapid increase in annual C input by litter can be expected, but further stabilizes with basal area increase.

Further studies should focus on impact of other carbon pools on soil C input, such as belowground litter and biomass, fine-roots, ground vegetation and harvesting residues, for better estimation of soil carbon stock and prediction of its changes due to natural disturbances or management that alters stand development trajectory

ACKNOWLEDGEMENTS

The research was funded by ERDF project “Tool for assessment of carbon turnover and greenhouse gas fluxes in broadleaved tree stands with consideration of internal stem decay” No. 1.1.1.1/21/A/063

REFERENCES

[1.] Feng, C., Wang, Z., Yan, M., Songling, F., & Chen, H. Y. H. Increased litterfall contributes to carbon and nitrogen accumulation following cessation of anthropogenic disturbances in degraded forests. Forest Ecology and Management, 432, 832–839, 2019. https://doi.org/10.1016/j.foreco.2018.10.025

[2.] Neumann, M., Ukonmaanaho, L., Johnson, J., Benham, S., Vesterdal, L., Novotný, R., Verstraeten, A., Lundin, L., Thimonier, A., Michopoulos, P., & Hasenauer, H.. Quantifying carbon and nutrient input from litterfall in European forests using field observations and modeling. Global Biogeochemical Cycles, 32(5), 784-798, 2018. DOI: 10.1029/2017GB005825

[3.] Berg, B., & Laskowski, R. Litter decomposition: A guide to carbon and nutrient turnover. Advances in Ecological Research, 38(1), 1-428, 2005. DOI: 10.1016/S0065-2504(05)38001-9

[4.] Viskari, T., Pusa, J., Fer, I., Repo, A., Vira, J., & Liski, J. Calibrating the soil organic carbon model Yasso20 with multiple datasets. Geoscientific Model Development, 15, 1735–1752, 2022. DOI: 10.5194/gmd-15-1735-2022

[5.] Liski, J., Palosuo, T., Peltoniemi, M., & Sievänen, R. Carbon and decomposition model Yasso for forest soils. Ecological Modelling, 189(1–2), 168-182, 2005. DOI: 10.1016/j.ecolmodel.2005.03.005

[6.] Bārdule, A., Petaja, G., Butlers, A., Purviņa, D., & Lazdiņš, A. Estimation of litter input in hemiboreal forests with drained organic soils for improvement of GHG inventories. Baltic Forestry, 27(2), 534, 2021. DOI: 10.46490/BF534

[7.] Butlers, A., Lazdiņš, A., Kalēja, S., & Bārdule, A. Carbon Budget of Undrained and Drained Nutrient-Rich Organic Forest Soil. Forests, 13(11), 1790, 2022. DOI: 10.3390/f13111790

[8.] Ahti, T., Hamet-Ahti, L., & Jalas, J. Vegetation zones and their sections in northwestern Europe. Annales Botanici Fennici, 5, 169-211, 1968

[9.] Starr, M., Saarsalmi, A., Hokkanen, T., Merilä, P., & Helmisaari, H.-S. Models of litterfall production for Scots pine (*Pinus sylvestris* L.) in Finland using stand, site, and climate factors. Forest Ecology and Management, 205, 215-225, 2005.

[10.] Uri, V., Kukumägi, M., Aosaar, J., Varik, M., Becker, H., Aun, K., Nikopensius, M., Uri, M., Buht, M., Sepaste, A., Padari, A., Asi, E., Sims, A., & Karoles, K. Litterfall dynamics in Scots pine (*Pinus sylvestris*), Norway spruce (*Picea abies*), and birch (*Betula*) stands in Estonia. Forest Ecology and Management, 520, 120417, 2022. DOI: 10.1016/j.foreco.2022.120417